City Research Online

City St George's, University of London

Citation: Baldwin, S. N. (2022). Sexual dimorphisms in vascular KV7 channels. (Unpublished Doctoral thesis, St George's, University of London)

This is the accepted version of the paper.

This version of the publication may differ from the final published version. To cite this item please consult the publisher's version.

Permanent repository link: https://openaccess.city.ac.uk/id/eprint/37181/

Copyright and Reuse: Copyright and Moral Rights remain with the author(s) and/or copyright holders. Copies of full items can be used for personal research or study, educational, or not-for-profit purposes without prior permission or charge, unless otherwise indicated, provided that the authors, title and full bibliographic details are credited, a hyperlink and/or URL is given for the original metadata page and the content is not changed in any way. For full details of reuse please refer to City Research Online policy.

City Research Online: http://openaccess.city.ac.uk/ publications@citystgeorges.ac.uk

Sexual dimorphisms in vascular K_V7 channels

Samuel Neil Baldwin

BSc (Hons)

A thesis presented for the degree of Doctor of Philosophy (Ph.D.)

Supervised by:

Prof. Iain A Greenwood

Prof. Anthony P Albert

St George's university, London

March 2022

General abstract

Introduction: *Kcnq*-encoded K_V7 channels (termed $K_V7.1$-5) are essential regulators of vascular physiology and are associated with pathophysiological states, however, vascular studies on Kv7 channels to date have focussed almost solely on arteries from males. Considering impact of sex, the oestrus cycle and sex-hormones on vascular reactivity, the aim of this project was to characterise properties of K_V7 channels within several arteries from male and female Wistar rats separated into Di-oestrus and Met-oestrus (F-D/M) and Pro-oestrus and Oestrus (F-P/E) from normotensive (NT) and spontaneously hypertensive rats (SHRs).

Methods: RT-qPCR, immunocytochemistry and proximity-ligation assay determined K_V7 expression and interactions. Wire myography characterised vascular reactivity. Circulating sex-hormone concentrations were determined by Enzyme linked immunosorbent assays (ELISA). Whole-cell electrophysiology determined the specificity of K_V7 channel modulators and revealed the effect of Estrogen receptor stimulation on K_V7 currents.

Key results: The molecular and functional characteristics of vascular K_V7 channels were impaired within arteries from F-P/E compared to F-D/M animals, which corelated with raised serum Oestradiol E2. Moreover, F-P/E like K_V7 characteristics could be replicated in arteries from F-D/M by supplemental Oestradiol E2. Interestingly, K_V7 channel function was preserved within female SHRs when compared to males. A novel functional role for $K_V7.1$ was identified within prostacyclin mediated relaxation. Finally, endothelial cells express functional K_V7 channels.

Conclusions and implications: This dissertation has revealed dramatic alterations in Kv7 channel role throughout the oestrus cycle. A novel G-protein coupled Oestrogen receptor mediates a post transcriptional decrease in K_V7 membrane abundance, giving rise to a

'pro-contractile state.' In addition, K_V7 channels potentially represent one of the many factors that differentiates the aetiology of hypertension between age-matched men and women. Finally, the contribution of $K_V7.1$ to receptor mediated relaxation and the expression of K_V7 within the endothelium adds new layers of complexity to the control of vascular tone by these channels.

Declaration by the candidate

I, Samuel Neil Baldwin, hereby declare that this thesis is my own work and that it has not been submitted elsewhere for any award.

Where other sources of work have been used, they have been acknowledged,

Signature:

Date: 01.03.2022

Acknowledgments

First and foremost, I would like to thank Professor Iain Greenwood. Since my undergraduate degree here at St George's, Iain has inspired in me a passion for pharmacology that I now intend to make my life's work. His enthusiasm and charisma as a lecturer made any subject matter engaging, exciting and surmountable. I knew that when the time came to choose my bachelor's degree dissertation project, any work that Iain offered was for me. After starting in the lab, it became clear my choice was justified. Iain provides an environment for any student to achieve high quality data, to engage in debate over a stunning range of topics and to promote oneself to the wider scientific community. With his continual and unwavering support and guidance, my Ph.D. experience has been one of academic fervour and good times. His dedication to my success during my time here and for my future has been invaluable to me, I will always be grateful to him, and I hope that we remain friends. A special thank you must also go to my co-supervisor Professor Anthony Albert. Though we weren't in daily contact, Anthony has always been a friendly and considerate ear. His calm presence and keen interest in my work has always been greatly appreciated.

During my project, I have had the pleasure to work alongside Dr Henry Askew-Page, Dr Vincenzo Barrese, Dr Jennifer Stott, Dr Miguel Aragon Baudel, Dr Sultana Jahana and Ms Simonette Carlton-Crew. With their help, I have slowly but surely developed into my own independent researcher, and I thank them all for their patience with me. Our lunches in Simply and the market and our nights in the bar have been a staple during my time here. A place to decompress, drink too much and eat great food. I've been lucky to make friends for life and want to thank them for introducing me to parts of Italian, Spanish and Scottish culture that I will take with me everywhere. Their company has been a pleasure and without them my experience here would have been far duller. To Elizabeth, and Zena, I leave the lab in great hands, good luck with your projects!

Next to my friends, Ed, Rob, Julia, Lowri, Craig and Emilie, who have let me rant and rave, who have helped me celebrate the highs, commiserate the lows and who have made me laugh to tears. I want to thank you all for your continual and generous friendship and love.

To Emily, I am so lucky to have had your unwavering support and understanding over the last five years. Her love, time and devotion have carried me through two degrees. Our weekends in Liverpool and London were always the perfect respite, and since moving to London life has only been the easier. I want to thank you for our Fridays in Heny's, our Sunday Bolognese, our love of Pizza, our cycling endeavours and so much more. Without her, this Ph.D. would have been much harder.

Lastly, to my family. I stand on the support that they have given me, and without them this work would not have been possible. A thank you seems insufficient for the time, love, patience, and support that my parents, Helen, and Craig, have always offered me. They have worked so hard to ensure that my brothers and I had every opportunity available to us. Always a phone call away, and no problem too mundane to listen too, I have always been able to rely on them both. To my Grandparents, Margaret, and Neil, the pride you take in all our achievements fills us with a sense of gratitude that I couldn't put into words. Finally, to Michael and Daisy, though you both passed during this degree, your thoughtful, earnest, and honest intellectualism, though sometimes brass, has always been my original source for interest in academic pursuits. Though I wish you could see the final product, I'm so grateful you helped me get this far.

‘In loving memory of Daisy and Michael’

Publications

- Baldwin, S. N., Barrese, V., Stott, J. B., Isakson, B. E., Albert, A. P., Greenwood, I. A. (2021): Marked Oestrus cycle-dependent regulation of rat arterial K_V7.4 channels driven by Oestradiol E2. Under review- BJP
- Baldwin, S. N., Forrester, E. A,. McEwan, L., Greenwood, I. A. (2021). Sexual dimorphism in prostacyclin-mimetic responses within rat mesenteric arteries: A novel role for KV7.1 in shaping IP-receptor mediated relaxation. 2021-BJP-0867-RP.R1. *British Journal of Pharmacology*, 1– 15. https://doi.org/10.1111/bph.15722
- Cil, O., Chen, X., Askew Page, H. R., Baldwin, S. N., Jordan, M. C., Myat Thwe, P., Anderson, M. O., Haggie, P. M., Greenwood, I. A., Roos, K. P., & Verkman, A. S. (2021). A small molecule inhibitor of the chloride channel TMEM16A blocks vascular smooth muscle contraction and lowers blood pressure in spontaneously hypertensive rats. *Kidney international*, *100*(2), 311–320. https://doi.org/10.1016/j.kint.2021.03.025
- Baldwin, S. N., Sandow, S. L., Mondéjar-Parreño, G., Stott, J. B., & Greenwood, I. A. (2020). K_V7 Channel Expression and Function Within Rat Mesenteric Endothelial Cells. *Frontiers in physiology*, *11*, 598779. https://doi.org/10.3389/fphys.2020.598779
- Barrese, V., Stott, J. B., Baldwin, S. N., Mondejar-Parreño, G., & Greenwood, I. A. (2020). SMIT (Sodium-Myo-Inositol Transporter) 1 Regulates Arterial Contractility Through the Modulation of Vascular Kv7 Channels. *Arteriosclerosis, thrombosis, and vascular biology*, *40*(10), 2468–2480. https://doi.org/10.1161/ATVBAHA.120.315096
- Askew Page, H. R., Dalsgaard, T., Baldwin, S. N., Jepps, T. A., Povstyan, O., Olesen, S. P., & Greenwood, I. A. (2019). TMEM16A is implicated in the regulation of coronary flow and is altered in hypertension. *British journal of pharmacology*, *176*(11), 1635–1648. https://doi.org/10.1111/bph.14598

Conference presentations

Oral communications

- *2019*- West-Palm beach, Florida- Federation of American societies for experimental biology, 'The Smooth Muscle Conference': Sex-dependent differences in vascular K_V7 channels
- *2019*- Copenhagen, Denmark- Scandinavian Physiological Society, Annual Scandinavian vascular research symposium: Investigation into the expression and function of K_V7 channels in arteries from male vs female rats

Poster presentations

- *2021*- British pharmacological Society, Pharmacology 2021: Oestrus cycle-dependent changes in arterial K_V7 activity
- *2019*- Edinburgh, UK- British pharmacological Society, Pharmacology 2019: Sex-dependent differences in vascular K_V7 channels
- *2019*- Naples, Italy- Italian Society of Pharmacology, International Kv7 channels symposium: Sex-dependent differences in vascular K_V7 channels
- *2019*- West-Palm beach, Florida- Federation of American societies for experimental biology, 'The Smooth Muscle Conference': Sex-dependent differences in vascular K_V7 channels
- *2018*- London, UK- The Physiological Society, Europhysiology 2018: K_V7 channels expression and function in rat mesenteric artery endothelium.

Table of contents

Chapter 1: Introduction **30**

1.1 The cardiovascular system and disease 30

1.2 Vascular contraction 31

1.2.1 $G_{q/11}$ mediated calcium dependent contraction 31

1.2.2 Calcium sensitization via MLCP 33

1.2.3 Calcium sensitization via actin polymerization 35

1.3 Depolarizing ion channels of the vasculature 36

1.3.1 CaCCs, molecular identity, structure, and function 36

1.3.2 Non-specific cation channels 37

1.3.2.1 Store operated channels 38

1.3.2.2 Receptor operated channels 38

1.4 Hyperpolarising ion channels 39

1.4.1 K_{Ca} channels 40

1.4.1.1 BK_{Ca} channels 40

BK_{Ca} structure, and function 40

A role for BK_{Ca} in vascular reactivity, myogenic tone and receptor mediated responses 41

1.4.1.2 IK_{Ca} / SK_{Ca} channels 44

Structure, function, and distribution 44

IK_{Ca}/SK_{Ca} within the endothelium and their role in the generation and spread of EDH 44

1.4.2 K_{IR} channels 46

1.4.2.1 Classic $K_{IR}2.x$ 47

Classic $K_{IR}2$ gating properties 47

$K_{IR}2.x$, end-stage boosters in neurovascular coupling and endothelial derived signalling 48

1.4.2.2 K_{ATP} channels 49

K_{ATP} gating properties 49

K_{ATP} channels are downstream target of receptor mediated vascular reactivity 51

1.4.3 K_{2P} channels 52

1.4.3.1 TREK-1, TRAAK-1 and TASK-1, K_{2P} channels in the vasculature, 53

1.4.4 K_V channels 54

1.4.4.1 K_V1 channels 55

1.4.4.2 K_V2 channels 56

1.4.4.3 $K_V11.1$ channels 56

1.5 K_V7 channels 57

1.5.1 K_V7 channel structure 57

1.5.2 K_V7 channel gating 59

1.5.3 K_V7 channel pharmacology 60

1.5.4 Vascular K_V7 63

1.5.4.1 Distribution 63

1.5.4.2 Function 65

Channel inhibition, PIP_2 depletion, CaM:Ca^{2+} activation and PKC binding 66

Channel modulation, the products of cAMP 68

Channel modulation, the products of cGMP 69

Auxiliary subunit regulation 70

1.5.4.3 K_V7 channels and hypertension 71

1.5.5 Extravascular K_V7 channels 73

1.5.5.1 Cardiac 73

1.5.5.2 Epithelial 74

1.5.5.3 Neuronal 75

1.5.5.4 Non-vascular smooth muscle 76

1.6 Sex, CVS and CVD 77

1.6.1 Sexual dimorphisms in cardiovascular physiology 77

1.6.1.1 Endothelium derived sex differences in vascular reactivity 78

1.6.1.2 Endothelium independent sex differences in vascular reactivity 79

1.6.2 Sexual dimorphisms in cardiovascular pathophysiology 80

1.6.3 The vascular effects of sex hormones and their receptors 80

1.6.3.1 An overview on sex-hormone mediated vascular effects 81

1.6.3.2 Oestrogen 83

Oestrogen receptors α/β 83

Novel G-protein coupled Oestrogen receptor 84

1.6.3.3 Progesterone 85

1.6.3.3 Testosterone 86

1.6.4 Sex and K_V7 channels 87

1.7 Thesis aims 88

Chapter 2: Methods and materials 90

2.1 Animal model 90

2.2 Oestrus cycle stage determination 90

2.3 Isometric tension recording, wire myography 94

2.3.1 Vessel mounting and normalisation 94

2.3.2 Isometric tension recording protocols 96

2.4 Reverse transcription quantitative polymerase chain reaction 101

2.4.1 mRNA extraction, quantification, and conversion to cDNA 101

2.4.2 Relative transcript abundance quantification 103

2.4.2.1 Normalising Cq values 104

2.4.3 In plate controls, RT-qPCR 105

2.5 Vascular smooth muscle staining 110

2.5.1 Vascular smooth muscle cell isolation 110

2.5.2 Immunocytochemistry 110

2.5.3 Proximity ligation assay 112

2.6 Cell culture 116

2.7 Single cell electrophysiology 118

2.7.1 The basic principles 118

2.7.2 Voltage-clamp 119

2.7.3 The set up 121

2.7.4 Protocols 122

2.8 Serum concentration of sex hormones 124

2.9 Data analysis 124

Chapter 3: K_V7 channels in the male vasculature, validating a molecular and pharmacological toolbox **126**

3.1 Introduction 126

3.2 Methods 127

3.2.1 Protein extraction and quantification 127

3.2.2 Gel electrophoresis, protein transfer, staining, and relative protein quantification 128

3.3 Results 130

3.3.1 Characterising K_V7 channel modulators 130

3.3.1.1 Ruptured whole cell electrical currents recorded in HEK-$K_V7.4$ cells demonstrates $K_V7.2$-5 channel modulator activity at the level of the channel 130

3.3.1.2 Ruptured whole cell current recordings in HEK-$K_V7.1$ cells demonstrates $K_V7.1$ channel modulator activity at the level of the channel 134

3.3.1.3 Isometric tension recoding of male mesenteric arteries validates K_V7 channel modulator specificity 138

3.3.2 K_V7 channels are essential regulators of male arterial vascular physiology 140

3.3.2.1 ML213 and S-1 are potent and efficacious vasorelaxants 140

3.3.2.2 U46619-mediated vasoconstriction is sensitive to $K_V7.2$-5 channel inhibition 143

3.3.2.3 Isoprenaline-mediated vasorelaxation is sensitive to $K_V7.2$-5 channel inhibition 145

3.3.3 K_V7 channels expression within the vasculature of the Wistar rat 147

3.3.3.1 K_V7 channels at the level of the transcript 147

3.3.3.2 K_V7 channels at the level of the protein 150

Validating anti-K_V7/Kcne4 antibodies 150

K_V7/KCNE staining in male isolated mesenteric and renal artery VSMCs 152

Protein quantification, Western blot 155

3.4 Discussion 157

3.4.1 Validating a pharmacological toolbox 157

3.4.1.1 K_V7 channel activators 157

3.4.1.2 K_V7 channel inhibitors 159

3.4.2 K_V7 channels are key regulators of vascular reactivity in arteries from male Wistars 160

3.4.3 Limitations 163

3.4.4 Conclusion 164

Chapter 4: Oestrus cycle dependent regulation of arterial $K_V7.4$ 165

4.1 Introduction 165

4.2 Methods 167

4.3 Results 168

4.3.1 Sex/Oestrus cycle dependent changes in sensitivity to K^+ channel modulators 168

4.3.2 Diminished K_V7 channel contribution to receptor mediated responses underpins Oestrus cycle dependent changes in contractility 174

4.3.3 Identification of K_V7 channel transcript and protein expression in female Wistar arteries 178

4.3.3.1 K_V7 at the level of the transcript 178

4.3.3.2 K_V7 at the level of the protein 179

4.3.4 Cyclical increases in serum E2 mediate reduction in $K_V7.4$ membrane abundance via GPER1, impairing ML213-mediated relaxation 183

4.3.4.1 An analysis of circulating sex-hormones 183

4.3.4.2 Expression of Oestrogen receptors 185

4.3.4.3 Time-dependent modulation of ML213-mediated relaxation by E2 186

4.3.4.4 E2 and G-1 analogously impair $K_V7.4$ 188

4.3.4.5 GPER1 activation reduced $K_V7.4$ currents in overexpression system 191

4.3.4.6 E2 reduces $K_V7.4$ interaction with forward trafficking molecular chaperone protein heat-shock protein 90 in F-D/M, but not F-P/E VSMCs 193

4.3.5 Oestrogenic signalling similarly diminishes $K_V7.4$ membrane abundance and functional properties in male arteries 195

4.3.6 Oestrus cycle dependent regulation of arterial reactivity is non-vascular bed specific and partially K_V7 dependent 197

4.3.6.1 Cyclical changes in sensitivity to K_V7 activators, but not inhibitors 197

4.3.6.2 K_V7 contribution to receptor-mediated responses 200

4.4 Discussion 203

4.4.1 Cyclical reduction in $K_V7.4$ membrane abundance correlates with a pro-contractile phenotype 204

4.4.1.1 K_V7 channel contribution to basal coronary and cerebral tone 205

4.4.1.2 Oestrus cycle dependent changes in vascular reactivity are partially K_V7 dependent 206

4.4.2 E2 diminishes $K_V7.4$ membrane abundance through reduced interaction with HSP90 via GPER1 signalling 207

4.4.3 Oestrogenic signalling within the male vasculature 209

4.4.3 Limitations 210

4.4.4 Conclusion 211

Chapter 5: Preservation of vascular K_V7 function within the hypertensive Female rat 212

5.1 Introduction 212

5.2 Methods 214

5.3 Results 215

5.3.1 Preservation of ML213-mediated relaxation in the female hypertensive rat 215

5.3.2 Receptor mediated contraction in the normotensive and hypertensive rat 218

5.3.2.1 Sex-dependent differences in U46619-mediated contraction 218

5.3.2.2 Ablation of oestrus cycle dependent regulation of arterial reactivity in the hypertensive model 221

5.3.2 Receptor mediated relaxation in the normotensive and hypertensive rat 223

5.3.2.1 Comparable Isoprenaline-mediated relaxation in male and female rats 223

5.3.2.2 β-adrenoreceptor mediated relaxation is ablated independent of the oestrus cycle 226

5.3.3 The molecular characteristics of $K_V7.4$ in the hypertensive rat 227

5.3.3.1 $K_V7.4$ at the level of the protein in the SHR 227

5.3.3.1 $K_V7.4$ at the level of the transcript in the SHR 230

5.4 Discussion 232

5.4.1 $K_V7.4$ and the hypertensive phenotype 233

5.4.2 Sexual dimorphisms in $K_V7.4$ handling in the hypertensive animal 234

5.4.3 Limitations 236

5.4.4 Perspectives 237

Chapter 6: An investigation into sex-dependent signalling of prostacyclin mimetics 238

6.1 Introduction 238

6.2 Materials and methods 240

6.2.1 Morpholino transfection 240

6.3 Results 241

6.3.1 Iloprost-mediated vasoactive responses 241

6.3.1.1 Delineating EP_3/IP receptor mediated vascular effects 244

6.3.1.2 Generating concentration effect curves to Iloprost on pre-contracted arteries 246

6.3.1.3 Prostanoid receptor expression within the vasculature 248

6.3.2 Characterising MRE-269-mediated relaxation. 250

6.3.3 A novel role for $K_V7.1$ in shaping IP receptor-specific agonists in mesenteric arteries. 251

6.3.3.1 Pharmacological inhibition of $K_V7.1$ 251

6.3.3.2 Molecular interference of $K_V7.1$ 253

6.3.3.3 IP-receptor mediated signalling cascade 255

6.3.3.4 Alternate targets for IP-receptor mediated signalling cascade 257

6.3.4 Oestrus cycle-dependent shifts in the sensitivity of MRE-269-mediated vasorelaxation to K_V7 channel modulators 258

6.4 Discussion 261

6.4.1 Iloprost evoked vasocontraction 262

6.4.2 $K_V7.1$ underpins IP receptor mediated relaxation 263

6.4.3 Perspectives 266

6.4.4 Limitations 267

6.4.5 Conclusion 267

Chapter 7: K_V7 channel expression and function within endothelial cells from rat mesenteric arteries 268

7.1 Introduction 268

7.2 Materials and methods 270

7.2.1 Reverse transcription quantitative polymerase chain reaction 270

7.2.2 Immunocytochemistry 270

7.2.3 Immunohistochemistry 271

7.3 Results 273

7.3.1 Identification of K_V7 channels within mesenteric artery ECs 273

7.3.2 The impact of the endothelium on K_V7 channel activator-mediated relaxation 277

7.3.2.1 ECs modulate $K_V7.2$-5 channel activator-mediated relaxation in a gap-junction sensitive manner 277

7.3.2.2 Oestrus cycle depend on modulation of EC contribution to K_V7 channel activator-mediated relaxation 280

7.3.3 EC K_{IR} channels modulate $K_V7.2$-5 activator sensitivity 283

7.3.4 IK_{Ca}/SK_{Ca} inhibitors had no impact on K_V7 activator-mediated relaxation 286

7.3.5 K_V7 channels contribute to CCh evoked vasorelaxation 287

7.3.5.1 CCh evoked relaxation is predominantly mediated via EDH in rat mesenteric arteries 287

7.3.5.2 $K_V7.2$-5 channels contribute to the NO axis of CCh evoked relaxation 289

7.3.5.3 $K_V7.2$-5 channels contribute to NO derived CCh-mediated relaxation upstream of NO 290

7.4 Discussion 291

7.4.1 K_V7 channel expression and function within ECs 291

7.4.1.1 Endothelial K_V7 channel function within the female 292

7.4.2 A novel functional interaction with endothelial K_{IR} channels 293

7.4.3 The contribution of K_V7 channels to CCh evoked relaxations within rat mesenteric arteries 295

7.4.4 Limitations 296

7.4.5 Conclusions 296

Chapter 8: General discussion **297**

8.1 Summary 297

8.2 Contrasts to the generally accepted role for E2 within the vasculature 300

8.3 Perspectives 301

8.3.1 A role for $K_V7.4$ in the adverse cardiovascular effects of hormone replacement therapy 301

8.2.2 Cyclical drop of Oestrogen within the female, aberrant levels of K_V7 within the membrane 302

8.3.3 Oestrogenic regulation of arterial reactivity in the male 303

8.4 Conclusion 303

Chapter 9: Bibliography **305**

List of figures

Chapter 1: 30

Figure 1.1: $G_{q/11}$-GPCR mediated vasoconstriction 33

Figure 1.2: MLCP derived calcium sensitization 35

Figure 1.3: The impact of K^+ channel activity of vascular tone 39

Figure 1.4 K_V7 and KCNE protein structure 58

Figure 1.5 Diagrammatic representation of the rodent and human reproductive cycles 81

Chapter 2: 90

Figure 2.1: Cervical histology throughout the oestrus cycle. 92

Figure 2.2: Diagrammatic representation of mounted vessels 94

Figure 2.2: Representative vessel normalisation 95

Figure 2.3: Equilibrium protocol 96

Figure 2.4: Isometric tension recording protocols 100

Figure 2.5: mRNA quantification. 102

Figure 2.6: Representative qPCR. 104

Figure 2.7: Representative melt curve analysis. 106

Figure 2.8: Representative no-template and no-reverse transcription control. 107

Figure 2.9: Immunocytochemistry 111

Figure 2.10: Diagrammatic representation of PLA 113

Figure 2.11: Diagrammatic representation of ruptured whole-cell voltage-clamp 120

Figure 2.12: Representative GPER1-GFP spark fluorescence. 122

Figure 2.13: Voltage-clamp protocol 1 123

Chapter 3: 126

Figure 3.1: Voltage activated currents in HEK cells are $K_V7.4$ dependent and are ablated by Linopirdine/XE-991. 131

Figure 3.2: The structurally dissimilar $K_V7.2$-5 activators ML213 and retigabine enhance HEK-$K_V7.4$ currents. 133

Figure 3.3: Voltage activated currents in HEK-$K_V7.1$ cells are dependent on $K_V7.1$ and are HMR-1556 sensitive. 135

Figure 3.4: $K_V7.1$ specific activator ML277 enhances HEK-$K_V7.1$ currents. 137

Figure 3.5: K_V7 channel activator-mediated relaxation in male mesenteric arteries is ablated by 10 µmol-L^{-1} Linopirdine pre-incubation. 139

Figure 3.6: K_V7 channel activator-mediated relaxation in various arteries 141

Figure 3.7: Contraction in response to K_V7 channel inhibitors in arteries from male Wistar rats. 142

Figure 3.8: U46619-mediated contraction in renal, mesenteric, and cerebral arteries from male Wistars are underpinned by $K_V7.2$-5 channels. 144

Figure 3.9: Isoprenaline-mediated relaxation in renal, mesenteric, cerebral and coronary arteries from male Wistars are underpinned by $K_V7.2$-5 channels. 146

Figure 3.10: Relative mRNA transcript for *Kcnq1-5* and *Kcne1-5* within positive control tissues from male Wistar rats 148

Figure 3.11: Relative mRNA transcript for *Kcnq1-5* and *Kcne1-5* within arteries from male Wistar rats 149

Figure 3.12: Validating Pineda Anti-$K_V7.1$, APC-164, ABN137 and HPA011. 151

Figure 3.13: Validating Anti-$K_V7.4$ (Ab reference, #APC-164) 152

Figure 3.14: Membrane abundance for $K_V7.4$ in mesenteric and renal arteries from male Wistar rats. 153

Figure 3.15: Membrane abundance for $K_V7.1$, $K_V7.5$ and Kcne4 in renal arteries from male Wistar rats. 154

Figure 3.16: Protein quantification of $K_V7.4$ 156

Figure 3.17: Graphical summary of K_V7 channel activity in the vasculature of the male 162

Chapter 4: 165

Figure 4.1: Oestrus cycle dependent differences in S-1-mediated relaxation of pre-contracted tone within arteries from female (P/E2) and female (D/M) Wistar rats. 169

Figure 4.2: ML213 is more efficacious and potent in arteries from female (D/M) Wistar rats when compared to female (P/E) rats. 170

Figure 4.3: Effect of K_V7 blockers on arterial tone. 172

Figure 4.4: Ion channel modulator mediated vasorelaxation in renal female (P/E) and female (D/M) Wistar rats. 173

Figure 4.5: U46619-mediated contraction in renal and mesenteric arteries from female D/M, but not female P/E Wistars are underpinned by $K_V7.2$-5 channels. 175

Figure 4.6: Isoprenaline-mediated relaxation in renal and mesenteric arteries from female D/M, but not female P/E Wistars are underpinned by $K_V7.2$-5 channels. 177

Figure 4.7: Relative mRNA transcript for *Kcnq1-5* and *Kcne1-5* within arteries from female (P/E2) and female (D/M) Wistar rats 178

Figure 4.8: Immunocytochemistry demonstrates an oestrus cycle dependent reduction in $K_V7.4$ subcellular distribution in mesenteric and renal artery myocytes. 180

Figure 4.9: Immunodetection of $K_V7.1$, $K_V7.5$ and KCNE4 in isolated renal artery vascular smooth muscle cells from female Wistars. 182

Figure 4.10: Plasma concentration of sex hormones from female Wistar rats 184

Figure 4.11: Relative mRNA transcript for *Esr1, Esr2* and *Gper1* within arteries from female P/E and female D/M Wistar rats. 185

Figure 4.12: Oestradiol E2 mediated vascular effects are time dependent. 187

Figure 4.13: Oestradiol E2 and G-protein coupled Estrogen receptor agonist G1 pre-incubation replicate female P/E $K_V7.4$ membrane abundance within female D/M. 189

Figure 4.14: Oestradiol and G-protein coupled Estrogen receptor agonist G1 pre-incubation impair K_V7.2-5 channel activator ML213-mediated relaxation in renal and mesenteric arteries of female D/M, but not female P/E arteries. 190

Figure 4.15: Oestradiol E2 and G1 pre-incubation impair K_V7.4 channel activity. 192

Figure 4.16: Oestradiol reduces K_V7.4-Heat shock protein 90 interactions in F-D/M, but not F-P/E mesenteric artery myocytes. 194

Figure 4.17: Relative mRNA transcript for *Esr1, Esr2* and *Gper1* within arteries male Wistar rats. 195

Figure 4.18: Oestradiol E2 and G1 pre-incubation impairs K_V7.4 membrane abundance and ML213-mediated relaxation in male mesenteric arteries. 196

Figure 4.19: K_V7 channel activators are more efficacious and potent arteries from female (D/M) Wistar rats when compared to female (P/E) rats. 198

Figure 4.20: K_V7 channel inhibitors are more insensitive to the oestrus cycle within coronary and cerebral arteries from female rats. 199

Figure 4.21: U46619-mediated contraction in cerebral and coronaryarteries from female Wistars are insensitive to K_V7 channels inhibition. 201

Figure 4.21: Determining K_V7.2-5 channel contribution to Isoprenaline-mediated relaxation in cerebral and coronary arteries from female D/M and P/E rats. 202

Figure 4.23: Graphical summary 203

Chapter 5: 212

Figure 5.1: Preservation of K_V7.2-5 channel activator-mediated relaxation in arteries from hypertensive female rats 216

Figure 5.2: Oestrus cycle dependent changes in sensitivity to K_V7 channel modulators in the hypertensive rat 217

Figure 5.3: U46619-mediated contraction within renal arteries from female rats is less potent in arteries from female rats compared to males. 219

Figure 5.4: K_V7 channel contribution to U46619-mediated contraction in normotensive and hypertensive rats. 220

Figure 5.5: Diminished functional contribution of K_V7 to U46619-mediated contraction accounts for the disparity between arteries taken from normotensive and hypertensive rats. 222

Figure 5.6: Isoprenaline-mediated relaxation of rat renal arteries is ablated in the hypertensive model 224

Figure 5.7: K_V7 channel contribution to U46619-mediated contraction in normotensive and hypertensive rats. 225

Figure 5.8: Diminished functional contribution of K_V7 to U46619-mediated contraction accounts for the disparity between arteries taken from normotensive and hypertensive rats. 226

Figure 5.9: Immunostaining reveals a reduction in KV7.4 staining in the hypertensive VSMCs 228

Figure 5.10: Membrane cytosol ratio for $K_V7.4$ staining in vascular cells isolated from normotensive and hypertensive rats 229

Figure 5.11: Relative mRNA transcript for *Kcnq4* within arteries from normotensive and hypertensive rats 231

Figure 5.12: Graphical summary of K_V7 channel activity in arteries from male and female rats. 233

Chapter 6: 238

Figure 6.1: Iloprost evokes bi-phasic vasoactive responses within male, but not female mesenteric arteries. 243

Figure 6.2: Iloprost evoked responses are not Oestrus cycle dependent. 243

Figure 6.3: Iloprost-mediated contraction ablated by EP_3- receptor inhibition. 244

Figure 6.4: Iloprost-mediated relaxation is ablated by IP-receptor inhibition. 245

Figure 6.5: Cumulative concentration effect curves generated from Iloprost-mediated vasoactive responses. 247

Figure 6.6: Prostanoid receptor expression within whole mesenteric artery lysates. 249

Figure 6.7: Selexipag-mediated relaxation was unaffected by CAY-10441 in male mesenteric arteries. 250

Figure 6.8: Linopirdine and HMR-1556 attenuate MRE-269-mediated vasorelaxation in mesenteric arteries from male and female rats. 252

Figure 6.9: Molecular interference of *Kcnq1* via targeted morpholino knockdown impairs MRE-269-mediated relaxation. 254

Figure 6.10: MRE-268 mediated relaxation is sensitive to adenylate cyclase, Gβγ and protein kinase A inhibition, but not effector protein activated by cAMP in male rat mesenteric arteries. 256

Figure 6.11: MRE-269-mediated relaxation is not attenuated K_{ATP} and BK_{Ca} inhibition. 257

Figure 6.12: K_V7 channel inhibition attenuates MRE-269-mediated vasorelaxation in mesenteric arteries from Di-oestrus/Met-oestrus (F-D/M), but not Pro-oestrus/Oestrus (F-P/E) female rats. 260

Figure 6.13: Iloprost mediated vascular responses in mesenteric arteries from male and female Wistar rats. 262

Figure 6.15: MRE-269 mediated vascular responses in mesenteric arteries from male and female Wistar rats. 266

Chapter 7: 268

Figure 7.1: Expression profile of *Kcnq* genes within isolated rat mesenteric vascular smooth muscle cells (VSMCs) and endothelial cells (ECs). 273

Figure 7.2: Immunocytochemistry demonstrates $K_V7.1$, $K_V7.4$ and $7_V.5$ localization in rat mesenteric artery isolated endothelial (EC) and smooth muscle cells (SMC). 275

Figure 7.3: Immunohistochemistry demonstrates Kv7.4 and 7.5 localization in rat mesenteric artery endothelium (EC) and smooth muscle cells (SMCs) with a focus on internal elastic lamina (IEL) hole sites in whole mount tissue. 276

Figure 7.4: K_V7.2-5 channel activator-mediated vasorelaxation was significantly attenuated by EC removal. 278

Figure 7.5: Carbenoxolone has no effect on ML213-mediated relaxation in the absence of endothelial cells (ECs). 279

Figure 7.6: K_V7.1 channel activator-mediated vasorelaxation was unaffected by endothelial cell (EC) removal. 279

Figure 7.7: K_V7.2-5 channel activator-mediated vasorelaxation was attenuated by endothelial cell (EC) removal in females during D-Oestrus and Met-oestrus (F-D/M), but not females during Pro-Oestrus and Oestrus (F-P/E). 281

Figure 7.8: K_V7.2-5 channel activator-mediated vasorelaxation was unaffected by carbenoxolone in the absence of endothelial cells (ECs) in females during D-Oestrus and Met-oestrus (F-D/M) and females during Pro-Oestrus and Oestrus (F-P/E). 282

Figure 7.9: K_V7.2-5 channel activator-mediated vasorelaxation was attenuated by two structurally different K_{IR} channel blockers, $BaCl_2$ and ML133. 284

Figure 7.10: K_V7.2-5 channel activator-mediated vasorelaxation was significantly attenuated by EC removal. 285

Figure 7.11: K_V7 channel activator-mediated vasorelaxation was not affected by preincubation with IK_{Ca}/SK_{Ca} channel antagonists. 286

Figure 7.12: CCh evoked vasorelaxation is mediated through both eNOS and IK_{Ca}/SK_{Ca} channels and is partially attenuated by inhibition of K_V7 channels. 288

Figure 7.13: K_V7 channel inhibition additivity inhibits the IK_{Ca} / SK_{Ca} axis of carbachol (CCh) evoked vasorelaxation only. 289

Figure 7.14: K_V7 channel prospectively upregulate endothelial nitric oxide production. 290

Figure 7.15: Schematic of K_V7.2-5 activator-mediated vasorelaxation. 295

List of tables

Chapter 1: **30**

Table 1.1: K_V7 activators 62

Table 1.2: K_V7 inhibitors 62

Table 1.3: Arterial K_V7 distribution 65

Chapter 2: **90**

Table 2.1: Cervical cell populations 93

Table 2.2: List of modulators 100

Table 2.3: List of primers 109

Table 2.4: List of primary anti-bodies 114

Table 2.5: List of secondary anti-bodies 115

List of abbreviations

1,4,5-inositol triphosphate	IP_3
17-β Oestradiol	*E2*
4′,6-diamidino-2-phenylindole	*DAPI*
A-kinase anchoring protein	*AKAP*
Amino	*N*
Amperes	*A*
Angiotensin II	*Ang-II*
Angiotensin II receptor	AT_1
Arbitrary units	*A.U.*
ATP sensitive potassium channel	K_{ATP}
Atrial natriuretic peptide	*ANP*
Blood pressure	*BP*
Calcitonin gene related peptide	*CGRP*
Calcium activated chloride channel	*CaCC*
Calcium activated chloride currents	$I_{Cl(Ca)}$
Calcium activated potassium channels	K_{Ca}
Calmodulin	*CaM*
Calnexin	*Canx*
Carbachol	*CCh*
Carboxy	*C*
Cardiovascular disease	*CD*
Cardiovascular system	*CVS*
Chinese hamster ovarian	*CHO*
Command voltage	V_{cmd}
Concentration effect curve	*CEC*
Conductance	*G*
Current	*I*
Current-voltage	*IV*
Cyclin adenosine monophosphate	*cAMP*
Cyclin guanine monophosphate	*cGMP*
Cyclooxygenase	*COX*
Cytochrome C1	*Cyc1*
Delayed-rectifier potassium current	I_{Ks}
Diacyl glycerol	*DAG*
Diethylamine NONOate diethylammonium	*DEA-NO*

Double stranded DNA	*dsDNA*
Echocardiogram	*ECG*
Endothelial cells	*ECs*
Endothelial derived hyperpolarisation	*EDH*
Endothelial nitric oxide synthase	*eNOS*
Equilibrium potential for Cl^-	E_{Cl}
Equilibrium potential for K^+	E_K
Equilibrium potential of an ion	E_{ion}
Ethylenediaminetetraacetic acid	*EDTA*
Exchange protein directly activated by cAMP	*EPAC*
Extracellular potassium concentration	$[K^+]_o$
Farads	*pF*
Females in Met-Oestrus and Di-Oestrus	*F-D/M*
Females in Pro-Oestrus and Oestrus	*F-P/E*
Follicular stimulating hormone	*FSH*
Fluorescence recovery after photobleaching	*FRAP*
G-protein coupled estrogen receptor	*GPER1*
G-protein kinase receptor	*GPCR*
Giga-ohm	*GΩ*
Globular actin	*G-actin*
Glyceraldehyde 3-phosphate dehydrogenase	*Gapdh*
Heart and Estrogen/progestin replacement study	*HERS*
Heat shock protein 70	*HSP70*
Heat shock protein 90	*HSP90*
HEK 293B stably expressing *Kcnq4*	*HEK-K_V7.4*
High K^+ physiological salt solution	*KPSS*
Hormone replacement therapy	*HRT*
Human embryonic kidney 293B	*HEK*
Intermediate conductance K_{Ca} channels	IK_{Ca}
Internal elastic lamina	*IEL*
Intracellular calcium concentration	$[Ca^{2+}]_i$
Inwardly rectifying potassium channels	K_{IR}
L-Nitroarginine methyl ester	*L-NAME*
Large conductance K_{Ca} channels	BK_{Ca}
Left anterior descending	*LAD*
Luria-Bertini	*LB*
Luteinizing hormone	*LH*
Mirco-RNA	*mi*

Mitogen activated protein kinase	*MAPK*
Myoendothelial gap junction	*MEGJ*
Myosin light chain kinase	*MLCK*
Myosin light chain phosphatase	*MLCP*
Myosin phosphatase targeting subunit-1	*MYPT-1*
Nitric oxide	*NO*
No-reverse transcription control	*NRT*
No-template control	*NTC*
Non-transfected	*N-T*
Normotensive	*NT*
Ohms	*Ω*
Phosphate buffered serum	*PBS*
Phosphatidylinositol-4,5-bisphosphate	*PIP2*
Phosphoinositide 3-kinase	*PI3K*
Phospholipase C-β	PLC_{β}
Physiological salt solution	*PSS*
Polyaimine transporter 1	*TPO-1*
Pore domain	*PD*
Prostacyclin	PGI_2
Protein kinase A	*PKA*
Protein Kinase C	*PKC*
Protein kinase G	*PKG*
Protein phosphatase 1	*PP1*
Protein phosphatase catalytic subunit	*PP1c-δ*
Proximity ligation assay	*PLA*
Pulmonary artery hypertension	*PAH*
Quantification cycle	*Cq*
Receptor operated channel	*ROC*
Resistance	*R*
Resting membrane potential	*RMP*
Reverse transcription quantitative polymerase chain reaction	*RT-qPCR*
Rho kinase	*RhoK*
Rho-guanine exchange factor	*RhoGEF*
Room temperature	*RT*
S-nitroprusside	*SNP*
Sarcoplasmic reticulum	*SR*
Sensor-stromal interaction molecule 1	*STIM1*

Small conductance K_{Ca} channels	*SK_{Ca}*
Sodium myoinositol transporter 1	*SMIT-1*
Spontaneously hypertensive rat	*SHR*
Store operated channel	*SOC*
Sulphonylurea receptor	*SUR*
Super optimum broth	*SOC*
Tandem of P domains in a Weak Inwardly rectifying K^+ channel	*TWIK-1*
Thromboxane	*TXA*
Total peripheral resistance	*TPR*
Transient potential receptor canonical	*TRPC*
Transmembrane potential	*V_m*
TWIK related acid sensitive K^+ channel	*TASK*
TWIK related arachidonic acid sensitive K^+ channel	*TRAAK*
TWIK-related K^+ channels	*TREK*
Two-pore domain channels	*K_{2P}*
Ubiquitin C	*UBC*
untranslated region	*UTR*
Vascular smooth muscle cell membrane potential	*$Vsmc_m$*
Vascular smooth muscle cells	*VSMCs*
Voltage at half-maximal activation	*$V_{½}$*
Voltage sensing domain	*VSD*
Voltage-gated calcium channels	*VGCCs/Ca_V*
Voltage-gated potassium channel	*K_V*
Volts	*V*
Wheat germ agglutinin	*WGA*

Chapter 1: Introduction

1.1 The cardiovascular system and disease

The cardiovascular system (CVS) is comprised of the heart, vascular network, and blood. The CVS perfuses organs with oxygen and nutrients, removes metabolic waste and facilitates immunological defense and systemic neurohormonal responses via blood flow, which is dependent on sufficient blood pressure (BP). BP is maintained by a plethora of factors including cardiac output and blood volume, which are in turn derived from central nervous control of the heart and fluid re-uptake from the kidney. Though, BP is dynamically regulated by total peripheral resistance (TPR), which according to Poiseuille's law, is inversely determined by the radius of the blood vessel to the power of 4 (r^4). Blood vessels are a multi-layer complex consisting of the tunica intima (endothelial cells (ECs) and internal elastic lamina), tunica media (vascular smooth muscle cells (VSMCs)), the adventitia (external elastic lamina, penetrating peri-vascular neurons and fat) and the hollow lumen through which blood flows. The diameter of the lumen is modulated through VSMC contractility. As VSMCs contract the lumen diameter decreases, resulting in an increases TPR and thus BP.

Whilst BP is necessary for healthy perfusion, sustained systolic and diastolic BP over 140mmHg and 90mmHg respectively, qualifies as hypertension. The outcomes of hypertension include amongst many others; arterial aneurism or hemorrhage, the rupture of atheroma and vessel blockage, and increased stress on the ventricle walls (termed afterload). Consequently, hypertension is a key risk factor in many cardiovascular diseases (CVDs) including stroke, ischemic heart disease and heart failure. Being that CVD is the leading cause of mortality in Europe (Wilkins. *et al.*, 2017), the factors governing BP, i.e VSMC contractility, represent a key area of interest.

1.2 Vascular contraction

Contraction of VSMC is driven by a rise in intracellular calcium that emanates from different sources with calcium influx through L-type voltage gated calcium channels (VGCCs), including $Ca_V1.2$, and intracellular calcium store release predominating. Calcium also enters the cell via non-selective cation channels and Na-Ca exchangers. A rise in free cytosolic calcium activates myosin light chain kinase (MLCK; Walsh *et al.*, 1982; Osol *et al.*, 2002; Kamm, 1985). MLCK binds and phosphorylates the 20kDa light chain of myosin II (LC_{20}) at Ser19 (Allen & Walsh, 1994), increasing myosinATPase activity and facilitating actin-myosin interaction, which gives rise to cross bridge cycling and cell shortening or an increase in tension (Kamm and Stull, 2001). Actomyosin is coupled to the extracellular matrix via interaction with a cortical network of actin filaments anchored to integrin proteins, allowing the cell to exert tension generated within the cell across the cell membrane and to the tissue as a whole (Gunst and Zhang, 2008). Due to the circular orientation of VSMCs within the tunica media, cell shortening results in a narrowing of the artery and an increase in vascular resistance. MLCK mediated vasoconstriction is opposed by the activity of myosin light chain phosphatase (MLCP; Hartshorne, Ito & Erdödi, 2004). MLCP removes the phosphate from LC_{20}-pSer19 causing the force of contraction to wane over time. VSMC contraction is ultimately regulated by the balance of VSMC contractile machinery including MLCK, MLCP and the coupling of actomyosin to the vessel wall. Myriad G-protein coupled receptors (GPCRs) regulate the activity of these elements. GPCRs respond to vasoactive ligands within circulation or from peri-vascular neurons, fat, ECs, and platelets or intrinsic factors including stretch of the vessel wall, giving rise to dynamic changes in tension in the form of contraction or relaxation. A brief overview of the signalling cascades governing VSMC contraction will be given here.

1.2.1 $G_{q/11}$ mediated calcium dependent contraction

$G_{q/11}$ associated-GPCR contraction is both agonist-dependent (noradrenaline, endothelin-1, vasopressin, 5-HT, thromboxane (TXA), etc.) and agonist-independent via

constitutively active receptors including mechanosensitive angiotensin II receptors (AT_1R; Mederos y Schnitzler *et al.*, 2008) . During vasoconstriction via $G_{q/11}$ coupled receptor signalling, GDP on $G_{q\alpha}$ is substituted for GTP. Active GTP-$G_{q\alpha}$ dissociates from the GPCR complex into the cytosol. GTP-$G_{q\alpha}$ activates phospholipase C-β (PLCβ) which in turn breaks down phosphatidylinositol-4,5-bisphosphate (PIP_2) into 1,4,5-inositol triphosphate (IP_3) and diacyl glycerol (DAG). Intracellular calcium stores are liberated via activation of the IP_3 receptor (IP_3R) along the sarcoplasmic reticulum (SR). Ryanodine receptors along the surface of the SR are activated during this response, driving calcium induced calcium release further depleting internal stores. Increased intracellular calcium concentration ($[Ca^{2+}]_i$) and raised DAG stimulate protein kinase C (PKC). A combination of these factors including; 1.) depletion of the SR; 2.) increased $[Ca^{2+}]_I$; 3.) activation of PKC and DAG depolarizes VSMC membrane potential ($Vsmc_m$) via the activation of depolarizing ion channels including non-specific cation channels and calcium activated chloride channels (CaCCs) and suppression of hyperpolarizing ion channels including potassium (K^+) channels. Depolarisation of $Vsmc_m$ increases the open probability of L-type VGCCs, including $Ca_V1.2$ or $Ca_V3.1$, allowing for the influx of extracellular Ca^{2+}. As $[Ca^{2+}]_i$ rises from a resting level of 120-150 nM to 300-500 μM, calmodulin (CaM) is saturated in a 1:4 ratio giving CaM:Ca^{2+} which in turn binds and activates MLCK via a change in its structural conformation, generating contraction (Walsh, 2011; Figure 1.1).

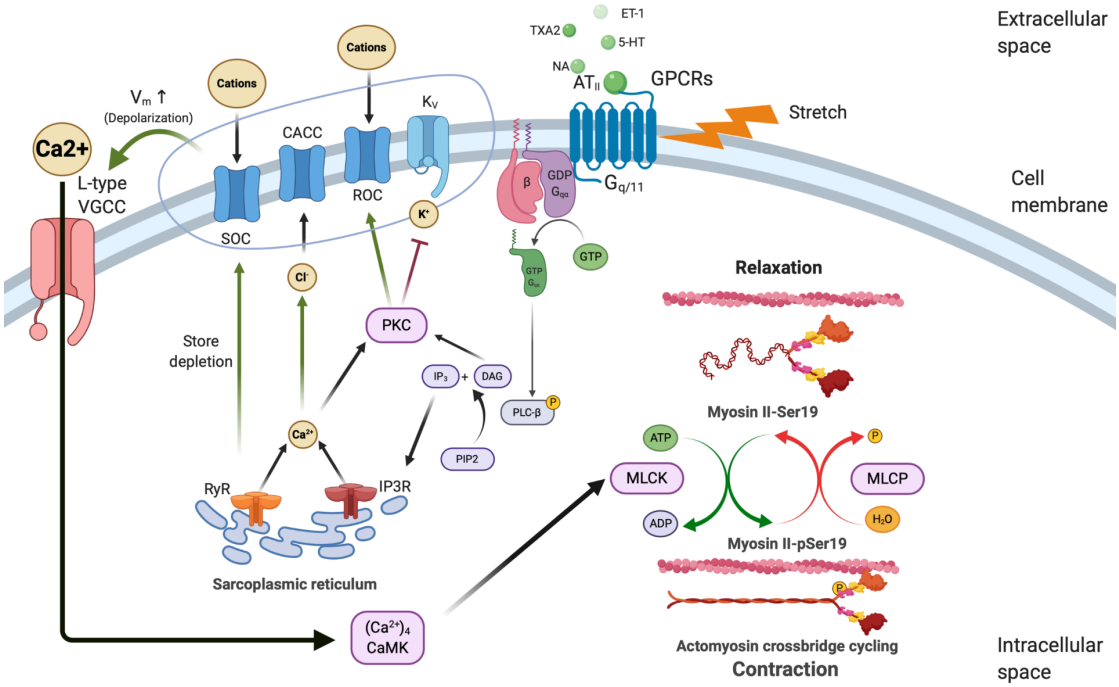

Figure 1.1: $G_{q/11}$-GPCR mediated vasoconstriction

VSMCs contract via calcium dependent $G_{q/11}$-GPCR mediated signalling cascades. Stimulation of $G_{q/11}$ results in liberation of intracellular calcium stores and depolarization of the membrane via activation of store-operated channels (SOCs), CaCCs and receptor operated channels (ROCs) and inactivation of potassium channels giving rise to the influx of extracellular calcium via VGCC. Raised $[Ca^{2+}]_I$ binds CaMK, which then activates myosin-light chain kinase (MLCK). MLCK activity phosphorylates myosin II-Ser19 allowing actomyosin cross-bridge cycling and vasoconstriction. (Author's product)

1.2.2 Calcium sensitization via MLCP

In various scenarios, smooth muscle contraction is maintained even when calcium has decreased due to suppression of MLCP. Vascular smooth muscle MLCP is a heterotrimeric holoenzyme comprised of a 38-kDa type-1 protein phosphatase δ isoform (PP1c-δ) catalytic subunit which targets LC20-pSer19 (Hartshorne, Ito & Erdödi, 1998; Hartshorne & Hirano, 1999; Hirano, 2007), a 110-kDa myosin binding subunit responsible for both targeting PP1c-δ to LC20 and regulating its enzymatic activity (myosin phosphatase targeting subunit-1 (MYPT-1; Hartshorne, Ito & Erdödi, 1998; Hirano, Phan & Hartshorne, 1997; Hartshorne & Hirano, 1999; Hirano, 2007) and a 20kDa structural subunit (Hirano, Phan and Hartshorne, 1997; Hartshorne, Ito and Erdödi, 1998). VSMCs can become sensitized to calcium via cascades including 1.) Rho

Kinase (RhoK) mediated phosphorylation of MYPT-1 at Thr696 and Thr858, preventing the association of MYPT-1 to myosin-II (Kawano *et al.*, 1999; Hirano, 2007), 2.) RhoK/PKC mediated phosphorylation of CPI-17, a 17kDa phosphatase enzyme, at Thr38, which subsequently inactivates PP1c via tightly binding its active domain (Eto *et al.*, 1995, 2007; Hayashi *et al.*, 2001). Inactivation of MLCP prevents LC_{20}-pSer19 turnover, augmenting vascular smooth muscle tension at a given concentration of $[Ca^{2+}]_i$. During GPCR signalling, $G_{q\alpha}$ (Lutz *et al.*, 2005) and $G_{12/13\alpha}$ (Fukuharaa, Chikumi and Silvio Gutkind, 2001; Dutt, Nguyen and Toksoz, 2004) phosphorylate Rho-guanine exchange factor (Rho-GEF), giving rise to GDP to GTP substitution at membrane associated RhoA, both of which are coupled to ligand and stretch activated receptors (Sagara *et al.*, 2007; Mederos Y Schnitzler *et al.*, 2008). $RhoA_{GTP}$ subsequently activates RhoK driving both pathways (1) and (2) described above (Fig 1.2). Pathways 1 and 2 are calcium independent means of calcium sensitization. Active $G_{q\alpha}$ also mediates a rise in $[Ca^{2+}]_I$ which activates PKC, driving pathways (2) via CPI-17 activation (Fig 1.2). A rise in $[Ca^{2+}]_I$ also activates class II-α phosphoinositide 3-kinase (PI3K-C2ç), which is reported to activated Rho-GEF (Wang *et al.*, 2006), stimulating pathways (1) and (2) as described above (Fig 1.2). These are calcium dependent mediums calcium sensitization. See Hirano, 2007 and Walsh & Cole, 2013 for review.

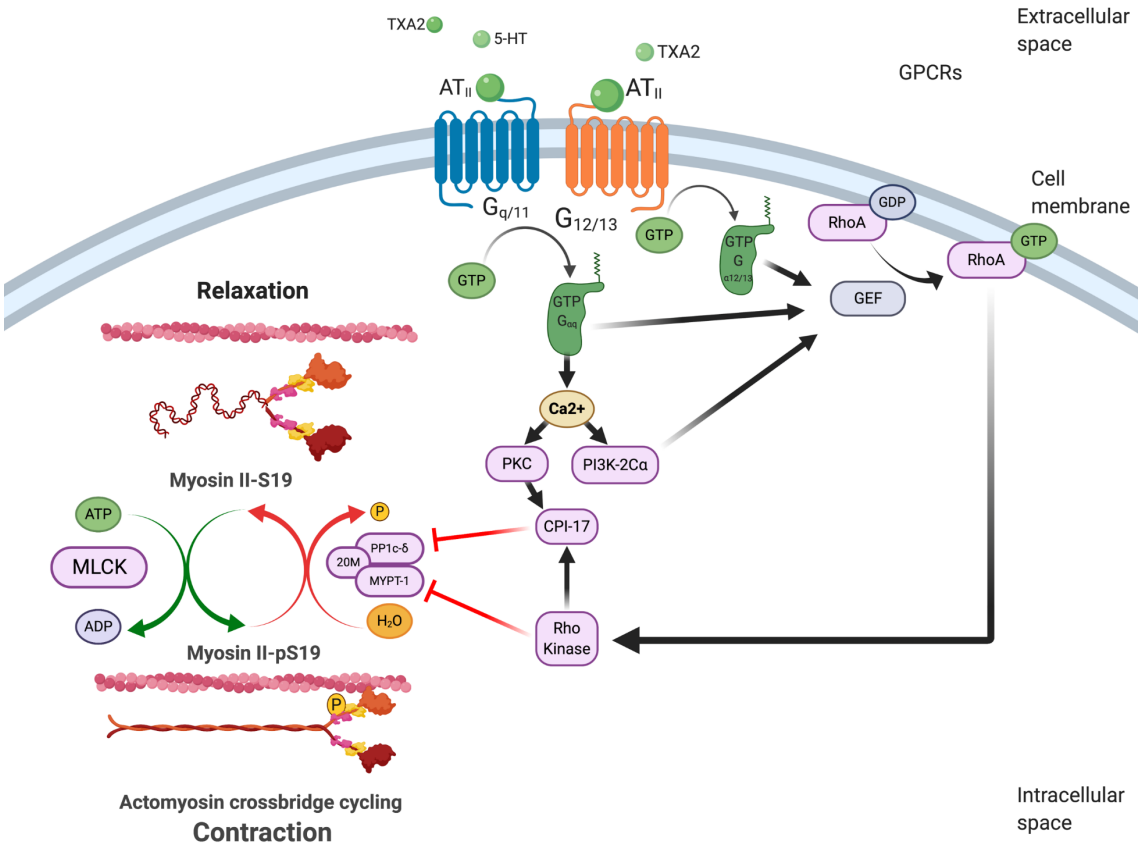

Figure 1.2: MLCP derived calcium sensitization

$G_{q/11}$/$G_{12/13}$-GPCR mediated calcium dependent and calcium independent calcium sensitization signalling cascades. Stimulation of $G_{q/11}$ or $G_{12/13}$ inhibits MLCP via RhoK mediated inhibition of MYPT-1 or CPI-17 mediated inhibition of PP1c-δ. Inhibition of MLCP augments actinomyosin cross-bridge cycling and vasoconstriction. (Author's product)

1.2.3 Calcium sensitization via actin polymerization

Filamentous actin is the fundamental factor that drives muscular and non-muscular cellular contraction. Interestingly, inhibition of free globular-actin (G-actin) polymerization within both vascular (Wright and Hurn, 1994; Cipolla, Gokina and Osol, 2002; Ohanian, Gatfield and Ohanian, 2005) and non-vascular (Tseng *et al.*, 1997; Dowell *et al.*, 2005) smooth muscle has been shown to attenuate receptor and stretch mediated contraction independent of actomyosin Mg-ATPase, MLCK and MLCP activity, see (Gunst and Zhang, 2008; Walsh and Cole, 2013) for review. It is hypothesized that dynamic reorganization of the cortical cytoskeleton as well as polymerization of contractile actin reduces the force required for sustained contraction (Walsh and Cole, 2013). Known

candidates for G-actin reorganization include RhoA (Hirshman and Emala, 1999; Corteling *et al.*, 2007; Zhang, Du and Gunst, 2010) and more recently PKC (El-Yazbi, Abd-Elrahman and Moreno-Dominguez, 2015), both of which are shown to be stimulated during ligand mediated GPCR and mechanosensitive AT_1R and α-integrin mediated signalling cascade (Hirshman and Emala, 1999; Colinas *et al.*, 2015; Hong *et al.*, 2016).

1.3 Depolarizing ion channels of the vasculature

The processes of myogenic reactivity described above account for a significant proportion of VSMC reactivity and are areas of key interest when understanding the dynamic contractile properties of the vasculature. Importantly, vessels will fail to contract in the absence of extracellular calcium (Osol *et al.*, 2002) and contraction can be ablated by VGCC inhibitors like Nicardipine (Tan, Hamner and Taylor, 2013). VSMC depolarization and the influx of calcium is therefore essential in the generation of VSMC contraction. In the following sections, the candidates for VSMC depolarisation will be addressed, with a basic overview of CaCCs, store and receptor operated channels.

1.3.1 CaCCs, molecular identity, structure, and function

Calcium activated chloride currents ($I_{Cl(Ca)}$) were first reported in VSMCs by Byrne & Large (1987) and have been identified in many arterial VSMCs since, see (Bulley and Jaggar, 2014) or (Dam, Boedtkjer, Aalkjaer, *et al.*, 2014) for review. Expression of Cl^-/HCO_3^- exchanger (Aickin and Brading, 1984), $Na^+K^+Cl^-$ co-transporter (Aiton *et al.*, 1981; Owen, 1984) and an as of yet unidentified 'pump III' (Davis, 1992) accumulates Cl^- ions within the cytosol of VSMCs. The equilibrium potential for Cl^- (E_{Cl}) within the vasculature is positive to the RMP, at roughly -30 to -20mV as a result of cytosolic Cl^- accumulation. As Cl^- channels open, Cl^- efflux mediates membrane depolarisation, increasing the open probability of VGCC, promoting vasoconstriction. $I_{Cl(Ca)}$ are evoked by a rise in $[Ca^{2+}]_I$ via release from the SR (Yuan, 1997) and entry through store operated channels including transient receptor potential canonical (TRPC1,4,6) or Orai1,2 (Forrest *et al.*, 2010) during

receptor mediated contraction (Kirkup *et al.*, 1996; He and Tabrizchi, 1997) and stretch mediated tone (Nelson *et al.*, 1997). The role of CaCCs in vascular contraction is highlighted by reduced vasoconstriction exhibited by arteries after application of either $Na^+K^+Cl^-$ co-transporter (Deth, Payne and Peecher, 1987; Stanke *et al.*, 1998; Stanke-Labesque *et al.*, 2000) or CaCC channel inhibitors (Davis *et al.*, 2013; Dam, Boedtkjer, Nyvad, *et al.*, 2014; Askew Page *et al.*, 2019).

Recently, $I_{Cl(Ca)}$ were attributed to TMEM16A (Schroeder *et al.*, 2008), a 10-transmembrane domain protein that forms functional dimers within the membrane (Fallah *et al.*, 2011). TMEM16A has been identified in an array of vascular beds including murine portal vein, thoracic aorta and carotid artery (Davis *et al.*, 2010, 2013), rabbit pulmonary (Davis *et al.*, 2013) and rat mesenteric (Dam, Boedtkjer, Nyvad, *et al.*, 2014), renal (Yip *et al.*, 2018), coronary (Askew Page *et al.*, 2019) pulmonary (Manoury, Tamuleviciute and Tammaro, 2010) and cerebral (Thomas-Gatewood *et al.*, 2011; Bulley *et al.*, 2012; Li *et al.*, 2016) arteries. Molecular interference or pharmacological inhibition of TMEM16A abrogates $I_{Cl(Ca)}$ within these vessels relaxes pre-contracted arterial tone (Davis *et al.*, 2013) and attenuates receptor (Manoury, Tamuleviciute and Tammaro, 2010; Dam, Boedtkjer, Nyvad, *et al.*, 2014; Askew Page *et al.*, 2019) and stretch (Bulley *et al.*, 2012; Yip *et al.*, 2018) mediated contraction, implicating TMEM16A in propagating calcium dependent contraction.

1.3.2 Non-specific cation channels

TRP channels encompass 28 distinct subtypes grouped into six-distinct subfamilies. Each member contains 6 conserved transmembrane domains (S1-6) with Carboxy (C) and amino (N) termini of variable length. Functional TRP channels are comprised of hetero/homotetramers of α-subunits (Clapham *et al.*, 2003) and allow for the flow of both Na^+ and Ca^{2+}. An array of TRP channels are expressed within the vasculature, however, only TRPC will be addressed here.

1.3.2.1 Store operated channels

Store operated channels are activated in response to depletion of intracellular calcium stores during PLC-mediated contraction and give rise to calcium induced calcium influx, augmenting contraction (Leung *et al.*, 2008). Thapsigargin and Cyclopiazonic acid inhibit Ca^{2+} re-uptake into the SR and deplete intracellular calcium stores. Both agents mediated sustained contractions of rat arteries (Kwan *et al.*, 1994), implicating store operated channels in VSMC contraction. Debate remains regarding the molecular correlate of store operated channels within native VSMCs, see (Baudel *et al.*, 2020) for review. Conflicting evidence argues for and against the role of an inwardly rectifying calcium channel Orai1, however, TRPC1 is a recognized store operated channel within the vasculature (Leung *et al.*, 2008). TRPC1 is purportedly activated by a confirmational change in shape of sensor-stromal interaction molecule 1 (STIM1) during Ca^{2+} depletion from the SR (Worley *et al.*, 2007; Shi *et al.*, 2017; Martín-Aragón Baudel *et al.*, 2020). Activation of TRPC1 contributes to VSMC contraction (Kunichika *et al.*, 2004) and proliferation (Li *et al.*, 2008) within pulmonary arteries and VSMC proliferation in cultured aortic cells (Rodríguez-Moyano *et al.*, 2013).

1.3.2.2 Receptor operated channels

Receptor operated channels are non-specific cation channels that are activated during $G_{q/11}$-coupled receptor mediated contraction independent of a change in Ca^{2+} store depletion. Receptor operated channels are activated in response to DAG, a product of PIP_2 hydrolyzation (Fig 1.1; Hofmann *et al.*, 1999). TRPC3/6/7 have been identified as receptor operated channels contributing to receptor mediated responses within rat aorta (Liu *et al.*, 2009) cerebral (Reading *et al.*, 2005; Xi *et al.*, 2008), renal (Facemire and Arendshorst, 2005; Fellner and Arendshorst, 2008) and mesenteric (Inoue *et al.*, 2009) arteries and rabbit coronary artery (Peppiatt-Wildman *et al.*, 2007). Activation of receptor operated channels including TRPC3/6/7 propagates membrane depolarisation and

accounts for sustained calcium entry during GPCR signalling, see (Earley and Brayden, 2015) for review.

1.4 Hyperpolarising ion channels

Potassium channels are a fundamental factor in the generation of VSMC resting membrane potential (RMP), which is roughly -70 to -55 mV. K^+ channels stabilises of the RMP in the face of depolarizing signals. As K^+ channels open, the cell becomes permeable to K^+. K^+ ions move down their electrochemical gradient, exiting the cell, thus moving $Vsmc_m$ towards the equilibrium potential for K^+ (E_k). As E_k within VSMC is roughly -90 mV, the cell membrane becomes hyperpolarized. As $Vsmc_m$ increases, the open probability of VGCC, predominantly $Ca_V1.2$ and $Ca_V3.1$, decreases, limiting Ca^{2+} influx into the cell preventing VSMC contraction (Figure 1.3). K^+ channels are therefore a breaking mechanism to VSMC contraction.

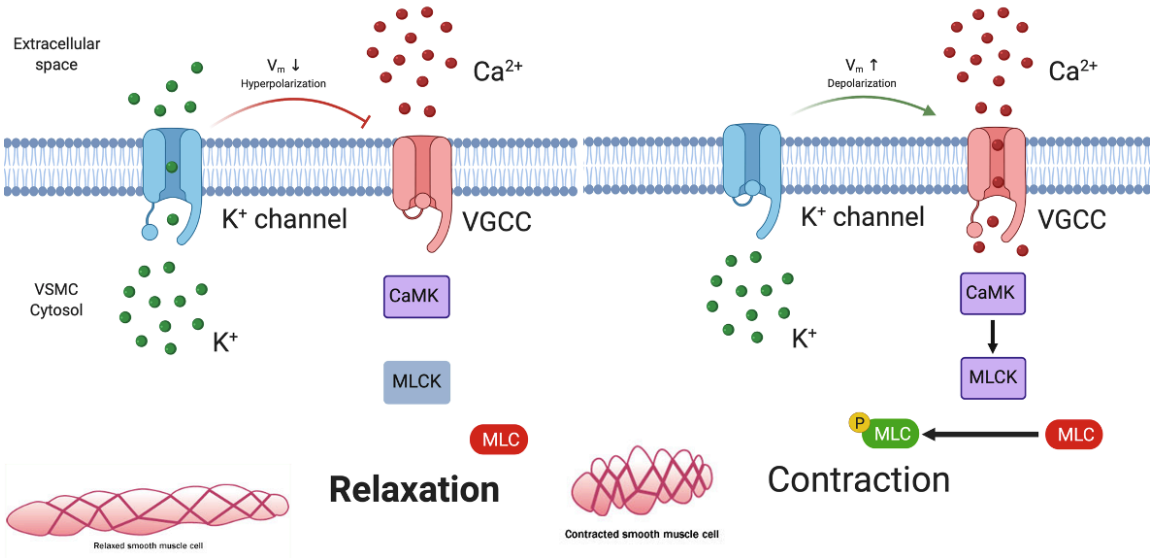

Figure 1.3: The impact of K^+ channel activity of vascular tone

When open, efflux of K^+ from vascular K^+ channels hyperpolarizes the VSMC membrane potential, negating calcium influx via the closure of VGCC resulting in vasorelaxation. When closed, the membrane becomes less permeable to K^+ depolarizing the membrane resulting in the opening of VGCC and Ca^{2+} influx.

K^+ channels are the largest family of ion channels encompassing 75 genes and four major classes divided into calcium activated (K_{Ca}), inward rectifier (K_{ir}), two-pore domain channels (K_{2P}) and voltage-dependent (K_V) K^+ channels. In the following section, a brief

description of the structure, function, and role of the key subtypes of each major class within the vasculature will be discussed.

1.4.1 K_{Ca} channels

Calcium evoked changes in membrane permeability to K^+ was first described by Gardos in 1958 and developed further by Meech & Strumwas (1970). Since which time, three broad classes of K_{Ca} channels have been identified and are differentiated by their conductance measured in picoSiemens (pS; Ghatta *et al.*, 2006); 100-300 pS, *KCNMA*-encoded $K_{Ca}1.1$ (a.k.a. large conductance K_{Ca} channels (BK_{Ca}; formerly MaxiK, dSlo; Marty, 1981); 25-100 pS, *KCNN4*-encoded $K_{Ca}3.1$ (a.k.a. intermediate conductance K_{Ca} (IK_{Ca}; Logsdon *et al.*, 1997)), and 2-25 pS, *KCNN1-3*-encoded $K_{Ca}2.1$-3 (a.k.a. small conductance K_{Ca} (SK_{Ca}; Blatz & Magleby, 1986).

1.4.1.1 BK_{Ca} channels

BK_{Ca} structure, and function

Large conductance calcium sensitive currents were first identified by Marty (1981). The molecular correlate of which was later cloned from Drosophila (Atkinson, Robertson and Ganetzky, 1991) and humans (Adelman *et al.*, 1992; Dworetzky, Trojnacki and Gribkoff, 1994; Tseng-Crank *et al.*, 1994) and is now termed *KCNMA1*. *KCNMA1* encodes for pore-forming α subunit $K_{Ca}1.1$, which in turn gives rise to homotetrameric channels within the membrane termed BK_{Ca} which are both calcium and voltage sensitive (Marty, 1981; Golowasch, Kirkwood and Miller, 1986; Zhang and Yan, 2014). $K_{Ca}1.1$ α-subunits are characterized by seven transmembrane domains. The intracellular C-terminus of $K_{Ca}1.1$ comprises roughly two thirds of its length and contains four subunits which confers calcium sensitivity to the channels gating properties (Y. Wu *et al.*, 2010; Yuan *et al.*, 2011). Moreover, each α-subunit contains an S5-6 pore domain (PD), and an S1-4 voltage sensing domain (VSD). Voltage sensitivity makes BK_{Ca} unique of the K_{Ca} channels, as they alone are modulated by membrane depolarisation. Finally, $K_{Ca}1.1$

subunits comprise an additional S0 domain comprising a long extracellular N-terminus. A seventh intracellular domain also makes BK_{Ca} unique of the voltage sensitive K^+ channels. The molecular properties of the α-subunit dictate that BK_{Ca} channels are activated in response to both an increase in $[Ca^{2+}]_I$ and membrane depolarisation and therefore act to oppose transient calcium sparks within cells.

Though the α-subunits of the channel are only encoded for by one gene, multiple splice variants (Atkinson, Robertson and Ganetzky, 1991; Adelman *et al.*, 1992; Yan *et al.*, 2008), protein modifications (Yan *et al.*, 2008) and alternate transcriptional promoters (Bohm *et al.*, 2000) within *KCNMA1* result in a diverse array of channel configurations. Furthermore, the extracellular N-terminus of $K_{Ca}1.1$ mediates the binding of β-auxiliary subunits, *KCNMB1-4* encoded $K_{Ca}\beta$1-4 (Knaus *et al.*, 1994; Wallner, Meera and Toro, 1999; Behrens *et al.*, 2000; Zhang and Yan, 2014), which also modulate channel activity. These variations ultimately underpin the heterogenicity of channel gating properties between cell types.

BK_{Ca} channels are ubiquitously expressed throughout the body, though are not necessary for life as deletion of the gene is not terminal in mice (Werner *et al.*, 2005). Within the rat, BK_{Ca} channels mediate calcium or voltage derived repolarization of ganglion (Scholz, Gruss and Vogel, 1998; Zhang, Gopalakrishnan and Shieh, 2003), retinal (Sun *et al.*, 2017) and cochlear neuronal cells (Langer, Gründer and Rüsch, 2003; Wersinger *et al.*, 2010) in addition to myometrial (Anwer *et al.*, 1993), gastrointestinal (Ren *et al.*, 2016), detrusor (Soder and Petkov, 2011), and vascular smooth muscle cells.

A role for BK_{Ca} in vascular reactivity, myogenic tone and receptor mediated responses

Within the vasculature, BK_{Ca} channels were first identified within mesenteric arteries taken from guinea pigs (Benham *et al.*, 1986). Subsequently, BK_{Ca} channels have been

identified within an array of vascular beds where expression is predominantly restricted to VSMCs, though some expression may be present within the endothelium (Sandow and Grayson, 2009). BK_{Ca} primarily couples with the auxiliary subunit $K_{Ca}\beta1$ within VSMCs, which improves calcium and voltage sensitivity when compared to $K_{Ca}1.1$ alone (McCobb *et al.*, 1995; McManus *et al.*, 1995; Meera *et al.*, 1996). BK_{Ca} downregulation is also implicated in several hypertensive phenotypes (Brenner *et al.*, 2000; Plüger *et al.*, 2000; Amberg and Santana, 2003; Amberg *et al.*, 2003). BK_{Ca} are now recognized as negative feedback regulators of myogenic tone and as down-stream targets of endogenous vasoactive responses.

In a vascular bed specific manner, Inhibitors of BK_{Ca} channels increase basal and pressure-induced tone established in rat tail (Schubert *et al.*, 1997), saphenous (Berczi *et al.*, 1992), cerebral (Howitt *et al.*, 2011) and mesenteric (Jackson-Weaver *et al.*, 2011) arteries but not rat or human cremasteric VSMCs (Jackson, Huebner and Rusch, 1997; Jackson, 1998). The current hypothesis states that a rise in $Vsmc_m$ and $[Ca_2^+]_I$ during stretch induced tone activates BK_{Ca} channels, modulating depolarisation of the membrane. This proposal is supported by an enhancement of stretch-induced membrane depolarisation within pig coronary arteries by BK_{Ca} blockers (Wu and Davis, 2001), which had no effect on resting cells, and a diminished effect of iberiotoxin on membrane depolarisation within pressurized coronary and cerebral arteries in the presence of calcium channel blockers (Brayden and Nelson, 1992; Nelson, 1993). This phenomenon appears to be dependent on the co-expression of $K_{Ca}\beta1$ (Tykocki, Boerman and Jackson, 2017).

BK_{Ca} has also been implicated as the downstream targets of an array of receptor mediated responses. BK_{Ca} is both downregulated and upregulated during receptor mediated contraction in a receptor dependent manner. For example, BK_{Ca} inhibition is crucial to pressure induced contraction whereby angiotensin-II (Ang-II) internalizes and

degrades BK_{Ca} (Wesselman *et al.*, 1997; Fallet *et al.*, 2001; Leo *et al.*, 2015) in a process purported to be dependent on PKC (Schubert, Noack and Serebryakov, 1999; Taguchi, Kaneko and Kubo, 2000). BK_{Ca} inhibition augments contraction in response to histamine (Hashemzadeh-Gargari and Rembold, 1992), vasopressin (Wakatsuki *et al.*, 1992), and norepinephrine (Jackson and Blair, 1998). Though these responses are PKC dependent, IP_3 also activates BK_{Ca} (Yang *et al.*, 2013). The current view states that elevated $[Ca^{2+}]_I$ and IP_3 during receptor mediated contraction activates BK_{Ca} channels, overcoming PKC mediated inhibition of the channel attenuating receptor mediated contraction (Tykocki, Boerman and Jackson, 2017). By comparison, the role of BK_{Ca} in receptor mediated vasodilatation is clearer. Upregulation of BK_{Ca} channel activity was first discovered in response to raised intracellular cyclic adenosine monophosphate (cAMP) during isoprenaline evoked responses (Sadoshima *et al.*, 1988), then later shown to be dependent on protein kinase A (PKA) binding of serine residue 869 $K_{Ca}1.1$ (Reinhart *et al.*, 1991; Nara *et al.*, 1998). Subsequently, BK_{Ca} has been identified as a downstream target of additional $G_{s\alpha}$-cAMP dependent signalling molecules including calcitonin gene related peptide (CGRP; Gozalov *et al.*, 2007), prostacyclin (PGI_2) IP receptor (Schubert *et al.*, 1996, 1997) and adenosine (Cabell, Weiss and Price, 1994). Additionally, BK_{Ca} channels are also upregulated by direct interaction with cyclic guanine monophosphate (cGMP) activated protein kinase G (PKG; Robertson *et al.*, 1993) during both receptor bound guanylyl cyclase mediated signalling including atrial natriuretic peptide (Otsuka *et al.*, 2002) and extraneous nitric oxide (NO) activated soluble guanylyl cyclase (Fukao *et al.*, 1999). These descriptions provide only a brief insight into the role of BK_{Ca} channels within the vasculature, for more detail see (Tykocki, Boerman and Jackson, 2017). In summary, BK_{Ca} channels are abundant within the vasculature, and represent key components of vascular reactivity.

1.4.1.2 IK_{Ca} / SK_{Ca} channels

Structure, function, and distribution

The remaining K_{Ca} channels are, as above, divided into IK_{Ca} and SK_{Ca}. IK_{Ca} is encoded for by only one gene, *KCNN4,* giving rise to $K_{Ca}3.1$. By contrast to IK_{Ca}, SK_{Ca} encompasses three separate genes, *KCNN1-3,* which give rise to $K_{Ca}2.1$-3 respectively (Wei *et al.*, 2005). By contrast to BK_{Ca} channels, IK_{Ca}/SK_{Ca} channels are constituted by homotetramers of six-transmembrane domain α-subunits which are voltage insensitive, express no inactivation at negative potentials and thus sustain hyperpolarization and are indirectly activated by Ca^{2+} by CaM, which is constitutively bound to the c-terminal domain of both channels in a 1:1 ratio (Xia *et al.*, 1998; Fanger *et al.*, 1999). Upon binding Ca^{2+}, Ca^{2+}:CaM complex causes a conformational shape in the channel and is responsible for the channel gating properties (Schumacher *et al.*, 2001; Wei *et al.*, 2005). The CaM binding domain within the C-terminus in essence acts as the β-auxiliary subunit proteins known to bind BK_{Ca}.

SK_{Ca} and IK_{Ca} distribution patterns vary widely. IK_{Ca} channels were originally thought to be expressed exclusively in non-excitable cells including lymphocytes (Partiseti *et al.*, 1992; Logsdon *et al.*, 1997) and erythrocytes (Vandorpe *et al.*, 1998), whereas SK_{Ca} expression was expressed in an array of neuronal cells (Villalobos *et al.*, 2004) and cardiac myocytes (Xu *et al.*, 2003; Tuteja *et al.*, 2005). More recent findings also implicate IK_{Ca} channels in the cardiac action potential of mice (Haron-Khun *et al.*, 2017) and rats (Zhao *et al.*, 2019). For the purpose of this thesis however, we will focus on the integral role of IK_{Ca}/SK_{Ca} channels in regulating endothelial-vascular coupling.

IK_{Ca}/SK_{Ca} within the endothelium and their role in the generation and spread of EDH

Within the vasculature, of the SK_{Ca} subtypes, $K_{Ca}2.3$ is principally expressed within the endothelium (Köhler *et al.*, 1996, 2001; Taylor *et al.*, 2003), with little to no $K_{Ca}2.2$

(Burnham *et al.*, 2002) and no expression of $K_{Ca}2.1$. Similarly, $K_{Ca}3.1$ has been demonstrated within the endothelium (Köhler *et al.*, 2000, 2001; Burnham *et al.*, 2002; Edwards and Weston, 2004; Sandow *et al.*, 2006). $K_{Ca}3.1$ is also present within proliferating arterial smooth muscle cells before they undergo a phenotypic switching, after which $K_{Ca}1.1$ becomes the predominant subtype (Neylon *et al.*, 1999). SK_{Ca}/IK_{Ca} expression is therefore typically restricted to the endothelium within several different vascular beds and animal models.

There is consensus within the literature regarding the fundamental role of IK_{Ca}/SK_{Ca} channels within the generation and spread of endothelial derived hyperpolarization (EDH) within resistance arteries. Resistance arteries in turn present with preferential dependence on EDH during endothelium dependent receptor mediated relaxation over the canonically associated NO signalling, reinforcing the importance of these channels. Hyperpolarization of ECs in response to raised $[Ca^{2+}]_I$ during receptor derived responses to bradykinin (Colden-Stanfield *et al.*, 1987), acetylcholine (Shimokawa *et al.*, 1996) and substance P (Brunet and Bény, 1989), and shear stress (Brähler *et al.*, 2009) is well documented. Transient increases in $[Ca^{2+}]_I$ activate IK_{Ca}/SK_{Ca} channels, which are located in close proximity to IP_3R and non-specific cation channels, giving rise to K^+ efflux and hyperpolarization of the cell, see (Goto, Ohtsubo and Kitazono, 2018) for review. Spatial distribution of IK_{Ca}/SK_{Ca} channels infers their functional role within the endothelium. IK_{Ca} channels are predominantly located within proximity of connexin proteins within myo-endothelial projections that span the internal elastic lamina and are responsible for heterocellular communication between the endothelium and the adjacent VSMCs (Sandow *et al.*, 2006), whereas SK_{Ca} channels are near structurally dissimilar connexin proteins within homocellular communicating domains (Goto *et al.*, 2004; Sandow *et al.*, 2006) and are responsible for endothelial cell communication. In summary, activation of IK_{Ca} channels in response to receptor stimulation in ECs causes hyperpolarization that spreads into VSMCs, where activation of SK_{Ca} channels causes the spread of hyperpolarization along the vessel wall.

Impaired expression of SK_{Ca} channels has been demonstrated in models of primary hypertension including spontaneously hypertensive rats (SHRs; Seki *et al.*, 2017; Giachini *et al.*, 2009; Kong *et al.*, 2015; Weston *et al.*, 2010) and Ang-II infused mice (Hilgers and Webb, 2007). Diminished SK_{Ca} expression contributes to impaired EDH and thus endothelial cell dysfunction, a typical feature of hypertension (Goto, Ohtsubo and Kitazono, 2018). Interestingly, upregulation of IK_{Ca} has also been reported in the aforementioned studies (Hilgers and Webb, 2007; Giachini *et al.*, 2009; Kong *et al.*, 2015), providing compensatory mechanism for diminished SK_{Ca} expression. Though the causative factors impairing SK_{Ca} expression remain unknown, recent evidence would suggest that oxidative stress diminishes K_{Ca} expression within the vasculature (Zhao *et al.*, 2014). Regulation of SK_{Ca} expression in hypertension remains a key area of interest in the treatment of hypertension and endothelial cell function recovery.

1.4.2 K_{IR} channels

Inwardly rectifying K^+ currents were first identified by Katz in skeletal muscle (Katz, 1949), wherein greater current passed into the cell than out of it. Later analysis would describe the non-linearity of current flow within embryonic cells that passed inward current more-readily at potentials more negative to E_k than outward current when at potentials more positive to E_k (Hagiwara and Takahashi, 1974; Miyazaki *et al.*, 1974), a phenomenon known as negative slope conductance. Inwardly rectifying K^+ channels were later purposed to account for the regulation of the resting membrane potential in ventricular myocytes (Sakmann and Trube, 1984; Hibino *et al.*, 2010). The molecular correlate of which would be later identified as the K_{IR} subfamily of K^+ channels (Ho *et al.*, 1993; Kubo *et al.*, 1993), now known to encompass 15 subtypes categorized into 7 subfamilies, K_{IR}1-7, encoded for by *KCNJ1-15* (Kubo *et al.*, 2005). K_{IR} channels can be further subcategorized based on their function, including; K^+ transporters K_{IR}1.1/4.1/4.3/5.1/7.1, classic K_{IR} channels K_{IR}2.1-4, G-protein gated channels K_{IR}3.1-4, and ATP-sensitive K^+ channels (K_{ATP}) K_{IR}6.1/2 (Hibino *et al.*, 2010). K_{IR} channels have

been identified in myriad tissues including cardiovascular (Beeler and Reuter, 1970), urinary (Tsai *et al.*, 2014), neuronal (Brown *et al.*, 1990) and skeletal (Sims and Dixon, 1989) and encompass a diverse array of physiological roles. Within the vasculature, classic inwardly rectifying ($K_{IR}2.x$) and K_{ATP} channels ($K_{IR}6.x$) act as key regulators of arterial reactivity.

1.4.2.1 Classic $K_{IR}2.x$

Classic $K_{IR}2$ gating properties

$K_{IR}2.x$ channels are a homo/heterotetramers of α-subunit proteins (Glowatzki *et al.*, 1995; Raab-Graham and Vandenberg, 1998). Each α-subunit is comprised of two transmembrane domains termed TM1 and TM2, an extracellular pore-forming component termed H5 (Heginbotham *et al.*, 1994) and intracellular C and N-termini (Raab-Graham and Vandenberg, 1998). Inward rectification is inherent to K_{IR} channels because of negatively changed amino acids within TM2 (e.g. D171 in $K_{IR}2.1$) and in C-terminal domains (e.g. E224 and E229 in $K_{IR}2.1$; Taglialatela *et al.*, 1995, 1994; Yang, Jan & Jan, 1995) which bind Mg^{2+} (Vandenberg, 1987; Nichols, Ho and Hebert, 1994) and polyamines (Lopatin, Makhina and Nichols, 1994). Polyamine/Mg^{2+} bind the intracellular surface of K_{IR} α-subunits in voltage-dependent manner blocking the channel with increasing affinity at more positive potentials. Moreover, conductance through K_{IR} channels increase in relation to the concentration of extracellular K^+ ions (Hagiwara and Takahashi, 1974; Kubo *et al.*, 1993; Lopatin and Nichols, 1996). It has been proposed that upon binding K^+ within domains in the extracellular P-loop of the selectivity filter, Mg^{2+}/polyamines are displaced from the intracellular C/N-terminal domains, allowing for current flow, see (Stanfield, Nakajima and Nakajima, 2002; Longden and Nelson, 2015) for review. These molecular features give rise to the aforementioned negative slope conductance, whereby as $Vsmc_m$ is hyperpolarized or $[K^+]_o$ rises, K_{IR} channels are unblocked moving $Vsmc_m$ towards E_K. Whereas at more depolarized $Vsmc_m$, K_{IR} open probability is decreases through intracellular pore blockage and the cell depolarizes.

K_{IR}2.x, end-stage boosters in neurovascular coupling and endothelial derived signalling

Of the K_{IR}2.x subtypes within the vasculature, K_{IR}2.1 is predominantly expressed, with little K_{IR}2.2 and no K_{IR}2.3 (Bradley *et al.*, 1999; Zaritsky *et al.*, 2000; Wu *et al.*, 2007), however, there are vascular bed specific differences in K_{IR}2.x distribution within the arterial wall. Though numerous examples have determined K_{IR}2.x expression within whole lysates of coronary, cerebral and mesenteric arteries (Bradley *et al.*, 1999; Zaritsky *et al.*, 2000; Crane, Walker, *et al.*, 2003; Smith *et al.*, 2008), expression of K_{IR}2.x channel is restricted to the endothelium of small mesenteric arteries (Crane, Walker, *et al.*, 2003; Smith *et al.*, 2008; Sonkusare *et al.*, 2016). This discrepancy in distribution gives rise to functional differences in response to raised external $[K^+]_o$.

Within the cerebral circulation, small increases in extracellular K^+ concentration ($[K^+]_o$) correlate with vasodilatation (Edwards, Hirst and Silverberg, 1988; Knot, Zimmermann and Nelson, 1996; Zaritsky *et al.*, 2000; Smith *et al.*, 2008). Local surges in K^+ are reported to come from astrocyte endfeet during nerve stimulation. Astrocytes encase the vascular wall of the cerebral microcirculation (Mathiisen *et al.*, 2010) and release K^+ into the perivascular space via IP_3R driven BK_{Ca} activation (Filosa *et al.*, 2006; Straub *et al.*, 2006; Girouard *et al.*, 2010; Longden and Nelson, 2015). Exposure to raised $[K^+]_o$ activates vascular K_{IR}2.x channels by removal of the polyamine / Mg^{2+} block mediating vasodilatation by hyperpolarization of $Vsmc_m$, increasing blood flow to the area. This phenomenon forms the basis for neurovascular coupling and underpins neuron induced functional hyperemia, see (Longden and Nelson, 2015) for review. A role for K_{IR}2.x within this phenomenon is evidenced by an inhibition of change in cerebral blood flow in responses to glutamate receptor activators, whisker stimulation (Girouard *et al.*, 2010), or sciatic nerve stimulation (Vetri *et al.*, 2012) by K_{IR}2.x blocker Ba^{2+}.

By contrast, raised $[K^+]_o$ had minimal effect on mesenteric artery vasodilatation in the rat when compared to coronary and cerebral arteries (Smith *et al.*, 2008). $K_{IR}2.x$ channels within the endothelium are purported to; 1.) contribute to the resting membrane potential of the cell within pig coronary artery ECs (Nilius, Schwarz and Droogmans, 1993; von Beckerath *et al.*, 1996); 2.) provide electrochemical driving force for the influx of Ca^{2+} for the generation of endothelial nitric oxide synthase (eNOS) products during flow mediated vasodilatation in rabbit cerebral arteries (Wellman and Bevan, 1995); 3.) propagate the spread of EDH in mouse mesenteric, acting as an endstage booster of IK_{Ca}/SK_{Ca} derived hyperpolarization in response to acetylcholine (Sonkusare *et al.*, 2016). These concepts will be revisited in greater detail in Chapter 7.

Degradation of endothelial $K_{IR}2.x$ channels has been implicated in the development of endothelial cell dysfunction in genetic models of hypertension (Goto *et al.*, 2004; Weston *et al.*, 2010). In secondary models of hypertension endothelial $K_{IR}2.x$ channels appeared unaltered (Sonkusare *et al.*, 2016). Moreover, vascular $K_{IR}2$ channels responsible for neurovascular coupling are thought to be implicated in an array of neurological diseases, see (Longden and Nelson, 2015) for review. Though some confusion remains regarding the role of endothelial $K_{IR}2$ in models of primary and secondary hypertension and the implication of $K_{IR}2.x$ channels in neurovascular disease is a currently novel field of research, $K_{IR}2.x$ channels are well established vascular $[K^+]_o$ sensors and hyperpolarization boosters within VSMCs and ECs, which play pivotal roles in vascular reactivity.

1.4.2.2 K_{ATP} channels

K_{ATP} gating properties

ATP sensitive currents were first identified by (Noma, 1983) within cardiac myocytes, then later confirmed by (Trube and Hescheler, 1984), whereby strong outward currents were enhanced by depletion of intracellular ATP. The molecular correlates of K_{ATP} channels were later cloned and identified as $K_{IR}6.1$ and $K_{IR}6.2$ (Inagaki *et al.*, 1995),

which were found to have homology with the K_{IR} subfamily. By comparison to $K_{IR}2$ channels, $K_{IR}6.x$ channels express poor inward rectification (Lu and MacKinnon, 1994; Taglialatela *et al.*, 1995). Additionally, expression of $K_{IR}6.x$ alone however does not form functional K^+ channels, but requires the co expression of sulphonylurea receptors (SURs; Inagaki *et al.*, 1995; Aguilar-Bryan *et al.*, 1995; Chutkow *et al.*, 1996; Yamada *et al.*, 1997; Isomoto *et al.*, 1996), including SUR1, SUR2A and SUR2B, see (Aguilar-Bryan *et al.*, 1998) for review. K_{ATP} are now recognized as intracellular sensors that convey changes in metabolic states to electrical signals across the membrane. As above, K_{IR} structure is preserved amongst the varying subtypes. $K_{IR}6$ channels are no exception to this. Functional K_{ATP} channels are constituted by heteromultimers of 4 $K_{IR}6.x$ α-subunits that comprise two transmembrane domains, a heavily conserved H5 selectivity filter and intracellular C and N-termini and 4 SURs (Clement *et al.*, 1997; Yamada *et al.*, 1997). ATP sensitivity is purported to be derived from multiple regions in the N and C-termini of $K_{IR}6.x$ α-subunit as demonstrated by mutagenesis studies (Tucker *et al.*, 1997, 1998; Takano *et al.*, 1998). The SURs infer sensitivity inhibitors of K_{ATP} termed Sulphonylureas including Glibenclamide (Panten *et al.*, 1989; Aguilar-Bryan *et al.*, 1998), an agent employed in Chapter 6.

The physiological role of K_{ATP} channels is best understood within β-pancreatic cells of the islet of Langerhans. Raised serum glucose sufficient to cause transport into β-pancreatic cells augments intracellular ATP. β-pancreatic cells express $K_{IR}6.2$/SUR1 complexes which are inhibited by free cytoplasmic ATP/Mg^{2+}, causing the depolarisation of the membrane, calcium entry and insulin mobilization (Ashcroft and Kakei, 1989; Hibino *et al.*, 2010). Sulphonylureas are one of the few K^+ channel modulators to have made it to clinical practice, which propagate β-pancreatic cell depolarisation and insulin release via $K_{IR}6.2$/SUR1 inhibition. VSMCs primarily express $K_{IR}6.1$/SUR2B complexes (Isomoto *et al.*, 1996), which are by comparison to $K_{IR}6.2$/SUR1 less sensitive to

intracellular ATP levels and express lower unitary conductance (Kajioka, Kitamura and Kuriyama, 1991; Beech *et al.*, 1993; Yamada *et al.*, 1997).

K_{ATP} channels are downstream target of receptor mediated vascular reactivity

The role of K_{ATP} in vascular reactivity has been demonstrated by murine knockout model lacking either $K_{IR}6.1$ or SUR2B. In these models, mice were hypertensive, resistant to vasodilators and prone to coronary artery vasospasm leading to sudden death (Chutkow *et al.*, 2002; Miki *et al.*, 2002; Aziz *et al.*, 2014). Other studies have also demonstrate K_{ATP} inhibitor-mediated contraction of coronary (Duncker *et al.*, 1995; Farouque, Worthley and Meredith, 2004) and renal arteries (Colburn *et al.*, 2020) in normotensive (NT) animals implicating K_{ATP} in the regulation of basal arterial tone. The mechanism of K_{ATP} contribution to basal tone however remains unclear. Theoretically, K_{ATP} express low activity at rest due to high levels of resting VSMC intracellular ATP (Beech *et al.*, 1993; Randak and Welsh, 2005; Shi *et al.*, 2012). K_{ATP} contribution to basal vascular tone is prospectively due to K_{ATP} activation by sympathetic nerve terminal neurotransmitter release (Colburn *et al.*, 2020) or in the case of coronary arteries a release of an as of yet undescribed ventricular myocyte factor (Takeda *et al.*, 2006).

The role and regulation of K_{ATP} in receptor mediated responses however is, comparably to K_{ATP} contribution to basal vascular tone, better understood. K_{ATP} is a target of $G_{q/11}$ receptor mediated PKC dependent contractions including histamine, serotonin, neuropeptide-y (Bonev and Nelson, 1996), Ang-II (Kubo, Quayle and Standen, 1997), vasopressin (Shi *et al.*, 2007), endothelin 1 (W. S. Park *et al.*, 2005) and noradrenaline (Tan, Al Abed and Brock, 2007). $K_{IR}6.1$ expresses PKC-binding domains within its intracellular C-terminal domain that are shown to decrease channel activity (Shi, Cui, *et al.*, 2008) and calveolin-1 mediated channel internalization (Jiao *et al.*, 2008). Diminished K_{ATP} channel activity promotes membrane depolarisation and contraction. Moreover, K_{ATP} is a target of G_s-coupled cAMP-PKA dependent receptor mediated relaxations including PGI_2 (Schubert *et al.*, 1997), CGRP (Kitazono, Heistad and Faraci, 1993) and

β-adrenoreceptor agonists (Ming, Parent and Lavallée, 1997). Both $K_{IR}6.1$ (Quinn, Giblin and Tinker, 2004) and SUR2B (Shi, Chen, *et al.*, 2008) contain residues that act as phosphorylation targets for PKA binding, which reportedly underpins G_s-coupled receptor mediated upregulation of channel activity. Moreover, activation of G_s-coupled receptors depletes intracellular ATP, relieving channel block. Finally, K_{ATP} channels are also implicated in guanylyl cyclase mediated cGMP-PKG relaxations in response to NO and receptor mediated responses (Kubo *et al.*, 1994; Murphy and Brayden, 1995), though not universally (Jackson *et al.*, 1993; Quayle *et al.*, 1994). The reason for the discrepancy between these studies may be due to differing animal models and vascular beds investigated, however the mechanism remains to be described. The role of K_{ATP} in vascular reactivity is therefore well evidenced, though still incompletely understood.

1.4.3 K_{2P} channels

Lesage *et al,* (1994) probed GenBank for transcripts expressing homology for the K^+ selectivity filter termed the P domain shown to be preserved within K_V, K_{Ca} and K_{IR} channels. Lesage *et al,* (1994) identified a transcript encoding for a K^+ channel they termed Tandem of P domains in a Weak Inwardly rectifying K^+ channel (TWIK-1), based on its molecular and electrophysiological properties (Lesage *et al.*, 1996). Since the first demonstrations of the electrical properties of excitable cells, strong background K^+ conductance's have been recorded, which was voltage independent, instantaneous and non-inactivating (Hodgkin & Huxley, 1947; Hodgkin & Huxley, 1952a; Enyedi & Czirják, 2010). Constitutive background K^+ conductance's, or leak, was suggested to stabilize the membrane potential. K_{2P} channel properties largely accounted for this unidentified channel. TWIK-1 expresses no-voltage sensitivity, linear current voltage relationship, instantaneous activation and no inactivation (Lesage *et al.*, 1996, 1997), however TWIK-1 channels also express weak outward rectification through Mg^{2+} block (Lesage *et al.*, 1996, 1997). Though not a perfect fit, K_{2P} was widely recognized as the correlate for the K^+ leak current (Enyedi and Czirják, 2010). The *KCNK1* encoded α-subunit of TWIK-1,

K_{2P}1.1 (Goldstein *et al.*, 2005), contains two P-domain selectivity filters and four transmembrane domains (Lesage *et al.*, 1996) that form homodimers within the membrane, making them unique of the K^+ channels discovered to date. This unique structure led to the rapid discovery of the remaining leak channels, which include 15 subtypes encoded for *Kcnk1-18*, see (Enyedi and Czirják, 2010) for review, though *Kcnk7,11,15* are now known not to exist. Though there are wide ranging differences in the sequence of the remaining leak channels, the two-pore domain is preserved across the subfamily. K_{2P} channels encompass several subfamilies including TWIK, TWIK-related K^+ channels (TREK), TWIK-related arachidonic acid sensitive K^+ channel (TRAAK), TWIK-related acid sensitive K^+ channel (TASK), TWIK-related alanine activate K^+ channel, Tandem-pore domain Halothane inhibited K^+ channel, and TWIK-related spinal cord K^+ channel. Recent literature has focused on the role of TREK-1, TRAAK-1 and TASK-1 within the vasculature and will be addressed here.

1.4.3.1 TREK-1, TRAAK-1 and TASK-1, K_{2P} channels in the vasculature,

TREK-1 channels unlike TWIK-1 channels display complex gating properties (Patel *et al.*, 1998; Dedman *et al.*, 2009), including voltage-gated outward rectification (Dedman *et al.*, 2009), whereby current increases at more positive potentials over time. Residues within the C-terminal domain contribute to voltage-sensitivity (Maingret *et al.*, 2002) and outward rectification is attributed to the two-pore selectivity domains in the α-subunit (Goonetilleke and Quayle, 2012). TREK-1 channels are expressed across the vasculature (Gurney *et al.*, 2003; Gardener *et al.*, 2004; Bryan *et al.*, 2006), mutagenesis has demonstrated a role for these channels in endothelium derived NO production (Garry *et al.*, 2007) and polyunsaturated fatty acid mediated relaxation of basilar arteries (Blondeau *et al.*, 2007). Moreover, TRAAK channels are known to be positively regulated by arachidonic acid (Fink *et al.*, 1998). A novel role for TRAAK in cerebral artery vasorelaxation in response to arachidonic acid was demonstrated by Byran *et al*,. (2006), independent of arachidonic acid metabolism or other K^+ channels. Finally, TASK-1, a K_{2P} channel gated by extracellular changes in pH (Duprat *et al.*, 1997) is reported to underpin

the resting membrane potential of pulmonary artery vascular smooth muscle (Gurney *et al.*, 2003), and contributes to hypoxia induced vasorelaxation (Gardener *et al.*, 2004; Gurney and Manoury, 2009). Though the literature regarding K_{2P} within the vasculature is by comparison to other K+ channels limited, there is growing appreciation for the role of these channels in vascular biology.

1.4.4 K_V channels

K_V channels encompass the largest number of K^+ channels with 40 individual sub members subcategorized into 12 subfamilies K_V1-12 (Gutman *et al.*, 2005; González *et al.*, 2012). K_V1-4,7,10-12 form functional homo/heterotetramers whereas K_V5,6,9 are electrically silent but co-assemble with K_V2/3 subunits to form functional channels (Gutman *et al.*, 2005; González *et al.*, 2012; Jackson, 2018). Voltage gated delayed rectifying currents were first described by Hodgkin and Huxley (1952b) within giant squid axons, wherein depolarisation of the membrane led to K^+ dependent current which underpinned the action potential duration and shape (Hodgkin & Huxley, 1952b). Heterogeneity in K_V current gating properties is well documented, and is reflected by wide diversity within the K_V family (González *et al.*, 2012; Jackson, 2018). Despite the vast array of K_V channels, K_V α-subunit protein structure is largely preserved across the subfamilies. Each α-subunits consists of six transmembrane domains (S1-6), with distinct sections including: 1.) S4 VSD, comprised of positively charged amino acids which cause a change in conformational shape of the channel pore to an open state at depolarized potentials (Larsson *et al.*, 1996; Mannuzzu, Moronne and Isacoff, 1996), 2.) S5-6 PD, including a P-loop structure between S5-6 that provides selectivity for K^+ (Lu, Klem and Ramu, 2001), 3.) intracellular C and N terminal domains responsible for channel inactivation properties (Hoshi, Zagotta and Aldrich, 1991) and tetramerization (Gulbis *et al.*, 2000). Channel complexity is further complicated by combinations of channel hetromers, β-auxiliary subunit proteins, splice variants and truncated channel expression, summarised in González *et al.*, 2012; Jackson, 2018. In general terms, K_V1.2, K_V1.5, K_V2.1 K_V2.2 and Kv7s are expressed in most arterial VSMCs, where they

regulate $Vsmc_m$ and in turn $[Ca^{2+}]_i$ during rest and during vasoactive signalling cascades (Cox, Folander and Swanson, 2001; Belevych *et al.*, 2002; Albarwani *et al.*, 2003; Tykocki, Boerman and Jackson, 2017).

1.4.4.1 K_V1 channels

Several studies have found positive, yet contrasting, expression of *KCNA2,4,5,6* (K_V1.2,4,5,6) transcripts and protein between vascular bed and animal model with no clear pattern discernable (Cheong *et al.*, 2001; Cheong, Dedman and Beech, 2001; Kerr *et al.*, 2001; Fergus, Martens and England, 2003; Cox and Fromme, 2016). For example, Cheong *et al,* (2001) argues that K_V1.2 is restricted to the endothelium of rabbit cerebral arterioles whereas Kerr *et al*, (2001) and Fergus *et al,* (2003) demonstrate that the molecular correlate of native delayed rectifier current is K_V1.2/K_V1.5 heterotetramers within rabbit portal vein and K_V1.2/K_V1.4 heterotetramers within rat renal vascular myocytes respectively. These discrepancies are further complicated by varying expression of K_V1 β-auxiliary subunit proteins $K_V\beta$1/2. Whereby, $K_V\beta$1 alters K_V1.5 gating properties giving rise to rapid inactivation in retinal arteries (McGahon *et al.*, 2007), $K_V\beta$2 regulates K_V1.5 membrane trafficking in mouse coronary arteries (Nystoriak *et al.*, 2017) and $K_V\beta$1 contributes to K_V1.2/5 heterotetramers in rat mesenteric arteries. Numerable reports have argued that of K_V1, K_V1.5 appears to be the predominant functional subtype within the VSMCs (Thorneloe *et al.*, 2001; Plane *et al.*, 2005; Chen *et al.*, 2006). K_V1.5 channels are implicated in hampering myogenic tone in rat mesenteric (Plane *et al.*, 2005) and cerebral (Chen *et al.*, 2006) arteries, K_V1.5 is internalized during 5-HT mediated contraction in rat pulmonary VSMCs (Cogolludo *et al.*, 2006) and $K_V\beta$1.3 inactivation of K_V1.5 is diminished during PKA mediated responses (Kwak *et al.*, 1999). The latter prospectively identifying a role for K_V1.5 in β-adrenoreceptor vasorelaxation (Aiello, Walsh and Cole, 1995; Aiello *et al.*, 1998; Johnson *et al.*, 2009; Jackson, 2018).

1.4.4.2 K_V2 channels

In addition to K_V1 channels, several studies have identified *KCNB* encoded K_V2.1 and K_V2.2 in whole lysates of arteries (Schmalz *et al.*, 1998; Xu *et al.*, 1999), and both contribute to native rat (Xu *et al.*, 1999) and canine (Schmalz *et al.*, 1998) vascular smooth muscle K_V currents. Of note, K_V2.2 is minimally expressed compared to K_V2.1 in rat middle cerebral artery (Zhong, Abd-Elrahman, *et al.*, 2010) and aorta (Tanaka *et al.*, 2006). Being that K_V2.1 and K_V2.2 form heteromultimers (Blaine and Ribera, 1998; Xu *et al.*, 1999), the effects of K_V2.2 can be difficult to delineate. The current literature has focused more heavily on K_v2.1 by comparison. K_V2.1 contributes to voltage sensitive delayed rectifying currents in rat pulmonary (Smirnov *et al.*, 2002), mesenteric (Lu *et al.*, 2002) and aortic (Belevych *et al.*, 2002; Tammaro *et al.*, 2004) VSMCs. Functionally, K_V2.1 regulates resting $Vsmc_m$ in rat middle cerebral artery and oppose myogenic tone in a pressure sensitive process (Amberg and Santana, 2006) in heteromultimeric configurations of K_V2.1/K_V9.3 (Zhong, Abd-Elrahman, *et al.*, 2010). K_V2.1 is also upregulated in response to atrial natriuretic peptide (ANP), NO dependent signalling within rat aorta (Tanaka *et al.*, 2006)

1.4.4.3 K_V11.1 channels

Isoforms of *KCNH2* encoded K_V11.1, commonly known as *ether-a-go-go* (ERG) related channels, including ERG1a and ERG1b contribute to the fast-component of the delayed rectifying current of the cardiac action potential (Lees-Miller *et al.*, 1997; Larsen *et al.*, 2008). More recently, ERG1 blocker E-4031 sensitive currents were demonstrated in murine portal vein (Ohya *et al.*, 2003; Yeung *et al.*, 2007) and protein and transcript were identified within isolated murine arterial smooth muscle cells (Barrese *et al.*, 2017), though no ERG currents were detectable. Inhibition of K_V11.1 did however prevent and activation enhanced VSMC proliferation (Barrese *et al.*, 2017). Moreover, K_V1.3 has been identified in proliferative VSMCs and is implicated in the phenotypic switch to contractile VSMCs via PLCγ independent of K^+ influx (Cidad *et al.*, 2012, 2015),

prospectively through their c-terminal domain (Jiménez-Pérez *et al.*, 2016). Implicating an unorthodox role for these channels outside of their commonly considered function.

1.5 K_V7 channels

K_V7 channels are encoded by the genes *KCNQ1-5*, which each give rise to distinct α-subunit proteins, termed $K_V7.1$-5 respectively. K_V7 channels activate slowly upon depolarization with a relatively low threshold (eg ~-40 mV) and exhibit little inactivation. They are widely expressed across the body and underpin many key physiological phenomena. As K_V7 channels are the primary focus of this thesis, a broad overview of K_V7 structure, distribution and function will be given in greater detail than above, covering both vascular and non-vascular K_V7 function.

1.5.1 K_V7 channel structure

K_V7 α-subunits consist of six transmembrane domains encapsulated by intracellular C and N-termini (Fig 1.4). By contrast to K_V1-4, K_V7 channels have a much larger C-terminus conserved across each subtype which can be broken down into four helical domains (A-D; summarised in Haitin & Attali, 2008). Parallel coiled-coil interactions within the distal section of the C-terminus domain determine subtype assembly (Schmitt *et al.*, 2000; Schwake, Jentsch and Friedrich, 2003; Howard *et al.*, 2007), giving rise to a cone like structure within the membrane with a highly conserved K^+ selectivity filter within S6 (Doyle *et al.*, 1998; del Camino and Yellen, 2001) and voltage sensitivity provided by positively charged amino acids within S4 (Larsson *et al.*, 1996; Mannuzzu, Moronne and Isacoff, 1996) as described above. K_V7 α-subunits form homo/heterotetrameric channels within the membrane that are therefore both voltage-sensitive and K^+ selective. K_V7 channel stoichiometry varies between systems. $K_V7.1$ is commonly thought of as exclusively homotetrameric (Schwake, Jentsch and Friedrich, 2003), although Oliveras *et al* (2014) speculated $K_V7.1$ could heteromerized with $K_V7.5$ in arterial VSMCs (Oliveras *et al.*, 2014). The remaining K_V7 channels, i.e $K_V7.2$-5, seem

to form hetromers within native tissue. Neuronal heterotetramers of K_V7.2/7.3 (Wang *et al.*, 1998), K_V7.3/7.4 (Kubisch *et al.*, 1999) and K_V7.2/7.5 (Schroeder, Hechenberger, *et al.*, 2000) increase plasma membrane abundance of K_V7.3, which forms weak channels individually. Vascular K_V7.4 readily forms heterotetramers of K_V7.4/7.5, though can also be abundantly found as a homotetramers, whereas K_V7.5 exist predominantly with K_V7.4 (Chadha *et al.*, 2014; Lyubov I. Brueggemann *et al.*, 2014). Moreover, channel complexity is further increased by β-auxiliary subunit proteins, KCNE1-5, that are encoded for by *KCNE1-5* respectively. KCNE proteins are single transmembrane proteins that are found in juxtaposition to K_V7 α-subunit proteins which modify the biophysical and pharmacological properties of the channels as well as regulate intracellular trafficking (McCrossan and Abbott, 2004; Kanda and Abbott, 2012). See Figure 1.4 for a diagrammatic representation of K_V7/KCNE structure.

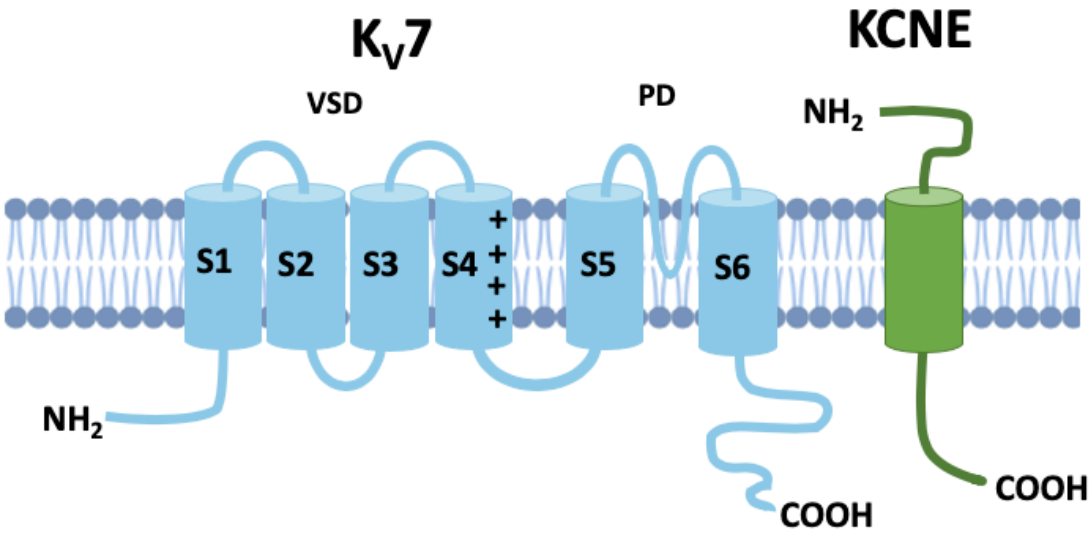

Figure 1.4 K_V7 and KCNE protein structure

K_V7 α-subunit proteins are constituted by 6-transmembrane domains including a voltage sensing domain (VSD; S1-4) and pore forming domain (PD; S5-6). K_V7 channels are found in close proximity with β-auxiliary subunit KCNE proteins that are comprised of a single transmembrane domain.

1.5.2 K_V7 channel gating

As above, K_V7 channels are activated by membrane voltage, though in contrast to other K_V subfamily members, are active at more negative membrane potentials and express little to no inactivation, allowing them to contribute to sustained membrane potentials, see (Barrese, Stott and Greenwood, 2018) for review. The gating properties of K_V7 channels are regulated by several secondary signalling molecules that interact with their intracellular C-terminal domains. K_V7 currents are universally dependent on PIP_2 (Zhang *et al.*, 2003; Li *et al.*, 2005). PIP_2 binds K_V7 within the proximal anti-parallel A/B helices of the C-terminal domain, S2-3 linker and S3-4 linkers (Zhang *et al.*, 2003; K.-H. Park *et al.*, 2005; Hernandez, Zaika and Shapiro, 2008), stabilizing the channel in its open state by coupling the VSD to the PD (Zaydman *et al.*, 2013; Pant *et al.*, 2021). PIP_2 binding diminished current rundown in all subtypes (Zhang *et al.*, 2003) and mediates a left-shift in the voltage dependance of activation (K.-H. Park *et al.*, 2005). Additionally, all K_V7 channels bind CaM (Yus-Najera, Santana-Castro and Villarroel, 2002) within the proximal A/B helices of the C-terminus (Xu *et al.*, 2013; Sachyani *et al.*, 2014; Sihn *et al.*, 2016) and is essential for $K_V7.1$ (Ghosh, Nunziato and Pitt, 2006), $K_V7.2$ (Etxeberria *et al.*, 2008) and $K_V7.4$ (Zhuang and Yan, 2020) membrane trafficking. Though the role of CaM differs between K_V7 subtypes. Overexpression of CaM augments currents evoked from $K_V7.1$ and $K_V7.3$, but inhibits $K_V7.2$, $K_V7.4$ and $K_V7.5$ (Gamper, Li and Shapiro, 2005). Current understanding implicates CaM as a calcium sensing regulator of K_V7 which, upon binding Ca^{2+} upregulates $K_V7.1$ currents (Shamgar *et al.*, 2006) but impairs $K_V7.2$-5 (Xu *et al.*, 2013) currents through a conformational change in shape of CaM:Ca^{2+}. The importance of CaM regulation of K_V7 is highlighted by Long-QT mutations associated with diminished C-terminal interaction with CaM (Ghosh, Nunziato and Pitt, 2006). $G_{\beta\gamma}$ is also a key determinant of $K_V7.4$ activity and crucial for receptor mediated increase in channel activity (Stott, Povstyan, *et al.*, 2015) in a synergistic interplay of $G_{\beta\gamma}$ and PIP_2 (Povstyan *et al.*, 2017), though the precise mechanisms is yet to be described. Channel gating properties are further complicated by dynamic regulation via of products

of cAMP including PKA and exchange protein directly activated by cAMP (EPAC), products of cGMP including PKG and PKC, and will be discussed in context across an array of tissues below.

1.5.3 K_V7 channel pharmacology

Due to the contribution of K_V7 channels to known heritable diseases of the cardiovascular and nervous systems, modulators of K_V7 channels activity have been a keen area of interest for the pharmaceutical industry. A slew of activators and inhibitors are available and are summarized by Barrese *et al,.* (2018) and expanded upon below in Table 1.1 (activators) and 1.2 (inhibitors). Activators of K_V7 can be crudely separated into those that bind the VSD or PD, whereas inhibitors of K_V7 block PD only. Within this thesis $K_V7.2$-5 channel activators S-1, ML213 and Retigabine, $K_V7.1$ channel activator ML277, pan-K_V7 channel inhibitors Linopirdine and XE991 and $K_V7.1$ channel inhibitors HMR-1556 and Chromanol 293B have been employed to delineate the functional role of K_V7 channels within the vasculature. Characterizing these modulators and establishing their specificity is the focus of Chapter 3 and is discussed at length there.

Compound name	***Target***	***Site of action***	***Reference***
S-1	$K_V7.2$-5: $K_V7.4$>$K_V7.2/3/5$	Tryptophan in S5 PD: $K_V7.4$-Trp242	(Bentzen *et al.*, 2006)
ML213	$K_V7.2$-5: $K_V7.2/4$>$K_V7.3/5$	Tryptophan in S5 PD: $K_V7.4$-Trp242	(H. Yu *et al.*, 2011; Jepps *et al.*, 2014)
Retigabine	$K_V7.2$-5	Tryptophan in S5 PD: $K_V7.2$-Trp236 $K_V7.3$-Trp265 $K_V7.4$-Trp242	(Schenzer *et al.*, 2005; Wuttke *et al.*, 2005; Lange *et al.*, 2009; Li *et al.*, 2021)
NS15370	$K_V7.2$-5	Tryptophan in S5 PD: $K_V7.4$-Trp242	(Jepps *et al.*, 2014)

ICA-27243	K_V7.2-5: K_V7.2/3>K_V7.4/5	S1-4 VSD: Potentially within S2/3	(Wickenden *et al.*, 2008; Padilla *et al.*, 2009)
ICA-069673	K_V7.2-5: K_V7.2>K_V7.3/4>K_V7.5	S1-4 VSD: K_V7.2-F168 / A181 (S3) K_V7.4-F143	(Lyubov I. Brueggemann *et al.*, 2014; Wang, Yang and Kurata, 2017)
PF-05020182	K_V7.2/3	N/A	(Davoren *et al.*, 2015)
ICA-110381	K_V7.2-5:K_V7.2/3>K_V7.4	Putative S1-4 VSD	(Boehlen *et al.*, 2013)
QO58-lysine	K_V7: K_V7.2/4>K_V7.1>K_V7.3	N/A	(Zhang *et al.*, 2013; Teng *et al.*, 2016)
Zinc pyrithione	K_V7.1-5	S6 PD: K_V7.1-S338 K_V7.2-Leu249,275 + Gly301	(Xiong, Sun and Li, 2007; Gao *et al.*, 2008)
Meclofenamic acid, diclofenac	K_V7.2/3	N/A	(Peretz *et al.*, 2005)
NH29	K_V7.2-5: K_V7.2>K_V7.4>K_V7.3	VSD, S1,2,4: K_V7.2-Multiple residues	(Peretz *et al.*, 2010)
BMS-204352	K_V7.2-5	Tryptophan in S5 PD: K_V7.4-Trp242	(Bentzen *et al.*, 2006)
Flupirtine	K_V7.2-5	Structural analogue of retigabine, prospectively PD Trp residues	(Martire *et al.*, 2004)
R-L3 (L-364,373)	K_V7.1	N/A	(Salata *et al.*, 1998)
Mefenamic acid	K_V7.1+KCNE1	KCNE1-K41	(Wang, Eldstrom and Fedida, 2020)

ML277	K_V7.1	VSD: K_V7.1-E160/R231	(Yu, 2013; Hou *et al.*, 2019; Eldstrom *et al.*, 2021)

Table 1.1: K_V7 activators

A list of the currently identified KCNQ/K_V7 activators, the subtype preference, site of action (if known) and references that identify them.

Compound name	***Target***	***Site of action***	***Reference***
Linopirdine/ XE-991	K_V7	Open state channel blocker, PD: K_V7.2-R214	(Costa and Brown, 1997; Schnee and Brown, 1998; Greene, Kang and Hoshi, 2017; Li *et al.*, 2021)
ML-252	K_V7.2	N/A	(H. Yu *et al.*, 2011)
Chromanol 293B	K_V7.1+KCNE1/3> K_V7.1	PD, H5 selectivity filter/S6: K_V7.1-Ile337, Phe340	(Busch *et al.*, 1996; Lerche *et al.*, 2007)
HMR-1556	K_V7.1+KCNE1>K $_V$7.1	N/A Chromanol derivative	(Gerlach *et al.*, 2001; Thomas, Gerlach and Antzelevitch, 2003)
Azilimide dihydrochloride	K_V7.1	N/A	(Karam *et al.*, 1998)

Table 1.2: K_V7 inhibitors

A list of the currently identified KCNQ/K_V7 inhibitors, the site of action (if known) and references that identify them.

1.5.4 Vascular K_V7

1.5.4.1 Distribution

Within the vasculature, *Kcnq* was first identified in mouse portal vein via reverse transcription -quantitative polymerase chain reaction (RT-qPCR; Ohya *et al.*, 2003). Ohya *et al*, (2003) observed that *Kcnq1, 4* and *5* were predominantly expressed with little contribution from *Kcnq3* and no expression of *Kcnq2.* Though, at the level of protein, $K_V7.4$ expression generally dominates (Jepps *et al.*, 2011; Ng *et al.*, 2011). See table 1.3 for a comprehensive list of the currently identified vascular KCNQ/K_V7 subtypes within vessels from both human and animal models. Further investigation has identified the most commonly occurring vascular channel stoichiometries as the following; $K_V7.4$/ $K_V7.5$ > $K_V7.4$ > $K_V7.5$ (Chadha *et al.*, 2014, Brueggemann et al., 2014). Moreover, as with other systems, vascular K_V7 proteins are also found in juxtaposition with KCNE proteins, especially KCNE4 in male Wistar rats (Jepps *et al.*, 2015). To date, no vascular bed has been found not to express K_V7 channel transcript or protein.

Vascular smooth muscle	***Models***	***Sub-types expression profile***	***Reference***
Carotid artery	Mouse	Transcript (qPCR): KCNQ4> KCNQ5> KCNQ1> KCNQ3/KCNQ2	(Yeung *et al.*, 2007)
(Middle) Cerebral artery	Rat	Transcript (qPCR): KCNQ4> KCNQ5> KCNQ1 Protein (immunocytochemistry): K_V7.4> K_V7.5> K_V7.1	(Zhong, Harhun, *et al.*, 2010)
(Left) Coronary artery	Rat	Transcript (qPCR): KCNQ4/KCNQ5/KCNQ1 Protein (immunocytochemistry): K_V7.1, K_V7.4, K_V7.5	(Khanamiri *et al.*, 2013; Oliveras *et al.*, 2014; Morales-Cano *et al.*, 2015)
(Right) Coronary	Rat	Transcript (qPCR): KCNQ4> KCNQ5/KCNQ1 Protein (immunocytochemistry): K_V7.1, K_V7.4, K_V7.5	(Morales-Cano *et al.*, 2015)
Chorionic plate arteries	Human	Transcript (qPCR): KCNQ4> KCNQ1> KCNQ5> KCNQ3 Protein (Western blot): K_V7.3, K_V7.4, K_V7.5 Protein (Immunocytochemistry): K_V7.1, K_V7.4, K_V7.5	(Mills *et al.*, 2015; Wei *et al.*, 2018)
Femoral artery	Mouse	Transcript (qPCR): KCNQ4> KCNQ5> KCNQ1	(Yeung *et al.*, 2007)
Mesenteric artery	Mouse, Rat, Human	Transcript (qPCR): KCNQ4> KCNQ5/KCNQ1> KCNQ3 Protein (Western blot): K_V7.4 Immunocytochemistry: K_V7.1, K_V7.4, K_V7.5	(Yeung *et al.*, 2007; Mackie *et al.*, 2008; Jepps *et al.*, 2011; Ng *et al.*, 2011; Baldwin *et al.*, 2020; D. Zhang *et al.*, 2021)
Penile artery	Rat	Transcript (qPCR): KCNQ5> KCNQ4/KCNQ3 Protein (immunocytochemistry): K_V7.4, K_V7.5	(Jepps *et al.*, 2016)

Portal Vein	Mouse	Transcript (qPCR): KCNQ1> KCNQ3/KCNQ4/KCNQ5 Protein (Immunocytochemistry): $K_V7.1$	(Ohya *et al.*, 2003)
Pulmonary artery	Rat, Human	Transcript (qPCR): KCNQ4> KCNQ1> KCNQ1 Protein (Immunocytochemistry): $K_V7.1$, $K_V7.4$, KCNE4 Protein (Western blot): $K_V7.1$, $K_V7.4$, $K_V7.5$, KCNE3, KCNE4	(Joshi *et al.*, 2009; Chadha, Zunke, Davis, *et al.*, 2012; Mondéjar-Parreño *et al.*, 2020)
Renal artery	Rat	Transcript (qPCR): KCNQ1> KCNQ4> KCNQ3> KCNQ5 Protein (immunofluorescence): $K_V7.1$, $K_V7.4$, $K_V7.5$	(Chadha, Zunke, Zhu, *et al.*, 2012; Jepps *et al.*, 2014; Barrese *et al.*, 2020)
Thoracic Aorta	Mouse Rat	Transcript (qPCR): KCNQ4> KCNQ1> KCNQ5> KCNQ3/KCNQ2 Protein (Western blot): $K_V7.1$, $K_V7.4$, $K_V7.5$	(Yeung *et al.*, 2007; Jepps *et al.*, 2011; Oliveras *et al.*, 2014)
Gracilis artery	Rat	Transcript (qPCR): KCNQ4> KCNQ1> KCNQ5> KCNQ3/KCNQ2	(Ma *et al.*, 2020; Zavaritskaya *et al.*, 2020)
Saphenous artery	Rat	Transcript (qPCR): KCNQ4> KCNQ1> KCNQ5> KCNQ3/KCNQ2 Protein (Western blot): $K_V7.4$/KCNE4	(Shvetsova *et al.*, 2019; Ma *et al.*, 2020)

Table 1.3: Arterial K_V7 distribution

A list of the currently identified vascular KCNQ/K_V7 subtypes and the methods used to identify them.

1.5.4.2 Function

Within the vasculature, pan K_V7 channel blockers depolarize rat VSMC RMP (Mackie *et al.*, 2008; Mani *et al.*, 2011) and mediate a rise in base-line tension in both human and rodent arteries (Yeung *et al.*, 2007; Zhong, Harhun, *et al.*, 2010; Ng *et al.*, 2011; Chadha,

Zunke, Zhu, *et al.*, 2012; Lee *et al.*, 2015). Though $K_V7.1$-specific blockers like HMR-1556 or chromanol 293B do not effect base-line tension in rat aorta, mesenteric nor interpulmonary arteries (Chadha, Zunke, Davis, *et al.*, 2012). As no expression of $K_V7.2/K_V7.3$ has been demonstrated within the vasculature, the generally accepted consensus is that $K_V7.4/K_V7.5$ are functionally important regulators of arterial smooth muscle $Vsmc_m$ and that their activity hyperpolarizes the membrane potential negating Ca^{2+} influx by the closure of VGCC. Functional vascular K_V7 channel activity is further evidenced by relaxation of pre-contracted arterial tone in response to several $K_V7.2$-5 channel activators across a number of rodent arteries (Ohya *et al.*, 2003; Yeung *et al.*, 2007; Jepps *et al.*, 2014). Though in contrast to channel inhibitors, activators of $K_V7.1$ including RL-3, Mefenamic acid and ML277 (Chadha, Zunke, Davis, *et al.*, 2012; Baldwin *et al.*, 2020) are effective and reversable relaxants of pre-contracted tone. Indicating that functional $K_V7.1$ channels are present within the vasculature. The role of $K_V7.1$ in the vasculature has remained elusive, however a novel contribution of $K_V7.1$ to PGI_2 IP receptor mediated relaxation is demonstrated within Chapter 6. In addition to regulating the RMP and tone of the vasculature, K_V7 channels are well documented functional end targets in a plethora of receptor mediated responses.

Channel inhibition, PIP_2 depletion, CaM:Ca^{2+} activation and PKC binding

Pre-incubating rodent and murine arteries with pan K_V7 blockers sensitizes vessels to vasoconstriction in response to various constrictors at low concentrations (Yeung *et al.*, 2007; Chadha, Zunke, Zhu, *et al.*, 2012; Chadha *et al.*, 2014). K_V7 channel open probability is thought to increase during receptor mediated depolarisation of the membrane, curtailing receptor contraction by hyperpolarization of the membrane. Although concurrent findings show vasoconstriction in response to vasopressin, endothelin-1 and 5HT suppresses native K_V7 currents rat aortic cell line A7r5 and mesenteric and basilar arteries (Brueggemann *et al.*, 2006; Mackie *et al.*, 2008; Mani *et al.*, 2013; Lioubov I Brueggemann, Mackie, *et al.*, 2014). Activation of $G_{q/11}$ coupled receptors mediates PIP_2 hydrolyzation and an increase in $[Ca^{2+}]_I$, both of which are

shown to impair K_V7.4/7.5 open probability (Zhang *et al.*, 2003; Li *et al.*, 2005; Xu *et al.*, 2013). Depletion of PIP_2 is responsible for Ang-II mediated inhibition of neuronal M-currents (K_V7.2/ K_V7.3; Zaika *et al.*, 2006), initial hypothesis argued for the same regulation of vascular K_V7 channels during receptor mediated contraction. Later, Mackie *et al.*, (2008) suggested that vasopressin mediated inhibition of K_V7.5 in mesenteric artery VSMCs, which was PKC dependent in A7r5 cells (Brueggemann *et al.*, 2006), also occurred via PKC independently of a change in PIP_2. Later, Mani *et al,* (2013) also demonstrated that supplemental PKC activator inhibits K_V7 currents and mediates vasoconstriction in rat basilar arteries (Mani *et al.*, 2013). More recently, within cultured human trachealis smooth muscle cells, PKC mediated suppression of K_V7.5 correlated with increased phosphorylation of the channel and its effects were abrogated by S441 mutation in K_V7.5 C-terminus (Haick *et al.*, 2017), a residue which is absent from K_V7.4 (Brueggemann, Cribbs and Byron, 2020b). Furthermore, supraphysiological concentrations of vasopressin diminished PIP_2 binding of K_V7.5 in A7r5 cells (Brueggemann, Cribbs and Byron, 2020b), which was argued as the underlying mechanism for diminished channel current. Indicating that in these primary cell culture lines, K_V7.5 is the target for PKC mediated K_V7 current suppression, however, PKC can interact with K_V7.4 via a-kinase anchoring protein (AKAP; (Bal *et al.*, 2010)). Moreover, within the heart, chronic Ang-II treatment internalize K_V7.1 via PKC, diminishing channel current (Gou *et al.*, 2021). In isolated murine mesenteric artery VSMCs, Ang-II internalizes K_V7.4 which is targeting for degradation via ubiquitination (Barrese *et al.*, 2018). Though the contribution of PKC to this was not investigated, a role for PKC in K_V7.4 channel internalization is plausible. Though the precise mechanism regarding PKC mediated inhibition of native vascular K_V7 is therefore yet to be described, whether it is diminished interaction of PIP_2 with K_V7.5, or internalization of K_V7.4. What is clear however is that K_V7 channels both functionally negate response to and are key targets during receptor mediated VSMC contraction.

Channel modulation, the products of cAMP

Within the rat, molecular knockdown of *Kcnq4/Kcnq5* and pharmacological blockade has implicated K_V7 as major components of cAMP mediated vasorelaxations including; isoprenaline in renal and mesenteric arteries (Chadha, Zunke, Zhu, *et al.*, 2012; Stott, Povstyan, *et al.*, 2015), adenosine in coronary arteries (Khanamiri *et al.*, 2013; Morales-Cano *et al.*, 2015), CGRP in cerebral arteries (Chadha *et al.*, 2014) and cAMP activator Forskolin in cerebral and renal arteries (Chadha, Zunke, Zhu, *et al.*, 2012; Lee *et al.*, 2015).

PKA is a heterotrimeric holoenzyme that binds cAMP in a 1:4 ratio. Active PKA subsequently phosphorylates serine and threonine residues in targeted substrate proteins (van der Horst, Greenwood and Jepps, 2020). PKA is bound by the aforementioned AKAP, a scaffolding protein which targets PKA to intercellular substrates (Dema *et al.*, 2015). Recently, β-adrenoreceptor stimulation was shown to increase the interaction of $K_V7.4$ and AKAP150 in isolated renal artery VSMCs (Stott, Barrese and Greenwood, 2016). A concurrent study in aortic cell line A7r5 cells revealed no change in $K_V7.4$ phosphorylation by β-adrenoreceptor activation, but did show an increase in $K_V7.5$ phosphorylation (Mani *et al.*, 2016). The reason for this discrepancy is currently unclear, though Mani *et al,* (2016) suggests that it may be a result of a lower number of consensus sites for PKA phosphorylation in $K_V7.4$ compared to $K_V7.5$ (Obenauer, Cantley and Yaffe, 2003). In support of this conjecture, mutation of S53 in the N-terminus of $K_V7.5$ prevented PKA-mediated upregulation of K_V7 derived currents in a primary culture of airway smooth muscle (Brueggemann *et al.*, 2018), a site which is absent from $K_V7.4$. As $K_V7.4/K_V7.5$ heterotetramers are purported to be the most abundant stoichiometry within native VSMCs, the importance of this discrepancy is therefore yet to be determined. Moreover, the mechanism by which PKA increases Linopirdine sensitive currents is also unclear. PKA phosphorylation of $K_V7.1$ increases the binding of PIP_2 to the channel (Lopes *et al.*, 2007). Similarly, Brueggemann *et al*, (2020)

demonstrated that $K_V7.5$ current run down was resistant to PIP_2 depletion after Forskolin mediated phosphorylation of the channel, which they argued was due to increased PIP_2 affinity. An increase in $K_V7.4/K_V7.5$ affinity for PIP_2 would increase channel open probability (Zhang *et al.*, 2003) mediating the aforementioned increase in linopirdine sensitive current in response to Forskolin (Chadha, Zunke, Zhu, *et al.*, 2012).

EPAC, a novel alternate down-stream target of cAMP is known to regulate vascular reactivity by activation of Guanine exchange factor, which targets small Ras-related G-proteins Rap1 and Rap2 (de Rooij *et al.*, 1998). Rap proteins have important cardiovascular effects, including inactivation of RhoA mediated calcium sensitisation (Zieba *et al.*, 2011) and upregulation of BK_{Ca} channel activity (Roberts *et al.*, 2013). Isoprenaline-mediated relaxation of rodent mesenteric arteries is known to be PKA independent (White *et al.*, 2001). Work by our laboratory has recently shown that like BK_{Ca}, within a heterologous over expression system and isolated mesenteric and renal artery myocytes, K_V7 sensitise currents were increased by a synthetic EPAC activator (Stott, Barrese and Greenwood, 2016). Moreover, PKA insensitive β-adrenoreceptor activator-mediated relaxation in mesenteric arteries was attenuated by EPAC inhibitor and pan-K_V7 channel inhibitor Linopirdine but showed no additive attenuation in the presence of both targets, indicating that K_V7 is downstream of EPAC (Stott, Barrese and Greenwood, 2016). Finally, β-adrenoreceptor activator isoprenaline increased $K_V7.4$: Rap1 interaction in isolated mesenteric VSMCs (Stott, Barrese and Greenwood, 2016), collectively demonstrating a novel mechanism for K_V7 activation and alternate intracellular signalling cascades between vascular beds which link K_V7 to the same receptor.

Channel modulation, the products of cGMP

K_V7 channels also contribute to cGMP mediated vasorelaxation. Atrial natriuretic peptide (ANP) activates membrane bound guanylyl cyclase, giving cGMP. Within renal arteries

and aorta, pan-K_V7 channel inhibitor linopirdine attenuates cGMP sensitive ANP mediated relaxation (Stott, Barrese, *et al.*, 2015). Nitric oxide donor S-nitroprusside (SNP) / diethylamine NONOate diethylammonium (DEA-NO) activates soluble guanylyl cyclase similarly giving rise to cGMP/K_V7 channel sensitive relaxations of aorta (Stott, Barrese, *et al.*, 2015), penile (Jepps *et al.*, 2016) and pulmonary (Mondéjar-Parreño *et al.*, 2019) arterial smooth muscle. Although, no role for K_V7 channels was identified in SNP mediated relaxation of rat renal arteries (Stott, Barrese, *et al.*, 2015), indicating a vascular bed specific sensitivity to soluble or membrane bound guanylyl cyclase activation. Moreover, within heterologous expression systems, supplemental cGMP enhanced $K_V7.4$ currents (Stott, Barrese, *et al.*, 2015) and guanylyl cyclase inhibition prevented DEA-NO increase in $K_V7.5$ currents (Mondéjar-Parreño *et al.*, 2019). The mechanism of action of cGMP mediated upregulation of K_V7 channel activity is currently unclear, though appears not to be channel nitrosylation due to cGMP sensitivity (Stott, Barrese, *et al.*, 2015; Mondéjar-Parreño *et al.*, 2019). cGMP activates PKG, which has consensus sites within K_V7 (Mondéjar-Parreño *et al.*, 2019), however high concentration of cGMP can activate PKA (Sausbier *et al.*, 2000), which as discussed at length above, can activate K_V7. Though the current mechanism and reason for vascular bed discrepancy in cGMP mediated K_V7 channel activation is unclear, both $K_V7.4$ and $K_V7.5$ channels appear to be targets for cGMP mediated relaxation.

Auxiliary subunit regulation

Within rat mesenteric VSMCs, $K_V7.4$ exists in close proximity with KCNE4 (Jepps *et al.*, 2015). Transfection with morpholinos targeted to *Kcne4* leads to a decreased membrane population of $K_V7.4$, a depolarized membrane potential and increased sensitivity to vasoconstrictors in male Wistar arteries (Jepps *et al.*, 2015). Additionally, co-expression of *KCNE4* and *KCNQ4* in heterologous expression system enhanced $K_V7.4$ membrane abundance and significantly enhanced K_V7 current properties (Jepps *et al.*, 2015). $K_V7.4$ is similarly dependent on KCNE4 within murine arteries (Abbott and Jepps, 2016). Providing evidence for a positive contribution of *Kcne4* to vascular K_V7 function. Little is

known of the other *Kcne* subtypes within the vasculature. Previous reports demonstrate *Kcne3* and *Kcne5* expression in addition to *Kcne4*, though Kcne3 negatively and Kcne5 positively regulated $K_V7.4$ currents, see (Jepps, 2017) for review.

More recent work has identified a novel ancillary subunit that associated with $K_V7.4$ within isolated rat renal and mesenteric artery VSMCs, sodium myoinositol transporter 1 (SMIT-1; Barrese *et al.*, 2020). SMIT-1 transports myo-inositol, a PIP_2 pre-cursor into the cell. Interestingly, direct functional interaction with $K_V7.4$/$K_V7.5$ is purported to regulate channel activity in addition to the generation of positive allosteric regulators of the channel (Barrese *et al.*, 2020). SMIT1 also couples to $K_V7.1$ (Abbott *et al.*, 2014) and $K_V7.2$/$K_V7.3$ (Manville, Neverisky and Abbott, 2017) in neurons and heterologous expression system and has led to the term 'Chansporter.' The novel and expanding field of research regarding ion channel regulation by auxiliary subunit proteins adds yet another lay of complexity to ion channel regulation across the body, which we are only beginning to understand.

1.5.4.3 K_V7 channels and hypertension

$K_V7.4$ channels are downregulated in primary and secondary of hypertension (Jepps *et al.*, 2011; Chadha, Zunke, Zhu, *et al.*, 2012; Stott, Barrese, *et al.*, 2015; Carr *et al.*, 2016; Barrese *et al.*, 2018) and are implicated in the hypertensive phenotype. SHRs present with an increased sensitivity to vasoconstrictors and a reduced sensitivity to both vasodilators and K_V7 channels activators (Jepps *et al.*, 2011; Chadha, Zunke, Zhu, *et al.*, 2012; Stott, Barrese, *et al.*, 2015), corresponding with a post-translational decrease in $K_V7.4$ protein abundance in renal and mesenteric arteries (Jepps *et al.*, 2011). Downregulation of $K_V7.4$ channels during hypertension is likely to underpin impaired β-adrenoreceptor mediated vasorelaxation within the renal arteries (Chadha, Zunke, Zhu, *et al.*, 2012) as well as natriuretic peptide/SNP mediated vasorelaxation in the renal artery and aorta (Stott, Barrese, *et al.*, 2015).

Carr et al (2016) showed a significant correlation between the upregulation of micro-RNA 153 (miR153) and diminished expression of $K_V7.4$ proteins in the SHRs (Carr *et al.*, 2016). Micro-RNA molecules are short 20-nucleotide sequences that target the 3'-untranslated region (UTR) of a sequence causing the degradation of a transcript or inhibition of protein synthesis. miR153 has been identified as having consensus sequence for KCNQ4 3'UTR. Carr et al (2016) postulated that a rise in miR153 underpinned the observed difference in $K_V7.4$ abundance between NT and SHRs. In support of this theory, overnight incubation in supplemental miR153 replicated the hypertensive phenotype in arteries harvested from NT animals (Carr *et al.*, 2016). No increase miR153 was seen in cerebral arteries taken from SHRs, where K_V7 channel abundance and function is shown to be preserved (Carr *et al.*, 2016). Recent investigations by Barrese *et al* (2018) revealed that in Ang-II infused mice, the interaction between heat shock protein 90 (HSP90) and K_V7 channels was dysregulated, disabling protein stability and promoting degradation through ubiquitination via interaction with the E3 ubiquitin ligase C-terminus of Heat-shock protein 70 (HSP70; Barrese *et al.*, 2018). This pathway promoted channel internalization and degradation at the proteosome and further, prevented forward trafficking and folding by diminished interaction with HSP90 (Barrese *et al.*, 2018). These insights provided, for the first time, a mechanism for the diminished K_V7 function and expression previously reported by Jepps *et al,* (2011) in both primary (Carr *et al.*, 2016) and secondary (Barrese *et al.*, 2018) hypertension.

By contrast, K_V7 channel function is upregulated in rat models of pulmonary artery hypertension (PAH) induced by prolonged exposure to hypoxia (Mondéjar-Parreño *et al.*, 2020). This paradoxical observation revealed an increase in contribution of K_V7 channels to gross whole-cell K^+ currents and an increased sensitivity to K_V7 channel modulator mediated change in arterial tone (Mondéjar-Parreño *et al.*, 2020). Interestingly, this was associated with an increase in β-auxiliary subunit protein KCNE4 within arteries taken from rat models of PAH when compared to arteries from NT animals, which was argued

to account for the increase in K_V7 channel function (Mondéjar-Parreño *et al.*, 2020), ultimately compensating for diminished $K_V1.5$ and TASK-1 channel expression/function (Mondéjar-Parreño *et al.*, 2020). The role of K_V7 in vascular disease has been established over the past decade, however, is still an incompletely understood phenomenon which warrants further investigation.

1.5.5 Extravascular K_V7 channels

1.5.5.1 Cardiac

$K_V7.1$ in association with β-auxiliary subunit protein KCNE1 is the correlate of the slow component of the delayed-rectifier K^+ current (I_{Ks}) of the cardiac action potential (Sanguinetti *et al.*, 1996). $K_V7.1$/KCNE1 gives a slowly activating delayed rectifier current that is active at negative potentials, though also strongly activates during the plateau phase of the cardiac action potential, repolarizing the heart. The rate of activation of $K_V7.1$/KCNE1 determines action potential pacing. During β-adrenoreceptor mediated sympathetic nerve stimulation, upregulated I_{Ks} shortens the cardiac action potential to allow for greater diastolic filing time between beats and is represented by a shortening of the QT interval during ECG. $K_V7.1$/KCNE1 is a downstream target of β-adrenoreceptor signalling via cAMP/PKA dependent pathways (Walsh and Kass, 1988, 1991). AKAP9 (Yotiao) is an essential scaffolding protein which associates $K_V7.1$/KCNE1 complexes via leucine zipper motif (Marx *et al.*, 2002). Yotiao targets PKA and protein phosphatase 1 (PP1) to the C-terminal domain of $K_V7.1$ (Marx *et al.*, 2002). Yotiao facilitates PKA phosphorylation of $K_V7.1$ N-terminus (Walsh and Kass, 1988, 1991; Marx *et al.*, 2002) and PP1 prevents cAMP degradation, maintaining stimulation of $K_V7.1$ (Marx *et al.*, 2002) increasing I_{Ks} currents shorten QT. Mutations of *KCNQ1* have been identified as a heritable factor that contributes to long QT syndrome (Chen *et al.*, 2007; Qureshi *et al.*, 2013), an arrhythmogenic disease that can lead to sudden cardiac death. Of which, Romano-Ward syndrome is the most common heritable form and is accounted for by 300 different loss of function mutations within KCNQ1 (Splawski *et al.*, 2000; Peroz *et*

al., 2008). Loss of function mutations commonly dysregulate voltage-sensitivity, PIP_2 binding, forward trafficking of the channel, aberrant channel assembly, or diminished PKA interaction amongst others (Barrese, Stott and Greenwood, 2018) and account for roughly 40% of hereditary long-QT syndromes (Shimizu and Horie, 2011). Moreover, gain of function mutations of *KCNQ1* underpin hereditary short-QT syndrome, which is characterized by truncated cardiac action potentials giving rise to atrial fibrillation (Restier, Cheng and Sanguinetti, 2008).

The role for $K_V7.1$/KCNE1 and their respective I_{Ks} current is well established within the literature, however novel findings also demonstrate $K_V7.4$ expression within cardiac myocyte ventricular mitochondria (Testai *et al.*, 2016). Where activation of the channel is proposed to protect cardiac myocytes from ischemia induced cell death, highlighting a potential role for $K_V7.4$ in protection against reperfusion injury (Testai *et al.*, 2016).

1.5.5.2 Epithelial

Throughout the body, essential roles for $K_V7.1$/KCNE complexes have been demonstrated within an array of epithelial tissue, including the stomach acid producing (parietal; Grahammer *et al.*, 2001a) and distal colonic (Diener *et al.*, 1996; Suessbrich *et al.*, 1996; Schroeder, Waldegger, *et al.*, 2000; O'Mahony *et al.*, 2007, 2009; Alzamora *et al.*, 2011; Rapetti-Mauss *et al.*, 2013) cells of the gastrointestinal tract, the proximal tubule (Vallon *et al.*, 2001, 2005) of the nephron, the follicular cells (Fröhlich *et al.*, 2011; Purtell *et al.*, 2012) of the thyroid gland, areolar (Trinh *et al.*, 2007), trachea (Florian Grahammer *et al.*, 2001) and airway epithelial cells (Mall *et al.*, 2000; Hynes and Harvey, 2019) of the lungs and β-pancreatic cells (Yasuda *et al.*, 2008) of the islets of Langerhans. Within these tissues, the activity of K_V7 channels hyperpolarizes the membrane and establishes electrochemical gradients that facilitate the movement of other ions including Cl^- for the purposes of fluid reuptake, H^+ secretion for the generation of stomach acid, the release of insulin and the production of thyroid hormones. Loss of function mutations within *KCNQ1* are associated with type 2 diabetes mellitus (Unoki *et*

al., 2008; Yasuda *et al.*, 2008) and hypothyroidism within a knockout mouse model (Fröhlich *et al.*, 2011).

1.5.5.3 Neuronal

K_V7.2/7.3 are the molecular correlates of the neuronal M-current (Brown and Adams, 1980; Wang *et al.*, 1998), and are principally regarded as the 'neuronal K_V7 channels.' Though this is erroneous, as K_V7.5 readily forms heterotetramers with K_V7.3 within the central and systemic nervous system (Lerche *et al.*, 2000), K_V7.2/7.3 are the predominant heteromeric structure within the nervous system. Moreover, though K_V7.4 is not present in sensory and peripheral neurons, it is present within dopaminergic (mesolimbic and substantia nigra) and serotonergic neurons of the dorsal raphe (Hansen *et al.*, 2008; Barrese, Stott and Greenwood, 2018). Within the peripheral nervous system, K_V7 channels are targeted to key areas of the nerve where their activity maintains the resting membrane potential and hampers action potential firing. K_V7.2/7.3 channels are inhibited by $G_{q/11}$ coupled receptor signalling including acetylcholine (M1,3,5) and bradykinin receptors potentiating action potential firing (Brown and Selyanko, 1985). K_V7.2 channel inhibition is purportedly mediated via PKC-phosphorylation, which is dependent on AKAP79/150 scaffolding protein (Hoshi *et al.*, 2003; Zhang and Shapiro, 2012). Conversely, K_V7.2/7.3 channels are upregulated by PKA-mediated phosphorylation of Ser52 in K_V7.2 channel N-terminus (Schroeder, Waldegger, *et al.*, 2000) and Ser438/Ser455 in K_V7.2 channel C-terminus (Salzer *et al.*, 2017), via AKAP79/150 (Hoshi *et al.*, 2003; Zhang and Shapiro, 2012) giving rise to neuronal quiescence. Similar to the principals listed above for arterial K_V7.4 regulation during receptor mediated signalling, phosphorylation of K_v7.2 regulates its affinity for PIP_2 as a means of determining channel activity (Salzer *et al.*, 2017; van der Horst, Greenwood and Jepps, 2020). Mutations to *KCNQ2-3* can give rise to a host of encephalopathies including benign neonatal familial convulsions (Cooper *et al.*, 2000; Robinson and Gardiner, 2000) and neonatal epileptic encephalopathy (Miceli *et al.*, 1993) as well as

age-related impairment of memory, psychiatric disorders and ischemic brain injuries (Barrese, Stott and Greenwood, 2018).

Though $K_V7.1$ is not present within the nervous system, both $K_V7.1$ and $K_V7.4$ are expressed in the stria vascularis of the cochlear and contribute to hearing via secretion of K^+ into the endolymph (Neyroud *et al.*, 1997; Kubisch *et al.*, 1999). The establishment of a high K^+ gradient within the endolymph is essential for signal transduction at the hair cells, and thus hearing. *KCNQ4* mutations are attributed to heritable dominant deafness (Kubisch *et al.*, 1999). Moreover, mutations in *KCNQ1* genes are linked to autosomal recessive Jervell and Lang-Nielsen syndrome, a disease of both the cardiovascular and auditory system responsible for the generation of bilateral deafness and long QT syndrome (Splawski *et al.*, 2000; Peroz *et al.*, 2008).

1.5.5.4 Non-vascular smooth muscle

In addition to arterial smooth muscle, K_v7 channels are expressed and functionally active in visceral smooth muscle including gastrointestinal, bladder, corpus cavernosum, uterine and airway smooth muscle. Briefly, within spontaneously contracting smooth muscles including gastrointestinal (Jepps *et al.*, 2009; Ipavec *et al.*, 2011) myometrium (McCallum, Greenwood and Tribe, 2008; McCallum *et al.*, 2011) and detrusor (Svalø *et al.*, 2012, 2015), pharmacological activation of K_V7 channels causes quiescence and inhibition of the channel increases the rate and amplitude of phasic contractions. By contrast, in quiescent smooth muscle including corpus cavernosum, inhibition of K_V7 channels causes an increase in intracellular $[Ca^{2+}]_I$ and K_V7 channel activators produces marked hyperpolarization of isolated smooth muscle cells (Jepps *et al.*, 2009). Similarly, inhibition of K_V7 channels contracts bronchial smooth muscle (Brueggemann *et al.*, 2012) and K_V7 channel activators are effective relaxants of pre-contracted pulmonary airway smooth muscle tone (Lioubov I Brueggemann, Haick, *et al.*, 2014). Moreover, Ser52 of $K_V7.5$ N-terminus is the target of β-adrenoreceptor mediated relaxation of airway smooth

muscle during cAMP-PKA mediated responses (Brueggemann *et al.*, 2018) which increases PIP_2 affinity (Brueggemann, Cribbs and Byron, 2020b).

Though the literature on these smooth muscles is limited when compared to arterial K_V7s, these channels clearly play a role in regulating basal and receptor mediated responses. Additionally, therapeutic potential for targeting these channels has been implicated in overactive bladder (Svalø *et al.*, 2012), erectile dysfunction (Jepps *et al.*, 2009) and as novel bronchodilators (Lioubov I Brueggemann, Haick, *et al.*, 2014).

1.6 Sex, CVS and CVD

Sexual dimorphisms in cardiovascular physiology and pathophysiology are a well-documented phenomenon (Pabbidi *et al.*, 2018). Within the following section, a brief overview of the literature regarding sexual dimorphisms in vascular biology will be given, followed by the current understanding of sex-dependent differences in K_V7 channel function.

1.6.1 Sexual dimorphisms in cardiovascular physiology

Numerable reports demonstrate that BP is lower in healthy women when compared to men (Gaffey *et al.*, 2021), indicative of sex-dependent differences in normal vascular function. Consistent with that postulation, Hitesh *et al* (2014) demonstrated in a population of young healthy adults, that women have smaller coronary arteries when compared to men (Hiteshi *et al.*, 2014). Further, women express greater coronary (Patel *et al.*, 2016) and cerebral (Liu, Lou and Ma, 2016) blood flow when compared to men. Greater end organ blood flow in women is attributed to increased shear stress along the endothelium, giving rise to enhanced flow via upregulated generation and release of NO, PGI_2 and EDH. Indeed, flow mediated dilatation is greater in brachial arteries from women when compared to age-matched men (Black *et al.*, 2009; Skaug *et al.*, 2013). Within animal models, basic pre-clinical scientific research has also identified an array

of molecular components which give rise to sex differences in vascular reactivity which can be split roughly into endothelium and non-endothelium derived and will be briefly discussed here.

1.6.1.1 Endothelium derived sex differences in vascular reactivity

As above, shear stress and flow mediated dilatation is greater within women when compared to males. The underlying mechanism may well be related to structural differences in wall structure, however, NO production in response to acetylcholine is reportedly higher in aortas from female rats when compared to males (Kauser and Rubanyi, 1997) in a process attributed to oestrogen mediated upregulation of eNOS. Similarly, PGI_2 production in response to vasopressin is also enhanced by oestrogen within female rats, and is greater when compared to males (Deer and Stallone, 2016). The effects of sex-hormones on vascular reactivity will be discussed in greater detail below. Soluble hydroxylase enzyme, an enzyme responsible for the breakdown of epoxyeicosatrienoic acid, a vasodilatory mediator produced by the breakdown of arachidonic acid during receptor mediated endothelium derived relaxation, is expressed to a smaller degree within ECs from female animals when compared to males (Qin *et al.*, 2015). Moreover, ECs from female animals also generate less superoxide anions when compared to males (Brandes and Mügge, 1997). The bulk of the current literature, however, describes sex-dependent differences in EDH contribution to EC function. Scotland *et al*,. (2005) demonstrated clear EDH signalling within female mice of a eNOS/COX knock-out model, which was absent from male animals. These findings were later repeated in swine coronary (Wong, Roberts and Randall, 2014), rat mesenteric (Zhang *et al.*, 2012) and murine femoral (Luksha *et al.*, 2006) arteries. The aggregated findings make clear that the endothelium from the female, by contrast to the male, favours vasodilatory signalling cascades. This in addition to the structural differences detailed above and a differential dependence on EDH rather than NO are proposed to underpin known differences in flow and shear stress mediated vasodilatation.

1.6.1.2 Endothelium independent sex differences in vascular reactivity

By contrast to the endothelium, sex differences in VSMCs themselves has been a secondary consideration within the literature, however, phenylephrine and KCl mediated contraction within rat aorta (Crews and Khalil, 1999b), Ang-II mediated contraction of middle cerebral arteries (De Silva *et al.*, 2009) and pressure induced contraction of cerebral arterioles (Wellman *et al.*, 1996) are smaller within female rats when compared to males. Further, Crews and Khalil (1999b) also demonstrated reduced receptor mediated increases in $[Ca^{2+}]_i$ when comparing aortas from females to males. These findings coincide with reduced VGCC current in VSMCs isolated from female swine coronary arteries compared with males (Bowles *et al.*, 2004). Sex-dependent differences in voltage-gated calcium currents are potentially underpinned by oestrogen mediated increase in Cav1β (Tharp *et al.*, 2014), which is known to downregulate Ca^{2+} currents. In addition, sex differences in VSMC calcium homeostasis and receptor mediated signalling intermediates are also evident and may contribute to diminished contraction within female arteries. For example, Sarcoplasmic reticulum Ca^{2+} ATPase, which stores $[Ca^{2+}]_I$ in the SR, is prospectively more active (Loukotová, Kunes and Zicha, 2002), Orai1/STIM1 is less active (Giachini *et al.*, 2012) and PKC (Kanashiro and Khalil, 1998) and Rho Kinase (Chrissobolis *et al.*, 2004) are less expressed within vascular myocytes from female arteries, diminishing receptor mediated contraction. Finally, sexual dimorphisms in K^+ channel activity where shown by Yang *et al*,. (2007) within swine coronary artery VSMCs, wherein outward K^+ currents were greater in cells from female pigs when compared to males. These findings were recently developed upon by (Reed *et al.*, 2020), where BK_{Ca} and K_V sensitive currents were greater were observed within isolated VSMCs from middle cerebral arteries from female rats when compared to males. Similar to the work described above within the endothelium, female vascular myocytes appear to favour factors that oppose vasoconstriction by comparison to males.

1.6.2 Sexual dimorphisms in cardiovascular pathophysiology

As described at the start of this chapter, hypertension is the key risk factor in the development of CVD. Yet, pre-menopausal women express an enigmatic cardioprotective factor or factors that differentiates the prevalence of CVD between young women compared to age matched men and post-menopausal women (Tunstall-Pedoe *et al.*, 1994; Usselman, Stachenfeld and Bender, 2016). In conjunction, female SHRs and female Ang-II infused mice express a smaller increases in systemic BP when compared to males (Reckelhoff, Zhang and Granger, 1998; Maris *et al.*, 2005; Tiwari *et al.*, 2010; Bubb, Khambata and Ahluwalia, 2012). There is large debate however regarding the factors that drive such significant differences. As described above, many studies show clear sex-dependent differences in the production of vasoregulatory molecules from the endothelium (Chan *et al.*, 2012; Ahmad, Randall and Roberts, 2017b, 2017a) and vascular ion channel activity (Pabbidi *et al.*, 2018), which all represent possible contributory factors.

1.6.3 The vascular effects of sex hormones and their receptors

The prime candidates for sex dependent differences in any system are typically sex hormones, predominantly, oestrogen, progesterone, and testosterone. Sex hormones fluctuate throughout the course of the oestrus (rodent) and menstrual (human) cycles. A direct comparison between rodent and human cycles is difficult, the rodent oestrus cycle last only 4-5 day and is split into four stages (Pro-oestrus, Oestrus, Met-oestrus and Di-oestrus), by comparison the human cycle last roughly 28 days and has two primary phases (follicular and luteal), followed by menses, see a diagrammatic representation of human and rodent reproductive cycles in Figure 1.5. Further, each of the listed sex hormones has beneficial and detrimental attributes associated with them, which makes for a complicated outlook on sex-hormone mediated vascular effects. Within the following section, a brief overview of the vascular effects of sex hormones and their receptors will be given

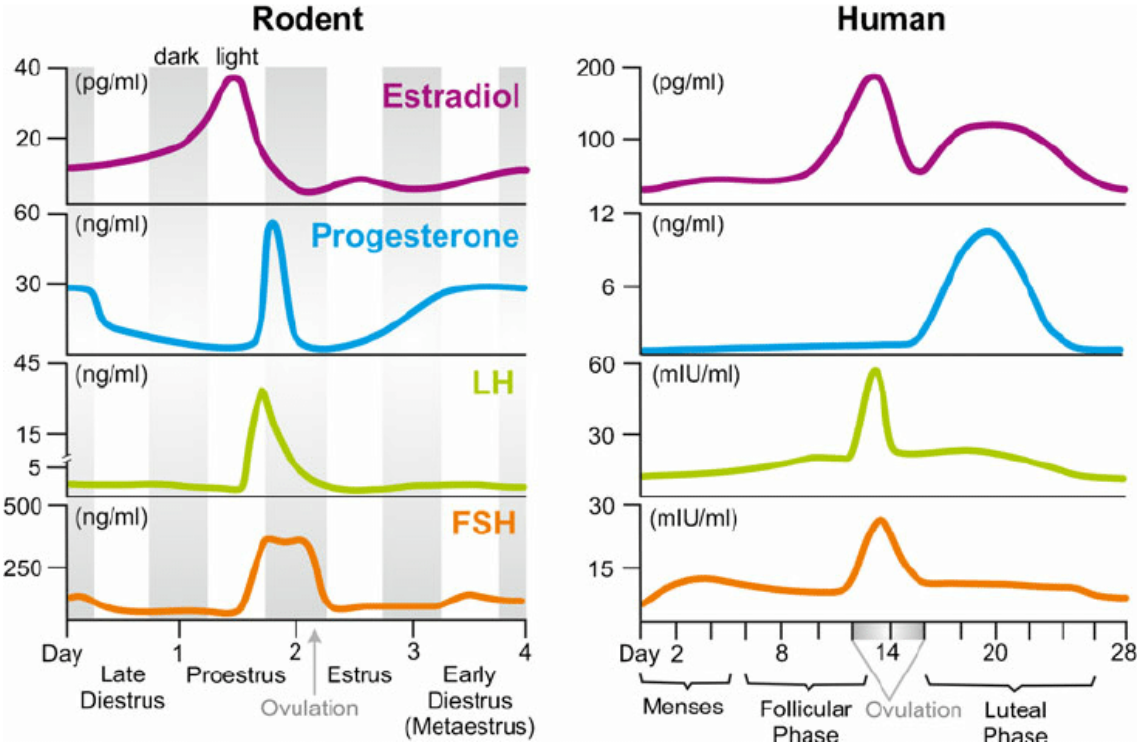

Figure 1.5 Diagrammatic representation of the rodent and human reproductive cycles

Diagrammatic representation of average fluctuating levels of circulating sex-hormones including; 1.) Oestradiol, pg/mL; 2.) Progesterone, ng/mL; 3.) Luteinising hormone (LH), ng/mL; 4.) Follicular stimulating hormone (FSH), ng/mL, in rodents (left) and humans (right). Figure taken from (Donner and Lowry, 2013).

1.6.3.1 An overview on sex-hormone mediated vascular effects

Initial hypothesis attributed the increase in BP post-menopause to the absence of oestrogen. In the late 1970's, ovariectomy SHR models mimicked the sharp increase in BP seen in the male and was inversed by pre-treatment with oestrogen (Iams and Wexler, 1979), supporting this hypothesis. Although several studies have since observed no difference in mean BP between the control (SHAM) and ovariectomy female SHR models (Reckelhoff, Zhang and Granger, 1998; Maris *et al.*, 2005). These conflicting results have similarly been demonstrated within humans, wherein during the hormone replacement therapy (HRT) trail, Estrogen/Progestin in the Heart and estrogen/progestin replacement study (HERS) I (Hulley *et al.*, 1998) and II (Hulley *et al.*, 2002) adverse cardiovascular events increased within women taking supplemental oestrogen. Adverse cardiovascular effects observed in women taking supplemental hormones has also

recently been recorded in a study of post-menopausal women who, upon receiving conjugated equine oestrogen, expressed an 18.8% increase in the prevalence of hypertension when compared to placebo control (Swica *et al.*, 2018). These findings contradicted initial animal and human studies on HRT prior to the HERS which had positive outcomes (Yang and Reckelhoff, 2011). Subsequent studies argued that, if prescribed at the 'right' time following menopause, oestrogen has been shown to reduce the prevalence of CVD (Karim *et al.*, 2005; Usselman, Stachenfeld and Bender, 2016), though the factors required to see a positive outcome are elusive.

Progesterone has historically been second thought of in consideration to oestrogen. That being said, progesterone has been identified as a natriuretic (Landau and Lugibihl, 1958), depressor of response to Ang-II in rats and humans (Gant *et al.*, 1973; Nakamura *et al.*, 1988), depressor of the norepinephrine response in Sprague-Daley rats (Barbagallo *et al.*, 2001), decreases the production of endothelin-1 (Morey *et al.*, 1998), relaxes precontracted arterial tone (Crews and Khalil, 1999a; Barbagallo *et al.*, 2001) and reduces blood pressure in ovariectomy models of rodent, which oestrogen did not (Nakamura *et al.*, 1988). Though not all reports are in agreement, Novak & Kaufman found no differences to pressor response to Ang-II in pregnant mice model wherein progesterone is consistently high (Novak and Kaufman, 2017).

The literature regarding impact of testosterone is also conflicting. Within animal models, testosterone mediates vasorelaxation in rabbit aorta and coronary arteries (Yue *et al.*, 1995), reduction in the size of myocardial infarction in rat models (Er *et al.*, 2004) by stabilizing the mitochondrial membrane potential preventing depolarization during reperfusion of the heart (Di Lisa and Bernardi, 2006) and protection against metabolic syndrome (Filippi *et al.*, 2009). Within humans, the concentration of testosterone within the blood is inversely correlated with mortality (Laughlin, Barrett-Connor and Bergstrom, 2008). Testosterone has conversely been implicated in myocardial-inflammation

(Crisostomo *et al.*, 2006) and augmenting contractions to 5-HT in rat thoracic aorta (Ammar, Said and Hassan, 2004).

Within the studies detailed above, the receptors responsible for the vascular effects of each hormone were largely unspecified. Within following section, a brief description of the distribution and function of the known sex-hormone receptors and their specific impact on vascular function will be described.

1.6.3.2 Oestrogen

The bioactive form of oestrogen, 17-β Oestradiol (E2), is synthesized in a two-cell one hormone process within the theca and granulosa cells of the ovaries. E2 is also produced within the adrenal glands and locally within the vasculature by aromatase enzymes. Via oestrogen receptors (ERs), E2 mediates both genomic and fast acting non-genomic vascular effects through nuclear and membrane bound receptors.

Oestrogen receptors α/β

The first ERs to be described were ERα/ERβ, which are canonically considered cytoplasmic nuclear receptors which dimerize upon binding E2 forming homo/hetromers which translocate to the nucleus. Active nuclear ERs bind oestrogen response elements within the genome and regulate transcription (Matsuda *et al.*, 2002; Caroccia *et al.*, 2016). E2 also exerts rapid non-genomic effects that derive from membrane bound ERα/β (Razandi *et al.*, 1999). Upon activation, membrane bound ERs evoke myriad intracellular signalling cascades attributed to mitogen activated protein kinase (MAPK)/extracellular signal- regulated kinases (ERK), serine and threonine kinases, PI3K, and cAMP (Traupe *et al.*, 2007; Meyer *et al.*, 2009; Ronda, Buitrago and Boland, 2010; Connelly *et al.*, 2021). Within the vasculature, both ERα and ERβ are present within the plasma membrane, cytosol and nucleus of ECs and VSMCs (Caroccia *et al.*, 2016). ERα activation upregulates eNOS synthesis within the endothelium and promotes

vasodilatation and angiogenesis (Klinge *et al.*, 2005; Traupe *et al.*, 2007; Meyer *et al.*, 2009). In contrast ERβ mediated eNOS independent, EDH sensitive relaxation of coronary arteries (Traupe *et al.*, 2007). The role of ERs in regulating ion channels however is less clear and is discussed in greater length within Chapter 4.4.2.

Novel G-protein coupled Oestrogen receptor

Novel g-protein coupled Oestrogen receptor (GPER1), initially designated GPR30, is expressed in an array of animal and human arteries (Haas *et al.*, 2007). GPER1 is present within the membrane of SR, the golgi apparatus and the plasma membrane of both VSMCs and ECs (Caroccia *et al.*, 2016). Activators of the receptor dilate human, rodent and porcine arteries (Haas *et al.*, 2007, 2009; Meyer *et al.*, 2010) in endothelium dependent (Broughton, Miller and Sobey, 2010; Meyer *et al.*, 2010) and independent (X. Yu *et al.*, 2011) cascades, attenuate receptor mediated contraction independent of a change of intracellular VSMC $[Ca^{2+}]_i$ (Haas *et al.*, 2007; Meyer *et al.*, 2010) and reduce BP in rats (Haas *et al.*, 2009) and ovariectomized mice (Lindsey *et al.*, 2009). Moreover, deletion of *Gper1* enhances endothelin-1 mediated contraction in mice when compared to wild-type control (Meyer *et al.*, 2012), and a hypo-functioning variant of *GPER1* in humans is associated with raised BP (Feldman *et al.*, 2014). GPER1 activation mediates PI3K derived intracellular calcium mobilization and cAMP production (Rubio-Gayosso *et al.*, 2000; Filardo *et al.*, 2002; Revankar *et al.*, 2005; Lin and Smrcka, 2011; Gaudet *et al.*, 2015), eNOS upregulation (Lindsey, Liu and Chappell, 2014) and PKA mediated MLCP activation (Yu *et al.*, 2014). Although conflicting reports also demonstrate GPER1 mediated contraction of renal arteries via a slew of kinase molecules including PKC (Kurt and Buyukafsar, 2013). GPER1 signalling is further complicated by receptor crosstalk. GPER1 mediated Ca^{2+} mobilization is dependent on transactivation of epidermal growth-factor (Filardo *et al.*, 2002; Thomas *et al.*, 2005). Though aldosterone cannot bind GPER1 (Cheng *et al.*, 2014), aldosterone mediates GPER1 sensitive vasodilatation (Gros *et al.*, 2011, 2013) and enhances Ang-II (Batenburg, Jansen and Bogaerdt, 2012)

and phenylephrine mediated contraction (Ferreira *et al.*, 2015). Current understanding indicates that aldosterone mediated GPER1 sensitive vascular effects may be derived from cross talk with mineralocorticoid receptors (Barton and Meyer, 2015).

1.6.3.3 Progesterone

Progesterone is a steroidal hormone produced within the adrenal cortex, gonads and within the corpus luteum of the pregnant rat. Its receptors have been found within both ECs and VSMCs of rats, mice and humans (Goletiani, Keith and Gorsky, 2007). Comparable to E2, the literature on progesterone within the vasculature is sparce, though can be broken down into nuclear and non-nuclear signalling. Like E2, progesterone binds two distinct cytoplasmic nuclear receptors termed progesterone receptor (PR) A/B which are derived from a single gene. Upon binding progesterone the receptors dimerize, forming homo/hetromers which translocate to the nucleus and bind progesterone response elements, which subsequently regulates gene transcription (Conneely *et al.*, 2002; Leonhardt, Boonyaratanakornkit and Edwards, 2003). Moreover, a novel class of membrane bound progesterone receptors (mPR) have also been discovered and include three subtypes α, β and γ. The activation of mPR is associated with $G_{\alpha i}$ and a decrease in cAMP as well as the activation of MAPKs, ERK1/2 and JNK1/2 (Zhu, Bond and Thomas, 2003; Karteris *et al.*, 2006; dos Santos *et al.*, 2014). Studies have argued for progesterone mediated genomic (Simoncini *et al.*, 2004) and non-genomic changes (Selles *et al.*, 2001; Simoncini *et al.*, 2004; Pang, Dong and Thomas, 2015) in the abundance of eNOS in ECs and an increase in oxidative stress (Wassmann, Wassmann and Nickenig, 2005) and the expression of AT_1R transcripts within cultured VSMCs (Nickenig *et al.*, 2000), however these findings, and the vascular effects of progesterone listed above, do not differentiate between receptors.

1.6.3.3 Testosterone

Testosterone, and its more potent analogue di-hydro testosterone are produced within the gonads and adrenal glands of both sexes. Like E2 and progesterone, testosterone activates both nuclear and membrane bound androgen receptors (ARs). Classic ARs include two isoforms, A/B, which are cytosolic nuclear transcription factors that dimerise and translocate to the nucleus and bind androgen response elements, mediating a change in gene transcription (Connelly *et al.*, 2021). Recently, a novel class of testosterone activated GPCRs have been discovered (Shihan, Bulldan and Scheiner-Bobis, 2014; Lorigo *et al.*, 2020), in addition to membrane associated nuclear ARs. Upon binding testosterone, activated membrane associated nuclear, and membrane bound G-protein coupled ARs undergo a conformational change in shape, and can mediated rapid non-genomic effects associated with the activation of PKC, PKA, MAPK, cAMP, ERK and PKG (Shihan, Bulldan and Scheiner-Bobis, 2014; Lorigo *et al.*, 2020; Connelly *et al.*, 2021). ARs are expressed within both VSMCs and ECs (Connelly *et al.*, 2021). Though testosterone can locally be converted to E2 via aromatase enzyme activity, several studies have demonstrated fast-acting non-genomic vasorelaxation in response to Testosterone in the presence of aromatase enzyme inhibition (Lorigo *et al.*, 2020). During fast acting non-genomic signalling via membrane receptors, testosterone mediates vasorelaxation in an array of arteries. Testosterone mediated relaxation is both endothelium dependent and endothelium independent, via processes including upregulation of eNOS activity and NO bioavailability (Yu *et al.*, 2012) or the inactivation of Ca^{2+} channels and activation of K_V/BK_{Ca} channels (Yue *et al.*, 1995; Ding and Stallone, 2001; Tep-areenan, Kendall and Randall, 2002; Hall *et al.*, 2006; Cairrão *et al.*, 2008; Lorigo *et al.*, 2020), depending on experimental model. Conversely, non-genomic AR signalling is also proposed to mediated contraction through activation of non-specific cation channels in an as of yet undescribed process (Lorigo *et al.*, 2020). In addition, the genomic effects of testosterone are thought to include a shift in the expression of

angiotensin converting enzyme and AT_1R, promoting vasoconstriction (Te Riet *et al.*, 2015; Mishra *et al.*, 2019).

1.6.4 Sex and K_V7 channels

The effects of sex hormones in the vasculature are diverse and inchoate, however the impact of sex hormones on K_V7 channels is forming. Busch *et al,* (1996) demonstrated supraphysiological concentrations of E2 (1µmol-L^{-1}) mediated I_{Ks} channel inhibition in heterologous expression system (Busch *et al.*, 1996). Later, more thorough investigations revealed E2 inhibition of $K_V7.1$ derived currents in rat distal colic crypt cells in a PKC- δ dependent manner independent of the classical Oestrogen receptors (O'Mahony *et al.*, 2007). Later work by the same laboratory demonstrated that basolateral currents responsible for Cl^- secretion known to be derived from $K_V7.1$/KCNE3 complexes are inhibited by E2 via dissociation of $K_V7.1$/KCNE3 (Alzamora *et al.*, 2011). Moreover, in HT29cl.19A cells, E2 abrogated $K_V7.1$ membrane expression through PKC-δ dependent channel endocytosis into early endosomes, which is then recycled to the membrane (Rapetti-Mauss *et al.*, 2013). Taken as a collective, the aforementioned studies provide strong evidence of Oestrogenic K_V7 channel regulation.

Nothing is known about the impact of progesterone on K_V7 channels, vascular or otherwise. In mouse myometrial tissue, cycle dependent upregulation in the total copy number for *Kcnq1, Kcnq5* and *Kcne1* has been demonstrated (McCallum, Greenwood and Tribe, 2009), with progesterone production from the corpus luteum hypothesized as being responsible. In male's, testosterone increases the relative expression of *Kcnq1* in cardiomyocytes (Masuda *et al.*, 2018). This has been postulated to underpin testosterone mediated short QT intervals (Masuda *et al.*, 2018).

Despite the known impact of sex on cardiovascular health and sex-hormone mediated channel regulation in extravascular tissue, the current literature regarding sex-impact on vascular K_V7 channels is comparatively limited. In one of the few studies to consider sex

as a factor, Abbott and Jepps revealed that deletion of *Kcne4* sex-dependently altered vascular reactivity (Abbott and Jepps, 2016). Whereby male *Kcne4-/-* knockout mouse model showed an increased sensitivity to the vasoconstrictor methoxamine and decreased sensitivity to Kv7.2-5 activator ML213, a phenotype not observed in the females (Abbott and Jepps, 2016). Moreover, K_V7 channel actviators hampered norepinephrine mediated increases in female Wistar Kyoto rat and SHR only, with no significant effect observed within the male (Berg, 2018). Providing inference for differential sex-dependent regulation of vascular K_V7 physiology and pathophysiology.

1.7 Thesis aims

Given the wealth of literature regarding the contribution of K_V7 channels to vascular reactivity and the known sexual dimorphisms in cardiovascular physiology, the aim of this thesis was to characterize and compare the expression and function of K_V7 channels within the vasculature of male and female Wistar rats. The primary questions proposed for this thesis included:

1. Are K_V7 channels expressed within the vasculature of the female Wistar and if so, what functional role do they play?
2. Is K_V7 channel function impaired within the female SHR? Do K_V7 channels represent a novel factor that differentiates the etiology of CVD between males and females?

Prior to approaching these questions, a variety of control experiments were undertaken to establish the specificity of the pharmacological and molecular tools employed in the following chapters. As well as to repeat previously published works, giving credence to novel findings discussed in later chapters.

To answer the first question, the relative transcript abundance and protein expression for the prime candidates for vascular K_V7 channel function (*Kcnq1,4,5* encoded $K_V7.1,4,5$ and *Kcne4* encoded KCNE4) was determined in mesenteric, renal, cerebral, and coronary arteries of both sexes. Moreover, within these vessels the effect of well-established K_V7 channel modulators was determined on basal and pre-contracted arterial tone and receptor mediated vasoconstriction and vasorelaxation. Due to the known regulation of extravascular K_V7 channels by E2 (O'Mahony *et al.*, 2007; Alzamora *et al.*, 2011; Rapetti-Mauss *et al.*, 2013) and the known cyclical changes in circulating serum concentration of sex hormones (Nilsson *et al.*, 2015) the Oestrus cycle stage of each female rat was considered as an experimental factor. The second question is founded in the previous discoveries that K_V7 channels are both impaired in and contribute to the hypertensive phenotype (Described in Chapter 1.5.4.3 and Jepps *et al.*, 2011; Chadha *et al.*, 2012; Stott *et al.*, 2015; Carr *et al.*, 2016; Barrese *et al.*, 2018; Mondéjar-Parreño *et al.*, 2020) and the novel finding that K_V7 channel modulator mediated reduction in TPR in female NT and SHRs but not male rats (Berg, 2018).

As secondary considerations, the contribution of K_V7 channels to prostacyclin mimetic mediated responses and the expression and function of K_V7 channels within mesenteric artery ECs was investigated. These investigations were undertaken in light of the known contribution of other K^+ channels to prostacyclin mediated vascular effects (Schubert *et al.*, 1996, 1997) and EC function as a regulator of VSMC contractility (Sandow *et al.*, 2009; Garland and Dora, 2017).

Chapter 2: Methods and materials

2.1 Animal model

Experiments were performed on tissues from male and female Wistar rats (Charles River, Margate, UK) ages 11-15 weeks (200-350g) kept at the Biological Research Facility (St George's University, London). The animals were housed in cages with free access to water and food (RM1; Dietex Inter-national, UK) on a 12-hour light/dark cycle and maintained at a constant temperature and humidity (21°C± 1°C; 50% ± 10% humidity) in accordance with the Animal (Scientific Procedures) Act 1986. Animals were kept in a bedding of LSB Aspen woodchip. Male and female rats were housed in separate rooms to ensure standard progression through the oestrus cycle. Animals were culled by cervical dislocation with secondary confirmation via cessation of the circulation by femoral artery severance in accordance with Schedule 1 of the Animal (Scientific Procedures) Act 1986. Organs were harvested and immediately placed in ice cold physiological salt solution (PSS), composition (mmol-L^{-1}): 119 NaCl, 4.5 KCl, 1.17 $MgSO_4.7H_20$, 1.18 NaH_2PO_4, 25 $NaHCO_3$, 5 glucose, 1.25 $CaCl_2$. Subsequently, arteries were dissected, cleaned of fat and adherent tissue, and placed on ice in PSS.

2.2 Oestrus cycle stage determination

Defined changes in cervical cell histology allowed for the determination of Oestrus cycle stage, these being: Pro-oestrus - 14 hrs; 2.) Oestrus - 24-48 hrs; 3.) Met-oestrus 6-8 hrs; 4.) Di-oestrus - 48-72 hrs (Cora, Kooistra and Travlos, 2015). Following euthanasia, 50 µL of PSS was inserted into the vaginal canal via a 2-200 µL tip and flushed 4-6 times to liberate cells from the surface of the cervix. PSS was removed from the vaginal canal, then placed into an *Eppendorf* tube on ice. 25 µL of the subsequent cell suspension was mounted on a glass slide and examined under light microscopy (Olympus CK40). Variation in the population of three principal cell types were used to identify each stage,

including; large keritanised (cornified) epithelial cells, nucleated epithelial cells and leukocytes. Table 2.1 is adapted from Cora, Kooistra and Travlos, (2015), which was the primary tool used for cycle stage determination during the course of this study, and describes at length the profile of cervical cell histology across the cycle) demonstrates representative images and a description of the abundance of each cell type in addition to changes in the total number of cells visible in each stage. Cycle stage determination was performed post-experiment during functional investigation as a means of blinding, this was not possible during molecular techniques as samples were stored for extended periods of time prior to use. To generate the representative images in Figure 2.1, 50 µL of cervical cell suspension was plated on a glass slide and left to adhere for 1 hr at RT. Subsequently, 1 mL of Toludine blue (made in house by the image resource facility, St George's university, London), was passed through a 0.2 µM syringe flooding the slide. Cells were left in dye for 45 seconds, before being submerged in distilled water on a rotating plate (20 rpm) for 1 min. Cells were left to dry, then imaged via Nikon Eclipse Ni.

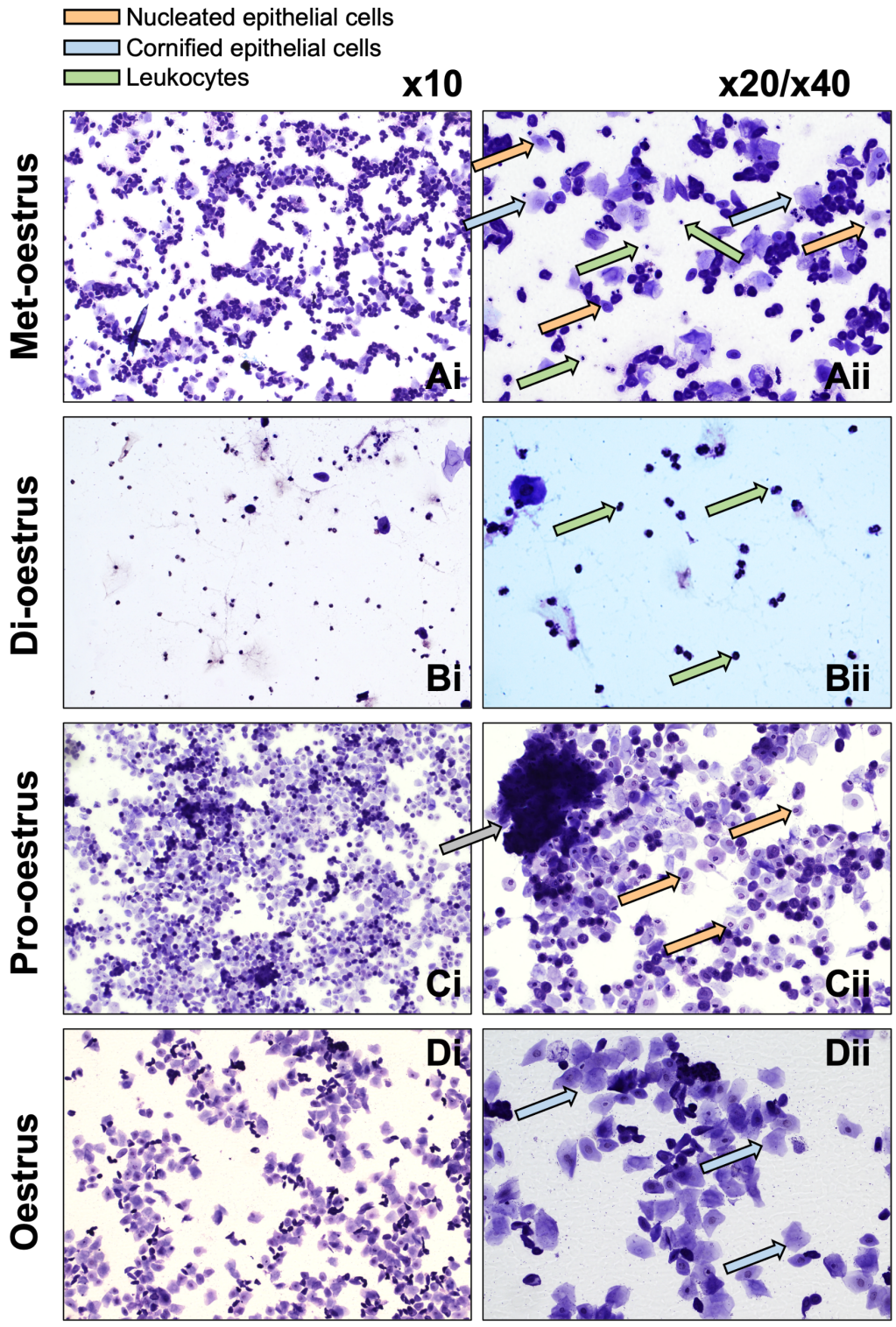

Figure 2.1: Cervical histology throughout the oestrus cycle.

Representative images of cell suspension lifted from the cervix during met-oestrus (Ai/Aii), di-oestrus (Bi/Bii), pro-oestrus (Ci/Cii) and oestrus (Di/Dii) at magnifications x10 (Ai-Di), x20 (Aii,Cii,Dii) and x40 (Bii) and stained in toluidine blue. Arrows demonstrate nucleated epithelial cells (orange), anucleated epithelial cells (blue) and leukocytes (green; Aii-Dii). Grey arrow demonstrates a 'swirl' of nucleated epithelial cells typical of pro-oestrus, used as an additive tool in determining cycle stage (Cii).

Cycle stage	*Leukocytes*	*Nucleated epithelial cells*	*Anucleated epithelial cells*	*Cell density*
Pro-oestrus	0 - +	++ - +++	0 - +	Low-moderate
Oestrus	0 - +	0 - ++	+++	Moderate- High
Met-oestrus	+ - +++	+ - ++	++	Moderate-high
Di-oestrus	++ - +++	+ - ++	+	Low - moderate

Table 2.1: Cervical cell populations

Changes in cervical cell population throughout the course of the oestrus cycle. This table is modified from Cora *et al.,* 2015.

2.3 Isometric tension recording, wire myography

2.3.1 Vessel mounting and normalisation

Arterial segments (~2 mm) of main renal, 2nd order mesenteric, basilar and left anterior descending coronary (LAD) arteries were mounted on either 200 µm pins (renal) or 40 µm tungsten wires (mesenteric, coronary and cerebral arteries) within a myograph chamber (Fig 2.2; Danish Myo Technology, Arhus, Denmark) containing 5 mL of PSS (composition described above) oxygenated with 95% O_2 and 5% CO_2 at 37°C. After mounting, vessels were left to equilibrate for 30 minutes.

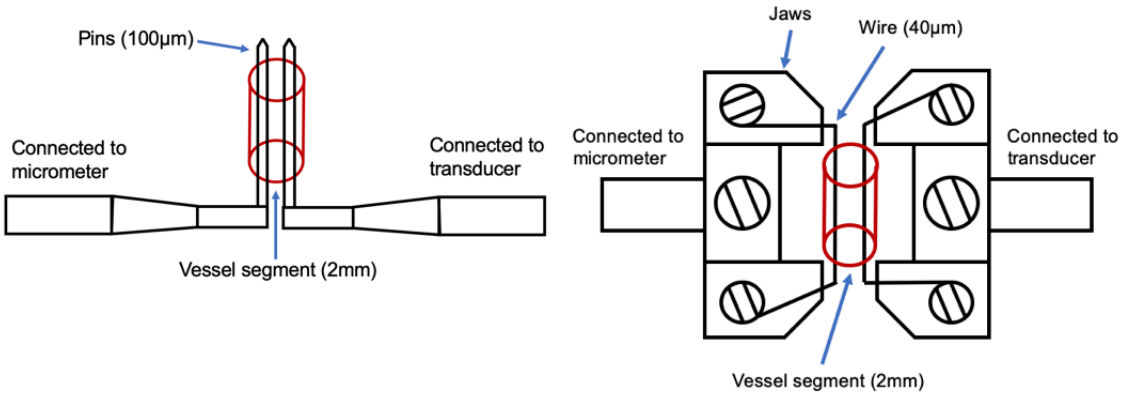

Figure 2.2: Diagrammatic representation of mounted vessels

A diagrammatic representation of 2mm segments of vessels mounted within a single chamber of a myograph (Daish MyoTechnology, Denmark) on either 100µm pins (left) or 40µm steel tungsten wire (right).

In the following experiments, force generated was first amplified by a PowerLab (ADInstruments, Oxford, UK), then recorded via LabChart software (ADInstruments, Oxford, UK). Vessels underwent a normalization process to achieve an internal luminal circumference at a transmural pressure of 100 mmHg (13.3 kPa), then set to 90% of this pressure to standardize pre-experimental conditions as demonstrated in Figure 2.2. 13.3 kPa is described as normal physiological blood pressure when the vessel is relaxed *in vivo* and as the optimal tension for experiments investigating VSMC contraction (Mulvany, 1977). Vessel normalization standardizes the degree of cell stretch between tissues with variable amounts of smooth muscle, allowing for effective comparison between vessels from the same and different animals, setting the base-line tension for

the following investigations. Vessels were then left to rest for 10 minutes. A minimal interval that was applied between all separate challenges to the vessels.

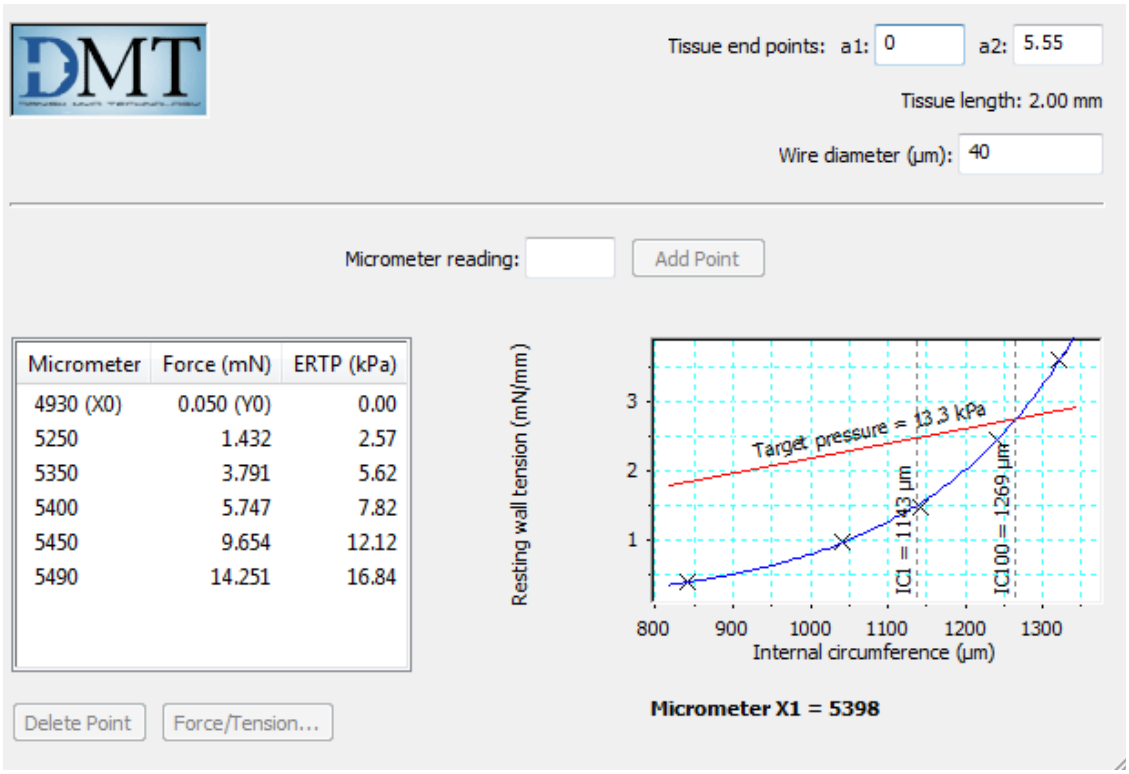

Figure 2.2: Representative vessel normalisation

Incrementally increasing tone allows for pre-experimental normalisation of vessel tension to achieve an internal luminal circumference as seen at 100mmHg (13.3kPa) via ADInstruments software in 'LabChart.'

Vessels were then challenged with isotonic high K^+ physiological salt solution (KPSS) of the following composition (mmol-L^{-1}); 63.5 NaCl, 60 KCl, 1.17 $MgSO_4.7H_20$, 1.18 NaH_2PO_4, 25 $NaHCO_3$, 5 glucose, 1.25 $CaCl_2$ to determine viability. By raising external K^+, the E_K is raised to -20mV, causing a depolarization of the membrane and opening of VGCC which mediates contraction. After the contraction had stabilized, vessels were washed in normal PSS until they returned to baseline. This challenge was then repeated to ensure maximal contraction to raised [K^+] was recorded (Fig 2.3). EC integrity was determined by relaxation of pre-constricted arterial tone (10 µmol-L^{-1} α1-adrenoceptor agonist Methoxamine; MO) in response to 10 µmol-L^{-1} synthetic acetylcholine analogue Carbachol (CCh). Only vessels that generated ≥80% relaxation were considered

endothelium positive. This 'equilibrium' protocol was repeated at the beginning of every experiment. Representative traces can be seen in Figure 2.3.

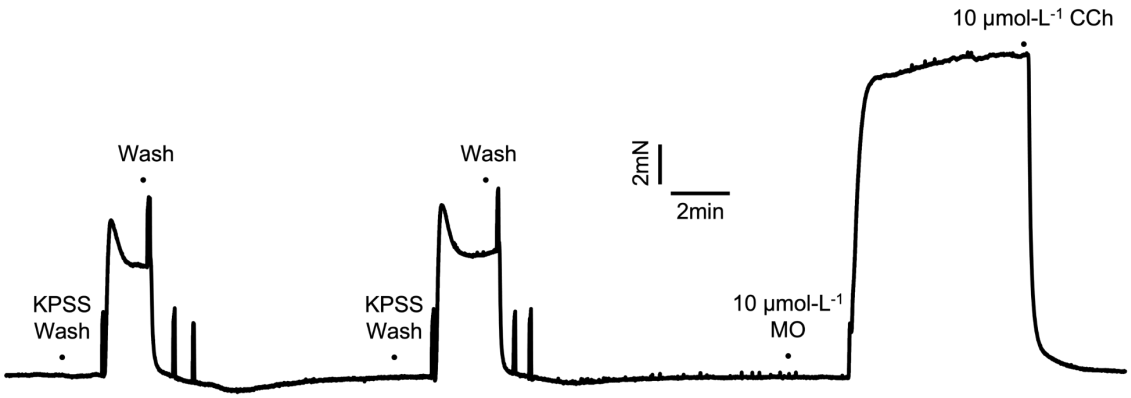

Figure 2.3: Equilibrium protocol

Representative 'warm-up' protocol trace within a male mesenteric artery segment.

2.3.2 Isometric tension recording protocols

Two protocols used during isometric tension recording form the basis for a large part of the work of this thesis. They include the generation of cumulative concentration effect curves (CECs) in response to either vasoconstrictors (Protocol 1) or vasorelaxants (Protocol 2). When generating CECs in response to vasoconstrictors, logarithmically increasing concentrations of an agent were added to the bath following the 'equilibrium' protocol, with incremental increase in tension allowed to plateau before the next concentration was added. Upon completion of the curve, vessels were washed in standard PSS and allowed to return to base-line tension. A variety of pharmacological modulators (see Table 2.2) where then added to the bath prior to starting a second concentration effect curve (Fig 2.3.A). All contractions were then normalized to the peak, stable contraction generated in response to KPSS. In contrast, when investigating vasorelaxants, vessels were first pre-constricted with 300 nmol-L^{-1} TXA_2 receptor agonist U46619. U46619 was chosen over other vasoconstrictors due to its ability to generate stable contractions with consistent potencies across the vasculature. Once tone had stabilized logarithmically increasing concentrations of an agent would be added to the bath. Similarly, vessels were then washed, pharmacological modulators were added, and a second curve was generated (Fig 2.3.B). This allowed for both vertical comparison

between different compounds and horizontal comparisons within the same vessel pre- and post the addition of a modulator. With experiments involving vasorelaxation in response to ion channel modulators, only one curve could be generated as these drugs do not readily wash out.

Name	***Description***	***Supplier***	***URL***
S-1	K_V7.2-5 channel activator	NeuroSearch, Ballerup, Denmark	N/A
ML213	K_V7.2-5 channel activator	Tocris Bioscience, Oxford, UK	https://www.tocris.com/products/ml-213_4519
Retigabine	K_V7 channel activator	Tocris Bioscience, Oxford, UK	https://www.tocris.com/products/retigabine_6233
ML277	K_V7.1 channel activator	Tocris Bioscience, Oxford, UK	https://www.tocris.com/products/ml-277_4777
BMS204352	K_V7.2-5 / BK_{Ca} channel activator	Sigma Aldrich, Oxford, UK	https://www.sigmaaldrich.com/GB/en/product/sigma/sml1313?context=product
Nicardipine	VGCC inhibitor	Sigma Aldrich, Oxford, UK	https://www.sigmaaldrich.com/GB/en/product/sigma/n7510
Pinacidil	K_{ATP} channel activator	Tocris Bioscience, Oxford, UK	https://www.tocris.com/products/pinacidil_1503
NS11021	BK_{Ca} channel activator	Tocris Bioscience, Oxford, UK	https://www.tocris.com/products/ns-11021_4788
Linopirdine	Pan-K_V7 channel inhibitor	Tocris Bioscience, Oxford, UK	https://www.tocris.com/products/linopirdine-dihydrochloride_1999
XE-991	Pan-K_V7 channel inhibitor	Tocris Bioscience, Oxford, UK	https://www.tocris.com/products/xe-991-dihydrochloride_2000

HMR-1556	K_V7.1 channel inhibitor	Tocris Bioscience, Oxford, UK	https://www.tocris.com/products/hmr-1556_5011
Chromanol 293B	K_V7.1 channel inhibitor	Tocris Bioscience, Oxford, UK	https://www.tocris.com/products/chromanol-293b_1412
Iberiotoxin	BK_{Ca} channel inhibitor	Tocris Bioscience, Oxford, UK	https://www.tocris.com/products/iberiotoxin_1086
Glibenclamide	K_{ATP} channel inhibitor	Tocris Bioscience, Oxford, UK	tocris.com/products/glibenclamide_0911
Isoprenaline	Mixed β-adrenoreceptor agonist	Tocris Bioscience, Oxford, UK	https://www.tocris.com/products/isoproterenol-hydrochloride_1747
U46619	TXA_2 receptor agonist	Tocris Bioscience, Oxford, UK	https://www.tocris.com/products/u-46619_1932
Methoxamine	α-1 adrenoreceptor agonist	Sigma Aldrich, Oxford, UK	https://www.sigmaaldrich.com/GB/en/product/sigma/m6524
β-Oestradiol	Oestradiol receptor agonist	Tocris Bioscience, Oxford, UK	https://www.tocris.com/products/b-estradiol_2824
G-1	GPER1 receptor agonist	Tocris Bioscience, Oxford, UK	https://www.tocris.com/products/g-1_3577
Iloprost	Prostacyclin receptor agonist	Tocris Bioscience, Oxford, UK	https://www.tocris.com/products/iloprost_2038
MRE-269	IP receptor agonist	Caymen chemical company, Ann Arbor, MI USA	https://www.caymanchem.com/product/10010412/mre-269
L-798,106	EP_3 receptor antagonist	Caymen chemical company, Ann Arbor, MI USA	https://www.caymanchem.com/product/11129/l-798%2C106
CAY-10441	IP receptor antagonist	Caymen chemical company, Ann Arbor, MI USA	https://www.caymanchem.com/product/10005186/cay10441
SQ22,536	Adenylate cyclase inhibitor	Tocris Bioscience, Oxford, UK	https://www.tocris.com/products/sq-22536_1435

Rp-8-Br-cAMP	PKA inhibitor	Sigma Aldrich, Oxford, UK	https://www.sigmaaldrich.com/GB/en/product/sigma/b2432?context=product
KT5720	PKA inhibitor	Tocris Bioscience, Oxford, UK	https://www.tocris.com/products/kt-5720_1288
ESI09	EPAC inhibitor	Biolog, Bermen, Germany	https://www.biolog.de/esi-09
M119K	$G_{\beta\gamma}$ inhibitor	National Cancer Institute Drug Development Programme	N/A
Carbachol	Non-selective cholinergic agonist	Tocris Bioscience, Oxford, UK	https://www.tocris.com/products/carbamoylcholine-chloride_2810
4-AP	Non-selective K^+ channel blocker	Sigma Aldrich, Oxford, UK	https://www.sigmaaldrich.com/GB/en/product/aldrich/275875
Tetraethylammonium	Non-selective K^+ channel blocker	Sigma Aldrich, Oxford, UK	https://www.sigmaaldrich.com/GB/en/product/sigma/t2265?gclid=CjwKCAjwh5qLBhALEiwAiooods0spjY4ifzWHtWfXZfm6TCwGgZeph6z95rbchOfOKN6VVtxtiHpJMxoC1gwQAvD_BwE
L-NAME	Endothelial nitric oxide inhibitor	Tocris Bioscience, Oxford, UK	https://www.tocris.com/products/l-name-hydrochloride_0665
TRAM-34	IK_{Ca} channel inhibitor	Tocris Bioscience, Oxford, UK	https://www.tocris.com/products/tram-34_2946
Apamin	SK_{Ca} channel inhibitor	Tocris Bioscience, Oxford, UK	https://www.tocris.com/products/apamin_1652
SNP	Nitric oxide donor	Sigma Aldrich, Oxford, UK	https://www.sigmaaldrich.com/GB/en/product/sigma/s0501
$BaCl_2$	K_{IR} channel inhibitor	Sigma Aldrich, Oxford, UK	https://www.sigmaaldrich.com/GB/en/substanc

			e/bariumchloride2082310361372?context=product
ML133	K_{IR} channel inhibitor	Tocris Bioscience, Oxford, UK	tocris.com/products/ml-133-hydrochloride_4549
Carbenoxolone	Gap junction inhibitor	Tocris Bioscience, Oxford, UK	tocris.com/products/carbenoxolone-disodium_3096

Table 2.2: List of modulators

A comprehensive list and short description of the modulators used throughout the course of this thesis.

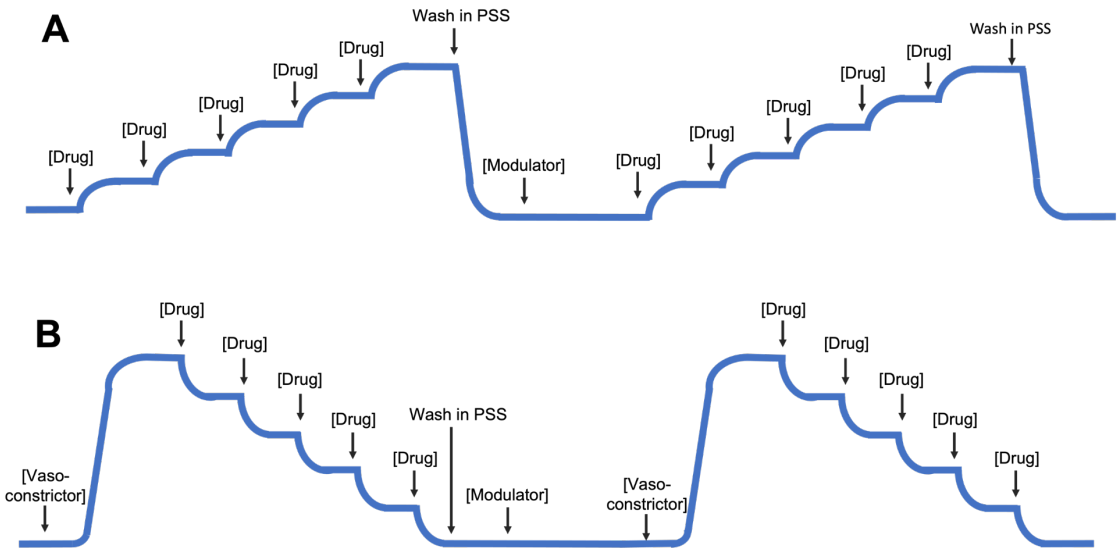

Figure 2.4: Isometric tension recording protocols

Diagrammatic representation of cumulative concentration effect curves generated in response to vasoconstrictors (Protocol 1, A) and vasodilators (Protocol 2, B).

2.4 Reverse transcription quantitative polymerase chain reaction

Relative fold-changes in expression levels of transcripts were determined in renal, mesenteric, cerebral, and coronary arteries in conjunction with whole brain, heart, and uterine samples via RT-qPCR.

2.4.1 mRNA extraction, quantification, and conversion to cDNA

mRNA was extracted using Monarch Total RNA Miniprep Kit (New England BioLabs, Ipswich, Massachusetts, USA). As per manufacturer's instruction, whole tissues were placed in a RNase free microfuge tube, 1.5 mL SafeLock *Eppendorff* (NextAdvance), with 2x DNA/RNA protection buffer (150 µL) diluted with nuclease free water (150 µL). Tissues were mechanically homogenized, first with scissors then via a bullet blender (NextAdvance) with 0.9-2 mm beads on a high intensity 5-minute spin protocol. Subsequently, tissues were supplemented with 30 µL Proteinase K, diluted in 60 µL 'proteinase K reaction buffer,' briefly vortexed then incubated for 15-30 mins at 55°C in a heat block. Samples were then centrifuged for 30 sec at 14,000 x g to pellet the cell debris. The supernatant was transferred to an RNase free microfuge tube and an equal volume of RNA lysis buffer (380 µL) was added. The sample was then transferred to a 'genomic DNA (gDNA) removal column' fitted with a collection tube and centrifuged at 14,000 g x for 30 sec. An equal volume of 100% ethanol (760 µL) was then added and gently mixed by pipetting, then up ≤ 800 µL was transferred to an 'RNA purification column,' and centrifuged at 14,000 g x for 30 sec. The elution was discarded, and the remaining sample was spun through. Following which, DNase I diluted in 'DNase reaction buffer' was incubated in the column at room temperature (RT) for 15 minutes for the enzymatic removal of any residual gDNA. Next, 500 µL RNA priming buffer was centrifuged through the column at 14,000 g x for 30 sec and the elution was discarded. Finally, RNA wash buffer was centrifuged through the column at 14,000 g x twice, first for 30 sec, then a second wash for 2 minutes. To elute the sample, the RNA purification column was moved to RNase free microfuge tube and 30 µL nuclease free water was

centrifuged through the column at 14,000 g x for 30 sec. This RNA containing elution was then placed on ice prior to quantification.

RNA was quantified via Nanodrop 1000 spectrophotometer (Thermo Fisher Scientific) and processed via ND-1000 V.3.8.1 programme (Thermo Fisher Scientific). A 1.5 µL sample droplet was placed on the end of a fiber optic cable, the surface tension of the droplet keeps it in position, a second fiber was then brought into contact with the first whereby the sample bridges the gap between the two. Absorbance at a wavelength of 260 nm was read as a pulsed xenon flash lamp, which passes light through the sample. Using the Beer-Lambert Law, the amount of light absorbed can be related to the concentration of the absorbing molecule. Readouts are given in (ng/µL) and are used to inform the volumes for the following steps. Quality control is assessed by the ratio of absorbance between 260/280nm ($A_{260/280}$), whereby a ratio of 2 is considered pure RNA. Any sample below a ratio 1.86 was discarded. See example trace of nano-drop reading for whole mesenteric artery plexus below in Figure 2.5.

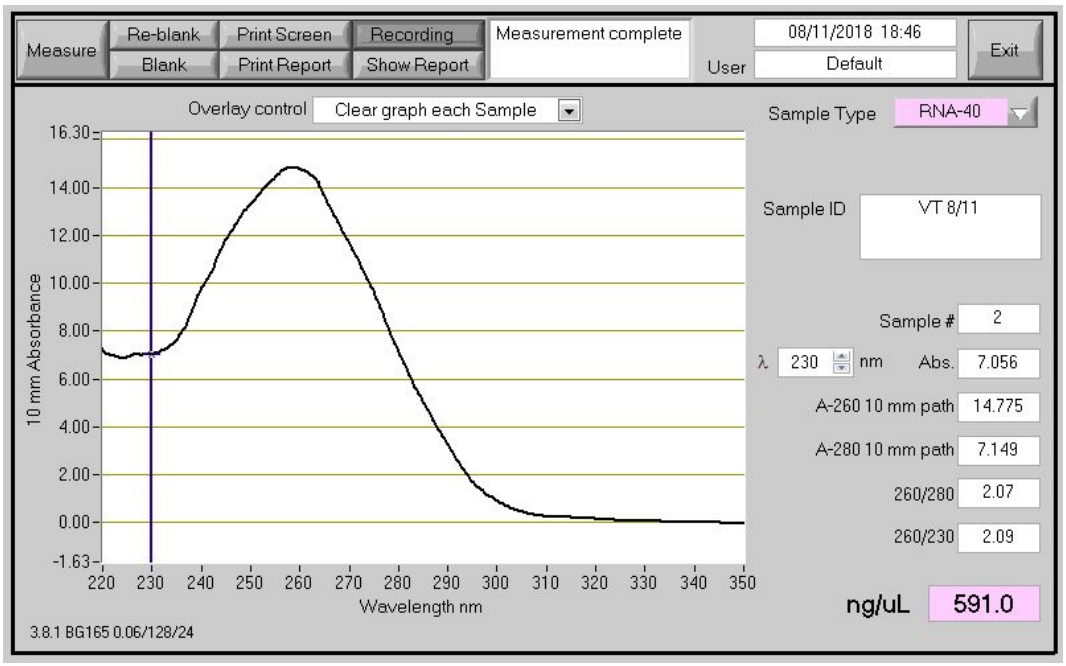

Figure 2.5: mRNA quantification.

Representative mRNA quantification via Nanodrop 1000 spectrophotometer processed by ND-1000 V.3.8.1 programme. Values in bottom right hand corner display $A_{260/280}$ ≥2 and mRNA amount expressed in ng / µL.

Extracted and quantified mRNA was then converted into complimentary DNA (cDNA) via LunaScript RT SuperMix Kit (New England BioLabs, Ipswich, Massachusetts, USA). Within a 20 µL mixture, up to 1 µg RNA sample was reverse transcribed in each reaction. As per manufacturer's instructions, 4 µL LunaScript RT SuperMix (x5) and RNA sample made up to 20 µL with nuclease free water was run in a thermocycler (Multigene gradient, Labnet) using the following steps; 1.) Primer annealing- 2 min at 25°C; 2.) cDNA synthesis- 10 min at 55°C; 3.) Heat inactivation- 1 min at 95°C. In conjunction, a no-reverse transcription control (NRT) was also made. NRT samples contained up to 1 µg of RNA sample and 4 µL LunaScript no-RT SuperMix made up to 20 µL with nuclease free water and run under the same conditions.

2.4.2 Relative transcript abundance quantification

Quantitative analysis of target genes was assessed via CFX-96 Real-Time PCR Detection System (BioRad, Hertfordshire, UK). Samples were run in BrightWhite qPCR plate (Primer Design, Camberley, UK) in combination with either SYBR green based dyes PrecisionPLUS qPCR Master Mix (Primer Design, Camberley, UK) or Luna Universal qPCR master mix (New England BioLabs, Ipswich, Massachusetts, USA), 300 nmol-L^{-1} of gene specific target primer (Thermofisher scientific, Waltham, Massachusetts, USA; table 2.3) and 10 ng cDNA as per manufacturer's instruction. SYBR green dye fluoresces when it non-selectively binds the major groove of double stranded DNA (dsDNA). Samples were run via the following protocol: 1.) activation step (15 minutes: 95°C); 2.) denaturation step (15 sec: 94°C); 3.) annealing step (30 sec: 55°C); 4.) extension step (30 sec: 70°C). Steps 2, 3, and 4 were repeated 40 times. Following which, a melt curve was also run. Quantification cycle (Cq) was determined via Bio-Rad CFX96 Manager 3.0 (see representative amplification as seen in Bio-Rad CFX96 Manager 3.0 in Figure 2.6). Cq is the number of cycles required to pass a pre-determined level of fluorescence, which is dependent on the preceding number of transcripts already within the sample. Cq was normalised to the average of two housekeeping genes chosen among ubiquitin C (*Ubc*), polyamine transporter 1 (*Tpo-1*),

cytochrome C1 (*Cyc1*), Calnexin (*Canx*), and glyceraldehyde 3-phosphate dehydrogenase (*Gapdh*) to give relative abundance of target genes of interest. See table 1 for a list of the primers targeted to genes of interest used in the following investigation (Thermofisher, Paisley, UK). Primers for house keepers were provided by Primer design (UK), as such sequences cannot be disclosed for proprietary reasons.

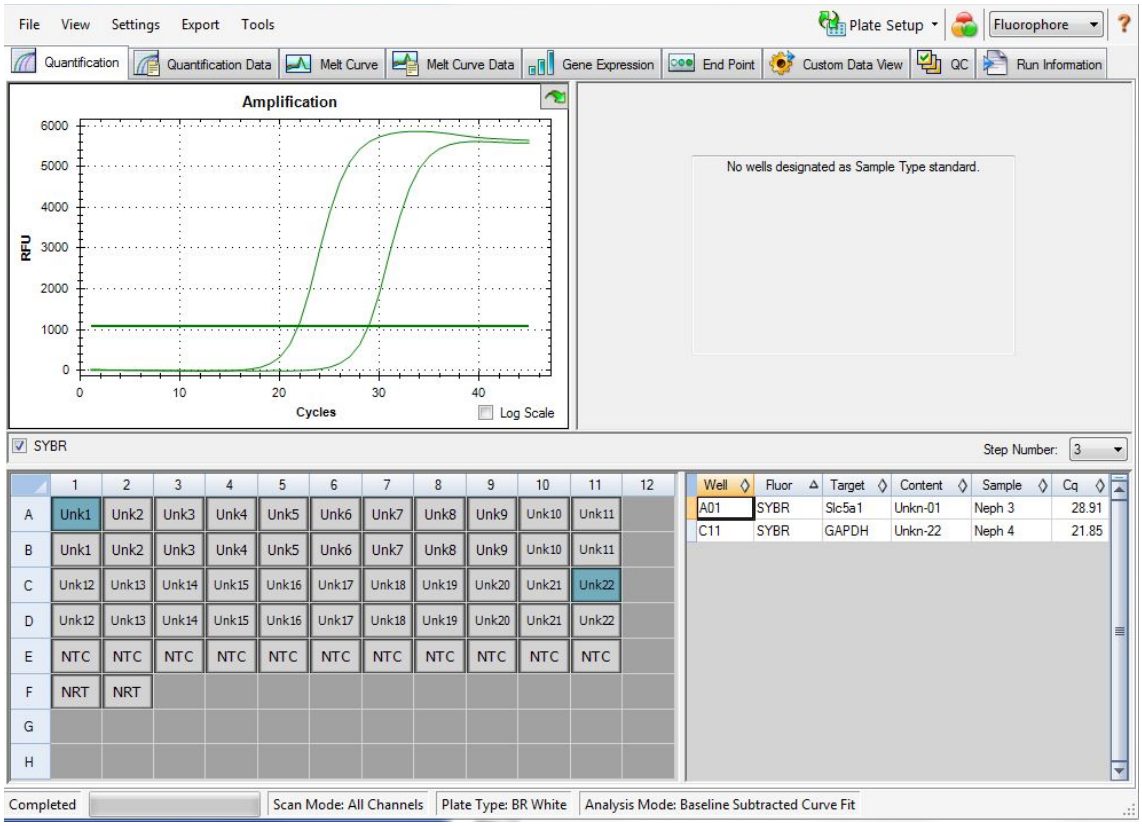

Figure 2.6: Representative qPCR.

Representative image of qPCR via BioRad CFX-96 run via Bio-Rad CFX96 Manager 3.0 demonstrating target gene (*Slc5a1*) and housekeeper gene (*Gapdh*) achieving Cq at 28.91 and 21.85 respectively.

2.4.2.1 Normalising Cq values

In the following investigations, ΔCq (Livak and Schmittgen, 2001) allowed for the comparison of gene expression between tissues and groups on the condition that the same house keepers have been used. Using the following equation,

$$Relative\ gene\ expression = 2^{-\Delta \mathrm{Cq}}$$

Relative gene expression is then expressed as a normalised value when compared to stable housekeeper genes. This method was used as the principal means of expressing RT-qPCR data.

In addition, when comparing hypertensive animals against normotensive controls, gene expression was expressed as fold changes. In the following equation,

$$Fold\ change\ in\ gene\ expression = 2^{-\Delta\Delta Cq}$$

ΔCq of target gene when compared to housekeeper in the normotensive sample is subtracted from the hypertensive sample to give $\Delta\Delta$Cq, then expressed as 2^{-}.

2.4.3 In plate controls, RT-qPCR

Melt curve analysis allowed for the determination of primer-dimer formation during amplification and excluded the possibility of false positive results. As we have used non-specific probe-based dye (SYBR green), it is possible that should the primer dimerise, it can amplify itself in addition to the target sequence producing an abundance of dsDNA within the reaction mixture. Non-specific probes such as SYBR green will bind and fluoresce, giving a false positive result. In performing a melt curve, the sample temperature is incrementally increased, and fluorescence is measured. As the melt temperature (T_m) for each sequence is reached, the dsDNA dissociates, and the dye fluorescence decreases. -ΔF/ΔT (change in fluorescence / change in temperature) is then plotted against the temperature to determine the melt dynamics. As T_m is dictated by the length of the product, CG content and mismatches it is a highly specific characteristic of each product. In a specific reaction, by the end of the run cycle only a single product should have been amplified and will therefore be the predominant transcript within the sample. Therefore, a decrease in fluorescence at a single temperature is indicative of only one amplification product. See figure 2.7 for representative melt curve analysis of both a specific reaction (Fig 2.7.A) and primer dimer

formation (Fig 2.7.B). In the presence of primer-dimer detection, the sample was discarded.

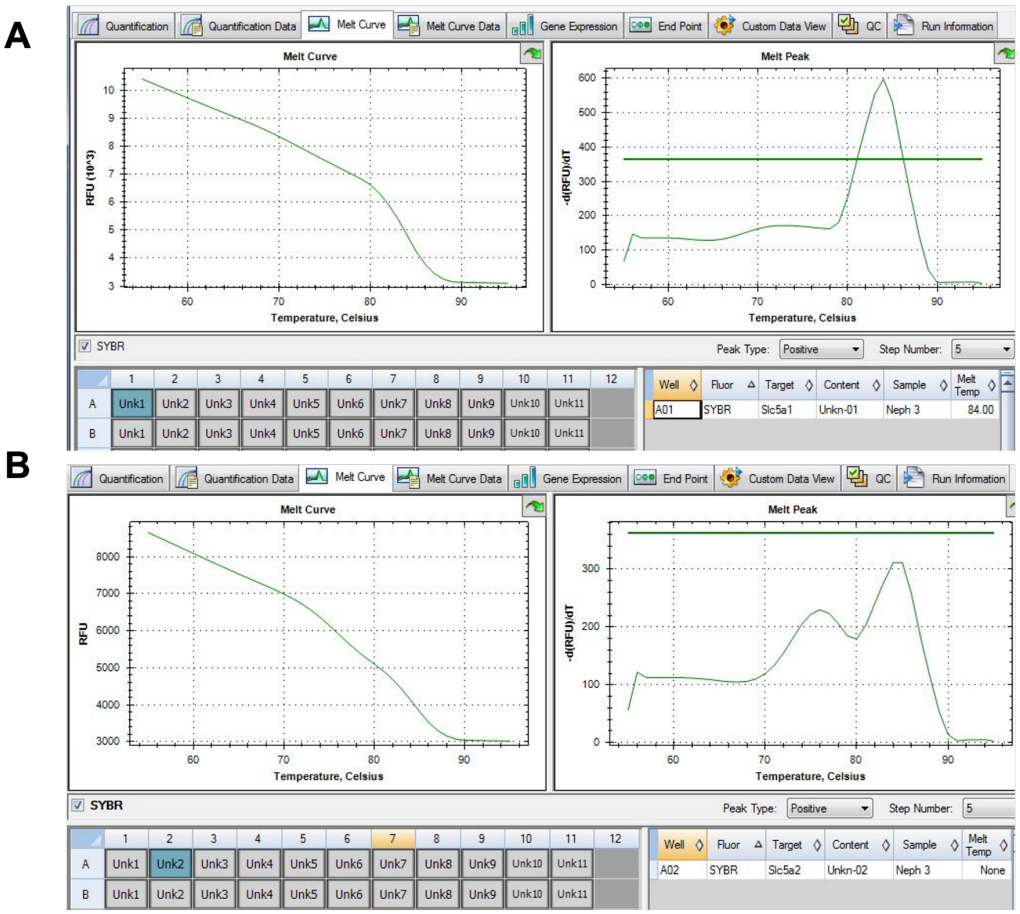

Figure 2.7: Representative melt curve analysis.

Representative images of melt curve analysis via BioRad CFX-96 run via Bio-Rad CFX96 Manager 3.0 of target genes *Slc5a1* (A), which presented with a single peak i.e no primer-dimer formation, and *Slc5a2* (B), which presented with two peaks i.e, primer-dimer formation.

In addition, no-template controls (NTC) were also run for each primer. This involved running each sample containing 10 µL PrecisionPLUS qPCR Master Mix or Luna Universal qPCR master mix and 300 nmol-L^{-1} of gene specific target primer made up to 20 µL with nuclease free water in the absence of any cDNA. This secondary control additionally screened for primer-dimer formation, and the contamination of the sample with exogenous DNA. Finally, at least one NRT was run in combination with target samples during RT-qPCR as a means for screening for gDNA contamination. If either NTC or NRT values were within 5 Cq of target samples, the sample would be discarded.

See figure 2.8 for representative images of sample vs NTC and NRT when targeting housekeeper gene *Gapdh.*

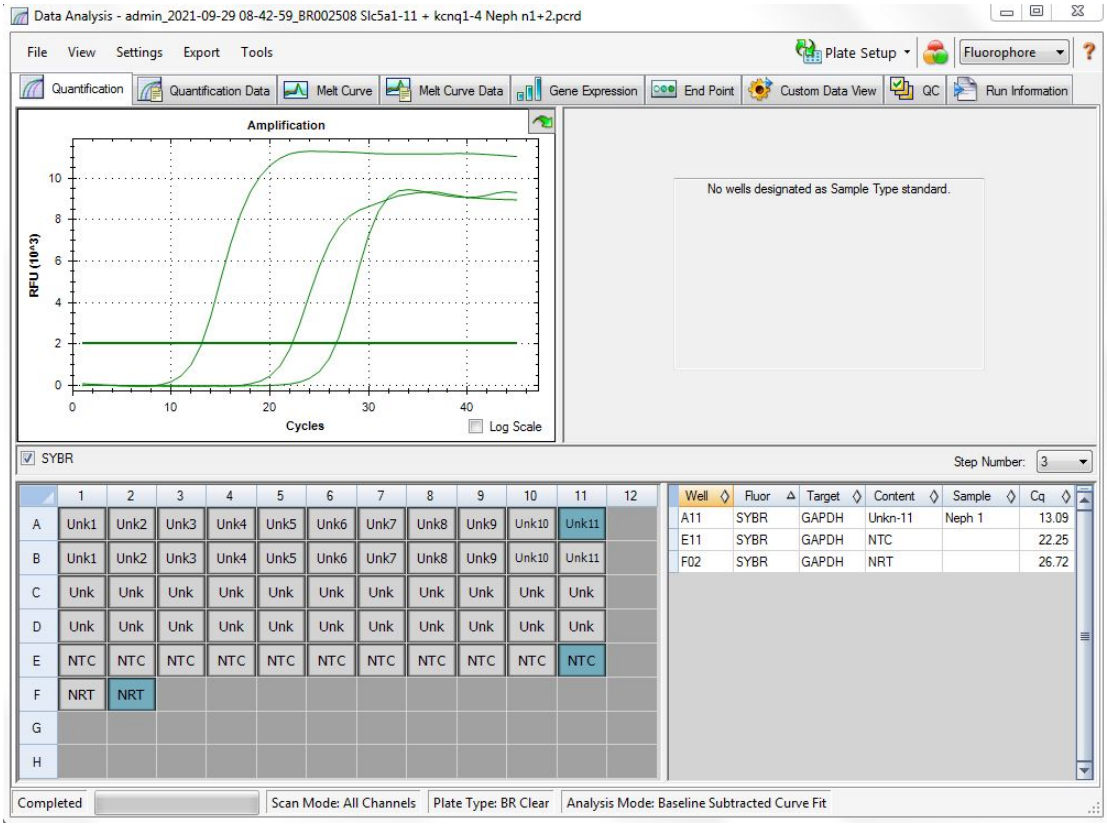

Well	Fluor	Target	Content	Sample	Cq
A11	SYBR	GAPDH	Unkn-11	Neph 1	13.09
E11	SYBR	GAPDH	NTC		22.25
F02	SYBR	GAPDH	NRT		26.72

Figure 2.8: Representative no-template and no-reverse transcription control.

Representative images of no-template (NTC) and no reverse transcription control (NRT) compared to sample. RT-qPCR run via BioRad CFX-96 run via Bio-Rad CFX96 Manager 3.0 of housekeper gene *Gapdh* run with cDNA vs *Gapdh* run with NTC and NRT.

Gene	(+) Forward primer sequence (-) Reverse primer sequence	Gene accession number	Amplicon (bp)
Kcnq1	TGGGTCTCATCTTCTCCTCC GTAGCCAATGGTGGTGACTG	NM_032073	124
Kcnq2	AAGAGCAGCATCGGCAAAAA GGTGCGTGAGAGGTTAGTAGCA	NM_133322	101
Kcnq3	CAGCAAAGAACTCATCACCG ATGGTGGCCAGTGTGATCAG	AF091247	161
Kcnq4	GAATGAGCAGCTCCCAGAAG AAGCTCCAGCTTTTCTGCAC	XM_233477.8	133
Kcnq5	AACTGATGAGGAGGTCGGTG GATGACCGTGACCTTCCAGT	XM_001071249.3	120
Kcne1	GTTTCCCCAAATCTCTCCATT AGCACACACTTCCCATTTCAA	NM_008424	111
Kcne2	CCTGGTATTTAACTGAGTTGGACAT GCACTGGGGGCTCTTGAAT	NM_134110	97
Kcne3	CTCAACCATATCAAGCCACAGT GCCTATCAGTCCCTCTTCTCT	NM_001190869	99
Kcne4	GGAGGAGGGGGCTGATGA CTGGTGGATGTTCTCGGAAGA	NM_021342	88
Kcne5	GCACGAAGAGACCTCAGACAT GGACAGGAAACAAGAACACCAT	NM_0214487	146
Esr1	TTCACCTTCTGGAGTGTGCC ACTTGACGTAGCCAGCAACA	NM_012689.1	173
Esr2	TGCCGACTTCGCAAGTGTTA ACCGTTTCTCTTGGCTTTGC	NM_012754.2	138

Gper1	TCATCGGCCTGTGCTATTCC GAAGACAAGGACCACTGCGA	NM_133573	119
Ptger1	AGTTCGAACGTTGGTCACGA TAAGGTTGCAGCATTGTGCG	NM_001278475.1	112
Ptger2	TATGCTCCCTGCCTTTCACAA GGAGGTCCCACTTTTCCTTT	NM_031088.2	*72*
Ptger3	GTGCAATTCCTTCCTAATCGCC TCAGGTTGTTCATCATCTGGCA	NM_012704.1	122
Ptger4	ATGAGCATTGAGCGCTACCT AGATGCATAGACGGCGAAGA	NM_032076.3	*102*
Ptgir	TGACACTTTCGCCTTCGCTA TAGATGGCAGGCAAAGCCAA	NP_001071112.1	156
Tbxa2r	TTGACATTCCCAGGCCCAAA ACGTGATAAGGGGGTCAACA	NM_017054.2	*141*
Acta2	ATCCGATAGAACACGGCATC AGGCATAGAGGGACAGCACA	NM_031004.2	228
Pecam1	CTCCTAAGAGCAAAGAGCAACTTC TACACTGGTATTCCATGTCTCTGG	NM_031591.1	100

Table 2.3: List of primers

A comprehensive list of primers used for RT-qPCR.

2.5 Vascular smooth muscle staining

2.5.1 Vascular smooth muscle cell isolation

Renal and mesenteric arteries were incubated in isolation PSS of the following composition (mmol-L^{-1}); 120 NaCl, 6 KCl, 12 glucose, 10 HEPEs and 1.2 $MgCl_2$ supplemented with 1.75 mg/mL Collagenase Type IA, 0.9 mg/mL protease, 1 mg/mL Trypsin inhibitor and 1 mg/mL bovine serum albumin (Sigma, UK) at 37°C for 30 min (renal artery) and 17 min (mesenteric artery). Next, vessels were gently triturated with wide-bore glass pipette to liberate VSMCs from their extracellular matrix. 75 µL of subsequent cell suspension was plated on 25 mm glass coverslips, supplemented with 75 µL of 2.5 mmol-L^{-1} Ca^{2+} and left to adhere for 1hr in an incubator at 37°C in 95% O_2 + 5% CO_2. Isolated myocytes were then either fixed immediately afterwards or were incubated in 1 mL isolation PSS containing DMSO + Ethanol, E2 (10 nmol-L^{-1}) or GPER1 agonist G-1 (1 µmol-L^{-1}) for 30 min.

2.5.2 Immunocytochemistry

As previously described (Barrese *et al.*, 2018); isolated VSMCs were fixed in 3% PFA containing phosphate buffered serum (PBS) for 15 min at RT. For membrane staining, cells were incubated in Alexa Fluor 488-conjugated wheat germ agglutinin (WGA; Thermo-Fisher, Paisley, UK; dil. 1:200 in PBS) for 10 mins, WGA is a lectin protein that binds glycoconjugates N-acetylglucosamine and N-acetylneuraminic acid at the cell membrane. This step was performed pre-permeabilization to ensure that WGA tagged only the extracellular surface. Subsequently, cells were washed in 0.1 mmol-L^{-1} glycine in PBS for 5 min to chelate any remaining formaldehyde. Next, coverslips were washed for 1 hr in blocking solution containing cell perforating agent (0.1% Triton X-100) and non-specific protein (10% foetal bovine serum in PBS) to allow antibody access into the cytosol and to reduce off-target binding. Cells were incubated overnight in primary antibodies (see table 2.4) at 4°C.

The following morning, cells were washed in PBS and incubated in secondary antibodies (see table 2.5 for a list of secondary antibodies), then mounted in Vectasheild (P4170; Sigma, UK) medium containing 4′,6-diamidino-2-phenylindole (DAPI). All anti-bodies were diluted in blocking solution. Cells were then imaged via Nikon A1R confocal microscope (inverted) on Ti2 chassis (Image Resource Facility, St George's University, London). For experiments determining Membrane:Cytosol ratio for $K_V7.4$ expression, fluorescence intensity profiles for $K_V7.4$ and WGA were plotted across three randomly drawn lines spanning the width of the cell measured in arbitrary units (A.U.) using image J software (https://imagej.nih.gov/ij/). Fluorescence intensity ≥ 200 A.U was considered as the plasma membrane and below the threshold was considered as the cytosol. Membrane:Cytosol ratio for $K_V7.4$ expression was calculated by measuring the average fluorescence intensity of $K_V7.4$ within the membrane and dividing it by the average fluorescence intensity of $K_V7.4$ within cytosol. 10-12 cells per *n*. Total cell fluorescence was measured by via Image J software (https://imagej.nih.gov/ij/). See figure 2.8 for a schematic demonstrating the principals of immunocytochemistry.

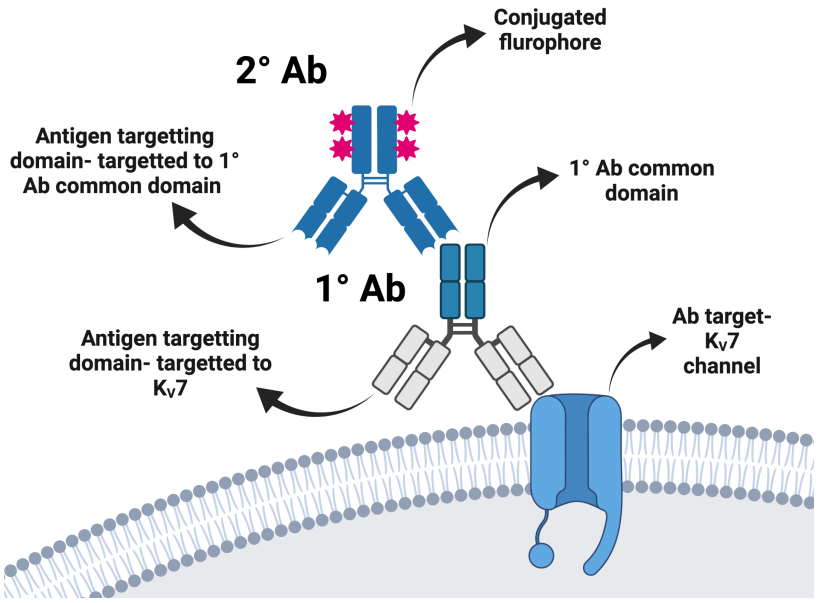

Figure 2.9: Immunocytochemistry

Diagrammatic representation of immunocytochemistry. Primary antibody (1° Ab) antigen targeting domain binds to K_V7, whilst the secondary antibody (2° Ab) conjugated with a fluorophore binds the common domain of the 1° Ab.

2.5.3 Proximity ligation assay

The interaction of $K_V7.4$ and HSP90 was determined by proximity ligation assay (PLA) similar to Barrese *et al.,* (2018). PLA is used to resolve protein-protein interactions ≤ 40 nm, which are expressed as red puncta within the cell during imaging. Mesenteric VSMCs were isolated, incubated in either Ethanol or 10 nmol-L^{-1} E2 and fixed as above. Cells were washed in 0.1 mmol-L^{-1} glycine containing PSS for 10 mins, permeabilised via 0.1 % triton X-100 for 5mins and blocked via Duolink blocking solution for 1 hr at 37°C, then incubated overnight in a combination of rabbit anti-$K_V7.4$ (APC-164, Alamone, Jerusalem, Israel; dil 1:200) and mouse-anti-HSP90 (ab13492, Abcam, Cambridge, UK; dil 1:200) overnight at 4°C. Cells were then incubated in a combination of Duolink In situ PLA probes, anti-mouse MINUS (DUO92004; Sigma-Aldrich, St Louis, MO, USA) and anti-rabbit PLUS (DUO92002; Sigma-Aldrich, St Louis, MO, USA) for 1hr at 37°C, as per manufacturer's instructions. Using Duolink In situ detections reagents (DUO92008; Sigma-Aldrich, St Louis, MO, USA) samples underwent ligation (30 min at 37°C in 5 x ligation buffer and 40 x ligase in distilled water) whereby anti-sense single stranded DNA sequences from the plus and minus probes within a proximity of ≤40 nm bind, and amplification (100 min at 37°C in 5 x amplification buffer and 80 x polymerase in distilled water) whereby the now dsDNA replicates into a large complex. Red fluorophore (568 nm) is present within the amplification buffer and binds the amplified product. Cells were then mounted on cover slides in vectasheild (P4170; Sigma, UK) containing DAPI. All anti-bodies and probes were diluted in blocking solution. Cells were then imaged via Nikon A1R confocal microscope (inverted) on Ti2 chassis (Image Resource Facility, St George's University, London). See Figure 2.9 for diagrammatic representation of PLA.

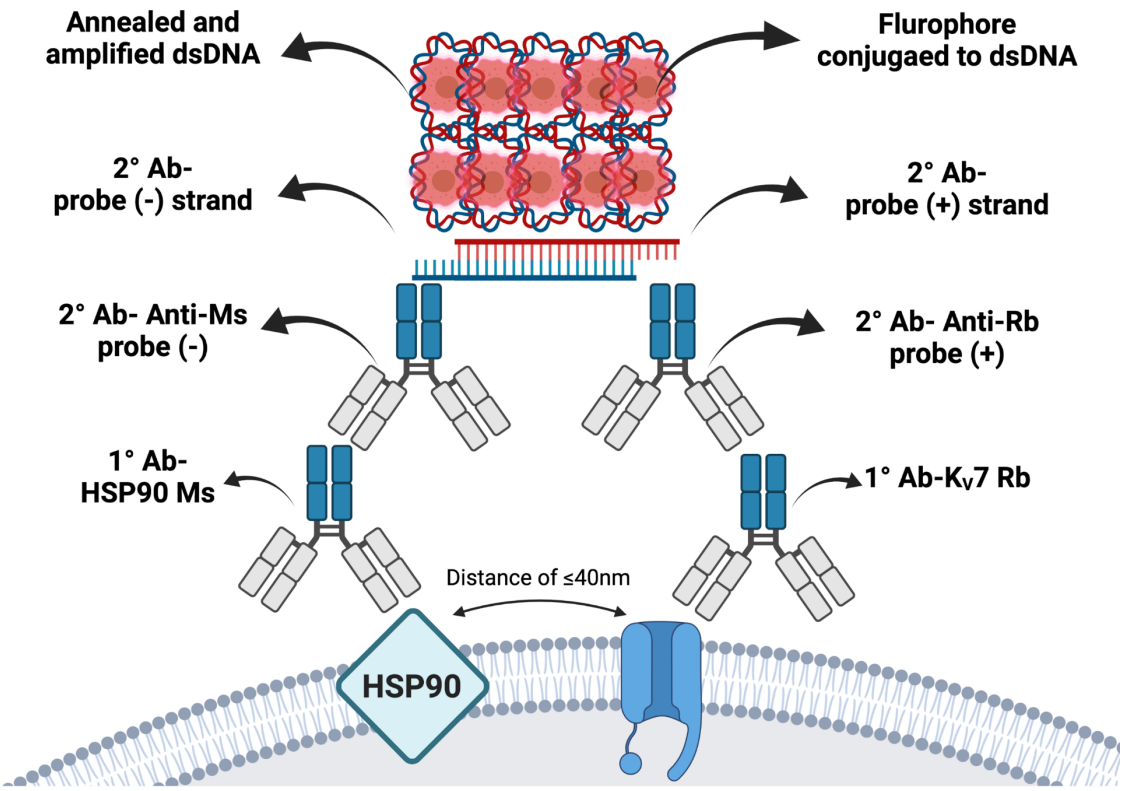

Figure 2.10: Diagrammatic representation of PLA

Diagrammatic representation of Proximity ligation assay (PLA). Both K_V7 and heat shock protein 90 are targeted for by primary antibodies (1° Ab) raised in rabbit and mice respectively. Secondary antibodies (probes), anti-mouse minus (Anti-Ms (-)) and anti-rabbit plus (Anti-Rb (+)) bind the common domain of the 1° Ab. The antisense sequence of the probes are then annealed, ligated and amplified whereby a fluorophore binds the amplified sequence and fluoresces.

Target antigen	*Source*	*Catalog #*	*Dilution*	*Lot #*	*URL*
Rabbit Anti-K_V7.1	Pineda, Antikörber-Service, Germany	N/A	1:100	N/A	N/A
Rabbit Anti-K_V7.4	Alomone, Jerusalem, Israel	#APC-164	1:200	APC164 AN0102	https://www.alomone.com/p/anti-kv7-4/APC-164
Rabbit Anti-K_V7.5	Millipore, Temecula, CA, USA	#ABN1372	1:100	3093511	https://www.merckmillipore.com/GB/en/product/Anti-Potassium-Channel-KCNQ5-Antibody,MM_NF-ABN1372?ReferrerURL=https%3A%2F%2Fwww.google.com%2F
Rabbit Anti-KCNE4	Atlas Antibodies, Sweden	#HPA011420	1:200	A104922	atlasantibodies.com/products/antibodies/primary-antibodies/triple-a-polyclonals/kcne4-antibody-hpa011420/
Mouse Anti-HSP90	Abcam, Cambridge, UK	Ab13492	1:200	GR3346139-4	https://www.abcam.com/hsp90-antibody-ac88-ab13492.html
Goat anti-Pecam-1 / Cd31	Santa Cruz Biotechnology,	Sc-1506	1:100		https://datasheets.scbt.com/sc-1506.pdf
Mouse anti-SM-α-actin	Sigma Aldrich	A2547	1:100		https://www.sigmaaldrich.com/GB/en/product/sigma/a2547

Table 2.4: List of primary anti-bodies

A list of primary anti-bodies used for immunocytochemistry and proximity ligation assay.

Target antigen	*Source*	*Catalog #*	*Dilution*	*Lot #*	*URL*
Goat Anti-Rabbit Alexa Fluor 568	Thermo-fisher, Paisley, UK	A-11036	1:100		https://www.thermofisher.com/antibody/product/Goat-anti-Rabbit-IgG-H-L-Highly-Cross-Adsorbed-Secondary-Antibody-Polyclonal/A-11036
Goat Anti-Mouse Alexa Fluor 488	Thermo-fisher, Paisley, UK	A-11001	1:100		https://www.thermofisher.com/antibody/product/Goat-anti-Mouse-IgG-H-L-Cross-Adsorbed-Secondary-Antibody-Polyclonal/A-11001
Goat-anti rabbit 488	Merk, St Louis, MO, USA	18772	1:100		https://www.sigmaaldrich.com/GB/en/product/sigma/18772?context=product
Donkey Anti-Goat 633	Thermo-fisher, Paisley, UK	A-21082	1:100		https://www.thermofisher.com/antibody/product/Donkey-anti-Goat-IgG-H-L-Cross-Adsorbed-Secondary-Antibody-Polyclonal/A-21082
Anti-mouse MINUS	Sigma-Aldrich, St Louis, MO, USA	DUO92004	1:500	SLCF4091	https://www.sigmaaldrich.com/GB/en/product/sigma/duo92004
Anti-Rabbit PLUS	Sigma-Aldrich, St Louis, MO, USA	DUO92002	1:500	SLCH5706	https://www.sigmaaldrich.com/GB/en/product/sigma/duo92002

Table 2.5: List of secondary anti-bodies

A list of secondary anti-bodies used for immunocytochemistry and proximity ligation assay.

2.6 Cell culture

Chinese hamster ovarian (CHO) cells, human embryonic kidney 293B (HEK) cells and HEK 293B stably expressing *KCNQ4* (HEK-K_V7.4) cells were grown in DMEM/F-12 (Sigma, UK) supplemented in 1% penicillin / streptomycin in an incubator with 5% CO_2 at 37°C. CHO / HEK / HEK K_V7.4 cells were transiently transfected by incubation in either a total of 4 µg of plasmid containing *Kcnq1, Kcnq4, Kcnq5, Kcne4* (University of Copenhagen, Denmark) or *Gper1* (SinoBiological, Eschbron, Germany) via Plasmid-Lipofectamine 3000 transfection reagent suspended in Opti-MEM mixture or lipofectamine / Opti-MEM only for 24 hrs as per manufactures instructions. Cells were mounted onto glass coverslips and left to attach for 1hr at RT. Cells were then used either to validate antibody specificity, or for single cell electrophysiology.

To maintain stock, plasmids were grown in bacteria. Autoclaved Luria-Bertini (LB) broth, agar (L2897, Sigma Aldrich, Oxford) and Plasmid resistance specific anti-biotic containing mixture was plated and left to set for 1 hr, then stored at 4°C. NEB 5-α high efficiency competent *E.coli* cells (#C2987H, New England BioLabs, Ipswich, Massachusetts, USA) were lifted from storage (-80°C) and left to defrost on ice. Competent cells are bacterial cells that readily take extraneous DNA including plasmids and replicate it as they replicate. Once defrosted, 1-5 µL of plasmid (1 pg-100 ng) was added to 50 µL of cells and mixed by flicking the tube, as per-manufactures instructions. Cell plasmid mixture was left to rest on ice for 30 minutes, then incubated at 42°C for 30 sec. This step is known as 'Heat-shock transformation,' during which the plasmid is taken up into the bacterial cell. After which, cells were supplemented with 200 µL super optimum broth medium, which supplies in excess vital nutrients for *E.coli* growth. Cells were then left for 30 min at 37°C on a shaker. Agar plates were simultaneously warmed in an incubator. After which the bacteria were spread on the anti-biotic containing agar, left to dry and incubated over night at 37°C inverted. The following morning, single colonies of bacteria were picked from the plate and transferred to an inoculation tube containing 3 mL of LB broth (L7275, Sigma Aldrich, Oxford) + antibiotic and left for 6-8

hrs at 37°C on a shaker. Cells were then incubated overnight in 100 mL of LB broth (L7275, Sigma Aldrich, Oxford) + antibiotic at 37°C on a shaker.

Plasmid was then extracted and purified via QIAGEN Plasmid Maxi Kit (12162, QIAGEN). As per-manufacturers instruction, cultured bacteria was centrifuged at 6000 x *g* for 15 min at 4°C, prepared in two separate 50 mL falcon tubes (CLS430828, Sigma Aldrich, Oxford). The bacterial pellet was then resuspended in 10 mL 'buffer P1,' then lysed at RT for 5 min via 10 mL buffer P2. Subsequently, 10 mL of buffer P3 was added and left on ice for 20 min, which halts the reaction. After which, the suspension was centrifuged at 150,000 x *g* for 30 min at 4°C. During which time the gravity filter column was calibrated by running 10 mL of buffer GC through the column. After centrifugation, the supernatant was then transferred to the filter column and left to run. The column was then washed 2 x 30 mL with buffer QC. DNA was then eluted into 15 mL falcon tubes (CLS430828, Sigma Aldrich, Oxford) via 10.5 mL of isopropanol and centrifuged at 15,000x *g* for 30 min at 4°C. The supernatant was discarded, and pelleted DNA was then washed in 70% ethanol and transferred to a 1.5 mL *Eppendorff* tube (NextAdvance) and centrifuged at 15,000x *g* for 10 min at 4°C. The supernatant was discarded, and the plasmid was resuspended in 200 µL of TE buffer, then quantified via Nanodrop 1000 spectrophotometer (Thermo Fisher Scientific) and processed via ND-1000 V.3.8.1 programme (Thermo Fisher Scientific) as above.

2.7 Single cell electrophysiology

2.7.1 The basic principles

The lipid membrane insulates the cell creating an impermeable barrier. This barrier allows for the formation of electrochemical gradients of charged ions, which are established by transporters within the membrane. Electrochemical gradients across the membrane create a potential difference measured in volts (*V*), which is the driving force of ions across the membrane (transmembrane potential; V_m). Ion channels form selective pores within the membrane. When open, the flow of ions carries electrical current (*I*) which is measured in amperes (A). Using electrophysiological techniques, including patch-clamp, the biophysical properties of ion channels can be investigated by measuring *I* in relationship to *V* using the following equations. Firstly, the most important electrical principal when concerning electrophysiology is Ohm's law,

$$I = \frac{V}{R}$$

In this context, resistance (*R*), is generated by the cell membrane and ion channels when closed as these impermeable barriers prevent the flow of *I* and can be measured in Ohms (Ω). Therefore, as *V* in the system increases, *I* increases. Additionally, as ion channels close *R* increases, and *I* decrease. For electrophysiology however, it is more appropriate to consider the conductance (*G*) of ion flow which is measured in Siemens and is the inverse of *R*,

$$G = \frac{1}{R}$$

As ion channels open, *G* increases. Additionally, *G* accumulates, thus, if one open channel is equal to 1*G*, then two open channels in the membrane is equal to 2*G*. Considering Ohm's law, we can instead substitute *R* for *G* to give,

$$I = GV$$

Using this equation, we can see that an increase in either *G* or *V*, *I* also increases. Therefore, increases in *I* in response to pre-determined increased *V* would relate to increases in *G*. As *G* directly relates to the open state of an ion channel, plotting current-voltage (*IV*) relationships can be used to study ion channel physiology.

Finally, we can apply these principles to individual ions. The equilibrium potential of an ion (E_{ion}) is the V_m whereby net movement of the ion is 0, which in turn is derived from the Nernst equation. The Nernst equation describes that the E_{ion} is largely dictated by the concentration of ions outside of the cell vs. the ions inside the cell. As the cell becomes permeable to an ion during the opening of its complimentary ion channel, the ion will diffuse across the membrane, causing a shift in V_m to E_{ion}. In the following investigations, heterologous over expression systems were used whereby HEK 293B transiently, or stably overexpressed $K_V7.1$ or $K_V7.4$ respectively. As such, the principal ion channel expressed within the membrane is selectively permeable to K^+ only. As the E_K for K^+ in the following experiment is -95 mV (V_K), the driving force for potassium K^+ can be more accurately described by,

$$I_K = G_K(V_m - V_K)$$

where the current for potassium is driven by the difference in V_m and V_K. As V_m becomes more positive, the driving force for K^+ increases resulting in outward current as represented by positive *I* values. If V_m is more negative than V_K, then current will flow into the cell represented by negative *I* values. This equation describes the basic principles of the currents represented in the following experiments.

2.7.2 Voltage-clamp

To characterise K_V7 channel activity, we opted for ruptured whole-cell continuous single electrode voltage clamp. In this system, a single electrode is used to both pass *I* and dictate a command voltage (V_{cmd}) via an amplifier. V_{cmd} is directly proportional to V_m and will be used synonymously forthwith. A glass pipette pulled to a low resistance was filled with internal solution and pressed against cells bathed in external solution. Within the pipette was a silver electrode connected to an amplifier. Back pressure in the pipette allows for a giga-ohm (GΩ) seal formation between the electrode and the cell membrane. Subsequently, a sharp increase in pressure was used to rupture the membrane, 'accessing' the cell. The electrode and the membrane then form a complete circuit with

the earth electrode in the bath and current passes through the cell. The experimenter then dictates V_m and measures *I* injection over a given period. The investigator can then plot *IV* relationships. See representative schematic in Figure 2.11.

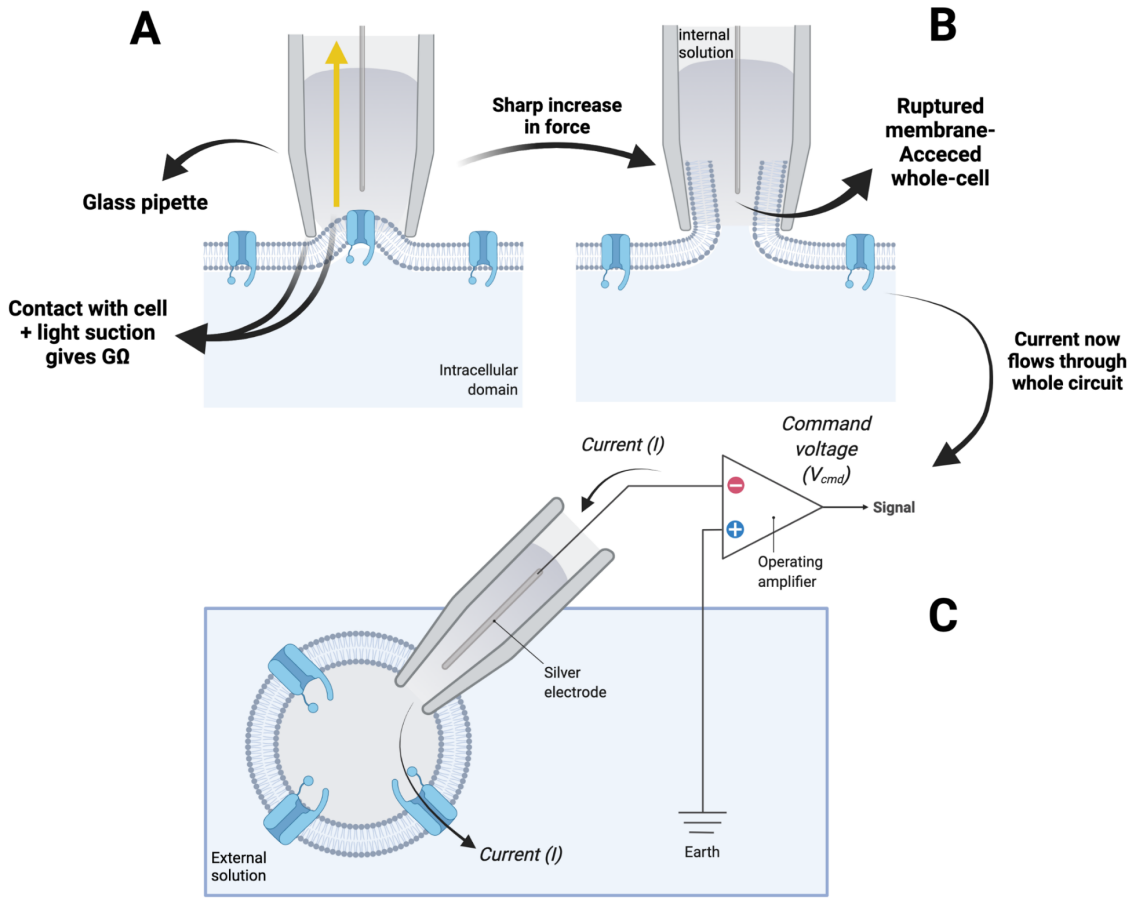

Figure 2.11: Diagrammatic representation of ruptured whole-cell voltage-clamp

A glass pipette makes contact with a cell, forming a tight gigaseal (GΩ) by slight backpressure in the pipette (A). A sharp increase in pressure in the pipette ruptures the membrane of the cell (B), giving access to the intracellular compartment creating a complete circuit (C). The investigator is then free to dictate V_m via the amplifier.

2.7.3 The set up

All currents in the following investigation were recorded using an AXOpatch 200B amplifier (Axon instruments) and Whole cell-electrical signals were made and digitized via Digidata 1550A series operated by pClamp 10.7 (molecular devices). Coverslips were mounted on an inverted Nikon Eclipse T5100 microscope fitted with a Nikon C-SHG mercury lamp. Cells were observed under a x40 objective + x10 eyepiece for x400 total magnification. The microscope was housed on an air-table inside a faraday cage to nullify vibration and electrical interference. Cells were bathed in an external solution composed of (in mmol-L^{-1}): 140 NaCl, 4 KCl, 2 $CaCl_2$, 10 HEPES, 1 $MgCl_2$ balanced to a pH of 7.4 with NaOH at RT. A 'static-bath' configuration was used, whereby cells were supplement with via a perfusion system that worked via gravity mediated flow. Short 20 sec intervals were used to wash the cells in drugs to ensure a total exchange of medium in the bath for new, drug containing medium. Gentle agitation of the microscope allowed for the determination of attached cells. Only firmly attached cells were used in the following investigation, as cell attachment was used as a crude metric of cell viability and enabled the formation of high quality GΩ. Glass pipettes (Plowden & Thompson) were pulled in house via PP-830 (Narishige, Japan) to a resistance of 6-10 MΩ. Pipettes were filled with an internal solution composed of (in mmol-L^{-1}): 110 K gluconate, 30 KCl, 0.5 $MgCl_2$, 5 HEPEs, 0.5 EGTA, 1 Na_2ATP.

For investigations involving HEK $K_V7.4$ cells transiently transfected with *GPER1* (pCMV3-GPER1-GFPSpark), fluorescence microscopy was used to identify transfected cells. As the plasmid containing *GPER1* contains a GFPSpark tag, upon exposure to excitation frequency (488 nm), transfected cells will fluoresce (510 nm). Cells that lacked fluorescence were considered non-transfected (see representative images in Figure 2.12).

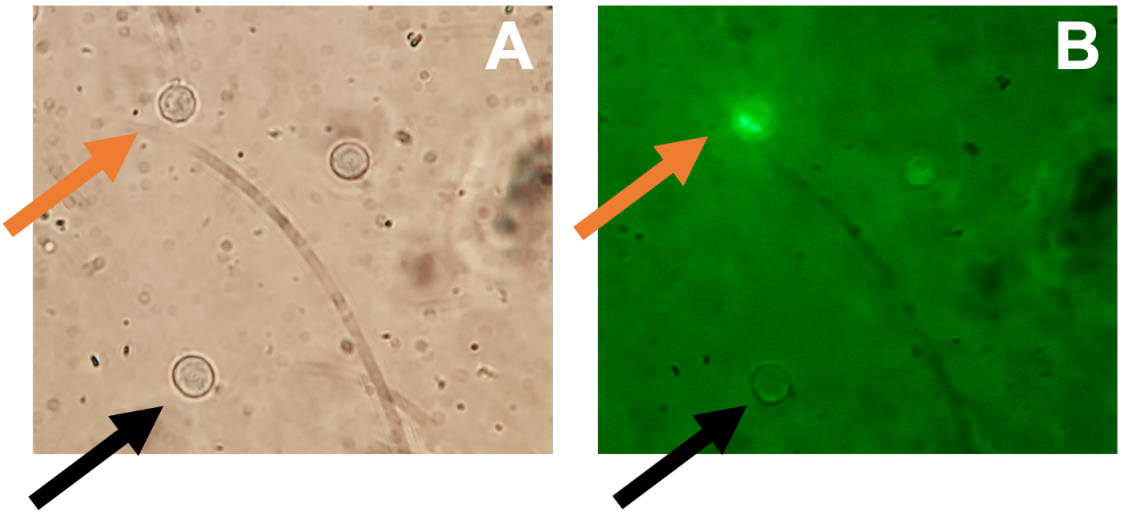

Figure 2.12: Representative GPER1-GFP spark fluorescence.

HEK K_V7.4 cells as observed under x40 magnification (Nikon Eclipse T5100) under bright field (A) or under fluorescence (B) microscopy (Nikon C-SHG). Red arrows indicate the same cell under light microscopy that fluorescence when the light source is exchanged for high-powered excitation wavelengths from the mercury lamp, which are therefore transfected. Black arrows indicate non-transfected cells that do not fluoresce under the same conditions and are therefore non-transfected. Authors photograph.

2.7.4 Protocols

Two protocols were used in the following investigations: 1.) post-access, the cell was held at -50 mV and in 20 sec intervals a 0.2 sec +20 mV step was run, and current amplitude measured. A minimum of three stable 'test pulses' were required to move on to the next stage of the protocol to account for 'run-up' or 'run-down' of the current amplitude (2.13.A). Subsequently, a '1.5 sec *IV* curve' protocol was run, whereby cells were held at -50 mV and every 15 sec for 1.5 sec V_m was stepped to a test V_m ranging from -70 - +40 mV increasing in 10 mV intervals, then stepped down to an inactivation step -40 mV for 0.1 sec before return to holding potential (2.13.B). This was used to generate 'Ctrl' current-voltage relationships. A secondary set of test pulses were run, in which three stable pulses were recorded prior to adding drug to the well, and post addition of a drug (2.13.C). After three stable test pulses, a final '1.5 sec *IV* curve' protocol was run (2.13.D). See representative voltage step protocols in figure 2.13.E,F. In this protocol, same-cell comparisons could be made in IV curves generated pre and

post application of drug. 2.) cells were pre-incubated in either solvent control, E2 (10 nmol-L^{-1}) or G-1 (1 µmol-L^{-1}) in the well for 30 minutes prior to cell access. Subsequently, one 'seal test' and one 'voltage-step' protocol was run. In this protocol, same cell comparisons could not be made, thus comparisons are between drug and transfection conditions.

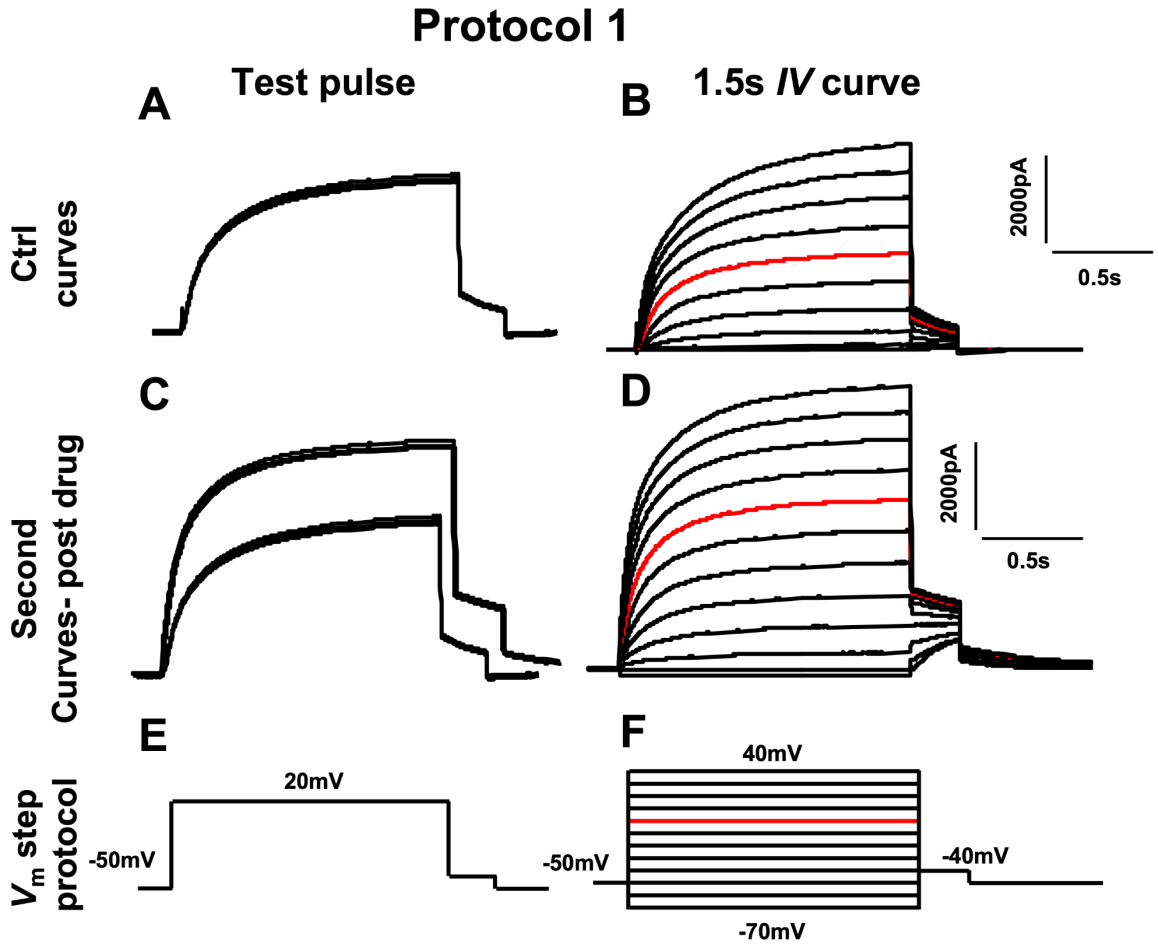

Figure 2.13: Voltage-clamp protocol 1

Representative figures of control (Ctrl) seal test (A) and 1.5 sec *IV* curve protocol (B) and second seal test (C) and voltage step protocol (D) after the addition of drug. Diagrammatic representation of the voltage steps in seal test (E) and voltage step (F) protocols below.

The investigator can then plot *IV* relationships, including; 1.) peak current, *I* expressed as pA divided by the cell capacitance, measured in Farads (pF) to give $I_{(pA/pF)}$. pF is directly proportional to the size of the phospholipid bilayer and was therefore used to normalise currents from cells of varying sizes. In investigations derived from protocol 1, pA/pF of second voltage-step protocol (post-drug) was normalised to Ctrl curve values

to reduce skew; 2.) tail currents, pA measured during inactivation step following each incremental increase in voltage was divided by current recorded at maximum step (+40 mV). A measurement of tail current gives inference of the amount of active channels at each *V*, expressed in units of *G*, to give *G/Gmax*; 3.) activation kinetics, τ, measured in milliseconds, is the measurement of the slope of current recorded at every voltage and is an inference of the rate of activation of ion channels.

2.8 Serum concentration of sex hormones

2 mL of blood was harvested following euthanasia into vials containing 100 µL of the anti-coagulant Ethylenediaminetetraacetic acid (EDTA). Samples were subsequently centrifuged at 2000 rpm for 20 minutes. Plasma was extracted and stored at -80ºC. Serum concentration of the following hormones were determined at the University of Virginia Ligand Core for clinical and basic scientific research projects via the following ELISAs; E2 (Calbiotech), Progesterone (IBL) and Testosterone (IBL). Additionally, Luteinizing hormone (LH) and follicular stimulating hormone (FSH) were analysed via an own in-house ELISA protocol. LH was measured in serum by a two-step sandwich immunoassay using monoclonal antibodies against bovine LH (no. 581B7) and against the human LH-beta subunit (no. 5303: Medix Kauniainen, Finland) as described previous (Haavisto *et al.*, 1993). FSH was assayed by RIA using mouse FSH reference prep AFP5308D for assay standards and Mouse FSH antiserum (guinea pig; AFP-1760191). See (https://med.virginia.edu/research-in-reproduction/ligand-assay-analysis-core/) for further detail.

2.9 Data analysis

All functional figures express mean data from at least 4 animals ±standard error of the mean (SEM). Power calculations, undertaken prior to the start of the project, demonstrated that *n*=4 was sufficient to determine the minimum number of subjects required to achieve sufficient statistical significance when comparing treatment

conditions. For functional experiments involving cumulative concentrations, a transformed data set was generated using; X=Log(X), to reduce representative skew. Following which a four parametric linear regression analysis was performed using the following equation; (Log(Agonist) vs. response – Variable slope (four parameters Bottom/Hillslope/top/EC_{50})) using GraphPad Prism (Version 8.2.0) to fit a concentration effect curve to the figure. For data comparing single groups, an unpaired student's t-test was used. For data comparing multiple groups, a Two way-ANOVA followed by a *post hoc* Bonferonni/Dunnet's test, to account for type 1 errors in multiple comparisons was performed for comparison of mean values. Significance values are represented as follows; $P<0.05$ (*/#/$). Investigations expressing groups of unequal numbers were gathered due to technical failure or an artefact of cycle stage determination post-experiment during functional investigations.

Chapter 3: K_V7 channels in the male vasculature, validating a molecular and pharmacological toolbox

3.1 Introduction

It is widely reported that *KCNQ*-encoded K_V7 channels are key regulators of vascular reactivity within rodent and human arteries, whereby activation of the channel mediates hyperpolarization of the membrane, closure of VGCCs and vasorelaxation. In vascular tissue, of the five subtypes; *KCNQ1*, *KCNQ4* and *KCNQ5* are the principally expressed transcripts (Ohya *et al.*, 2003; Ng *et al.*, 2011), $K_V7.4$ is the predominantly expressed protein (Yeung *et al.*, 2007; Ng *et al.*, 2011) and the $K_V7.4/K_V7.5$ heterotetramer is purported to be the most common channel stoichiometry (Chadha *et al.*, 2014; Lyubov I. Brueggemann *et al.*, 2014; Brueggemann, Cribbs and Byron, 2020a). Moreover, pharmacological and molecular evidence demonstrates that $K_V7.4/K_V7.5$ activity regulates RMP and therefore basal tone of the artery (Mackie *et al.*, 2008) and is functionally important for cAMP- and cGMP-linked receptor mediated vasorelaxation (Chadha, Zunke, Zhu, *et al.*, 2012; Chadha *et al.*, 2014; Stott, Barrese, *et al.*, 2015; Stott, Barrese and Greenwood, 2016; Mondéjar-Parreño *et al.*, 2019) and PKC-mediated contraction (Brueggemann *et al.*, 2006). See chapter 1.5.4 for greater detail. Throughout the course of this thesis, I have relied on a selection of pharmacological and molecular tools to derive conclusions regarding vascular K_V7 channel physiology and pathophysiology within the Wistar rat. The aim of this chapter was to establish the specificity of said tools and to replicate previously published findings regarding the molecular and functional properties of K_V7 channels within the vasculature of the male.

The findings detailed herein confirm the currently accepted role of K_V7 channels within the male vasculature.

3.2 Methods

The methods and materials applied in the following chapter are described in detail in Chapter 2.

3.2.1 Protein extraction and quantification

Arteries from male and female arteries were dissected of fat and adherent tissues then placed on ice in 100 µL of a cell lysis buffer of the following constitution, in mmol/L^{-1}; 20 Tris base, 137 NaCl, 2 EDTA, 1% NP40, 10% glycerol, pH 8, and 10 µL/mL protease inhibitor cocktail (Sigma-Aldrich, P8340). Samples were mechanically homogenised via dissection scissors and mechanical bead mill then placed on ice for 30 mins before centrifugation of cell debris. Cell supernatant was extracted and stored at -85°C.

Sample protein concentration was determined via Bradford assay prior to gel running. A bovine serum albumin (BSA; Sigma, A2153) standard curve diluted in PBS was made fresh prior to each assay. BSA standard curve included the following concentrations in µg/mL; 0 (blank), 0.5, 1, 2, 4, 8, 16. 80 µL BSA samples were placed into 96 well plate. Additionally, 2 µL of sample was diluted in 318 µL of PBS. 3x 80 µL of sample diluted in PBS was then placed into the same 96 well plate. Via multi-channel pipette, 20 µL of Bradford reagent (Sigma Aldrich, B6916) was placed into each well simultaneously. Giving a final dilution of sample at 1:200. Samples were run in triplicate. Blanks were made of 2 µL of cell lysis buffer diluted in 318 µL of PBS. Samples were then taken to a spectrophotometer (Promega GloMax) and absorbances at 595 nm were read. A linear regression analysis of the absorbance values recorded for the BSA standard curve was then calculated. The absorbance value for each sample was then subtracted from the blank value, and the linear regression analysis is then used to calculate the concentration

of the sample, then multiplied by 200 to account for the initial sample dilution, given in µg/mL.

3.2.2 Gel electrophoresis, protein transfer, staining, and relative protein quantification

A solution of the following composition; 40 µg of sample made up to 28 µL with cell lysis buffer, 10 µL TruPAGE™ Sample buffer x4 (Sigma, PCG3009) and 2µL NuPAGE™ sample reducing agent x10 (Invitrogen, NP0009), was denatured at 95°C for 5 min. 12 well TruPAGE™ SDS-PAGE (4-12% Bis-Tris) Precast Gel (Invitrogen, NP0335BOX) were loaded into a cartridge containing NuPAGE™ MOPS SDS running buffer (x20, 2062902) diluted in water. Samples were then loaded into the gel wells in combination with Chameleon duo pre-stained protein ladder (Li-Cor Bioscience, 928-60000). Samples then underwent electrophoresis at 200 V for 50 min via Invitgrogen Power Ease 500. The gel was then removed from its cast, mounted into a transfer chamber bathed in NuPAGE™ transfer buffer (x20, 2035702) diluted in water. Protein was then transferred from the gel to Polyvinylidene fluoride membrane (Milipore, UK) on ice under the following conditions: 50 V for 90 min. The membrane was then washed 3x 10 min in blocking solution (0.1% PBS-Tween20, 5% Milk). The membrane was then probed with anti-K_V7.4 (1:100, Alamone labs, #APC-164) and anti-β-actin (1:5,000, Sigma-Aldrich, A1978) overnight at 4°C diluted in blocking solution. The following morning, the membrane was washed 3x 10 min in blocking solution and secondary antibodies IRDye ® 800 CW Goat anti-mouse (Li-Cor bioscience, 925-32210) and IRDye ® 680 CW Donkey anti-rabbit (Li-Cor bioscience, 925-68073) diluted in blocking solution for 1 hr at rt. The membrane was then washed in blocking solution for 3x 10 min, then PBS 1x 10 min before imaging. Protein bands were visualised by immunofluorescence via Odyssey Clx (Li-Cor Bioscience) and analysed via Image Studio™ (Li-cor Bioscience) software. Values expressed as fluorescence intensity of target normalised to fluorescence intensity of β-actin.

3.3 Results

3.3.1 Characterising K_V7 channel modulators

3.3.1.1 Ruptured whole cell electrical currents recorded in HEK-$K_V7.4$ cells demonstrates $K_V7.2$-5 channel modulator activity at the level of the channel

As $K_V7.4$ is regarded as the principal functional component of the vascular $K_V7.4/7.5$ heterotetramer, initial electrophysiological investigations sought to characterise putative activators of K_V7 channels on *KCNQ4* encoded current. In whole cell current recordings, cells transfected with $K_V7.4$ exhibited larger time and voltage-dependent currents than non-transfected cells ($P \leq 0.05$; $n=8$; Fig 3.1.A). Both linopirdine, and its more potent analogue XE-991 are well characterised inhibitors of *KCNQ*-encoded K_V7 channels (Costa and Brown, 1997; Schnee and Brown, 1998) that preferentially block the open state channel by binding to individual subunits of the hetero/homotetramer (Greene, Kang and Hoshi, 2017). Similar to previous reports (Costa and Brown, 1997; Schnee and Brown, 1998), currents recorded in the presence of 10 μmol-L^{-1} XE-991 or Linopirdine were significantly smaller compared to cells incubated with DMSO solvent control ($P \leq 0.05$; n=6-11; Fig 3.1.B). Representative traces of voltage-evoked currents during ruptured whole cell current recordings and their respective voltage-step protocol are shown in figure 3.1.C. Overall, HEK cells expressing $K_V7.4$ produced slowly activating voltage dependent outward currents typical of K^+ channels that were sensitive to both linopirdine and XE991 and greater than currents from untransfected cells.

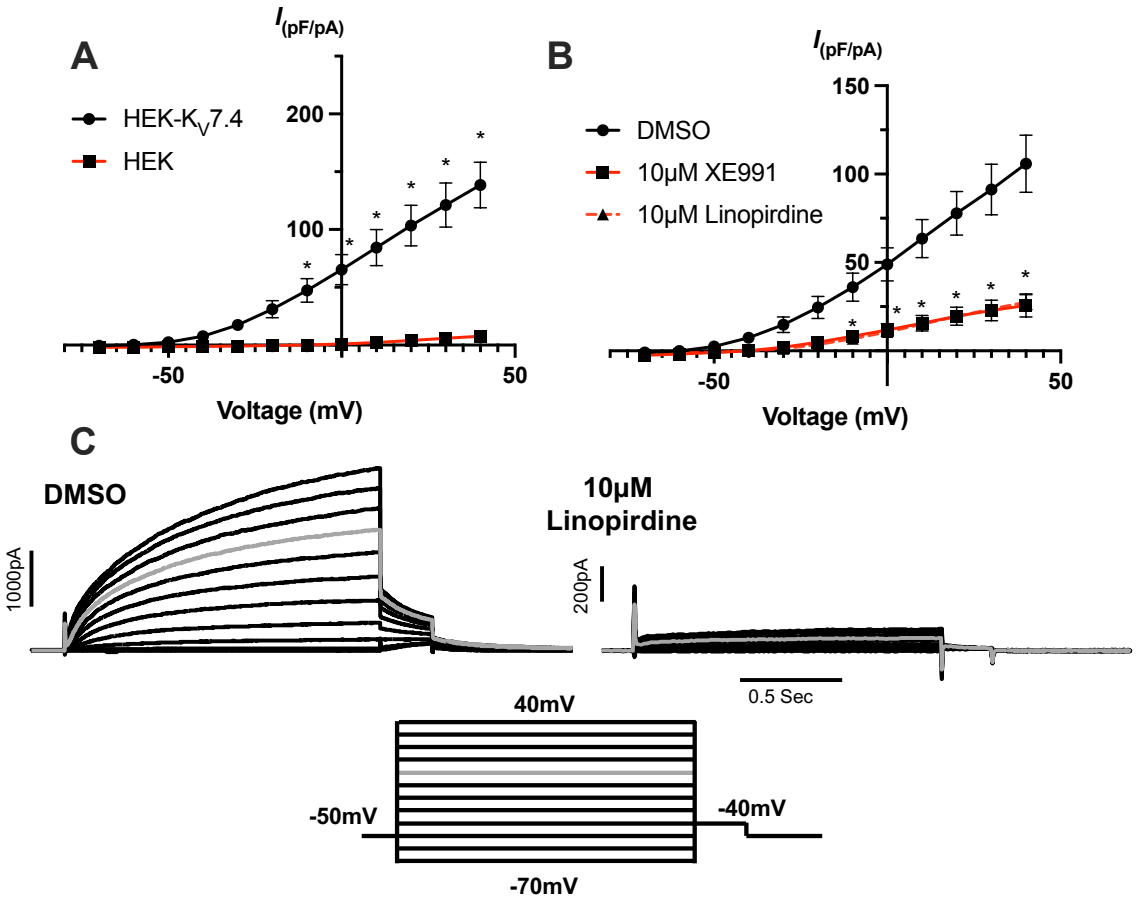

Figure 3.1: Voltage activated currents in HEK cells are K_V7.4 dependent and are ablated by Linopirdine/XE-991.

Current voltage (*IV*) relationship plotted for mean data generated from human embryonic kidney (HEK) cells stably expressing *KCNQ4* (HEK-K_V7.4; black; *n*= 8) vs non-transfected HEK cells (red; *n*=8) during ruptured whole cell current recording (A). Mean data for *IV* curves for HEK-K_V7.4 cells pre-incubated in solvent control (DMSO; black; *n*=8) or either pan-K_V7 channel inhibitors XE-991 (10 μmol-L^{-1}; red; *n*=11) or the structurally dissimilar Linopirdine (10 μmol-L^{-1}; red, dashed line; *n*=6; B). Representative traces of *IV* curves for HEK-K_V7.4 cells pre-incubated in DMSO (left) or linopirdine (right) and the voltage-step protocol used to generate the data below (C). Grey line demonstrates current recorded at +10mV (C). All values are expressed as mean + SEM. A two-way statistical ANOVA with either a post-hoc Bonferroni (A) or Dunnet's's (B) test was used to generate significance values (*= $P \leq 0.05$).

ML213 and the structurally dissimilar retigabine stimulate *KCNQ4*-encoded $K_V7.4$ channels via a binding site, tryptophan-242 residue, in the S5 pore-forming domain (Schenzer, 2005; Jepps *et al.*, 2014). Similarly to previous reports, when using protocol 1 (see Chapter 2.7.2), ML213 (10 μmol-L^{-1}) and retigabine (30 μmol-L^{-1}) significantly enhanced currents when compared to control ($P \leq 0.05$; n=11-24; Fig 3.2.B,E), as demonstrated in representative traces in figure 3.2.A. In addition, a significant leftward shift in the voltage at half-maximal activation ($V_{½}$) was observed in response to ML213 (Δ -17.05±2.8 mV; n=11) and Retigabine (Δ-7.85±2.5 mV; n=11) when compared to control currents ($P \leq 0.05$; Fig 3.2.C,F). Finally, ML213, but not retigabine enhanced the activation kinetics for $K_V7.4$ derived currents plotted for -40 mV – +40m mV, as demonstrated by a significant reduction in τ, a measurement of time function which represents time taken to achieve stable current amplitude ($P \leq 0.05$; n=11-24; Fig 3.2.D,H).

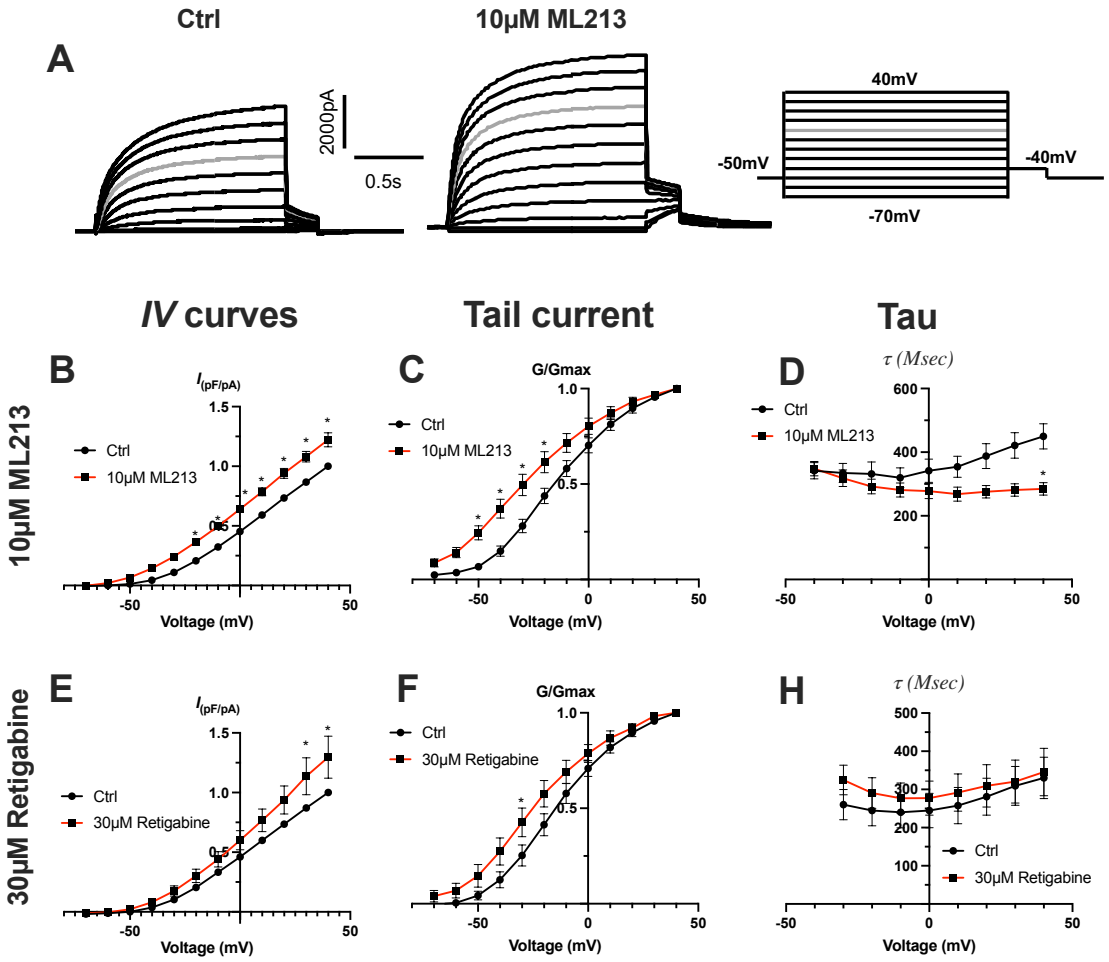

Figure 3.2: The structurally dissimilar K_V7.2-5 activators ML213 and retigabine enhance HEK-K_V7.4 currents.

Representative traces of control *IV* curves from HEK-K_V7.4 cells pre-addition (Ctrl) and post-addition of K_V7.2-5 activator ML213 (10μmol-L^{-1}) and the voltage-step protocol used to generate the data (A). Grey line demonstrates current recorded at +10 mV. *IV* curves plotted for mean data generated from HEK-K_V7.4 before (Ctrl; black; *n*= 11; B-E) and after addition of either K_V7.2-5 channel activators ML213 (10 μmol-L^{-1}; red; *n*= 11; B-D) or retigabine (10 μmol-L^{-1}; red; *n*= 11; E-H). Values expressed as either; 1.) peak current (B,E); 2.) tail current (C,F); 3.) activation kinetics (D,H). All values are expressed as mean + SEM. A two-way statistical ANOVA with a post-hoc Bonferroni test was used to generate significance values (*= *P* ≤0.05). (*n*=) number of cells used.

3.3.1.2 Ruptured whole cell current recordings in HEK-K_V7.1 cells demonstrates K_V7.1 channel modulator activity at the level of the channel

As described in chapter 1.5.5.1, K_V7.1 along with the β-auxiliary subunit protein KCNE1 is the molecular correlate of I_{Ks}. Mutations of this channel underpin Long-QT syndrome, giving rise to life threatening cardiac arrythmias (Schwartz, Crotti and Insolia, 2012). An array of pharmacological modulators has been developed to study K_V7.1 channel activity. Similar to above, cells transiently transfected with *KCNQ1* exhibited currents that were considerably larger than currents from un-transfected HEK cells ($P \leq 0.05$; n=8-11; Fig 3.3.A).

HMR-1556 is a selective and potent inhibitor of I_{Ks} currents in heterologous over expression systems and IPS cells (Gerlach *et al.*, 2001; Thomas, Gerlach and Antzelevitch, 2003). Here, HMR-1556 (10 µmol-L^{-1}) significantly reduced $I_{(pA/pF)}$ amplitude in HEK-K_V7.1 cells when compared to cells pre-incubated in DMSO solvent control ($P \leq 0.05$; n=3-4; Fig 3.3.B) but had no effect on currents in HEK-K_V7.4 cells (n=8-11; Fig 3.3.D). See representative traces in Figure 3.3.C. In summary, HMR-1556 is a selective blocker of K_V7.1 channels, with little to no effect on K_V7.4 channels.

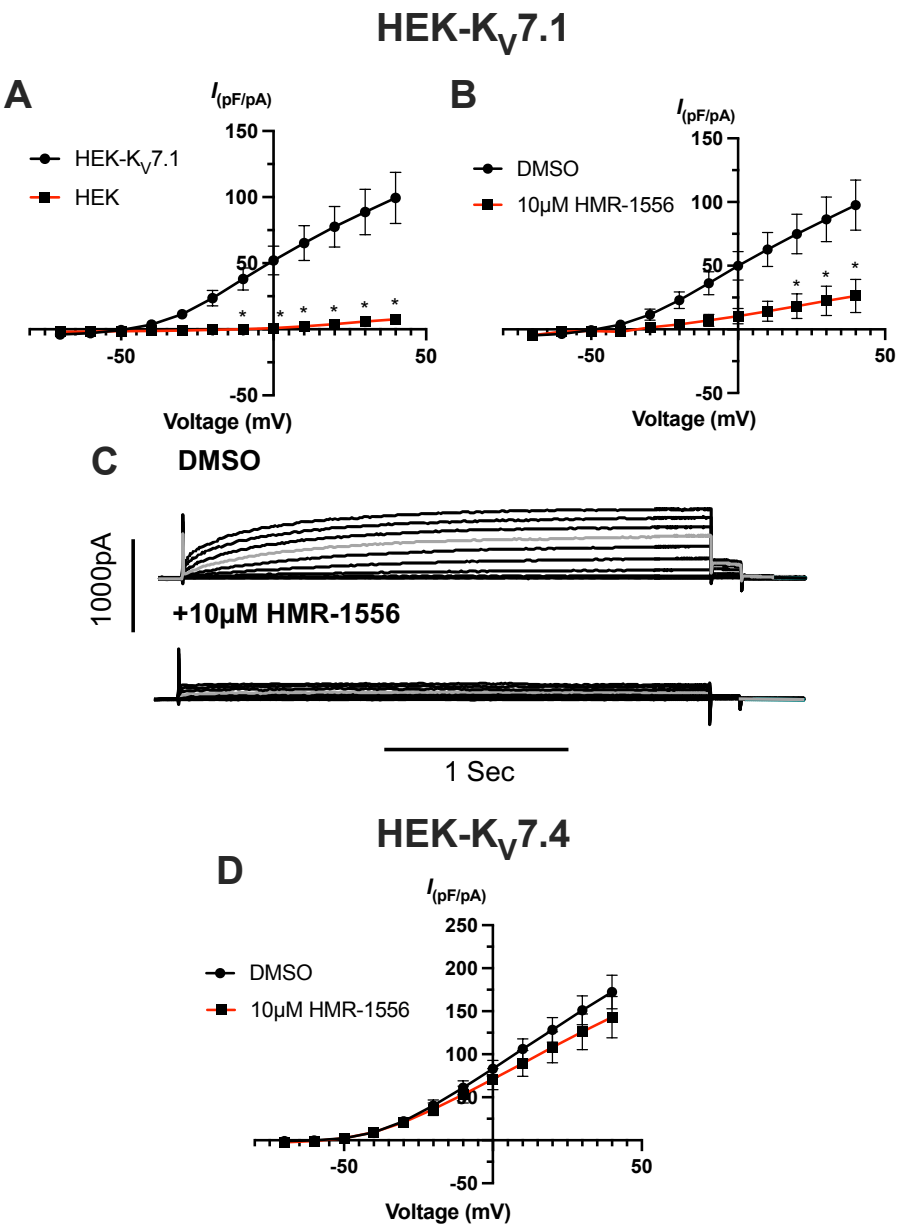

Figure 3.3: Voltage activated currents in HEK-K$_V$7.1 cells are dependent on K$_V$7.1 and are HMR-1556 sensitive.

Current voltage (*IV*) relationship plotted for mean data generated from human embryonic kidney (HEK) cells transiently expressing *KCNQ1* (HEK-K$_V$7.1; black; *n*= 11) vs non-transfected HEK cells (red; *n*=8) during ruptured whole-cell current recording (A). Mean data for *IV* curves generated in HEK-K$_V$7.1 pre-incubated in either DMSO solvent control (Black; *n*=4) vs HEK-K$_V$7.1 cells pre-incubated in K$_V$7.1 specific blocker HMR-1556 (10 μmol-L^{-1}; red; *n*=3; B). Representative traces of *IV* curves for HEK-K$_V$7.4 cells pre-incubated in DMSO (upper) or HMR-1556 (lower) (C). Grey line demonstrates current recorded at +10mV (C). Mean data for *IV* curves generated in HEK-K$_V$7.4 pre-incubated in either DMSO solvent control (Black; *n*=8) vs HEK-K$_V$7.4 cells pre-incubated in K$_V$7.1 specific blocker HMR-1556 (10 μmol-L^{-1}; red; *n*=8; D). All values are expressed as mean + SEM. A two-way statistical ANOVA with a post-hoc Bonferroni test was used to generate significance values (*= $P \leq 0.05$). (*n*=) number of cells used.

The $K_V7.1$ modulator ML277 and the putative $K_V7.2$-5 activator ML213 were screened on HEK-$K_V7.1$ cells. Similar to previous reports (Yu, 2013; Hou *et al.*, 2019), 1 μmol-L^{-1} ML277 evoked an increase in $I_{(pA/pF)}$ independent of a change in $V_{½}$ within HEK-$K_V7.1$ cells when compared to control curve (P≤0.05; n=4; Fig 3.4.B.C). See representative traces in Figure 3.4.A. In contrast to Hou *et al.,* (2019), no difference in current kinetics were observed after the addition of ML277 (Fig 3.4.D). Additionally, ML213 (10 μmol-L^{-1}), significantly enhanced HEK-$K_V7.1$ currents (P≤0.05; n=4; Fig 3.3.E), though to a lesser extent than HEK-$K_V7.4$ cells. Moreover, ML213 had no effect on the $V_{½}$ nor activation kinetics of the current (n=4; Fig 3.4.F,G). Finally, ML277 had no effect on *IV* curves generate in HEK-$K_V7.4$ cells (n=6; Fig 3.4.H).

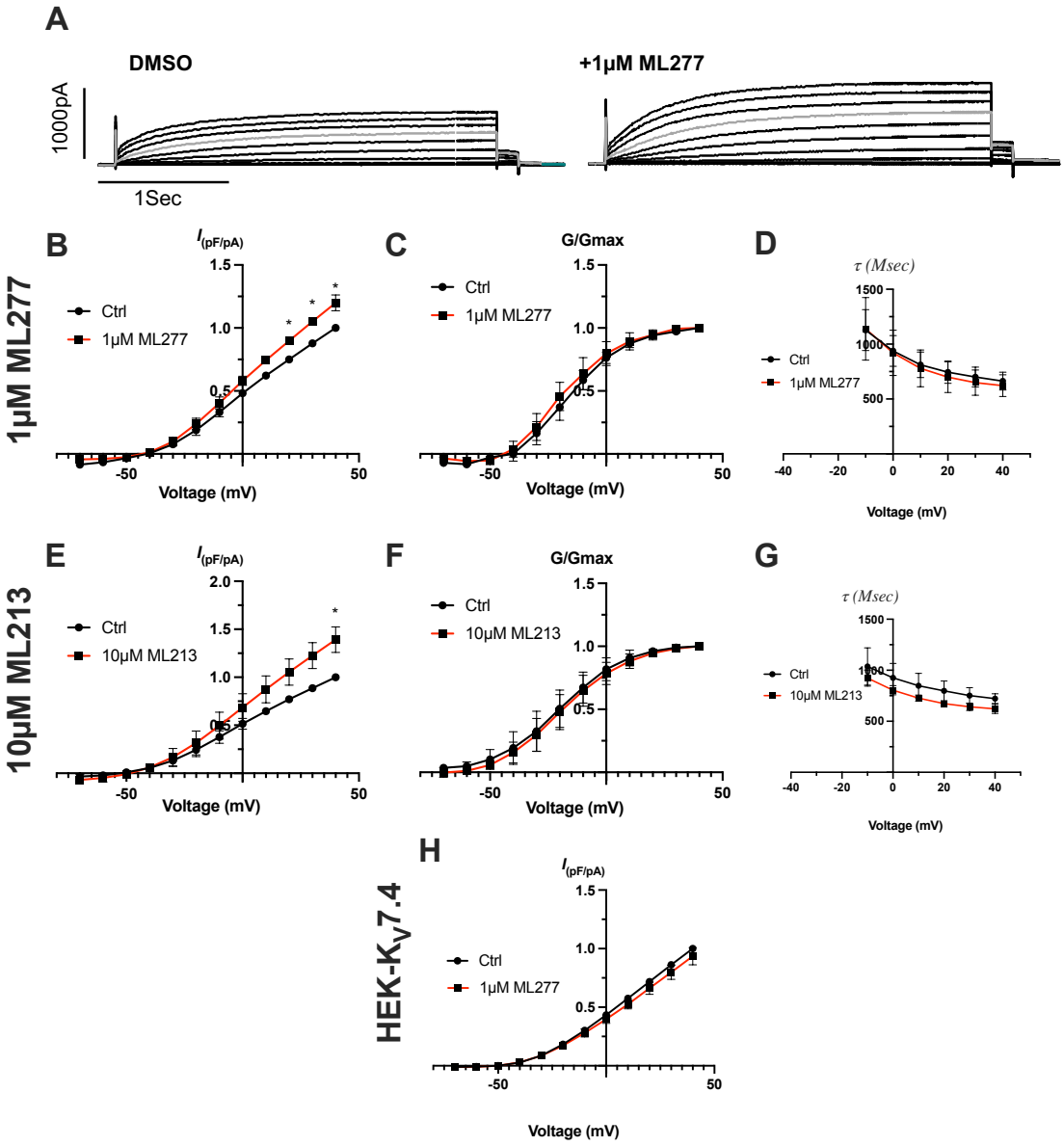

Figure 3.4: K_V7.1 specific activator ML277 enhances HEK-K_V7.1 currents.

Representative traces of control *IV* curves form HEK-K_V7.1 cells pre-addition (Ctrl) and post-addition (+1μM ML2277) of K_V7.1 activator (A). Grey line demonstrates current recorded at +10m V. *IV* curves plotted for mean data generated from HEK-K_V7.1 (A-G) or HEK-K_V7.4 (H) cells before (Ctrl; black; *n*=4; B-H) and after addition of either K_V7.1 channel activator ML277 (1 μmol-L^{-1}; red; *n*= 4-g; B-D,H) or K_V7.2-5 channel activator ML213 (10 μmol-L^{-1}; red; *n*= 4; E-H). Values expressed as either; 1.) peak current (B,E,H); 2.) tail current (C,F)' 3.) rate of activation (D,G). All values are expressed as mean + SEM. A two-way statistical ANOVA with a post-hoc Bonferroni test was used to generate significance values (*= *P* ≤0.05). (*n*=) number of cells used.

3.3.1.3 Isometric tension recoding of male mesenteric arteries validates K_V7 channel modulator specificity

Isometric tension recordings were generated in 2nd order mesenteric arteries from male Wistar rats in accordance with protocol 2 (see Figure 2.4 in Chapter 2). Three structurally different activators of $K_V7.2$-5 were studied, namely retigabine, ML213 and S-1. The latter also interacts with the same pharmacophore centered around a tryptophan in the S5 domain utilized by retigabine (Bentzen et al., 2006; Brueggemann et al, 2014; Jepps et al., 2014; Schenzer, 2005). Due to the collapse of NeuroSearch, a Danish Biotechnology company and the sole producer of S-1, our stock of this drug was exhausted before it could be screened on HEK-$K_V7.4$ cells via ruptured whole-cell current recording, however previous work by Bentzen *et al,.* (2006) provides a comprehensive electrophysiological description of S-1-mediated effects on $K_V7.4$ derived currents, whereby S-1 increases peak amplitude and channel conductance mediating a left-ward shift in $V_{½}$.

Consistent with previous findings (Chadha, Zunke, Zhu, *et al.*, 2012; Khanamiri *et al.*, 2013; Jepps *et al.*, 2014), S-1, ML213 and retigabine-mediated vasorelaxation (0.1-10/30 µmol-L^{-1}) of pre-contracted arterial tone (300 nmol-L^{-1} U46619), which was ablated by pre-incubation with 10 µmol-L^{-1} of the pan-K_V7 channel inhibitor linopirdine ($P \leq 0.05$; n=4-5; Fig 3.5.A-D). See representative trace of S-1-mediated relaxation in figure 3.5.A. The relaxation in response to K_V7 channel activators was considerably different than a loss of vascular tone, as application of equal volumes of DMSO solvent control had no effect (n=5; Fig 3.5.B). ML277-mediated relaxations were also prevented by incubation with linopirdine, although only at concentrations of <1 µmol-L^{-1} (P0.05; n=4-5; Fig 3.5.E). Therefore, relaxation in response to ML277 above <1 µmol-$L^{-1}$are not driven by $K_V7.1$. In summary, ML213, S-1, Retigabine and concentrations of ML277 not exceeding 300 nmol-L^{-1} are selective and potent modulators of K_V7 channels and were used to investigate functional K_V7 responses in our vessels.

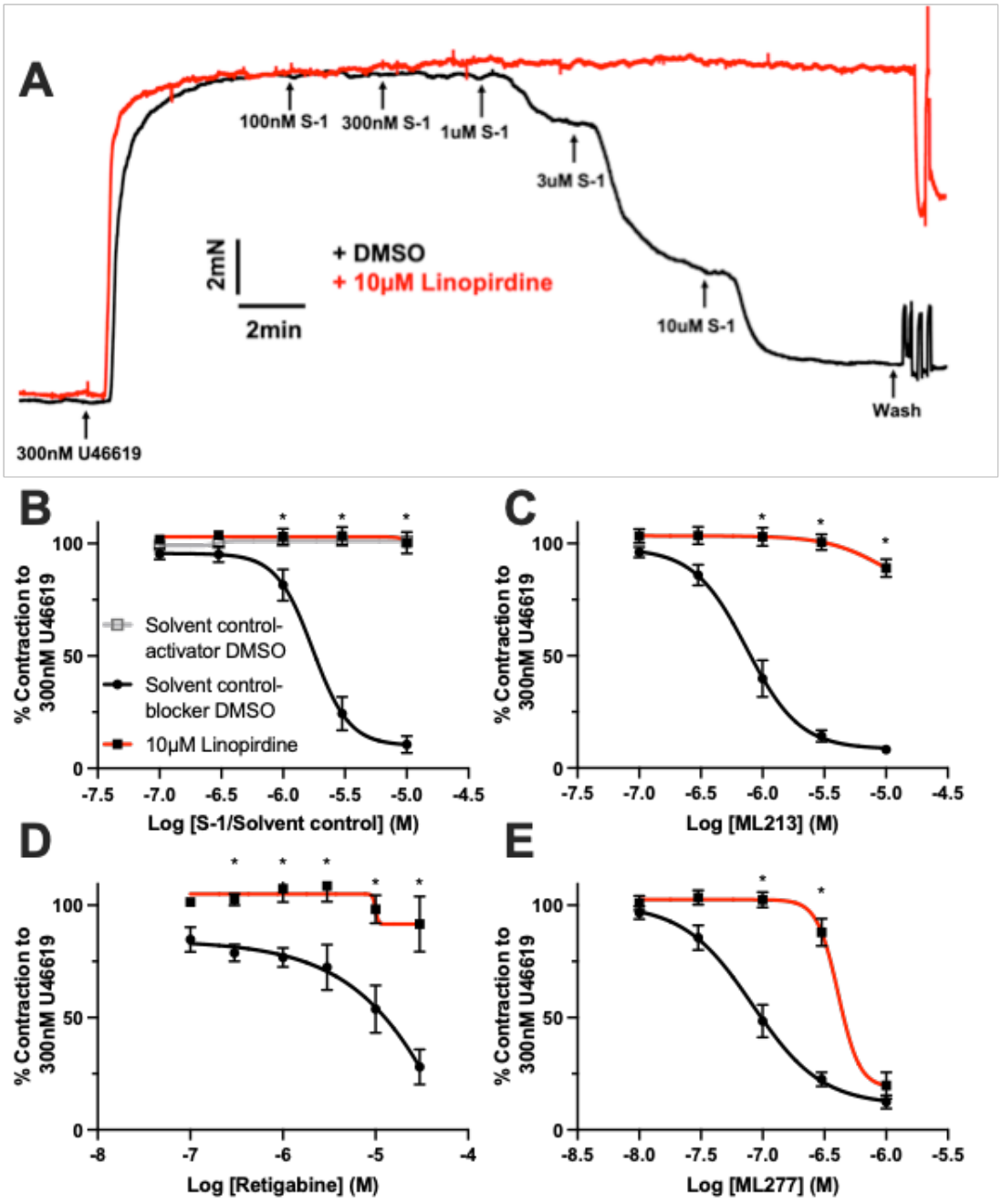

Figure 3.5: K_V7 channel activator-mediated relaxation in male mesenteric arteries is ablated by 10 μmol-L^{-1} Linopirdine pre-incubation.

A representative trace of S-1-mediated vasorelaxation (1-10 μmol-L^{-1}) in male mesenteric arteries pre-incubated in either DMSO solvent control (black) or 10 μmol-L^{-1} linopirdine (red; D). Mean data for vasorelaxation of pre-constricted arterial tone (300 nmol-L-1 U46619) in vessels pre-incubated in either DMSO solvent control (black; B-D) or pan K_V7 channel inhibitor linopirdine (10 μmol-L^{-1}; red; *n*= 5; B-D) in response to $K_V7.2$-5 channel activators S-1 (0.1-10 μmol-L^{-1}; *n*=4; B), ML213 (0.1-10 μmol-L^{-1}; *n*=4; C) and retigabine (0.1-30 μmol-L^{-1}; *n*=5; D) or $K_V7.1$ channel activator ML277 (0.01-1 μmol-L^{-1}; *n*=4; E. Application of DMSO solvent control to pre-contracted arteries has no effect (*n*=5; B). All values are expressed as mean + SEM. A 2-way statistical ANOVA with a post-hoc Bonferroni test was used to generate significance values. Statistical significance is defined as *$P \leq 0.05$ (A-C).

3.3.2 K_V7 channels are essential regulators of male arterial vascular physiology

In this section, we aimed to characterise the effect of K_V7 channel modulators on an array of vascular beds including main renal, 2nd order mesenteric, basilar, and left-anterior descending to delineate and ratify the contribution K_V7 channels to vascular tone and receptor mediated vasoactive responses within the male.

3.3.2.1 ML213 and S-1 are potent and efficacious vasorelaxants

Having established the specificity of these K_V7 channel modulators, concentration effect curves were generated in response to S-1, ML213 and retigabine (0.1-10/30 μmol-L^{-1}) on arterial tone generated by application of U46619 300 nmol-L^{-1}. Similar to previous reports (Jepps *et al.*, 2014), ML213 and S-1-mediated relaxations were more potent or efficacious in all arteries when compared to Retigabine (Fig 3.6.A-C).

K_V7, channels contribute to the resting membrane potential of VSMCs (Mackie *et al.*, 2008) and inhibitors of the channel mediated an increase in basal tone across and array of arteries (Mackie *et al.*, 2008; Ng *et al.*, 2011; Chadha, Zunke, Zhu, *et al.*, 2012; Khanamiri *et al.*, 2013; Mani *et al.*, 2013). Here, the pan-K_V7 channel inhibitor Linopirdine, but not the K_V7.1 specific inhibitor HMR-1556 (10 μmol-L^{-1}) increased basal tone in all arteries (P≤0.05; n=10-14; Fig 3.7). Though this failed to reach statistical significance in mesenteric artery.

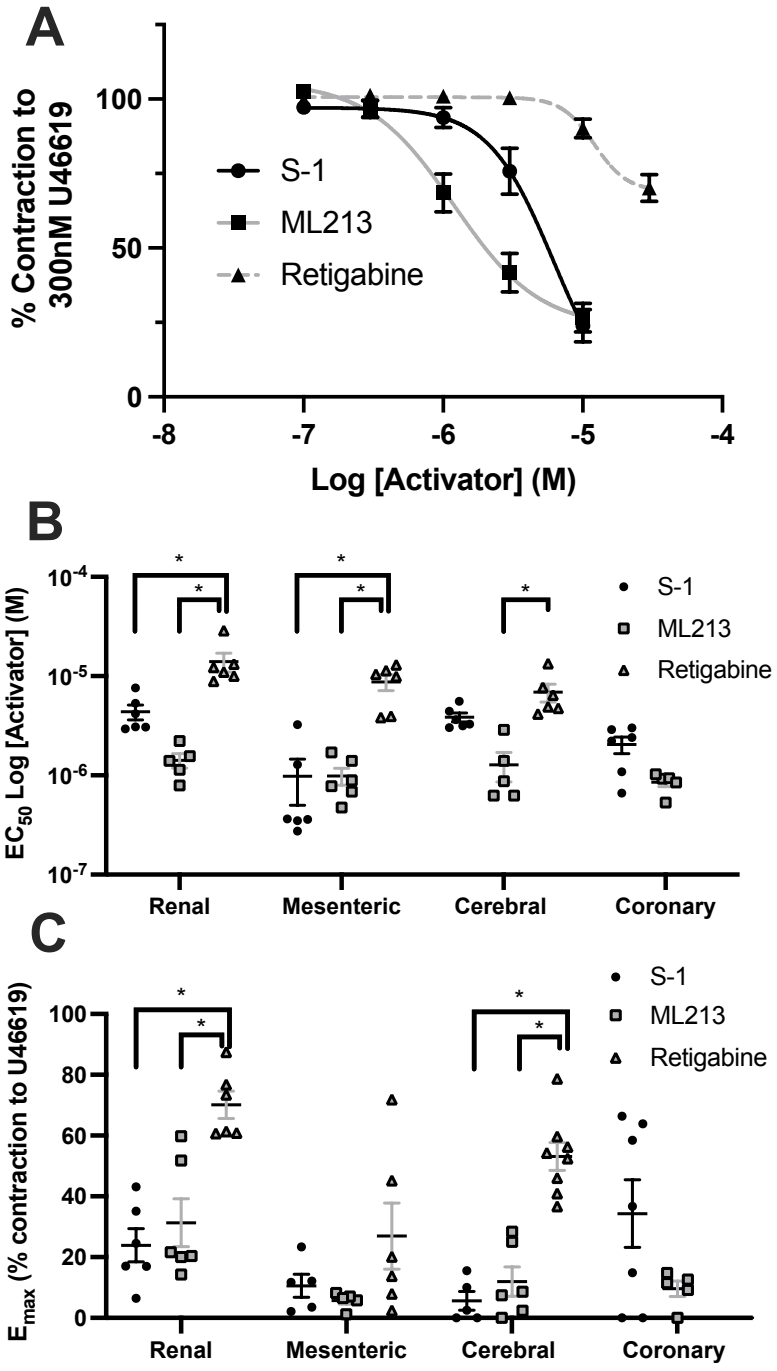

Figure 3.6: K_V7 channel activator-mediated relaxation in various arteries

$K_V7.2$-5 channel activators S-1 (0.1-10 μmol-L^{-1}; black; *n*=5), ML213 (0.1-10 μmol-L^{-1}; grey; *n*=5) and retigabine (0.1-30 μmol-L^{-1}; grey, dashed line; *n*=6) mediate relaxation of pre-constricted arterial tone (300 nmol-L-1 U46619) in male renal arteries (A). Scatter graph plot with mean ±SEM of EC_{50} (B) and E_{max} (C) vales for S-1 (dot), ML213 (square) and retigabine-mediated relaxation in renal (*n*=5-6), mesenteric (*n*=5-6), cerebral (*n*=5-8) and coronary (*n*=5-7) arteries. All values are expressed as mean + SEM. A 2-way statistical ANOVA with a post-hoc Bonferroni test was used to generate significance values. Statistical significance is defined as **P*≤0.05 (A-C).(*n*=) number of samples used.

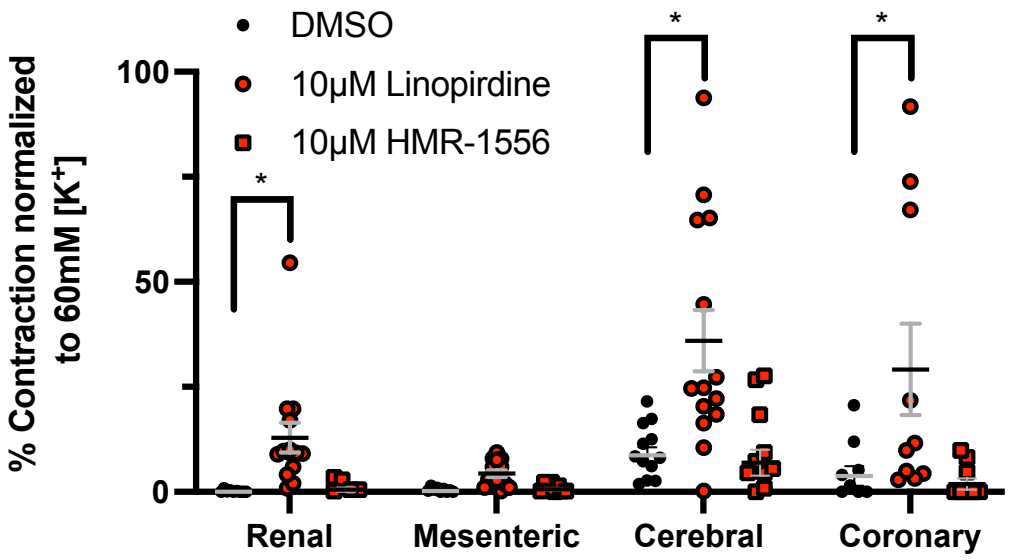

Figure 3.7: Contraction in response to K_V7 channel inhibitors in arteries from male Wistar rats.

Mean data for increase in basal tone normalised to contraction in response to 60mM K^+ was in response to DMSO solvent control (black), 10 μmol-L^{-1} pan K_V7 channel inhibitor Linopirdine (red,) or 10μmol-L^{-1} $K_V7.1$ specific inhibitor HMR-1556 (red pattern, black boarder) renal (A) (*n*=11-14), mesenteric arteries (*n*=10-14), cerebral (*n*=13-14) and coronary (*n*=12) arteries. All values are expressed as means ± SEM error bars. A two-way statistical ANOVA with a post-hoc Dunnet's test was used to generate significance values (*= $P \leq 0.05$). (*n*=) number of animals used (A-D).

3.3.2.2 U46619-mediated vasoconstriction is sensitive to K_V7.2-5 channel inhibition

K_V7 channel contribution to TXA_2 receptor agonist, U46619, mediated vasoconstriction was pharmacologically discerned via the use of the K_V7 channel inhibitors linopirdine (10 μmol-L^{-1}) and HMR-1556 (10 μmol-L^{-1}).

Concentration-dependent vasoconstriction in response to U46619 (0.003-3 μmol-L^{-1}) was observed within all arteries (Fig 3.8.A-E). Linopirdine pre-incubation significantly enhanced U46619-mediated vasoconstriction at concentrations ≤0.3 μmol-L^{-1} in renal arteries (*P*0.05; *n*=10-11; Fig 3.8.A) and at concentrations ≥0.3 and ≥1 μmol-L^{-1} in mesenteric and cerebral arteries respectively (*P*0.05; *n*=6-11; Fig 3.8.B,C). Additionally, Linopirdine increased the potency of U46619-mediated vasoconstriction in mesenteric and renal as demonstrated reduction in EC_{50} (in μmol-L^{-1}); mesenteric, DMSO-0.097±0.01, Linopirdine- 0.057±0.007 (*P*0.057); renal, DMSO- 0.058±0.012, Linopirdine-0.034±0.006 (Fig 3.8.E), though this failed to reach statistical significance. In contrast, Linopirdine pre-incubation had no effect on U46619 within coronary arteries (*n*=5; Fig 3.8.D). Finally, HMR-1556 had no effect on U46619-mediated contraction any artery (Fig 3.8.A-E). These data support a role for K_V7.4/7.5 in dampening TXA_2-mediated contractions.

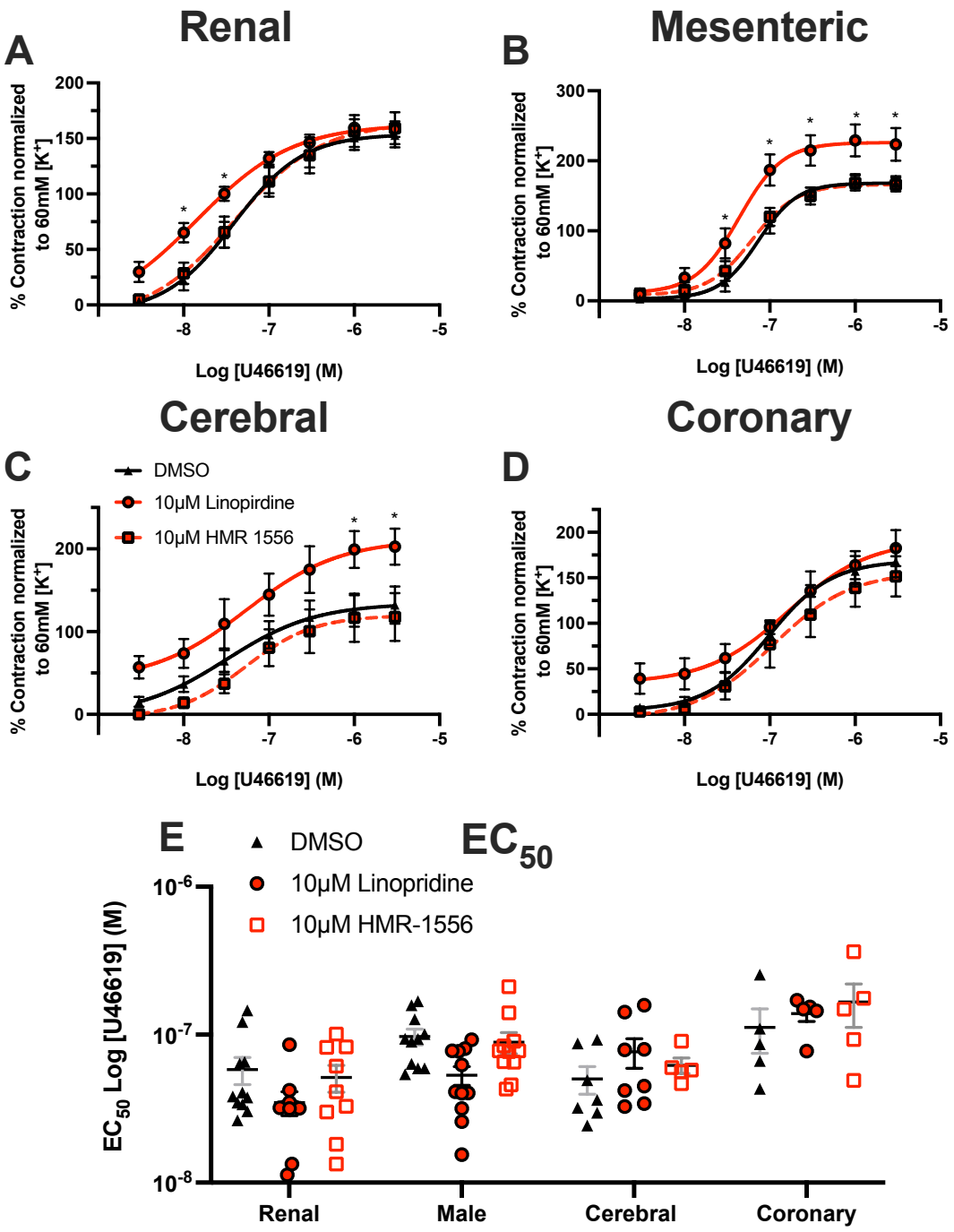

Figure 3.8: U46619-mediated contraction in renal, mesenteric, and cerebral arteries from male Wistars are underpinned by K_V7.2-5 channels.

Mean data of contraction in response to U46619 (0.003-3μmol-L^{-1}) within renal (*n*=10-11; A), mesenteric (*n*=10-11; B), cerebral (*n*=6-8; C) and coronary (*n*=5; D) arteries preincubated within DMSO solvent control (black), Linopirdine (10 μmol-L^{-1}; red) or HMR-1556 (10 μmol-L^{-1}; red, dashed-line). Scatter graph representing the raw EC_{50} values of U46619-mediated contraction within arteries of the mean data above, in addition to vessels pre-incubated in (E). A two-way statistical ANOVA with a post-hoc Dunnet's correction was used to generate significance values; values (*= $P \leq 0.05$) (*n*=) number of animals used.

3.3.2.3 Isoprenaline-mediated vasorelaxation is sensitive to K_V7.2-5 channel inhibition

K_V7 channels are strongly implicated in cAMP-PKA dependent β-adrenoreceptor mediated vasorelaxation within male rat RA (Chadha, Zunke, Zhu, *et al.*, 2012; van der Horst, Greenwood and Jepps, 2020). Here, we also demonstrate inhibition of K_V7 with Linopirdine (10 μmol-L^{-1}) attenuated relaxations generated by the β-adrenoreceptor agonist, isoprenaline (0.03-3 μmol-L^{-1}), mediated vasorelaxation in renal and cerebral arteries ($P \leq 0.05$; n=6-11; Fig 3.9.A-C). This was associated with an increase the EC_{50} (in μmol-L^{-1}) of Isoprenaline-mediated relaxation in mesenteric and renal arteries ($P \leq 0.05$; n=6-12; Fig 3.9.E). EC_{50} could not be calculated in some renal arteries where linopirdine totally ablated the response to Isoprenaline. As with U46619-mediated vasoconstriction, K_V7 channel inhibition had no effect on Isoprenaline-mediated relaxation of coronary arteries (Fig 3.9.D). In contrast, HMR-1556 did not alter isoprenaline-mediated relaxations in any artery (Fig 3.9.A-E). Therefore, K_V7.2-5 represent downstream targets of β-adrenoreceptor mediated vasorelaxation in a vascular bed specific manner.

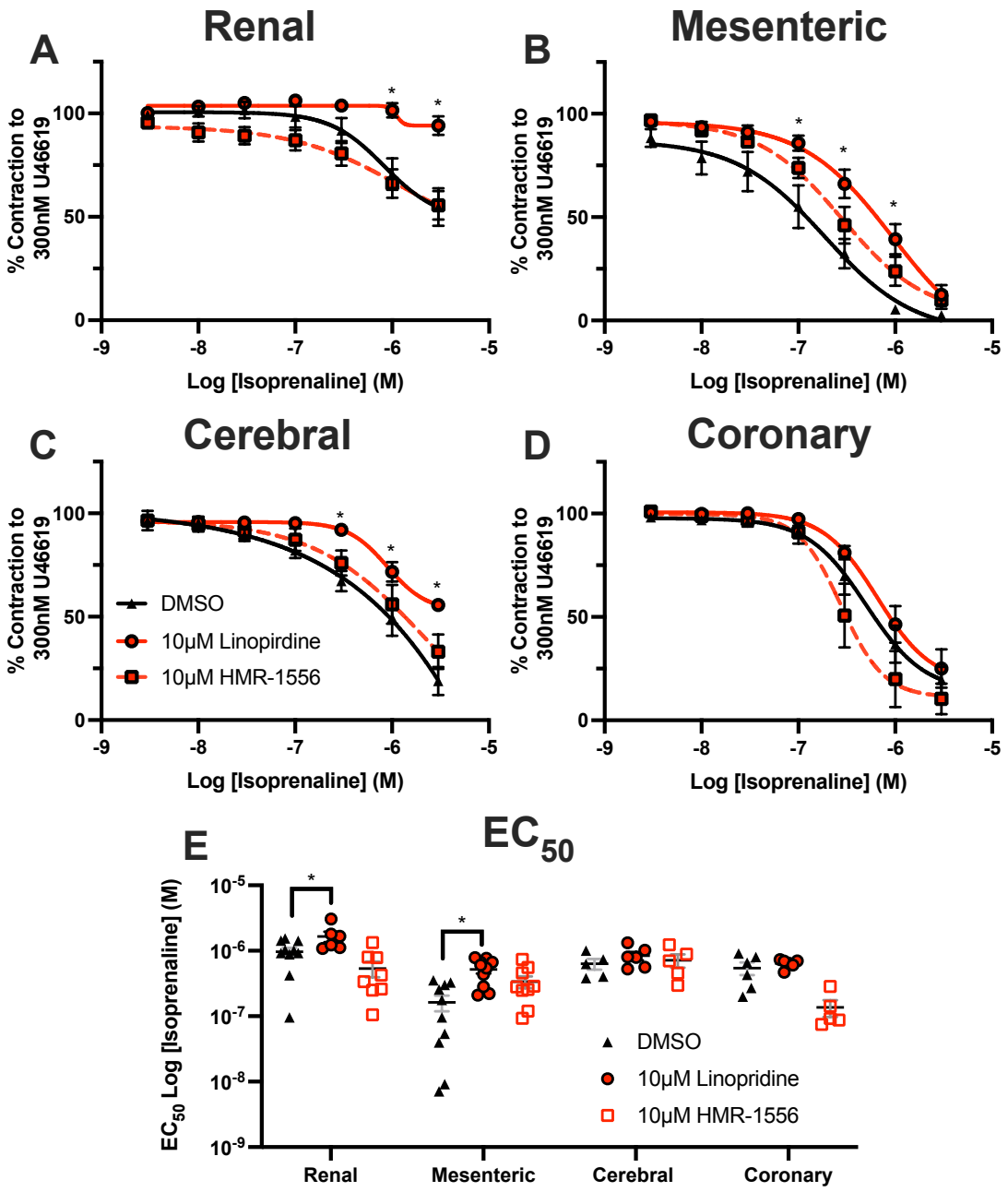

Figure 3.9: Isoprenaline-mediated relaxation in renal, mesenteric, cerebral and coronary arteries from male Wistars are underpinned by K_V7.2-5 channels.

Mean data of Isoprenaline (0.003-3μmol-L^{-1}) mediated relaxation of pre-contracted arterial tone U46619 (300 nmol-L^{-1}) within renal (*n*=9-12; A), mesenteric (*n*=8-10; B), cerebral (*n*=5-6; C) and coronary (*n*=6-7; D) arteries preincubated within DMSO solvent control (black), Linopirdine (10 μmol-L^{-1}; red) or HMR-1556 (10 μmol-L^{-1}; red, dashed-line). Scatter graph representing the raw EC_{50} values of Isoprenaline-mediated relaxation within arteries of the mean data above (E). A two-way statistical ANOVA with a post-hoc Dunnet's correction was used to generate significance values; values (*= $P \leq 0.05$) (*n*=) number of animals used.

3.3.3 K_V7 channels expression within the vasculature of the Wistar rat

3.3.3.1 K_V7 channels at the level of the transcript

RT-qPCR was used to determine the relative transcript abundance of *Kcnq1-5* and *Kcne1-5* in whole artery lysates. Though the primers used herein have also been used in a number of previously published works (Jepps *et al.*, 2011, 2014; Chadha, Zunke, Zhu, *et al.*, 2012; Khanamiri *et al.*, 2013; Carr *et al.*, 2016; Barrese *et al.*, 2020), the expression profile of *Kcnq1-5* and *Kcne1-5* was first determined in whole Heart and Brain lysates (Fig 3.10.A-D), where *Kcnq/Kcne* expression is well established, see Barrese *et al,.* (2018) for review and Chapter 1.5.5 for more detail. Similar to previous reports, *Kcnq2* and *Kcnq3* were absent, whilst *Kcnq1*, 4, *5* and *Kcne1- 5* were readily abundant in rat whole heart lysates (Fig 3.10.A,B). In contrast, *Kcnq2, 3* and *5* and *Kcne5* were predominant in brain lysates (Fig 3.10.C,D).

Subsequently, the data presented here demonstrates that similar to previous reports (Yeung *et al.*, 2007; Jepps *et al.*, 2011, 2014; Chadha, Zunke, Zhu, *et al.*, 2012; Khanamiri *et al.*, 2013), *Kcnq4* > *Kcnq5* > *Kcnq1* and *Kcne4* were the most abundance K_V7 and KCNE channel encoding transcripts respectively within whole lysates of rat arteries (Fig 3.11.A-H).

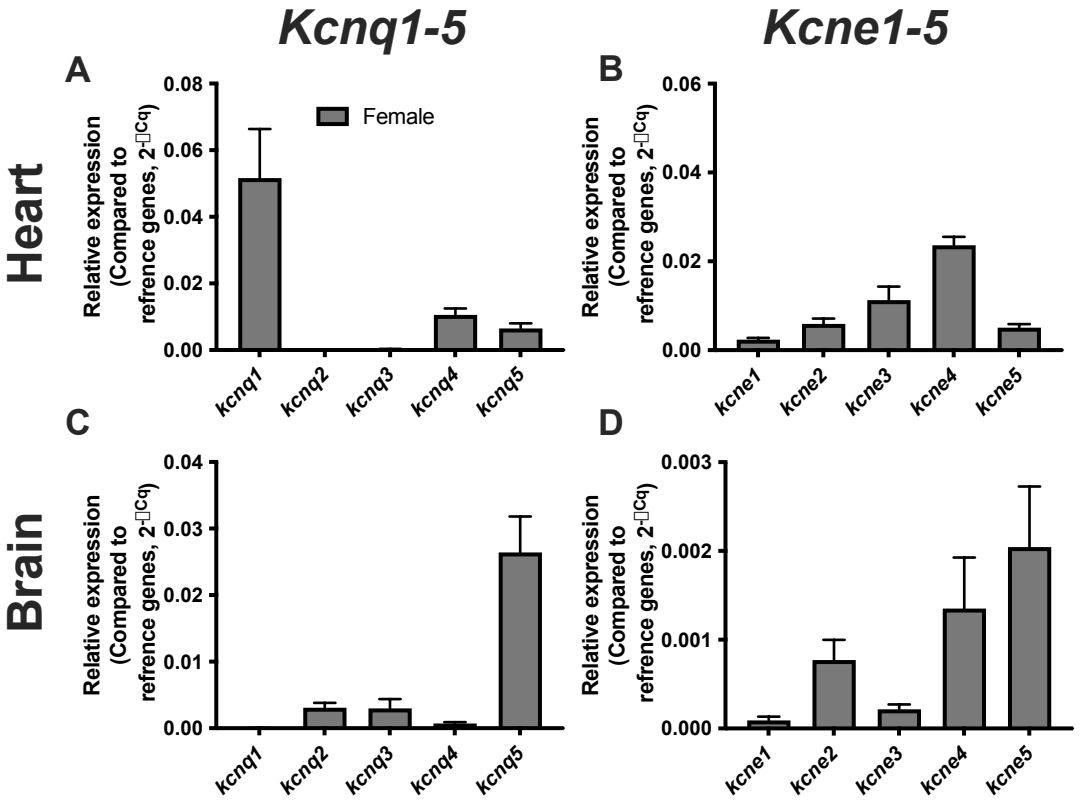

Figure 3.10: Relative mRNA transcript for *Kcnq1-5* and *Kcne1-5* within positive control tissues from male Wistar rats

Relative expression levels for *Kcnq1-5* and *Kcne1-5* were measured within Heart (*n*=4; A,B) and Brain (*n*=4; C,D) lysates from male Wistar rats when compared to appropriate reference gene (*Gapdh*; $2^{-\Delta Cq}$). (*n*=) number of animals used.

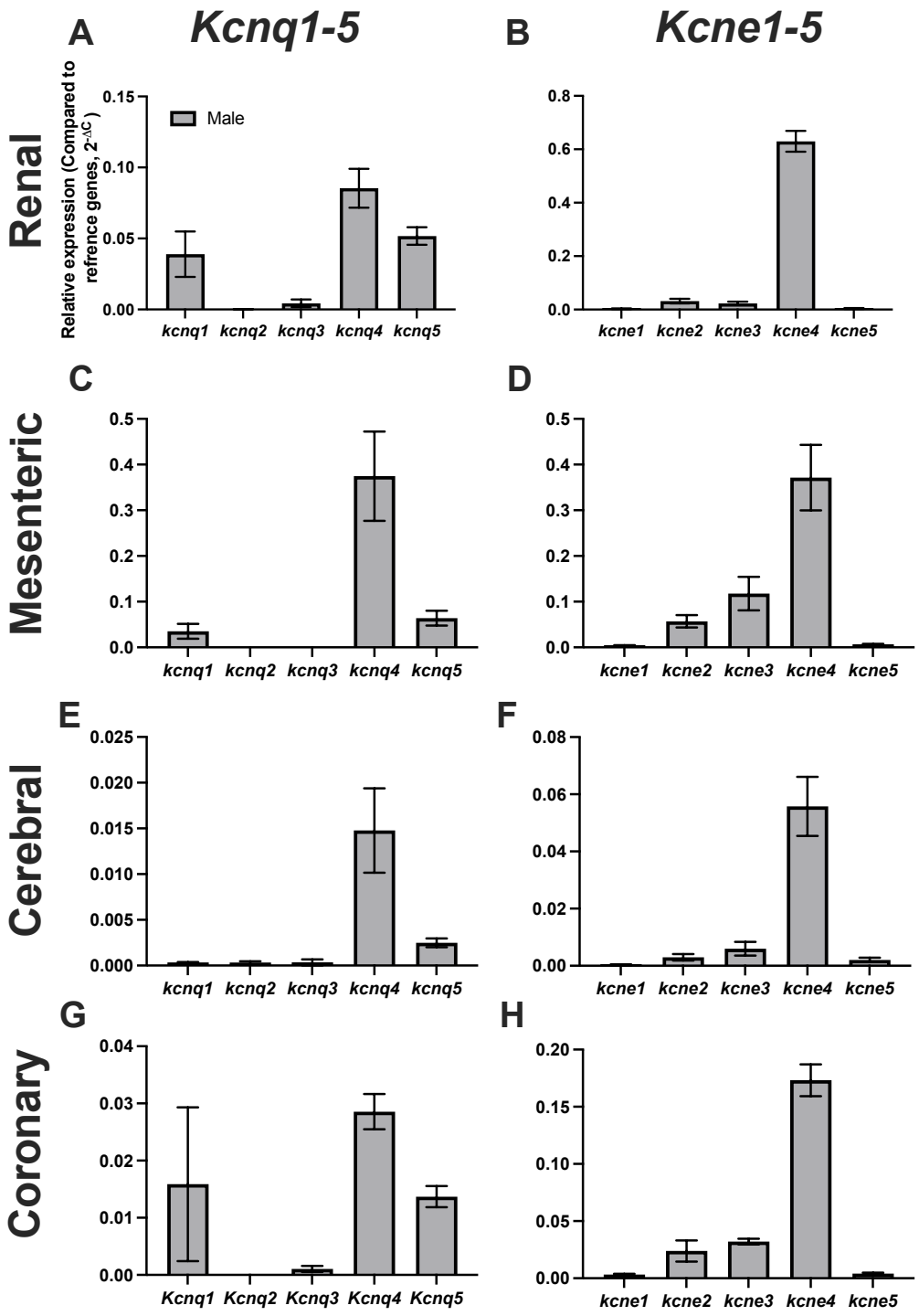

Figure 3.11: Relative mRNA transcript for *Kcnq1-5* and *Kcne1-5* within arteries from male Wistar rats

Relative expression levels for *Kcnq1-5* and *Kcne1-5* were measured within lysates of whole renal (*n*=4; A,B), mesenteric (*n*=5; C,D), cerebral (*n*=5; E,F) and coronary (G,H; *n*=3*) arteries from male Wistar rats when compared to appropriate reference genes ($2^{-\Delta Cq}$). Appropriate reference genes included the following; renal (*Tpo1, Ubc*; A,B), mesenteric (*Canx*, *Cyc1*; C,D), cerebral (*Cyc1*; E-F) and coronary (Y*wahz, Cyc1*; G,H). (*n*=) number of animals used, (*)= 3 animals per *n*.

3.3.3.2 K_V7 channels at the level of the protein

Validating anti-K_V7/Kcne4 antibodies

Initial investigations sought first to validate the antibodies primarily used hereafter. CHO cells were used as heterologous overexpression systems whereby they were transiently transfected with *KCNQ1, KCNQ4, KCNQ5 and KCNE4* and subsequently stained for their respective proteins and compared with non-transfected controls. Under the same laser intensity settings, we observed positive staining for $K_V7.1$ via Rabbit anti-$K_V7.1$ (Pineda, Antikörber-Service; Fig 3.12.A), $K_V7.4$ via Rabbit anti-$K_V7.4$ (APC-164; Alomone; Fig 3.12.C), $K_V7.5$ via Rabbit anti-$K_V7.5$ (ABN1372; Millipore; Fig 12.E) and KCNE4 via Rabbit anti-KCNE4 (HPA01142; Atlas antibodies; Fig 12.G) in red, that was absent when compared to non-transfected controls (Fig 3.12.B,D,F,H). Insets show nuclear labelling with DAPI (Fig 3.12).

Additional investigations sought to further validate Rabbit anti-$K_V7.4$ APC-164, as this antibody would be used to a greater extent. During overnight incubation with primary antibody (see Chapter 2.5.2 for protocol) *KCNQ4* transfected-CHO cells were incubated with either Rabbit anti-$K_V7.4$ or Rabbit anti-$K_V7.4$ plus antigenic blocking peptide (#BLP-PC164). Under the same laser intensity settings, no staining was observed in the presence of the antigenic peptide (Fig 13.B). Finally, no staining for $K_V7.4$ was observed in *KCNQ4*-transfected CHO cells in the absence of primary antibody (Fig 13.C), and therefore the staining observed could not be attributed to off target effects of the secondary antibody.

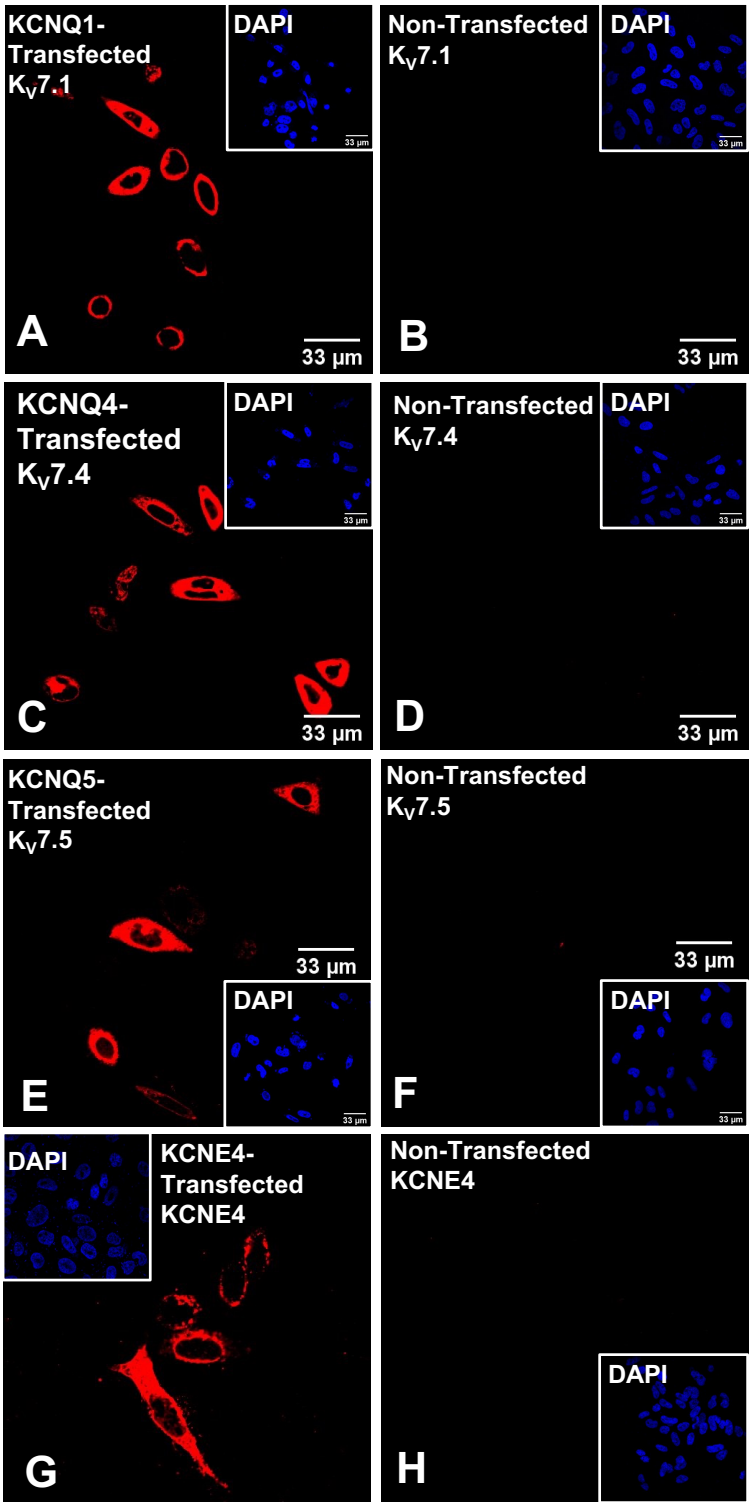

Figure 3.12: Validating Pineda Anti-K_V7.1, APC-164, ABN137 and HPA011.

Chinese hamster ovarian (CHO) cells transfected with plasmids containing either *KCNQ1* (A), *KCNQ4 (C), KCNQ5* (E) or *KCNE4* (G) presented with diffuse staining for anti; K_V7.1 (Pineda, Antikörber-Service, Germany), K_V7.4 (Alomone, Jerusalem, Israel), K_V7.5 (Millipore, Temecula, CA, USA) and KCNE4 (Atlas antibodies, Sweden) respectively. No staining was observed in non-transfected CHO cells (B,D,F). 4′,6-diamidino-2-phenylindole (DAPI; e.g. inset).

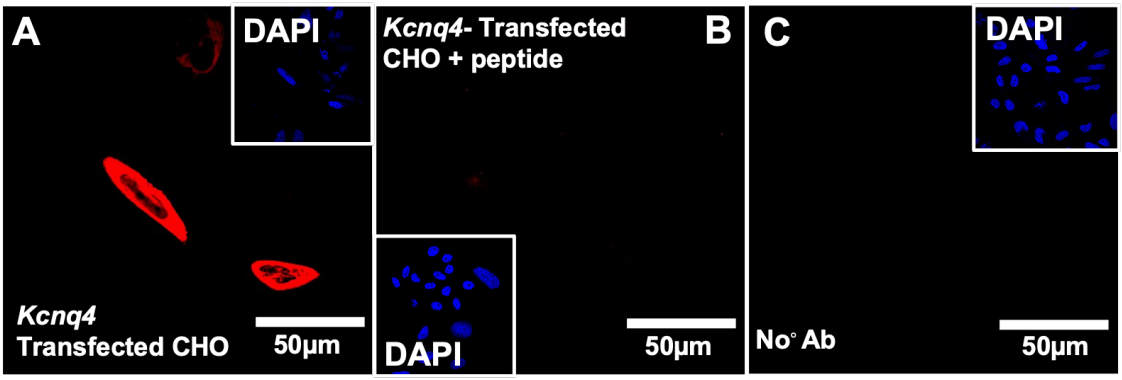

Figure 3.13: Validating Anti-K_V7.4 (Ab reference, #APC-164)

Chinese hamster ovarian (CHO) cells transfected with plasmids containing *KCNQ4* presented with diffuse labelling for K_V7.4 (A; red). Comparably, no staining was observed in *KCNQ4*-transfected CHO cells supplemented with blocking peptide (#BLP-PC164; B) nor in the absence of primary antibody (C). 4′,6-diamidino-2-phenylindole (DAPI; blue; A-F), wheat germ agglutinin membrane marker (green) merged image (merge; D-F) insets.

K_V7/KCNE staining in male isolated mesenteric and renal artery VSMCs

In agreement with previous reports (Barrese *et al.*, 2018), K_V7.4 staining was identified at the membrane by overlap with WGA in VSMCs from male mesenteric and renal arteries (see representative images, Fig 3.14.A and fluorescence intensity profiles, Fig 3.14.B). Fluorescence intensity for WGA, measured in A.U, at ≥200 A.U is indicative of staining at the membrane. K_V7.4 distribution was quantified by dividing the florescence intensity for K_V7.4 staining that overlaps with WGA ≥200 A.U by K_V7.4 within the cytosol. In the present study, Membrane:Cytosol ratios for K_V7.4 were 1.4±0.1 and 1.38±0.09 respectively (Fig 3.14.C). As such, K_V7.4 was predominantly found within the membrane. As above, no staining was observed in the absence or presence of primary antibody or blocking peptide respectively (Fig 14.A). Similarly to (Oliveras *et al.*, 2014; Jepps *et al.*, 2015; Morales-Cano *et al.*, 2015), within renal artery VSMCs, K_V7.1 and KCNE4 were also expressed within the membrane (Fig 15). In contrast to (Oliveras *et al.*, 2014; Morales-Cano *et al.*, 2015) the staining observed for K_V7.5 was predominately cytoplasmic within these cells (Fig 15). In summary, the protein and transcripts of the key candidates known to underpin K_V7 channel vascular activity were readily expressed within the investigated vascular beds.

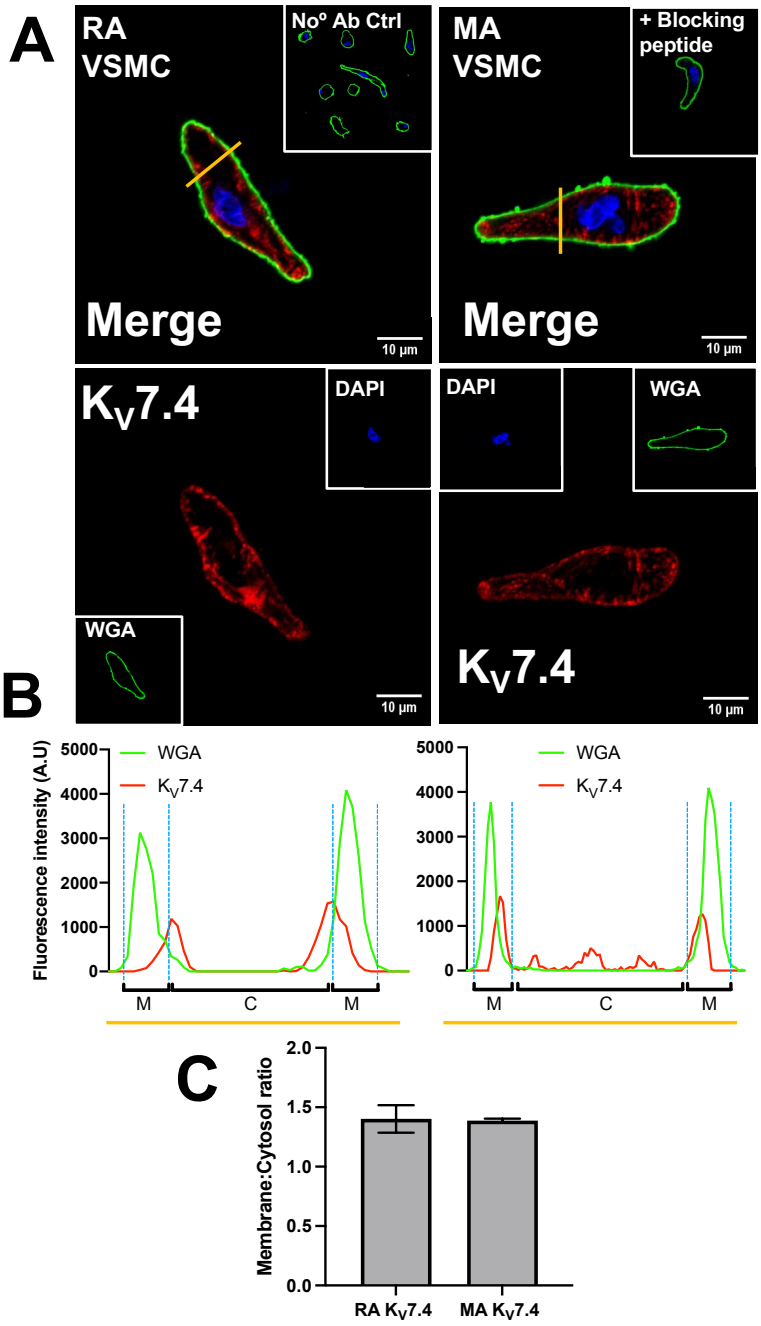

Figure 3.14: Membrane abundance for $K_V7.4$ in mesenteric and renal arteries from male Wistar rats.

Representative images of immunocytochemistry demonstrates $K_V7.4$ expression (red) from male (*n*=3) renal (RA) and mesenteric (MA; A) artery vascular smooth muscle cells. Plasma membrane and nuclear markers, wheat germ agglutinin (WGA; green) and 4′,6-diamidino-2-phenylindole (DAPI; blue) respectively, are also shown. Fluorescence intensity profiles were plotted for $K_V7.4$ and WGA measured in arbitrary units (A.U) along the yellow line seen in the merged image above (B). Bar chart demonstrating mean data of the Membrane:Cytosol ratio for $K_V7.4$ expression in RA and MA (C). Insets show staining in RA in the absence of primary antibody (upper left) and MA in the presence of blocking peptide (BLP-PC164; upper right) or split WGA/DAPI staining (bottom left/right). All values are expressed as means ± SEM error bars.

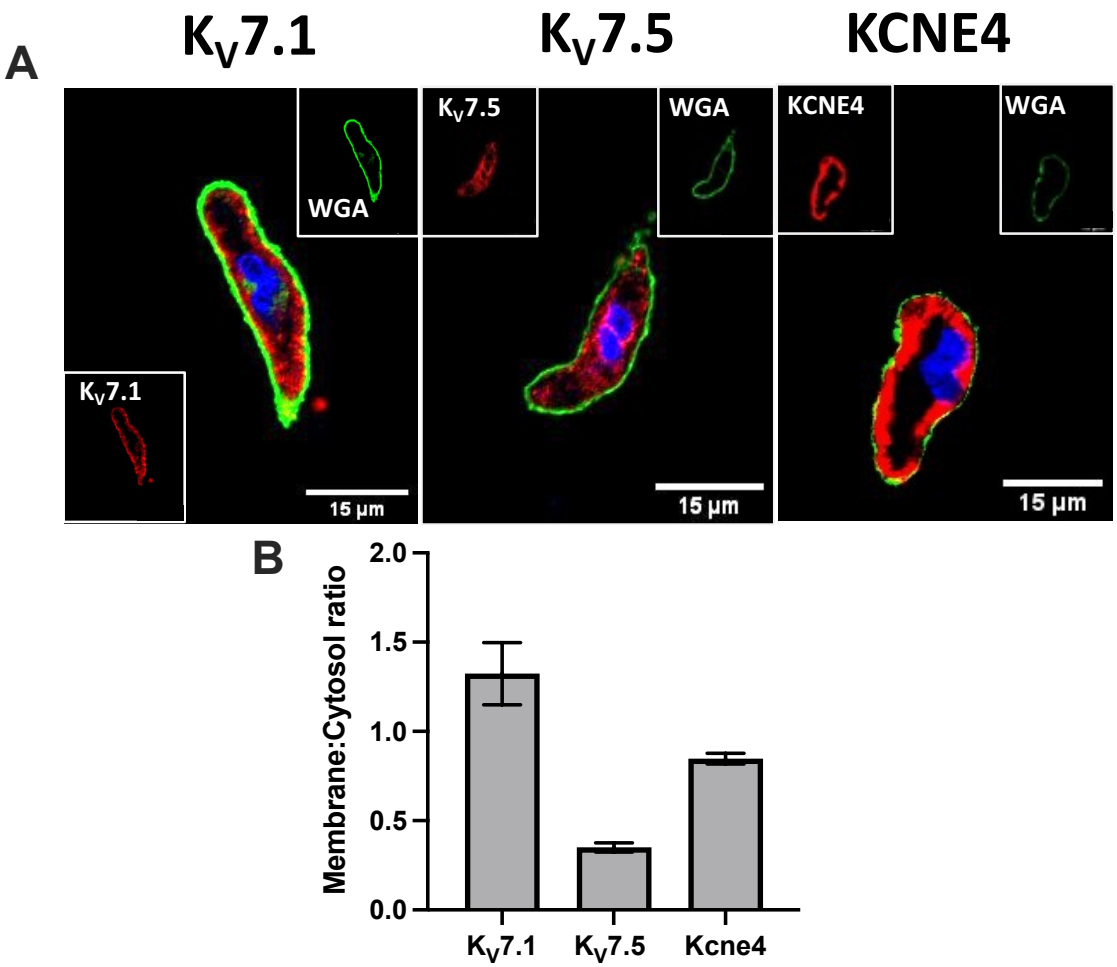

Figure 3.15: Membrane abundance for $K_V7.1$, $K_V7.5$ and Kcne4 in renal arteries from male Wistar rats.

Representative images of immunocytochemistry demonstrates $K_V7.1$, $K_V7.5$ and Kcne4 expression (red) from female male (*n*=3) artery vascular smooth muscle cells. Plasma membrane and nuclear markers, wheat germ agglutinin (WGA; green) and 4′,6-diamidino-2-phenylindole (DAPI; blue) respectively, are also shown. Bar chart demonstrating mean data of the Membrane:Cytosol ratio for $K_V7.1$, $K_V7.5$ and Kcne4 in RA (B). Membrane:Cytosol ratio for $K_V7.4$ expression was calculated by measuring the fluorescence intensity of $K_V7.4$ within the membrane and dividing it by the fluorescence intensity of $K_V7.4$ within cytosol from three randomly drawn lines in 10-12 cells pre *n.* Mean data for total cell fluorescence (A.U; D). All values are expressed as means ± SEM error bars

Protein quantification, Western blot

Protein quantification via western blot was attempted for $K_V7.4$ in both heterologous overexpression system and in whole artery lysates, however, we failed to achieve bands. See representative images in Figure 3.16. In collaboration with Thomas Jepp's Ph.D. students at the University of Copenhagen, a total of five different antibodies were screened, all of which failed to produce bands at 77kDa within lysates of whole arteries. Trialled anti-$K_V7.4$ antibodies included the following; Alamone APC-164 (Rb), SantaCruz sc-271329 (F-10; Ms), UC Davis 75-082 (NeuroMab), ThermoFisher PA5-77657 (Rb) and Abcam ab84820 (Ms). Consequently, single cell immunocytochemistry alone was employed to determine the intracellular distribution of K_V7 channels within VSMCs.

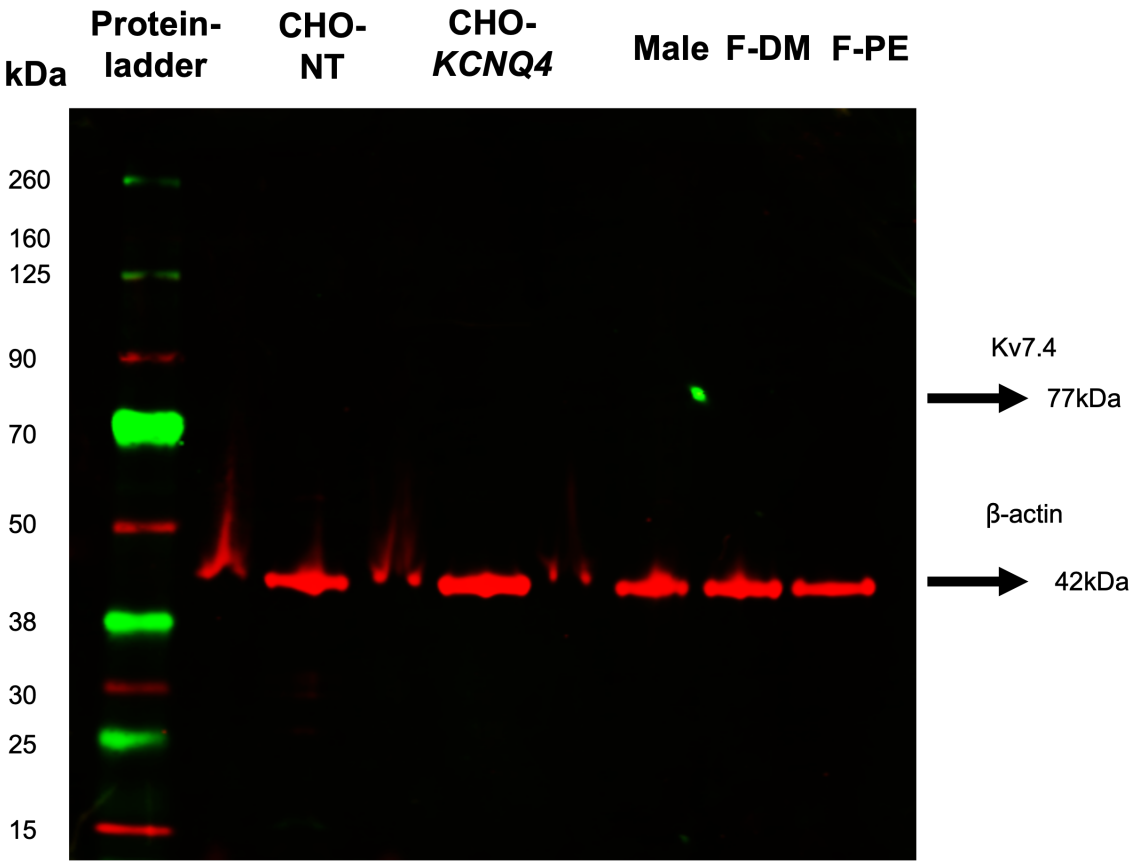

Figure 3.16: Protein quantification of $K_V7.4$

Representative western blot of staining for $K_V7.4$ (77 kDa) and β-actin (42 kDa) in protein lysates from Chinese hamster ovarian (CHO) cells non-transfected (NT) or *KCNQ4* transfected and whole renal arteries from male, females in Di-oestrus / Met-oestrus (F-D/M) and females in Pro-oestrus / Oestrus (P/E).

3.4 Discussion

The results of this chapter confirm the previously well-established notion that K_V7 channels are key regulators arterial smooth muscle tone. Moreover, ML213 and retigabine upregulate $K_V7.4$ activity at the level of the channel with preferential affinity for $K_V7.4$ over $K_V7.1$, ML277 selectively upregulates $K_V7.1$ channel activity, Linopirdine ablated $K_V7.4$ channel activity and HMR-1556 selectively inhibits $K_V7.1$ channels. Further, ML213, retigabine and S-1 were effective and potent relaxants of pre-contracted arterial tone in a linopirdine-sensitive manner, and linopirdine increased basal tone in myogenic arteries, enhanced receptor mediated contraction and depressed receptor mediated relaxation (Fig 3.17). Finally, *Kcnq* transcripts and K_V7 proteins were identified in an array of arteries in a fashion analogous to previous reports.

3.4.1 Validating a pharmacological toolbox

3.4.1.1 K_V7 channel activators

$K_V7.2$-5 channel activators are effective tools in the treatment of both epilepsy (Rostock *et al.*, 1996) and pain (Ilyin *et al.*, 2002) and are to date, the only K_V channel activators that have been approved for use in humans. Of the activators chosen, the mechanism by which channel activity is regulated is a well understood process. As described in table 1.1, retigabine (Schenzer *et al.*, 2005), ML213 (H. Yu *et al.*, 2011; Jepps *et al.*, 2014) and S-1 (Bentzen *et al.*, 2006) bind a tryptophan residue within the S-5 region of *KCNQ2-5* channels ($hK_V7.4$-Try242 / $hK_V7.5$-Trp235) which is absent from *KCNQ1.* ML213, Retigabine and S-1 bind $K_V7.2$-5 via formation of hydrogen bonds (Kim *et al.*, 2015) when the channel is in an open-state (Wuttke *et al.*, 2005), stabilizing the voltage-sensing domain in an activated configuration in a PIP_2 dependent process (Telezhkin *et al.*, 2013; Kim, Pless and Kurata, 2017). Subsequently giving rise to a negative shift in the voltage-dependence of activation and an increase in channel conductance, however, the precise molecular scaffolding that links activator binding to a change in gating properties remains elusive.

Here, similar to previous reports (Tatulian *et al.*, 2001; H. Yu *et al.*, 2011; Jepps *et al.*, 2014) we demonstrate that retigabine and ML213 upregulate the peak amplitude and decrease $V_{½}$ of $K_V7.4$ channel derived currents in heterologous over expression systems during ruptured whole-cell electrical recordings. Moreover, ML213, but not retigabine increased the activation kinetics for voltage evoked $K_V7.4$ derived currents. Additionally, vasorelaxation seen in response to retigabine, S-1 and ML213 was ablated by pre-incubation with Linopirdine, giving credence to their action and specificity, however, 10 μmol-L^{-1} ML213 significantly enhanced $K_V7.1$ derived currents at +40mV, independent of a change in $V_{½}$ or τ. Though the effect of ML213 was comparably smaller in $K_V7.1$ when compared to $K_V7.4$ currents, concentrations of ≥10 μmol-L^{-1} ML213 appear to influence $K_V7.1$ channel activation independent of the S5 tryptophan residue.

There is current debate regarding the channel configuration requirement for retigabine-mediated activation of K_V7. During the initial characterisation of retigabine binding properties, Schenzer *et al,.* (2005) described a dependence on four individual tryptophan containing S5 regions within the channel for retigabine-mediated effects on channel gating properties. Though, (Yau *et al.*, 2018) recently disputed this statement by demonstrating that only one tryptophan containing subunit of the heterotetramer was required for near full drug activity. This minutia is relevant, as though $K_V7.1$ is typically considered a homotetrameric channel and that tryptophan binding $K_V7.2$-5 channel activators have no effect on currents derived from these channels (Main *et al.*, 2000; Tatulian *et al.*, 2001; Schenzer, 2005; Wuttke *et al.*, 2005), $K_V7.1$ is capable of forming heterotetramers with $K_V7.5$ within coronary artery myocytes (Oliveras *et al.*, 2014). The capability of these agents in selectively studying $K_V7.2$-5 channels over $K_V7.1$ may be diminished by; 1.) a propensity for $K_V7.2$-5 activators to upregulate $K_V7.1$ containing heteromultimers; 2.) h$K_V7.4$-Try242 independent effect of ML213 on HEK-$K_V7.1$ cells at concentrations of ≥10 μmol-L^{-1}, however, the effects of ML213, retigabine and S-1 appear largely preferential for $K_V7.2$-5 channels over $K_V7.1$ and make effective tools in

the characterisation of K_V7 channel activity within the vasculature despite these limitations.

As above, activators of $K_V7.1$ are of clinical importance as mutations in *KCNQ1* give rise to long-QT syndrome (Schwartz, Crotti and Insolia, 2012), a life threatening cardiac arrythmia. ML277 has been identified as a potent activator of $K_V7.1$ via high throughput investigation (Yu, 2013), expressing a 100 fold increase in selectivity for $K_V7.1$ when compared to $K_V7.2$-5 (Yu, 2013). The binding properties of ML277 to $K_V7.1$ are, comparably to $K_V7.2$-5 activators, poorly understood. Though ML277 putatively alters the electromechanical coupling of the voltage sensing and pore forming domains of the channel, stabilising $K_V7.1$ in its active state (Hou *et al.*, 2019). Within this study, similar to (Hou *et al.*, 2019), we demonstrated an increase in peak current amplitude independent of a change in the voltage-dependence for activation of the channel in response to 1 μmol-L^{-1} ML277. Though in contrast, we observed no change in the activation kinetics of the current (Hou *et al.*, 2019). Moreover, ML2177 had no effect on voltage-evoked currents in HEK-$K_V7.4$ cells, consistent with ML277 being selective for $K_V7.1$, however, application of concentrations of ML277 >300 nmol-L^{-1} gave rise to relaxation pre-contracted arterial tone in the presences of linopirdine, indicating off-target effects at concentrations of ML277 ≥1 μmol-L^{-1} on a target natively expressed within the vasculature which is yet to be identified.

3.4.1.2 K_V7 channel inhibitors

Pan-K_V7 blockers Linopirdine and XE-991 are state dependent inhibitors of the channel that favour K_V7 in the open state, binding one single subunit as opposed to open channel inhibition (Schnee and Brown, 1998; Greene, Kang and Hoshi, 2017; Li *et al.*, 2021). Our initial configuration during current recording (see protocol 1 in chapter 2.7.4) yielded no response to either linopirdine or XE-991, wherein inhibitors of the channel were washed onto the cell during +20 mV pulse for ≥1 min, however, when pre-incubating HEK-$K_V7.4$ cells in either analogue (10 min), voltage-evoked current was ablated. Both Linopirdine

and XE-991 have slow binding kinetics (Greene, Kang and Hoshi, 2017). Indicating that five-minute incubation used during protocol 1 was insufficient. As such, in the following chapters, Linopirdine was pre-incubated for no less than 10 minutes.

$K_V7.1$ specific inhibitor HMR-1556 is a highly selective and potent inhibitor of *KCNQ1* encoded currents within an array of tissues (Gögelein *et al.*, 2000; Gerlach *et al.*, 2001). Chromanol 293B inhibits I_{Ks} through interaction with Ile337 and Phe340 within the selectivity filter of the S6 pore forming domain of $K_V7.1$ (Lerche *et al.*, 2007). Though its precise mechanism remains uncharacterised, HMR-1556 is a chromanol compound which prospectively works via the same mechanism as Chromanol 293B. Here, we demonstrate HMR-1556 mediated inhibition of $K_V7.1$ currents that had no effect on $K_V7.4$, in support of those conjectures.

3.4.2 K_V7 channels are key regulators of vascular reactivity in arteries from male Wistars

Myriad papers have demonstrated the ability for K_V7 channel activators to relax pre-contracted arterial tone (eg Yeung *et al.*, 2007; Mackie *et al.*, 2008; Jepps *et al.*, 2011; Ng *et al.*, 2011; Jepps *et al.*, 2014; Carr *et al.*, 2016; Stott *et al.*, 2015a, 2018; Barrese *et al.*, 2018, 2020; Baldwin *et al.*, 2020; Chadha *et al.*, 2012a; Khanamiri *et al.*, 2013; Oliveras *et al.*, 2014; Morales-Cano *et al.*, 2015; Fig 3.17). Similar to Jepps *et al,.* (2014) ML213 and S-1 were more potent when compared to both Retigabine across a range of arteries. As such, the principal tools used in the following investigations were ML213 and S-1, in favour of retigabine. As above, relaxation in response to these agents was due to an opening of $K_V7.4/7.5$ channels, hyperpolarisation of the membrane and closure of VGCC resulting in diminished $[Ca^{2+}]_I$. Our findings support this theory. Additionally, pan-K_V7 channel inhibition increases basal tone and depolarises the membrane (Ohya *et al.*, 2003; Yeung *et al.*, 2007; Mackie *et al.*, 2008; Jepps *et al.*, 2011; Ng *et al.*, 2011; Chadha, Zunke, Zhu, *et al.*, 2012; Khanamiri *et al.*, 2013), implicating a role for K_V7 channels in the resting membrane potential and resting tone of the vasculature (Fig 3.17). We

similarly demonstrate that Linopirdine, but not HMR-1556 increased basal tone, supporting a role for $K_V7.4/7.5$, but not $K_V7.1$ in regulating the basal tone of the vasculature.

Suppression of neuronal M-currents in response to $G_{q/11}$ receptor has previously been attributed to depletion of PIP_2 (Suh and Hille, 2002; Zhang *et al.*, 2003) and calcium-calmodulin complex interaction with the C-terminal domain of the channel (Gamper, Li and Shapiro, 2005). As above and in Chapter 1.5.4.2, PKCα, a downstream intracellular signalling molecule of $G_{q/11}$ receptor mediated contraction has recently been implicated in K_V7 channel suppression during vasoconstriction in response to vasopressin (Brueggemann *et al.*, 2006; Lioubov I Brueggemann, Mackie, *et al.*, 2014) and 5-HT (Mani *et al.*, 2013) within the vasculature. PKCα prospectively binds $K_V7.5$ c-terminal domain diminishing PIP_2 binding (Haick *et al.*, 2017; Brueggemann, Cribbs and Byron, 2020b). Suppression of native K_V7 channels during TXA_2 mediated PKC-derived (Cogolludo *et al.*, 2003) contraction in these vessels is yet to be described, however, within this chapter we observed an augmentation of U46619 mediated contraction by inhibition of $K_V7.4/7.5$ channels. Indicating that $K_V7.4/7.5$ oppose TXA_2 mediated contraction. Though it is plausible that TXA_2 receptor mediated contraction suppresses channel activity, K_V7 channels still appear active to a significant functional degree (Fig 3.17).

Though the molecular identity of K_V7 was yet to be characterised, the first identification of receptor mediated increases in K_V7 channel activity was in response to β-adrenoreceptor activation of gastrointestinal cells that evoked neuronal-like M-currents (Sims, Singer and Walsh, 1988). Since which time, cAMP dependent β-adrenoreceptor mediated relaxation has been shown to upregulate K_V7 channel activity within vascular myocytes (Chadha, Zunke, Zhu, *et al.*, 2012; Stott, Povstyan, *et al.*, 2015) via either PKA, coupled by AKAP, in conjunction with G$\beta\gamma$ (Stott, Povstyan, *et al.*, 2015; Mani *et al.*, 2016;

Brueggemann *et al.*, 2018) or EPAC (Stott, Barrese and Greenwood, 2016) in a vascular bed specific manner (Chapter 1.5.4.2). Here, we similarly demonstrate that pharmacological inhibition of $K_V7.4/5$, but not $K_V7.1$ attenuated β-adrenoreceptor mediated relaxation (Fig 3.17).

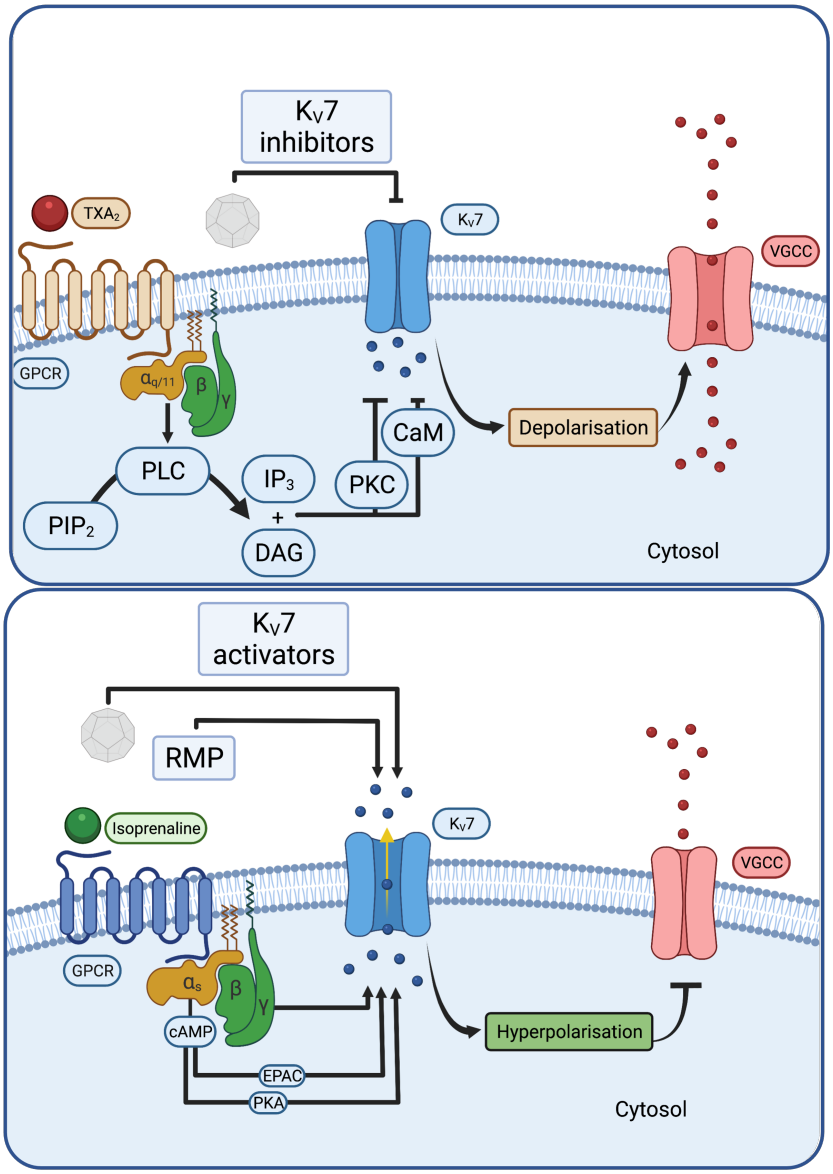

Figure 3.17: Graphical summary of K_V7 channel activity in the vasculature of the male

Diagrammatic representation of K_V7 channel inhibition via thromboxane A2 receptor mediated vasocontraction or synthetic inhibitors of the channel (upper). Diagrammatic representation of K_V7 channel basal activity at resting membrane potential (RMP) enhancement via β-adrenoreceptor mediated vasorelaxation and synthetic activators of the channel (lower).

3.4.3 Limitations

The work of this chapter relies heavily on isometric tension recording and immunocytochemistry, both of which have limitations that carry throughout the remainder of this thesis. Firstly, with regards to deducing K_V7 contribution to receptor mediated responses by reductive approach during isometric tension recording, i.e adding Linopirdine or HMR-1556 prior to generating CECs to vasodilators or vasoconstrictors, our findings are limited by possible 'functional antagonism,' which suggests that when inhibiting K_V7 channels, which are active at rest within the vasculature, observation of antagonism of receptor mediated relaxation or augmentation of receptor mediated contraction could be due to inhibiting basal activity of the channel. To curtail this limitation, future investigations will include perforated whole cell current recordings, wherein linopirdine sensitive currents will be pharmacologically dissected and recorded in the presence and absence of receptor agonists in native smooth muscle cells, as previously (Mackie *et al.*, 2008; Chadha, Zunke, Zhu, *et al.*, 2012; Stott, Barrese and Greenwood, 2016). Further, an inability of our vessels to contract again after the application of high concentration of channel activators, i.e ML213 or S-1, is a possible indication of the toxicity of these compounds as opposed to their action at the site of the channel. A refute to this claim is the previously demonstrated reversal of K_V7 activator mediated relaxation to near full pre-contracted tone by application of pan-K_V7 channel inhibitors post addition of the pan-K_V7 activators (Yeung *et al.*, 2007) or $K_V7.1$ specific activators (Chadha, Zunke, Davis, *et al.*, 2012). With regards to immunocytochemistry, our findings are limited to the specificity of the molecular tools we have employed. Though we show positive controls for the candidates associated with vascular-K_V7 function, negative controls would add credence to the specificity of these anti-bodies. In the future, diminishing total K_V7 abundance via targeted morpholinos or short-inhibiting RNAs, or inhibition of K_V7 derived currents during ruptured whole cell current recording via antibody transfection will be employed to further ratify these tools.

3.4.4 Conclusion

In summary, the results of this chapter reinforce the previously validated specificity of the K_V7 channel modulators used in the remaining chapters and the notion that $K_V7.4/7.5$ channels are key regulators of both basal vascular reactivity and as key functional end targets in vasoactive responses. The results of this chapter give credence to the novel findings and remarks detailed hereafter.

Chapter 4: Oestrus cycle dependent regulation of arterial $K_V7.4$

4.1 Introduction

Sexual dimorphisms in cardiovascular physiology and pathophysiology are a well-documented phenomenon (Pabbidi *et al.*, 2018). Pre-menopausal women exhibit greater coronary and cerebral blood flow (Pabbidi *et al.*, 2018), greater protection against systemic inflammation induced EC dysfunction (Rathod *et al.*, 2017) and the incidence of adverse cardiovascular events is significantly lower (Pabbidi *et al.*, 2018). As the female cardioprotective phenotype diminishes post-menopause, the most likely candidates that drive sexual dimorphisms within the vasculature are sex-hormones, primarily oestrogen, however, the role of oestrogen within the CVS remains enigmatic, being shown to be both protective and detrimental to the vasculature (Hulley *et al.*, 1998, 2002; Yang and Reckelhoff, 2011).

To date the literature on vascular K_V7 channels focuses primarily on arteries from male animals. Considering the known sexual dimorphisms in vascular reactivity and the growing appreciation for sex as an experimental factor (Docherty *et al.*, 2019), we aimed to address this deficit. We characterised K_V7 channel functional and molecular properties within arteries from Female Wistar rats. In light of previously demonstrated oestrus cycle dependent changes in vascular reactivity (Jaimes *et al.*, 2019), the oestrus cycle was a key consideration in the following study. The rat oestrus cycle lasts only 4-5 days, with each stage lasting the following: 1.) Pro-oestrus - 14 hrs; 2.) Oestrus - 24-48 hrs; 3.) Met-oestrus 6-8 hrs; 4.) Di-oestrus - 48-72 hrs (Cora, Kooistra and Travlos, 2015). As sex-hormones peak in Pro-oestrus (Nilsson *et al.*, 2015), females were separated into Pro-oestrus and Oestrus (F-P/E) and Di-oestrus and Met-oestrus (F-D/M) stages of the

oestrus cycle. The observations detailed herein demonstrate a remarkable oestrus cycle derived reduction in $K_V7.4$ membrane abundance by E2 signalling via GPER1 which underpins a pro-contractile vascular state.

4.2 Methods

The methods used within this chapter are described at length within Chapter 2, however, to reiterate, females in the following chapters separated into Pro-oestrus and Oestrus and Di-oestrus and Met-oestrus as identified by distinct histological changes in cells lifted from the surface of the cervix. The methods by which this was achieved are described in Chapter 2.2 and are derived from (Cora, Kooistra and Travlos, 2015).

4.3 Results

4.3.1 Sex/Oestrus cycle dependent changes in sensitivity to K^+ channel modulators

The K_V7.2-5 specific activator S-1 (0.1-10 μmol-L^{-1}; Fig 3.5; Bentzen *et al.*, 2006; Baldwin *et al.*, 2020) evoked concentration dependent relaxation of pre-constricted arterial tone (300 nmol-L^{-1} U46619) in arteries from both F-D/M and F-P/E rats (see representative traces in Figure 4.1.A,B). S-1 was approximately 10-fold more potent in renal arteries from F-D/M (EC_{50} = 0.45±0.07 μmol-L^{-1}) rats when compared to arteries from F-P/E rats (EC_{50}= 4±0.3 μmol-L^{-1}; Fig 4.1.C; *n*=6-8; *P*≤0.05). The same oestrus-cycle-dependent phenomenon was observed within mesenteric as well as coronary and cerebral arteries (Fig 4.1.D-F; *n*=4-8; *P*≤0.05). Vasorelaxation of precontracted tone in response to a structurally dissimilar Kv7.2-7.5 activator, ML213 (0.1-10 μmol-L^{-1}; Fig 3.2/5; Jepps *et al.*, 2014; Baldwin *et al.*, 2020) was also significantly more potent within mesenteric and renal arteries from F-D/M rats than arteries from F-P/E rats (Fig 4.2.A-D; *n*=6; *P*≤0.05).

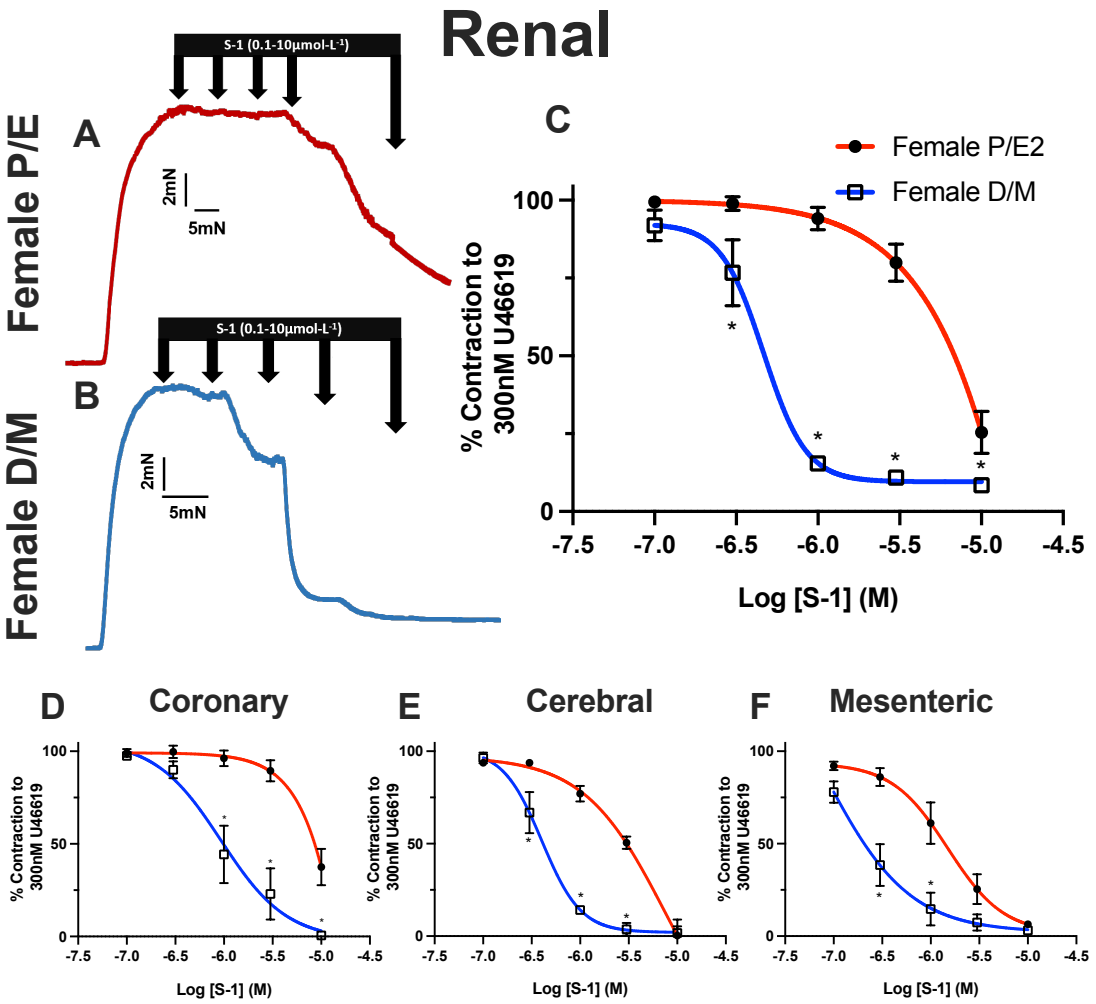

Figure 4.1: Oestrus cycle dependent differences in S-1-mediated relaxation of pre-contracted tone within arteries from female (P/E2) and female (D/M) Wistar rats.

Representative traces of relaxation of pre-contracted arterial tone (U46619; 300nmol-L^{-1}) in renal arteries from female pro-oestrus/oestrus (P/E; red; A) and female di-oestrus/met-oestrus (D/M; blue; B) in response to K_V7.2-5 activator S-1 (0.1-10µmol-L^{-1}). Mean data of S-1-mediated relaxation in renal (*n*= 5-8; C), coronary (*n*=4-8; D), cerebral (*n*=5-7; E) and mesenteric (*n*=5-6; F) arteries. Values are expressed as means ± SEM error bars (C-F). A two-way statistical ANOVA with a post-hoc Bonferroni test was used to generate significance values (*= *P*≤0.05). (*n*=) number of animals.

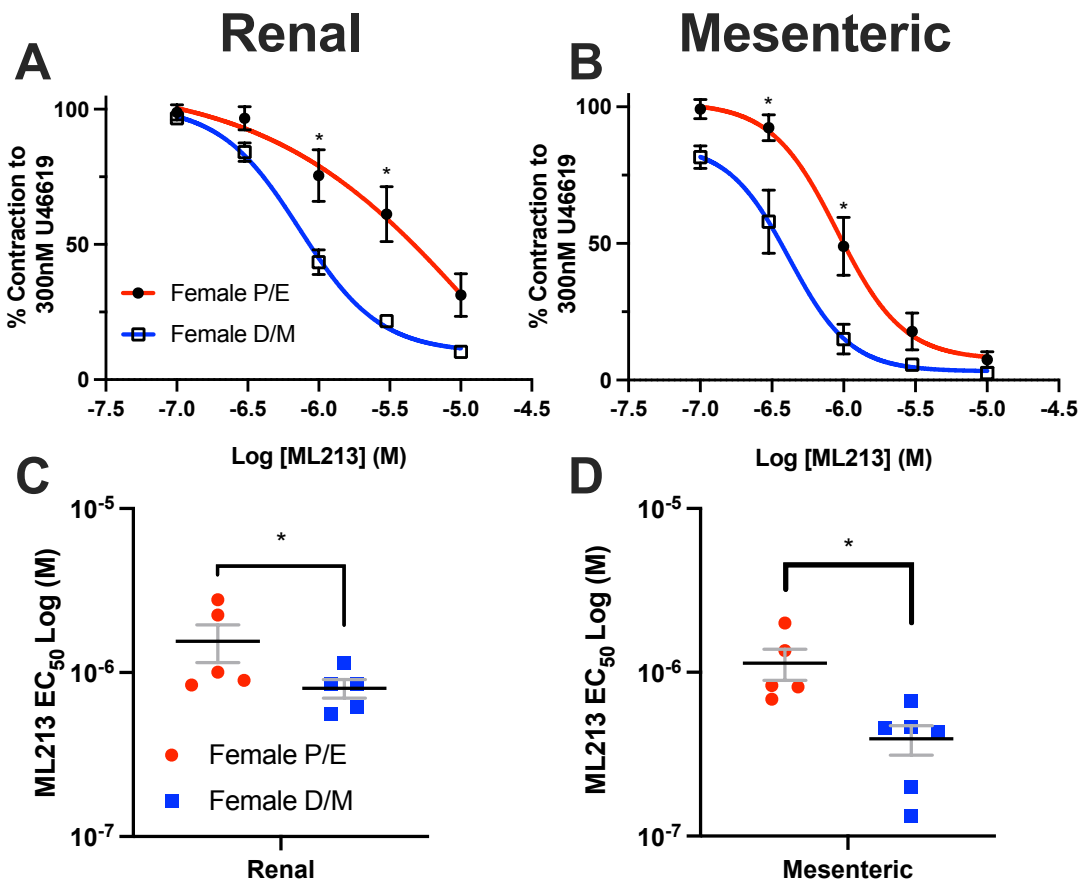

Figure 4.2: ML213 is more efficacious and potent in arteries from female (D/M) Wistar rats when compared to female (P/E) rats.

Mean data of relaxation of pre-contracted tone (U46619; 300nmol-L^{-1}) in response to ML213 (0.01-10µmol-L^{-1}) in renal (*n*=5; A) and mesenteric (*n*=5; B) arteries from female pro-oestrus/oestrus (P/E; red) and female di-oestrus/met-oestrus (D/M; blue) rats. Scatter graph representing the raw EC_{50} values of ML213-mediated relaxation within renal (C) and mesenteric (D) arteries of the mean data above. All values are expressed as means ± SEM error bars. A two-way statistical ANOVA with a post-hoc Bonferoni correction was used to generate significance values (*= $P \leq 0.05$). (*n*=) number of animals.

Inhibitors of K_V7 channels depolarise VSMC membrane potential and produce contraction in arteries from male animals (Fig 3.7; Mackie *et al.*, 2008; Yeung & Greenwood, 2005; Yeung *et al.*, 2007). Figure 4.3.C,D shows that 10 μmol-L^{-1} of the pan-K_V7 channel blocker Linopirdine (Schnee and Brown, 1998) produced robust contractions in renal arteries from F-D/M Wistars. Linopirdine also produced contractions in mesenteric arteries from F-D/M rats which were significantly greater than application of DMSO solvent control, though smaller in amplitude than those observed in renal arteries (Fig 4.3B,C; n=10-13; $P \leq 0.05$). Comparably, contractions to linopirdine were far smaller in renal and mesenteric arteries from F-P/E rats (Fig 4.3.A-C), see representative trace in Figure 4.3.A. Application of 10 μmol-L^{-1} $K_V7.1$ specific blocker HMR-1556 had no effect on basal tone in any group (Thomas, Gerlach & Antzelevitch, 2003; Fig 4.3.B,C), consistent with previous reports (e.g Chadha *et al.*, 2012). These data indicate a significant $K_V7.2$-5 channel contribution to base-line tension within arteries from F-D/M rats, which was diminished within arteries from F-P/E rats, collectively demonstrating a clear oestrus cycle dependent shift in sensitivity to K_V7 modulators.

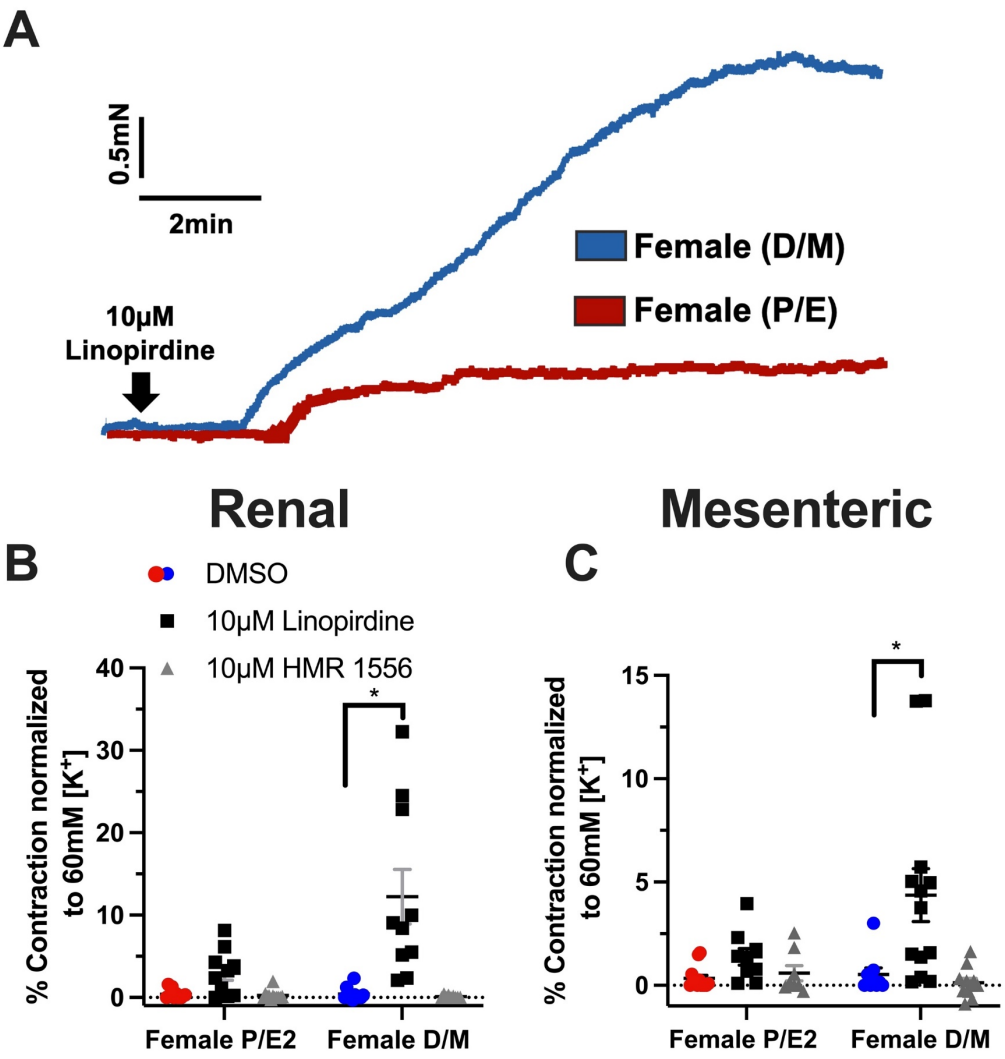

Figure 4.3: Effect of K_V7 blockers on arterial tone.

Representative traces of contraction of renal arteries from female P/E (red) and female D/M (blue) rats in response to pan K_V7 channel blocker Linopirdine (10μmol-L^{-1}; A). Mean data of increases in basal tone in response to solvent control DMSO (Female P/E, red; Female D/M, blue), Linopirdine (10μmol-L^{-1}; black) and HMR-1556 (10μmol-L^{-1}; grey) in renal (*n*= 10-12; B) and mesenteric arteries (*n*= 10-13; BC). All values are expressed as means ± SEM error bars. A two-way statistical ANOVA with a post-hoc Dunnet's's correction was used to generate significance values (*= $P \leq 0.05$). (*n*=) number of animals.

In an effort to identify if oestrus cycle-dependent changes in activity were specific to K_V7 channels, the effect of BK_{Ca} activator NS11021 (0.1-10µmol-L^{1}), the K_{ATP} activator pinacidil (0.1-10µmol-L^{1}) and the VGCC inhibitor nicardipine (0.001-1µmol-L^{-1}) were studied in arteries from both groups of females. Within renal arteries, NS11021 failed to relax pre-contracted arterial tone (Fig 4.4.A; *n*=4-6), however, pinacidil and nicardipine relaxed pre-contracted arterial tone in both groups independent of oestrus cycle stage (Fig 4.4.B,C; *n*=5-7). Similarly, NS11021 and nicardipine relaxed pre-contracted tone in mesenteric arteries independent of oestrus cycle stage (Fig 4.4.D,F; *n*=5-6), however, pinacidil evoked relaxations were more potent within mesenteric arteries from F-D/M rats when compared to F-P/E (Fig 4.4.E; *n*=5-6; *P*≤0.05).

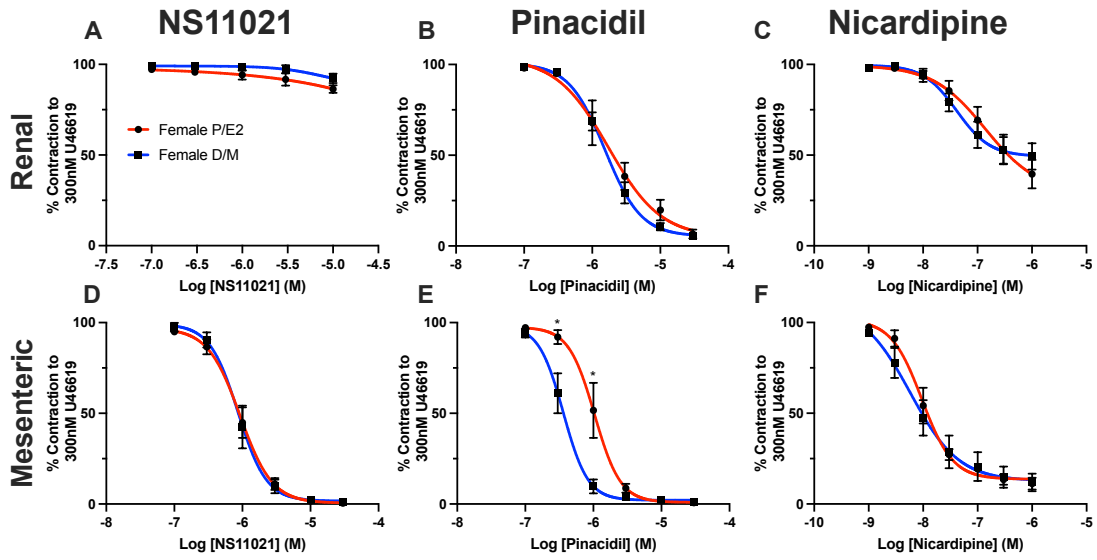

Figure 4.4: Ion channel modulator mediated vasorelaxation in renal female (P/E) and female (D/M) Wistar rats.

NS11021 (0.1-30µmol-L^{-1}; A,D), pinacidil (0.1-30µmol-L^{-1}; B,E) and nicardipine (0.001-1µmol-L^{-1}; C,F) mediated relaxation of pre-constricted arterial tone (300nmol-L^{-1} U46619) in renal (A-C) and mesenteric (D-F) arteries from female pro-oestrus/oestrus (red; *n*=4-5) and female di-oestrus/met-oestrus (D/M; blue; *n*=5-7) Wistar rats. All values are expressed as means ± SEM error bars. A two-way statistical ANOVA with a post-hoc Bonferroni test was used to generate significance values (*=*P*≤0.05). (*n*=) number of animals used (A-F).

4.3.2 Diminished K_V7 channel contribution to receptor mediated responses underpins Oestrus cycle dependent changes in contractility

Previous studies in arteries from male rats have shown that K_V7 blockers like linopirdine enhance receptor-mediated contractions (see Fig 3.8; Brueggemann *et al.*, 2006) and diminish cAMP-PKA dependent β-adrenoreceptor mediated vasorelaxation (see Fig 3.9; e.g Chadha et al., 2012, Stott et al., 2018). Experiments were undertaken to determine if Linopirdine affected receptor-mediated contractions and relaxations in arteries from female rats.

U46619 (0.003-3 μmol-L^{-1}) evoked vasocontraction was significantly less efficacious at lower concentrations within renal and mesenteric arteries from F-D/M when compared to vessels from F-P/E rats (Fig 4.5.A,B $P \leq 0.05$; n=8-10). Linopirdine significantly augmented the sensitivity of renal and mesenteric arteries to U46619-mediated vasocontraction within vessels from F-D/M, but not F-P/E rats (Fig 4.5.A-D; $P \leq 0.05$; n=5-10). Within arteries from F-D/M rats pre-incubated in linopirdine, the response to U46619 was equipotent to arteries from F-P/E rats preincubated in either DMSO solvent control or linopirdine (Fig 4.5.A,B,C,D). In contrast, pre-incubation with HMR-1556 had no effect within any group (Fig 4.5.C,D).

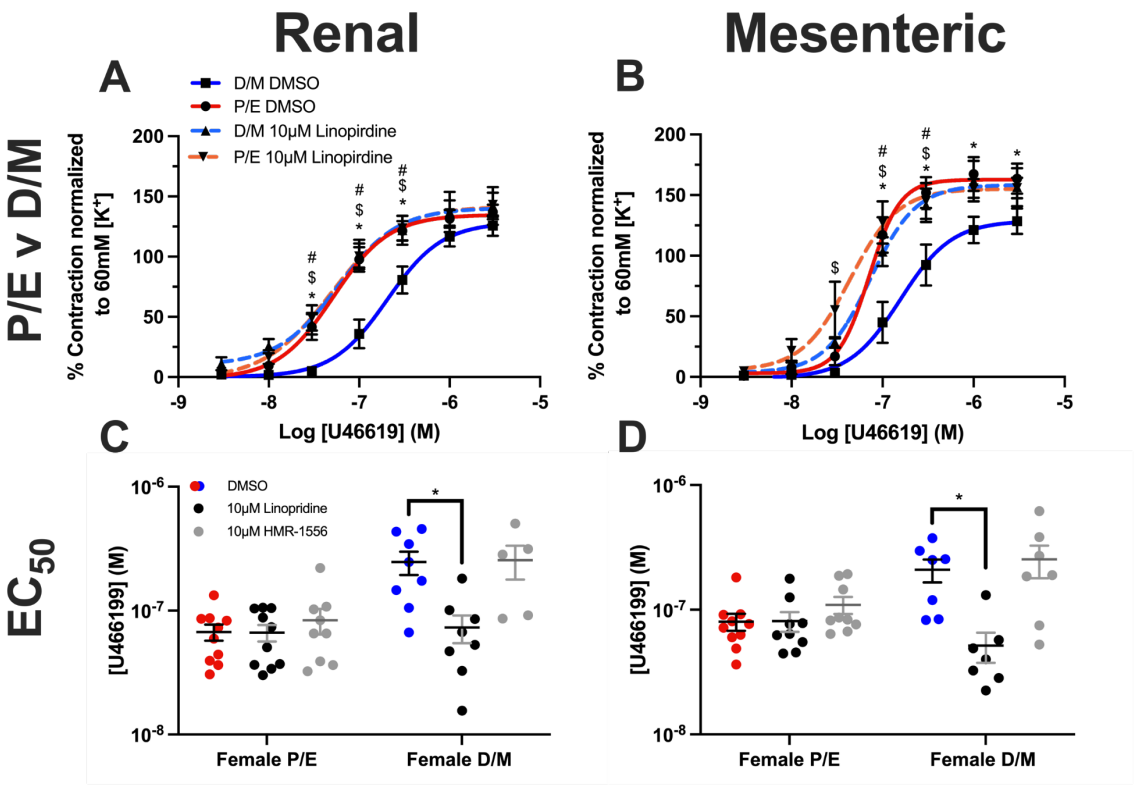

Figure 4.5: U46619-mediated contraction in renal and mesenteric arteries from female D/M, but not female P/E Wistars are underpinned by K_V7.2-5 channels.

Mean data of contraction in response to U46619 (0.003-3μmol-L^{-1}) within renal (*n*=7-10; A) and mesenteric (*n*=7-10; B) arteries preincubated within DMSO solvent control (Female di-oestrus/met-oestrus (D/M), blue; Female pro-oestrus/oestrus (P/E), red; or Linopirdine (10μmol-L^{-1}; Female D/M, blue-dashed line; Female P/E, red-dashed line). Scatter graph representing the raw EC_{50} values of U46619-mediated contraction within renal (C) and mesenteric (D) arteries of the mean data above, in addition to vessels pre-incubated in K_V7.1 specific blocker HMR1556 (10μmol-L^{-1}; grey). A two-way statistical ANOVA with a post-hoc Bonferroni (A,B) or Dunnet's (C,D) correction was used to generate significance values; values (*/#/$= $P \leq 0.05$). Post-hoc Bonferroni statistical comparisons include Ctrl v Ctrl (*= D/M DMSO v P/E DMSO), Ctrl v Same group condition (#= D/M DMSO v D/M 10μmol-L^{-1} Linopirdine) and Ctrl v Different group condition ($= D/M DMSO v P/E 10μmol-$L^{-1}$ Linopirdine; A,B). Dunnet's statistical comparisons include (*= DMSO v Condition, C,D). (*n*=) number of animals used (A-D).

Isoprenaline was significantly less potent in renal and mesenteric arteries from F-P/E rats when compared to vessels from F-D/M rats (Fig 4.6.A,B; *n*=5-6; *P*≤0.05). Similar to previous reports (Fig 3.9; Chadha *et al.*, 2012; Stott, Barrese & Greenwood, 2016), linopirdine significantly attenuated Isoprenaline-mediated vasorelaxation in arteries from F-D/M (Fig 4.6.A-D; *n*=5; *P*≤0.05) but had comparably minor effect on isoprenaline-mediated vasorelaxation in arteries from F-P/E rats (Fig 4.6.A-D; *n*=5; *P*≤0.05). The response to isoprenaline in arteries from F-D/M rats pre-incubated in linopirdine, was equipotent to arteries from F-P/E rats preincubated in either DMSO solvent control or linopirdine (Fig 4.6.C,D). Moreover, in all vessels pre-incubation with HMR-1556 had no effect (Fig 4.6.C,D).

The aggregated findings indicate that the K_V7.2-5 channel contribution to isoprenaline, and U46619-mediated vascular response was diminished within arteries from F-P/E rats. This phenomenon potentially underpins the observed oestrus cycle dependent increased sensitivity of arteries to TXA2-receptor-mediated contraction and decreased sensitivity to β-adrenoreceptor-mediated relaxation in arteries from F-P/E when compared to F-D/M rats.

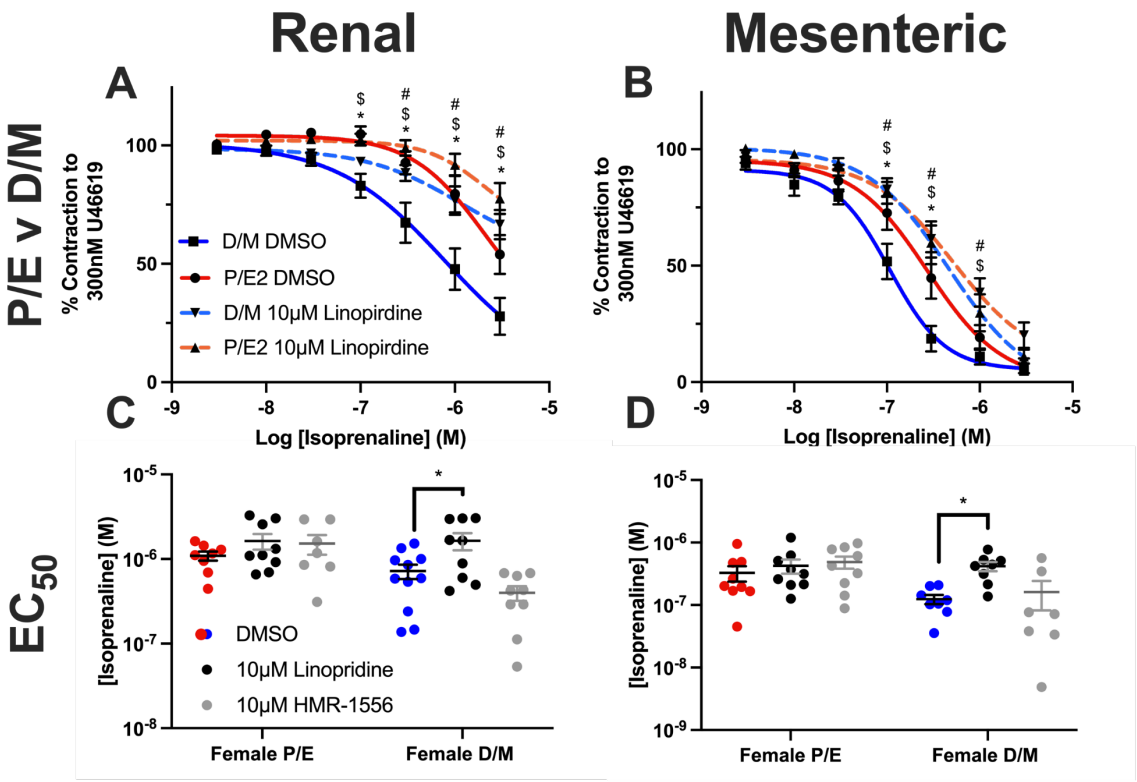

Figure 4.6: Isoprenaline-mediated relaxation in renal and mesenteric arteries from female D/M, but not female P/E Wistars are underpinned by K_V7.2-5 channels.

Mean data of relaxation of pre-contracted tone (U46619; 300nmol-L^{-1}) in response to Isoprenaline (0.003-3μmol-L^{-1}) in renal (*n*=9-10; A,C) and mesenteric (*n*=8-9; B,D) arteries preincubated in DMSO solvent control (female di-oestrus/metestrus (D/M), blue; female pro-oestrus/oestrus (P/E), red) or Linopirdine (10μmol-L^{-1}; Female D/M, blue-dashed line; Female P/E, red-dashed line). Scatter graph representing the raw EC_{50} values of Isoprenaline-mediated relaxation within renal (C) and mesenteric (D) arteries of the mean data above, in addition to vessels pre-incubated in K_V7.1 specific blocker HMR1556 (10μmol-L^{-1}; grey). A two-way statistical ANOVA with a post-hoc Bonferroni (A,D) or Dunnet's (C,D) correction was used to generate significance values; values (*/#/$= *P*≤0.05). Post-hoc Bonferroni statistical comparisons include Ctrl v Ctrl (*= D/M DMSO v P/E DMSO), Ctrl v Same group condition (#= D/M DMSO v D/M 10μmol-L^{-1} Linopirdine) and Ctrl v Different group condition ($= D/M DMSO v P/E 10μmol-$L^{-1}$ Linopirdine; A,B). Dunnet's statistical comparisons include (*= DMSO v Condition, C,D). (*n*=) number of animals used (A-D).

4.3.3 Identification of K_V7 channel transcript and protein expression in female Wistar arteries

4.3.3.1 K_V7 at the level of the transcript

Determination of *Kcnq* gene expression by RT-qPCR showed no significant difference in *Kcnq1-5* and β-auxiliary subunit *Kcne1-5* relative transcript abundance within renal and mesenteric arteries from both groups (Fig 4.7.A-D; *n*=5).

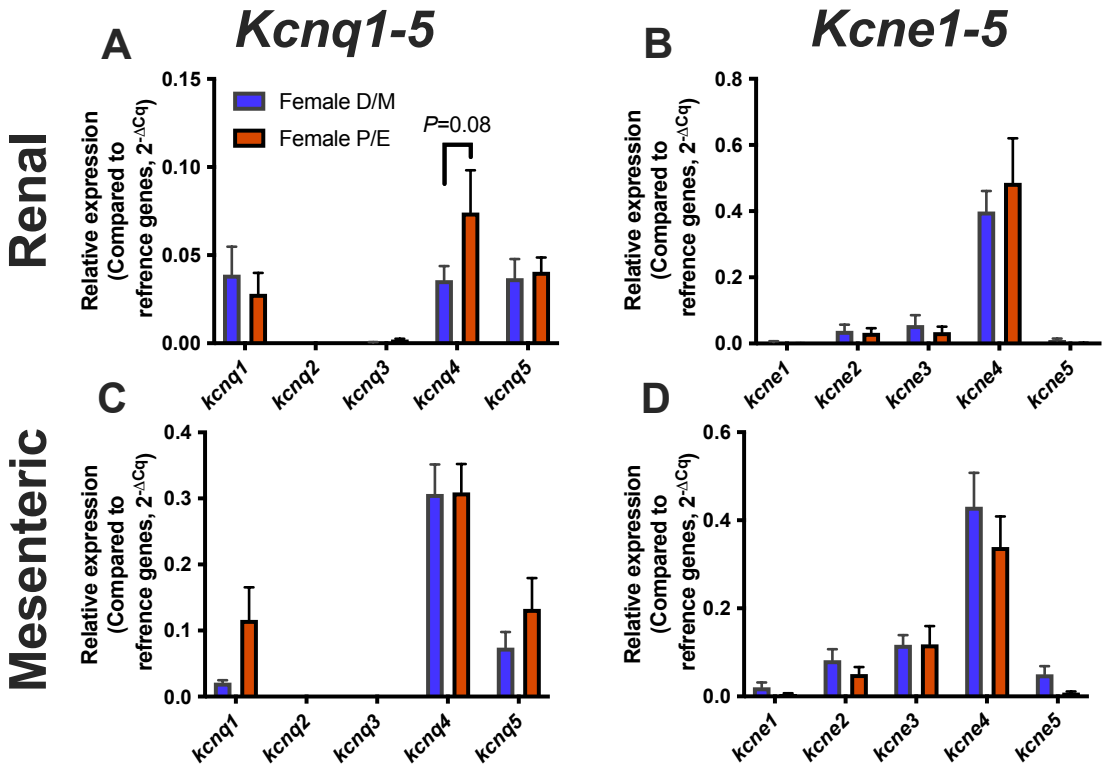

Figure 4.7: Relative mRNA transcript for *Kcnq1-5* and *Kcne1-5* within arteries from female (P/E2) and female (D/M) Wistar rats

Relative transcript abundance for *Kcnq1-5* and *Kcne1-5* were measured within renal (*n*=4-5; A,B) and mesenteric arteries (*n*=4-5; C,D) and heart (E,F; *n*=4) and brain (G,H; *n*=4) from female pro-oestrus/oestrus (P/E; red) and female di-oestrus/met-oestrus (D/M; blue) and mixed female (Grey) Wistar rats when compared to appropriate reference genes ($2^{-\Delta Cq}$) included the following; renal (*Top1, Ubc*) and mesenteric (*Canx, Cyc*1), heart *(Cyc1),* brain (*Gapdh*). All values are expressed as means ± SEM error bars. A 2-way statistical ANOVA with a post-hoc Bonferroni test was used to generate significance values. (*n*=) number of animals used.

4.3.3.2 K_V7 at the level of the protein

Immunocytochemistry of VSMCs isolated from renal and mesenteric arteries from F-D/M Wistar rats revealed K_V7.4 associated fluorescence to be predominantly in the periphery of the cell, overlapping with the membrane marker WGA. In contrast, in VSMCs from F-P/E rats K_V7.4 staining was diffuse throughout the cytosol (Fig 4.8.A,B). Fluorescence intensity profiles for WGA and K_V7.4 drawn randomly across the cell revealed a reduction in the Membrane:Cytosol ratio for K_V7.4 from 1.2±0.19 and 1.8±0.2 in renal and mesenteric artery myocytes from F-D/M rats respectively to 0.5±0.03 and 0.8±0.02 within cells from F-P/E Wistars (Fig 4.8.C; n=3; P≤0.05), however, no reduction in total cell fluorescence (A.U) was observed between the groups (Fig 4.8.D). Indicative of an oestrus cycle dependent shift in K_V7.4 cellular distribution.

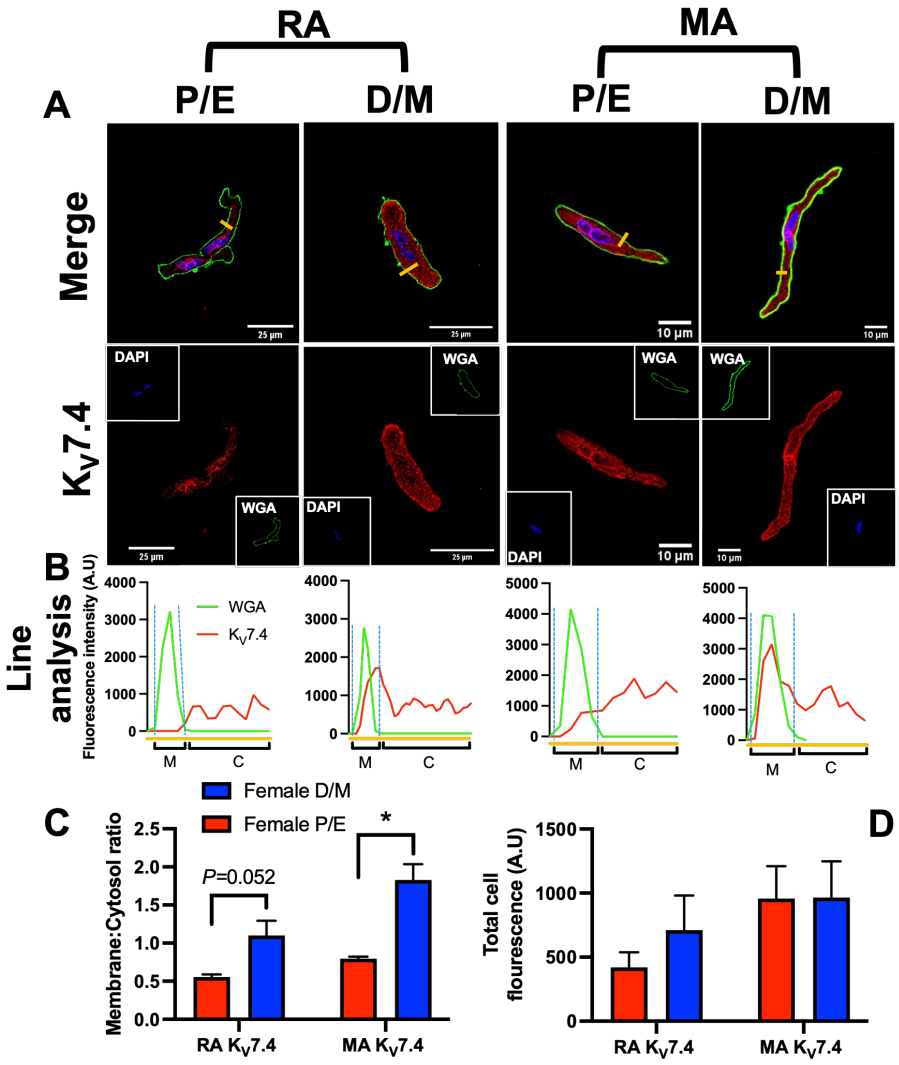

Figure 4.8: Immunocytochemistry demonstrates an oestrus cycle dependent reduction in K_V7.4 subcellular distribution in mesenteric and renal artery myocytes.

Representative images of immunocytochemistry demonstrate K_V7.4 expression (red) from female pro-oestrus/oestrus (P/E; *n*=3) and female di-oestrus/met-oestrus (D/M; *n*=3) renal (RA) and mesenteric (MA; A) artery vascular smooth muscle cells. Plasma membrane and nuclear markers, wheat germ agglutinin (WGA; green) and 4′,6-diamidino-2-phenylindole (DAPI; blue) respectively, are also shown. Fluorescence intensity profiles were plotted for K_V7.4 and WGA measured in arbitrary units (A.U) along the yellow line seen in the merged image above (B). Bar chart demonstrating mean data of the Membrane:Cytosol ratio for K_V7.4 expression in P/E (red) and D/M (blue) RA and MA myocytes (C). Membrane:Cytosol ratio for K_V7.4 expression was calculated by measuring the fluorescence intensity of K_V7.4 within the membrane and dividing it by the fluorescence intensity of K_V7.4 within cytosol from three randomly drawn lines in 10-12 cells pre *n.* Mean data for total cell fluorescence measured in myocytes from MA and RAs from F-P/E (Red) and F-D/M rats (A.U; D). All values are expressed as means ± SEM error bars. A 2-way statistical ANOVA with a post-hoc Bonferroni correction was used to generate significance values. (*n*=) number of animals used.

Similar to previous reports in male arteries (Oliveras *et al.*, 2014; Jepps *et al.*, 2015; Morales-Cano *et al.*, 2015) and our own findings (see Fig 3.14), $K_V7.1$ and KCNE4 staining was typical of ion channels, being found predominantly at the membrane with diffuse staining throughout the cytosol. Similar to our observations in myocytes isolated form male animals however, $K_V7.5$ was diffuse throughout the cytoplasm, with little to no overlap with WGA. As no comparable oestrus cycle dependent differences in the mean analysis of staining for the other K_V7 subtypes associated with vascular function, $K_V7.1$ and $K_V7.5$, nor the β-auxiliary subunit protein Kcne4 were observed in isolated renal artery VSMCs, subsequent experiments focused on $K_V7.4$ alone.

Whilst antibodies for each K_V7 subunit were validated by over-expression studies (see Fig 3.12/3.13) and allowed for effective immunocytochemical imaging (Fig 4.8/9) no $K_V7.4$ antibody was effective in Western blot studies (as illustrated in representative blot in Fig 3.15). Consequently, identification of protein expression relied upon immunocytochemical data alone.

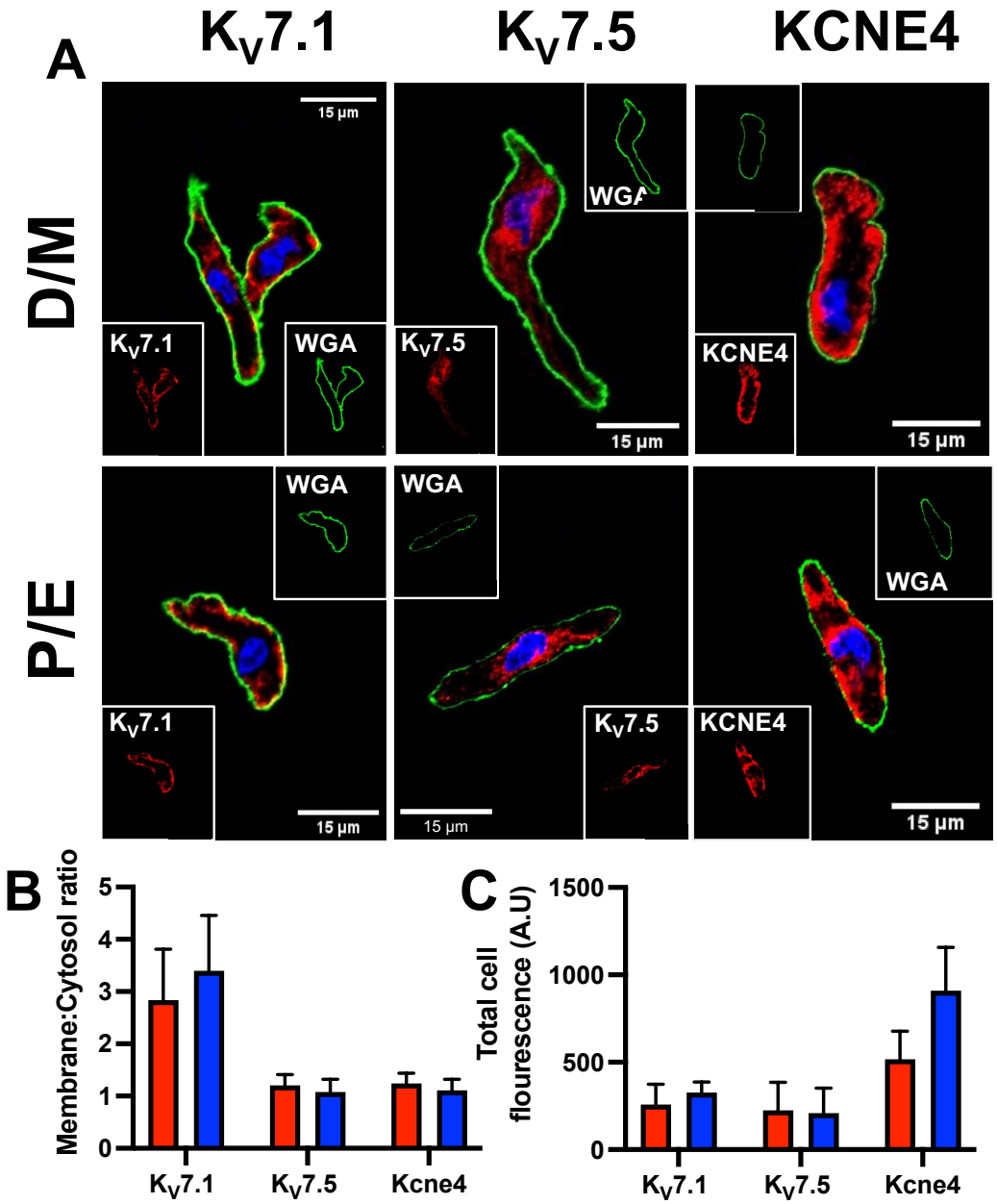

Figure 4.9: Immunodetection of $K_V7.1$, $K_V7.5$ and KCNE4 in isolated renal artery vascular smooth muscle cells from female Wistars.

Representative images of immunocytochemistry demonstrates $K_V7.1$ (A,D), $K_V7.5$ (B,E) and KCNE4 (C,F) staining (red) from female di-oestrus/met-oestrus (D/M; A-C; *n*=3) and female pro-oestrus/oestrus (P/E; D-F; *n*=3) in isolated renal artery vascular smooth muscle cells. Plasma membrane and nuclear markers, wheat germ agglutinin (WGA; green) and 4′,6-diamidino-2-phenylindole (DAPI; blue) respectively, are also shown. Insets demonstrate separated target protein ($K_V7.1$, $K_V7.5$, Kcne4) and membrane marker (WGA). Mean data for Membrane:Cytosol ratio (B) and total cell fluorescence measured in arbitrary units (A.U; D/M, blue; P/E, red; C). All values are expressed as means ± SEM error bars. (*n*=) number of animals used, 8-12 cells per *n*.

4.3.4 Cyclical increases in serum E2 mediate reduction in K_V7.4 membrane abundance via GPER1, impairing ML213-mediated relaxation

4.3.4.1 An analysis of circulating sex-hormones

To identify potential candidates that drive the observed oestrus cycle dependent fluctuation in K_V7.4 membrane abundance and function, plasma was extracted from animals' post-euthanasia. Concentrations of testosterone, E2, progesterone P4, FSH and LH were analysed via ELISA at the Core Facility at the University of Virginia, Charlottesville, USA (Fig 4.10.A-E). Though no statistical significance was achieved, E2 rose from 4±0.5 pg/mL in serum from F-D/M Wistars to 5.6±0.5 pg/mL in F-P/E Wistars (Fig 4.10.B; *P*0.07; *n*=13-14) consistent with published data (Nilsson *et al.*, 2015). No differences between F-D/M and F-P/E were observed within the other hormones investigated. We proposed that a rise in serum E2 during Pro-oestrus mediates a reduction in K_V7.4 membrane abundance that does not recover until Met-oestrus. Therefore, E2 signalling became the focus of the following investigations.

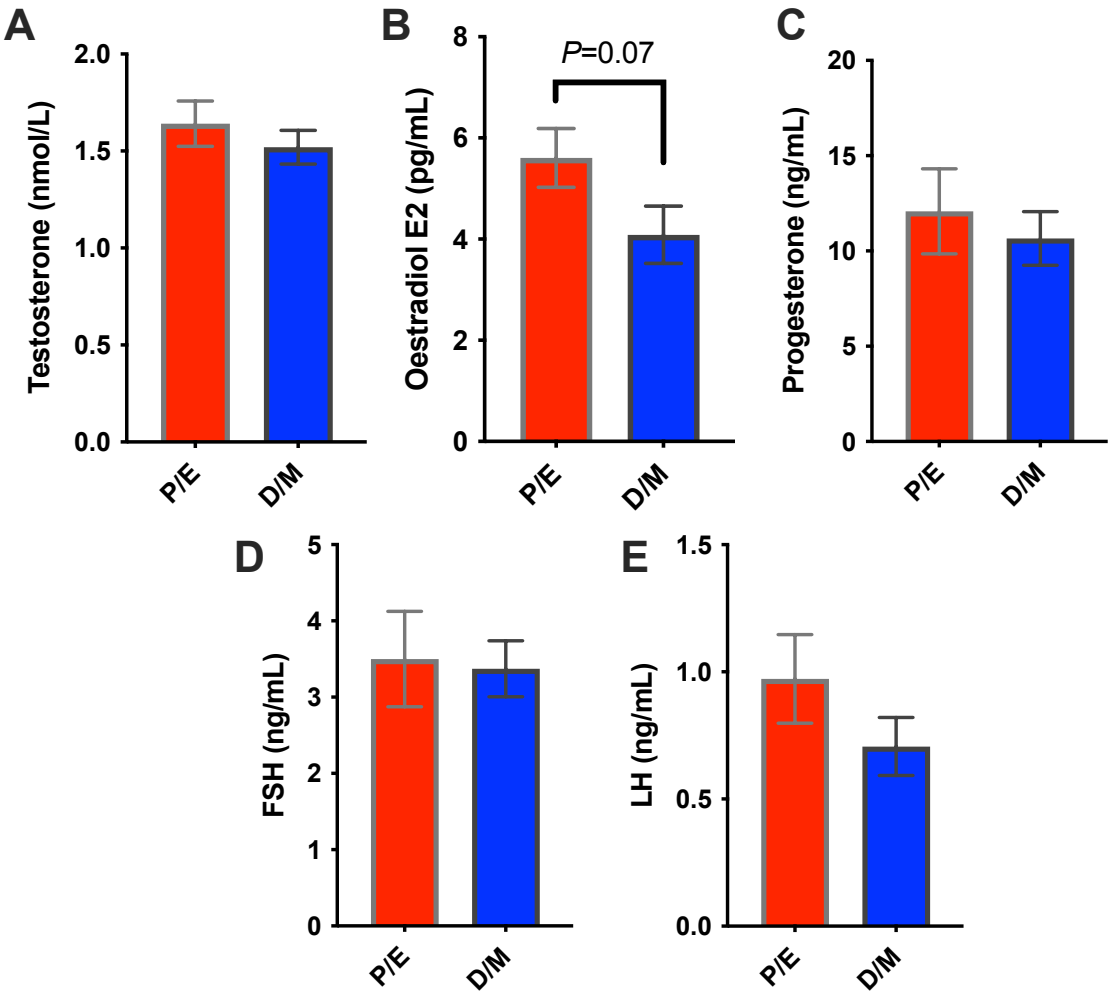

Figure 4.10: Plasma concentration of sex hormones from female Wistar rats

Serum concentration of testosterone (nmol/L; *n*= 13-14; A), Oestradiol E2 (pg/mL; *n*= 13-14; B), progesterone (ng/mL; *n*= 13-14; C), follicular stimulating hormone (ng/mL; *n*= 13-14; D) luteinizing hormone (LH; ng/mL; *n*= 13-14; E) within pro-oestrus/oestrus (P/E; red) and met-oestrus/di-oestrus (D/M; blue) Wistar rats. A students T-test was used to generate significance values. (*n*=) number of animals used (A-E).

4.3.4.2 Expression of Oestrogen receptors

As described in chapter 1.6.1.1, the three principal E2 receptors are ERα and ERβ, canonically considered nuclear receptors, and a novel membrane bound receptor, GPER1, encoded for by *Ers1, Ers2* and *Gper1* respectively. We ascertained the expression of these receptors in rat arteries using whole uterine lysates as a positive control. Rat mesenteric and renal artery lysates from both groups had an expression profile of *Esr1>Gper1>Esr2* whilst the expression profile in uterus was *Esr1>Esr2>Gper1* (Fig 4.11.A,B).

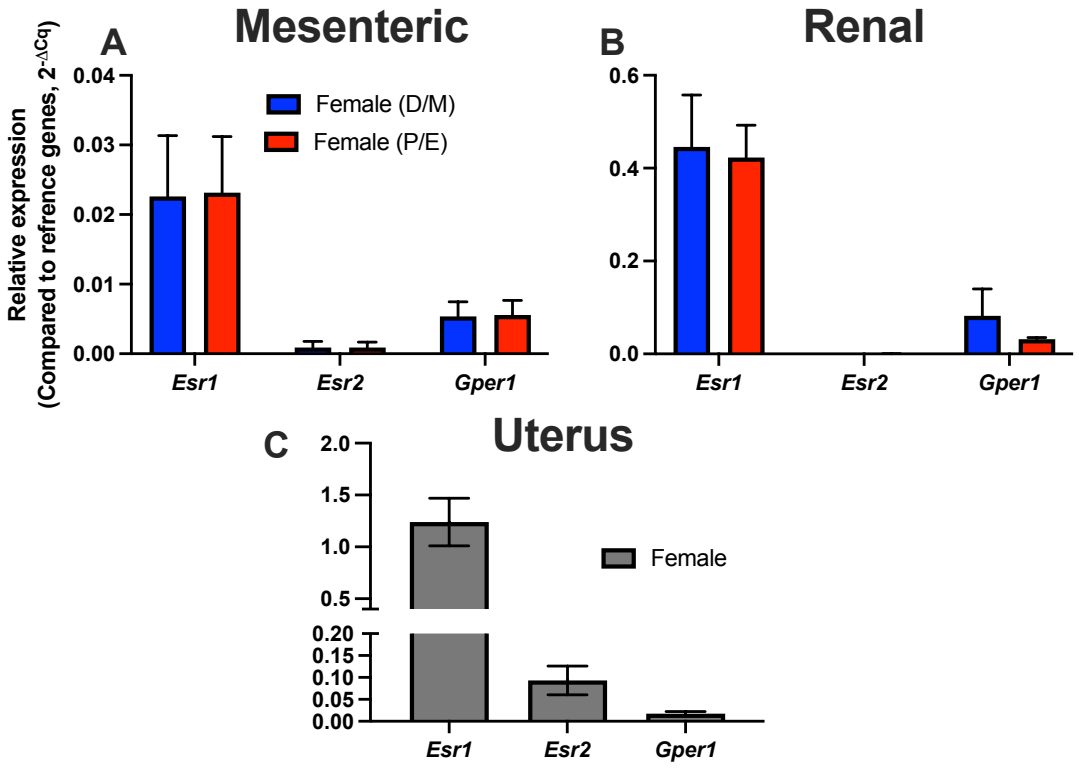

Figure 4.11: Relative mRNA transcript for *Esr1, Esr2* and *Gper1* within arteries from female P/E and female D/M Wistar rats.

Relative transcript abundance for *Esr1, Esr2* and *Gper1* were measured within mesenteric (*n*=5; A) and renal arteries (*n*=5; B) and uterus (*n*=4) from female pro-oestrus/oestrus (P/E; red) and female di-oestrus/met-oestrus (D/M; blue) and mixed female (Grey; C) Wistar rats when compared to appropriate reference genes ($2^{-\Delta Cq}$) including the following; mesenteric (*Canx, Cyc1*), renal (*Top1, Ubc*) and uterus *(Cyc1, Canx*). (*n*=) number of animals used.

4.3.4.3 Time-dependent modulation of ML213-mediated relaxation by E2

The onset of a pro-contractile phenotype in arteries from F-P/E occurs within a narrow time frame in the absence of a change in the relative abundance of *Kcnq*/*Kcne* transcripts. In addition, E2 mediated internalisation of K_V7.1 occurs via a fast acting, 'non-genomic' signalling cascade (Alzamora *et al.*, 2011; Rapetti-Mauss *et al.*, 2013). As such, experiments were undertaken to ascertain if non-genomic E2 signalling could underlie the oestrus cycle-dependent change in K_V7.4.

Initial investigations sought to determine the minimum-time required to evoke E2 mediated effects on K_V7 channel modulator activity. Renal and mesenteric arteries from female Wistar rats were incubated with E2 for a period of 5, 15 or 30mins. Within mesenteric and renal arteries from F-D/M, 30 mins (grey, triangle) of E2 pre-incubation significantly impaired ML213-mediated relaxation (Fig 4.12.A,C; $P \leq 0.05$; n=4-5), however, 5 mins (black, circle) pre-incubation was comparably more effective than 30 min in mesenteric arteries from F-D/M when compared to solvent control (Fig 4.12.A; $P \leq 0.05$; n=4-5). E2 had no effect in arteries form F-P/E animals (Fig 4.12.B,D). Consequently, a minimal pre-incubation time of 30 mins or 5 mins for renal and mesenteric arteries respectively was used for E2 receptor agonists in the following investigations.

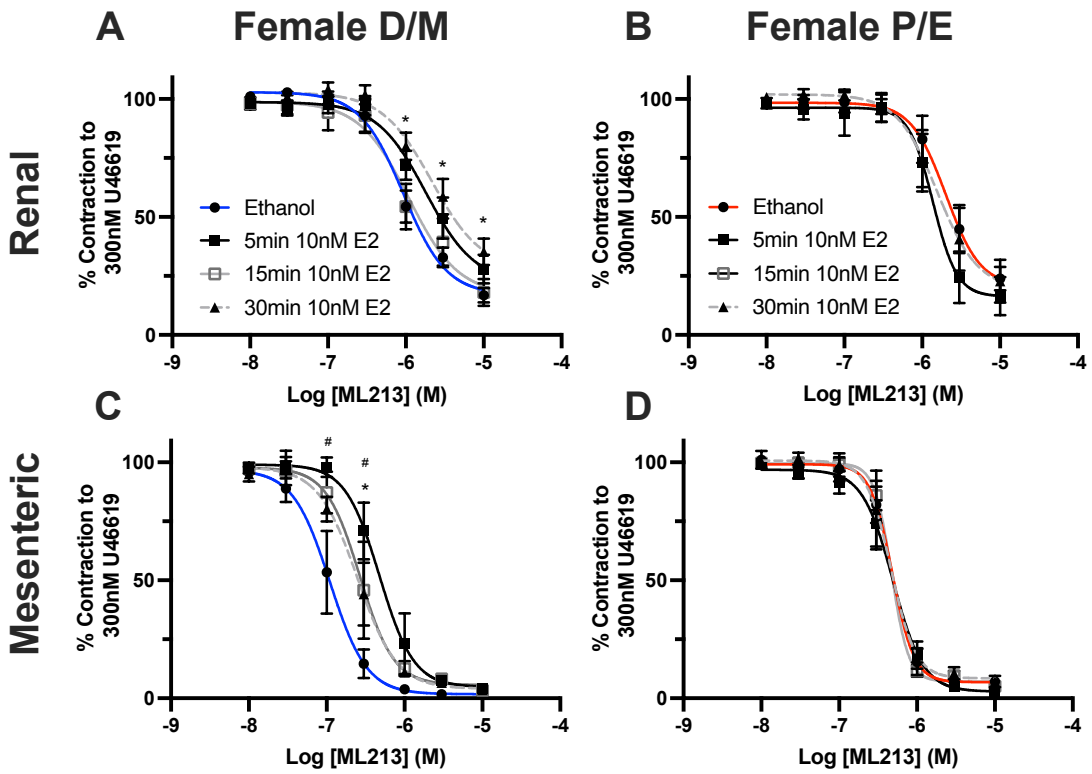

Figure 4.12: Oestradiol E2 mediated vascular effects are time dependent.

Mean data for ML213 mediated relaxation (0.01-10µmol-L^{-1}) of pre-contracted arterial tone in (U46619; 300 nmol-L^{-1}) in renal (A,B *n*=5) and mesenteric (C,D; *n*= 4-5) arteries from female D/M and female P/E Wistars pre-incubated in solvent control (DMSO/Ethanol; blue / red), Oestradiol E2 (0.01µmol-L^{-1}; E2) pre-incubated for 5mins (black), 15min (grey) or 30mins (grey, dashed line). All values are expressed as means ± SEM error bars. A 2-way statistical ANOVA with a post-hoc Dunnet's correction was used to generate significance values (*/#= *P*≤0.05; *= Ethanol v 30min E2; #= Ethanol v 5min E2). (*n*=) number of animals used.

4.3.4.4 E2 and G-1 analogously impair K_V7.4

The candidates for fast-acting oestrogenic signalling include membrane associated GPER1 (Filardo *et al.*, 2000) and ERα following palmitoylation at cysteine residue 446 (Simoncini *et al.*, 2000). Incubating isolated mesenteric artery VSMCs from F-D/M Wistars in either pan-oestrogen receptor agonist E2 (10 nmol-L^{-1}) or GPER1 specific agonist G-1 (1 µmol-L^{-1}; Dennis *et al.*, 2009) for 30 mins reduced the overlap of K_V7.4 staining (Fig 4.13.A; red) with WGA (Fig 4.13.A; green) when compared to DMSO/Ethanol control. This resulted in a significant reduction in the Membrane:Cytosol ratio for K_V7.4 staining ($P \leq 0.05$; $n = 3$). In contrast, E2 or G-1 had no effect on the predominantly cytosolic staining for K_V7.4 in VSMCs from mesenteric arteries from F-P/E Wistars (Fig 4.13). Interestingly, the Membrane:Cytosol for K_V7.4 in myocytes from F-D/M rats after treatment with G-1 or E2 was analogous to the reduction observed when comparing myocytes from F-D/M and F-P/E (Fig 4.13). Pre-incubating mesenteric arteries from F-D/M Wistars with E2 / G-1 (5mins) significantly attenuated ML213 (0.01-10µmol-L^{-1}) mediated relaxations of pre-contracted arterial tone (300 nmol-L^{-1} U46619; Fig 4.14.A-C). This response mirrored the potency for ML213-mediated relaxation seen in mesenteric arteries from F-P/E Wistars in control conditions (Fig 4.14.A). Comparable attenuation of ML213-mediated relaxation by E2 and G-1 was observed in renal arteries from female Wistars (Fig 4.14.D-E). Therefore, the structurally dissimilar GPER1 agonists E2 and G-1 impair K_V7.4 membrane abundance and function only in arteries harvested from female rats in a 'low serum E2' stage of the Oestrus cycle.

G-15 is reported to be an effective inhibitor of GPER1 signalling at concentrations ≥1 µmol-L^{-1} (Dennis *et al.*, 2009), however, when pre-incubating isolated cells for immunodetection of K_V7.4 or whole arteries within a wire myograph chamber, G-15 precipitated in both solutions. This left us unable to pharamcologically select against GPER1, however, GPER1 knockout in murine models has repeatedly been shown to ablate physiological responses seen to G-1 (Dennis *et al.*, 2009), and within the literature it is considered to be a highly selective tool for studying GPER1 mediated signalling.

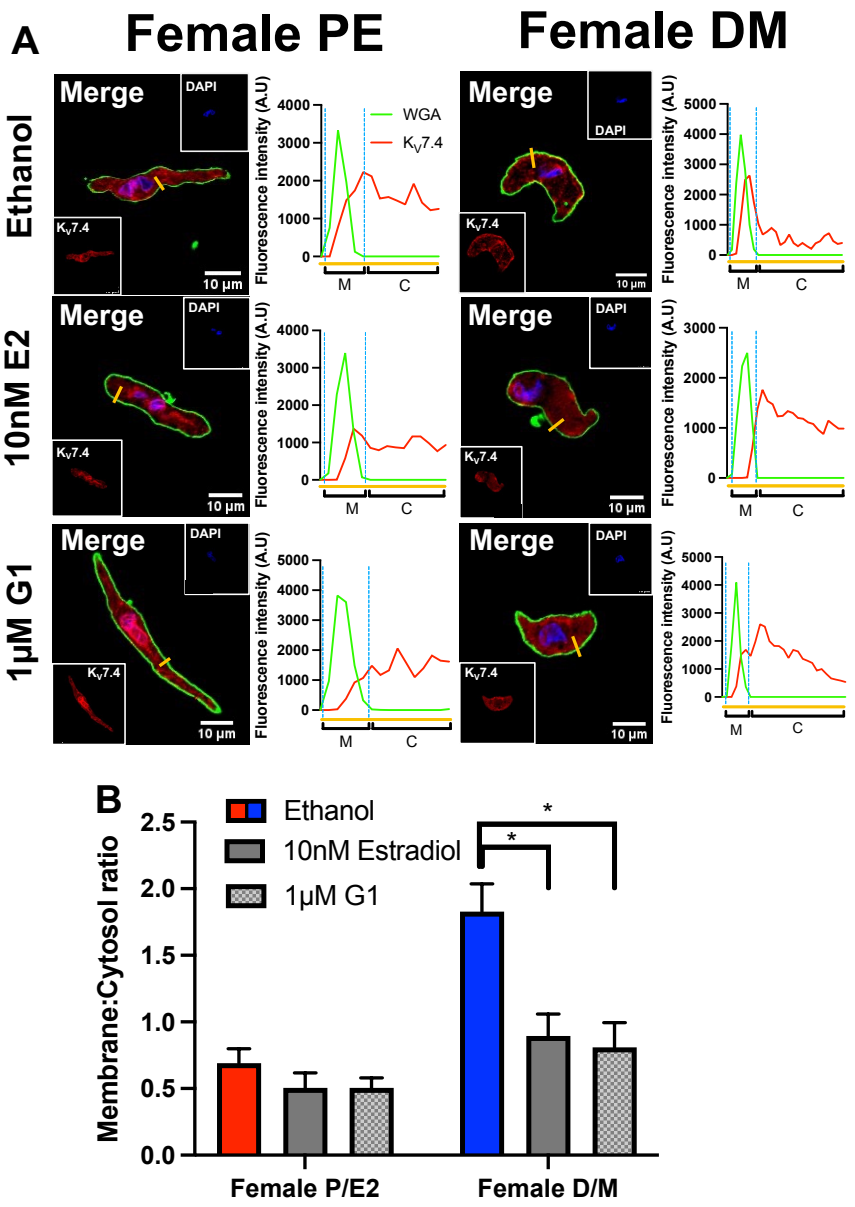

Figure 4.13: Oestradiol E2 and G-protein coupled Estrogen receptor agonist G1 pre-incubation replicate female P/E $K_V7.4$ membrane abundance within female D/M.

Representative images of immunocytochemistry demonstrate $K_V7.4$ expression (red) from female pro-oestrus/oestrus (P/E; *n*=3) and female di-oestrus/met-oestrus (D/M; *n*=3) mesenteric artery vascular smooth muscle cells pre-incubated in either solvent control (ethanol/DMSO), oestradiol (E2; 10nmol-L^{-1}) or G1 (1µmol-L^{-1}; A). Plasma membrane and nuclear markers wheat germ agglutinin (WGA; green) and 4′,6-diamidino-2-phenylindole (DAPI; blue) are also shown. Bar chart demonstrating mean data of the Membrane:Cytosol ratio for $K_V7.4$ expression solvent control (D/M, blue; P/E, red), E2 (grey) or G1 (grey, square pattern; C). Membrane:Cytosol ratio for $K_V7.4$ expression was calculated by measuring the fluorescence intensity of $K_V7.4$ within the membrane and dividing it by the fluorescence intensity of $K_V7.4$ within cytosol from three randomly drawn lines in 10-12 cells pre *n.* A 2-way statistical ANOVA with a post-hoc Dunnet's's correction was used to generate significance values. (*n*=) number of animals used.

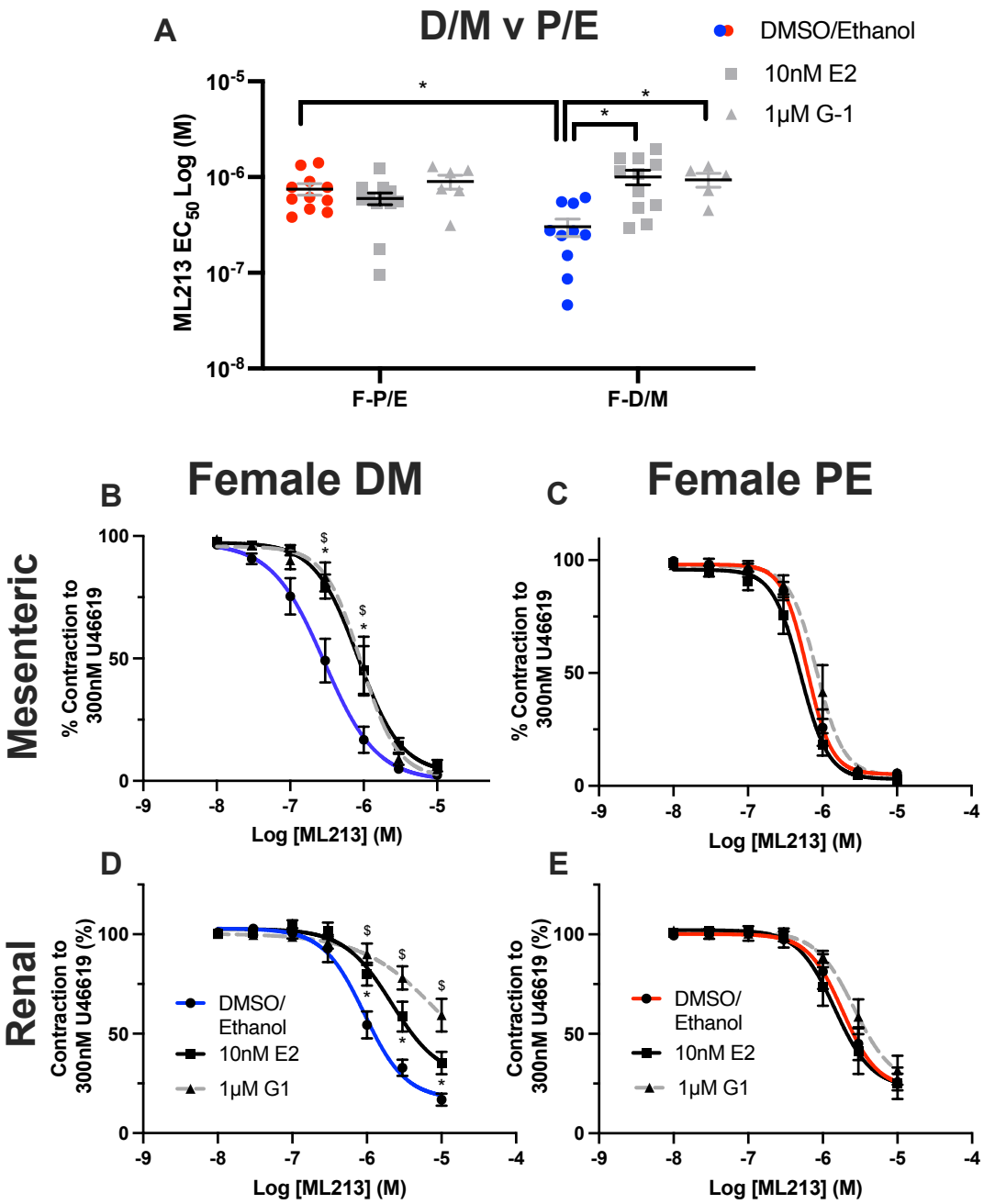

Figure 4.14: Oestradiol and G-protein coupled Estrogen receptor agonist G1 pre-incubation impair K_V7.2-5 channel activator ML213-mediated relaxation in renal and mesenteric arteries of female D/M, but not female P/E arteries.

Scatter graph plot and mean data for EC_{50} values (A) and mean data for ML213-mediated relaxation (0.01-10μmol-L^{-1}, B-E) of pre-contracted arterial tone in (U46619; 300nmol-L^{-1}) in mesenteric (A-C; *n*= 6-10) and renal (D,E; *n*=6-8) arteries from female D/M and female P/E Wistars pre-incubated in solvent control (DMSO/Ethanol; blue / red), Oestradiol E2 (0.01μmol-L^{-1}; E2; black) or G1 (1μmol-L^{-1}; grey, dashed line). All values are expressed as means ± SEM error bars. A 2-way statistical ANOVA with a post-hoc Dunnet's's correction was used to generate significance values (*/$= *P*≤0.05; *= DMSO/Ethanol v E2; $= DMSO/Ethanol v G1). (*n*=) number of animals used.

4.3.4.5 GPER1 activation reduced K_V7.4 currents in overexpression system

Ruptured whole cell current recording from HEK-K_V7.4 was used as a secondary means of determining the effect of GPER1 activation on K_V7.4 channel activity. As per Figure 2.7.3, cells transfected with pCMV3-GPER1-GFPSpark were identified under fluorescence microscopy via Nikon C-SHG mercury lamp attached to the head stage. Cells fluorescing green to high intensity UV light were considered *GPER1*-transfected (GPER1), whilst translucent cells were considered non-transfected (N-T).

As representative traces and mean data show in Figure 4.15.A,B, incubation of HEK-K_V7.4 cells with the GPER1 agonist G-1 (1 µmol-L^{-1}) for 30 mins produced a considerable reduction in currents recorded from HEK-K_V7.4 cells only when the GPER1 receptor was co-expressed ($P \leq 0.05$; $n = 6$). Analogous to G-1, E2 (10 nmol-L^{-1}; red, square) pre-incubation reduced K_V7.4 currents at +20mV when compared to N-T solvent control (black, circle; $P \leq 0.05$; $n = 6$-7; Fig 4.15.C) only in cells expressing GPER1. GPER1 stimulation by either G-1 or E2 did not affect the voltage-dependence of activation, as shown by no change in $V_{1/2}$ when compared to controls (Fig 4.15.D). Currents recorded under solvent control conditions were identical in un-transfected and GPER1-expressing HEK cells (Fig 4.15). In summary, GPER1 stimulation diminishes *KCNQ4*-encoded currents independent of a change in current gating properties, indicative of a reduction in total channel number.

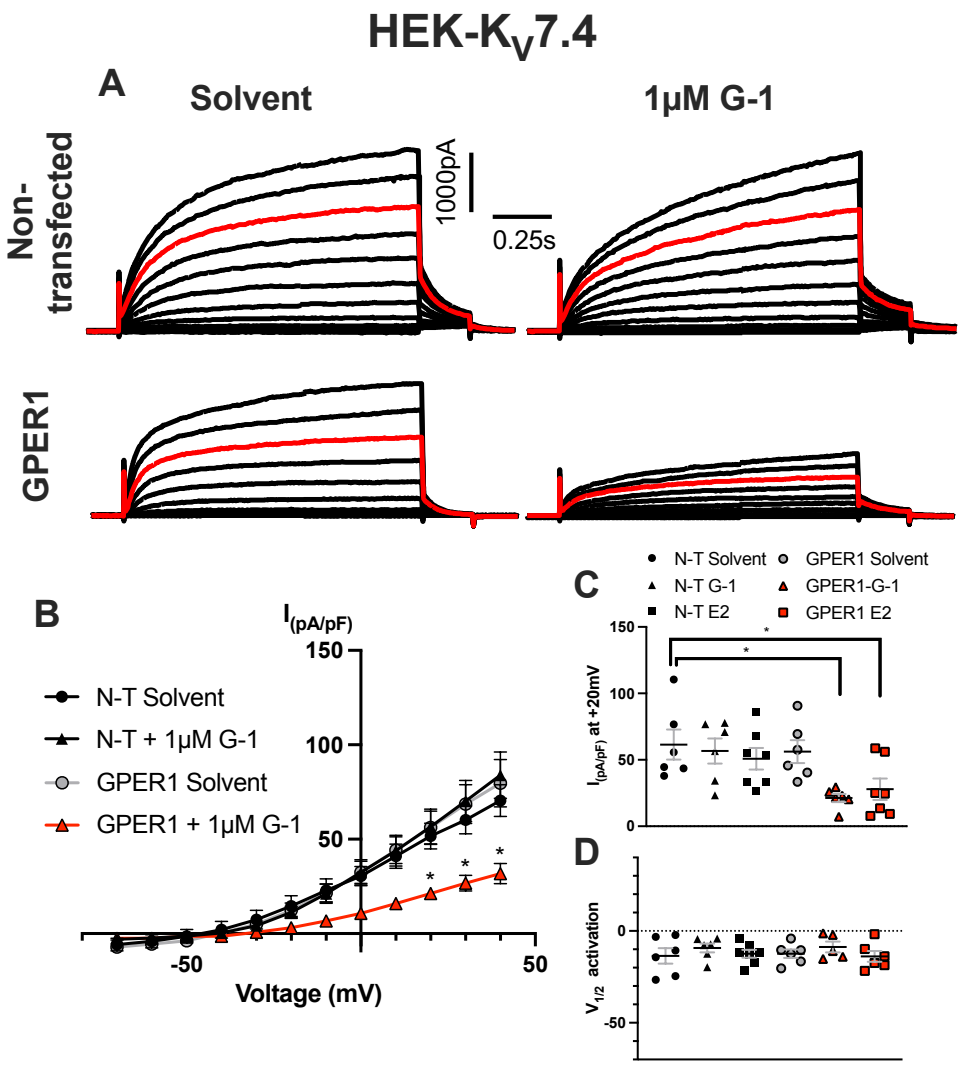

Figure 4.15: Oestradiol E2 and G1 pre-incubation impair K_V7.4 channel activity.

Representative current recordings during ruptured whole cell patch-clamp in non-transfected (N-T) HEK-K_V7.4 pre-incubated (30min) in solvent control (upper left) or G-1 (1µmol-L^{-1}; upper right) and GPER1-transfected cells pre-incubated in solvent control (lower left) or G-1 (lower right; A). Red line represents current flow in response to +20mV. Cells were held at a holding potential of -60mV, then stepped to test voltage for 1.5sec every 15 sec ranging from -70mV to +40mV increasing in 10mV intervals. Before returning to rest potential, voltage was stepped to an inactivation potential of -40mV. Mean *IV* relationships plotted for HEK-K_V7.4 cells; NT in solvent control (black, circle; *n*= *5*) or G-1 (black, triangle; *n*= 6) and GPER1 transfected cells in solvent (grey, circle; DMSO; *n*= 6) or G-1 (red, triangle; red; *n*= 6; B). Scatter graph demonstrates peak current amplitude at +20mV in non-transfected cells pre-incubated in solvent control (black, circle; *n*=6), G-1 (black tringle; *n*=6), Oestradiol E2 (10 nmol-L^{-1}; black, square; *n*=7) and GPER1 transfected cells solvent control (grey, circle; *n*=6), G-1 (red tringle; *n*=6), Oestradiol E2 (red, square; *n*=7; C). Voltage dependence of activation for K_V7.4 currents (D). All values are expressed as means ± SEM error bars. A 2-way statistical ANOVA (B) with a post-hoc Dunnet's's correction or a 1-way statistical ANOVA (C,D) was used to generate significance values. (*= *P*≤0.05) condition vs non-transfected solvent control. (*n*=) number of cells used.

4.3.4.6 E2 reduces K_V7.4 interaction with forward trafficking molecular chaperone protein heat-shock protein 90 in F-D/M, but not F-P/E VSMCs

The molecular chaperone protein HSP90 is critical in the folding and biogenesis of K^+ channels including K_{ATP} (Yan *et al.*, 2010), K_V11.1 (Ficker, 2003) and K_V7.4 (Gao *et al.*, 2013). Additionally, GPER1 activation increases human myometrial contractility by phosphorylation of heat shock protein 27 (Maiti *et al.*, 2011) and Ang-II application decreased the interaction of K_V7.4 and HSP90 diminishing K_V7.4 membrane abundance in mesenteric arteries (Barrese *et al.*, 2018). Therefore, we proposed that the reduction in Membrane:Cytosol ratio observed in response to E2 / G-1 was underpinned by a reduction in interaction of K_V7.4 and HSP90 in a process similar to Ang-II. PLA was used to resolve protein-protein interactions ≤40 nm, which are expressed as red puncta within the cell. 30 min pre-incubation with 10 nmol-L^{-1} E2 gave rise to a significant reduction in the interaction between K_V7.4 : HSP90 within mesenteric VSMCs from F-D/M Wistars when compared to Ethanol solvent control (P<0.05; n=3; Fig 4.16). Comparably, no change in K_V7.4 : HSP90 interaction was observed in VSMCs from F-P/E Wistars by E2 (Fig 4.16.B). Additionally, the puncta per cell in VSMCs from F-P/E rats was equivalent to the that observed in VSMCs from F-D/M pre-incubated in E2.

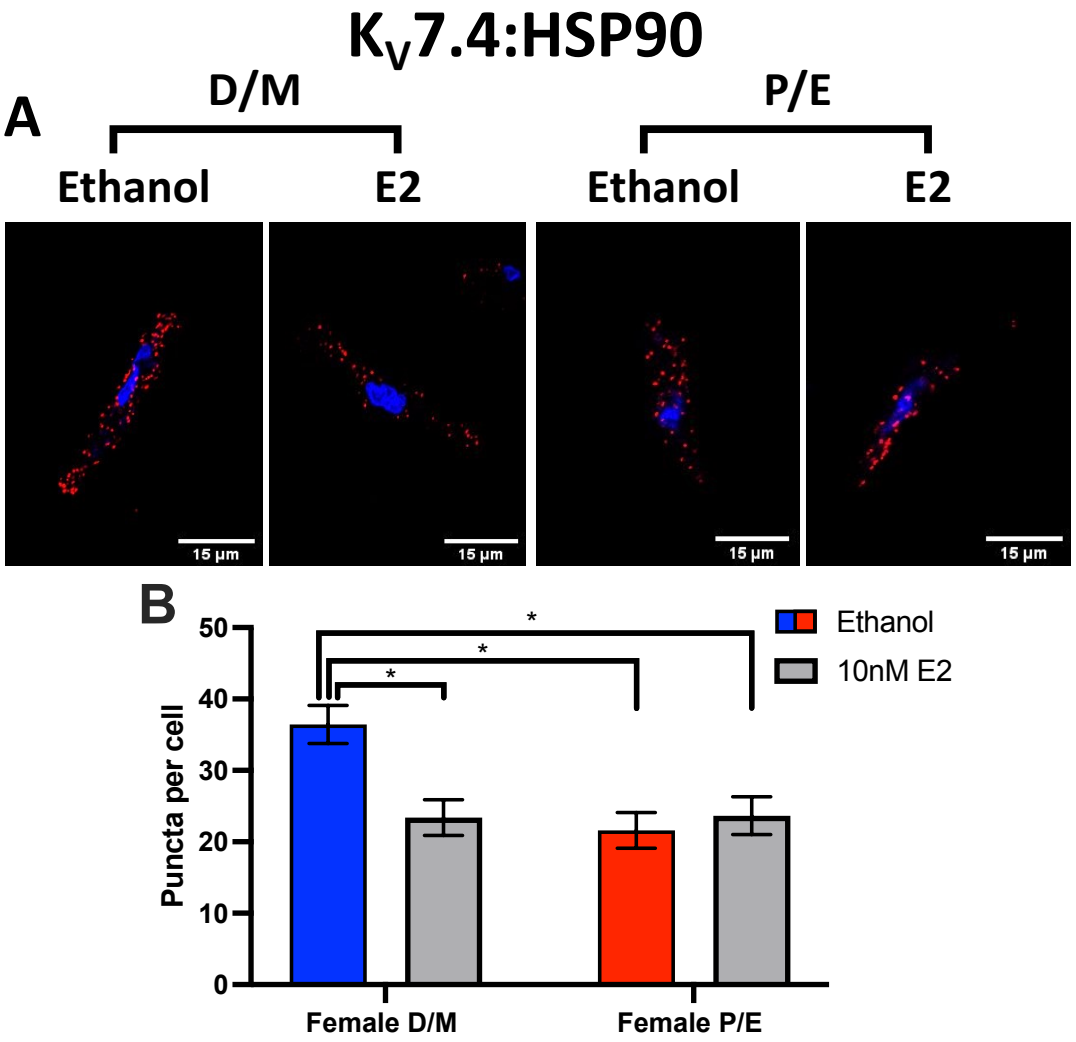

Figure 4.16: Oestradiol reduces K_V7.4-Heat shock protein 90 interactions in F-D/M, but not F-P/E mesenteric artery myocytes.

Proximity ligation assay (PLA) for K_V7.4 and Heat shock protein 90 (HSP90) interaction within female di-oestrus/met-oestrus (D/M) and female pro-oestrus/oestrus (P/E) mesenteric artery myocytes pre-incubated in either ethanol or 10nmol-L^{-1} Oestradiol E2 (E2; 30min; *n*=3). Representative images of mesenteric artery myocyte mid-cell cross section exhibit fluorescent puncta which illustrate K_V7.4:HSP90 interactions within a distance of <40nm (red) and the nucelli via 4′,6-diamidino-2-phenylindole (DAPI; blue). Bar graph of mean data for puncta per-cell in an xy cross section for myocytes taken from mesenteric arteires incubated in solvent control (D/M, blue; P/E, red) or 10 nmol-L^{-1} E2 (grey; B). All values are expressed as mean ± SEM. A 2-way statistical ANOVA with a post-hoc Turkey correction was used to generate significance values. (*n*=) number of animals used, 10-15 cells per *n*.

4.3.5 Oestrogenic signalling similarly diminishes K_V7.4 membrane abundance and functional properties in male arteries

Oestrogenic signalling is often only considered when regarding the female. Males produce both testosterone and small amounts of oestrogen in the testes, however, aromatase expression within the vasculature causes the conversion of androgens to oestrogens locally within arterial smooth muscle. As such the effect of E2 and G-1 on K_V7.4 abundance and function were also determined in males. Like females, we observed *Esr1>Gper1>Esr2* expression in mesenteric and renal arteries (Fig 4.17). Moreover, both E2 and G-1 pre-incubation analogously reduced K_V7.4 membrane abundance (Fig 4.18.A-C) and inhibited ML213-mediated relaxation of pre-contacted tone in mesenteric and renal arteries (Fig 4.18.A-C; $P \leq 0.05$; n=5-8). These effects were comparable to those seen in arteries from females in D/M.

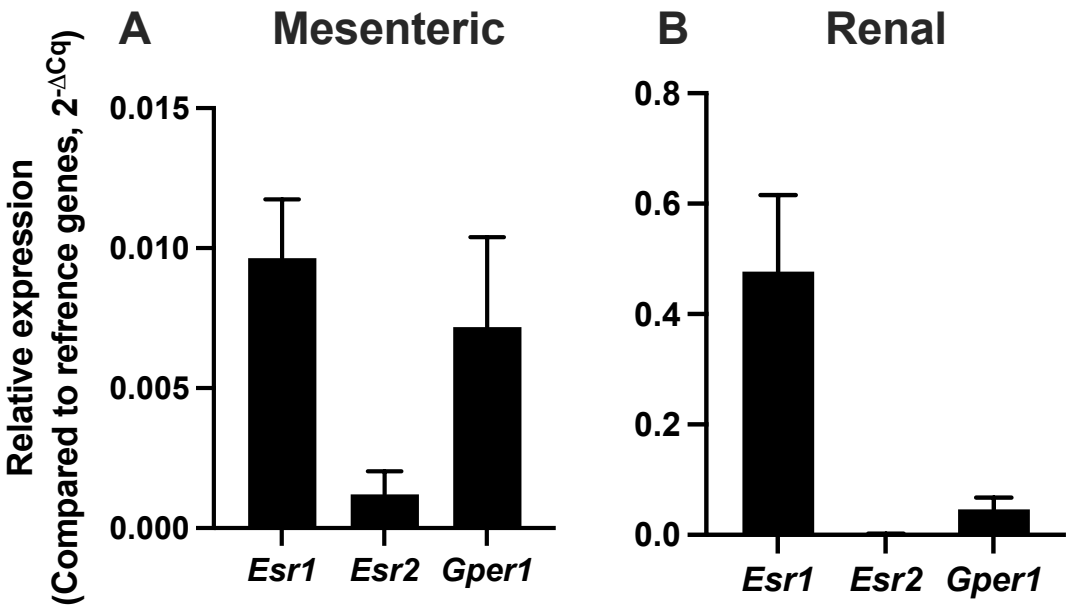

Figure 4.17: Relative mRNA transcript for *Esr1, Esr2* and *Gper1* within arteries male Wistar rats.

Relative transcript abundance for *Esr1, Esr2* and *Gper1* were measured within mesenteric (n=5; A) and renal arteries (n=5; B) male Wistar rats when compared to appropriate reference genes ($2^{-\Delta Cq}$) included the following; mesenteric (*Canx, Cyc1*), renal (*Top1, Ubc)*. All values are expressed as means ± SEM error bars. (n=) number of animals used.

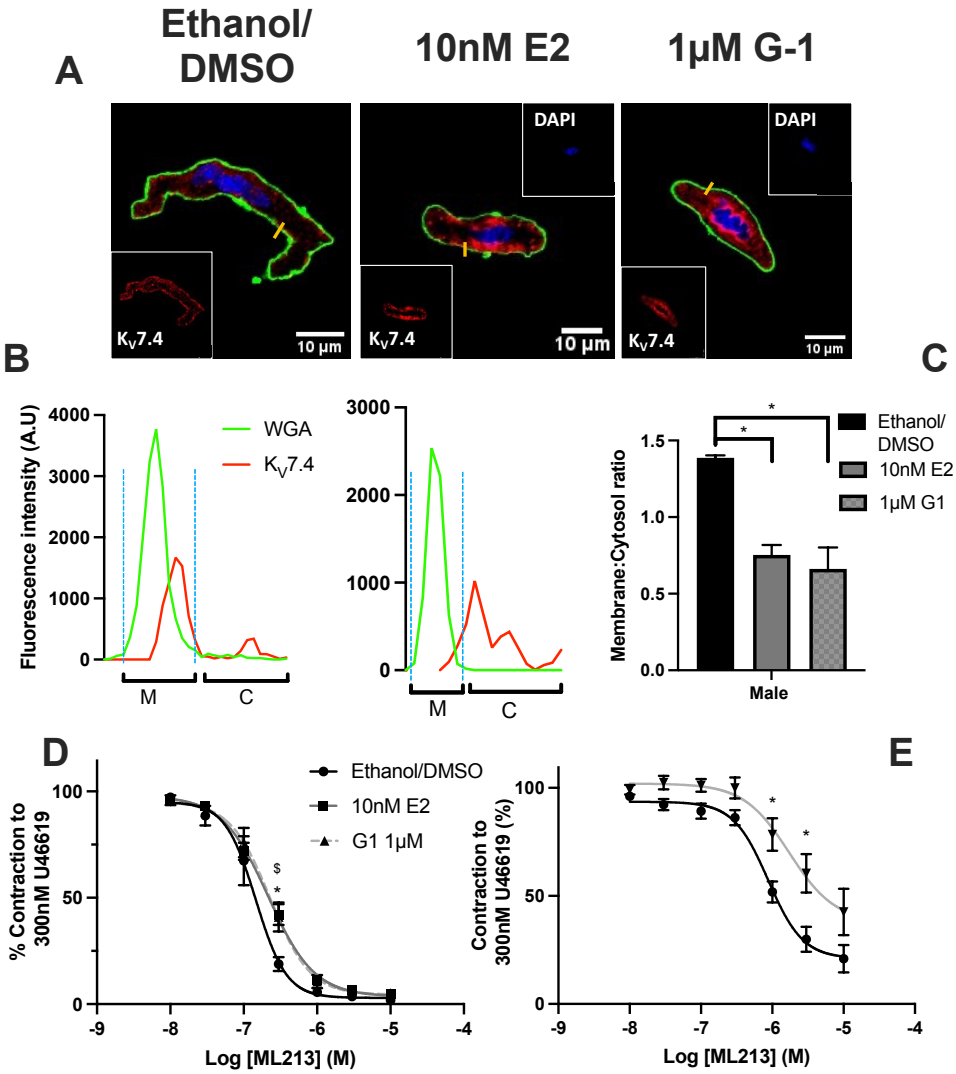

Figure 4.18: Oestradiol E2 and G1 pre-incubation impairs $K_V7.4$ membrane abundance and ML213-mediated relaxation in male mesenteric arteries.

Representative images of immunocytochemistry demonstrates $K_V7.4$ expression (red) from male (*n*=3) mesenteric artery vascular smooth muscle cells pre-incubated in either solvent control (ethanol/DMSO), Oestradiol (E2; 10nmol-L^{-1}) or G1 (1μmol-L^{-1}; A). Plasma membrane and nuclear markers wheat germ agglutinin (WGA; green) and 4′,6-diamidino-2-phenylindole (DAPI; blue) are also shown. Fluorescence intensity profiles were plotted for $K_V7.4$ and WGA measured in arbitrary units (A.U) along the yellow line seen in the merged image above. Representative fluorescence intensity profiles (B) for Solvent (left) and E2 (right). Bar chart demonstrating mean data of the Membrane:Cytosol ratio for $K_V7.4$ expression solvent control (black), E2 (grey) or G1 (grey, square pattern; C). Mean data for ML213-mediated relaxation (0.01-10μmol-L^{-1}) of pre-contracted arterial tone in (U46619; 300nmol-L^{-1}) in mesenteric (D) and renal (E) arteries from male Wistars pre-incubated in solvent control (DMSO/Ethanol; black; *n*=5), E2 (grey; *n*=5) or G1 (grey, dashed line; *n*=5; D/E). All values are expressed as means ± SEM error bars. A 2-way statistical ANOVA with a post-hoc Dunnet's's correction was used to generate significance values. (*n*=) number of animals used.

4.3.6 Oestrus cycle dependent regulation of arterial reactivity is non-vascular bed specific and partially K_V7 dependent

4.3.6.1 Cyclical changes in sensitivity to K_V7 activators, but not inhibitors

Similar to renal and mesenteric arteries, ML213 (0.1-10 μmol-L^{-1}) was a more effective relaxant of cerebral and coronary arteries from F-D/M when compared to arteries from F-P/E ($P \leq 0.05$; n=4-6; Fig 4.19). In contrast to renal and mesenteric arteries, the pan-K_V7 channel inhibitor linopirdine (10 μmol-L^{-1}) evoked significant contraction of basal tone when compared to DMSO solvent control within both groups ($P \leq 0.05$; n=8-12; Fig 4.20).

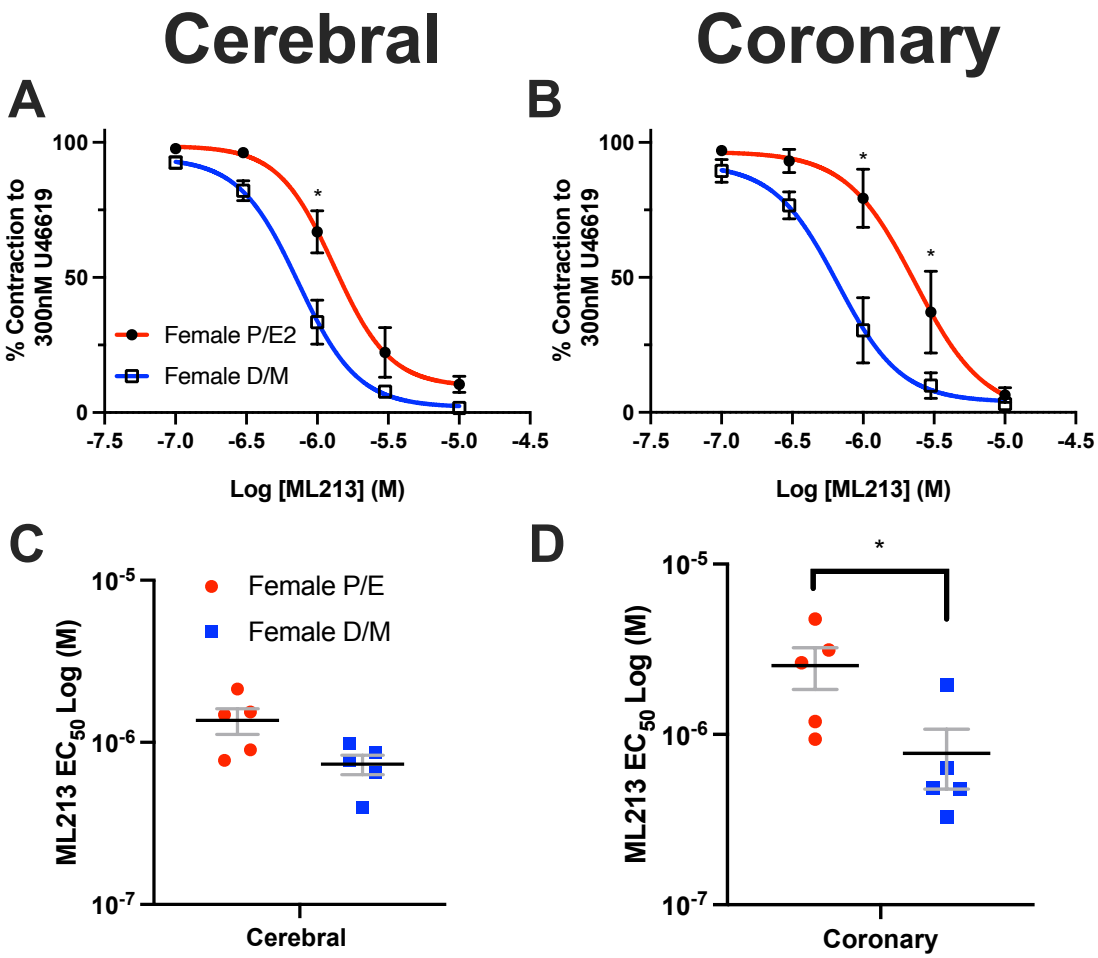

Figure 4.19: K_V7 channel activators are more efficacious and potent arteries from female (D/M) Wistar rats when compared to female (P/E) rats.

Mean data of relaxation of pre-contracted tone (U46619; 300nmol-L^{-1}) in response to ML213 (0.01-10µmol-L^{-1}) in cerebral (*n*=4-6; A) and coronary (*n*=5; B) arteries from female pro-oestrus/oestrus (P/E; red) and female di-oestrus/met-oestrus (D/M; blue) rats. Scatter graph representing the raw EC_{50} values of ML213-mediated relaxation within cerebral (C) and coronary (D) arteries of the mean data above. All values are expressed as means ± SEM error bars. A two-way statistical ANOVA with a post-hoc Bonferoni correction was used to generate significance values (*= *P*≤0.05). (*n*=) number of animals.

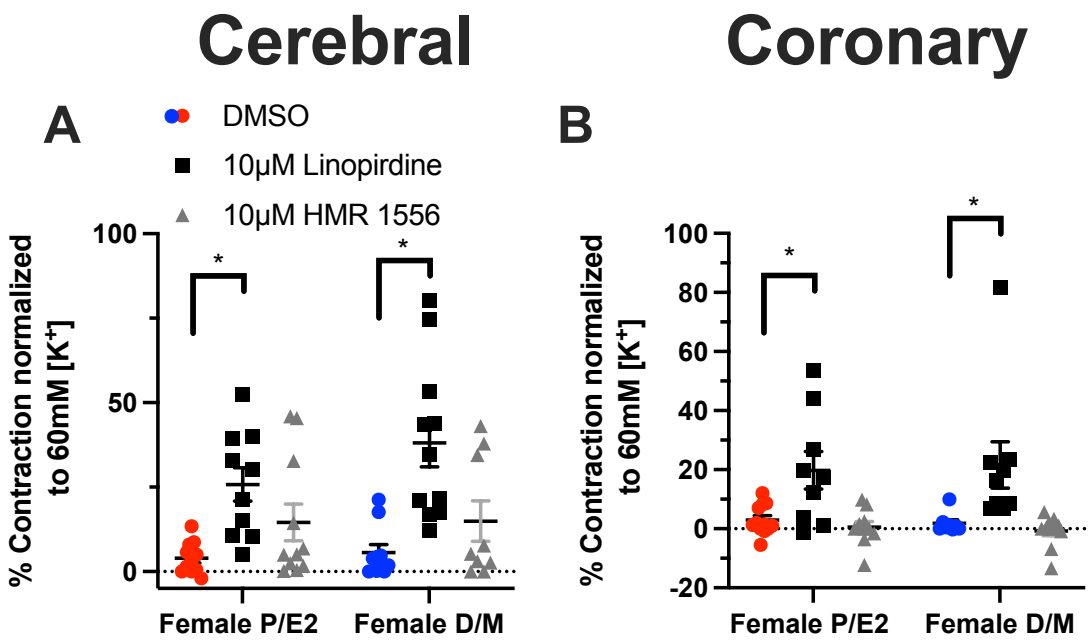

Figure 4.20: K_V7 channel inhibitors are more insensitive to the oestrus cycle within coronary and cerebral arteries from female rats.

Mean data of increases in basal tone in response to solvent control DMSO (Female P/E, red; Female D/M, blue), Linopirdine (10μmol-L^{-1}; black) and HMR-1556 (10μmol-L^{-1}; grey) in cerebral (*n*= 9-11; A) and coronary arteries (*n*= 8-12; B). All values are expressed as means ± SEM error bars. A two-way statistical ANOVA with a post-hoc Dunnet's's (A,B) correction was used to generate significance values (*= *P*≤0.05). (*n*=) number of animals.

4.3.6.2 K_V7 contribution to receptor-mediated responses

The contribution of K_V7 channels to TXA2 and β-adrenoreceptor mediated contraction and relaxation respectively, was determined within coronary and cerebral arteries. In contrast to above, Linopirdine pre-incubation had no significant effect on U46619 (0.003-3 μmol-L^{-1}) mediated contraction in either artery from female rats (Fig 4.21). Within cerebral arteries, no significant oestrus cycle-dependent change in receptor mediated contraction was observed between control conditions (Fig 4.21.A,C), however, U46619-mediated contraction in coronary arteries from F-P/E was significantly more efficacious when compared to those from F-D/M ($P \leq 0.05$; n=4-7; Fig 4.21.B).

Isoprenaline (0.003-3 μmol-L^{-1}) mediated relaxation was significantly more efficacious within cerebral arteries form F-D/M when compared to F-P/E ($P \leq 0.05$; n=5; Fig 4.22.A). In addition, Isoprenaline-mediated relaxation of cerebral arteries was attenuated by linopirdine pre-incubation in arteries from F-D/M only, whereby these responses were equipotent to those observed in control conditions in arteries from F-P/E ($P \leq 0.05$; n=5; Fig 4.22.A,C). In contrast to previous reports (Khanamiri *et al.*, 2013), we observed no inhibition of Isoprenaline-mediated relaxation by linopirdine in coronary arteries from either groups of female rats (Fig 4.22.B,D). Moreover, within these arteries there were no oestrus cycle dependent changes in sensitivity to receptor mediated relaxation (Fig 4.22.B,D).

In summary, both cerebral and coronary arteries from female Wistar rats showed Oestrus cycle dependent changes in arterial reactivity and sensitivity to K_V7 channel modulators. Though these changes were less well-defined by comparison to mesenteric and renal arteries there were clear oestrus-cycle dependent changes in vascular responses which partially correlated with changes in sensitivity to linopirdine, indicative of a K_V7 component.

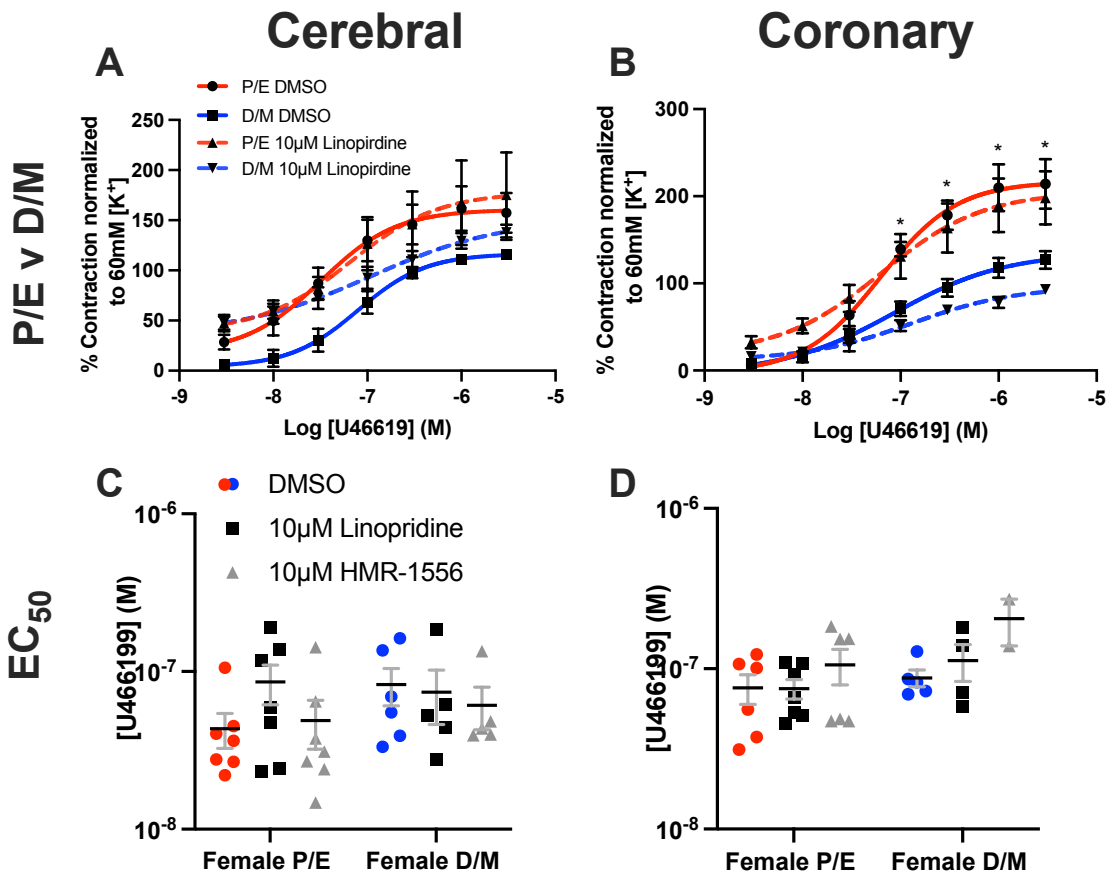

Figure 4.21: U46619-mediated contraction in cerebral and coronary arteries from female Wistars are insensitive to K_V7 channels inhibition.

Mean data of contraction in response to U46619 (0.003-3μmol-L^{-1}) within cerebral (*n*=5-7; A) and coronary (*n*=4-7; B) arteries preincubated within DMSO solvent control (Female di-oestrus/met-oestrus (D/M), blue; Female pro-oestrus/oestrus (P/E), red) or Linopirdine (10μmol-L^{-1}; Female D/M, blue-dashed line; Female P/E, red-dashed line). Scatter graph representing the raw EC_{50} values of U46619-mediated contraction within cerebral (C) and coronary(D) arteries of the mean data above, in addition to vessels pre-incubated in $K_V7.1$ specific blocker HMR1556 (10μmol-L^{-1}; grey). A two-way statistical ANOVA with a post-hoc Bonferroni (A,B) or Dunnet's (C,D) correction was used to generate significance values $P \leq 0.05$. Post-hoc Bonferroni statistical comparisons include Ctrl v Ctrl (*= D/M DMSO v P/E DMSO; B). (*n*=) number of animals used (A-D).

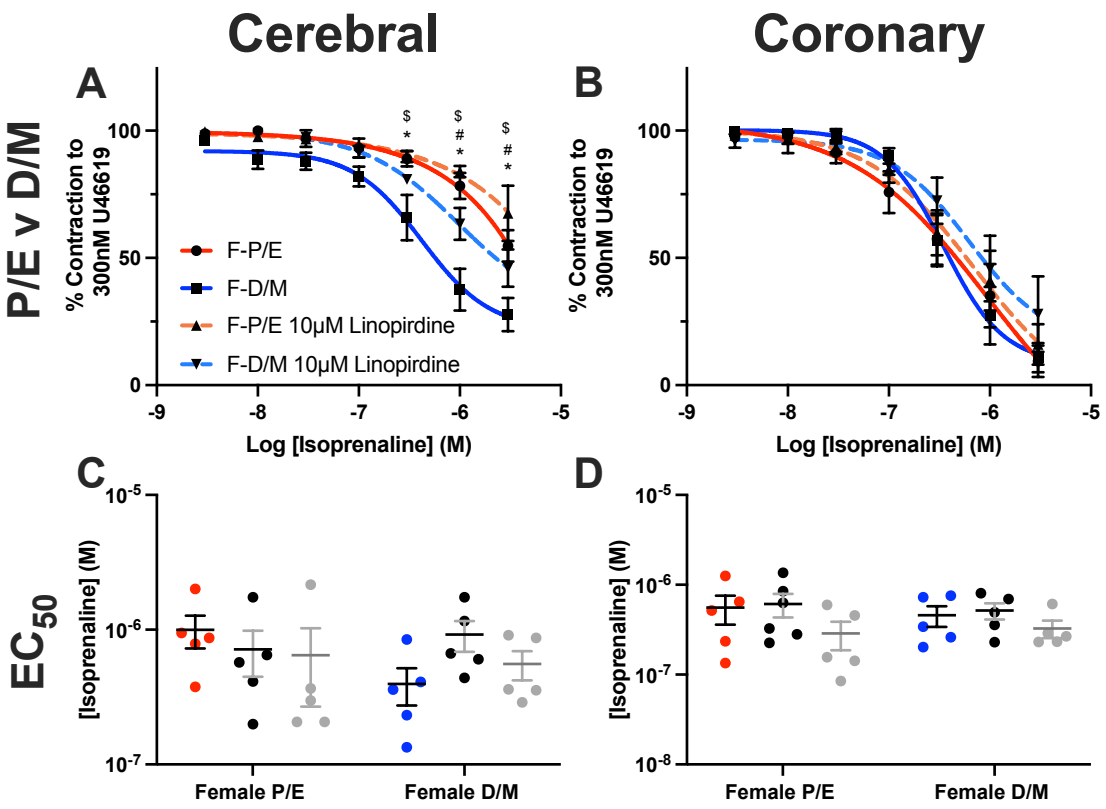

Figure 4.21: Determining K_V7.2-5 channel contribution to Isoprenaline-mediated relaxation in cerebral and coronary arteries from female D/M and P/E rats.

Mean data of relaxation of pre-contracted tone (U46619; 300nmol-L^{-1}) in response to Isoprenaline (0.003-3μmol-L^{-1}) in cerebral (*n*=5; A,C) and coronary (*n*=5-6; B,D) arteries preincubated in DMSO solvent control (female di-oestrus/metestrus (D/M), blue; female pro-oestrus/oestrus (P/E), red) or Linopirdine (10μmol-L^{-1}; Female D/M, blue-dashed line; Female P/E, red-dashed line). Scatter graph representing the raw EC_{50} values of Isoprenaline-mediated relaxation within cerebral (C) and coronary (D) arteries of the mean data above, in addition to vessels pre-incubated in K_V7.1 specific blocker HMR1556 (10μmol-L^{-1}; grey). A two-way statistical ANOVA with a post-hoc Bonferroni (A,D) or Dunnet's (C,D) correction was used to generate significance values; values (*/#/$= $P \leq 0.05$; *= D/M DMSO v P/E DMSO; #= D/M DMSO v D/M 10μmol-L^{-1} Linopirdine; $= D/M DMSO v P/E 10μmol-$L^{-1}$ Linopirdine; A,B; *= condition v DMSO solvent control, C,D), (*n*=) number of animals used (A-D).

4.4 Discussion

In this study, stark oestrus cycle dependent changes in vascular reactivity were observed, whereby phenotypically pro-contractile vessels from F-P/E rats exhibit diminished $K_V7.4$ channel function and membrane abundance in conjunction with moderately raised serum E2. Moreover, both E2 and novel GPER1 activator G-1 impaired K_V7 membrane abundance and function in F-D/M only, replicating a F-P/E pro-contractile vascular phenotype. In heterologous overexpression system, both E2 and G-1 diminished human $K_V7.4$ currents in *GPER1* transfected cells only, independent of a change in the biophysical properties of the current, consistent with a reduction in channel number. Finally, E2 diminished $K_V7.4$ interaction with its forward trafficking molecular chaperone protein HSP90 only in rats in a 'low serum E2' stage of the oestrus cycle (Fig 4.23).

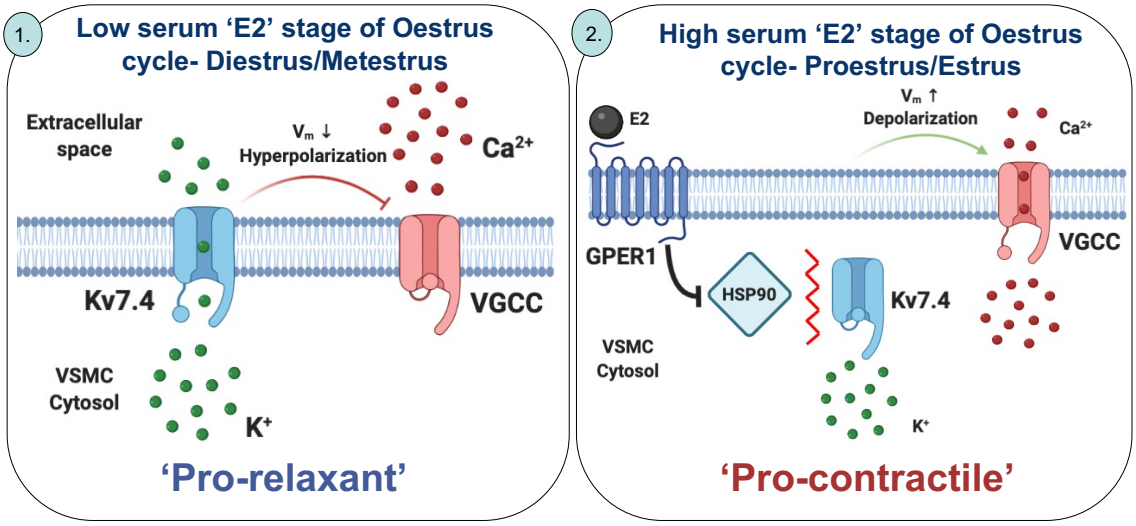

Figure 4.23: Graphical summary of GPER1 regulation of arterial $K_V7.4$

Diagrammatic representation of GPER1 mediated reduction of $K_V7.4$ membrane abundance through diminished interaction with HSP90 during high serum Oestradiol E2 (E2) stages of the oestrus cycle.

4.4.1 Cyclical reduction in K_V7.4 membrane abundance correlates with a pro-contractile phenotype

The role of K_V7 channels within male VSMCs is well established (Chapter 1.5; Barrese, Stott & Greenwood, 2018), however, in spite of the known sexual dimorphisms in cardiovascular physiology and pathophysiology (Pabbidi *et al.*, 2018), comparably little is known about K_V7 channel activity in arteries from females. Of the few studies to consider sex as a factor, K_V7 channels within the female are shown to; 1.) be differentially regulated by its β-auxiliary subunit protein Kcne4 (Abbott and Jepps, 2016); 2.) impair norepinephrine induced increases in total peripheral resistance in NT and SHRs, a phenomenon not present in males (Berg, 2018). As such, there is already strong inferences of sexual dimorphisms in vascular K_V7 activity, structure, and regulation within the literature.

This study demonstrates that similar to previous reports in arteries from male animals, K_V7.2-5 channel activators S-1 and ML213 relaxed pre-contracted arterial tone in a range of arteries from female rats and the pan-K_V7 channel inhibitor linopirdine but not K_V7.1 specific inhibitor HMR-1556 increased basal tone in these arteries (Mackie *et al.*, 2008; Ng *et al.*, 2011; Chadha, Zunke, Zhu, *et al.*, 2012). Additionally, K_V7.2-5 channel inhibition enhanced TXA2-mediated contractions and impaired β-adrenoreceptor-driven relaxations, however, U46619-mediated contraction was more potent and Isoprenaline-mediated relaxation was less efficacious in in arteries from F-P/E when compared to F-D/M under control conditions. Though this conclusion is drawn with the caveat that maximal response to Isoprenaline was not achieved in these vessels. Similarly, K_V7.2-5 channel activator-mediated relaxation and pan K_V7 channel inhibition mediated increase in basal tone and modulation of receptor mediated responses was more efficacious in arteries from F-D/M rats. Immunocytochemistry revealed staining for K_V7.4 located predominantly in the plasmalemmal membrane of myocytes from F-D/M renal and mesenteric arteries. Strikingly this was absent in myocytes from F-P/E, however, neither

total cell fluorescence nor the relative abundance of the *Kcnq4* transcripts were altered. Thus, our findings indicate a post-transcriptional cyclical reduction in K_V7.4 membrane abundance, which correlates with diminished contribution of K_V7 channels to both basal tone and receptor mediated responses, underpinning a pro-contractile phenotype. This conclusion was drawn with the caveat that more accurate protein quantification via western blot was unattainable. Upon identification / production of an antibody suitable for K_V7.4 staining during western blot, this experiment will be revisited. With regards to the current literature, K_V7.4 channel activity during P/E may account for the significantly greater mean arterial pressure observed in F-P/E rats compared to di-oestrus rats by (Takezawa *et al.*, 1994).

No change in transcript nor membrane abundance of the other candidates for vascular K_V7 channel function were observed (K_V7.1, K_V7.5 and KCNE4), reinforcing the previously reported notion that K_V7.4 is the fundamental component of the functional K_V7.4/K_V7.5 heterotetramer (Barrese, Stott and Greenwood, 2018).

4.4.1.1 K_V7 channel contribution to basal coronary and cerebral tone

Coronary and cerebral circulation are dependent on a constant stable supply of blood. To facilitate these demands, these vascular beds are intrinsically myogenic whereby arteries contract and relax in response to changes in intravascular flow or pressure. Mechanosensitive arteries respond to an increase in either factor by depolarisation of the membrane, opening of VGCC and a narrowing of arterial diameter by actin-myosin cross bridge cycling. K_V7 channels are known to contribute the resting state and basal flow of both cerebral (Zhong, Harhun, *et al.*, 2010) and coronary (Khanamiri *et al.*, 2013) arteries. Here, we observed efficacious contractions in response to Linopirdine, but not K_V7.1-specific blockers in these arteries. Indicting that K_V7.4/5 channels also contribute to basal tone. In spite of an oestrus cycle dependent shift in sensitive to both S-1 and ML213-mediated relaxation, we observed no differences in the contraction evoked in

response to Linopirdine between cerebral or coronary arteries harvested from F-D/M or F-P/E rats.

4.4.1.2 Oestrus cycle dependent changes in vascular reactivity are partially K_V7 dependent

$K_V7.2$-5 channel inhibition significantly attenuated Isoprenaline-mediated relaxation in cerebral arteries, giving rise to a response profile within F-D/M arteries similar to that seen in F-P/E, where linopirdine was ineffective. Indicating a role for K_V7 channels in the observed oestrus cycle dependent changes in vascular reactivity. Vascular bed specific contribution of K_V7 channels to receptor mediated vasorelaxation has been demonstrated in response to C-type atrial natriuretic peptide and nitric oxide donor S-nitroprusside (Stott, Barrese, *et al.*, 2015). Here, we similarly demonstrate that unlike renal or mesenteric arteries, pan-K_V7 channel inhibition failed to significantly attenuate U46619-mediated contraction in cerebral arteries from female rats. Additionally, Linopirdine pre-incubation had no effect on Isoprenaline-mediated relaxation within coronary arteries. In these instances where receptor mediated responses were not sensitive to K_V7 blockers, there was no observed Oestrus-cycle dependent change in arterial reactivity giving further credence to the role of K_V7 channels in underpinning oestrus cycle regulation of arterial reactivity, however, U46619-mediated contraction in coronary arteries was insensitive to Linopirdine, though also presented with stark differences in the efficacy of receptor mediated contraction, indicative of an alternate candidate for Oestrus cycle-dependent changes in arterial reactivity (e.g. pinacidil-sensitive K_{ATP}).

Further work is required to establish an oestrus cycle dependent regulation of K_V7 channels within these vessels from both a functional and molecular standpoint and will form the basis of future investigations.

4.4.2 E2 diminishes K_V7.4 membrane abundance through reduced interaction with HSP90 via GPER1 signalling

The role for E2 in modulating vascular activity is complex. E2 upregulates the bioavailability of nitric oxide and prostaglandin PGI_2 within ECs, and decreases intracellular calcium availability in VSMCs in a K^+ channel independent process (Mazzuca *et al.*, 2015; Novella *et al.*, 2019), however, there is less consensus within the literature concerning ion channel modulation by E2. In myriad examples E2 is shown to both increase and decrease the activity of ion channels such as BK_{Ca}, K_{ATP} and K_V (Kow and Pfaff, 2016). With regards to K_V7, E2 internalises K_V7.1 in female rat distal colic crypt cells (O'Mahony *et al.*, 2007; Rapetti-Mauss *et al.*, 2013) and diminished I_{Ks} currents in overexpression models and rabbit cardiac myocytes (Busch *et al.*, 1996; Möller and Netzer, 2006), however, E2 also increases M-currents (K_V7.2/7.3) in Neuropeptide-Y neurons in mice (Roepke *et al.*, 2011). Comparably, little is known of the effect of E2 on vascular K_V7 channels, however, E2 injection into rats post bi-lateral ovariectomy significantly increased mean arterial pressure (Takezawa *et al.*, 1994). The results of this chapter demonstrate an increase in serum E2 in F-P/E rats (*P*0.07). Moreover, short incubation with supplemental E2 or novel GPER1 activator G-1 significantly reduced K_V7.4 membrane abundance, interaction with its forward trafficking molecular chaperone protein HSP90 and the potency ML213-mediated relaxation in mesenteric and renal arteries from F-D/M rats only. No additive inhibition of K_V7 channel membrane abundance, function nor interaction with HSP90 by E2 or G-1 was observed in F-P/E rats where serum E2 was higher, supporting a role for oestrogenic signalling in driving the observed cyclical dependent shifts in vasoreactivity.

As above, E2 rapidly reduces colonic crypt cell conductance purportedly via ERα downregulation of K_V7.1 via fast acting and genomic processes which were PKA-PKCδ dependent (O'Mahony *et al.*, 2007, 2009), however, G-1 expresses a high degree of selectivity for GPER1 over ERα (Bologa *et al.*, 2006), whereas E2 binds

ERα/ERβ/GPER1 equally at 10nmol-L^{-1} (Bologa *et al.*, 2006). As the effects of E2 and G-1 were analogous, we attributed the observed effects to GPER1, and not ERα. This was supported by single cell electrophysiology in a heterologous over expression system, whereby, Oestrogenic regulation of K_V7.4 was dependent on GPER1 expression. GPER1 activation via either G-1 or E2 mediated a reduction in total K_V7.4 current independent of a change in the conductance of the individual channel, however, we cannot rule out a contribution of from nuclear E2 receptors as cross talk between these pathways (Meyer *et al.*, 2009; Romano and Gorelick, 2018) and oestrogen response elements within ion channel transcripts (Kow and Pfaff, 2016) are well documented. Future investigations will aim to selected against nuclear E2 signalling via agents including ERα/β antagonists Tamoxifen / Raloxifene or GPER1 antagonist G36 (Dennis *et al.*, 2011), which will constitute future experiments.

E2 mediated reduction in K_V7.1 conductance in colon cells is also derived from an uncoupling of K_V7.1 and its β-auxiliary subunit protein KCNE3 (Alzamora *et al.*, 2011). An orthologue, KCNE4, is purported to be essential to K_V7.4 activity in the vasculature (Jepps *et al.*, 2015), though we observed no change in the membrane abundance of KCNE4 across the oestrus cycle, and deletion of Kcne4 does not impair K_V7 channel function in female murine arteries (Abbott and Jepps, 2016). Moreover, KCNE3 negatively regulates K_V7.4 currents in over-expression systems (Lundby *et al.*, 2008). Finally, the work undertaken by Alzamora *et al.,* (2011) concerns a structurally different subunit of the K_V7 channel subfamily in a different cell type. Interestingly oestrus cycle dependent changes in the contribution of K_V7.1 to IP-receptor-mediated relaxations have been reported in mesenteric arteries (Baldwin *et al.*, 2021; Chapter 6) but this was not associated with a change in response to K_V7.1-specific activators. As the role of KCNE subunits in regulating K_V7 has yet to be defined within the vasculature of the female and appear not to contribute to E2 mediated regulation of arterial K_V7.4, they remain outside the scope of this study.

Our data suggest that GPER1 activation alters the forward trafficking of K_V7.4 through altered interaction with chaperone HSP90. Ang-II also alters HSP90:K_V7.4 association that results in ubiquitination and proteasomal degradation (Barrese *et al.*, 2018). We don't know whether similar occurs during the oestrus cycle and channel protein is created *de novo* or ultimate degradation is prevented and the existing K_V7.4 can recycle back to the membrane. Moreover, we do not know the signals linking GPER1 activation to HSP90 instability. As there is growing appreciation for the importance of ion channel membrane trafficking as the basis for many channelopathies (Curran and Mohler, 2015) the mechanisms linking GPER1 to HSP90 be the focus of future studies.

4.4.3 Oestrogenic signalling within the male vasculature

Within the male, circulating Testosterone is converted into oestrogens by aromatase enzymes in a process known as aromatisation. As human vascular smooth muscle expresses aromatase (Harada *et al.*, 1999), E2 is produced locally within the vasculature of the male. Oestrogenic signalling within male animals enhances endothelial derived vasorelaxation (Geary, Krause and Duckles, 2000) and G-1 mediated GPER1 activation attenuates receptor mediated vasocontraction (Haas *et al.*, 2009), however, exogenous E2 supplementation in males has historically been associated with high risk. The findings of the 'The coronary drug project,' (Group, 1973), revealed that high E2 treatment was associated with an increased risk of myocardial infarction and death. Though these finding have since been put into question, as long-term observation of male to female transexuals who are given exogenous E2 over the course of years revealed increased endothelial function and arterial reactivity (McCrohon *et al.*, 1997; New *et al.*, 2000). Within this chapter, we show that in contrast to previous reports (New *et al.*, 2000; Haas *et al.*, 2009), E2 and G-1 diminished K_V7.4 functional and molecular properties within the male vasculature in a fashion analogous to F-D/M.

4.4.3 Limitations

The results of this chapter are limited by several errors in study design. The level of pre-contracted arterial tone generated prior to application of vasorelaxants, was, according to CEC generated in response to U46619, uneven when comparing arteries from F-D/M and F-P/E animals. Initial characterisation of U46619 mediated contraction had demonstrated that EC_{80} was roughly 300 nmol-L^{-1} across the various arterial beds investigated within the female, however, upon separation of the females after observation of an oestrus cycle dependent change in vascular reactivity, a significant difference in pre-contracted tone was clear. This begs the question, was the increased sensitivity to K_V7.2-5 channel activator and isoprenaline mediated responses due to physiological agonism by diminished U46619 potency within arteries from F-D/M rats, or an oestrus cycle dependent regulation of K_V7 function? Whilst this is a plausible limitation to the findings of this chapter, no differences were seen in response to either NS11021 or Nicardipine in mesenteric arteries, nor Pinacidil or Nicardipine within renal arteries from F-D/M or F-P/E rats, arguing against physiological agonism. Additional limitations with the functional data generated include a lack of maximal responses achieved when generating CEC effect curves to isoprenaline. 0.003-3 µmol-L^{-1} was chosen as the range for isoprenaline mediated CECs in light of previous work by our laboratory regarding K_V7 channel contribution to β-adrenoreceptor mediated relaxation (Chadha, Zunke, Zhu, *et al.*, 2012). In future investigations, determination of maximal Isoprenaline mediated responses will allow for an accurate comparison of drug efficacy within renal arteries.

With regards to the molecular data, the principal findings of this chapter, E2/G-1 mediated decrease in K_V7.4 membrane abundance, is limited by the confidence in our K_V7.4 antibody. As described in Chapter 3.4.3, further work is required to validate anti-K_V7.4 (#APC-164) to increase the confidence in the findings described here. Further, alternative supplementary means of determining K_V7.4 membrane abundance or trafficking will be employed to give credibility to said findings. For example, Fluorescence recovery after photobleaching (FRAP) in combination with a biotin internalisation and

recycling assay will allow for the determination of diminished $K_V7.4$ forward trafficking to the membrane in addition to protein internalisation respectfully. Though the latter is dependent on the identification of an anti-body suitable for western blot.

The work of this chapter and thesis relies heavily on the accurate identification of the stage of female rats throughout the oestrus cycle. The methods employed here (described in Chapter 2.2) are derived from (Cora, Kooistra and Travlos, 2015), and have been employed within myriad papers. Some leniencies in accuracy maybe allowed for, as females were split between pro-oestrus/oestrus and di-oestrus/met-oestrus, as opposed to determining individual stages of the oestrus cycle, reducing the margin for error in categorising females into appropriate groups. Moreover, circulating levels of E2 was higher in serum from F-P/E rats, a stage previously shown to have considerably greater serum E2 (Nilsson *et al.*, 2015), however, the study is limited by a lack of secondary means of stage determination. Alternative supplementary methods to be considered in future investigations include histological analysis of the cyclical changes in the uterine wall (Westwood, 2008) or visual changes in the vagina (Byers *et al.*, 2012), though the latter has only been demonstrated in mice.

Finally, we opted not to make a male-female comparison in K_V7 channel function for the sake of clarity in the study, however, functional comparisons in male-female vascular reactivity and the molecular properties of $K_V7.4$ will be the focus of the following chapter.

4.4.4 Conclusion

The results of this chapter confirm the previously published notion that vascular reactivity changes over the course of the oestrus cycle (Jaimes *et al.*, 2019), and argues for a novel GPER1 mediated regulation of $K_V7.4$ membrane abundance and functional output which drives a robust component of this phenomenon.

Chapter 5: Preservation of vascular K_V7 function within the hypertensive Female rat

5.1 Introduction

Hypertension is the key risk factor in the development and pathogenesis of CVD (Lund-Johansen, 1980; Messerli, Williams and Ritz, 2007; Giles *et al.*, 2009; Hermida *et al.*, 2018). CVD is known to be the leading cause of mortality in both the United States and Europe (Mosca, Barrett-Connor and Wenger, 2011; Wilkins E. *et al.*, 2017), however, whilst the absolute number of patients suffering with CVD in the USA as of 2011 were women, CVD mortality rates were highest in men (Mosca, Barrett-Connor and Wenger, 2011). This is because women were more likely to survive to older age demographics than men. It is well accepted that women express a cardioprotective phenotype that differentiates the aetiology of CVD between male and females. Sexual dimorphisms in CVD is further supported by a comparably smaller increases in BP within female hypertensive animal models including SHRs and Ang-II infused mice when compared to males (Reckelhoff, Zhang and Granger, 1998; Maris *et al.*, 2005; Tiwari *et al.*, 2010; Bubb, Khambata and Ahluwalia, 2012), however the root cause of hypertension remains elusive. Importantly, arterial myocytes of hypertensive animals are more depolarised contributing to raised $[Ca^{2+}]_i$ (Gebremedhin *et al.*, 1990; Wellman *et al.*, 2001; Jepps *et al.*, 2011), therefore, the factors that govern $Vsmc_m$ are of key interest.

As discussed in chapter 1.5.4.3, previous works by our lab and others have identified vascular K_V7 channels as novel therapeutic targets in the treatment of CVD (Stott, Jepps and Greenwood, 2014; Haick and Byron, 2016; Barrese, Stott and Greenwood, 2018).

Notably, K_V7.4 channels are downregulated in SHRs (Jepps *et al.*, 2011) via post-transcriptional mechanisms affecting protein synthesis, trafficking and degradation (Carr *et al.*, 2016; Barrese *et al.*, 2018), impairing receptor mediated responses (Chadha, Zunke, Zhu, *et al.*, 2012; Li *et al.*, 2013; Stott, Barrese, *et al.*, 2015). Consequently, K_V7.4 is implicated in the hypertensive phenotype (see (Barrese, Stott and Greenwood, 2018) for review). Recently, Berg (2018) demonstrated that K_V7 channel activators hamper norepinephrine mediated increases in total peripheral resistance in female, but not male SHRs. In light of these findings, we proposed that vascular K_V7 channels represent one of the cardioprotective factors that differentiate the rise in BP between male and female hypertensive animal models males (Reckelhoff, Zhang and Granger, 1998; Maris *et al.*, 2005; Tiwari *et al.*, 2010). The aim of this chapter was to characterize the response of vessels from male and female SHRs to K_V7 channel activators, the contribution of K_V7 channels to receptor mediated responses and the molecular characteristics of K_V7.4. The data detailed herein demonstrates a preservation of K_V7.2-5 channel activator-mediated relaxation and K_V7.4 membrane abundance when comparing arteries from female SHRs to males. Suggestive of a role for K_V7 in the cardioprotective phenotype.

5.2 Methods

The methods employed in the following chapter are described at length in Chapter 2. Of note, male and female SHRs were used as a means of investigating vascular K_V7 channel activity in the hypertensive model. SHRs were purchased from Envigo (Inotiv, In, USA) at 250-300 g. Blood pressure monitoring was performed by Envigo and on shipment, each rat was guaranteed to be at a stable blood pressure of ≥200 mmHg. Animals were then kept in house and culled as per Chapter 2.1. SHRs were compared to Wistar rats purchased from Charles River (Margate, UK). Wistar rats purchased from Charles River (Margate, UK) are reported to express a resting BP of 100 mmHg (Luo *et al.*, 2008) and will be denoted as NT in the following study.

5.3 Results

5.3.1 Preservation of ML213-mediated relaxation in the female hypertensive rat

Experiments were performed to investigate the effect of K_V7 activators in arteries from normotensive and hypertensive rats. Mean data for ML213 (0.01-10 μmol-L^{-1}) mediated relaxation of pre-contracted arterial tone (0.3 μmol-L^{-1} U46619) was generated in main renal arteries harvested from male and female NT and SHRs (Fig 5.1). ML213-mediated relaxation was equally efficacious (Fig 5.1.A) and potent (Fig 5.1.E) within arteries taken from male and female NT animals (*n*=8-20). Similar to previous reports (Jepps *et al.*, 2011; Chadha, Zunke, Zhu, *et al.*, 2012), ML213-mediated relaxation was impaired significantly in arteries taken from male (Fig 5.1.B,E; *P*0.05; *n*=4-8) and, as a novel finding female (Fig 5.1.C,E; *P*0.05; *n*=7-20), SHRs when compared to NT rats, however, ML213 was significantly more efficacious in arteries taken from female SHR when compared to male SHRs (Fig 5.1.D; *P*0.05; *n*=4-7).

When separated into arteries from F-D/M and F-P/E, ML213-mediated relaxation was significantly impaired in SHRs when compared to NT in both groups (Fig 5.2.A,B; *P*≤0.05; *n*=3-10), however, ML213 evoked relaxation was significantly more efficacious (Fig 5.2.C) and potent (Fig 5.2.D) in arteries from SHRs in F-D/M compared to arteries from SHRs in F-P/E (*P*≤0.05; *n*=3-10). The aggregated findings are indicative of a degradation of K_V7 function within both male and female animals, however significantly less so in female animals. Moreover, an Oestrus cycle dependent regulation of K_V7 channel modulator sensitivity was still present in the hypertensive model.

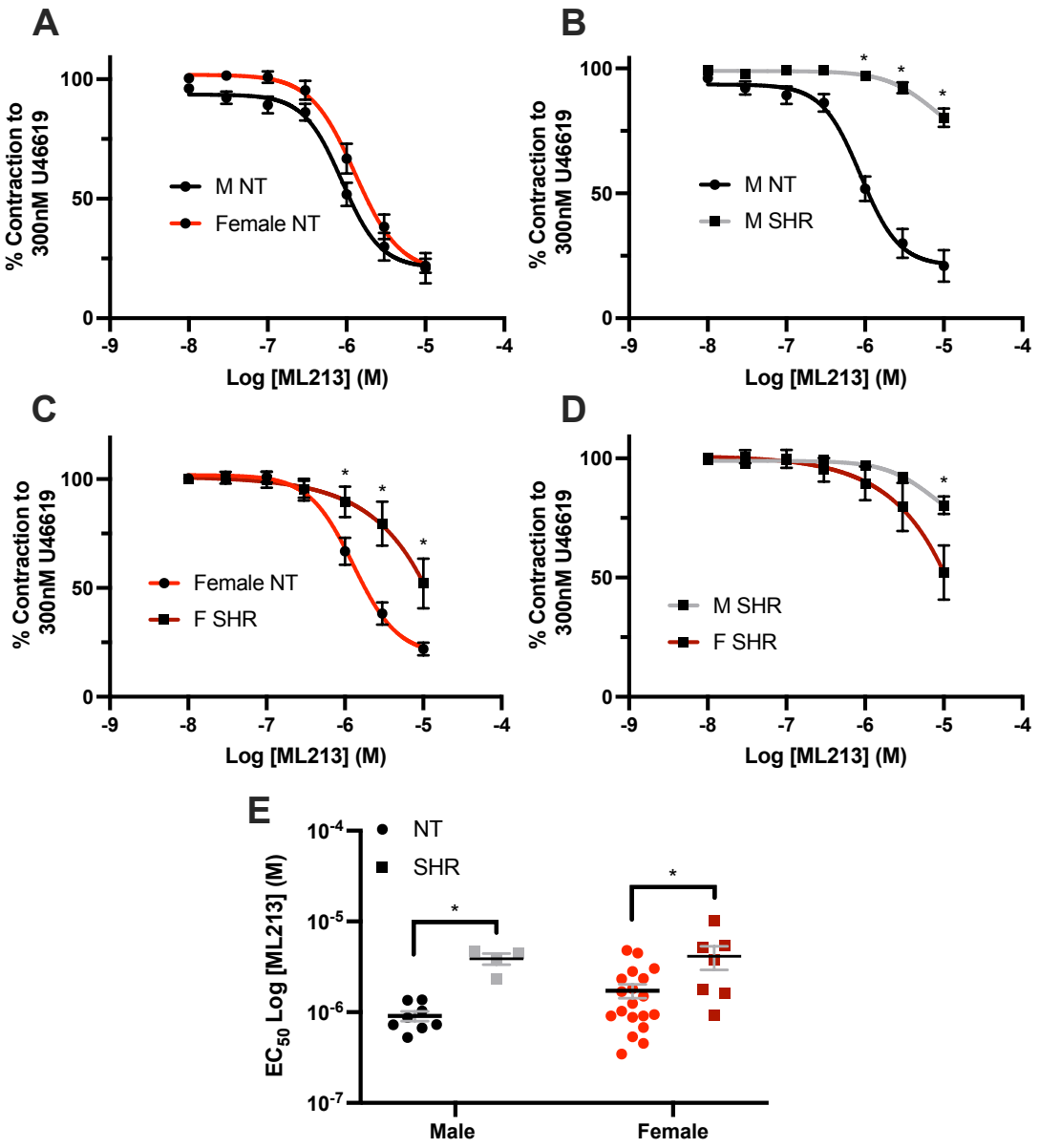

Figure 5.1: Preservation of K_V7.2-5 channel activator-mediated relaxation in arteries from hypertensive female rats

K_V7.2-5 channel activator ML213 (0.01-10 µmol-L^{-1}) mediate relaxation of pre-constricted arterial tone (300 nmol-L-1 U46619) in renal arteries from male (black, grey) and female (red, dark red) normotensive (NT; circle; *n*=10-19) and spontaneously hypertensive rats (SHR; square; *n*=4-7; A-D). Scatter graph plot with mean ±SEM of EC_{50} vales for ML213-mediated relaxation in renal arteries (*n*=4-11; E). All values are expressed as mean + SEM. A 2-way statistical ANOVA with a post-hoc Bonferroni (A-E) test was used to generate significance values. Statistical significance is defined as *$P \leq 0.05$ (A-C).

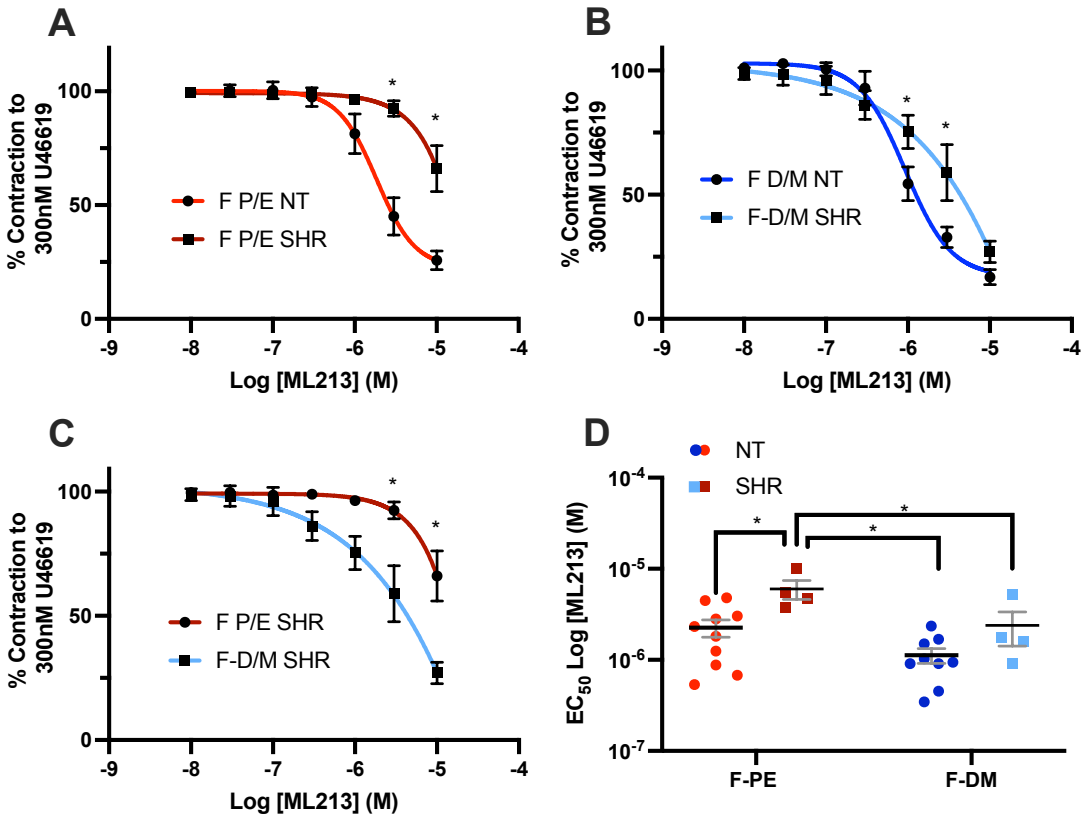

Figure 5.2: Oestrus cycle dependent changes in sensitivity to K_V7 channel modulators in the hypertensive rat

$K_V7.2$-5 channel activator ML213 (0.01-10 µmol-L^{-1}) mediate relaxation of pre-constricted arterial tone (300 nmol-L-1 U46619) in renal arteries from female Wistars in either Pro-oestrus / Oestrus (P/E; red) or Di-oestrus / Met-oestrus (D/M; blue) that were normotensive (NT; circle; *n*=5) or spontaneously hypertensive rats (SHR; square; *n*=4; A-C). Scatter graph plot with mean ±SEM of EC_{50} vales for ML213-mediated relaxation in renal arteries (*n*=4-5; D). All values are expressed as mean + SEM. A 2-way statistical ANOVA with a post-hoc Bonferroni (A-E) test was used to generate significance values. Statistical significance is defined as **P*≤0.05 (A-C).

5.3.2 Receptor mediated contraction in the normotensive and hypertensive rat

5.3.2.1 Sex-dependent differences in U46619-mediated contraction

Application of U46619 (0.003-3 μmol-L^{-1}) produced a contraction in main renal arteries that was significantly more efficacious at low concentrations when comparing NT males to NT females (Fig 5.3.A; $P \leq 0.05$; n=7-17), NT males to SHR males (Fig 5.3.B; $P \leq 0.05$; n=4-7) and NT female to SHR females (Fig 5.3.C; $P \leq 0.05$; n=7-17), however, the vascular response to U46619 was significantly less efficacious (Fig 5.3.D) and potent (Fig 5.3.E) within renal arteries taken from female SHRs when compared to males ($P \leq 0.05$; n=4-7). In short, when comparing within the sex, arteries taken from the hypertensive rat were more contractile compared to arteries from the normotensive rat, however, arteries taken from female animals were less contractile when compared to those from males.

U46619-derived responses were significantly enhanced by pre-incubation with Linopirdine (10 μmol-L^{-1}) in arteries taken from NT rats of both sexes (Fig 5.4.A,B; $P \leq 0.05$; n=7-17). Additionally, linopirdine failed to augment U46619-mediated contraction in arteries from SHRs of either sex (Fig 5.4.C-E), consistent with a reduction in vascular K_V7 function within these animals.

These findings taken in context with the preserved response to ML213 are indicative of a female cardioprotective phenotype, whereby comparably to males the responses to vasorelaxants are preserved, and the response to vasoconstrictors are less sensitised, however, K_V7 channel sensitivity to U46619-mediated responses was diminished. Indicative of reduced K_V7 channel functional activity.

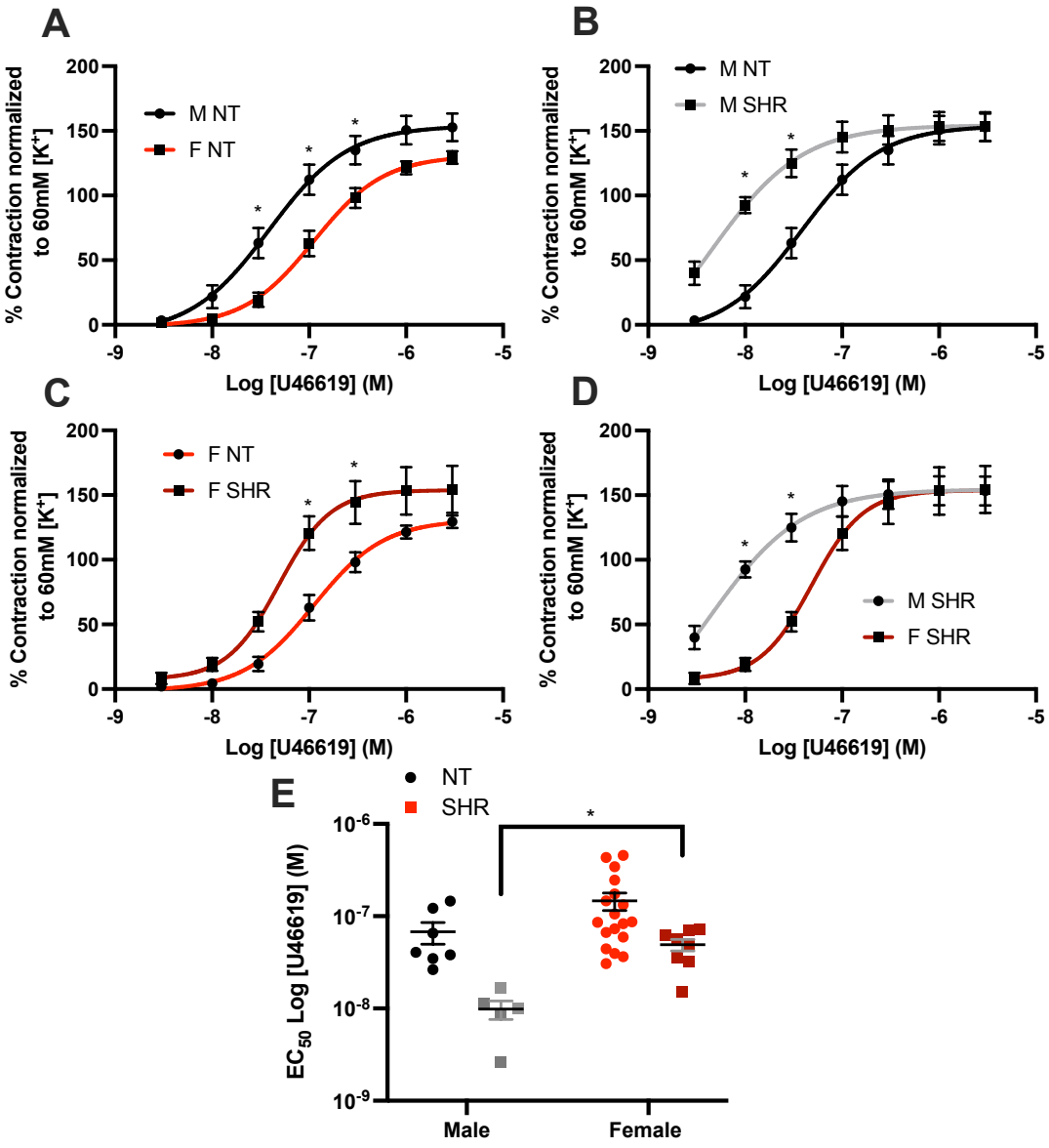

Figure 5.3: U46619-mediated contraction within renal arteries from female rats is less potent in arteries from female rats compared to males.

Mean data of contraction in response to U46619 (0.003-3μmol-L^{-1}) within arteries from male (black, grey) or female (red, dark red) Wistar rats that were normotensive (circle; *n*=7-17) or hypertensive (square; *n*=5-8; A-D). Scatter graph representing the raw EC_{50} values of U46619-mediated contraction within renal arteries of the mean data above (E). All values expressed as mean ±SEM. A two-way statistical ANOVA with a post-hoc Bonferroni (correction was used to generate significance values, *=*P*≤0.05. (*n*=) number of animals used.

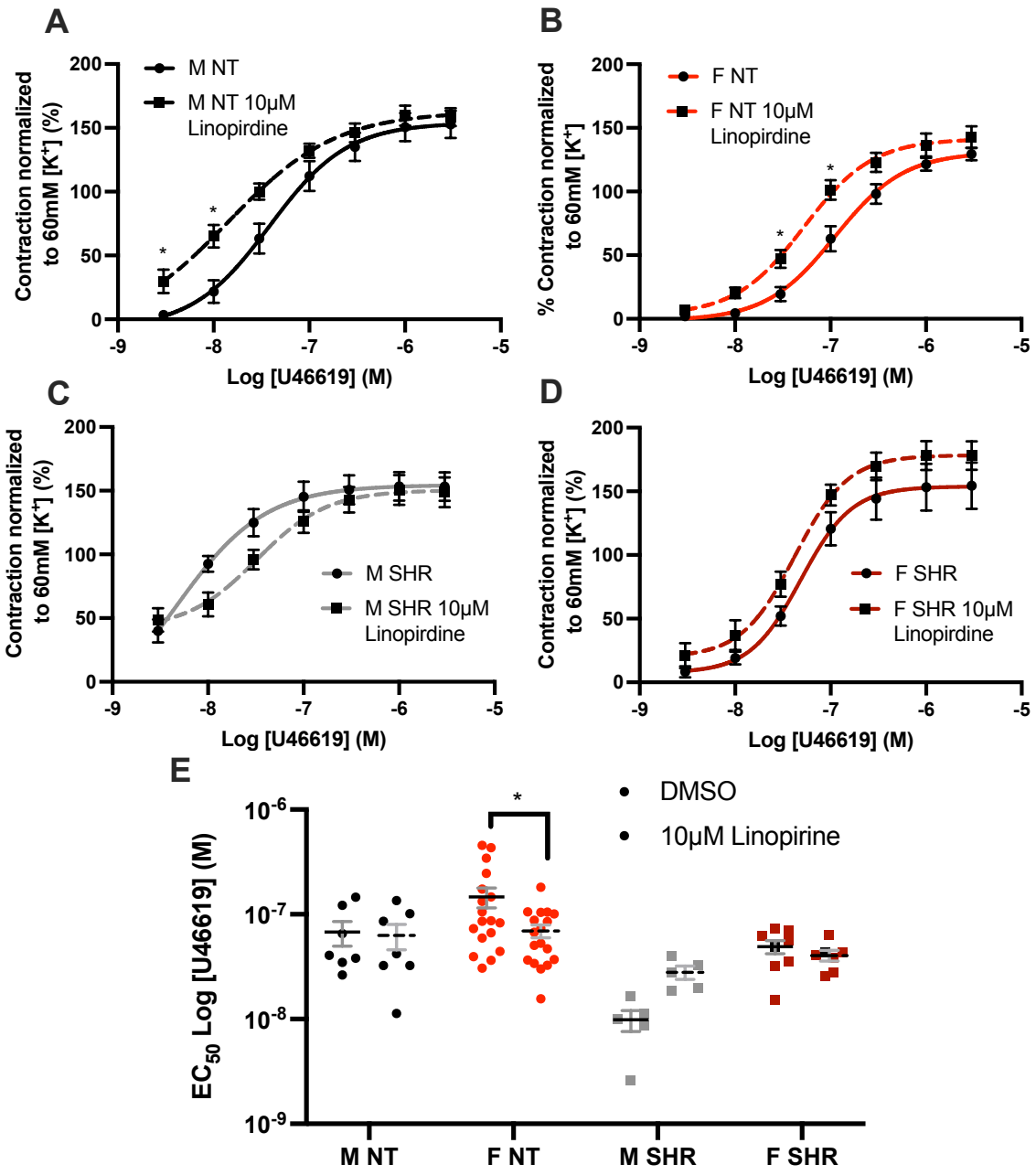

Figure 5.4: K_V7 channel contribution to U46619-mediated contraction in normotensive and hypertensive rats.

Mean data of contraction in response to U46619 (0.003-3μmol-L^{-1}) within arteries from male (black, grey) or female (red, dark red) Wistar rats that were normotensive (circle; *n*=7-17) or hypertensive (square; *n*=5-8) in vessels pre-incubated in either DMSO (block line) or pan-K_V7 channel inhibitor Linopirdine (10 μmol-L^{-1}; dashed line; A-D). Scatter graph representing the raw EC_{50} values of U46619-mediated contraction within renal arteries of the mean data above (E). All values expressed as mean ±SEM. A two-way statistical ANOVA with a post-hoc Bonferroni (correction was used to generate significance values, *=*P*≤0.05. (*n*=) number of animals used.

5.3.2.2 Ablation of oestrus cycle dependent regulation of arterial reactivity in the hypertensive model

The influence of oestrus stage on hypertension induced changes in function was ascertained. U46619-mediated contractions were enhanced considerably in arteries from SHRs in D/M compared to the NT, illustrated by a large leftward shift in the U46619 concentration-effect curve (Fig 5.5). In contrast, the shift in the U44619 concentration-effect curve was minimal in arteries from F-P/E SHR compared to NT F-P/E. Moreover, linopirdine had no effect on U46619 mediated contraction in arteries from SHRs in either oestrus stage.

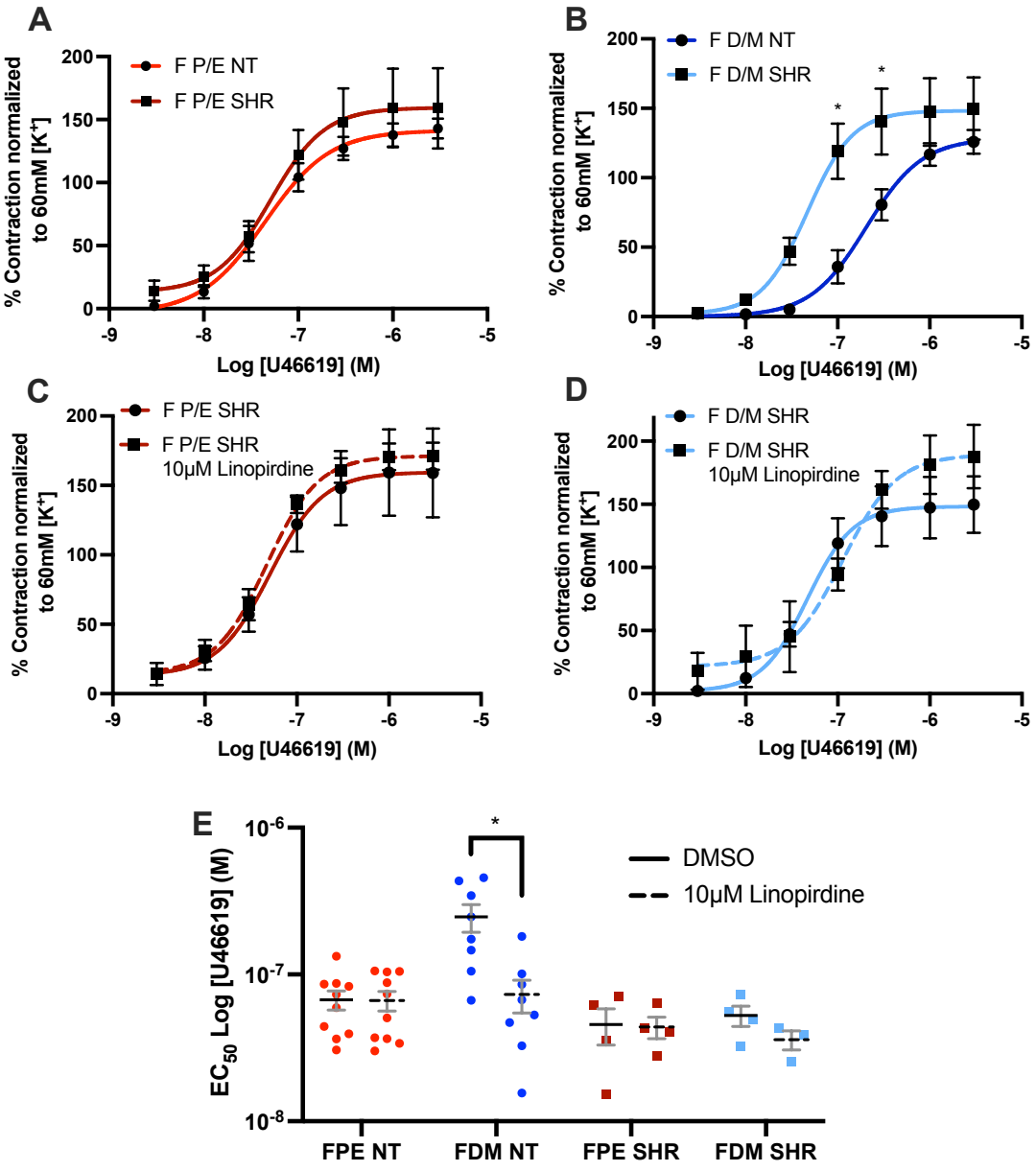

Figure 5.5: Diminished functional contribution of K_V7 to U46619-mediated contraction accounts for the disparity between arteries taken from normotensive and hypertensive rats.

Mean data of contraction in response to U46619 (0.003-3μmol-L^{-1}) within arteries from female Wistars in either Pro-oestrus / Oestrus (P/E; red) or Di-oestrus / Met-oestrus (D/M; blue) that were normotensive (NT; circle; *n*=8-10) or spontaneously hypertensive rats (SHR; square; *n*=3-5) in vessels pre-incubated in either DMSO (block line) or pan-K_V7 channel inhibitor Linopirdine (10 μmol-L^{-1}; dashed line; A-D). Scatter graph representing the raw EC_{50} values of U46619-mediated contraction within renal arteries of the mean data above (E). All values expressed as mean ±SEM. A two-way statistical ANOVA with a post-hoc Bonferroni (correction was used to generate significance values, *=$P \leq 0.05$. (*n*=) number of animals used.

5.3.2 Receptor mediated relaxation in the normotensive and hypertensive rat

5.3.2.1 Comparable Isoprenaline-mediated relaxation in male and female rats

In contrast to U46619, no sex-dependent differences in isoprenaline (0.03-3 μmol-L^{-1}) mediated responses on pre-contracted arterial tone (0.3 μmol-L^{-1} U46619) were observed between male and female NT (Fig 5.6.A; *n*=10-18) or SHRs (Fig 5.D; *n*=5-8), however, like (Chadha, Zunke, Zhu, *et al.*, 2012) we observed reduced relaxation in response to isoprenaline in SHRs compared to NT rats (Fig 5.6.B,C; *n*=5-18). In vessels where no responses were observed to isoprenaline, no EC_{50} values could be generated.

When taken as a collective, male and female NT animals were equally sensitive to linopirdine pre-incubation (Fig 5.7.A,B; *n*=10-18). Additionally, in arteries taken form hypertensive animals where the response to isoprenaline was ablated, Linopirdine had no additional effect (Fig 5.7.C,D; *n*=5-8).

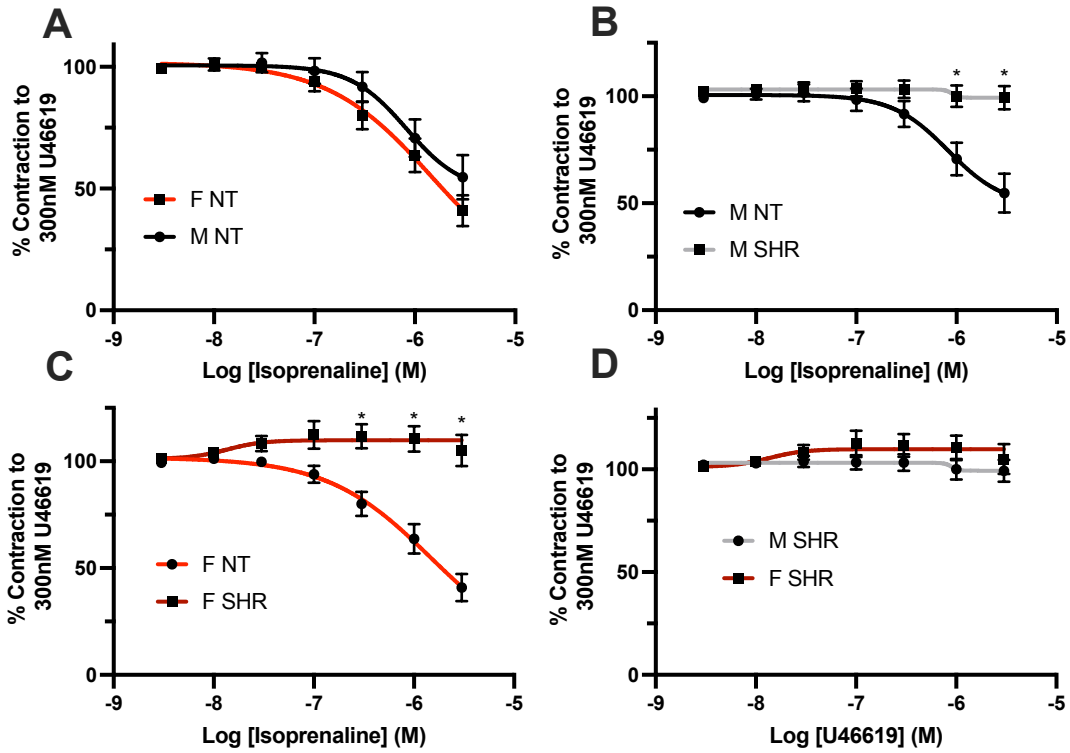

Figure 5.6: Isoprenaline-mediated relaxation of rat renal arteries is ablated in the hypertensive model

Mean data for Isoprenaline (0.003-3 μmol-L^{-1}) mediated relaxation of pre-contracted arterial tone (U46619, 0.3 μmol-L^{-1}) in renal arteries from male (black, grey) and female (red, dark red) normotensive (circle; *n*=10-18) and spontaneously hypertensive (SHR; square; *n*=5-8) rats (A-D). All values expressed as mean ±SEM. A two-way statistical ANOVA with a post-hoc Bonferroni (correction was used to generate significance values, *=*P*≤0.05. (*n*=) number of animals used.

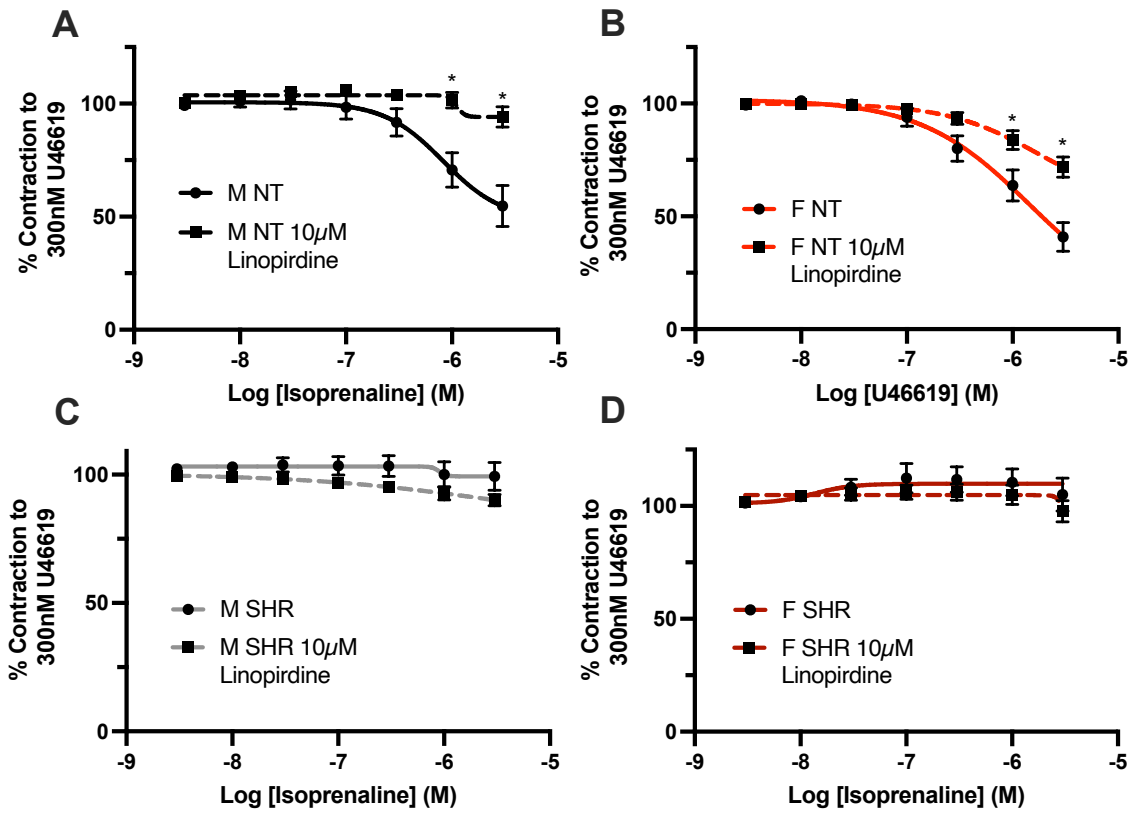

Figure 5.7: K_V7 channel contribution to U46619-mediated contraction in normotensive and hypertensive rats.

Mean data of for Isoprenaline (0.003-3 μmol-L^{-1}) mediated relaxation of pre-contracted arterial tone (U46619, 0.3 μmol-L^{-1}) in renal arteries from male (black, grey) or female (red, dark red) Wistar rats that were normotensive (circle; *n*=10-18) or hypertensive (square; *n*=5-8) in vessels pre-incubated in either DMSO (block line) or pan-K_V7 channel inhibitor Linopirdine (10 μmol-L^{-1}; dashed line; A-D). A two-way statistical ANOVA with a post-hoc Bonferroni (correction was used to generate significance values, *=*P*≤0.05. (*n*=) number of animals used.

5.3.2.2 β-adrenoreceptor mediated relaxation is ablated independent of the oestrus cycle

Similarly to above, when separating out into the Oestrus cycle, no differences in β-adrenoreceptor mediated relaxation was observed (Fig 5.8.A,B). In summary, β-adrenoreceptor evoked responses were absent in all hypertensive groups, independent of sex or Oestrus cycle. As such, these responses seem not to account for the well documented cardioprotective phenotype.

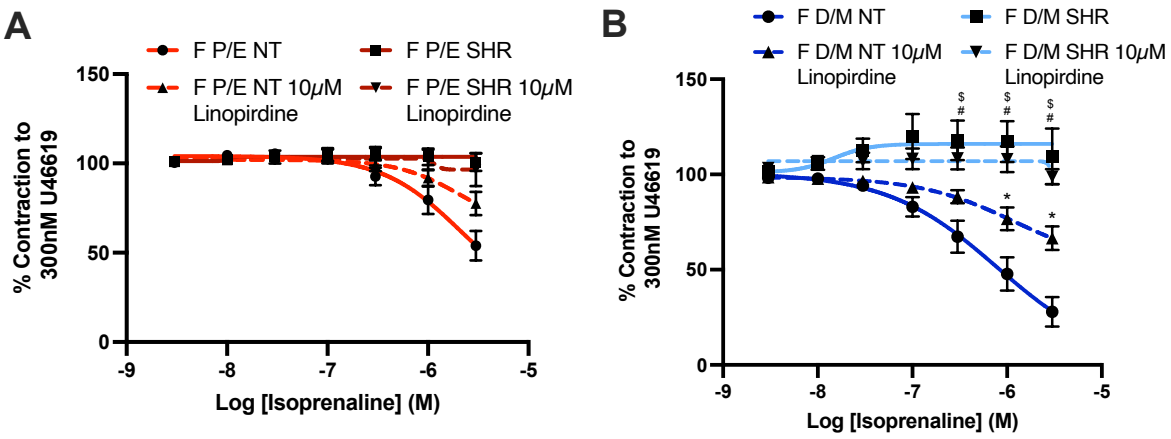

Figure 5.8: Diminished functional contribution of K_V7 to U46619-mediated contraction accounts for the disparity between arteries taken from normotensive and hypertensive rats.

Mean data for Isoprenaline (0.003-3 μmol-L^{-1}) mediated relaxation of pre-contracted arterial tone (U46619, 0.3 μmol-L^{-1}) in renal arteries from female Wistars in either Pro-oestrus / Oestrus (P/E; red) or Di-oestrus / Met-oestrus (D/M; blue) that were normotensive (NT; circle; *n*=9-12) or spontaneously hypertensive rats (SHR; square; *n*=4) in vessels pre-incubated in either DMSO (block line) or pan-K_V7 channel inhibitor Linopirdine (10 μmol-L^{-1}; dashed line). All values expressed as mean ±SEM. A two-way statistical ANOVA with a post-hoc Bonferroni correction was used to generate significance values, *=*P*≤0.05. (*n*=) number of animals used.

5.3.3 The molecular characteristics of K_V7.4 in the hypertensive rat

Previously, of the *Kcnq* subtype known to influence vascular reactivity, *Kcnq4* alone was shown to be aberrant in the hypertensive rat (Jepps *et al.*, 2011). As such, *Kcnq4* and its respective protein were the focus of the following molecular investigations.

5.3.3.1 K_V7.4 at the level of the protein in the SHR

The distribution of K_V7.4 was determined by immunocytochemistry as described in Chapter 3.3.3.2 and 4.3.3.2, where the distribution of K_V7.4 in myocytes taken from NT animals is described. In these studies, immunostaining revealed a diffuse staining for K_V7.4 throughout the cytoplasm, with some clustered staining around the nucleus within male mesenteric artery myocytes taken from hypertensive animals (Fig 5.9). When plotting fluorescence intensity across the cell, there were no-peaks in intensity that correlated with WGA marker, indicating a lack of protein at the membrane. Similarly, staining for K_V7.4 in mesenteric artery myocytes from F-P/E SHRs was predominantly cytoplasmic, with more intense staining observed around the nucleus. Comparably, K_V7.4 associated fluorescence which overlapped with WGA was still observable in VSMCs from F-D/M, however the fluorescence intensity of the peaks at the membrane were diminished when compared to the NT control myocytes (Fig 5.9). These findings could be quantified by determining the Membrane:Cytosol ratio for K_V7.4. The abundance of K_V7.4 was significantly decreased in both male and F-D/M SHRs when compared to NT rats (Fig 5.10.A; $P \leq 0.05$; $n=3$ (8-12 cells per n)), however, when re-plotted into Membrane:Cytosol ratios for K_V7.4 in myocytes isolated from hypertensive rats alone, the membrane cytosol ratio for K_V7.4 was significantly higher in cells from F-D/M (0.83±0.03) when compared to males (0.28±0.09; $P<0.5$; Fig 5.10.B). Correlating with the preserved response to ML213 within vessels taken from these animals.

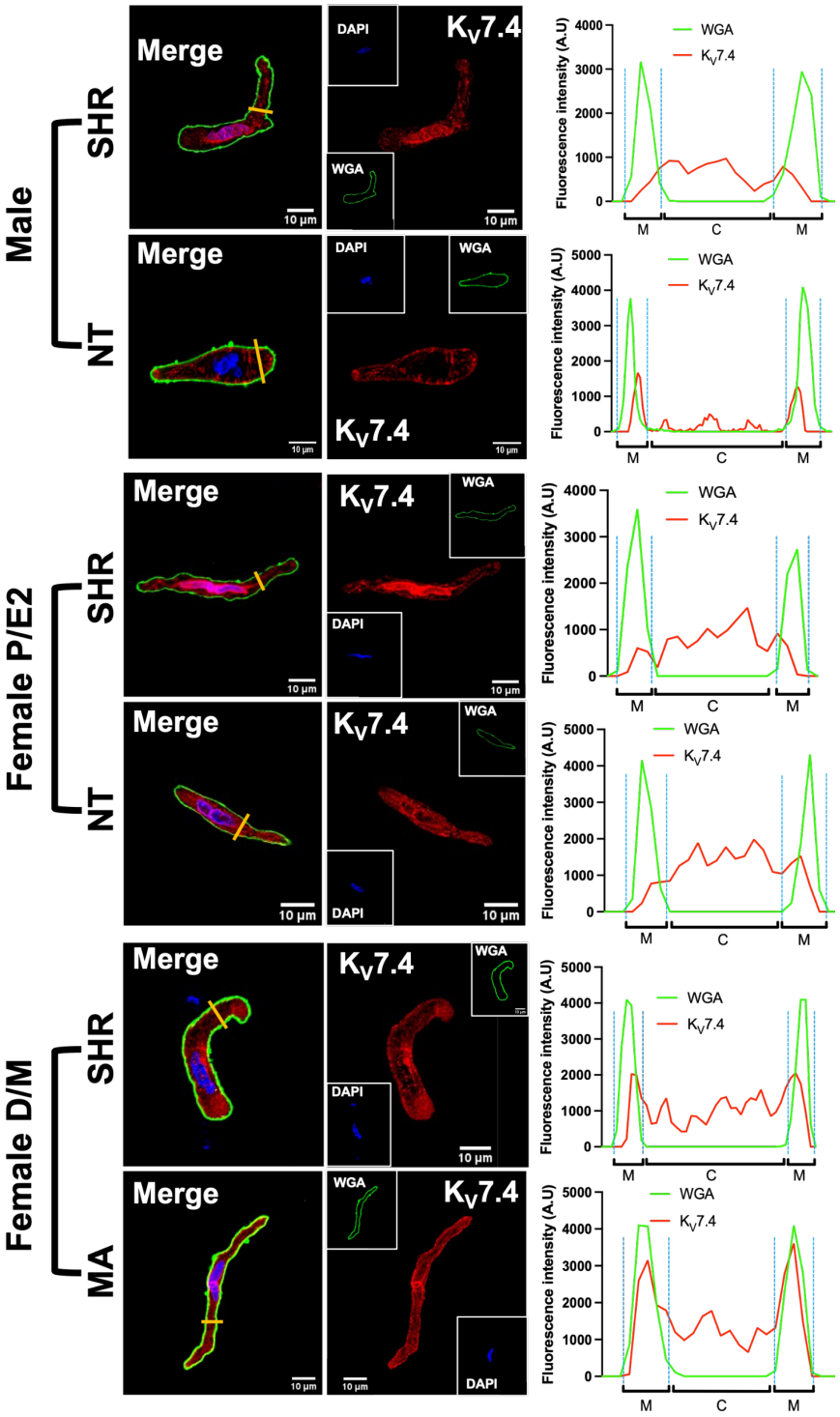

Figure 5.9: Immunostaining reveals a reduction in KV7.4 staining in the hypertensive VSMCs

Representative images of immunostaining from isolated mesenteric artery vascular smooth muscle cells from normotensive and spontaneously hypertensive (SHR) male, females in pro-oestrus / oestrus (P/E) and females in di-oestrus / met-oestrus (D/M) demonstrates $K_V7.4$ expression (red). Plasma membrane and nuclear marker wheat-germ agglutinin (WGA; green) and 4'-6-diamino-2-phenylindole (DAPI; blue) are also shown.

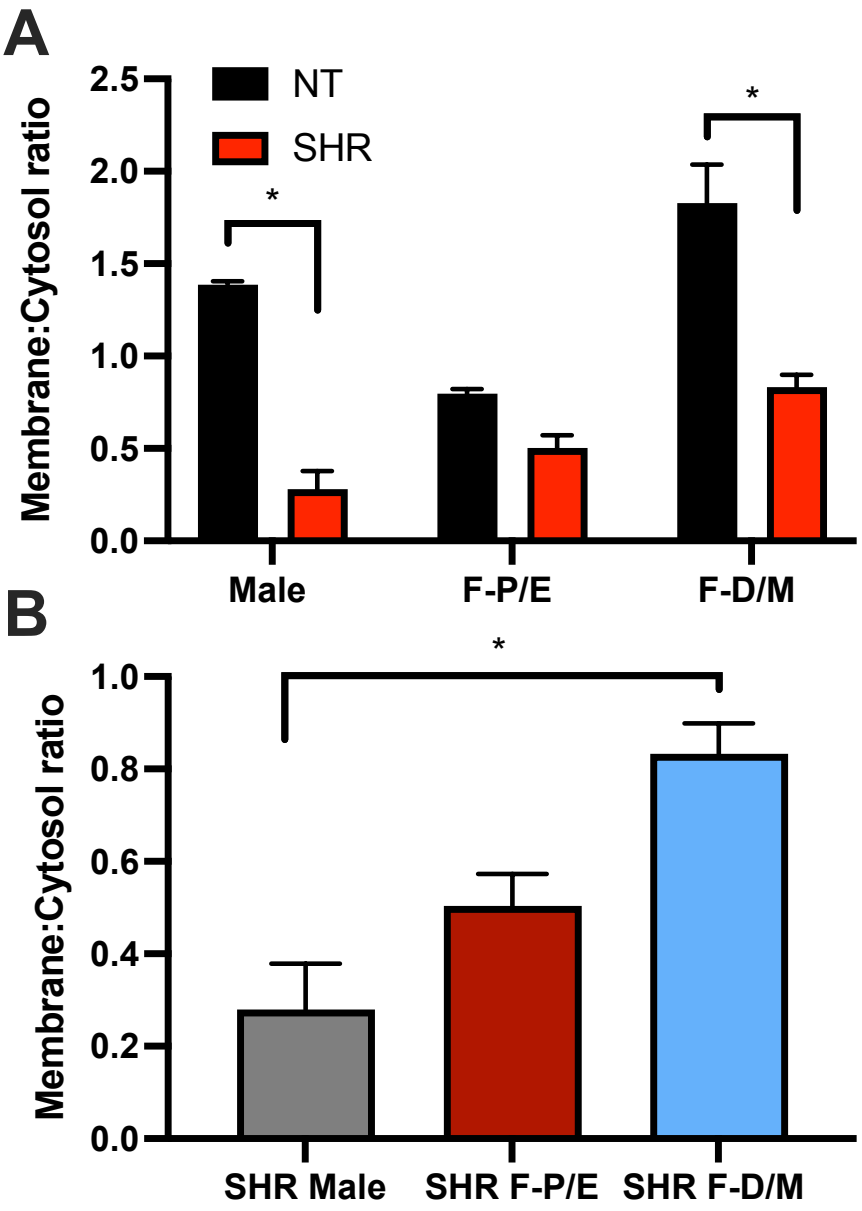

Figure 5.10: Membrane cytosol ratio for K_V7.4 staining in vascular cells isolated form normotensive and hypertensive rats

Mean data from isolated mesenteric artery vascular smooth muscle cells from normotensive (black) and spontaneously hypertensive (SHR; red) male, females in pro-oestrus / oestrus (P/E) and females in di-oestrus / met-oestrus (D/M) demonstrates K_V7.4 Membrane : Cytosol ratio (A; *n*=3). Re-plotted data for K_V7.4 Membrane : Cytosol ratio for K_V7.4 in myocytes from hypertensive male (grey), P/E (red) and D/M (blue) only (B). All values are expressed as mean values ± SEM. Statistical significance values generated via two-way ANOVA (A) or one way ANOVA (B) in combination with a post-hoc Bonferroni (A) or Turkey (B) test, (*= *P*<0.5). (*n*=) number of animals used, 8-12 cells per *n*.

5.3.3.1 K_V7.4 at the level of the transcript in the SHR

When looking at the level of the transcript, *Kcnq4* was increased when expressed as $2^{-\Delta\Delta Cq}$ in lysates from female hypertensive rats when compared to NT controls (Fig 5.11). No change in *Kcnq4* expression was seen in males, similar to previous reports (Jepps *et al.*, 2011). The collective findings indicate a post-transcriptional down regulation of K_V7.4 membrane abundance. Due to issues with protein quantification as described in chapter 3.3.2.3, Western blot was not achievable.

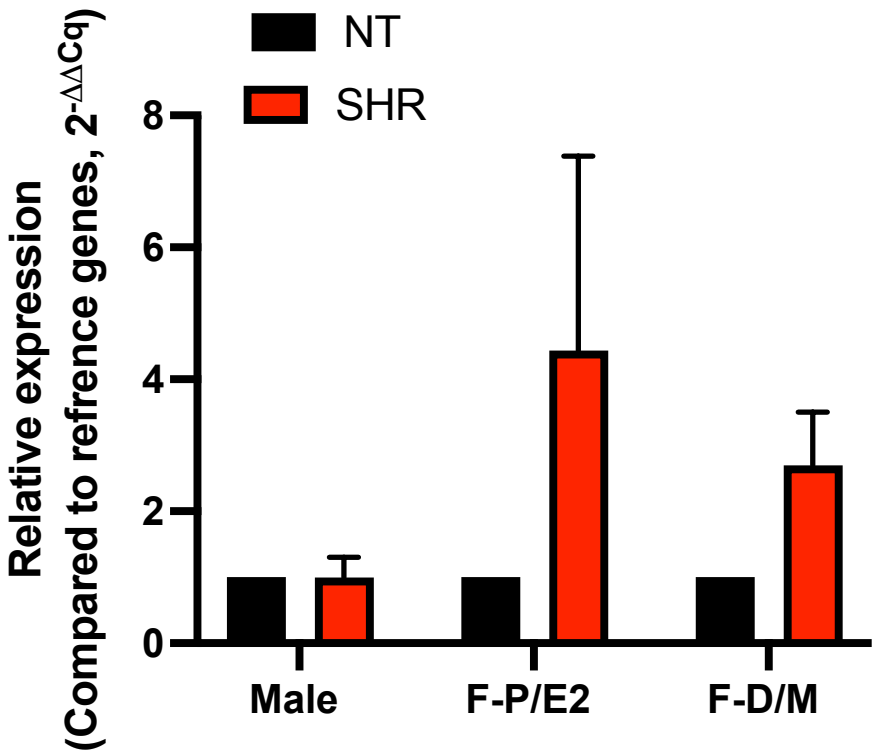

Figure 5.11: Relative mRNA transcript for *Kcnq4* within arteries from normotensive and hypertensive rats

Relative transcript abundance for *Kcnq4* was measured within whole lysates from mesenteric arteries (*n*=4) from male, female pro-oestrus/oestrus (P/E) and female di-oestrus/met-oestrus (D/M) isolated from normotensive (black) and spontaneously hypertensive (red) rats. Values are expressed as fold expression of SHR when compared to normotensive animals ($2^{-\Delta\Delta Cq}$). Initial values normalised to appropriate reference genes ($2^{-\Delta Cq}$; *Canx, Cyc*1). (*n*=) number of animals used.

5.4 Discussion

The results of this chapter demonstrate that within arteries from SHRs of both sexes; 1.) K_V7 channels activator evoked relaxation was diminished; 2.) K_V7 inhibitor mediated modulation of receptor mediated responses was diminished; 3.) $K_V7.4$ membrane abundance in vascular myocytes was reduced independent of a change in *Kcnq4* transcript abundance, indicating an impairment of vascular K_V7 channel function. Interestingly, degradation of K_V7 function was less severe in arteries from female rats when compared to males. Moreover, arteries form female hypertensive rats presented with Oestrus cycle sensitive changes in vascular reactivity similar to those described at length in Chapter 4. These observations coincided with a significantly higher $K_V7.4$ membrane abundance within myocytes harvested from F-D/M SHRs when compared to male (Fig 5.12). Preservation of K_V7 channel function and membrane abundance within the F-D/M hypertensive rat potentially underpins the decreased sensitivity to vasoconstrictor U46619 when compared to hypertensive males, however, sex-dependent preservation of NT vascular reactivity was not universal, as Isoprenaline-mediated relaxation was ablated in the hypertensive animal of both sexes.

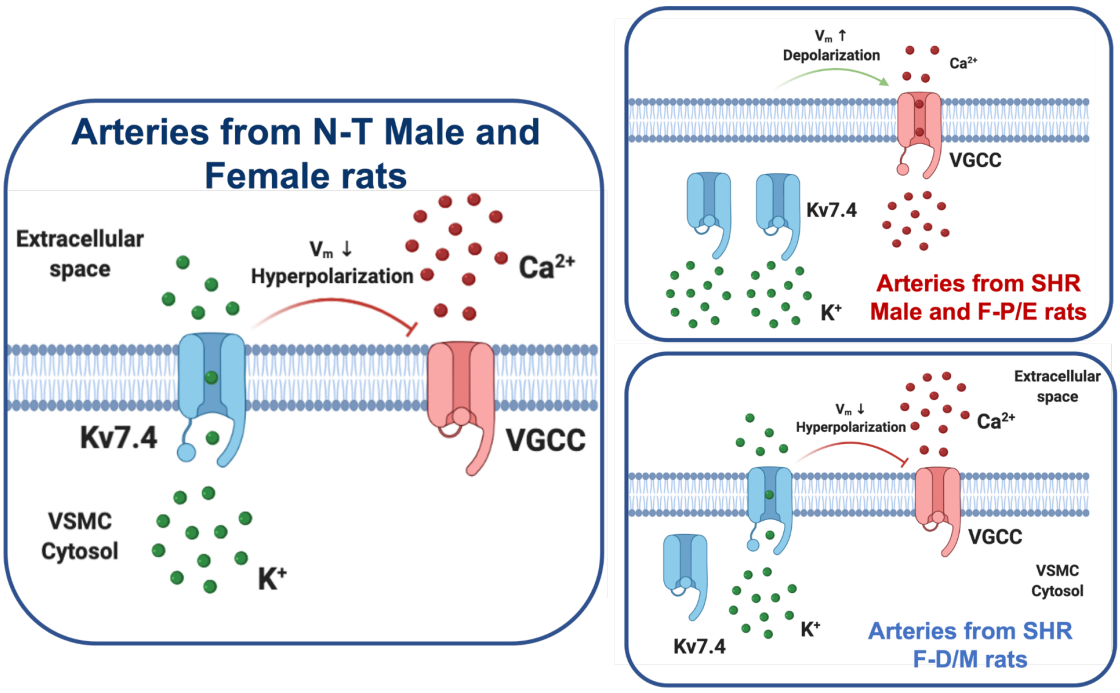

Figure 5.12: Graphical summary of K_V7 channel activity in arteries form male and female rats.

Diagrammatic representation of K_V7 channel membrane abundance and function within arteries from male and female (F; di-oestrus/met-oestrus (F-D/M); pro-oestrus/oestrus (F-P/E)) normotensive (N-T; right) and spontaneously hypertensive rats (SHRs; left).

5.4.1 $K_V7.4$ and the hypertensive phenotype

The role of $K_V7.4$ in male animal models of hypertension is well-established. Within primary and secondary models of hypertension, $K_V7.4$ protein expression is reduced via post-transcriptional processes including; 1.) diminished interaction with forward trafficking chaperone protein HSP90 and increased ubiquitination (Barrese *et al.*, 2018); 2.) translation inhibition by an aberrant rise of miR153, a microRNA with consensus for the 3'- untranslated region of *Kcnq4* (Carr *et al.*, 2016). These processes correlate with diminished K_V7 channel modulator sensitivity (Jepps *et al.*, 2011; Chadha, Zunke, Zhu, *et al.*, 2012) and impaired β-adrenoreceptor (Chadha, Zunke, Zhu, *et al.*, 2012), natriuretic peptide (Stott, Barrese, *et al.*, 2015) and peri-vascular adipose tissue factor (Li *et al.*, 2013) mediated relaxation. Though the underlying mechanisms remain outside the scope of this brief investigation, the data presented here similarly demonstrates a reduction in K_V7 channel modulator sensitivity whereby $K_V7.2$-5 channel activator

ML213-mediated relaxation of pre-contracted tone was diminished and pan-K_V7 channel inhibitor Linopirdine failed to augment or attenuate U46619 and Isoprenaline-mediated vasoactive responses respectively within arteries from male hypertensive animals. Moreover, we also demonstrate a reduction in $K_V7.4$ membrane abundance independent of a change in the transcript level of *Kcnq4*, indicative of a post-translational decrease in $K_V7.4$ trafficking, or protein expression, however, other candidates have been shown to be impaired within male renal arteries from SHRs including K_{ATP} (Kawata *et al.*, 1998; Mimuro *et al.*, 1998) and K_{Ca} (Martens and Gelband, 1996; Michel, Man and Vanhoutte, 2007). Though BK_{Ca} channel activator NS11021 failed to relax pre-contracted arterial tone in Chapter 4 (Fig 4.4), rat renal artery myocytes are known to express BK_{Ca} currents which are implicated in receptor mediated contraction (Betts and Kozlowski, 2000). Therefore, degradation or impairment of K_{Ca} or K_{ATP} cannot be ruled out as a potential means for the discrepancies observed in responses to U46619 or isoprenaline when comparing arteries from NT or SHRs. In summation, the results of this chapter support the previously established notion that $K_V7.4$ is implicated in the hypertensive phenotype within male animals.

5.4.2 Sexual dimorphisms in $K_V7.4$ handling in the hypertensive animal

As described in Chapter 1, pre-menopausal women express an enigmatic cardioprotective factor or factors that differentiates the etiology of CVD between age-matched men and women (Tunstall-Pedoe *et al.*, 1994; Usselman, Stachenfeld and Bender, 2016). Similarly, within animal models of hypertension females develop smaller increases in BP when compared to males (Reckelhoff, Zhang and Granger, 1998; Maris *et al.*, 2005; Tiwari *et al.*, 2010). Though to date little is known of the role of K_V7 channels within the hypertensive female, a study by Berg (2018) demonstrated a blunting of norepinephrine mediated increases in total peripheral resistance in response to intravenous retigabine within female NT and SHRs alone. Indicating that K_V7 channels potentially play a role in the sexual dimorphisms in the etiology of CVD. The data in this chapter would partially substantiate Berg's (2018) findings, whereby K_V7 channel

activator-mediated relaxation is preserved within female SHRs when compared to males, however, throughout this thesis, K_V7 channel activators have proven effective agents in relaxing pre-contracted arterial tone in NT males. Moreover, we observed no sex-dependent differences when comparing ML213 in arteries taken from NT animals. Berg infused 4.3 µmol/kg retigabine into male and female rats. Being that retigabine-mediated relaxation within in renal arteries from male Wistars is, comparably to the other agents used in Chapter 3 (Fig 3.6) and in previously published works (Jepps *et al.*, 2014), a poor relaxant of pre-contracted tone, the agent chosen may account for the discrepancies between the two studies.

When separated dependent on the Oestrus cycle, K_V7 channel activator-mediated relaxation in arteries taken from SHRs in F-D/M was equipotent to NT arteries from F-P/E. We have yet to determine the process of $K_V7.4$ handling during the Oestrus cycle. Previously, oestrogenic signalling in distal colic crypt cells was shown to internalize $K_V7.1$ via Rab4 and Rab11 trafficking to recycling endosomes (Rapetti-Mauss *et al.*, 2013), before later transport back to the membrane. Other studies have also demonstrated preferential recycling of ion channels targeted to endosomes in cardiac myocytes (Seebohm *et al.*, 2007; Hardel *et al.*, 2008; Conrad *et al.*, 2018), epithelia (van de Graaf *et al.*, 2008; Rapetti-Mauss *et al.*, 2013), and vascular myocytes (Leo *et al.*, 2014). Ion channel recycling is purported to be essential for the homeostasis of membrane surface ion channel density. Work by Conrad *et al*,. (2018) indicates that ion channels targeted for endosomal recycling are protected from protein degradation at the proteosome and when recycled back to the membrane, maintain ion channel membrane density during long (20hr) periods of disrupted *de novo* synthesis of protein. Though pure speculation, it is possible that E2 mediated internalization during P/E pulls $K_V7.4$ from the membrane. During which time $K_V7.4$ is protected from the degradative processes observed within the male, as reserved $K_V7.4$ is maintained within the recycling endosome. Protein stored within the recycling endosome may account for the preserved $K_V7.4$ membrane abundance observed within myocytes isolated from female SHRs in F-D/M.

However, it is also possible that Females express smaller increases in MicroRNAs known to rise during hypertension within the male (Carr *et al.*, 2016), preventing translation of *Kcnq4*. Paradoxical 4.4±2.9 and 2.69±0.8-fold increases in *Kcnq4* abundance were observed within whole artery lysates from F-P/E and F-D/M respectively when comparing arteries from SHRs against NT. Similar increases were observed by Jepps *et al,.* (2011) and Carr *et al,.* (2016), which was proposed to be because of a negative feedback loop on transcript expression due to diminished translation. Whole transcriptome was extracted from lysates of mesenteric and renal arteries from NT and SHRs, with the aim of screening for miR133a and miR153 in addition to *Kcnq4*. Unfortunately, though these experiments were attempted, no signal was observed with either miR153 or microRNA housekeeper gene RNU6-2 (MS00033740, Qiagen, UK). These experiments were undertaken at the end of the project, by which time the funds required to repeat the experiments had been exhausted. As such, they will form the basis of future investigations.

5.4.3 Limitations

A functional characterization of vascular reactivity by isometric tension recordings via wire myograph provides valuable insight into vascular function, however, its inferences are isolated to small 2 mm segments of arteries. This study is limited by a lack of BP measurements. As detailed above, previous work by Berg (2018), provided strong inference of sexual dimorphism in the impact of K_V7 modulators on BP. BP recordings were always intended to be included in this thesis, however, the unfortunate closure of the animal facilities at St George's took place before this work could be undertaken. BP measurements in future investigations will allow for a comparison of systemic cardiovascular and K_V7 function, with the aim of repeating Berg's (2018) findings.

As described in Figure 5.5, 300 nmol-L^{-1} U46619 evokes significantly greater contraction within arteries from male animals when compared to females. When comparing multiple

vascular beds and multiple groups, the same concentration of pre-contractile agent was chosen as a means to reduce the number of variables within the investigation, however, this error introduces the caveat of physiological agonism into the sex-dependent differences in ML213 mediated responses, like those described in chapter 4.4.3. Appropriate levels of pre-contracted tone when comparing multiple groups will be of key consideration within investigations moving forwards.

5.4.4 Perspectives

While in its infancy, the data of this chapter provide strong evidence for a preservation of K_V7 channel function within the female SHR. Though myriad factors may account for the sexual dimorphisms in CVD, vascular K_V7 function may represent a novel candidate for these differences. A better understanding of how vascular K_V7 channels operate in the female, and in particular, the SHR female model will allow us to answer these questions and possibly help ameliorate the hypertensive phenotype.

Chapter 6: An investigation into sex-dependent signalling of prostacyclin mimetics

6.1 Introduction

Within the following chapter, a change in approach to study vascular reactivity within the female rat was employed, whereby K_V7 channels were investigated as a secondary consideration. PGI_2, a product of cyclooxygenase-1 and 2 (COX-1/2) mediated metabolism of arachidonic acid, exhibits anti-thrombotic, anti-inflammatory and potent vasodilatory properties in a process attributed to the activation of G_s-coupled IP prostanoid receptor signalling (Fetalvero, Martin and Hwa, 2007). In addition to IP receptors, PGI_2 and stable analogues including Iloprost also bind to other GPCR including $EP_{1,2,3,4}$, TP, FP and DP_1 (Katusic, Santhanam and He, 2012), though with different affinities. For instance, in human and rat pulmonary arteries Iloprost binds to IP / EP_1 with high affinity, FP > $EP_{3/4}$ with moderate affinity and – DP_1 > EP_2 > TP with low affinity (Whittle *et al.*, 2012). As such, the potential effect of PGI_2 / Iloprost within the vasculature includes both $EP_{1/3}$ / FP prostanoid receptor evoked contraction (Tang *et al.*, 2008; Orie & Clapp, 2011; Kobayashi *et al.*, 2011) and EP_4 / IP prostanoid receptor mediated relaxation (Schubert *et al.*, 1996, 1997; Dumas *et al.*, 1997; Lombard *et al.*, 1999; Namkoong *et al.*, 2005). These diverse responses to prostacyclin mimetics remain largely uncharacterised. Moreover, few studies have considered sex as a factor when characterising prostacyclin-memetic mediated vascular responses.

Previously, BK_{Ca} (eg Schubert *et al.*, 1997), K_{ATP} (Lombard *et al.*, 1999; Schubert *et al.*, 1997) and K_{IR} (Orie *et al*, 2006) have been identified as the downstream targets of IP-

receptor mediated vasorelaxation. As the contribution of K_V7 channels to prostanoid receptor-mediated relaxations is unknown, the aim of this chapter was to determine whether K_V7 channels were involved with prostacyclin mimetic mediated responses in rat mesenteric arteries from aged-matched male and female rats. This artery was chosen because; 1.) K_V7 expression has been established (Mackie *et al.*, 2008; Jepps *et al.*, 2011, 2015, Present study - Figure 3.11/14), 2.) K_V7 activators are effective relaxants (Jepps *et al.*, 2014, Figure 3.5), 3.) a role for K_V7 channels in $G_{\alpha s}$-linked responses has been identified (eg Stott *et al.* , 2016; Stott *et al.*, 2018; Lindman *et al.*, 2018, Figure 3.9); 4.) endothelium dependent production of PGI_2 mediates concomitant IP-receptor mediated relaxation (Liu *et al.*, 2012) and TP/EP_3 mediated contraction (Liu *et al.*, 2012, 2017). To circumvent the short half-life of prostacyclin we characterised the contribution of EP_3 and IP receptors to responses mediated by its stable analogue Iloprost and defined the contribution of K_V7 channels to IP receptor mediated vasorelaxation using a selective IP receptor agonist, MRE-269. The findings of this chapter demonstrate a striking sex-dependent difference in response to Iloprost and a role for $K_V7.1$ channels in shaping IP-receptor evoked vasorelaxation within rat mesenteric arteries which within the female rat, similar to chapter 4, was Oestrus cycle-sensitive.

6.2 Materials and methods

The methods used in the following chapter are described at length in Chapter 2. For a list of drugs employed, please see table 2.1.

6.2.1 Morpholino transfection

Knockdown of $K_V7.1$ in both whole plexuses of mesenteric arteries for immunostaining, and 2nd order of mesenteric arteries for isometric tension recording was performed by transfection with morpholinos that prohibit protein translation but do not affect transcript levels, see; Jepps *et al.*, 2015; Barrese *et al.*, 2020. Either *Kcnq1* targeted morpholino nucleotides or mismatch controls (5 μmol-L^{-1}, Genetools, USA) were mixed with Lipofectamine 2000 (ThermoFisher, Paisley, UK) and Opti-MEM (Sigma, UK) and left at room temperature for 2hrs. Morpholino/Lipofectamine/Opti-MEM mixture was added to Dulbecco's modified eagle medium (DMEM) F-12 (Sigma, UK) containing 1%-penicillin/streptomycin. Mesenteric arteries were added and left for 48hrs at 37°C with 5% CO_2.

6.3 Results

6.3.1 Iloprost-mediated vasoactive responses

Initial investigations determined the vasoactive effect of Iloprost on both basal, and pre-contracted arterial tone. In mesenteric arteries from male rats stably contracted by U46619 (300 nmol-L^{-1}), Iloprost evoked a bi-phasic response, producing relaxation at lower concentrations followed by contraction at concentrations ≥1 µmol-L^{-1} (Fig 6.1.A,B; black). This phenomenon was notably absent in mesenteric arteries from female rats, wherein Iloprost only evoked concentration dependent vasorelaxation (P>0.05; Fig 6.1.A,B; red). See representative traces in Figure 6.1.A. Application of solvent control had negligible effect on established tone in mesenteric arteries from either male or female rats (Fig 6.1.B). Further, no differences were observed in the levels of pre-contracted arterial tone in response to U46619 when comparing arteries from male and female animals (Fig 6.1.C). As seen in Figure 6.2, no Oestrus cycle dependent changes in vascular reactivity were observed in response to Iloprost. As such, females have been combined into one group for the following experiments.

Prostacyclin-mediated relaxations are conventionally mediated via activation of IP receptors, and EP_3 receptors have been implicated in contractile responses to Iloprost in mesenteric arteries from hypertensive rats (Liu *et al.*, 2017). To establish a role for these receptors in the bi-phasic or mono-phasic response observed in male and female rats respectively, vessels were pre-incubated in either the EP_3 receptor antagonist L-798,106 (300 nmol-L^{-1}; Belley *et al.*, 2006, 2005) or IP receptor antagonist CAY-10441 (100 nmol-L^{-1}; Bley *et al.*, 2006).

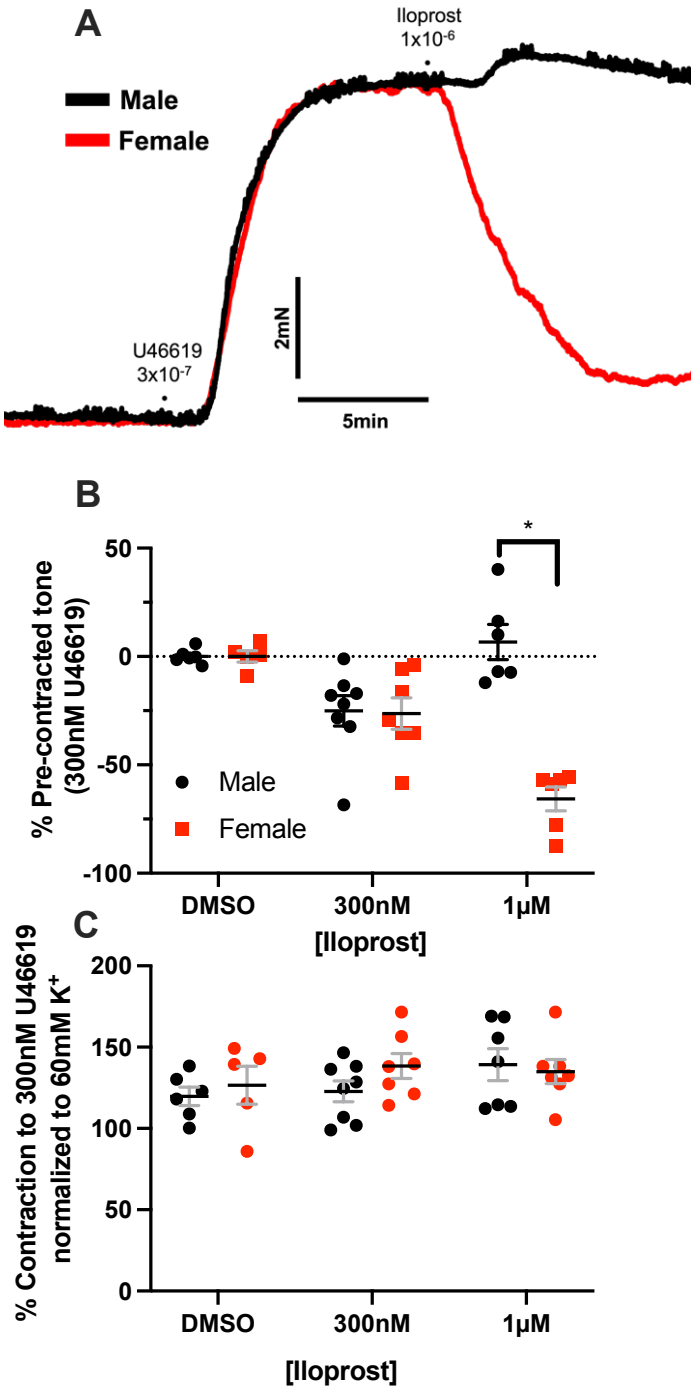

Figure 6.1: Iloprost evokes bi-phasic vasoactive responses within male, but not female mesenteric arteries.

Representative traces of Iloprost (1 µmol-L^{-1}) mediated vasoactive responses on pre-contracted tone (300 nmol-L^{-1} U46619) within mesenteric arteries from male (A; black) or female (A; red) Wistar rats. Scatter graph plot and mean data for DMSO solvent control and Iloprost (0.3-1 µmol-L^{-1}) mediated vasoactive responses on pre-contracted (300nmol-L^{-1} U46619) mesenteric arteries (B; *n*=6-8). Scatter graph showing individual and mean values of stable pre-contracted tone from male and female arteries prior to adding Iloprost to the chamber. All values are expressed as mean ± SEM. A two-way statistical ANOVA with a post-hoc Bonferroni test was used to generate significance values (*=*P*<0.05). (*n*=) number of animals used.

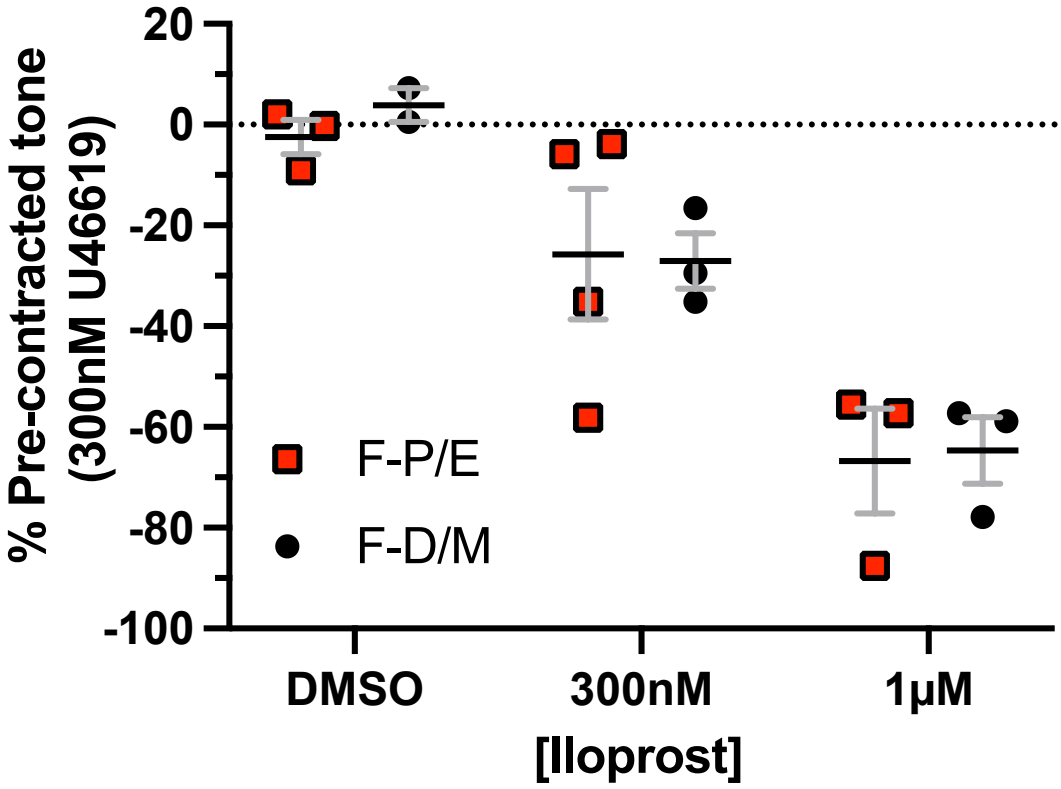

Figure 6.2: Iloprost evoked responses are not Oestrus cycle dependent.

Scatter graph plot and mean data for DMSO solvent control and Iloprost (0.3-1 µmol-L^{-1}) mediated vasoactive responses on pre-contracted (300nmol-L^{-1} U46619) mesenteric arteries from females in Pro-oestrus / Oestrus (F-P/E; red square; *n*=3-4) or females in Di-oestrus / Oestrus (F-D/M; B; *n*=3-4). All values are expressed as mean ± SEM. A two-way statistical ANOVA with a post-hoc Bonferroni test was used to generate significance values (*=*P*<0.05). (*n*=) number of animals used.

6.3.1.1 Delineating EP_3/IP receptor mediated vascular effects

In mesenteric arteries from male rats, the presence of the EP_3 receptor antagonist L-798,106, 1 µmol-L^{-1} Iloprost-mediated contraction was converted to a near full relaxation of pre-contracted tone (Fig 6.3.A). In contrast, within mesenteric arteries from females, EP_3 receptor inhibition had no significant effect on Iloprost evoked relaxation (Fig 6.3.A).

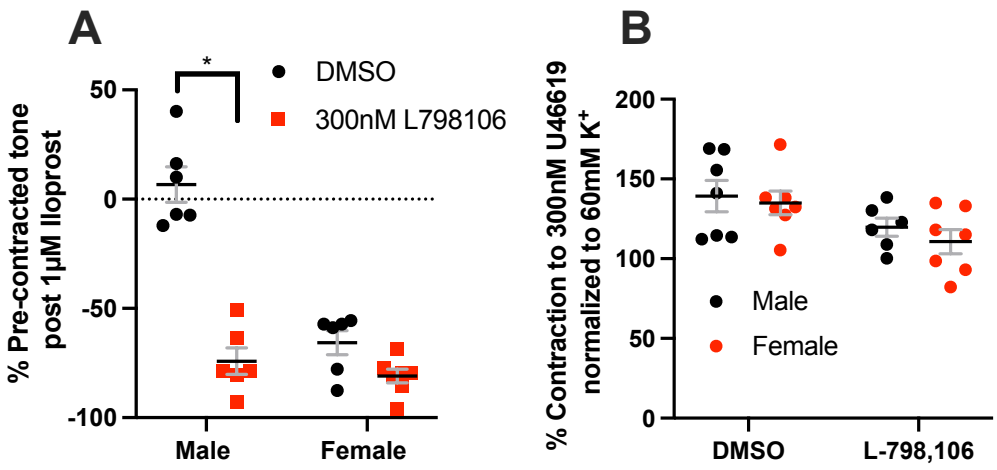

Figure 6.3: Iloprost-mediated contraction ablated by EP_3- receptor inhibition. Mean data for Iloprost-mediated vasoactive responses (A; 1 µmol-L^{-1}) within pre-contracted (300 nmol-L^{-1} U46619) mesenteric arteries from male and female rats pre-incubated in either solvent control (DMSO; *n*=6-8), 300 nmol-L^{-1} L-798,106 (A,B; *n*=6-7). Scatter graph showing individual and mean values of stable pre-contracted tone from male and female arteries prior to adding Iloprost to the chamber (B). A two-way statistical ANOVA with a post-hoc Bonferroni test was used to generate significant values (*=*P*<0.05). (*n*=) number of animals used.

Conversely, in the presence of the IP receptor antagonist CAY-10441, relaxation in response to 0.3 µmol-L^{-1} Iloprost was ablated in both groups (Fig 6.4.A; *P*≤0.05). Moreover, 3 µmol-L^{-1} Iloprost evoked significantly greater contraction from base-line tone in mesenteric arteries from male rats pre-incubated in CAY-10441 compared to DMSO (Fig 6.4.C). Whereas CAY-10441 pre-incubation had no significant effect on Iloprost-mediated increase in basal tone within mesenteric arteries from female rats (Fig 6.4.C). No differences were observed in pre-contracted tone in vessels pre-incubated in either L-798,106 or CAY-10441 when compared to DMSO solvent control or between the sexes (Fig 6.3.B/ 6.4.B).

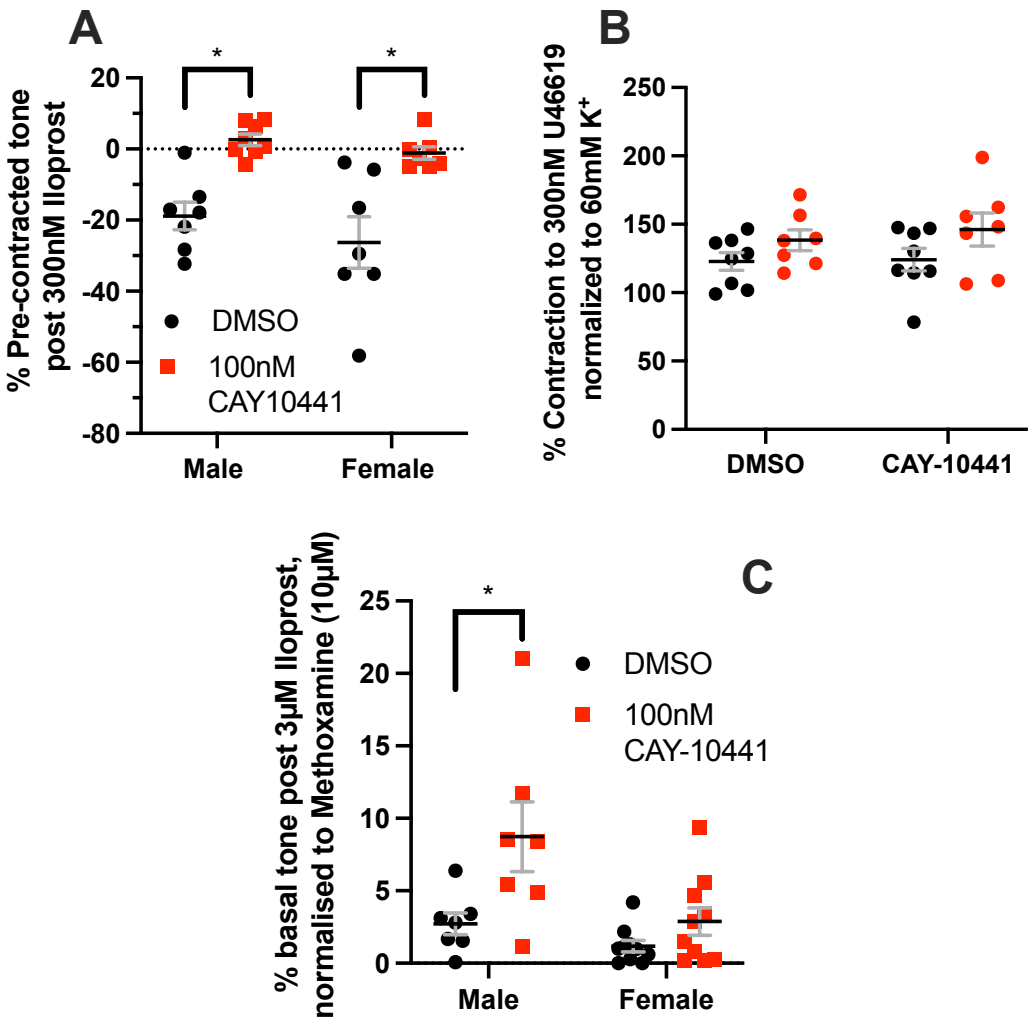

Figure 6.4: Iloprost-mediated relaxation is ablated by IP-receptor inhibition.

Mean data for Iloprost-mediated vasoactive responses (300 nmol-L^{-1}) within pre-contracted (300 nmol-L^{-1} U46619) mesenteric arteries from male and female rats pre-incubated in either solvent control (DMSO; A; *n*=7-8), 100 nmol-L^{-1} CAY-10441 (C; *n*=7-8). Scatter graph showing individual and mean values of stable pre-contracted tone from male and female arteries prior to adding Iloprost to the chamber (B). Mean data for vasoconstriction from base line tension in response to 3 µmol-L^{-1} Iloprost in male (black; *n*=7) and female (red; *n*=10) mesenteric arteries in the presence of DMSO or 100nmol-L^{-1} CAY-10441 normalised to peak contraction in response to 10µmol-L^{-1} methoxamine (C). A two-way statistical ANOVA with a post-hoc Bonferroni test was used to generate significant values (*=*P*<0.05). (*n*=) number of animals used.

6.3.1.2 Generating concentration effect curves to Iloprost on pre-contracted arteries

Cumulatively increasing concentrations of Iloprost (0.001-10 μmol-L^{-1}) were applied to pre-contracted arteries in the absence and presence of either CAY-10441 or L-798,106, see figure 6.5. In this protocol, Iloprost gave ill-defined concentration dependent effects, however, bi-phasic vascular responses in arteries from male rats, and mono-phasic relaxation in arteries form female rats were still present that were distinct from a time-dependent loss of tone or solvent mediated relaxation (Fig 6.5.A/B; n=6-8; P≤0.05). Moreover, EP_3 inhibition enhanced Iloprost-mediated relaxation in female arteries at concentrations ≥100 nmol-L^{-1} (Fig 6.5.D; n=6-8; P≤0.05). Finally, Iloprost-mediated contraction was more efficacious in male arteries when compared to females (Fig 6.5.E,F; n=6-8).

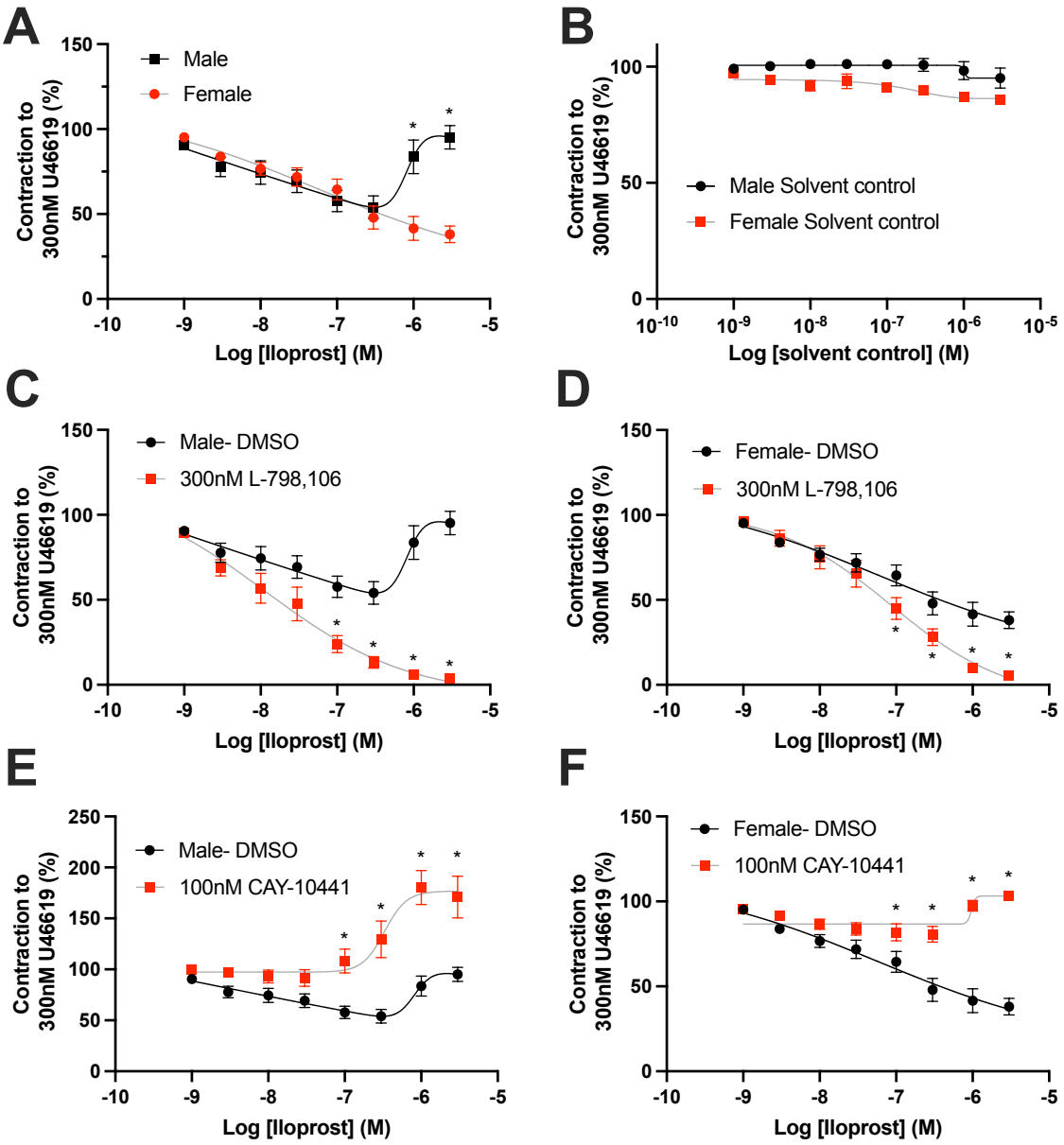

Figure 6.5: Cumulative concentration effect curves generated from Iloprost-mediated vasoactive responses.

Mean data for Iloprost-mediated vasoactive responses (A; 0.001-1 µmol-L^{-1}) within pre-contracted (300 nmol-L^{-1} U46619) mesenteric arteries arteries from male (black) and female (red) and female Wistar rats (A). The effect of equivalent cumulatively increasing volumes of DMSO solvent controls on pre-contracted vessels from male and female Wistars (B). Iloprost-mediated responses in vessels from male and female Wistars pre-incubated in either solvent control (DMSO; C-F; *n*=6-8), 300 nmol-L^{-1} L-798,106 (C,D; *n*=6-8) or 100 nmol-L^{-1} CAY-10441 (E,F; *n*=6-8). All values are expressed as mean ± SEM (A-F). A two-way statistical ANOVA with a post-hoc Bonferroni test was used to generate significant values (*=*P*<0.05). (*n*=) number of animals used.

6.3.1.3 Prostanoid receptor expression within the vasculature

Quantitative PCR was performed to determine the relative expression of prostanoid receptors (see table 2.2) in mesenteric arteries from both sexes. Figure 6.6 shows that expression of *Ptger2/4* ($EP_{2/4}$) was negligible in mesenteric arteries from both sexes compared to, *Ptger3* > *Ptgir* > *Ptger1,* (EP_3; IP; EP_1) which were well expressed, however, *Ptger3* was expression was significantly smaller in mesenteric arteries from female rats compared to mesenteric arteries from males (Fig 6.6; *n*=5-10; *P*≤0.05). In summary, our data demonstrates that Iloprost-mediated relaxation in rat mesenteric arteries occurs predominantly via IP receptors, whilst contraction at higher concentrations was driven by EP_3 receptors in males. Further, the absence of a bi-phasic response to Iloprost in female mesenteric arteries was observed in association with a significantly lower expression of *Ptger3* when compared to arteries from male rats.

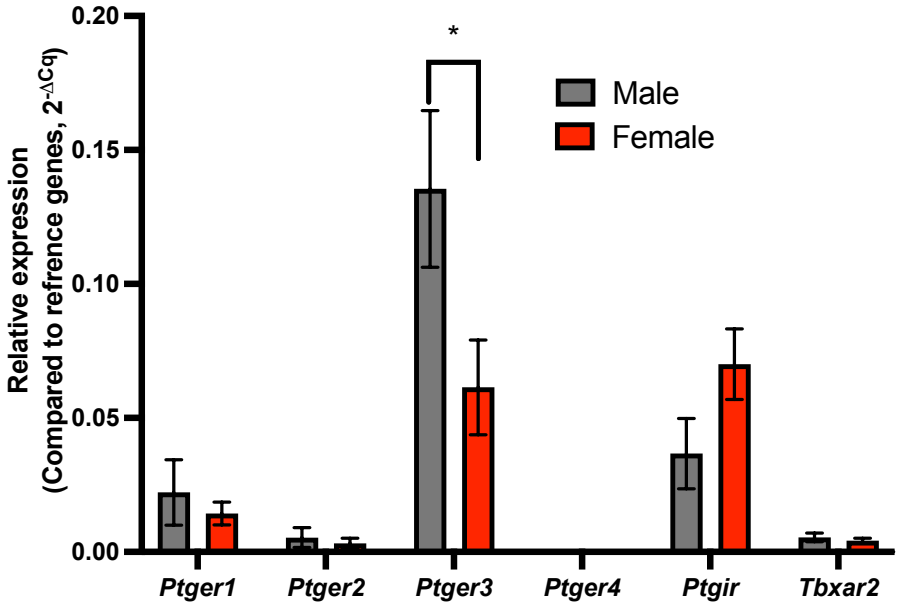

Figure 6.6: Prostanoid receptor expression within whole mesenteric artery lysates.

Relative gene expression of prostanoid receptors (*Ptger1-4* = EP_{1-4}, *Ptgi* = IP, *Tbxar2* = TXA2) normalised to stable housekeeper genes (*Canx, Cyc1*) expressed as $2^{-\Delta Cq}$ from male (black; *n*=5) and female (red; *n*=6-10) whole mesenteric artery lysates (F). A two-way statistical ANOVA with a post-hoc Bonferroni test was used to generate significant values (*=*P*<0.05). (*n*=) number of animals used.

6.3.2 Characterising MRE-269-mediated relaxation.

As Iloprost has a plethora of potential targets, we chose the clinically used IP receptor agonist, Selexipag (NS-304) to delineate the mechanisms underlying IP-mediated relaxation. Application of Selexipag produced concentration dependent relaxations of pre-contracted mesenteric arteries from male rats, however this effect was insensitive to pre-incubation with IP receptor antagonist CAY-10441 (Fig 6.7.A), thus its effects are non-IP receptor dependent. In the body, Selexipag is metabolized into the active compound, MRE-269. Application of MRE-269 to mesenteric arteries from male rats produced a relaxation that was ablated by CAY-10441 pre-incubation up to threshold of 1 µmol-L^{-1} (6.7.B; $P \leq 0.05$; $n=5$). At concentrations beyond this value, MRE-269-mediated relaxation was not sensitive to CAY-10441 and therefore not driven by IP receptor activation. Non-IP receptor mediated relaxation is highlighted by the grey box in Figure 6.7.B. Therefore in following investigations, MRE-269 was used at concentrations ≤1 µmol-L^{-1} to ensure only IP receptor-mediated effects were investigated.

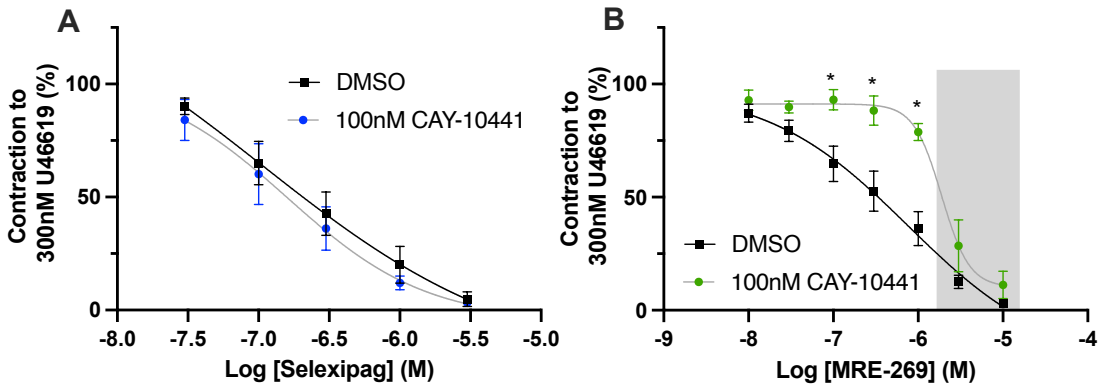

Figure 6.7: Selexipag-mediated relaxation was unaffected by CAY-10441 in male mesenteric arteries.

Mean data Selexipag (B; 0.03-3 µmol-L^{-1}) mediated relaxation in vessels pre-incubated in DMSO solvent control (black; $n=6$) or 100 nmol-L^{-1} CAY-10441 ($n=5$) in male mesenteric arteries. All values are expressed as mean ± SEM. A two-way statistical ANOVA with a post-hoc Bonferroni test was used to generate significant values (*=$P<0.05$). ($n=$) number of animals used.

6.3.3 A novel role for K_V7.1 in shaping IP receptor-specific agonists in mesenteric arteries.

6.3.3.1 Pharmacological inhibition of K_V7.1

K_V7 channels, especially K_V7.4 and K_V7.5, are functional endpoints for several G_s-linked receptors (see Chapter 1.5.4.2 / Barrese et al., 2018, Byron & Brueggmann, 2018). As such, we characterised the potential contribution of K_V7 channels to IP- receptor selective MRE-269-mediated relaxation. In mesenteric arteries from male rats, MRE-269-mediated relaxation was significantly attenuated by pre-incubation with the pan-K_V7 channel inhibitor Linopirdine (10 μmol-L^{-1}; yellow) when compared to DMSO solvent control (Fig 6.8; black; P<0.05). Strikingly, pre-incubation with the K_V7.1 specific inhibitor HMR-1556 (10 μmol-L^{-1}), also impaired MRE-269-induced relaxations to the same extent as Linopirdine (Fig 6.8.A,B; green; P<0.05). The structurally dissimilar K_V7.1 inhibitor Chromanol 293B also significantly attenuated MRE-269-mediated relaxation of male mesenteric arteries (P<0.05; Fig 6.8.C). In contrast, and consistent with previous reports (Stott *et al*., 2016), relaxations of mesenteric arteries induced by the mixed β-adrenoceptor agonist isoprenaline were not affected by 10 μmol-L^{-1} HMR-1556 pre-incubation but was impaired by linopirdine (Fig 6.8.D; Fig 3.9). These data suggest that unlike other GPCR-driven vasorelaxations, IP-generated relaxations involve K_V7.1 channels rather than K_V7.4/ 7.5.

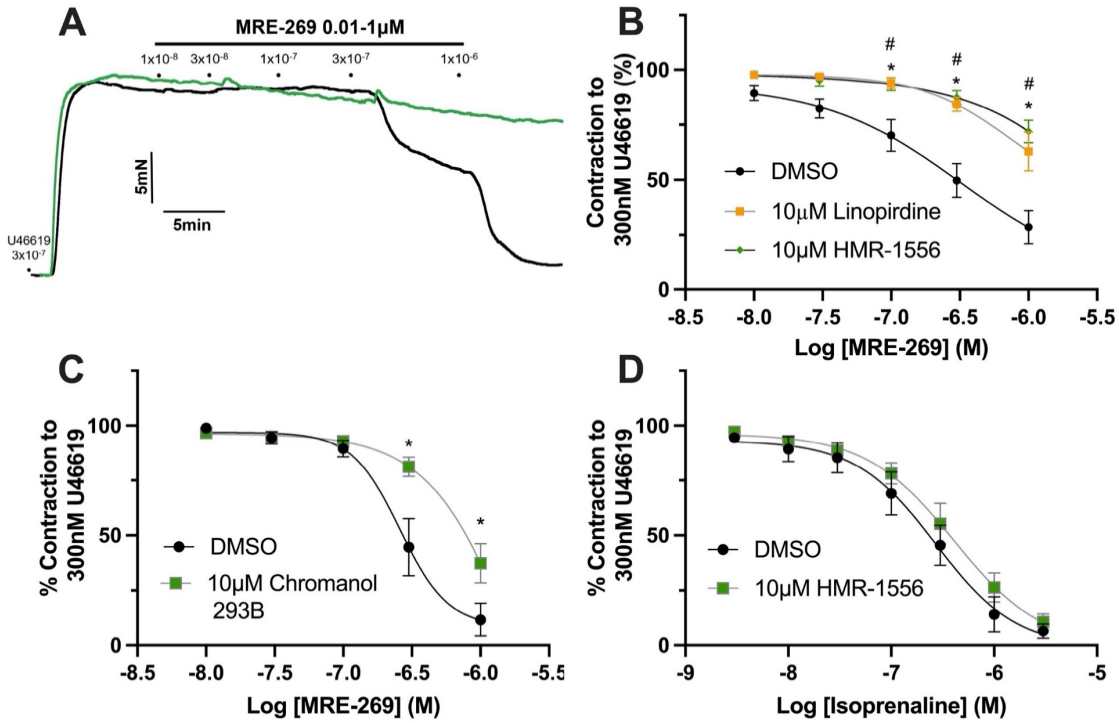

Figure 6.8: Linopirdine and HMR-1556 attenuate MRE-269-mediated vasorelaxation in mesenteric arteries from male and female rats.

Representative traces of MRE-269-mediated (0.01-1µmol-L^{-1}) relaxation of pre-contracted tone (300 nmol-L^{-1} U46619) within mesenteric arteries pre-incubated in either DMSO solvent control (A; black) or 10µmol-L^{-1} $K_V7.1$ specific blocker HMR-1556 (A; green) from male Wistar rats. Mean data for MRE-269-mediated vasorelaxation (0.01-1 µmol-L^{-1}) of pre-contracted tone (300 nmol-L^{-1} U46619) within mesenteric arteries pre-incubated in either DMSO (B; black) solvent control, 10 µmol-L^{-1} pan-K_V7 channel blocker linopirdine (B; yellow) or HMR-1556 (B; green) or 10µmol-L^{-1} $K_V7.1$ specific blocker Chromanol 293B (C; green; *n*=7-10). Mean data for Isoprenaline-mediated relaxation in vessels pre-incubated in DMSO (black) or 10 µmol-L^{-1} HMR-1556 (green) in male mesenteric arteries (D; *n*=9). All values are expressed as mean ± SEM (A-F). A two-way statistical ANOVA with a post-hoc Dunnet's's (B) or Bonferroni (C-D) test was used to generate significant values (*=*P*<0.05). (*n*=) number of animals used.

6.3.3.2 Molecular interference of K_V7.1

To corroborate the contribution of K_V7.1 to IP-receptor mediated vasorelaxation we transfected mesenteric arteries with either a morpholino that prevented translation of K_V7.1 or a scrambled control. Immunocytochemistry with an antibody for K_V7.1 validated by over-expression studies (See chapter 3, Fig 3.13) showed a significant reduction in total cell fluorescence (A.U) in *Kcnq1* morpholino transfected arteries when compared to mismatch control (Fig 6.9.A-C; P>0.05). Functionally, within arteries incubated with mismatch control, 300 nmol-L^{-1} of the K_V7.1 activator ML277 ((Yu, 2013); Fig 3.4/5) produced a significantly greater relaxation when compared to *Kcnq1* morpholino-transfected arteries (Fig 6.9.D; P>0.05; n=7-10). Similarly, relaxation produced by 1 µmol-L^{-1} MRE-269 was greater in arteries transfected with mismatch control morpholino when compared *Kcnq1* morpholino transfected arteries (Fig 6.9.E; P>0.05; n=7-10). Thus, a reduction in K_V7.1 protein was observed in conjunction with an diminished relaxation in response to ML277 and MRE-269.

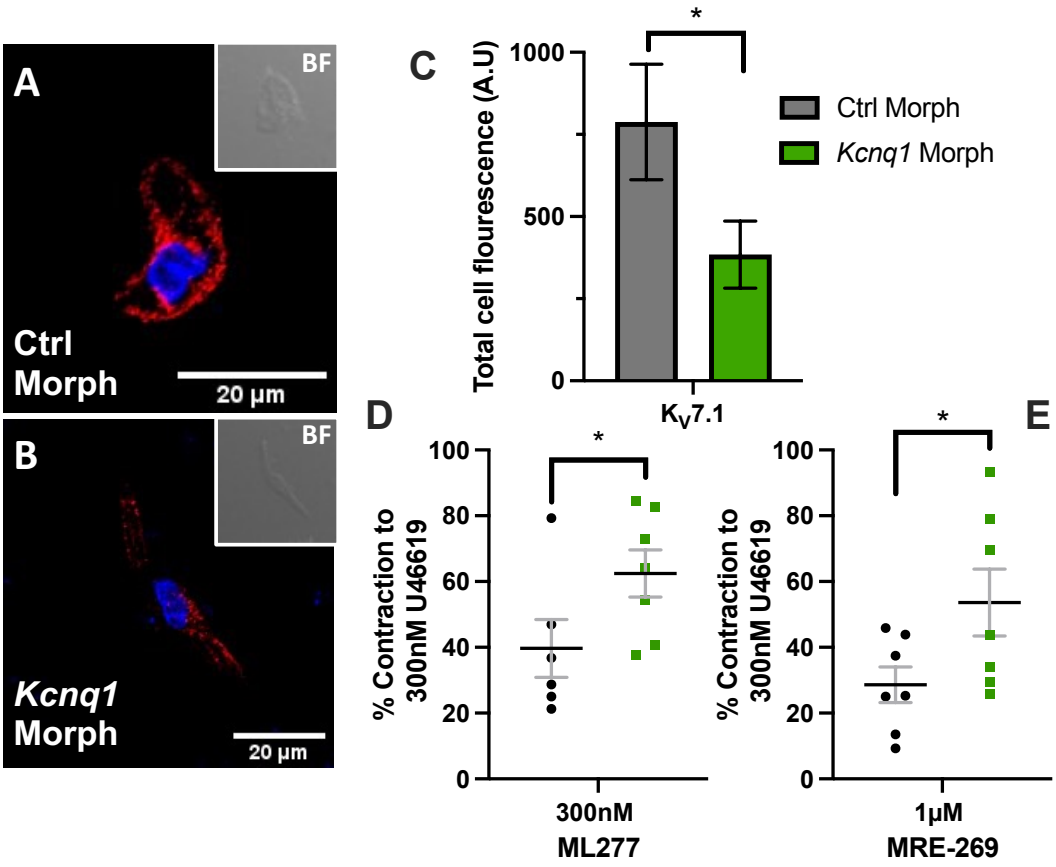

Figure 6.9: Molecular interference of *Kcnq1* via targeted morpholino knockdown impairs MRE-269-mediated relaxation.

Representative immunofluorescence showing $K_V7.1$ in isolated vascular smooth muscle cells from either scrambled control (Ctrl morph; A) or *Kcnq1 (Kcnq1* morph*;* B) morpholino transfected mesenteric arteries. $K_V7.1$ shown in red, nuclear staining in blue (DAPI [4',6-diamidino-2-phenylindole, dihydrochloride]). Insets show brightfield (BF) images of the cell. Mean data for total cell fluorescence measured in arbitrary units (A.U) for Ctrl morph (grey; *n*=3; N=10) and *Kcnq1* morph (green; *n*=3; N=10; D) transfected cells. Scatter graph and mean data for 300nmol-L^{-1} ML277 mediated relaxation (*n*=7; E). Mean data for 1µmol-L^{-1} MRE-269-mediated relaxation (*n*=7; F). All values are expressed as mean ± SEM (A-F). A paired Student's t test was used to generate significant values (*=*P*<0.05). (*n*=) number of animals used, (N=) number of cells per biological repeat.

6.3.3.3 IP-receptor mediated signalling cascade

Subsequent experiments aimed to determine the signalling cascade activated in response to IP-receptor stimulation. Iloprost evoked hyperpolarization of rat tail artery VSMCs is mediated via G_s – cAMP/PKA stimulation of K^+ currents (Schubert *et al.*, 1996) in a process attributed to IP receptors although not fully defined. Here we similarly demonstrate that adenylate cyclase inhibitor SQ22,562 (10 μmol-L^{-1}) and PKA inhibitors Rp-8-Br-cAMP (1 μmol-L^{-1}) and KT5720 (1 μmol-L^{-1}) significantly attenuated MRE-269-mediated relaxation (1 μmol-L^{-1}; $P \leq 0.05$; Fig 6.7.A-C; n=7-9). Inhibition of an alternative secondary signalling molecule activated by G_s -cAMP, EPAC, via ESI-09 had no effect (100 nmol-L^{-1}; Fig 6.10.D). Finally, $G_{\beta\gamma}$ inhibition by M119K (1 μmol-L^{-1}) also significantly attenuated MRE-269-mediated relaxations (Fig 6.10.E; P>0.05; n=7).

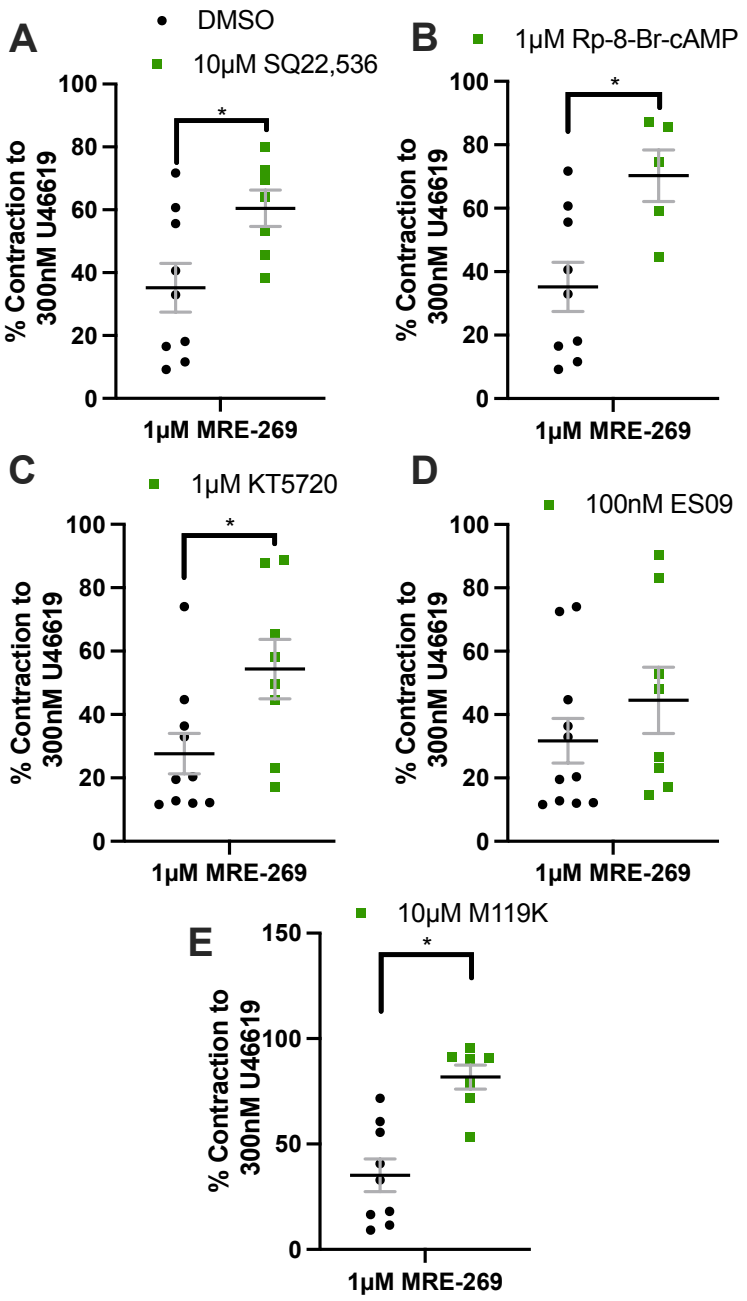

Figure 6.10: MRE-268 mediated relaxation is sensitive to adenylate cyclase, Gβγ and protein kinase A inhibition, but not effector protein activated by cAMP in male rat mesenteric arteries.

Mean data for MRE-269-mediated vasorelaxation (1 μmol-L^{-1}) of pre-contracted tone (300 nmol-L^{-1} U46619) within mesenteric arteries pre-incubated in either DMSO (A-E; *n*= 9; grey) solvent control or inhibitors of the following (green); adenylate cyclase- SQ22,562 (10 μmol-L^{-1}; *n*=7; A), protein kinase A- Rp-8-Br-cAMP (1μmol-L^{-1}; *n*=5; B) / KT5720 (1μmol-L^{-1}; *n*=8; C), effector protein inhibited by cAMP- ES09 (100nmol-L^{-1}; *n*=8; D) and Gβγ- ML119K (1μmol-L^{-1}; *n*=7; E). All values are expressed as mean ± SEM (A-E). An unpaired students T-test was used to generate significant values (*=*P*<0.05). (*n*=) number of animals used.

6.3.3.4 Alternate targets for IP-receptor mediated signalling cascade

BK_{Ca} and K_{ATP} channels have also been identified as down-stream targets of cAMP-PKA dependent relaxations evoked by Iloprost (Schubert *et al.*, 1997). Here, we demonstrate that BK_{Ca} inhibitor iberiotoxin (100 nmol-L^{-1}) but not K_{ATP} inhibitor glibenclamide (1 µmol-L^{-1}) partially inhibited MRE-269-mediated relaxation in male mesenteric arteries (Fig 6.11.A,B), though this failed to reach statistical significance.

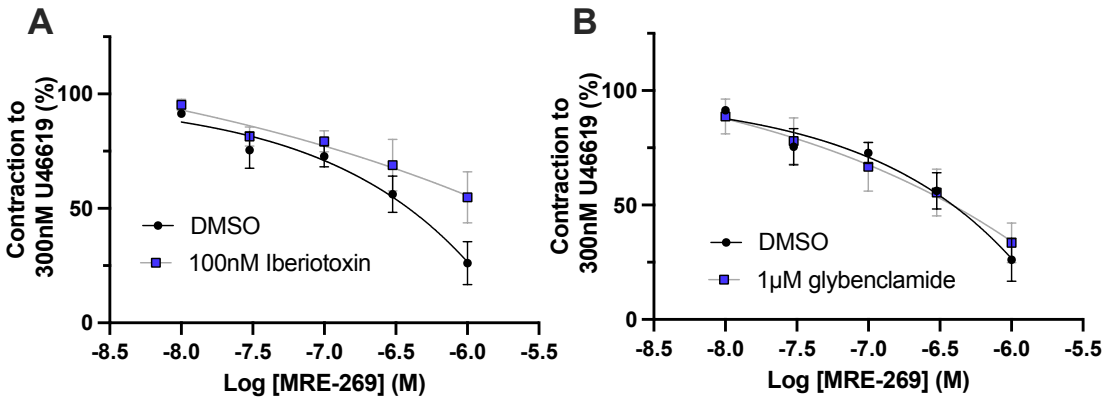

Figure 6.11: MRE-269-mediated relaxation is not attenuated K_{ATP} and BK_{Ca} inhibition.

Mean data for MRE-269 (A,B,C 0.01-10 µmol-L^{-1}) mediated relaxation in vessels pre-incubated in DMSO solvent control (A,B,C; black; *n*=4), 100 nmol-L^{-1} BK_{Ca} channel inhibitor Iberiotoxin (A; blue; *n*=5) or 1 µmol-L^{-1} K_{ATP} channel inhibitor glibenclamide (B; blue; *n*=5) in male mesenteric arteries. All values are expressed as mean ± SEM (A-F). A two-way statistical ANOVA with a post-hoc Bonferroni test was used to generate significant values (*=*P*<0.05). (*n*=) number of animals used.

6.3.4 Oestrus cycle-dependent shifts in the sensitivity of MRE-269-mediated vasorelaxation to K_V7 channel modulators

The pan K_V7 channel inhibitor Linopirdine also attenuated MRE-269-mediated relaxation in mesenteric arteries from female rats when compared to DMSO solvent control (Fig 6.12.A; P<0.05). Moreover, the K_V7.1 channel inhibitor HMR-1556 also significantly attenuated Iloprost-mediated relaxations (Fig 6.12.A; P<0.05), though to a smaller degree when compared to Linopirdine.

In contrast to Iloprost, when selecting for IP-receptor mediated responses, we observed oestrus cycle dependent changes in vascular reactivity like those observed in Chapters 4 and 5, again categorised into F-D/M and F-P/E. Both the pan-K_V7 channel inhibitor Linopirdine and K_V7.1 specific inhibitor HMR-1556 analogously impaired MRE-269-mediated relaxation in arteries from F-D/M (Fig 6.9.B; n=5-7; P<0.05), however, neither agent had any effect on MRE-269 responses in arteries from rats in F-P/E (Fig 6.12.C; n=6-8). Moreover, MRE-269-mediated relaxation in arteries from female F-P/E rats was significantly less potent within arteries from rats in F-P/E when compared to F-D/M (Fig 6.12.D; n=6-8; P<0.05). Interestingly, no oestrus-stage difference in the response to the K_V7.1 activator ML277 (0.1-0.3 μmol-L^{-1}) was observed (Fig 6.12.E; n=5-6). These data reveal an oestrus cycle stage dependent contribution of K_V7.1 to IP-receptor mediated relaxation, which coincides with diminished sensitivity to MRE-269-mediated relaxation. This phenomenon was observed independent of a change in sensitivity to K_V7.1 activator-mediated relaxation.

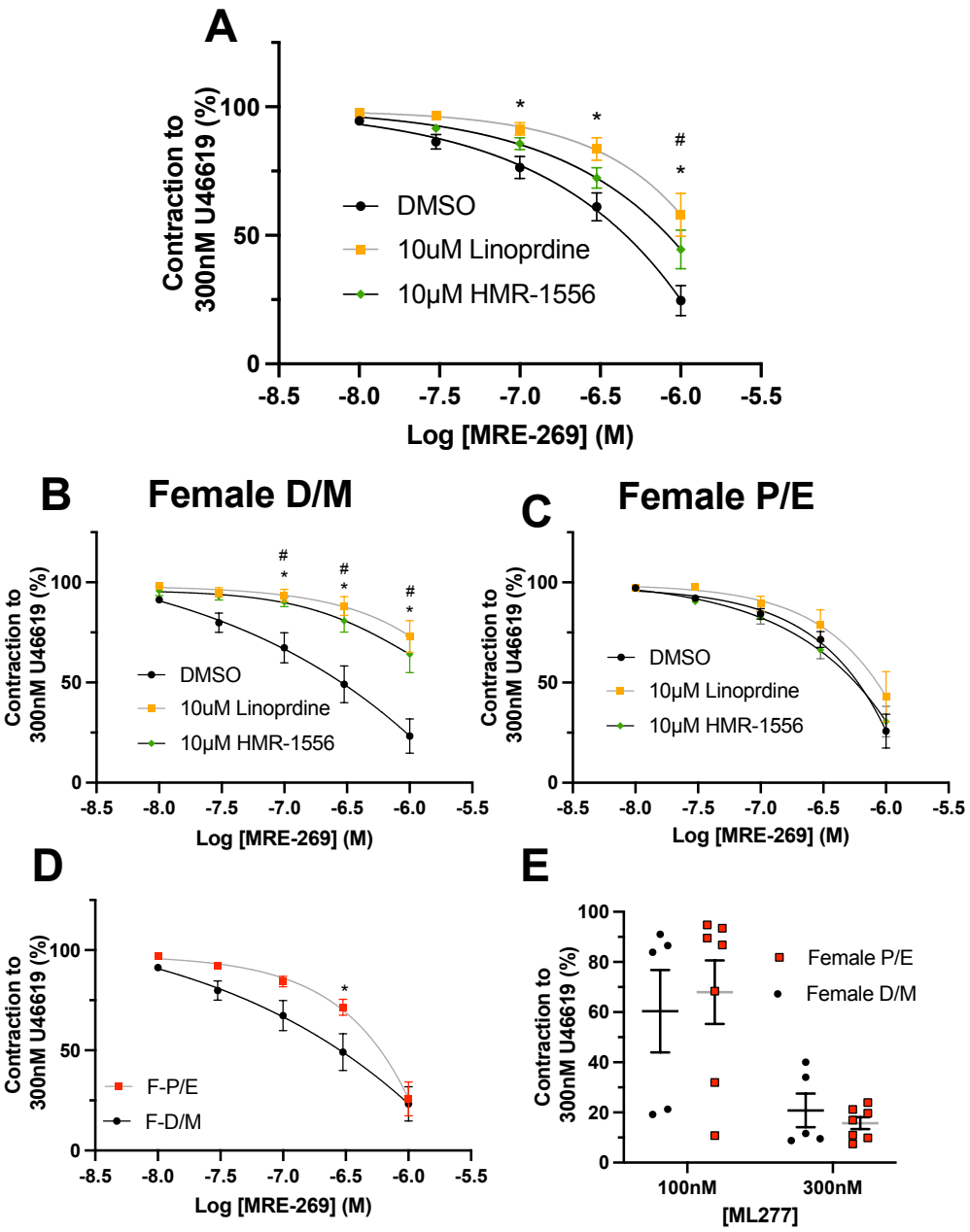

Figure 6.12: K_V7 channel inhibition attenuates MRE-269-mediated vasorelaxation in mesenteric arteries from Di-oestrus/Met-oestrus (F-D/M), but not Pro-oestrus/Oestrus (F-P/E) female rats.

Mean data for MRE-269-mediated vasorelaxation (0.01-1 µmol-L^{-1}) within mesenteric arteries pre-incubated in DMSO solvent control (A-C; black), 10 µmol-L^{-1} pan K_V7 channel inhibitor linopirdine (A-C; yellow) or 10 µmol-L^{-1} $K_V7.1$ specific inhibitor HMR-1556 (A-C; green) from female Wistar rats. Data is expressed as either all female (A), F-D/M (*n*=5-7, B) and F-P/E (*n*=6-8; C). MRE-269 (0.01-1 µmol-L^{-1}; D) and ML277 (0.01-0.03 µmol-L^{-1}) mediated relaxation in vessels from either F-P/E (red; *n*=6-8) or F-D/M (black; *n*=5-6). All values are expressed as mean ± SEM (A-E). A two-way statistical ANOVA with a post-hoc Dunnet's's (A-C) or Bonferroni (D,E) test was used to generate significant values (*=*P*<0.05). (*n*=) number of animals used.

6.4 Discussion

The present study is the first to highlight sex as a factor in the arterial response to prostacyclin mimetics. Whereby, application of Iloprost to pre-contacted mesenteric arteries from male rats produced bimodal responses, relaxation at low concentrations, followed by contraction at higher concentrations, whereas mesenteric arteries from female arteries presented with mono-phasic relaxation only. In arteries from both sexes the relaxant effect of Iloprost was enhanced by EP_3 receptor antagonist L-798,106 and was ablated by IP receptor antagonist CAY-10441. The data presented here demonstrates that Iloprost-mediated contractions in mesenteric arteries from male rats were more efficacious when compared to vessels from females, correlating with a higher level of *Ptger*$_3$ expression. See diagrammatic representation of prostanoid mimetic mediated responses in mesenteric arteries from male and female rats (Fig 6.13). Finally, the data shows that the selective IP receptor agonist MRE-269 was a potent relaxant of pre-contracted mesenteric arteries from both sexes. This relaxation was inhibited by both the pan-K_V7 blocker Linopirdine and $K_V7.1$ specific blocker HMR-1556 in arteries from males and F-D/M but strikingly, not F-P/E rats. These findings are the first observation of $K_V7.1$ as a downstream target of an endogenous vasoactive signalling cascade within the vasculature and reveal an Oestrus cycle dependent regulation of K_V7 channels.

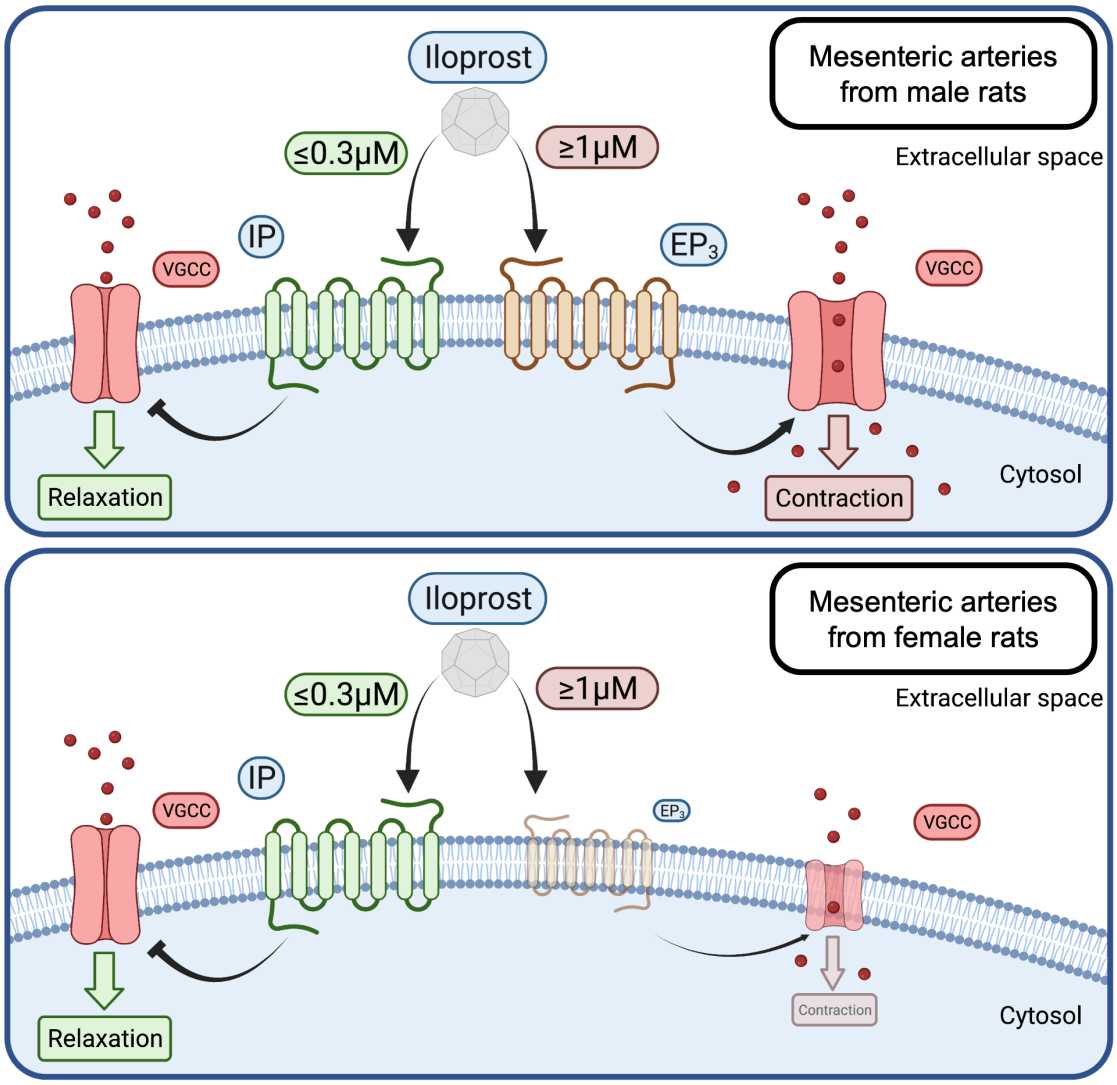

Figure 6.13: Graphical summary of Iloprost mediated vascular responses in mesenteric arteries from male and female Wistar rats.

Diagrammatic representation of Iloprost mediated activation of IP-prostanoid receptor (IP) at ≤0.3 μmol-L^{-1}, then activation of EP_3-prostanoid (EP_3) receptor at ≥1 μmol-L^{-1}, giving rise to relaxation and contraction respectively within arteries from male rats (upper). Comparable mono-phasic Iloprost mediated IP dependent relaxation within arteries from female rats (lower).

6.4.1 Iloprost evoked vasocontraction

Whilst principally regarded as a vasodilator, PGI_2 mediates both relaxation and contraction of smooth muscle (Moncada *et al.*, 1976; Dusting, Moncada and Vane, 1977; Liu *et al.*, 2017). PGI_2 has subsequently been identified as an endothelial derived contracting factor produced in response to acetylcholine within rat aorta (Gluais *et al.*, 2005), mesenteric (Liu *et al.*, 2017), iliac (Y. Zhang *et al.*, 2021) and renal arteries (Zhang

et al., 2021) in a process attributed to the activation of both EP and TP prostanoid receptors. Consistent with Liu *et al* (2017), we show that high concentrations of Iloprost evoked contractions that were ablated by the EP_3 receptor antagonist L-798,106. As Iloprost has a low affinity for TP receptors (Whittle *et al.*, 2012), TP receptor knockout has no effect on PGI_2 mediated contraction in mesenteric arteries (Li et al., 2017) and all vessels in this study were precontracted with U46619, a TP receptor agonist, TP receptors were not considered for the scope of this investigation. Additionally, EP_1 receptor agonists do not elicit contractions in male mesenteric arteries (Kobayashi *et al.*, 2011) and in agreement with previous findings (Kobayashi *et al.*, 2011), a reduced expression of *Ptger1* was observed when compared to *Ptger3*. Furthermore, Iloprost evokes negligible contractions in mesenteric arteries from female rats, which was associated with a lower expression level of *Ptger3* in these arteries.

6.4.2 K_V7.1 underpins IP receptor mediated relaxation

The results of this chapter show that relaxations of mesenteric arteries mediated by low concentrations of Iloprost were driven primarily through CAY-10441-sensitive IP receptor activation. We subsequently showed that CAY-10441-sensitive relaxations produced by the selective IP receptor agonist MRE-269 were impaired by the selective K_V7 channel blocker, linopirdine. As described in Chapter 1.5.4.2, pharmacological inhibition or molecular knockdown of K_V7.4/7.5 impairs relaxations to many different relaxants including isoprenaline, CGRP, adenosine (G_s linked), atrial natriuretic peptide (cGMP linked) and adipose derived relaxant factors in several arteries (Khanamiri *et al.*, 2013; Chadha *et al.*, 2014; Morales-Cano *et al.*, 2015; Stott, Barrese, *et al.*, 2015; Stott, Barrese and Greenwood, 2016; Gollasch, 2017; Byron and Brueggemann, 2018). Our data suggests that IP receptor activation in male mesenteric arteries is another GPCR that also relies on K_V7 channels for functional responses. In contrast to previous reports (Schubert *et al.*, 1997; Lombard *et al.*, 1999) IP-receptor mediated relaxation was not affected by K_{ATP} nor BK_{Ca} blockade, however, this discrepancy is potentially accounted

for by a difference in vascular model used as Lombard *et al* (1999), investigated rat middle cerebral artery and Schubert *et al* (1997), used rat tail artery.

Surprisingly, MRE-269 evoked CAY-10441-sensitive relaxations in mesenteric arteries from male rats were also inhibited considerably by two structurally dissimilar $K_V7.1$ specific inhibitors (HMR-1556, Chromanol 293B). In contrast to $K_V7.4$/ $K_V7.5$, the role of $K_V7.1$ within the vasculature remains enigmatic. Though $K_V7.1$ is expressed within VSMCs (Chadha, Zunke, Zhu, *et al.*, 2012; Tsvetkov *et al.*, 2017; Baldwin *et al.*, 2020) and $K_V7.1$ specific activators RL-1 and ML277 are effective relaxants of pre-contracted arterial tone (Chadha, Zunke, Davis, *et al.*, 2012; Baldwin *et al.*, 2020), $K_V7.1$ has not been identified as the downstream target of any endogenous vasoactive signalling cascades (Chadha *et al.*, 2014; Stott, Barrese, *et al.*, 2015; Stott, Barrese and Greenwood, 2016). Yet in the present study HMR-1556 produced as full an inhibition as linopirdine, which suggests $K_V7.1$, and not $K_V7.4/7.5$ contribute to MRE-269-mediated relaxations. Under the same conditions the mixed β-adrenoceptor agonist isoprenaline produced relaxations that were linopirdine but not HMR1556 sensitive. Moreover, a role for $K_V7.1$ in MRE-269-mediated relaxation was substantiated by morpholino-induced reduction in $K_V7.1$ protein levels. Whilst further work is required to validate these findings, to our knowledge our data is the first to describe an effect on vascular reactivity by $K_V7.1$ inhibition.

The results of this chapter also support the notion that IP-receptor mediated responses are cAMP-PKA mediated. In agreement with previous work done by our lab (Stott, Povstyan, *et al.*, 2015; Stott, Barrese and Greenwood, 2016; Stott *et al.*, 2018), relaxations that were sensitive to PKA, but not EPAC inhibition, were also sensitive to $G_{\beta\gamma}$ inhibition. The identification of $G_{\beta\gamma}$ contribution to IP-receptor mediated relaxation adds new complexity to GPCR derived vasoactive responses and gives credence to the

novel role for $G_{\beta\gamma}$-PKA synergism in the functional relationship between GPCRs and K_V7s.

To date, comparably little is known as to how K_V7 channels operate within the female, however, K_V7 has been shown to regulate both human and murine myometrium (McCallum, Greenwood and Tribe, 2009) and human chorionic plate artery (Mills *et al.*, 2015) contractility. Tissues where prostanoids are known key regulators of smooth muscle. When separated into oestrus cycle stages, arteries from F-D/M expressed sensitivities to HMR-1556 and Linopirdine equivalent to the male, whereas arteries from F-P/E were entirely insensitive to either, however, the response to the $K_V7.1$ activator-ML277 was identical in arteries from female rats in D/M or P/E. As the functional output of pharmacological activation of the channel remains the same, the data indicates an oestrus cycle dependent impairment of $K_V7.1$ channel coupling to IP-receptor mediated relaxation. Oestrus cycle dependent regulation of vascular reactivity is a known, but incompletely understood phenomenon (Jaimes *et al.*, 2019) largely attributed to endogenous sex-hormones, primarily, E2. As discussed in Chapter 1 and 4, E2 negatively regulates $K_V7.1$ in distal colic crypt cells and cardiac myocytes (Waldegger *et al.*, 1996; O'Mahony *et al.*, 2007; Alzamora *et al.*, 2011; Rapetti-Mauss *et al.*, 2013). As previous work and present findings demonstrates that within the Wistar rat, E2 peaks within Pro-oestrus/Oestrus rats followed by comparably diminished levels in, met-oestrus and di-oestrus (Nilsson *et al.*, 2015), our current hypothesis proposes that during Pro-oestrus, Oestradiol levels rise, impairing $K_V7.1$ coupling to IP-receptor during F-P/E, thus reducing the potency of MRE-269-mediated relaxation and its HMR-1556 / Linopirdine sensitivity, which does not recover until F-D/M. The mechanism coupling E2 to $K_V7.1$ remains to be described, however we would argue that it differs from previously generated work (O'Mahony *et al.*, 2007, 2009; Alzamora *et al.*, 2011; Rapetti-Mauss *et al.*, 2013), as $K_V7.1$ function appears to be preserved in these tissues.

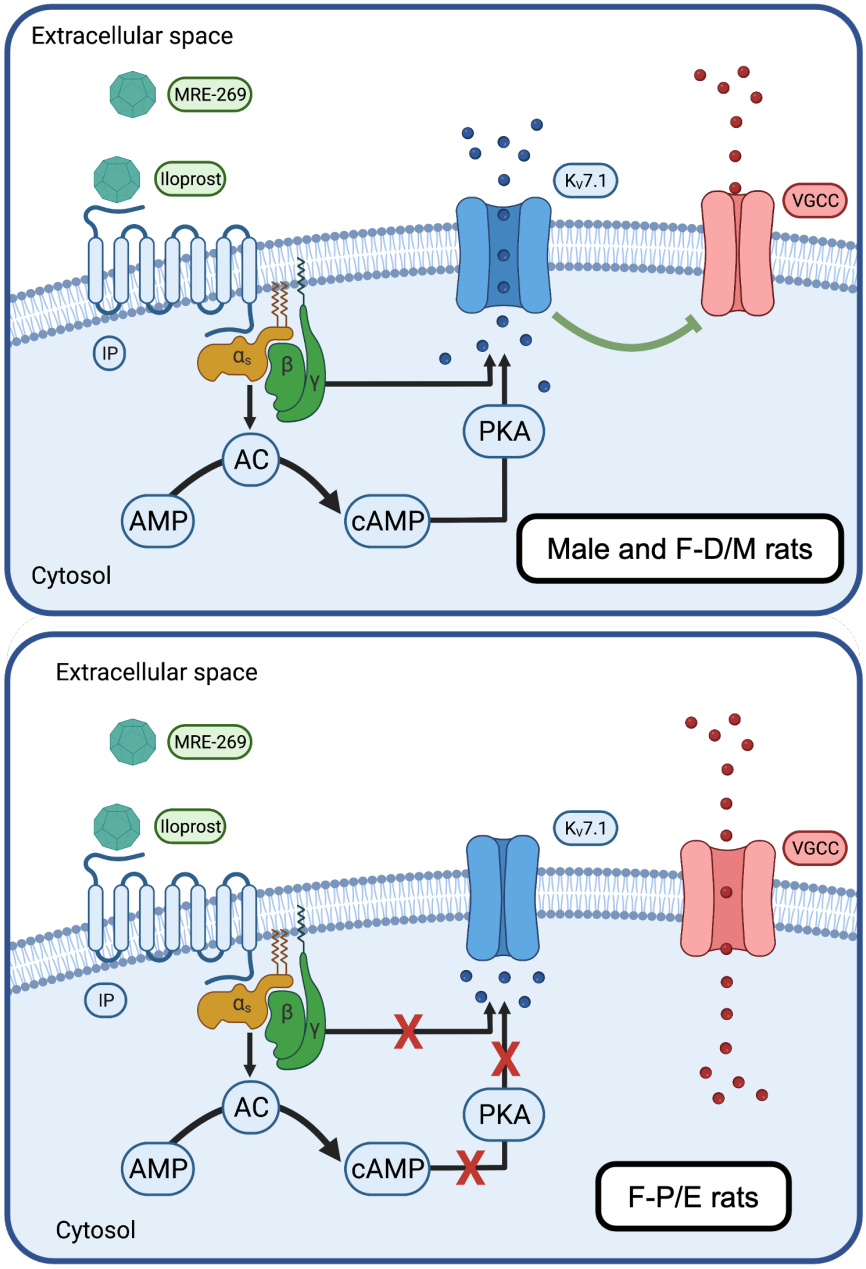

Figure 6.15: Graphical summary of MRE-269 mediated vascular responses in mesenteric arteries from male and female Wistar rats.

Diagrammatic representation of MRE-269 mediated activation of IP-prostanoid receptor (IP), which in turn activates $K_V7.1$ via adenylate cyclase (AC), cAMP-protein kinase A (PKA) and $G_{\beta\gamma}$ subunits within arteries from male and female di-oestrus/met-oestrus (F-D/M) rats (upper). Comparable decoupling of IP mediated signalling to $K_V7.1$ in arteries from female pro-oestrus/oestrus (F-P/E) rats (lower).

6.4.3 Perspectives

Chronic aldosterone treatment in male Wistar-Kyoto rats induces hypertension through endothelial dysfunction attributed to upregulated COX-2 production of PGI_2 (Blanco-Rivero *et al.*, 2005). Diminished EP_3 mediated contraction/expression in female rats may

potentially negate the pathophysiological levels of PGI_2 production observed by Blanco-Rivero *et al* (2005), contributing to the known cardioprotective phenotype expressed by females, though further work is required to validate this hypothesis.

As above, PGI_2 has a short half-life. In using prostacyclin mimetics at concentrations of ≥1 μmol-L^{-1}, the physiological relevance of the signalling cascades described within this chapter could be questioned, however, Selexipag and Iloprost are currently prescribed to myriads of patients with PAH. As such, deliniating the underlying components of the systemic vascular effects of prostacyclin mimeteics is of key importance from a clinical perspective, warranting further investigation.

6.4.4 Limitations

As described above, the results of this chapter provide strong evidence for the contribution of $K_V7.1$ to IP-receptor mediated responses via reductive pharmacological and molecular approaches. This study is limited however, but a lack of direct IP-receptor mediated enhancement of $K_V7.1$ sensitive currents within native mesenteric artery VSMCs. Single cell electrophysiological recordings will form the basis for future investigations.

6.4.5 Conclusion

The data of the present study demonstrates a remarkable sexual dimorphism in the vascular response to synthetic prostacyclin analogues and highlights the importance of considering sex as a determinant in vascular physiology. Strikingly, the potent relaxations to the selective IP receptor agonist MRE-269 were sensitive to the $K_V7.1$-specific blocker HMR1556 in mesenteric arteries from males and females in F-D/M but not at all in F-P/E, a novel demonstration of both a functional role for $K_V7.1$ and cyclical changes in K_V7 channel activity across the oestrus cycle.

Chapter 7: K_V7 channel expression and function within endothelial cells from rat mesenteric arteries

7.1 Introduction

Like Chapter 6, the approach of this study differs from previous chapters. The aim of this chapter was to determine the function of K_V7 channels within the endothelium of rat mesenteric arteries. ECs form the inner layer of blood vessels and constitute a paracrine signalling platform which regulates VSMC contractility, vascular resistance and ultimately blood flow through the release of NO, PGI_2, epoxyeicosatrienoic acid, C-type natriuretic peptide, and generation and spread of EDH amongst others (McGuire, Ding and Triggle, 2001; Ahluwalia and Hobbs, 2005; Garland and Dora, 2017). Myoendothelial projections within fenestrations of the internal elastic lamina (IEL) facilitate the presence gap junctions at roughly ~50% of such sites in adult rat 1^{st}-3^{rd} order 'large' mesenteric arteries (Sandow *et al.*, 2009). Myoendothelial gap junctions within IELs permits heterocellular electrochemical coupling via connexin proteins (Sandow et al,, 2012). These sites enable the transfer of EC-derived signals via the flow of both small molecules <~1 kDa and current between the cells. In endothelium-dependent relaxation of rat mesenteric arteries, a fundamental role for SK_{Ca} and IK_{Ca} (Sandow et al, 2006, Dora et al., 2008; Chapter 1.4.1.2), TRPC3 (Senadheera *et al.*, 2012), $K_{IR}2.x$ (Goto et al, 2004, Chapter 1.4.2.1), and IP_3R (Fukao *et al*., 1997) has been demonstrated.

Despite the contribution of K_V7 channels to baseline arterial diameter and receptor-mediated vasodilatations, their expression and function within ECs remains unknown.

Identification of K_V7 expression in ECs would open up a new layer of control by these channels and is a necessary requisite for understanding the role of these channels in vascular health and disease. This chapter aims to ascertain whether rat mesenteric ECs express K_V7 channels, what their functional implications may be and to identify any potential sexual dimorphisms in endothelial K_V7 activity. The results of this chapter reveal expression of K_V7 channels in rat mesenteric artery ECs and a contribution of these channels to both K_V7 activator-mediated relaxation via a potential functional interaction with $K_{IR}2$ channels and eNOS-dependent axis of CCh-mediated vasorelaxation.

7.2 Materials and methods

7.2.1 Reverse transcription quantitative polymerase chain reaction

2nd and 3rd order mesenteric artery segments were enzymatically digested to obtain either freshly isolated ECs (Greenberg *et al.*, 2016) or VSMCs. Vessels were washed in Hanks' Balanced Salt Solution (HBSS; ThermoFisher Scientific, GIBCO, 14170-088) containing 50 μmol-L^{-1} $CaCl_2$ for 5 min at 37°C, the media was then replaced in HBSS containing 1 mg/mL collagenase IA (Sigma Aldrich, C9891, UK) for 15 min at 37°C. Vessels were washed in HBSS containing 50 μmol-L^{-1} $CaCl_2$ for 10 min at 37°C. The supernatant was removed, and the vessels suspended in fresh HBSS containing 75 μmol-L^{-1} $CaCl_2$. For RT-qPCR, ECs were dissociated using a wide-bore smooth-tipped pipette and identified under the microscope (x10) as sheets of cells independent from the vessel which were harvested and stored separately from the residual VSMCs. Isolated VSMCs and ECs were then homogenised, and whole transcriptome was extracted, and reverse transcribed as described in Chapter 2.4.1.

7.2.2 Immunocytochemistry

For immunodetection of K_V7s within the endothelium, freshly dispersed ECs (as above), together with residual VSMCs were loaded onto 13mm glass coverslips and left to attach for 1hr. Cells were then fixed in 4% paraformaldehyde (Sigma-Aldrich, UK) in PBS for 15 min at RT as previously described (Barrese et al., 2018). Cells were treated with 0.1 mol-L^{-1} glycine for 5 min and incubated for 1 hr with blocking solution (PBS-0.1% Triton X-100, 10% bovine serum albumin) at RT. Cells were then incubated overnight at 4°C with primary antibodies including the following: anti-PECAM-1 for ECs, anti-α-actin for VSMCs and anti-K_V7.1, K_V7.4 or K_V7.5 channel for ECs/VSMCs (Table 2.3; alternate K_V7.4 antibody 'Mouse anti-Kv7.4, NeuroMab, 75-082' was used for immunocytochemistry) diluted in blocking solution. The following morning, cells were washed for 20 min with PBS, incubated for 1 hr at RT with the secondary conjugated antibodies diluted in blocking solution. Excess secondary antibody was removed by

washing with PBS. Coverslips were then mounted onto glass slides, placed in mounting media containing DAPI for nuclear counterstaining. Using triple staining on cells present mounted on the same coverslips, ECs and VSMC were differentiated via the following: ECs were positive for anti PECAM-1 and negative for anti-α-actin, while VSMC was positive for anti-α-actin and negative for anti-PECAM-1. Cells were analysed using a Zeiss LSM 510 Meta argon/krypton laser scanning confocal microscope (Image Resource Facility, St George's University, London).

7.2.3 Immunohistochemistry

Immunohistochemistry of *en face* 2nd order mesenteric arteries were performed by Dr Sandow at the University of the Sunshine Coase, Australia. The following methods and materials were provided by Dr Sandow. Animals were anaesthetized with sodium pentathol (intraperitoneal, 100 mg/kg) and perfusion fixed (Sandow et al., 2004) in 2% paraformaldehyde in 0.1 mol-L^{-1} PBS. 3rd to 4th order mesenteric artery segments were dissected, opened laterally and pinned as a sheet to a Sylgard dish. Segments were washed in PBS (3 x 5 min), incubated in blocking buffer (PBS with 1% BSA and 0.2% Triton) at RT for 2 hrs and then overnight with primary antibodies for K_V7.4 and K_V7.5 (Table 2.3; alternate K_V7.4 antibody 'Rabbit anti-K_V7.4, Abcam ab65797' was used for immunohistochemistry) in blocking buffer at 4°C, washed again (3 x 5 min with gentle agitation), and incubated in secondary antibody (Table 2.4) in PBS with 0.1% Triton in PBS for 2 hrs at RT. Tissue was mounted on slides in anti-fade media containing propidium iodide (PI; P4170, Sigma) or DAPI and imaged with uniform confocal settings. Incubation of tissue with secondary only was used as a 'zero' setting for confocal imaging. Controls involved substitution of primary with isotype control, with concentration (where provided by manufacturer) matched, or 10-fold higher than the respective antibody of interest (Table 1.2). Working Ab dilutions were prepared in accordance with previous work (Chadha et al., 2012; Jepps et al, 2009). Confocal image stacks were collected at 0.2 µm intervals. The optimal rinsing protocol was determined by incubating in secondary only; and rinsing after successive 5 min incubations until fluorescence was

reduced to background. Note that if this was not done secondary alone was specifically and highly localized to IEL hole sites; as potential false positives at such sites; suggesting that such sites have an affinity for IgG-secondary label alone.

7.3 Results

7.3.1 Identification of K_V7 channels within mesenteric artery ECs

Initial investigation sought to identify *Kcnq/*K_V7 transcript and protein within mesenteric artery ECs. Transcript levels for *Kcnq1-5*, endothelial and vascular smooth muscle markers were determined in lysates of isolated populations of either predominantly mesenteric artery VSMC or ECs. Both ECs and VSMCs expressed *Kcnq4* > *Kcnq5* > *Kcnq1* with no expression of *Kcnq2/3* (Fig 7.1.A) similar to previous studies (Ng et al., 2011; Ohya et al, 2003; Yeung et al., 2007), however, a comparative reduction in the relative abundance of *Kcnq1* was observed in mesenteric artery ECs when compared to VSMCs (Fig 7.1.A). Cell isolation efficiency is demonstrated by a reduction in EC marker *Pecam* within VSMCs cell lysates when compared to ECs (P<0.05) and a reduction in VSMCs marker *Acta2* in EC cell lysates when compared to VSMCs (P0.065, Fig 7.1.B,C).

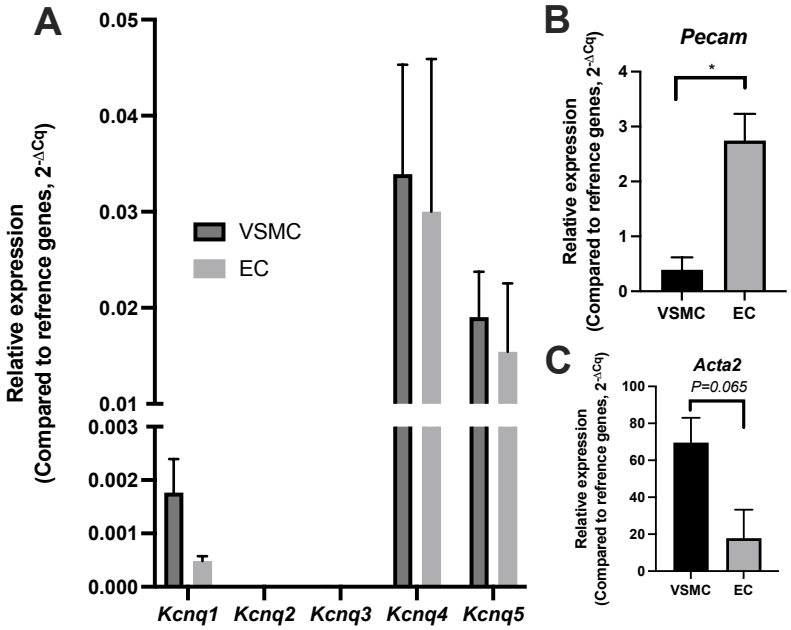

Figure 7.1: Expression profile of *Kcnq* genes within isolated rat mesenteric vascular smooth muscle cells (VSMCs) and endothelial cells (ECs).

RT-qPCR analysis of relative expression of *Kcnq1-5* in isolated VSMCs and ECs (A). Cell specific markers *Acta2* and *Pecam,* for VSMCs and ECs respectively, were measured to determine sample purity (B,C). Values expressed as mean ± SEM of ($2^{-\Delta Cq}$) of ΔCq values generated from appropriate housekeeper genes (n = 3). An unpaired T-test was used to generate significance values (*=P≤0.05). (n=) number of animals used.

K_V7.1, K_V7.4 and K_V7.5 were detected in isolated ECs by immunodetection (Fig 7.2A,C,E). K_V7.4 had a punctate distribution in isolated ECs (Fig 7.2.C) whereas K_V7.5 label appeared to be predominantly cytoplasmic with some diffuse label around the nucleus (Fig 7.2.E). Similar to previous reports (Zhong *et al.*, 2010; Oliveras *et al.*, 2014; Mills *et al.*, 2015; Morales-Cano *et al.*, 2015, Barrese et al., 2018) K_V7.1, K_V7.4 and K_V7.5 were also identified in isolated mesenteric artery VSMCs (Fig 2B,D,F). Kv7.1 staining in ECs was negligible compared to VMSCs (Fig 2.A,B). Importantly, as ion channel expression can alter in isolated cells, K_V7.4 and K_V7.5 were also detected in both ECs and VSMCs in *en face* whole-mount arteries (Fig 7.3.A,B,E,F). Notably, both K_V7.4 and 7.5 were expressed at a proportion of IEL hole sites at an apparently higher level than the associated EC membrane label (Fig 7.3.C,D,G,H). These studies identify K_V7.4 and K_V7.5 in ECs as well as smooth muscle cells.

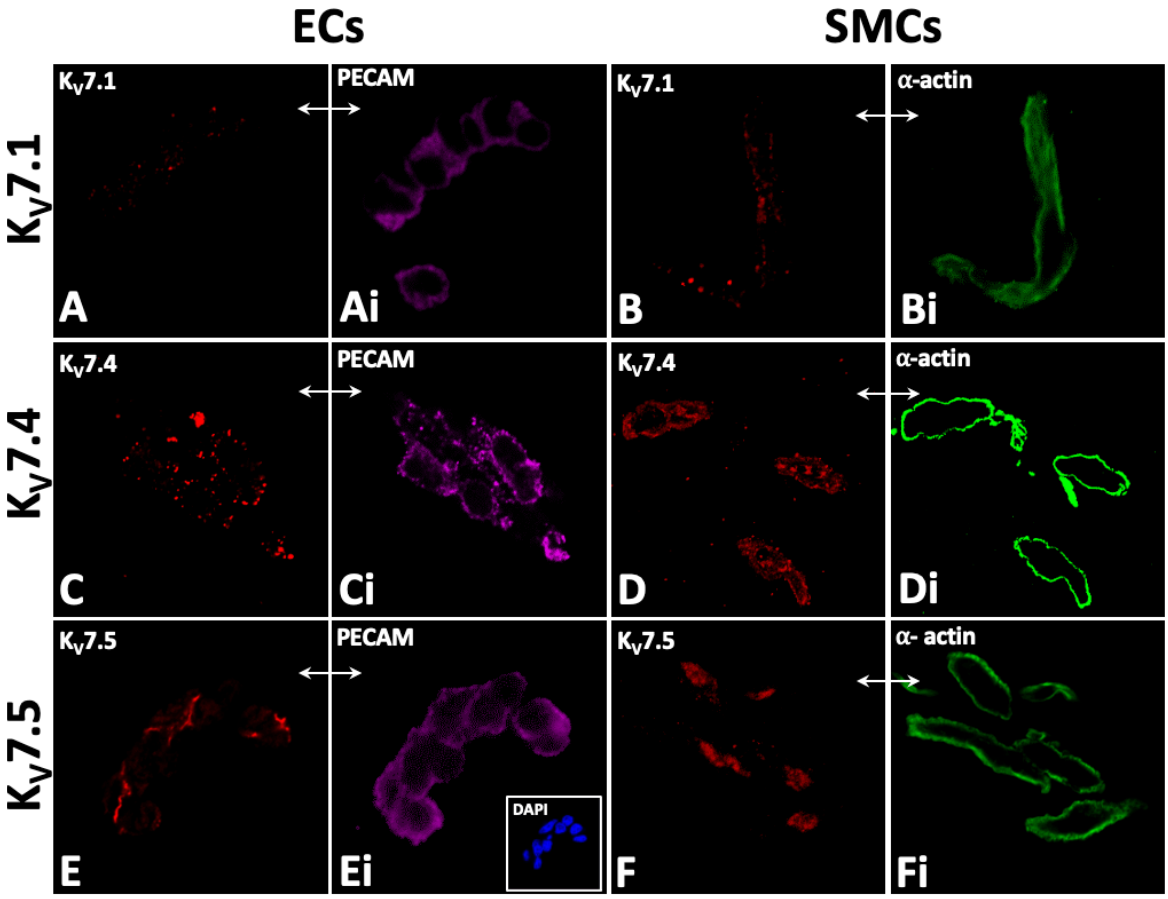

Figure 7.2: Immunocytochemistry demonstrates K_V7.1, K_V7.4 and 7$_V$.5 localization in rat mesenteric artery isolated endothelial (EC) and smooth muscle cells (SMC).

Punctate labelling for Kv7.1, Kv7.4 and 7.5 was present in isolated EC and SMCs (A,C and B,D, respectively). PECAM and smooth muscle α-actin were used as markers for isolated endothelial and smooth muscle cells, respectively (Ai,Ci,Ei and Bi,Di,Fi, respectively; e.g. comparative-same cells, double arrows, A-Fi). 4′,6-diamidino-2-phenylindole (DAPI; e.g. inset, C) were used as nuclear markers to verify cell patency. *n* = 4-6, representative of different source tissue (A-Fi). Double arrows from insets indicate same panel as main, but to different marker.

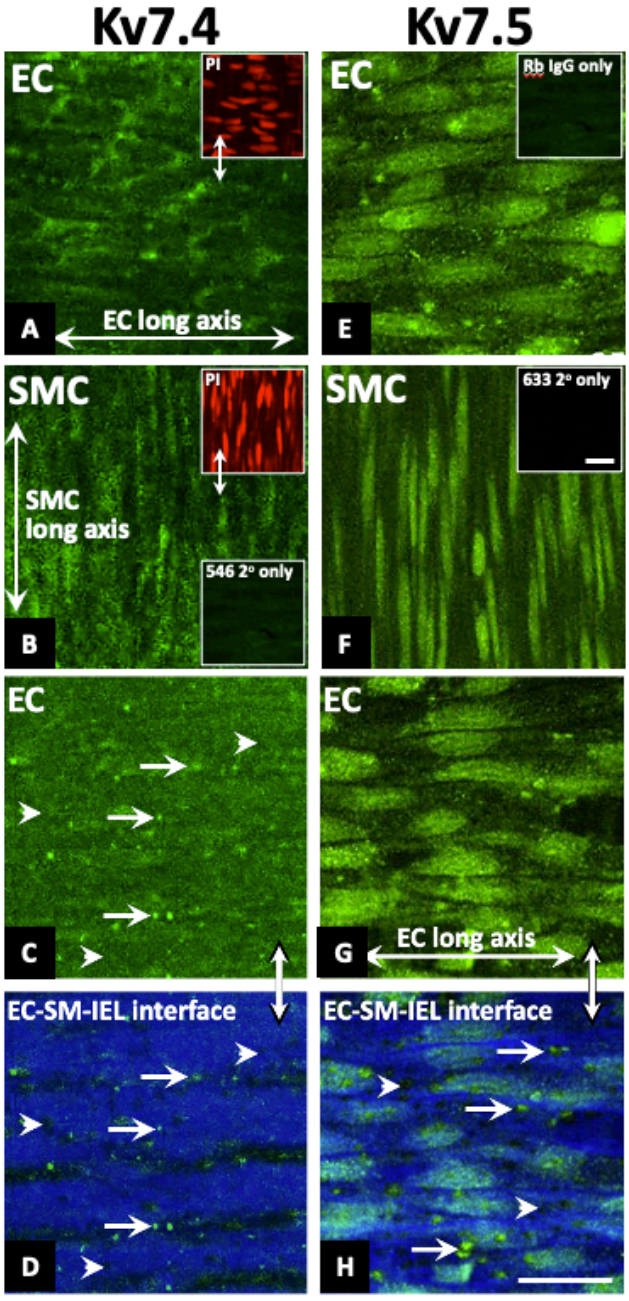

Figure 7.3: Immunohistochemistry demonstrates Kv7.4 and 7.5 localization in rat mesenteric artery endothelium (EC) and smooth muscle cells (SMCs) with a focus on internal elastic lamina (IEL) hole sites in whole mount tissue.

Whole mounts of confocal stacks through the EC and SMC of Kv7.4 (A,B respectively) and Kv7.5 (E,F respectively). Confocal image stacks through the luminal EC to SM border (C,G) show diffuse/punctate Kv7.4/K_V7.5 across the cell membrane with some punctate higher-level fluorescence at localized sites (e.g. full arrows; C). When single images were taken at the EC-IEL-SM interface (D,H), punctate higher-level fluorescence densities were present (e.g. D,H arrows; H, higher magnification inset) at *a proportion* of IEL hole sites (e.g. D,H arrowheads). Propidium iodide (PI; e.g. upper left inset, A,B) were used as nuclear markers to verify cell and layer patency. Double arrows indicate same site, but at different focal planes (C,D; G,H), and location of inset (D). Bar, 25 μm. Image provided by Dr Sandow.

7.3.2 The impact of the endothelium on K_V7 channel activator-mediated relaxation

7.3.2.1 ECs modulate K_V7.2-5 channel activator-mediated relaxation in a gap-junction sensitive manner

To determine if K_V7 channels have a functional role in mesenteric arteries ECs, vasorelaxation to K_V7 channel activators was compared between endothelium intact and denuded vessels. Endothelial removal for the following experiments was determined by addition of 10 μmol-L^{-1} CCh to pre-constricted arterial tone (10 μmol-L^{-1} MO). Vessels in the following investigations categorised as EC+ displayed ≥90% relaxation in response to CCh, whereas those categorised as EC- displayed ≤10% relaxation in response to 10 μmol-L^{-1} CCh (Fig 7.4.A). Endothelium denudation by mechanical abrasion has no impact on the peak contraction produced by 300 nmol-L^{-1} U46619 (Fig 7.4.B), but significantly attenuated the potency of S-1-mediated vasorelaxation increasing EC_{50} from 2±0.2 μmol-L^{-1} to 3±0.7 μmol-L^{-1} (Fig 7.4.C,D). S-1-mediated relaxation was also impaired via 100 μmol-L^{-1} of the non-selective gap junction inhibitor carbenoxolone (Tare *et al*., 2002; Fig 7.4.E). Similarly, ML213-mediated relaxation was also impaired by endothelial removal and by carbenoxolone in a fashion analogous to S-1 (Fig 7.4.F,G). Carbenoxolone pre-incaution had no effect on ML213-mediated relaxation of pre-contracted arterial tone in vessels that had been denuded of the endothelium (Fig 7.5). In contrast, the linopirdine-sensitive relaxation produced by the Kv7.1 activator, ML277 was not affected by endothelial removal (Fig 7.6). The aggregated findings indicate a contribution of endothelial K_V7.4/K_V7.5 channels to S-1/ML213-mediated relaxation in a gap-junction sensitive manner.

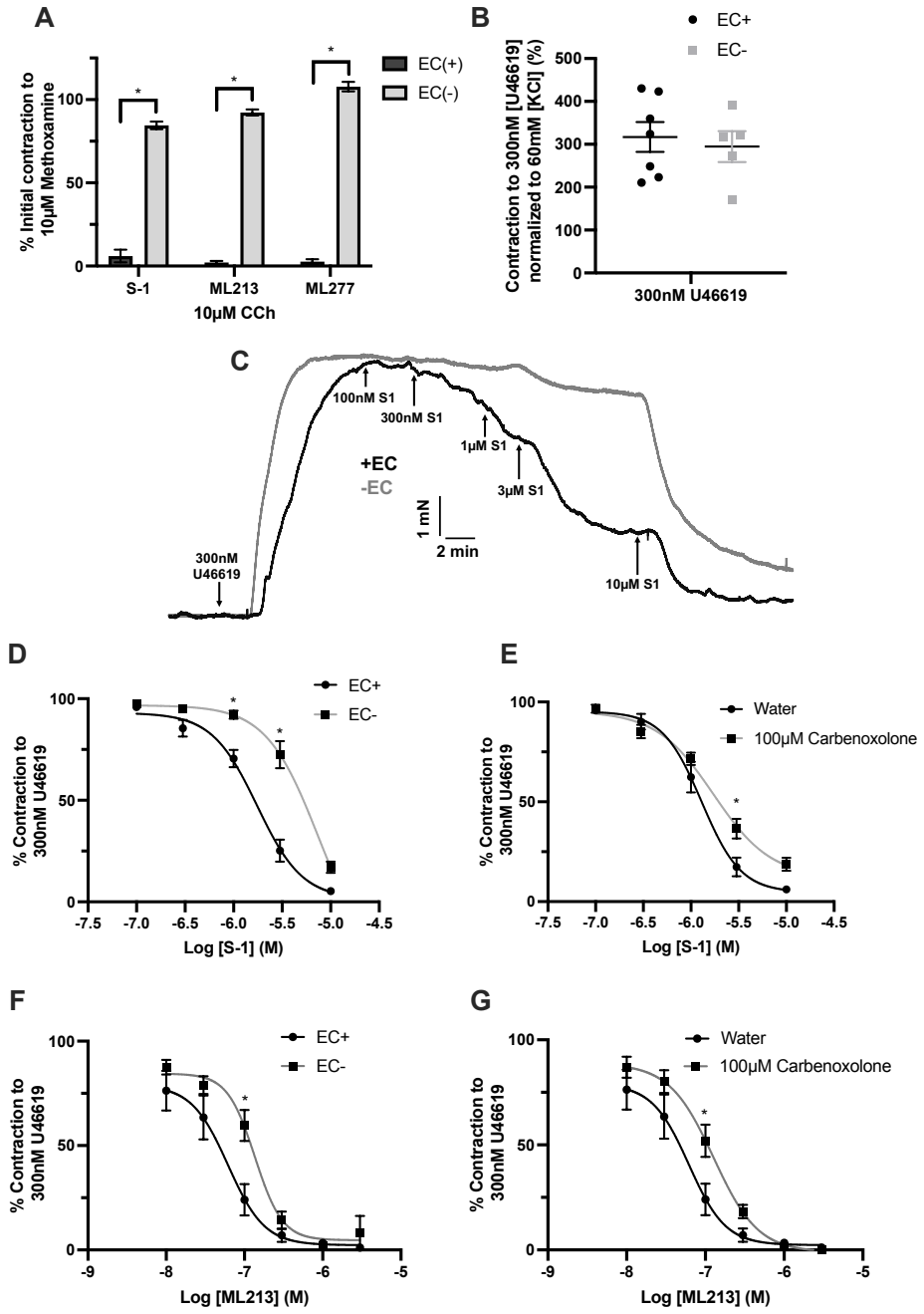

Figure 7.4: K_V7.2-5 channel activator-mediated vasorelaxation was significantly attenuated by EC removal.

Removal of ECs ablated vasorelaxation in response to 10 µmol-L^{-1} CCh following pre-constriction with 10 µmol-L^{-1} MO (A,D-F). Removal of ECs (grey) has no effect on vasoconstriction to U46619 (300 nmol-L^{-1}) when normalized to vasoconstriction to KCl (60 mmol-L^{-1}; *n* = 5-7; *N* = 15-21; B). Representative trace of EC S-1-mediated vasorelaxation in EC(-) denuded vessels (grey) vs EC(+) vessels (black; C). Mean data for S-1 (*n*=5-7; D,E) and ML213 (*n*=5-7; F,G) mediated vasorelaxation in the presence and absence of EC removal and 100 µmol-L^{-1} carbenoxolone. All values are expressed as mean +SEM (A-G). A 2-way statistical ANOVA with a post-hoc Bonferroni test was used to generate significance values. Statistical significance is defined as **P*<0.05 (A-G). (*n*=) number of animals used, (*N*=) number of segments used.

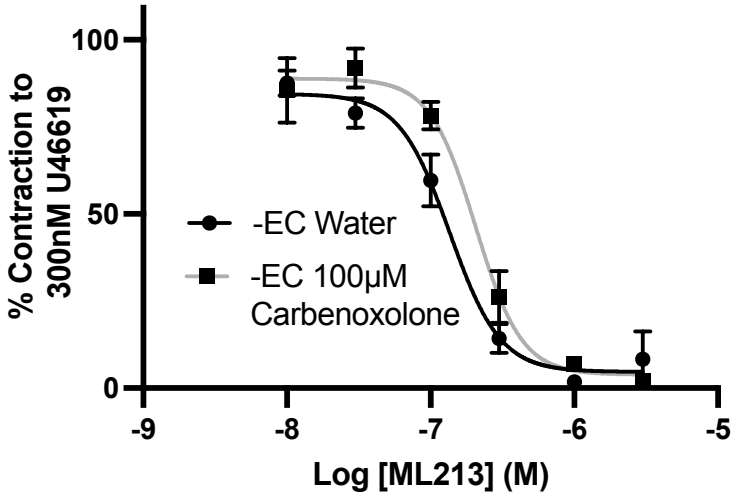

Figure 7.5: Carbenoxolone has no effect on ML213-mediated relaxation in the absence of endothelial cells (ECs).

Mean data for and ML213-mediated vasorelaxation in vessels denuded ECs pre-incubated in water (black; *n*=5) or 100 μmolL^{-1} carbenoxolone (grey; *n*=4). All values are expressed as mean +SEM (A-G). A 2-way statistical ANOVA with a post-hoc Bonferroni test was used to generate significance values. Statistical significance is defined as **P*<0.05 (A-G). (*n*=) number of animals used.

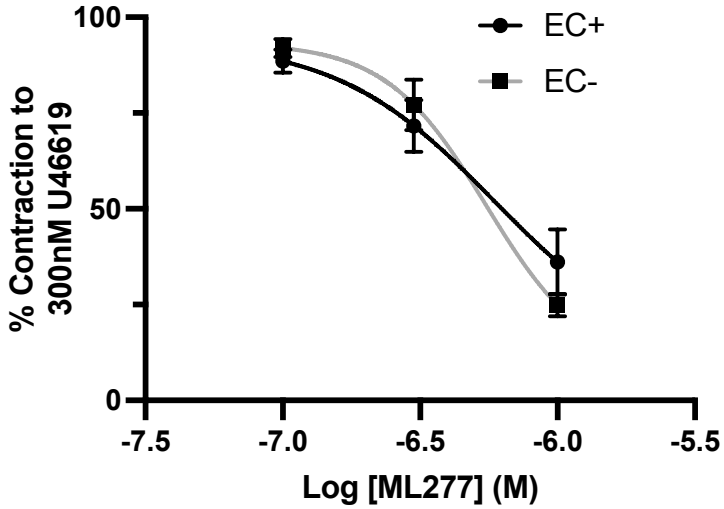

Figure 7.6: K_V7.1 channel activator-mediated vasorelaxation was unaffected by endothelial cell (EC) removal.

Mean data for ML2177 mediated vasorelaxation in the presence (black; *n*=5) and absence (grey; *n*=5) of EC removal. All values are expressed as mean +SEM (A-G). A 2-way statistical ANOVA with a post-hoc Bonferroni test was used to generate significance values. (*n*=) number of animals used.

7.3.2.2 Oestrus cycle depend on modulation of EC contribution to K_V7 channel activator-mediated relaxation

The contribution of ECs to K_V7 channel activator mediated relaxation was also screened within arteries from female Wistars. Similarly, to previous chapters, females were split into F-D/M and F-P/E. Removal of the endothelium (*n*=4; Fig 7.7.A) and pre-incubating vessels in the putative gap-junction inhibitor carbenoxolone (100 µmol-L^{-1}; *n*=4; Fig 7.7.B) significantly attenuated K_V7.2-5 channel activator ML213-mediated relaxation in arteries from F-D/M in a fashion analogous to male arteries. Comparably, neither removing the endothelium nor carbenoxolone impaired ML213-mediated relaxation in arteries from F-P/E when compared to solvent control (Fig 7.7.B). Furthermore, similarly to males, carbenoxolone had no effect in ML213-mediated relaxation in arteries from F-D/M (*n*=3-4) nor F-P/E (*n*=4) denuded of the endothelium (Fig 7.8). These findings indicate an Oestrus cycle dependent contribution of ECs to K_V7 channel activator-mediated relaxation within the female Wistar.

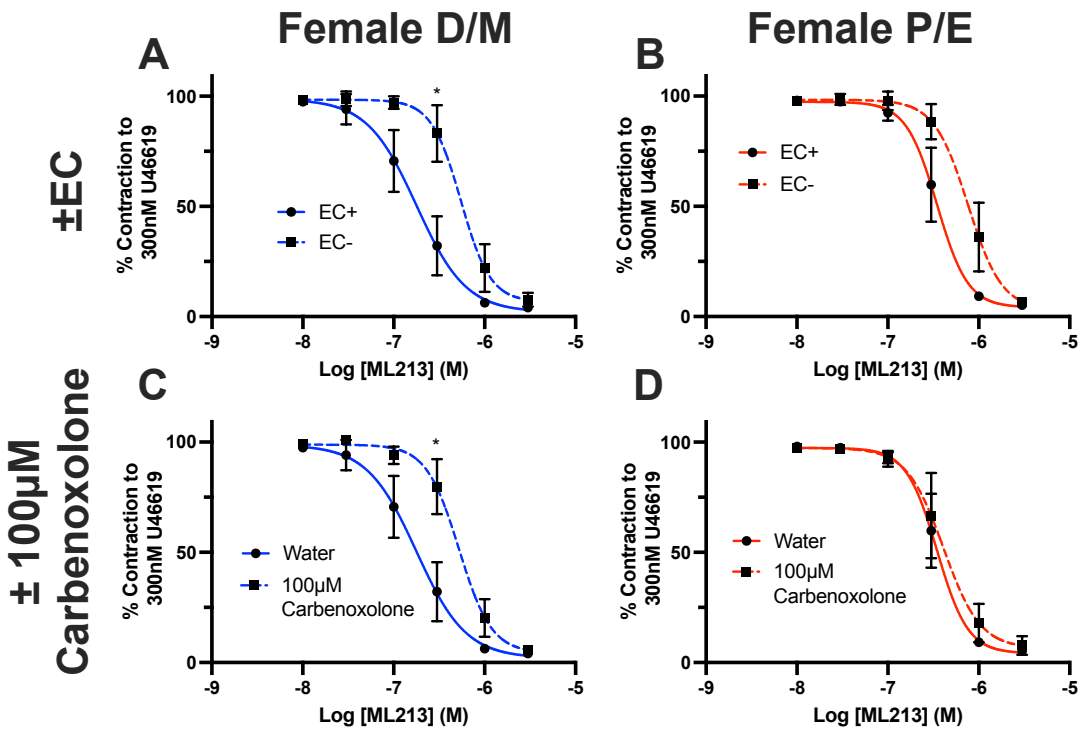

Figure 7.7: K_V7.2-5 channel activator-mediated vasorelaxation was attenuated by endothelial cell (EC) removal in females during D-Oestrus and Met-oestrus (F-D/M), but not females during Pro-Oestrus and Oestrus (F-P/E).

Mean data for ML213-mediated vasorelaxation in vessels from F-D/M (blue, A,C; *n*=4) and F-P/E (red, B,D; *n*=4) in the presence and absence of ECs (A,B) and 100 µmol-L^{-1} carbenoxolone (C,D) in. All values are expressed as mean +SEM (A-G). A 2-way statistical ANOVA with a post-hoc Bonferroni test was used to generate significance values. Statistical significance is defined as **P*<0.05 (A-G). (*n*=) number of animals used.

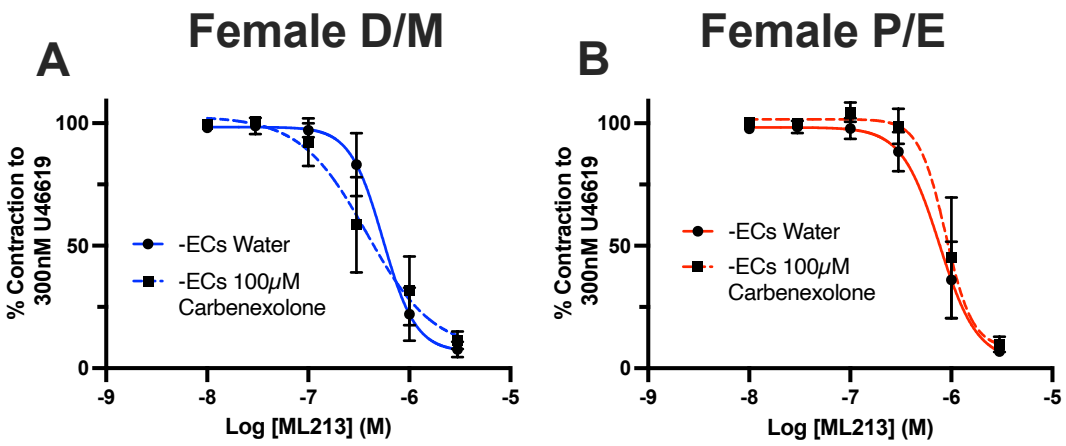

Figure 7.8: K_V7.2-5 channel activator-mediated vasorelaxation was unaffected by carbenoxolone in the absence of endothelial cells (ECs) in females during D-Oestrus and Met-oestrus (F-D/M) and females during Pro-Oestrus and Oestrus (F-P/E).

Mean data for ML213-mediated vasorelaxation in vessels from F-D/M (blue, A; *n*=3-4) and F-P/E (red, B; *n*=4) in denuded of ECs in the presence and absence of 100 μmol-L^{-1} carbenoxolone (A,B) in. A 2-way statistical ANOVA with a post-hoc Bonferroni test was used to generate significance values. Statistical significance is defined as **P*<0.05 (A-G). (*n*=) number of animals used.

7.3.3 EC K_{IR} channels modulate K_V7.2-5 activator sensitivity

Murine endothelial *Kcnj2*-encoded $K_{IR}2.1$ channels have been identified as 'signal boosters' that enhance EC-derived relaxation (Sonkusare *et al.*, 2016; Chapter 1.4.2.1). Comparatively, the current literature regarding rat mesenteric $K_{IR}2$ channels is limited. In brief, rat mesenteric artery endothelium expresses $K_{IR}2.1$ (Dora et al., 2008), inwardly rectifying Ba^{2+} sensitive channels are restricted to the endothelial layer (Crane et al., 2003) and K_{IR} channels contribute to acetylcholine-mediated responses (Goto *et al.*, 2004). We propose that like mice, rat mesenteric ECs express functional $K_{IR}2$ channels that propagate EC signals in a similar process. Therefore, a series of studies was performed to investigate the effect of two characterized $K_{IR}2$ blockers, $BaCl_2$ (Hagiwara et al,. 1978) and ML133 (Wang et al., 2011) on K_V7 activator-mediated vasorelaxation.

In arteries with a functional endothelium, $K_{IR}2$ blockers $BaCl_2$ (100 μmol-L^{-1}) and ML133 (20 μmol-L^{-1}) significantly impaired relaxations produced by S-1 and ML213 when compared to DMSO solvent control (Fig 7.9.A-D). In contrast, no attenuation of the response to ML277 was observed, consistent with the studies on EC removal. Furthermore, in arteries where the endothelium had been removed neither ML133 nor $BaCl_2$ had any effect on ML213-mediated relaxations (Fig 7.10.A,B).

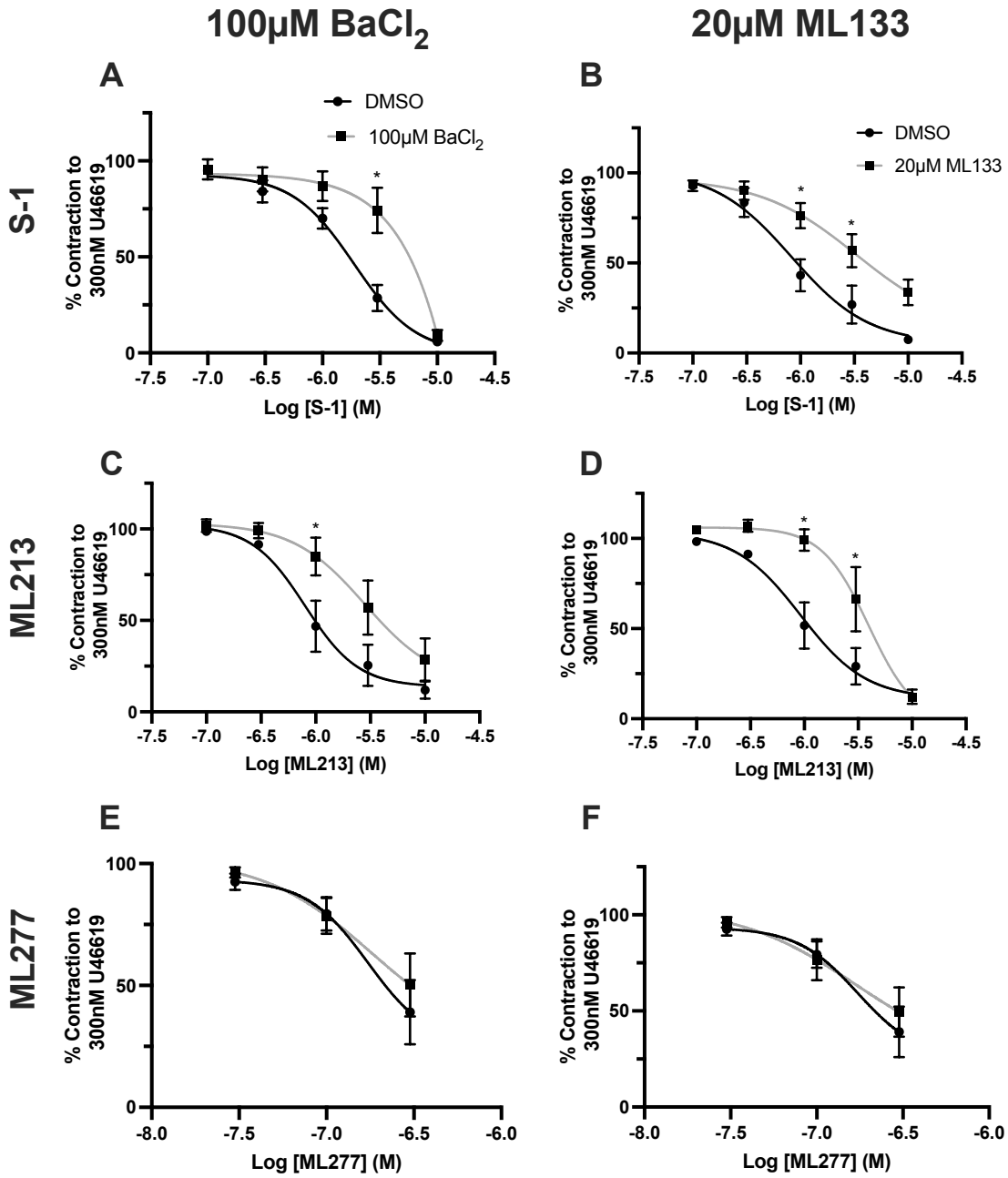

Figure 7.9: K_V7.2-5 channel activator-mediated vasorelaxation was attenuated by two structurally different K_{IR} channel blockers, $BaCl_2$ and ML133.

Mean data for K_V7.2-5 channel activator S-1 (A,B) and ML213 (C,D) and K_V7.1 (E,F) channel activator ML277 mediated relaxation in vessels pre-incubated with the K_{IR}2 channel inhibitor $BaCl_2$ (100 μmol-L^{-1}; grey; *n* = 5; A,C) or K_{ir} 2.1 channel inhibitor, ML133 (20 μmol-L^{-1}; grey; *n* = 5; B,D) when compared to solvent control (DMSO, black, *n*=7). All values are expressed as mean +SEM (A-F). A 2-way statistical ANOVA with a post-hoc Bonferroni test was used to generate significance values. Statistical significance is defined as **P*<0.05 (A-F). (*n*=) number of animals used.

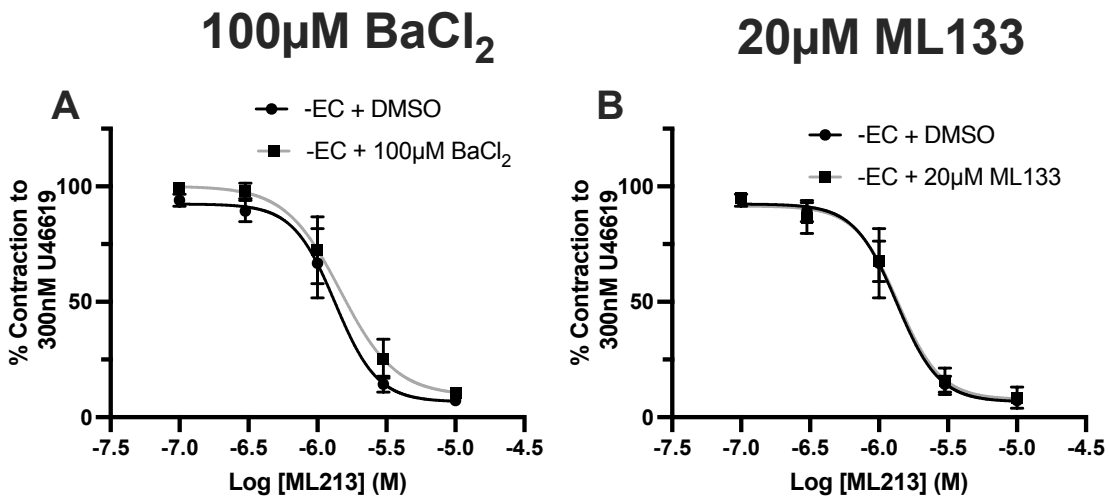

Figure 7.10: K_V7.2-5 channel activator-mediated vasorelaxation was significantly attenuated by EC removal.

Mean data for ML213-mediated relaxation in EC denuded vessels in vessels pre-incubation with either K_{IR}2 channel inhibitor $BaCl_2$ (100 μmol-L^{-1}; grey; *n* = 5; A) or ML133 (20 μmol-L^{-1}; grey; *n* = 5-6; B). A 2-way statistical ANOVA with a post-hoc Bonferroni test was used to generate significance values. (*n*=) number of animals used.

7.3.4 IK_{Ca}/SK_{Ca} inhibitors had no impact on K_V7 activator-mediated relaxation

Endothelial IK_{Ca} and SK_{Ca} channels contribute to relaxation responses in rat mesenteric arteries (Crane et al,. 2003). Thus, it is feasible that K_V7 channels interact with other key endothelial K^+ channels; particularly those expressed within microdomains (Sandow *et al.*, 2009), however, consistent with previous reports (Jepps et al,. 2016), pre-incubation with a combination of IK_{Ca} inhibitor TRAM-34 (1 μmol-L^{-1}; Wulff *et al.*, 2000) and SK_{Ca} inhibitor apamin (100 nmol-L^{-1}; Spoerri et al, 1975) had no effect on K_V7 activator-mediated vasorelaxation (Fig 7.11.A-C). Indicating that the endothelium-contribution to K_V7 activator-mediated relaxation involves endothelial K_{IR}, but not IK_{Ca} or SK_{Ca} channels.

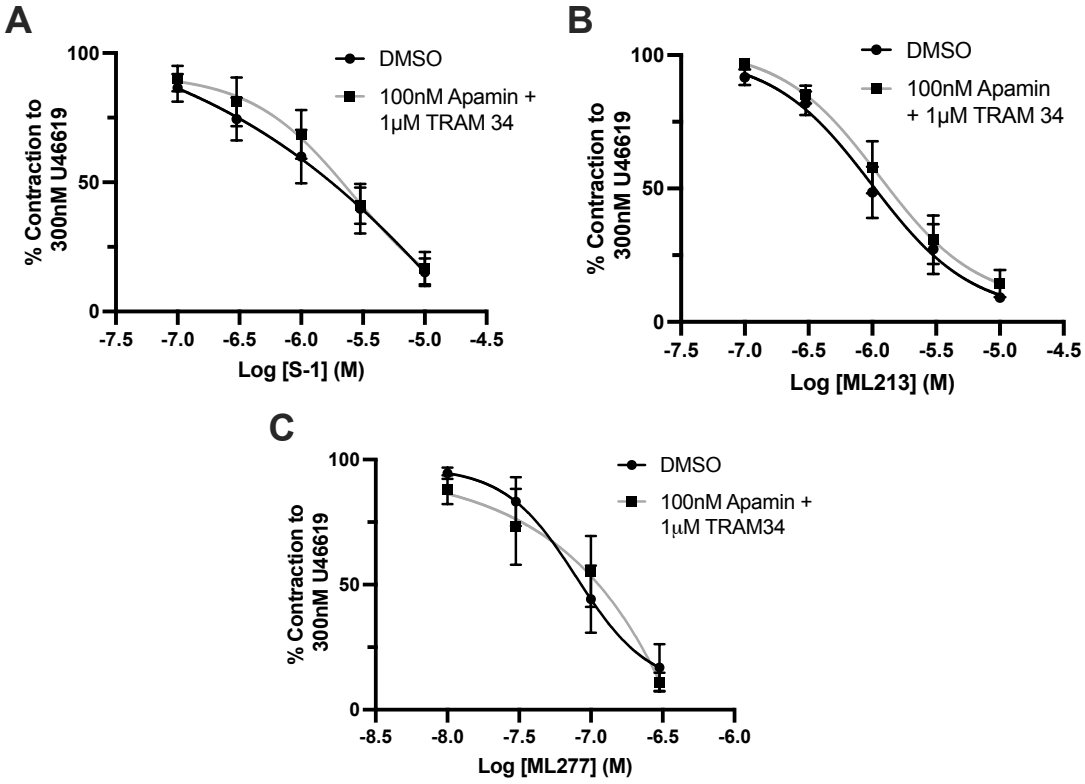

Figure 7.11: K_V7 channel activator-mediated vasorelaxation was not affected by preincubation with IK_{Ca}/SK_{Ca} channel antagonists.

Pre-incubation with both IK_{Ca} channel inhibitor TRAM34 (1 μmol-L^{-1}) and SK_{Ca} channel inhibitor Apamin (100 nmol-L^{-1}) had no effect on S-1, ML213 nor ML277 mediated vasorelaxation (*n* = 5-7; grey, A-C). All values are expressed are expressed as mean values ±SEM. A 2-way statistical ANOVA with a post-hoc Bonferroni test was used to generate significance values; no significant values were observed (A-C).

7.3.5 K_V7 channels contribute to CCh evoked vasorelaxation

7.3.5.1 CCh evoked relaxation is predominantly mediated via EDH in rat mesenteric arteries

The expression of functional K_V7 channels within ECs begs the question - do they contribute to EC-derived responses? Acetylcholine produces endothelium-dependent relaxation through NO-, EDH- and prostanoid-dependent mechanisms in rat mesenteric arteries (Parsons et al., 1994; Peredo et al., 1997; Shimokawa et al., 1996). Here, we observed a distinct rightward shift in the sensitivity to vasorelaxation in response to CCh, a synthetic acetylcholine analogue, when vessels were pre-incubated eNOS inhibitor L-nitroarginine methyl ester (L-NAME; 100 μmol-L^{-1}; Víteček *et al.*, 2012) when compared to DMSO control (*n*= 5-6; Fig 7.12.A). A combination IK_{Ca} and SK_{Ca} inhibitors, TRAM-34 (1 μmol-L^{-1}) and apamin (100 nmol-L^{-1}) respectively, suppresses EDH in rat mesenteric arteries (Garland and Dora, 2017). Here, EDH inhibition produced greater attenuation of CCh-mediated relaxation when compared to L-NAME (Fig 7.12.A). Furthermore, pre-incubating vessels with pan-K_V7 channel inhibitor linopirdine (10 μmol-L^{-1}) significantly attenuated CCh-mediated relaxation when compared to DMSO control (Fig 7.12.B). In contrast, pre-incubating vessels with either the K_V7.1 specific inhibitor HMR-1556 (10 μmol-L^{-1}) or a combination of non-specific K_V channel inhibitors tetraethylammonium (1 mmol-L^{-1}; (Choi et al., 1991) and 4-aminopyridine (4-AP; 1 μmol-L^{-1}; Kurata and Fedida, 2006) had no effect on CCh-evoked vasorelaxation (Fig 7.12.C,D).

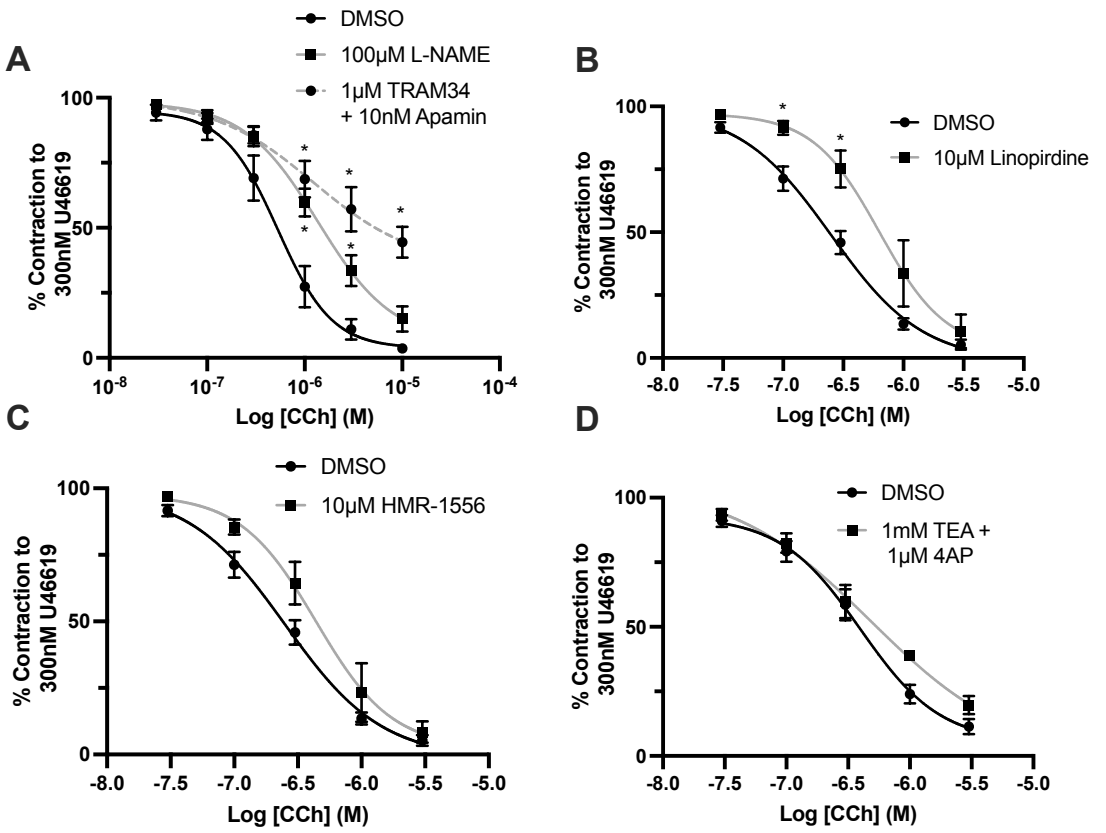

Figure 7.12: CCh evoked vasorelaxation is mediated through both eNOS and IK_{Ca}/SK_{Ca} channels and is partially attenuated by inhibition of K_V7 channels.

CCh-mediated relaxation of pre-contracted arterial tone (300 nmol-L^{-1} U46619) in vessels pre-incubated in either DMSO solvent control (black) eNOS inhibitor L-nitroarginine methyl ester (L-NAME; 100 μmol-L^{-1}; grey) or IK_{Ca}/SK_{Ca} channel inhibitors TRAM-34 (1 μmol-L^{-1}) and apamin (100 nmol-L^{-1}; grey, dashed line; *n* = 5-6; A). CCh-mediated relaxation in the vessels pre-incubated in DMSO solvent control (black), pan K_V7 channel inhibitor linopirdine (10 μmol-L^{-1}; grey; *n* = 6; B), $K_V7.1$ channel inhibitor HMR-1556 (10 μmol-L^{-1}; grey; *n* = 6; C) or non-specific K_V channel inhibitors 4-aminopyridine (4-AP; 1 mmol-L^{-1}) and tetraethylamonium (TEA; 1 mmol-L^{-1}; grey; *n*=5; D). All values are expressed as mean + SEM. A 2-way statistical ANOVA with a post-hoc Bonferroni test was used to generate significance values (*); Statistical significance is defined as **P*<0.05 (A-D).

7.3.5.2 K_V7.2-5 channels contribute to the NO axis of CCh evoked relaxation

When delineating the contribution of K_V7 channels to the NO or EDH axis of CCh-mediated relaxation, CCh-evoked relaxations were significantly attenuated in vessels pre-incubated in TRAM34/apamin (1 μmol-L^{-1}/100 nmol-L^{-1}) and linopirdine (10 μmol-L^{-1}) compared to vessels only pre-incubated in TRAM34/apamin alone (EC_{50} DMSO = 0.24±0.05 μmol-L^{-1}; TRAM34/Apamin = 0.27±0.03 μmol-L^{-1}; TRAM34/Apamin + linopirdine = 0.61±0.2 μmol-L^{-1}; Fig 7.13.B). In contrast, linopirdine failed to attenuate CCh relaxation in arteries pre-incubated with L-NAME (100 μmol-L^{-1}; Fig 7.13.A), suggesting K_V7 channels contribute to the eNOS sensitive proportion of CCh-mediated relaxation.

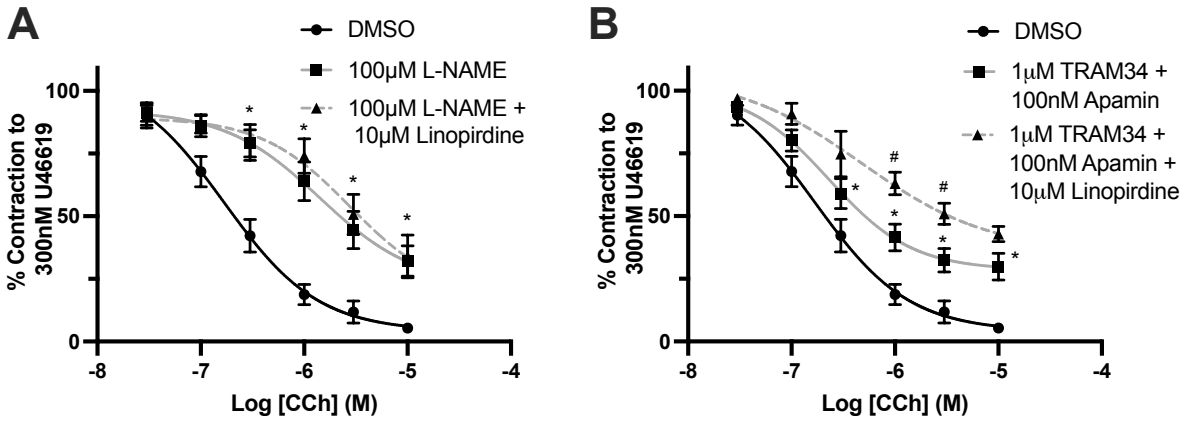

Figure 7.13: K_V7 channel inhibition additivity inhibits the IK_{Ca} / SK_{Ca} axis of carbachol (CCh) evoked vasorelaxation only.

Mean data of CCh-mediated relaxation of pre-contracted arterial tone (300 nmol-L^{-1}) in vessels pre-incubated in DMSO solvent controls (black), L-NAME (grey; 100 μmol-L^{-1}) L-NAME and Linopirdine (grey dashed line; 100 / 10 μmol-L^{-1}; *n*=5; A). Mean data of CCh-mediated relaxation of pre-contracted arterial tone in vessels pre-incubated in DMSO solvent controls (black), TRAM34 and apamin (grey; 1 / 0.1 μmol-L^{-1}), TRAM34, apamin and linopirdine (grey, dashed line; 1 / 0.1 /1 μmol-L^{-1}; B). All values are expressed as mean + SEM. A 2-way statistical ANOVA with a post-hoc Bonferroni test was used to generate significance values (*, drug v DMSO solvent control; #=Group B vs Group C) Statistical significance is defined as $^{\#/*}P<0.05$. (*n*=) number of animals used.

7.3.5.3 K_V7.2-5 channels contribute to NO derived CCh-mediated relaxation upstream of NO

Pre-incubating mesenteric arteries from male rats with linopirdine (10 μmol-L^{-1}) had no effect on vasorelaxation produced by the NO-donor SNP (Fig 7.14.A), however, in contrast with previous reports (Jepps et al., 2016), pre-incubation with L-NAME (100 μmol-L^{-1}) significantly attenuated K_V7.2-5 activator-mediated vasorelaxation (Fig 7.14.B). Suggesting that K_V7 channels upregulate NO production, rather than representing down-stream targets of NO mediated relaxation.

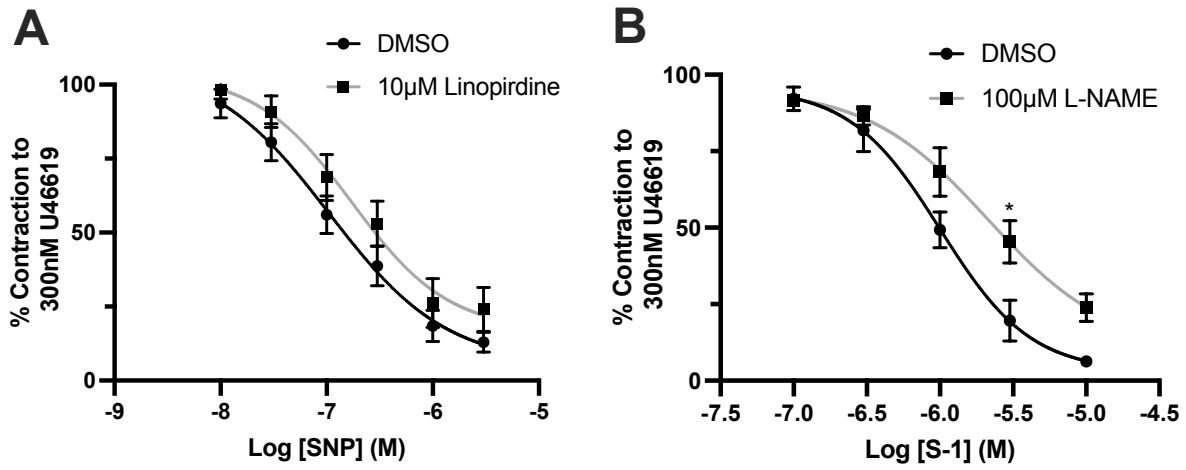

Figure 7.14: K_V7 channel prospectively upregulate endothelial nitric oxide production.

SNP-mediated vasorelaxation of pre-contracted tone (300 nmol-L^{-1}, U46619) in vessels pre-incubated in DMSO solvent control (black) or pan-K_V7 channel inhibitor linopirdine (10 μmol-L^{-1}; grey; *n*=5-6; A). K_V7.2-5 channel activator S-1-mediated relaxation in vessels pre-incubated with L-NAME (100 μmol-L^{-1}; grey; *n* = 5; B). All values are expressed as mean + SEM. A 2-way statistical ANOVA with a post-hoc Bonferroni test was used to generate significance values. Statistical significance is defined as **P*<0.05 (A). (*n*=) number of animals used.

7.4 Discussion

The results of this chapter identified *Kcnq1, Kcnq4* and *Kcnq5* transcripts in EC marker expressing cells and consequent $K_V7.1$, $K_V7.4$ and $K_V7.5$ protein in isolated and whole mount rat mesenteric artery ECs/VSMCs. Moreover, relaxation produced by two structurally different $K_V7.2$-5 activators, but not a $K_V7.1$ activator, were modulated by the presence of the endothelium and gap junction inhibition. ML277 mediated relaxation was also sensitive to $K_{IR}2$ inhibition, which was dependent on the presence of ECs, suggestive of a novel functional interaction between K_V7 and endothelial $K_{IR}2.x$ channels. Furthermore, the present data suggest that $K_V7.4$/$K_V7.5$ channels contribute to the NO-mediated axis of CCh-evoked endothelium-dependent relaxation upstream of eNOS. Thus, K_V7 channels are expressed in ECs, when pharmacologically upregulated, are functionally coupled to other EC K^+ and contribute to endothelium-derived responses channels in rat mesenteric arteries.

7.4.1 K_V7 channel expression and function within ECs

A caveat of the current literature regarding vascular K_V7 channels is a lack of differentiation between VSMCs and ECs, however, recently K_V7 channels were identified in pig coronary artery ECs (Chen *et al.*, 2016). The novel findings presented here expand on those findings and demonstrate K_V7 transcript and channel expression, functional activity and contribution to EC-derived vasodilatory signalling cascades in rat mesenteric artery endothelium.

In most arteries, the endothelium and smooth muscle are electrochemically linked via myoendothelial gap junctions formed from connexin proteins within heterocellular communicating domains present within holes in the IEL, see Sandow et al., (2012), for review. Via these connections, current injection in to ECs passes into VSMCs (Sandow, et al, 2002). The present data suggests a potential role for electrochemical heterocellular communication during $K_V7.2$-5 activator-mediated vasorelaxation. This conjecture is

supported by a higher-level of expression of K_V7.4/K_V7.5 in a proportion of IEL holes than that at the EC membrane as well as a significant attenuation of relaxation of pre-constricted arterial tone by two structurally different K_V7.2-5 activators in the absence of ECs and presence of a (putative) gap junction inhibitor. In contrast, EC removal had no impact on K_V7.1 activator-mediated vasorelaxation, which was observed in conjunction with reduced expression of *Kcnq1* transcript and K_V7.1 labelling within ECs compared to VSMCs. Collectively suggesting that only K_V7.4/K_V7.5 channels of the K_V7 sub-family are functionally expressed within mesenteric artery ECs.

An extrapolation of these results indicates a novel role for K_V7.4/K_V7.5 channels in the regulation of EC membrane potential within myoendothelial projections. It is plausible, that localised EC K_V7 channels negate the influx of depolarisation from VSMCs into the endothelium, providing tight regulation of EC V_m during VSMC contraction, however, further studies would be required to validate this hypothesis.

7.4.1.1 Endothelial K_V7 channel function within the female

This study demonstrates an oestrus cycle-dependent shift in sensitivity to K_V7 channel modulator responses similar to those observed in Chapters 4 and 5, whereby ML213 was more potent in vessels from F-D/M when compared to F-P/E. Additionally, EC removal had no effect in vessels from F-P/E, where K_V7.4 expression is shown to be reduced in mesenteric artery VSMCs (Fig 4.7). GPER1 signalling is partially attributed to endothelial dependent signalling (Prossnitz and Barton, 2011) and GPER1 has been identified in human ECs (Fredette, Meyer and Prossnitz, 2018). Though a molecular characterisation of K_V7 channels and GPER1 signalling within the endothelium of the female remain outside the scope of this study, we propose that during high-serum E2 stages of the oestrus cycle, GPER1 activation causes a global reduction in membrane abundance of K_V7.4 within the vasculature, including those prospectively in the endothelium. Therefore, during P/E, diminished membrane abundance of K_V7.4 within

the endothelium ablates the sensitivity of K_V7.2-5 channel activator-mediated relaxation to the presence of the endothelium.

7.4.2 A novel functional interaction with endothelial K_{IR} channels

K_{IR}2.x channels have been characterized in a variety of rat vascular beds including cerebral and coronary arteries (Smith *et al.*, 2008), where selective inhibition by Ba^{2+} revealed K_{IR} channel amplification of K^+ channel activator conductance (Smith *et al.*, 2008), however, there is a degree of conflict regarding the role of K_{IR}2.x channels within rat mesenteric arteries. As above, Ba^{2+} sensitive currents and K_{IR}2.x expression has been demonstrated in rat mesenteric artery ECs (Crane et al., 2003; Smith et al., 2008) which are purported to contribute to K_{Ca} mediated-hyperpolarization during ACh-derived EC-dependent responses (Goto *et al.*, 2004). In contrast, Smith *et al.*, (2008) demonstrate that within 3rd order mesenteric arteries, ACh-mediated K^+ conductance-dependent relaxation was insensitive to Ba^{2+}, indicating that K_{IR}2.x channels do not augment K^+ conductance in these vessels during receptor-mediated vasorelaxation.

In the present study, significant attenuation of both S-1 and ML213-mediated vasorelaxation was found following pre-incubation with two structurally different K_{IR}2.x blockers ML133 (M. Wu *et al.*, 2010) and Ba^{2+} (Hagiwara *et al.*, 1978) when compared to a solvent control. ML133 has been identified via high-throughput and mutagenesis investigation as a novel inhibitor of K_{IR}2.1 channels via interaction with D172 and I176 residues within the M2 region of K_{IR}2.1 (Wang *et al.*, 2011) with an IC_{50} of 1.8 μmol-L^{-1} at pH 7.4, with little to no selectivity against other K_{IR}2.x family members (M. Wu *et al.*, 2010; Wang *et al.*, 2011). Presently, ML133 is the most selective inhibitor of the K_{IR}2 family. In analogous fashion to our endothelium denudation experiments, K_{IR} inhibition had no effect on ML277-mediated vasorelaxation; implying a specific interplay with K_V7.4 and 7.5 channels. Furthermore, K_{IR}2 blockers had no effect on K_V7.2-7.5 activator-mediated relaxation in EC-denuded arteries, supporting the notion that functional K_{IR}2 channels (in the rat mesenteric artery bed) are restricted to the endothelium (Crane et

al., 2003). The present study suggests that pharmacological activation of endothelial $K_V7.4/7.5$ channels also activates an endothelial $K_{IR}2$ channels, increasing K^+ conductance, which in turn accounts for a proportion of EC augmentation of $K_V7.2$-5 activator-mediated vasorelaxation (Fig 7.15). This may be due to a localized increase in K^+ ion concentration in the proximity of the $K_{IR}2$ channels or an alternative modulation, however, based on the findings described by Goto *et al.,* (2004) and Smith *et al.,* (2008), the collective data suggest that this phenomenon is dependent on the branch order of mesenteric arteries. Furthermore, it remains unclear if this occurs during receptor mediated signalling, or if it is only present during pharmacological activation of endothelial K_V7 channels.

A primary concern for identification of novel functional interactions between ion channels using pharmacological tools is potential off-target effects, however, K_V7 activator-mediated relaxation in vessels pre-incubated in 10 μmol-L^{-1} linopirdine was abolished (Fig 3.5). If S-1 or ML213 were activating non-K_V channels such as K_{IR}, a degree of relaxation would still be observed in the presence of linopirdine. The present findings and those shown in chapter 3 therefore suggest that both S-1 and ML213 work exclusively via K_V7 channels and that a proportion of their response within rat mesenteric arteries occurs via a novel functional coupling of $K_V7.4/7.5$ and $K_{IR}2$ within ECs.

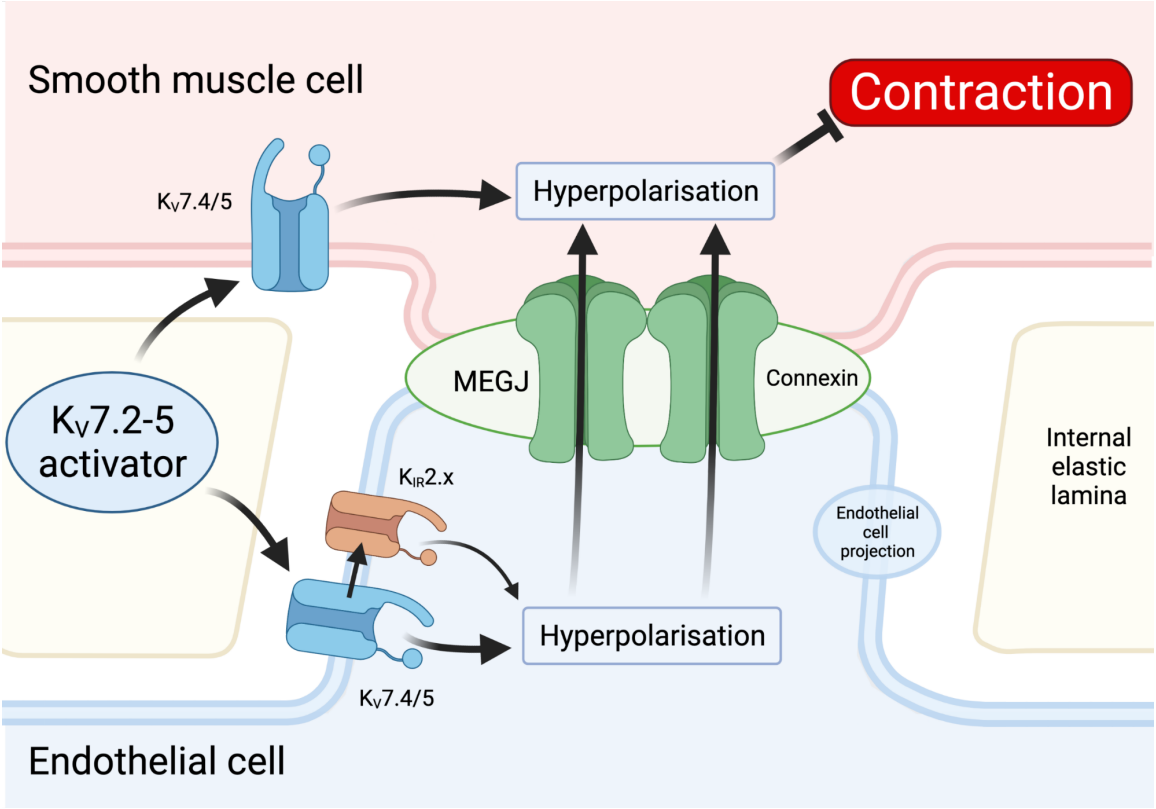

Figure 7.15: Schematic of K_V7.2-5 activator-mediated vasorelaxation.

K_V7.2-5 activator-mediated vasorelaxation occurs predominantly via K_V7.4/7.5 activation within VSMCs in addition to endothelial-K_V7.4/7.5 channels in a process sensitive to both gap-junction and endothelial-K_{IR}2.x inhibition.

7.4.3 The contribution of K_V7 channels to CCh evoked relaxations within rat mesenteric arteries

Our findings demonstrate that both NO- and EDH-dependent signalling contributes to CCh-mediated vasorelaxation, though the main contributor to endothelial-dependent vasorelaxation in 2nd order mesenteric arteries appears to be EDH, consistent with previous studies (Shimokawa *et al.*, 1996). In light of the significant impact of K_V7 inhibition on CCh-mediated vasorelaxation during the suppression of EDH, the present study suggests that K_V7 channels contribute to the eNOS sensitive axis of CCh-evoked relaxation within rat mesenteric arteries.

However, in a similar manner to rat renal artery (Stott et al., 2015), rat mesenteric artery K_V7 channels do not represent downstream targets of NO signalling as K_V7 inhibition does not impair NO-donor SNP-mediated relaxation, however, eNOS inhibition does

impair relaxation to a K_V7 activator, potentially implying K_V7 channel involvement in the production or release of NO in response to CCh. Interestingly, this appears to be a vascular bed specific phenomenon, as L-NAME has no effect on K_V7 activator-mediated relaxation within rat penile artery (Jepps et al., 2016).

7.4.4 Limitations

Ideally, direct functional evidence for a functional role of K_V7 channels in ECs would be provided by either single cell electrophysiology or sharp microelectrode impalement in whole arteries, however, this was not possible within the constraints of this study. Instead, we inferred a functional role for EC K_V7 channels using a reductive approach i.e comparison of functional responses without or with EC ablation. These studies implicate K_V7 channels as functional component of EC physiology that merit consideration in future studies.

7.4.5 Conclusions

In conclusion, the present data reveal that mesenteric ECs express $K_V7.4$/$K_V7.5$ channels and their presence boosts K_V7 activator-mediated relaxation. Furthermore, the data indicated a novel functional interaction with endothelial $K_{IR}2$ channels and supports the proposition that endothelial K_V7 channels contribute to endogenous endothelium-derived responses. These findings highlight the complex nature of the vascular response to K_V7 channel upregulation and emphasize the importance of these channels to vascular signalling.

Chapter 8: General discussion

8.1 Summary

The aim of this thesis was to determine the expression and function of K_V7 channels within the female rat from a physiological and pathophysiological perspective. The results detailed throughout argue for an essential role for K_V7 channels in receptor mediated vasoactive responses and as basal regulators of arterial tone within the vasculature of the female, mirroring those observed within the male, however, distinct Oestrus cycle dependent changes in vascular reactivity, underpinned by fluctuations in K_V7 membrane trafficking and functional output, reported within the first few months of the project rapidly became the primary focus of following investigations and provides a solid basis for future frontiers of investigations regarding vascular K_V7.

The data presented in Chapter 3 corroborated previous research done by our lab and others by showing that within the vasculature of the male, blockers of K_V7 channels contracted basal tone, enhanced receptor mediated contraction and impaired receptor mediated responses whilst various structurally different K_V7 activators relaxed pre-contracted tone (Fig 3.17). In addition, control experiments validated the pharmacological and molecular toolbox employed to investigate vascular K_V7 channel activity within the vasculature of the female Wistar. In short, the data in Chapter 3 on arteries from male rats added credence to the findings throughout the rest of the dissertation.

Chapter 4 by comparison details the principal novel contribution to the field of vascular K_V7 physiology within this thesis. Historically speaking, sex as an experimental factor has been neglected in basic science, with pharmacology at the forefront of male biased research (Beery and Zucker, 2011). This error in pre-clinical science study design has

culminated in a greater prevalence in adverse drug reactions within females when compared with age-matched men (Zopf *et al.*, 2008). One common explanation for the prejudice against investigations involving females is exclusion due to their inherent variability in physiology during the Oestrus cycle, culminating in greater workload (Wald and Wu, 2010; Klein *et al.*, 2015). The results of Chapter 4 substantiate that claim, however, also make clear that opting to exclude females based on an increased workload has led to the omission of unique and impactful Oestrus cycle derived process from the current literature. Chapter 4 argues for an E2 mediated, GPER1 receptor-derived, reduction in $K_V7.4$ function and membrane abundance (Fig 4.23). As evidenced by a considerably greater sensitivity to relaxation in response to K_V7 channel activators and K_V7 channel blocker mediated modulation of receptor derived responses and basal tone in addition to greater overlap of $K_V7.4$-membrane marker during ICC in arteries from F-D/M when compared to F-P/E. Interrogation of rat serum hormone levels by ELISA revealed a modest rise E2 in F-P/E rats when compared to F-D/M. Having identified E2 as a potential candidate for the Oestrus cycle dependent changes in K_V7 function, further investigation demonstrated an analogous inhibition of K_V7 activator mediated relaxation and $K_V7.4$ membrane abundance by physiological levels of extraneous E2 and selective GPER1 agonist G-1 in F-D/M rats only. Further, GPER1 activation mediated decrease in human KCNQ4 encoded currents in heterologous expression system. Finally, E2 decreased in the interaction of $K_V7.4$ and its forward trafficking molecular chaperone protein HSP90 in isolated mesenteric artery myocytes. The signalling cascades linking GPER1 activation to $K_V7.4$ channels and the fate of the channel remains to be determined. Previously, E2 was shown to internalise $K_V7.1$ via PKC into recycling endosomes which were later re-trafficked to the membrane (Rapetti-Mauss *et al,.* 2013), whereas angiotensin II was shown to promote $K_V7.4$ internalisation and degradation at the proteasome by increased ubiquitination (Barrese, Stott and Greenwood, 2018). Delineating the process of $K_V7.4$ handling after GPER1 activation will form the basis of future investigations. A key focus will be to determine changes in protein-protein interaction of $K_V7.4$ with chaperone proteins known to promote protein degradation

including Ubiquitin and C-terminal of HSP70 interacting protein (Barrese *et al,.* 2018) or recycling determinants including Rab11/Rab4 (Rapetti-Mauss *et al,.* 2013).

Chapter 5 expands the observations detailed in Chapter 4 into the hypertensive animal. When comparing K_V7 activator mediated relaxation in renal arteries harvested from male and female NT Wistar rats, no differences were observed, however, these similarities did not carry through to the hypertensive model, within which arteries from female SHRs were significantly more sensitive to ML213 mediated relaxation and less sensitive to U46619 mediated contraction compared to arteries from male SHRs. Moreover, when separated into F-D/M and F-P/E, $K_V7.4$ membrane abundance was significantly greater in myocytes form F-D/M when compared to males (Fig 5.12). Though in its infancy, the results of Chapter 5 indicate that preserved K_V7 function within the vasculature of the female may contribute to the female cardioprotective phenotype. Like Chapter 4, the findings of Chapter 5 provide the first inferences in a change in vascular $K_V7.4$ protein handling between the sexes of the rat. It is plausible that female SHRs exhibit a smaller increase in miR153/miR133 (Carr *et al.,* 2015), micro RNAs with consensus for $K_V7.4$ which impede translation of the channel in the male, however, arteries from female SHRs were still sensitive to the oestrus cycle. As argued in chapter 5, ion channel internalisation may preserve total protein levels within the cell (Conrad *et al*., 2018), accounting for the disparity between male and female SHRs. Steps taken to determine $K_V7.4$ handling within the NT animal will also be replicated within the SHR in future investigations.

Though recognised as a central component of both cardiomyocyte electrophysiology, and fluid movement across the epithelia of the gastrointestinal system (Barrese, Stott, and Greenwood., 2018), the role of $K_V7.1$ within the vasculature has remained enigmatic. $K_V7.1$ activators are effective relaxants of pre-contracted arterial tone (Chadha *et al*., 2012; Fig 3.5), however $K_V7.1$ blockers do not alter basal tone nor modulate receptor mediated responses. Experiments in Chapter 6 show clearly that two structurally

dissimilar inhibitors of $K_V7.1$ and molecular interference of the channel impaired relaxation to the IP receptor agonist MRE-269 (Fig 6.14). The identification of $K_V7.1$ contribution to endogenous vasoactive responses provides, to our knowledge, the first time a functional role for $K_V7.1$ within the vasculature.

Finally, the evidence provided in Chapter 7 provides new inference for K_V7 control of vascular tone. Wherein putative distribution of $K_V7.4$ within myoendothelial projections through the IEL would, in theory, provide tight regulation of electrical signals transmitted from the VSMC into the endothelium (Fig 7.15). This brief investigation into endothelial K_V7 expression and function provides novel, albeit preliminary, evidence for a role in K_V7 channels within the vasculature. Moreover, endothelial K_V7 channels within the female appear sensitive to oestrus cycle dependent regulation, a cell type which has previously been shown to express functional GPER1 channels.

8.2 Contrasts to the generally accepted role for E2 within the vasculature

Within the literature, oestrogens are generally regarded as a cardioprotective factor that enhances vascular relaxation. The data presented within this thesis, at first glance, opposes that idea, as E2 signalling via GPER1 diminished K_V7 membrane abundance and impaired relaxation of pre-contracted arterial tone in response to K_V7 channel activators. Previously, GPER1 stimulation in rat renal arteries contracted basal tone (Kurt and Buyukafsar, 2013). Further, Takezawa *et al.*, (1994) demonstrated an increase in mean arterial pressure in rats during pro-oestrus and after E2 injection into rats post-ovariectomy, collectively supporting the idea that E2 can negatively regulate arterial pressure, in line with the general conclusion of this thesis. This may however be an issue of perspective. The long-term effects of E2 on vascular reactivity were not determined within the course of this investigation, further, for the sake of clarity, a male v F-P/E v F-D/M comparison was not made, however, if we compared the relaxation in response to S-1 within in renal arteries from F-D/M vs males, S-1 was significantly more potent within arteries from F-D/M (EC_{50} = 0.4±0.35 μmol-L^{-1}) when compared to males (EC_{50} = 4±0.7

μmol-L^{-1}; *P*0.05; Fig 3.6/Fig 4.1). As proposed in Chapter 5.4.2, oestrus cycle dependent recycling of K_V7 channels into early endosomes may preserve K_V7 channel function within the hypertensive animals, giving rise to sex differences in the development of pathophysiology. Within the physiological context of the Wistar rat however, E2 mediated K_V7 recycling may enhance the functional output of K_V7 channels within F-D/M animals when compared to males. Indicating that the plausible long-term effect of E2 on vascular K_V7s is closer to the generally accepted role for oestrogens within the vasculature. An additional consideration is validity of the human-rodent comparison. As described in Chapter 1.6.3, a direct comparison between human and rodent reproductive cycles is complicated by large differences in cycle length and hormone fluctuations. Further, there is a growing concern within the literature regarding human-animal comparisons and the conclusions drawn from pre-clinical scientific research due to a fallacy known as 'false-analogy' (Sjoberg, 2017). It may well be that GPER1 mediated cycling of vascular K_V7 function occurs in rodents only, as such, before any definite statements can be made as to how the findings of this thesis translate to the human, further work is required. There are some interesting potential perspectives regarding GPER1 regulation of vascular K_V7 channels within the human, and will be described below, they are however discussed in the context of the caveats described above.

8.3 Perspectives

8.3.1 A role for $K_V7.4$ in the adverse cardiovascular effects of hormone replacement therapy

Within humans, HRT has become one of the most controversial topics of women's health of the last three decades. Trends in disease outcomes for patients on combined Estrogen/Progestin in the HERS I (Hulley *et al.*, 1998) and II (Hulley *et al.*, 2002) were not favourable, whereby adverse cardiovascular events increased, however there is conflict within the literature (Yang and Reckelhoff, 2011), as animal and human investigations on HRT prior to the HERS had positive outcomes. Though the effect of

exogenous E2 on the prevalence of CVD in women remains enigmatic, an extrapolation of the findings detailed herein could implicate diminished K_V7 channel function in the detrimental attributes of exogenous E2 in rodents and humans, as reduced K_V7 channel membrane abundance is implicated in a hypertensive phenotype. GPER1 is largely viewed as a promising therapeutic target in the treatment of CVD, as a hypo-functioning genetic variation of *GPER1* is associated with hypotension (Feldman *et al*., 2014), however we would argue that its effects are currently incompletely understood, meriting further investigation.

8.2.2 Cyclical drop of Oestrogen within the female, aberrant levels of K_V7 within the membrane

A link between migraine prevalence in women and the onset in menses is well established. By their late teens, females are twice as likely to suffer a migraine as males (Kornstein and Parker, 1997; Lipton and Bigal, 2005), and are 2.5 times as likely to suffer an attack within the first three days of menses (MacGregor and Hackshaw, 2004). The onset of menstrual migraines has been attributed to the withdrawal of E2 and are typically resistant to symptomatic treatment (Hu *et al.*, 2013). During migraines, pathophysiological vasodilatation and inflammation of the cephalic vasculature stretches the pial arteries which supply the cortex of the brain, which accounts for the pain associated with migraine. Current treatments for migraine symptoms are centred around vasoconstriction of the extracranial arteries via stimulation of the $5HT_{1B}$ receptor to reduce excess blood flow. As E2 drops to its lowest level of the cycle during menses, the results of this thesis would indicate that a lack of stimulation of GPER1 would lead to increased trafficking of K_V7 to the membrane. This would, in theory, give rise to pathological vasodilatation of the cerebral vasculature. Recently, novel strategies targeting CGRP ligand and receptor in women suffering from menstrual migraines have had positive outcomes (Silvestro *et al.*, 2021). K_V7 channels represent downstream targets of CGRP mediated relaxation in cerebral arteries (Chadha *et al.*, 2014), indicating a possible relationship between this novel treatment strategy and aberrant levels of K_V7

channel activity. In summary, we propose a bell-curve of stimulation of GPER1, whereby in either excess, or scarcity the result would be pathophysiological.

8.3.3 Oestrogenic regulation of arterial reactivity in the male

The pathogenesis of PAH is typified by raised pulmonary artery vascular resistance and mean pulmonary artery pressure of ≥20 mmHg in conjunction with raised serum E2. Sexual dimorphisms in the pathogenesis of PAH is a well described phenomenon (see (Ma *et al.*, 2017) for review). Women are more likely to develop PAH when compared to men, however PAH has a higher mortality rate in men compared to women (Badesch *et al.*, 2010; Frost *et al.*, 2011; Sun *et al.*, 2021). Recently, it was proposed that the sex-dependent differences in PAH aetiology was due to raised local concentration of E2 within the pulmonary vasculature of the male when compared to the female that leads to angiogenesis and vasocontraction (Assaggaf and Felty, 2017). Whilst the molecular mechanisms underlying this disease remain elusive, GPER1 mediated decrease in arterial $K_V7.4$ membrane abundance, as observed in both male and female Wistars in Chapter 4, potentially plays a role in PAH. Future experiments will seek to determine the effects of G-1/ E2 on pulmonary arterial K_V7 activity within both sexes.

8.4 Conclusion

This thesis demonstrates distinct sexual dimorphisms in vascular K_V7 physiology and pathophysiology. K_V7 channels are fundamental components of vascular reactivity within the female arteries in a fashion analogous to the male, however, fluctuations in vascular reactivity and K_V7 function across the Oestrus cycle differentiates females from the males. Whereby diminished $K_V7.4$ membrane abundance correlates with a 'pro-contractile' vascular phenotype, sensitising the vessel to vasoconstrictors and diminishing the effect of vasorelaxants. This phenomenon is prospectively driven via E2 signalling via GPER1. The central role for E2 mediated vascular K_V7 regulation has plausible and widespread implications of great interest and serves to re-enforce the

importance of the inclusion of females in basic pre-clinical science research. In conclusion, before a clear male-female comparison can be made, further work is required to better understand this unique phenomenon.

Chapter 9: Bibliography

Abbott, G. W. et al. (2014) 'KCNQ1, KCNE2, and Na+-coupled solute transporters form reciprocally regulating complexes that affect neuronal excitability.', Science signaling, 7(315), p. ra22. doi: 10.1126/scisignal.2005025.

Abbott, G. W. and Jepps, T. A. (2016) 'Kcne4 Deletion Sex-Dependently Alters Vascular Reactivity', Journal of Vascular Research. doi: 10.1159/000449060.

Adelman, J. P. et al. (1992) 'Calcium-activated potassium channels expressed from cloned complementary DNAs', Neuron. Elsevier, 9(2), pp. 209–216.

Aguilar-Bryan, L. et al. (1995) 'Cloning of the beta cell high-affinity sulfonylurea receptor: a regulator of insulin secretion', Science. American Association for the Advancement of Science, 268(5209), pp. 423–426.

Aguilar-Bryan, L. et al. (1998) 'Toward understanding the assembly and structure of KATP channels.', Physiological reviews. United States, 78(1), pp. 227–245. doi: 10.1152/physrev.1998.78.1.227.

Ahluwalia, A. and Hobbs, A. J. (2005) 'Endothelium-derived C-type natriuretic peptide: more than just a hyperpolarizing factor.', Trends in pharmacological sciences. England, 26(3), pp. 162–167. doi: 10.1016/j.tips.2005.01.005.

Ahmad, A. A., Randall, M. D. and Roberts, R. E. (2017a) 'Sex differences in the regulation of porcine coronary artery tone by perivascular adipose tissue: a role of adiponectin?', British Journal of Pharmacology. doi: 10.1111/bph.13902.

Ahmad, A. A., Randall, M. D. and Roberts, R. E. (2017b) 'Sex differences in the role of phospholipase A2-dependent arachidonic acid pathway in the perivascular adipose tissue function in pigs', Journal of Physiology. doi: 10.1113/JP274831.

Aickin, C. C. and Brading, A. F. (1984) 'The role of chloride-bicarbonate exchange in the regulation of intracellular chloride in guinea-pig vas deferens.', The Journal of physiology, 349, pp. 587–606. doi: 10.1113/jphysiol.1984.sp015175.

Aiello, E. A. et al. (1998) 'Beta-adrenoceptor activation and PKA regulate delayed rectifier K+ channels of vascular smooth muscle cells.', The American journal of physiology. United States, 275(2), pp. H448-59. doi: 10.1152/ajpheart.1998.275.2.H448.

Aiello, E. A., Walsh, M. P. and Cole, W. C. (1995) 'Phosphorylation by protein kinase A enhances delayed rectifier K+ current in rabbit vascular smooth muscle cells.', The American journal of physiology. United States, 268(2 Pt 2), pp. H926-34. doi: 10.1152/ajpheart.1995.268.2.H926.

Aiton, J. F. et al. (1981) 'Occurrence of passive furosemide-sensitive transmembrane potassium transport in cultured cells.', Biochimica et biophysica acta. Netherlands,

646(3), pp. 389–398. doi: 10.1016/0005-2736(81)90307-2.

Albarwani, S. et al. (2003) 'Voltage-gated K+ channels in rat small cerebral arteries: Molecular identity of the functional channels', Journal of Physiology, 551(3), pp. 751–763. doi: 10.1113/jphysiol.2003.040014.

Allen, B. G. and Walsh, M. P. (1994) 'The biochemical basis of the regulation of smooth-muscle contraction', Trends in Biochemical Sciences. doi: 10.1016/0968-0004(94)90112-0.

Alzamora, R. et al. (2011) 'Sexual dimorphism and oestrogen regulation of KCNE3 expression modulates the functional properties of KCNQ1 K+channels', Journal of Physiology. doi: 10.1113/jphysiol.2011.215772.

Amberg, G. C. et al. (2003) 'Modulation of the molecular composition of large conductance, Ca(2+) activated K(+) channels in vascular smooth muscle during hypertension.', The Journal of clinical investigation, 112(5), pp. 717–724. doi: 10.1172/JCI18684.

Amberg, G. C. and Santana, L. F. (2003) 'Downregulation of the BK channel beta1 subunit in genetic hypertension.', Circulation research. United States, 93(10), pp. 965–971. doi: 10.1161/01.RES.0000100068.43006.36.

Amberg, G. C. and Santana, L. F. (2006) 'Kv2 channels oppose myogenic constriction of rat cerebral arteries.', American journal of physiology. Cell physiology. United States, 291(2), pp. C348-56. doi: 10.1152/ajpcell.00086.2006.

Ammar, E. M., Said, S. A. and Hassan, M. S. (2004) 'Enhanced vasoconstriction and reduced vasorelaxation induced by testosterone and nandrolone in hypercholesterolemic rabbits', Pharmacological Research. doi: 10.1016/j.phrs.2004.03.010.

Anwer, K. et al. (1993) 'Calcium-activated K+ channels as modulators of human myometrial contractile activity.', The American journal of physiology. United States, 265(4 Pt 1), pp. C976-85. doi: 10.1152/ajpcell.1993.265.4.C976.

Ashcroft, F. M. and Kakei, M. (1989) 'ATP-sensitive K+ channels in rat pancreatic beta-cells: modulation by ATP and Mg2+ ions.', The Journal of physiology, 416, pp. 349–367. doi: 10.1113/jphysiol.1989.sp017765.

Askew Page, H. R. et al. (2019) 'TMEM16A is implicated in the regulation of coronary flow and is altered in hypertension', British Journal of Pharmacology. doi: 10.1111/bph.14598.

Assaggaf, H. and Felty, Q. (2017) 'Gender, Estrogen, and Obliterative Lesions in the Lung.', International journal of endocrinology, 2017, p. 8475701. doi: 10.1155/2017/8475701.

Atkinson, N. S., Robertson, G. A. and Ganetzky, B. (1991) 'A component of calcium-activated potassium channels encoded by the Drosophila slo locus', Science.

American Association for the Advancement of Science, 253(5019), pp. 551–555.

Aziz, Q. et al. (2014) 'The ATP-sensitive potassium channel subunit, Kir6. 1, in vascular smooth muscle plays a major role in blood pressure control', Hypertension. Am Heart Assoc, 64(3), pp. 523–529.

Badesch, D. B. et al. (2010) 'Pulmonary arterial hypertension: baseline characteristics from the REVEAL Registry.', Chest. United States, 137(2), pp. 376–387. doi: 10.1378/chest.09-1140.

Bal, M. et al. (2010) 'Ca2+/calmodulin disrupts AKAP79/150 interactions with KCNQ (M-Type) K+ channels.', The Journal of neuroscience : the official journal of the Society for Neuroscience, 30(6), pp. 2311–2323. doi: 10.1523/JNEUROSCI.5175-09.2010.

Baldwin, S. N. et al. (2020) 'KV7 Channel Expression and Function Within Rat Mesenteric Endothelial Cells', Frontiers in Physiology, 11(December), pp. 1–16. doi: 10.3389/fphys.2020.598779.

Barbagallo, M. et al. (2001) 'Vascular effects of progesterone: Role of cellular calcium regulation', Hypertension. doi: 10.1161/01.HYP.37.1.142.

Barrese, V. et al. (2017) 'Proliferative Role of Kv11 Channels in Murine Arteries.', Frontiers in physiology, 8, p. 500. doi: 10.3389/fphys.2017.00500.

Barrese, V. et al. (2018) 'Angiotensin II Promotes K V 7.4 Channels Degradation Through Reduced Interaction With HSP90 (Heat Shock Protein 90)Novelty and Significance', Hypertension. doi: 10.1161/HYPERTENSIONAHA.118.11116.

Barrese, V. et al. (2020) 'SMIT (Sodium-Myo-Inositol Transporter) 1 Regulates Arterial Contractility Through the Modulation of Vascular Kv7 Channels.', Arteriosclerosis, thrombosis, and vascular biology, 40(10), pp. 2468–2480. doi: 10.1161/ATVBAHA.120.315096.

Barrese, V., Stott, J. B. and Greenwood, I. A. (2018) 'KCNQ-Encoded Potassium Channels as Therapeutic Targets', Annual Review of Pharmacology and Toxicology. doi: 10.1146/annurev-pharmtox-010617-052912.

Barton, M. and Meyer, M. R. (2015) 'Nicolaus Copernicus and the rapid vascular responses to aldosterone', Trends in Endocrinology & Metabolism. Elsevier, 26(8), pp. 396–398.

Batenburg, W. W., Jansen, P. M. and Bogaerdt, A. J. van den (2012) 'Angiotensin II-aldosterone interaction in human coronary microarteries involves GPR30, EGFR, and endothelial NO synthase', Cardiovascular Research, 94, p. 136.

Baudel, M. A. S. M.-A. et al. (2020) 'Insights into Activation Mechanisms of Store-Operated TRPC1 Channels in Vascular Smooth Muscle.', Cells, 9(1). doi: 10.3390/cells9010179.

von Beckerath, N. et al. (1996) 'Inwardly rectifying K+ channels in freshly dissociated coronary endothelial cells from guinea-pig heart.', The Journal of physiology, 491 (

Pt 2(Pt 2), pp. 357–365. doi: 10.1113/jphysiol.1996.sp021221.

Beech, D. J. et al. (1993) 'K channel activation by nucleotide diphosphates and its inhibition by glibenclamide in vascular smooth muscle cells.', British journal of pharmacology, 110(2), pp. 573–582. doi: 10.1111/j.1476-5381.1993.tb13849.x.

Beeler, G. W. J. and Reuter, H. (1970) 'Voltage clamp experiments on ventricular myocarial fibres.', The Journal of physiology, 207(1), pp. 165–190. doi: 10.1113/jphysiol.1970.sp009055.

Beery, A. K. and Zucker, I. (2011) 'Sex bias in neuroscience and biomedical research.', Neuroscience and biobehavioral reviews, 35(3), pp. 565–572. doi: 10.1016/j.neubiorev.2010.07.002.

Behrens, R. et al. (2000) 'hKCNMB3 and hKCNMB4, cloning and characterization of two members of the large-conductance calcium-activated potassium channel beta subunit family.', FEBS letters. England, 474(1), pp. 99–106. doi: 10.1016/s0014-5793(00)01584-2.

Belevych, A. E. et al. (2002) 'Developmental changes in the functional characteristics and expression of voltage-gated K+channel currents in rat aortic myocytes', Cardiovascular Research. doi: 10.1016/S0008-6363(02)00227-4.

Belley, M. et al. (2005) 'Structure-activity relationship studies on ortho-substituted cinnamic acids, a new class of selective EP(3) antagonists.', Bioorganic & medicinal chemistry letters. England, 15(3), pp. 527–530. doi: 10.1016/j.bmcl.2004.11.051.

Belley, M. et al. (2006) 'Comparison between two classes of selective EP(3) antagonists and their biological activities.', Bioorganic & medicinal chemistry letters. England, 16(21), pp. 5639–5642. doi: 10.1016/j.bmcl.2006.08.025.

Benham, C. D. et al. (1986) 'Calcium-activated potassium channels in single smooth muscle cells of rabbit jejunum and guinea-pig mesenteric artery.', The Journal of physiology, 371, pp. 45–67. doi: 10.1113/jphysiol.1986.sp015961.

Bentzen, B. H. et al. (2006) 'The acrylamide (S)-1 differentially affects Kv7 (KCNQ) potassium channels', Neuropharmacology. doi: 10.1016/j.neuropharm.2006.07.001.

Berczi, V. et al. (1992) 'Pressure-induced activation of membrane K+ current in rat saphenous artery.', Hypertension (Dallas, Tex. : 1979). United States, 19(6 Pt 2), pp. 725–729. doi: 10.1161/01.hyp.19.6.725.

Berg, T. (2018) 'Kv7(KCNQ)-K+-Channels influence total peripheral resistance in female but not male rats, and hamper catecholamine release in hypertensive rats of both sexes', Frontiers in Physiology. doi: 10.3389/fphys.2018.00117.

Betts, L. C. and Kozlowski, R. Z. (2000) 'Electrophysiological effects of endothelin-1 and their relationship to contraction in rat renal arterial smooth muscle.', British journal

of pharmacology, 130(4), pp. 787–796. doi: 10.1038/sj.bjp.0703377.

Black, M. A. et al. (2009) 'Impact of age, sex, and exercise on brachial artery flow-mediated dilatation.', American journal of physiology. Heart and circulatory physiology, 297(3), pp. H1109-16. doi: 10.1152/ajpheart.00226.2009.

Blaine, J. T. and Ribera, A. B. (1998) 'Heteromultimeric potassium channels formed by members of the Kv2 subfamily.', The Journal of neuroscience : the official journal of the Society for Neuroscience, 18(23), pp. 9585–9593. doi: 10.1523/JNEUROSCI.18-23-09585.1998.

Blanco-Rivero, J. et al. (2005) 'Participation of prostacyclin in endothelial dysfunction induced by aldosterone in normotensive and hypertensive rats', Hypertension, 46(1), pp. 107–112. doi: 10.1161/01.HYP.0000171479.36880.17.

Blatz, A. L. and Magleby, K. L. (1986) 'Single apamin-blocked Ca-activated K+ channels of small conductance in cultured rat skeletal muscle', Nature. Nature Publishing Group, 323(6090), pp. 718–720.

Bley, K. R. et al. (2006) 'RO1138452 and RO3244794: characterization of structurally distinct, potent and selective IP (prostacyclin) receptor antagonists.', British journal of pharmacology, 147(3), pp. 335–345. doi: 10.1038/sj.bjp.0706554.

Blondeau, N. et al. (2007) 'Polyunsaturated fatty acids are cerebral vasodilators via the TREK-1 potassium channel.', Circulation research. United States, 101(2), pp. 176–184. doi: 10.1161/CIRCRESAHA.107.154443.

Boehlen, A. et al. (2013) 'The new KCNQ2 activator 4-Chlor-N-(6-chlor-pyridin-3-yl)-benzamid displays anticonvulsant potential.', British journal of pharmacology, 168(5), pp. 1182–1200. doi: 10.1111/bph.12065.

Bohm, R. A. et al. (2000) 'Transcriptional control of Ca(2+)-activated K(+) channel expression: identification of a second, evolutionarily conserved, neuronal promoter.', The Journal of experimental biology. England, 203(Pt 4), pp. 693–704.

Bologa, C. G. et al. (2006) 'Virtual and biomolecular screening converge on a selective agonist for GPR30.', Nature chemical biology. United States, 2(4), pp. 207–212. doi: 10.1038/nchembio775.

Bonev, A. D. and Nelson, M. T. (1996) 'Vasoconstrictors inhibit ATP-sensitive K+ channels in arterial smooth muscle through protein kinase C.', The Journal of general physiology, 108(4), pp. 315–323. doi: 10.1085/jgp.108.4.315.

Bowles, D. K. et al. (2004) 'Endogenous testosterone increases L-type Ca2+ channel expression in porcine coronary smooth muscle.', American journal of physiology. Heart and circulatory physiology. United States, 287(5), pp. H2091-8. doi: 10.1152/ajpheart.00258.2004.

Bradley, K. K. et al. (1999) 'Kir2.1 encodes the inward rectifier potassium channel in rat arterial smooth muscle cells.', The Journal of physiology, 515 (Pt 3(Pt 3), pp. 639–

651. doi: 10.1111/j.1469-7793.1999.639ab.x.

Brähler, S. et al. (2009) 'Genetic deficit of SK3 and IK1 channels disrupts the endothelium-derived hyperpolarizing factor vasodilator pathway and causes hypertension.', Circulation. United States, 119(17), pp. 2323–2332. doi: 10.1161/CIRCULATIONAHA.108.846634.

Brandes, R. P. and Mügge, A. (1997) 'Gender differences in the generation of superoxide anions in the rat aorta.', Life sciences. Netherlands, 60(6), pp. 391–396. doi: 10.1016/s0024-3205(96)00663-7.

Brayden, J. E. and Nelson, M. T. (1992) 'Regulation of arterial tone by activation of calcium-dependent potassium channels.', Science (New York, N.Y.). United States, 256(5056), pp. 532–535. doi: 10.1126/science.1373909.

Brenner, R. et al. (2000) 'Vasoregulation by the beta1 subunit of the calcium-activated potassium channel.', Nature. England, 407(6806), pp. 870–876. doi: 10.1038/35038011.

Broughton, B. R. S., Miller, A. A. and Sobey, C. G. (2010) 'Endothelium-dependent relaxation by G protein-coupled receptor 30 agonists in rat carotid arteries.', American journal of physiology. Heart and circulatory physiology. United States, 298(3), pp. H1055-61. doi: 10.1152/ajpheart.00878.2009.

Brown, D. A. et al. (1990) 'Membrane currents in hippocampal neurons.', Progress in brain research. Netherlands, 83, pp. 141–160. doi: 10.1016/s0079-6123(08)61247-9.

Brown, D. A. and Adams, P. R. (1980) 'Muscarinic suppression of a novel voltage-sensitive K+current in a vertebrate neurone [18]', Nature, pp. 673–676. doi: 10.1038/283673a0.

Brown, D. A. and Selyanko, A. A. (1985) 'Membrane currents underlying the cholinergic slow excitatory post-synaptic potential in the rat sympathetic ganglion.', The Journal of physiology, 365, pp. 365–387. doi: 10.1113/jphysiol.1985.sp015777.

Brueggemann, L. I. et al. (2006) 'Vasopressin stimulates action potential firing by protein kinase C-dependent inhibition of KCNQ5 in A7r5 rat aortic smooth muscle cells', AJP: Heart and Circulatory Physiology, 292(3), pp. H1352–H1363. doi: 10.1152/ajpheart.00065.2006.

Brueggemann, L. I. et al. (2012) 'Kv7 potassium channels in airway smooth muscle cells: signal transduction intermediates and pharmacological targets for bronchodilator therapy.', American journal of physiology. Lung cellular and molecular physiology, 302(1), pp. L120-32. doi: 10.1152/ajplung.00194.2011.

Brueggemann, Lyubov I. et al. (2014) 'Differential activation of vascular smooth muscle Kv7.4, Kv7.5, and Kv7.4/7.5 channels by ML213 and ICA-069673', Molecular Pharmacology. doi: 10.1124/mol.114.093799.

Brueggemann, Lioubov I, Mackie, A. R., et al. (2014) 'Differential protein kinase C-dependent modulation of Kv7.4 and Kv7.5 subunits of vascular Kv7 channels.', The Journal of biological chemistry, 289(4), pp. 2099–2111. doi: 10.1074/jbc.M113.527820.

Brueggemann, Lioubov I, Haick, J. M., et al. (2014) 'KCNQ (Kv7) potassium channel activators as bronchodilators: combination with a β2-adrenergic agonist enhances relaxation of rat airways.', American journal of physiology. Lung cellular and molecular physiology, 306(6), pp. L476-86. doi: 10.1152/ajplung.00253.2013.

Brueggemann, L. I. et al. (2018) 'Mechanisms of PKA-dependent potentiation of Kv7.5 channel activity in human airway smooth muscle cells', International Journal of Molecular Sciences. doi: 10.3390/ijms19082223.

Brueggemann, L. I., Cribbs, L. L. and Byron, K. L. (2020a) 'Heteromeric Channels Formed From Alternating Kv7.4 and Kv7.5 α-Subunits Display Biophysical, Regulatory, and Pharmacological Characteristics of Smooth Muscle M-Currents.', Frontiers in physiology, 11, p. 992. doi: 10.3389/fphys.2020.00992.

Brueggemann, L. I., Cribbs, L. L. and Byron, K. L. (2020b) 'Structural Determinants of Kv7.5 Potassium Channels That Confer Changes in Phosphatidylinositol 4,5-Bisphosphate (PIP(2)) Affinity and Signaling Sensitivities in Smooth Muscle Cells.', Molecular pharmacology. United States, 97(3), pp. 145–158. doi: 10.1124/mol.119.117192.

Brunet, P. C. and Bény, J. L. (1989) 'Substance P and bradykinin hyperpolarize pig coronary artery endothelial cells in primary culture.', Blood vessels. Switzerland, 26(4), pp. 228–234. doi: 10.1159/000158770.

Bryan, R. M. J. et al. (2006) 'Evidence for two-pore domain potassium channels in rat cerebral arteries.', American journal of physiology. Heart and circulatory physiology. United States, 291(2), pp. H770-80. doi: 10.1152/ajpheart.01377.2005.

Bubb, K. J., Khambata, R. S. and Ahluwalia, A. (2012) 'Sexual dimorphism in rodent models of hypertension and atherosclerosis.', British journal of pharmacology, 167(2), pp. 298–312. doi: 10.1111/j.1476-5381.2012.02036.x.

Bulley, S. et al. (2012) 'TMEM16A/ANO1 channels contribute to the myogenic response in cerebral arteries.', Circulation research, 111(8), pp. 1027–36. doi: 10.1161/CIRCRESAHA.112.277145.

Bulley, S. and Jaggar, J. H. (2014) 'Cl− channels in smooth muscle cells.', Pflügers Archiv : European journal of physiology, 466(5), pp. 861–72. doi: 10.1007/s00424-013-1357-2.

Burnham, M. P. et al. (2002) 'Characterization of an apamin-sensitive small-conductance Ca(2+)-activated K(+) channel in porcine coronary artery endothelium: relevance to EDHF.', British journal of pharmacology, 135(5), pp. 1133–1143. doi:

10.1038/sj.bjp.0704551.

Busch, A. E. et al. (1996) 'Inhibition of IKs in guinea pig cardiac myocytes and guinea pig IsK channels by the chromanol 293B', Pflügers Archiv - European Journal of Physiology, 432(6), pp. 1094–1096. doi: 10.1007/s004240050240.

Byers, S. L. et al. (2012) 'Mouse estrous cycle identification tool and images.', PloS one, 7(4), p. e35538. doi: 10.1371/journal.pone.0035538.

Byrne, N. G. and Large, W. A. (1987) 'Membrane mechanism associated with muscarinic receptor activation in single cells freshly dispersed from the rat anococcygeus muscle.', British journal of pharmacology, 92(2), pp. 371–379. doi: 10.1111/j.1476-5381.1987.tb11333.x.

Byron, K. L. and Brueggemann, L. I. (2018) 'Kv7 potassium channels as signal transduction intermediates in the control of microvascular tone', Microcirculation. doi: 10.1111/micc.12419.

Cabell, F., Weiss, D. S. and Price, J. M. (1994) 'Inhibition of adenosine-induced coronary vasodilation by block of large-conductance Ca(2+)-activated K+ channels.', The American journal of physiology. United States, 267(4 Pt 2), pp. H1455-60. doi: 10.1152/ajpheart.1994.267.4.H1455.

Cairrão, E. et al. (2008) 'Potassium channels are involved in testosterone-induced vasorelaxation of human umbilical artery.', Naunyn-Schmiedeberg's archives of pharmacology. Germany, 376(5), pp. 375–383. doi: 10.1007/s00210-007-0213-3.

del Camino, D. and Yellen, G. (2001) 'Tight steric closure at the intracellular activation gate of a voltage-gated K(+) channel.', Neuron. United States, 32(4), pp. 649–656. doi: 10.1016/s0896-6273(01)00487-1.

Caroccia, B. et al. (2016) 'Estrogen signaling in the adrenal cortex: implications for blood pressure sex differences', Hypertension. Am Heart Assoc, 68(4), pp. 840–848.

Carr, G. et al. (2016) 'MicroRNA-153 targeting of KCNQ4 contributes to vascular dysfunction in hypertension', Cardiovascular Research. doi: 10.1093/cvr/cvw177.

Chadha, P. S., Zunke, F., Davis, A. J., et al. (2012) 'Pharmacological dissection of Kv7.1 channels in systemic and pulmonary arteries', British Journal of Pharmacology, 166(4), pp. 1377–1387. doi: 10.1111/j.1476-5381.2012.01863.x.

Chadha, P. S., Zunke, F., Zhu, H. L., et al. (2012) 'Reduced KCNQ4-encoded voltage-dependent potassium channel activity underlies impaired β-adrenoceptor-mediated relaxation of renal arteries in hypertension', Hypertension, 59(4), pp. 877–884. doi: 10.1161/HYPERTENSIONAHA.111.187427.

Chadha, P. S. et al. (2014) 'Contribution of Kv7.4/Kv7.5 heteromers to intrinsic and calcitonin gene-related peptide-induced cerebral reactivity', Arteriosclerosis, Thrombosis, and Vascular Biology, 34(4), pp. 887–893. doi: 10.1161/ATVBAHA.114.303405.

Chan, M. V. et al. (2012) 'Distinct endothelial pathways underlie sexual dimorphism in vascular auto-regulation', British Journal of Pharmacology. doi: 10.1111/j.1476-5381.2012.02012.x.

Chen, L. et al. (2007) 'Mutation of an A-kinase-anchoring protein causes long-QT syndrome.', Proceedings of the National Academy of Sciences of the United States of America, 104(52), pp. 20990–20995. doi: 10.1073/pnas.0710527105.

Chen, T. T. et al. (2006) 'Key role of Kv1 channels in vasoregulation.', Circulation research. United States, 99(1), pp. 53–60. doi: 10.1161/01.RES.0000229654.45090.57.

Chen, X. et al. (2016) 'Novel Roles for Kv7 Channels in Shaping Histamine-Induced Contractions and Bradykinin-Dependent Relaxations in Pig Coronary Arteries', PLoS ONE. doi: 10.1371/journal.pone.0148569.

Cheng, S.-B. et al. (2014) 'Anatomical location and redistribution of G protein-coupled estrogen receptor-1 during the estrus cycle in mouse kidney and specific binding to estrogens but not aldosterone', Molecular and cellular endocrinology. Elsevier, 382(2), pp. 950–959.

Cheong, A. et al. (2001) 'K(V)alpha1 channels in murine arterioles: differential cellular expression and regulation of diameter.', American journal of physiology. Heart and circulatory physiology. United States, 281(3), pp. H1057-65. doi: 10.1152/ajpheart.2001.281.3.H1057.

Cheong, A., Dedman, A. M. and Beech, D. J. (2001) 'Expression and function of native potassium channel [K(V)alpha1] subunits in terminal arterioles of rabbit.', The Journal of physiology, 534(Pt 3), pp. 691–700. doi: 10.1111/j.1469-7793.2001.00691.x.

Choi, K. L. et al. (1991) 'Tetraethylammonium blockade distinguishes two inactivation mechanisms in voltage-activated Ki channels (quaternary ammonium ions/open channel block/ball-and-chain model)', Proc. Natl. Acad. Sci. USA.

Chrissobolis, S. et al. (2004) 'Evidence that estrogen suppresses rho-kinase function in the cerebral circulation in vivo.', Stroke. United States, 35(9), pp. 2200–2205. doi: 10.1161/01.STR.0000136951.85586.c8.

Chutkow, W. A. et al. (1996) 'Cloning, tissue expression, and chromosomal localization of SUR2, the putative drug-binding subunit of cardiac, skeletal muscle, and vascular KATP channels.', Diabetes. United States, 45(10), pp. 1439–1445. doi: 10.2337/diab.45.10.1439.

Chutkow, W. A. et al. (2002) 'Episodic coronary artery vasospasm and hypertension develop in the absence of Sur2 K ATP channels', The Journal of clinical investigation. Am Soc Clin Investig, 110(2), pp. 203–208.

Cidad, P. et al. (2012) 'Kv1.3 channels can modulate cell proliferation during phenotypic

switch by an ion-flux independent mechanism.', Arteriosclerosis, thrombosis, and vascular biology. United States, 32(5), pp. 1299–1307. doi: 10.1161/ATVBAHA.111.242727.

Cidad, P. et al. (2015) 'Kv1.3 channels modulate human vascular smooth muscle cells proliferation independently of mTOR signaling pathway.', Pflugers Archiv : European journal of physiology. Germany, 467(8), pp. 1711–1722. doi: 10.1007/s00424-014-1607-y.

Cipolla, M. J., Gokina, N. I. and Osol, G. (2002) 'Pressure-induced actin polymerization in vascular smooth muscle as a mechanism underlying myogenic behavior', The FASEB Journal. doi: 10.1096/cj.01-0104hyp.

Clapham, D. E. et al. (2003) 'International Union of Pharmacology. XLIII. Compendium of voltage-gated ion channels: transient receptor potential channels.', Pharmacological reviews. United States, 55(4), pp. 591–596. doi: 10.1124/pr.55.4.6.

Clement, J. P. 4th et al. (1997) 'Association and stoichiometry of K(ATP) channel subunits.', Neuron. United States, 18(5), pp. 827–838. doi: 10.1016/s0896-6273(00)80321-9.

Cogolludo, A. et al. (2003) 'Thromboxane A2-induced inhibition of voltage-gated K + channels and pulmonary vasoconstriction role of protein kinase Cζ', Circulation Research. doi: 10.1161/01.RES.0000095245.97945.FE.

Cogolludo, A. et al. (2006) 'Serotonin inhibits voltage-gated K+ currents in pulmonary artery smooth muscle cells: role of 5-HT2A receptors, caveolin-1, and KV1.5 channel internalization.', Circulation research. United States, 98(7), pp. 931–938. doi: 10.1161/01.RES.0000216858.04599.e1.

Colburn, T. D. et al. (2020) 'ATP-sensitive K(+) channel inhibition in rats decreases kidney and skeletal muscle blood flow without increasing sympathetic nerve discharge.', Respiratory physiology & neurobiology, 278, p. 103444. doi: 10.1016/j.resp.2020.103444.

Colden-Stanfield, M. et al. (1987) 'Bradykinin-induced increases in cytosolic calcium and ionic currents in cultured bovine aortic endothelial cells.', Circulation research. United States, 61(5), pp. 632–640. doi: 10.1161/01.res.61.5.632.

Colinas, O. et al. (2015) 'α5-Integrin-mediated cellular signaling contributes to the myogenic response of cerebral resistance arteries', Biochemical Pharmacology. doi: 10.1016/j.bcp.2015.08.088.

Conneely, O. M. et al. (2002) 'Reproductive functions of progesterone receptors.', Recent progress in hormone research. United States, 57, pp. 339–355. doi: 10.1210/rp.57.1.339.

Connelly, P. J. et al. (2021) 'Sex steroids receptors, hypertension, and vascular ageing.',

Journal of human hypertension. England. doi: 10.1038/s41371-021-00576-7.

Conrad, R. et al. (2018) 'Rapid Turnover of the Cardiac L-Type Ca(V)1.2 Channel by Endocytic Recycling Regulates Its Cell Surface Availability.', iScience, 7, pp. 1–15. doi: 10.1016/j.isci.2018.08.012.

Cooper, E. C. et al. (2000) 'Colocalization and coassembly of two human brain M-type potassium channel subunits that are mutated in epilepsy', Proc. Natl. Acad. Sci. U. S. A. doi: 10.1073/pnas.090092797.

Cora, M. C., Kooistra, L. and Travlos, G. (2015) 'Vaginal Cytology of the Laboratory Rat and Mouse:Review and Criteria for the Staging of the Estrous Cycle Using Stained Vaginal Smears', Toxicologic Pathology. doi: 10.1177/0192623315570339.

Corteling, R. L. et al. (2007) 'The functional consequence of RhoA knockdown by RNA interference in rat cerebral arteries', American Journal of Physiology - Heart and Circulatory Physiology. doi: 10.1152/ajpheart.01374.2006.

Costa, A. M. and Brown, B. S. (1997) 'Inhibition of M-current in cultured rat superior cervical ganglia by linopirdine: mechanism of action studies.', Neuropharmacology. England, 36(11–12), pp. 1747–1753. doi: 10.1016/s0028-3908(97)00155-x.

Cox, R. H., Folander, K. and Swanson, R. (2001) 'Differential expression of voltage-gated K+channel genes in arteries from spontaneously hypertensive and wistar-kyoto rats', Hypertension. doi: 10.1161/01.HYP.37.5.1315.

Cox, R. H. and Fromme, S. (2016) 'Functional Expression Profile of Voltage-Gated K(+) Channel Subunits in Rat Small Mesenteric Arteries.', Cell biochemistry and biophysics, 74(2), pp. 263–276. doi: 10.1007/s12013-015-0715-4.

Crane, G. J., Walker, S. D., et al. (2003) 'Evidence for a differential cellular distribution of inward rectifier K channels in the rat isolated mesenteric artery', Journal of Vascular Research. doi: 10.1159/000070713.

Crane, G. J., Gallagher, N., et al. (2003) 'Small-and intermediate-conductance calcium-activated K+ channels provide different facets of endothelium-dependent hyperpolarization in rat mesenteric artery', Journal of Physiology. doi: 10.1113/jphysiol.2003.051896.

Crews, J. K. and Khalil, R. A. (1999a) 'Antagonistic effects of 17 beta-estradiol, progesterone, and testosterone on Ca2+ entry mechanisms of coronary vasoconstriction.', Arteriosclerosis, thrombosis, and vascular biology. United States, 19(4), pp. 1034–1040. doi: 10.1161/01.atv.19.4.1034.

Crews, J. K. and Khalil, R. A. (1999b) 'Gender-specific inhibition of Ca2+ entry mechanisms of arterial vasoconstriction by sex hormones.', Clinical and experimental pharmacology & physiology. Australia, 26(9), pp. 707–715. doi: 10.1046/j.1440-1681.1999.03110.x.

Crisostomo, P. R. et al. (2006) 'Brief exposure to exogenous testosterone increases

death signaling and adversely affects myocardial function after ischemia', American Journal of Physiology-Regulatory Integrative and Comparative Physiology. doi: 10.1152/ajpregu.00833.2005.

Curran, J. and Mohler, P. J. (2015) 'Alternative paradigms for ion channelopathies: Disorders of ion channel membrane trafficking and posttranslational modification', Annual Review of Physiology, 77, pp. 505–524. doi: 10.1146/annurev-physiol-021014-071838.

Dam, V. S., Boedtkjer, D. M. B., Aalkjaer, C., et al. (2014) 'The bestrophin- and TMEM16A-associated Ca(2+)- activated Cl(–) channels in vascular smooth muscles.', Channels (Austin, Tex.), 8(4), pp. 361–369. doi: 10.4161/chan.29531.

Dam, V. S., Boedtkjer, D. M. B., Nyvad, J., et al. (2014) 'TMEM16A knockdown abrogates two different Ca(2+)-activated Cl (-) currents and contractility of smooth muscle in rat mesenteric small arteries.', Pflügers Archiv : European journal of physiology, 466(7), pp. 1391–409. doi: 10.1007/s00424-013-1382-1.

Davis, A. J. et al. (2010) 'Expression profile and protein translation of TMEM16A in murine smooth muscle.', American journal of physiology. Cell physiology, 299(5), pp. C948-59. doi: 10.1152/ajpcell.00018.2010.

Davis, A. J. et al. (2013) 'Potent vasorelaxant activity of the TMEM16A inhibitor T16A(inh) -A01.', British journal of pharmacology, 168(3), pp. 773–84. doi: 10.1111/j.1476-5381.2012.02199.x.

Davis, J. P. (1992) 'The effects of Na(+)-K(+)-Cl- co-transport and Cl(-)-HCO3-exchange blockade on the membrane potential and intracellular chloride levels of rat arterial smooth muscle, in vitro.', Experimental physiology. England, 77(6), pp. 857–862. doi: 10.1113/expphysiol.1992.sp003652.

Davoren, J. E. et al. (2015) 'Discovery of a novel Kv7 channel opener as a treatment for epilepsy.', Bioorganic & medicinal chemistry letters. England, 25(21), pp. 4941–4944. doi: 10.1016/j.bmcl.2015.04.074.

Dedman, A. et al. (2009) 'The mechano-gated K(2P) channel TREK-1.', European biophysics journal : EBJ. Germany, 38(3), pp. 293–303. doi: 10.1007/s00249-008-0318-8.

Deer, R. R. and Stallone, J. N. (2016) 'Effects of estrogen on cerebrovascular function: age-dependent shifts from beneficial to detrimental in small cerebral arteries of the rat.', American journal of physiology. Heart and circulatory physiology, 310(10), pp. H1285-94. doi: 10.1152/ajpheart.00645.2015.

Dema, A. et al. (2015) 'Pharmacological targeting of AKAP-directed compartmentalized cAMP signalling.', Cellular signalling. England, 27(12), pp. 2474–2487. doi: 10.1016/j.cellsig.2015.09.008.

Dennis, M. K. et al. (2009) 'In vivo effects of a GPR30 antagonist', Nature Chemical

Biology, 5(6), pp. 421–427. doi: 10.1038/nchembio.168.

Dennis, M. K. et al. (2011) 'Identification of a GPER/GPR30 antagonist with improved estrogen receptor counterselectivity.', The Journal of steroid biochemistry and molecular biology, 127(3–5), pp. 358–366. doi: 10.1016/j.jsbmb.2011.07.002.

Deth, R. C., Payne, R. A. and Peecher, D. M. (1987) 'Influence of furosemide on rubidium-86 uptake and alpha-adrenergic responsiveness of arterial smooth muscle.', Blood vessels. Switzerland, 24(6), pp. 321–333. doi: 10.1159/000158709.

Diener, M. et al. (1996) 'Cyclic AMP-dependent regulation of K+ transport in the rat distal colon.', British journal of pharmacology, 118(6), pp. 1477–1487. doi: 10.1111/j.1476-5381.1996.tb15563.x.

Ding, A. Q. and Stallone, J. N. (2001) 'Testosterone-induced relaxation of rat aorta is androgen structure specific and involves K+ channel activation.', Journal of applied physiology (Bethesda, Md. : 1985). United States, 91(6), pp. 2742–2750. doi: 10.1152/jappl.2001.91.6.2742.

Docherty, J. R. et al. (2019) 'Sex: A change in our guidelines to authors to ensure that this is no longer an ignored experimental variable', British Journal of Pharmacology, 176(21), pp. 4081–4086. doi: 10.1111/bph.14761.

Donner, N. C. and Lowry, C. A. (2013) 'Sex differences in anxiety and emotional behavior.', Pflugers Archiv : European journal of physiology, 465(5), pp. 601–626. doi: 10.1007/s00424-013-1271-7.

Dora, K. A. et al. (2008) 'Modulation of endothelial cell KCa3.1 channels during endothelium-derived hyperpolarizing factor signaling in mesenteric resistance arteries', Circulation Research. doi: 10.1161/CIRCRESAHA.108.172379.

Dowell, M. L. et al. (2005) 'Latrunculin B increases force fluctuation-induced relengthening of ACh-contracted, isotonically shortened canine tracheal smooth muscle', Journal of Applied Physiology. doi: 10.1152/japplphysiol.01378.2003.

Doyle, D. A. et al. (1998) 'The structure of the potassium channel: Molecular basis of K+conduction and selectivity', Science. doi: 10.1126/science.280.5360.69.

Dumas, M. et al. (1997) 'Role of potassium channels and nitric oxide in the effects of iloprost and prostaglandin E1 on hypoxic vasoconstriction in the isolated perfused lung of the rat', British Journal of Pharmacology. doi: 10.1038/sj.bjp.0700912.

Duncker, D. J. et al. (1995) 'Endogenous adenosine mediates coronary vasodilation during exercise after K(ATP)+ channel blockade.', The Journal of clinical investigation, 95(1), pp. 285–295. doi: 10.1172/JCI117653.

Duprat, F. et al. (1997) 'TASK, a human background K+ channel to sense external pH variations near physiological pH', The EMBO journal. John Wiley & Sons, Ltd, 16(17), pp. 5464–5471.

Dusting, G. J., Moncada, S. and Vane, J. R. (1977) 'Prostacyclin (PGI2) is a weak

contractor of coronary arteries of the pig', European Journal of Pharmacology. doi: 10.1016/0014-2999(77)90014-0.

Dutt, P., Nguyen, N. and Toksoz, D. (2004) 'Role of Lbc RhoGEF in Gα12/13-induced signals to Rho GTPase', Cellular Signalling. doi: 10.1016/S0898-6568(03)00132-3.

Dworetzky, S. I., Trojnacki, J. T. and Gribkoff, V. K. (1994) 'Cloning and expression of a human large-conductance calcium-activated potassium channel', Molecular Brain Research. Elsevier, 27(1), pp. 189–193.

Earley, S. and Brayden, J. E. (2015) 'Transient receptor potential channels in the vasculature.', Physiological reviews, 95(2), pp. 645–90. doi: 10.1152/physrev.00026.2014.

Edwards, F. R., Hirst, G. D. and Silverberg, G. D. (1988) 'Inward rectification in rat cerebral arterioles; involvement of potassium ions in autoregulation.', The Journal of physiology, 404, pp. 455–466. doi: 10.1113/jphysiol.1988.sp017299.

Edwards, G. and Weston, A. H. (2004) 'Potassium and potassium clouds in endothelium-dependent hyperpolarizations', Pharmacological Research, pp. 535–541. doi: 10.1016/j.phrs.2003.11.013.

El-Yazbi, A. F., Abd-Elrahman, K. S. and Moreno-Dominguez, A. (2015) 'PKC-mediated cerebral vasoconstriction: Role of myosin light chain phosphorylation versus actin cytoskeleton reorganization', Biochemical Pharmacology. doi: 10.1016/j.bcp.2015.04.011.

Eldstrom, J. et al. (2021) 'ML277 regulates KCNQ1 single-channel amplitudes and kinetics, modified by voltage sensor state.', The Journal of general physiology, 153(12). doi: 10.1085/jgp.202112969.

Enyedi, P. and Czirják, G. (2010) 'Molecular background of leak K+ currents: two-pore domain potassium channels.', Physiological reviews. United States, 90(2), pp. 559–605. doi: 10.1152/physrev.00029.2009.

Er, F. et al. (2004) 'Testosterone induces cytoprotection by activating ATP-sensitive K+channels in the cardiac mitochondrial inner membrane', Circulation. doi: 10.1161/01.CIR.0000146900.84943.E0.

Eto, M. et al. (1995) 'A novel protein phosphatase-1 inhibitory protein potentiated by protein kinase C. Isolation from porcine aorta media and characterization.', Journal of biochemistry, 118(6), pp. 1104–7.

Eto, M. et al. (2007) 'Phosphorylation-Induced Conformational Switching of CPI-17 Produces a Potent Myosin Phosphatase Inhibitor', Structure. doi: 10.1016/j.str.2007.10.014.

Etxeberria, A. et al. (2008) 'Calmodulin regulates the trafficking of KCNQ2 potassium channels.', FASEB journal : official publication of the Federation of American Societies for Experimental Biology. United States, 22(4), pp. 1135–1143. doi:

10.1096/fj.07-9712com.

Facemire, C. S. and Arendshorst, W. J. (2005) 'Calmodulin mediates norepinephrine-induced receptor-operated calcium entry in preglomerular resistance arteries.', American journal of physiology. Renal physiology. United States, 289(1), pp. F127-36. doi: 10.1152/ajprenal.00397.2004.

Fallah, G. et al. (2011) 'TMEM16A(a)/anoctamin-1 shares a homodimeric architecture with CLC chloride channels.', Molecular & cellular proteomics : MCP, 10(2), p. M110.004697. doi: 10.1074/mcp.M110.004697.

Fallet, R. W. et al. (2001) 'Influence of Ca(2+)-activated K(+) channels on rat renal arteriolar responses to depolarizing agonists.', American journal of physiology. Renal physiology, 280(4), pp. F583-91. doi: 10.1152/ajprenal.2001.280.4.F583.

Fanger, C. M. et al. (1999) 'Calmodulin mediates calcium-dependent activation of the intermediate conductance KCa channel, IKCa1.', The Journal of biological chemistry. United States, 274(9), pp. 5746–5754. doi: 10.1074/jbc.274.9.5746.

Farouque, H. M. O., Worthley, S. G. and Meredith, I. T. (2004) 'Effect of ATP-sensitive potassium channel inhibition on coronary metabolic vasodilation in humans.', Arteriosclerosis, thrombosis, and vascular biology. United States, 24(5), pp. 905–910. doi: 10.1161/01.ATV.0000125701.18648.48.

Feldman, R. D. et al. (2014) 'A common hypofunctional genetic variant of GPER is associated with increased blood pressure in women', British Journal of Clinical Pharmacology, 78(6), pp. 1441–1452. doi: 10.1111/bcp.12471.

Fellner, S. K. and Arendshorst, W. J. (2008) 'Angiotensin II-stimulated Ca2+ entry mechanisms in afferent arterioles: role of transient receptor potential canonical channels and reverse Na+/Ca2+ exchange.', American journal of physiology. Renal physiology. United States, 294(1), pp. F212-9. doi: 10.1152/ajprenal.00244.2007.

Fergus, D. J., Martens, J. R. and England, S. K. (2003) 'Kv channel subunits that contribute to voltage-gated K+ current in renal vascular smooth muscle.', Pflugers Archiv : European journal of physiology. Germany, 445(6), pp. 697–704. doi: 10.1007/s00424-002-0994-7.

Ferreira, N. S. et al. (2015) 'Diabetes impairs the vascular effects of aldosterone mediated by G protein-coupled estrogen receptor activation', Frontiers in Pharmacology, 6, p. 34.

Fetalvero, K. M., Martin, K. A. and Hwa, J. (2007) 'Cardioprotective prostacyclin signaling in vascular smooth muscle.', Prostaglandins & other lipid mediators. United States, 82(1–4), pp. 109–118. doi: 10.1016/j.prostaglandins.2006.05.011.

Ficker, E. (2003) 'Role of the Cytosolic Chaperones Hsp70 and Hsp90 in Maturation of the Cardiac Potassium Channel hERG', Circulation Research. doi: 10.1161/01.RES.0000079028.31393.15.

Filardo, E. J. et al. (2000) ‘Estrogen-induced activation of Erk-1 and Erk-2 requires the G protein-coupled receptor homolog, GPR30, and occurs via trans-activation of the epidermal growth factor receptor through release of HB-EGF.’, Molecular endocrinology (Baltimore, Md.). United States, 14(10), pp. 1649–1660. doi: 10.1210/mend.14.10.0532.

Filardo, E. J. et al. (2002) ‘Estrogen action via the G protein-coupled receptor, GPR30: stimulation of adenylyl cyclase and cAMP-mediated attenuation of the epidermal growth factor receptor-to-MAPK signaling axis.’, Molecular endocrinology (Baltimore, Md.). United States, 16(1), pp. 70–84. doi: 10.1210/mend.16.1.0758.

Filippi, S. et al. (2009) ‘Testosterone partially ameliorates metabolic profile and erectile responsiveness to PDE5 inhibitors in an animal model of male metabolic syndrome’, Journal of Sexual Medicine. doi: 10.1111/j.1743-6109.2009.01467.x.

Filosa, J. A. et al. (2006) ‘Local potassium signaling couples neuronal activity to vasodilation in the brain.’, Nature neuroscience. United States, 9(11), pp. 1397–1403. doi: 10.1038/nn1779.

Fink, M. et al. (1998) ‘A neuronal two P domain K+ channel stimulated by arachidonic acid and polyunsaturated fatty acids’, The EMBO journal. John Wiley & Sons, Ltd, 17(12), pp. 3297–3308.

Forrest, A. S. et al. (2010) ‘Intricate interaction between store-operated calcium entry and calcium-activated chloride channels in pulmonary artery smooth muscle cells.’, Advances in experimental medicine and biology, 661, pp. 31–55. doi: 10.1007/978-1-60761-500-2_3.

Fredette, N. C., Meyer, M. R. and Prossnitz, E. R. (2018) ‘Role of GPER in estrogen-dependent nitric oxide formation and vasodilation.’, The Journal of steroid biochemistry and molecular biology, 176, pp. 65–72. doi: 10.1016/j.jsbmb.2017.05.006.

Fröhlich, H. et al. (2011) ‘Hypothyroidism of gene-targeted mice lacking Kcnq1.’, Pflugers Archiv : European journal of physiology, 461(1), pp. 45–52. doi: 10.1007/s00424-010-0890-5.

Frost, A. E. et al. (2011) ‘The changing picture of patients with pulmonary arterial hypertension in the United States: how REVEAL differs from historic and non-US Contemporary Registries.’, Chest. United States, 139(1), pp. 128–137. doi: 10.1378/chest.10-0075.

Fukao, M. et al. (1999) ‘Cyclic GMP-dependent protein kinase activates cloned BKCa channels expressed in mammalian cells by direct phosphorylation at serine 1072.’, The Journal of biological chemistry. United States, 274(16), pp. 10927–10935. doi: 10.1074/jbc.274.16.10927.

Fukuharaa, S., Chikumi, H. and Silvio Gutkind, J. (2001) ‘RGS-containing RhoGEFs:

The missing link between transforming G proteins and Rho?', Oncogene. doi: 10.1038/sj.onc.1204182.

Gaffey, A. E. et al. (2021) 'Effects of ambulatory blood pressure monitoring on sleep in healthy, normotensive men and women.', Blood pressure monitoring, 26(2), pp. 93–101. doi: 10.1097/MBP.0000000000000494.

Gamper, N., Li, Y. and Shapiro, M. S. (2005) 'Structural requirements for differential sensitivity of KCNQ K+ channels to modulation by Ca2+/calmodulin.', Molecular biology of the cell, 16(8), pp. 3538–3551. doi: 10.1091/mbc.e04-09-0849.

Gant, N. F. et al. (1973) 'A study of angiotensin II pressor response throughout primigravid pregnancy', Journal of Clinical Investigation. doi: 10.1172/JCI107462.

Gao, Y. et al. (2013) 'Distinct Roles of Molecular Chaperones HSP90α and HSP90β in the Biogenesis of KCNQ4 Channels', PLoS ONE. doi: 10.1371/journal.pone.0057282.

Gao, Z. et al. (2008) 'Desensitization of chemical activation by auxiliary subunits: convergence of molecular determinants critical for augmenting KCNQ1 potassium channels.', The Journal of biological chemistry, 283(33), pp. 22649–22658. doi: 10.1074/jbc.M802426200.

Gardener, M. J. et al. (2004) 'Functional evidence of a role for two-pore domain potassium channels in rat mesenteric and pulmonary arteries.', British journal of pharmacology, 142(1), pp. 192–202. doi: 10.1038/sj.bjp.0705691.

GARDOS, G. (1958) 'The function of calcium in the potassium permeability of human erythrocytes.', Biochimica et biophysica acta. Netherlands, 30(3), pp. 653–654. doi: 10.1016/0006-3002(58)90124-0.

Garland, C. J. and Dora, K. A. (2017) 'EDH: endothelium-dependent hyperpolarization and microvascular signalling', Acta Physiologica, pp. 152–161. doi: 10.1111/apha.12649.

Garry, A. et al. (2007) 'Altered acetylcholine, bradykinin and cutaneous pressure-induced vasodilation in mice lacking the TREK1 potassium channel: the endothelial link.', EMBO reports, 8(4), pp. 354–359. doi: 10.1038/sj.embor.7400916.

Gaudet, H. M. et al. (2015) 'The G-protein coupled estrogen receptor, GPER: The inside and inside-out story', Molecular and cellular endocrinology. Elsevier, 418, pp. 207–219.

Geary, G. G., Krause, D. N. and Duckles, S. P. (2000) 'Gonadal hormones affect diameter of male rat cerebral arteries through endothelium-dependent mechanisms', American Journal of Physiology - Heart and Circulatory Physiology, 279(2 48-2), pp. 610–618. doi: 10.1152/ajpheart.2000.279.2.h610.

Gebremedhin, D. et al. (1990) 'Enhanced vascular tone in the renal vasculature of spontaneously hypertensive rats.', Hypertension (Dallas, Tex. : 1979). United

States, 16(6), pp. 648–654. doi: 10.1161/01.hyp.16.6.648.

Gerlach, U. et al. (2001) 'Synthesis and activity of novel and selective Iks-channel blockers', Journal of Medicinal Chemistry. doi: 10.1021/jm0109255.

Ghatta, S. et al. (2006) 'Large-conductance, calcium-activated potassium channels: Structural and functional implications', Pharmacology & Therapeutics, 110(1), pp. 103–116. doi: https://doi.org/10.1016/j.pharmthera.2005.10.007.

Ghosh, S., Nunziato, D. A. and Pitt, G. S. (2006) 'KCNQ1 assembly and function is blocked by long-QT syndrome mutations that disrupt interaction with calmodulin', Circulation Research. doi: 10.1161/01.RES.0000218863.44140.f2.

Giachini, F. R. C. et al. (2009) 'Upregulation of intermediate calcium-activated potassium channels counterbalance the impaired endothelium-dependent vasodilation in stroke-prone spontaneously hypertensive rats.', Translational research : the journal of laboratory and clinical medicine, 154(4), pp. 183–193. doi: 10.1016/j.trsl.2009.07.003.

Giachini, F. R. C. et al. (2012) 'STIM1/Orai1 contributes to sex differences in vascular responses to calcium in spontaneously hypertensive rats.', Clinical science (London, England : 1979), 122(5), pp. 215–226. doi: 10.1042/CS20110312.

Giles, T. D. et al. (2009) 'Definition and classification of hypertension: an update.', Journal of clinical hypertension (Greenwich, Conn.), 11(11), pp. 611–614. doi: 10.1111/j.1751-7176.2009.00179.x.

Girouard, H. et al. (2010) 'Astrocytic endfoot Ca2+ and BK channels determine both arteriolar dilation and constriction.', Proceedings of the National Academy of Sciences of the United States of America, 107(8), pp. 3811–3816. doi: 10.1073/pnas.0914722107.

Glowatzki, E. et al. (1995) 'Subunit-dependent assembly of inward-rectifier K+ channels.', Proceedings. Biological sciences. England, 261(1361), pp. 251–261. doi: 10.1098/rspb.1995.0145.

Gluais, P. et al. (2005) 'Acetylcholine-induced endothelium-dependent contractions in the SHR aorta: The Janus face of prostacyclin', British Journal of Pharmacology. doi: 10.1038/sj.bjp.0706390.

Gögelein, H. et al. (2000) 'Inhibition of IKs channels by HMR 1556', Naunyn-Schmiedeberg's Archives of Pharmacology, 362(6), pp. 480–488. doi: 10.1007/s002100000284.

Goldstein, S. A. N. et al. (2005) 'International Union of Pharmacology. LV. Nomenclature and molecular relationships of two-P potassium channels.', Pharmacological reviews. United States, 57(4), pp. 527–540. doi: 10.1124/pr.57.4.12.

Goletiani, N. V, Keith, D. R. and Gorsky, S. J. (2007) 'Progesterone: review of safety for clinical studies.', Experimental and clinical psychopharmacology. United States,

15(5), pp. 427–444. doi: 10.1037/1064-1297.15.5.427.

Gollasch, M. (2017) 'Adipose-Vascular Coupling and Potential Therapeutics', Annual Review of Pharmacology and Toxicology. doi: 10.1146/annurev-pharmtox-010716-104542.

Golowasch, J., Kirkwood, A. and Miller, C. (1986) 'Allosteric effects of Mg2+ on the gating of Ca2+-activated K+ channels from mammalian skeletal muscle.', The Journal of experimental biology. England, 124, pp. 5–13.

González, C. et al. (2012) 'K(+) channels: function-structural overview.', Comprehensive Physiology. United States, 2(3), pp. 2087–2149. doi: 10.1002/cphy.c110047.

Goonetilleke, L. and Quayle, J. (2012) 'TREK-1 K(+) channels in the cardiovascular system: their significance and potential as a therapeutic target.', Cardiovascular therapeutics. England, 30(1), pp. e23-9. doi: 10.1111/j.1755-5922.2010.00227.x.

Goto, K. et al. (2004) 'Attenuation of conducted vasodilatation in rat mesenteric arteries during hypertension: role of inwardly rectifying potassium channels.', The Journal of physiology, 561(Pt 1), pp. 215–31. doi: 10.1113/jphysiol.2004.070458.

Goto, K., Ohtsubo, T. and Kitazono, T. (2018) 'Endothelium-Dependent Hyperpolarization (EDH) in Hypertension: The Role of Endothelial Ion Channels.', International journal of molecular sciences, 19(1). doi: 10.3390/ijms19010315.

Gou, X. et al. (2021) 'Specific protein kinase C isoform exerts chronic inhibition on the slowly activating delayed-rectifier potassium current by affecting channel trafficking.', Channels (Austin, Tex.), 15(1), pp. 262–272. doi: 10.1080/19336950.2021.1882112.

Gozalov, A. et al. (2007) 'Role of BK(Ca) channels in cephalic vasodilation induced by CGRP, NO and transcranial electrical stimulation in the rat.', Cephalalgia : an international journal of headache. England, 27(10), pp. 1120–1127. doi: 10.1111/j.1468-2982.2007.01409.x.

van de Graaf, S. F. J. et al. (2008) 'TRPV5 is internalized via clathrin-dependent endocytosis to enter a Ca2+-controlled recycling pathway.', The Journal of biological chemistry. United States, 283(7), pp. 4077–4086. doi: 10.1074/jbc.M706959200.

Grahammer, F et al. (2001) 'The cardiac K+ channel KCNQ1 is essential for gastric acid secretion.', Gastroenterology. United States, 120(6), pp. 1363–1371. doi: 10.1053/gast.2001.24053.

Grahammer, Florian et al. (2001) 'The small conductance K+ channel, KCNQ1: expression, function, and subunit composition in murine trachea', Journal of Biological Chemistry. ASBMB, 276(45), pp. 42268–42275.

Greenberg, H. Z. E. et al. (2016) 'Stimulation of calcium-sensing receptors induces endothelium-dependent vasorelaxations via nitric oxide production and activation

of IKCa channels', Vascular Pharmacology. doi: 10.1016/j.vph.2016.01.001.

Greene, D. L., Kang, S. and Hoshi, N. (2017) 'XE991 and linopirdine are state-dependent inhibitors for Kv7/KCNQ channels that favor activated single subunits', Journal of Pharmacology and Experimental Therapeutics. doi: 10.1124/jpet.117.241679.

Gros, R. et al. (2011) 'GPR30 expression is required for the mineralocorticoid receptor–independent rapid vascular effects of aldosterone', Hypertension. Am Heart Assoc, 57(3), pp. 442–451.

Gros, R. et al. (2013) 'Aldosterone mediates its rapid effects in vascular endothelial cells through GPER activation.', American journal of physiology. Cell physiology. United States, 304(6), pp. C532-40. doi: 10.1152/ajpcell.00203.2012.

Group, C. D. P. R. (1973) 'The Coronary Drug Project: findings leading to discontinuation of the 2.5 mg/day estrogen group', Jama, 226, pp. 652–657.

Gulbis, J. M. et al. (2000) 'Structure of the cytoplasmic beta subunit-T1 assembly of voltage-dependent K+ channels.', Science (New York, N.Y.). United States, 289(5476), pp. 123–127. doi: 10.1126/science.289.5476.123.

Gunst, S. J. and Zhang, W. (2008) 'Actin cytoskeletal dynamics in smooth muscle: A new paradigm for the regulation of smooth muscle contraction', American Journal of Physiology - Cell Physiology. doi: 10.1152/ajpcell.00253.2008.

Gurney, A. M. et al. (2003) 'Two-pore domain K channel, TASK-1, in pulmonary artery smooth muscle cells.', Circulation research. United States, 93(10), pp. 957–964. doi: 10.1161/01.RES.0000099883.68414.61.

Gurney, A. and Manoury, B. (2009) 'Two-pore potassium channels in the cardiovascular system.', European biophysics journal : EBJ. Germany, 38(3), pp. 305–318. doi: 10.1007/s00249-008-0326-8.

Gutman, G. A. et al. (2005) 'International Union of Pharmacology. LIII. Nomenclature and molecular relationships of voltage-gated potassium channels.', Pharmacological reviews. United States, 57(4), pp. 473–508. doi: 10.1124/pr.57.4.10.

Haas, E. et al. (2007) 'Differential effects of 17beta-estradiol on function and expression of estrogen receptor alpha, estrogen receptor beta, and GPR30 in arteries and veins of patients with atherosclerosis.', Hypertension (Dallas, Tex. : 1979). United States, 49(6), pp. 1358–1363. doi: 10.1161/HYPERTENSIONAHA.107.089995.

Haas, E. et al. (2009) 'Regulatory role of G protein-coupled estrogen receptor for vascular function and obesity.', Circulation research, 104(3), pp. 288–291. doi: 10.1161/CIRCRESAHA.108.190892.

Haavisto, A. M. et al. (1993) 'A supersensitive immunofluorometric assay for rat luteinizing hormone', Endocrinology. doi: 10.1210/endo.132.4.8462469.

Hagiwara, S. et al. (1978) 'Blocking effects of barium and hydrogen ions on the

potassium current during anomalous rectification in the starfish egg.', The Journal of Physiology. doi: 10.1113/jphysiol.1978.sp012338.

Hagiwara, S. and Takahashi, K. (1974) 'The anomalous rectification and cation selectivity of the membrane of a starfish egg cell.', The Journal of membrane biology. United States, 18(1), pp. 61–80. doi: 10.1007/BF01870103.

Haick, J. M. et al. (2017) 'PKC-dependent regulation of Kv7.5 channels by the bronchoconstrictor histamine in human airway smooth muscle cells.', American journal of physiology. Lung cellular and molecular physiology. United States, 312(6), pp. L822–L834. doi: 10.1152/ajplung.00567.2016.

Haick, J. M. and Byron, K. L. (2016) 'Novel treatment strategies for smooth muscle disorders: Targeting Kv7 potassium channels', Pharmacology and Therapeutics. doi: 10.1016/j.pharmthera.2016.05.002.

Haitin, Y. and Attali, B. (2008) 'The C-terminus of Kv7 channels: A multifunctional module', in Journal of Physiology, pp. 1803–1810. doi: 10.1113/jphysiol.2007.149187.

Hall, J. et al. (2006) 'Selective inhibition of L-type Ca2+ channels in A7r5 cells by physiological levels of testosterone.', Endocrinology. United States, 147(6), pp. 2675–2680. doi: 10.1210/en.2005-1243.

Hansen, H. H. et al. (2008) 'Kv7 channels: interaction with dopaminergic and serotonergic neurotransmission in the CNS.', The Journal of physiology, 586(7), pp. 1823–1832. doi: 10.1113/jphysiol.2007.149450.

Harada, N. et al. (1999) 'Localized expression of aromatase in human vascular tissues.', Circulation research. United States, 84(11), pp. 1285–1291. doi: 10.1161/01.res.84.11.1285.

Hardel, N. et al. (2008) 'Recycling endosomes supply cardiac pacemaker channels for regulated surface expression.', Cardiovascular research. England, 79(1), pp. 52–60. doi: 10.1093/cvr/cvn062.

Haron-Khun, S. et al. (2017) 'SK4 K(+) channels are therapeutic targets for the treatment of cardiac arrhythmias.', EMBO molecular medicine, 9(4), pp. 415–429. doi: 10.15252/emmm.201606937.

Hartshorne, D. J. and Hirano, K. (1999) 'Interactions of protein phosphatase type 1, with a focus on myosin phosphatase', Molecular and Cellular Biochemistry. doi: 10.1007/978-1-4615-5543-8_10.

Hartshorne, D. J., Ito, M. and Erdödi, F. (1998) 'Myosin light chain phosphatase: Subunit composition, interactions and regulation', Journal of Muscle Research and Cell Motility. doi: 10.1023/A:1005385302064.

Hartshorne, D. J., Ito, M. and Erdödi, F. (2004) 'Role of protein phosphatase type 1 in contractile functions: Myosin phosphatase', Journal of Biological Chemistry. doi:

10.1074/jbc.R400018200.

Hashemzadeh-Gargari, H. and Rembold, C. M. (1992) 'Histamine activates whole cell K+ currents in swine carotid arterial smooth muscle cell.', Comparative biochemistry and physiology. C, Comparative pharmacology and toxicology. England, 102(1), pp. 33–37. doi: 10.1016/0742-8413(92)90039-a.

Hayashi, Y. et al. (2001) 'Defining the Structural Determinants and a Potential Mechanism for Inhibition of Myosin Phosphatase by the Protein Kinase C-potentiated Inhibitor Protein of 17 kDa', Journal of Biological Chemistry. doi: 10.1074/jbc.M107302200.

He, Y. and Tabrizchi, R. (1997) 'Effects of niflumic acid on alpha1-adrenoceptor-induced vasoconstriction in mesenteric artery in vitro and in vivo in two-kidney one-clip hypertensive rats.', European journal of pharmacology. Netherlands, 328(2–3), pp. 191–199. doi: 10.1016/s0014-2999(97)83045-2.

Heginbotham, L. et al. (1994) 'Mutations in the K+ channel signature sequence.', Biophysical journal, 66(4), pp. 1061–1067. doi: 10.1016/S0006-3495(94)80887-2.

Hermida, R. C. et al. (2018) 'Hypertension: New perspective on its definition and clinical management by bedtime therapy substantially reduces cardiovascular disease risk.', European journal of clinical investigation. England, 48(5), p. e12909. doi: 10.1111/eci.12909.

Hernandez, C. C., Zaika, O. and Shapiro, M. S. (2008) 'A carboxy-terminal inter-helix linker as the site of phosphatidylinositol 4,5-bisphosphate action on Kv7 (M-type) K+ channels.', The Journal of general physiology, 132(3), pp. 361–381. doi: 10.1085/jgp.200810007.

Hibino, H. et al. (2010) 'Inwardly rectifying potassium channels: their structure, function, and physiological roles.', Physiological reviews. United States, 90(1), pp. 291–366. doi: 10.1152/physrev.00021.2009.

Hilgers, R. H. P. and Webb, R. C. (2007) 'Reduced expression of SKCa and IKCa channel proteins in rat small mesenteric arteries during angiotensin II-induced hypertension.', American journal of physiology. Heart and circulatory physiology. United States, 292(5), pp. H2275-84. doi: 10.1152/ajpheart.00949.2006.

Hirano, K. (2007) 'Current topics in the regulatory mechanism underlying the Ca2+ sensitization of the contractile apparatus in vascular smooth muscle', Journal of Pharmacological Sciences. doi: 10.1254/jphs.CP0070027.

Hirano, K., Phan, B. C. and Hartshorne, D. J. (1997) 'Interactions of the subunits of smooth muscle myosin phosphatase', Journal of Biological Chemistry. doi: 10.1074/jbc.272.6.3683.

Hirshman, C. A. and Emala, C. W. (1999) 'Actin reorganization in airway smooth muscle cells involves G(q) and G(i-2) activation of Rho', American Journal of Physiology -

Lung Cellular and Molecular Physiology. doi: 10.1152/ajplung.1999.277.3.l653.

Hiteshi, A. K. et al. (2014) 'Gender differences in coronary artery diameter are not related to body habitus or left ventricular mass.', Clinical cardiology, 37(10), pp. 605–609. doi: 10.1002/clc.22310.

Ho, K. et al. (1993) 'Cloning and expression of an inwardly rectifying ATP-regulated potassium channel.', Nature. England, 362(6415), pp. 31–38. doi: 10.1038/362031a0.

Hodgkin, A. L. and Huxley, A. F. (1947) 'Potassium leakage from an active nerve fibre.', The Journal of physiology, 106(3), pp. 341–367. doi: 10.1113/jphysiol.1947.sp004216.

HODGKIN, A. L. and HUXLEY, A. F. (1952a) 'A quantitative description of membrane current and its application to conduction and excitation in nerve.', The Journal of physiology, 117(4), pp. 500–544. doi: 10.1113/jphysiol.1952.sp004764.

HODGKIN, A. L. and HUXLEY, A. F. (1952b) 'Currents carried by sodium and potassium ions through the membrane of the giant axon of Loligo.', The Journal of physiology, 116(4), pp. 449–472. doi: 10.1113/jphysiol.1952.sp004717.

Hofmann, T. et al. (1999) 'Direct activation of human TRPC6 and TRPC3 channels by diacylglycerol.', Nature. England, 397(6716), pp. 259–263. doi: 10.1038/16711.

Hong, K. et al. (2016) 'Mechanical activation of angiotensin II type 1 receptors causes actin remodelling and myogenic responsiveness in skeletal muscle arterioles', Journal of Physiology. doi: 10.1113/JP272834.

van der Horst, J., Greenwood, I. A. and Jepps, T. A. (2020) 'Cyclic AMP-Dependent Regulation of Kv7 Voltage-Gated Potassium Channels.', Frontiers in physiology, 11, p. 727. doi: 10.3389/fphys.2020.00727.

Hoshi, N. et al. (2003) 'AKAP150 signaling complex promotes suppression of the M-current by muscarinic agonists.', Nature neuroscience, 6(6), pp. 564–571. doi: 10.1038/nn1062.

Hoshi, T., Zagotta, W. N. and Aldrich, R. W. (1991) 'Two types of inactivation in Shaker K+ channels: Effects of alterations in the carboxy-terminal region', Neuron. doi: 10.1016/0896-6273(91)90367-9.

Hou, P. et al. (2019) 'ML277 specifically enhances the fully activated open state of KCNQ1 by modulating VSD-pore coupling.', eLife, 8. doi: 10.7554/eLife.48576.

Howard, R. J. et al. (2007) 'Structural Insight into KCNQ (Kv7) Channel Assembly and Channelopathy', Neuron. doi: 10.1016/j.neuron.2007.02.010.

Howitt, L. et al. (2011) 'Differential effects of diet-induced obesity on BKCa {beta}1-subunit expression and function in rat skeletal muscle arterioles and small cerebral arteries.', American journal of physiology. Heart and circulatory physiology. United States, 301(1), pp. H29-40. doi: 10.1152/ajpheart.00134.2011.

Hu, Y. et al. (2013) ‘Triptans in prevention of menstrual migraine: a systematic review with meta-analysis.’, The journal of headache and pain, 14(1), p. 7. doi: 10.1186/1129-2377-14-7.

Hulley, S. et al. (1998) ‘Randomized trial of estrogen plus progestin for secondary prevention of coronary heart disease in postmenopausal women. Heart and Estrogen/progestin Replacement Study (HERS) Research Group.’, JAMA. United States, 280(7), pp. 605–613. doi: 10.1001/jama.280.7.605.

Hulley, S. et al. (2002) ‘Noncardiovascular disease outcomes during 6.8 years of hormone therapy: Heart and Estrogen/progestin Replacement Study follow-up (HERS II)’, Journal of the American Medical Association. doi: 10.1001/jama.288.1.58.

Hynes, D. and Harvey, B. J. (2019) ‘Dexamethasone reduces airway epithelial Cl(-) secretion by rapid non-genomic inhibition of KCNQ1, KCNN4 and KATP K(+) channels.’, Steroids. United States, 151, p. 108459. doi: 10.1016/j.steroids.2019.108459.

Iams, S. G. and Wexler, B. C. (1979) ‘Inhibition of the development of spontaneous hypertension in SH rats by gonadectomy or estradiol.’, The Journal of laboratory and clinical medicine.

Ilyin, V. I. et al. (2002) ‘Flupirtine–a positive modulator of heteromeric KCNQ2/3 channels’, in Soc Neurosci Abstr.

Inagaki, N. et al. (1995) ‘Cloning and Functional Characterization of a Novel ATP-sensitive Potassium Channel Ubiquitously Expressed in Rat Tissues, including Pancreatic Islets, Pituitary, Skeletal Muscle, and Heart (∗)’, Journal of Biological Chemistry. ASBMB, 270(11), pp. 5691–5694.

Inoue, R. et al. (2009) ‘Synergistic activation of vascular TRPC6 channel by receptor and mechanical stimulation via phospholipase C/diacylglycerol and phospholipase A2/omega-hydroxylase/20-HETE pathways.’, Circulation research. United States, 104(12), pp. 1399–1409. doi: 10.1161/CIRCRESAHA.108.193227.

Ipavec, V. et al. (2011) ‘KV7 channels regulate muscle tone and nonadrenergic noncholinergic relaxation of the rat gastric fundus.’, Pharmacological research, 64(4), pp. 397–409. doi: 10.1016/j.phrs.2011.06.016.

Isomoto, S. et al. (1996) ‘A novel sulfonylurea receptor forms with BIR (Kir6.2) a smooth muscle type ATP-sensitive K+ channel.’, The Journal of biological chemistry. United States, 271(40), pp. 24321–24324. doi: 10.1074/jbc.271.40.24321.

Jackson-Weaver, O. et al. (2011) ‘Intermittent hypoxia in rats increases myogenic tone through loss of hydrogen sulfide activation of large-conductance Ca(2+)-activated potassium channels.’, Circulation research, 108(12), pp. 1439–1447. doi: 10.1161/CIRCRESAHA.110.228999.

Jackson, W. F. et al. (1993) 'Prostacyclin-induced vasodilation in rabbit heart is mediated by ATP-sensitive potassium channels.', The American journal of physiology. United States, 264(1 Pt 2), pp. H238-43. doi: 10.1152/ajpheart.1993.264.1.H238.

Jackson, W. F. (1998) 'Potassium channels and regulation of the microcirculation.', Microcirculation (New York, N.Y. : 1994). United States, 5(2–3), pp. 85–90.

Jackson, W. F. (2018) 'K(V) channels and the regulation of vascular smooth muscle tone.', Microcirculation (New York, N.Y. : 1994), 25(1). doi: 10.1111/micc.12421.

Jackson, W. F. and Blair, K. L. (1998) 'Characterization and function of Ca(2+)-activated K+ channels in arteriolar muscle cells.', The American journal of physiology. United States, 274(1), pp. H27-34. doi: 10.1152/ajpheart.1998.274.1.H27.

Jackson, W. F., Huebner, J. M. and Rusch, N. J. (1997) 'Enzymatic isolation and characterization of single vascular smooth muscle cells from cremasteric arterioles.', Microcirculation (New York, N.Y. : 1994). United States, 4(1), pp. 35–50. doi: 10.3109/10739689709148316.

Jaimes, L. et al. (2019) 'A Review of the Actions of Endogenous and Exogenous Vasoactive Substances during the Estrous Cycle and Pregnancy in Rats.', Animals : an open access journal from MDPI, 9(6). doi: 10.3390/ani9060288.

Jepps, T. A. et al. (2009) 'Molecular and functional characterization of K v 7 K + channel in murine gastrointestinal smooth muscles', American Journal of Physiology-Gastrointestinal and Liver Physiology. doi: 10.1152/ajpgi.00057.2009.

Jepps, T. A. et al. (2011) 'Downregulation of Kv7.4 channel activity in primary and secondary hypertension', Circulation. doi: 10.1161/CIRCULATIONAHA.111.032136.

Jepps, T. A. et al. (2014) 'Vasorelaxant effects of novel Kv7.4 channel enhancers ML213 and NS15370', British Journal of Pharmacology, 171(19), pp. 4413–4424. doi: 10.1111/bph.12805.

Jepps, T. A. et al. (2015) 'Fundamental role for the KCNE4 ancillary subunit in Kv7.4 regulation of arterial tone', Journal of Physiology. doi: 10.1113/JP271286.

Jepps, T. A. et al. (2016) 'Molecular and functional characterization of Kv7 channels in penile arteries and corpus cavernosum of healthy and metabolic syndrome rats', British Journal of Pharmacology. doi: 10.1111/bph.13444.

Jepps, T. A. (2017) 'Unravelling the complexities of vascular smooth muscle ion channels: Fine tuning of activity by ancillary subunits.', Pharmacology & therapeutics. England, 178, pp. 57–66. doi: 10.1016/j.pharmthera.2017.03.010.

Jiao, J. et al. (2008) 'Protein kinase C-epsilon induces caveolin-dependent internalization of vascular adenosine 5'-triphosphate-sensitive K+ channels.', Hypertension (Dallas, Tex. : 1979). United States, 52(3), pp. 499–506. doi: 10.1161/HYPERTENSIONAHA.108.110817.

Jiménez-Pérez, L. et al. (2016) 'Molecular Determinants of Kv1.3 Potassium Channels-induced Proliferation.', The Journal of biological chemistry, 291(7), pp. 3569–3580. doi: 10.1074/jbc.M115.678995.

Johnson, R. P. et al. (2009) 'Identification and functional characterization of protein kinase A-catalyzed phosphorylation of potassium channel Kv1.2 at serine 449.', The Journal of biological chemistry, 284(24), pp. 16562–16574. doi: 10.1074/jbc.M109.010918.

Joshi, S. et al. (2009) 'KCNQ modulators reveal a key role for KCNQ potassium channels in regulating the tone of rat pulmonary artery smooth muscle.', The Journal of pharmacology and experimental therapeutics, 329(1), pp. 368–76. doi: 10.1124/jpet.108.147785.

Kajioka, S., Kitamura, K. and Kuriyama, H. (1991) 'Guanosine diphosphate activates an adenosine 5'-triphosphate-sensitive K+ channel in the rabbit portal vein.', The Journal of physiology, 444, pp. 397–418. doi: 10.1113/jphysiol.1991.sp018885.

Kamm, K. (1985) 'The Function of Myosin and Myosin Light Chain Kinase Phosphorylation in Smooth Muscle', Annual Review of Pharmacology and Toxicology. doi: 10.1146/annurev.pharmtox.25.1.593.

Kamm, K. E. and Stull, J. T. (2001) 'Dedicated myosin light chain kinases with diverse cellular functions.', The Journal of biological chemistry, 276(7), pp. 4527–30. doi: 10.1074/jbc.R000028200.

Kanashiro, C. A. and Khalil, R. A. (1998) 'Signal transduction by protein kinase C in mammalian cells', Clinical and Experimental Pharmacology and Physiology. doi: 10.1111/j.1440-1681.1998.tb02170.x.

Kanda, V. A. and Abbott, G. W. (2012) 'KCNE regulation of K+channel trafficking - A Sisyphean task?', Frontiers in Physiology. doi: 10.3389/fphys.2012.00231.

Karam, R. et al. (1998) 'Azimilide dihydrochloride, a novel antiarrhythmic agent.', The American journal of cardiology. United States, 81(6A), pp. 40D-46D. doi: 10.1016/s0002-9149(98)00152-0.

Karim, R. et al. (2005) 'Determinants of the effect of estrogen on the progression of subclinical atherosclerosis: Estrogen in the Prevention of Atherosclerosis Trial', Menopause. doi: 10.1097/01.GME.0000153934.76086.A4.

Karteris, E. et al. (2006) 'Progesterone signaling in human myometrium through two novel membrane G protein-coupled receptors: potential role in functional progesterone withdrawal at term', Molecular endocrinology. Oxford University Press, 20(7), pp. 1519–1534.

Katusic, Z. S., Santhanam, A. V. and He, T. (2012) 'Vascular effects of prostacyclin: Does activation of PPARδ play a role?', Trends in Pharmacological Sciences. doi: 10.1016/j.tips.2012.05.005.

Katz, B. (1949) ‘Les constantes électriques de la membrane du muscle.’, Arch. Sci. Physiol., 2, pp. 285–299.

Kauser, K. and Rubanyi, G. M. (1997) ‘Potential cellular signaling mechanisms mediating upregulation of endothelial nitric oxide production by estrogen.’, Journal of vascular research. Switzerland, 34(3), pp. 229–236. doi: 10.1159/000159227.

Kawano, Y. et al. (1999) ‘Phosphorylation of myosin-binding subunit (MBS) of myosin phosphatase by Rho-kinase in vivo’, Journal of Cell Biology. doi: 10.1083/jcb.147.5.1023.

Kawata, T. et al. (1998) ‘The K(ATP) channel opener nicorandil: effect on renal hemodynamics in spontaneously hypertensive and Wistar Kyoto rats.’, Kidney international. Supplement. United States, 67, pp. S231-3. doi: 10.1046/j.1523-1755.1998.06758.x.

Kerr, P. M. et al. (2001) ‘Heteromultimeric Kv1.2-Kv1.5 channels underlie 4-aminopyridine-sensitive delayed rectifier K(+) current of rabbit vascular myocytes.’, Circulation research, 89(11), pp. 1038–1044. doi: 10.1161/hh2301.100803.

Khanamiri, S. et al. (2013) ‘Contribution of KV7 channels to basal coronary flow and active response to ischemia’, Hypertension, 62(6), pp. 1090–1097. doi: 10.1161/HYPERTENSIONAHA.113.01244.

Kim, R. Y. et al. (2015) ‘Atomic basis for therapeutic activation of neuronal potassium channels.’, Nature communications, 6, p. 8116. doi: 10.1038/ncomms9116.

Kim, R. Y., Pless, S. A. and Kurata, H. T. (2017) ‘PIP2 mediates functional coupling and pharmacology of neuronal KCNQ channels.’, Proceedings of the National Academy of Sciences of the United States of America, 114(45), pp. E9702–E9711. doi: 10.1073/pnas.1705802114.

Kirkup, A. J. et al. (1996) ‘Modulation of membrane currents and mechanical activity by niflumic acid in rat vascular smooth muscle.’, European journal of pharmacology. Netherlands, 317(1), pp. 165–174. doi: 10.1016/s0014-2999(96)00713-3.

Kitazono, T., Heistad, D. D. and Faraci, F. M. (1993) ‘Role of ATP-sensitive K+ channels in CGRP-induced dilatation of basilar artery in vivo.’, The American journal of physiology. United States, 265(2 Pt 2), pp. H581-5. doi: 10.1152/ajpheart.1993.265.2.H581.

Klein, S. L. et al. (2015) ‘Opinion: Sex inclusion in basic research drives discovery.’, Proceedings of the National Academy of Sciences of the United States of America, 112(17), pp. 5257–5258. doi: 10.1073/pnas.1502843112.

Klinge, C. M. et al. (2005) ‘Resveratrol and estradiol rapidly activate MAPK signaling through estrogen receptors α and β in endothelial cells’, Journal of Biological Chemistry. ASBMB, 280(9), pp. 7460–7468.

Knaus, H. G. et al. (1994) ‘Covalent attachment of charybdotoxin to the beta-subunit of

the high conductance Ca(2+)-activated K+ channel. Identification of the site of incorporation and implications for channel topology.', The Journal of biological chemistry. United States, 269(37), pp. 23336–23341.

Knot, H. J., Zimmermann, P. A. and Nelson, M. T. (1996) 'Extracellular K(+)-induced hyperpolarizations and dilatations of rat coronary and cerebral arteries involve inward rectifier K(+) channels.', The Journal of physiology, 492 (Pt 2(Pt 2), pp. 419–430. doi: 10.1113/jphysiol.1996.sp021318.

Kobayashi, K. et al. (2011) 'Prostaglandin E2-prostanoid EP3 signal induces vascular contraction via nPKC and ROCK activation in rat mesenteric artery', European Journal of Pharmacology. doi: 10.1016/j.ejphar.2011.03.032.

Köhler, M. et al. (1996) 'Small-conductance, calcium-activated potassium channels from mammalian brain.', Science (New York, N.Y.). United States, 273(5282), pp. 1709–1714. doi: 10.1126/science.273.5282.1709.

Köhler, R. et al. (2000) 'Expression and function of endothelial Ca(2+)-activated K(+) channels in human mesenteric artery: A single-cell reverse transcriptase-polymerase chain reaction and electrophysiological study in situ.', Circulation research. United States, 87(6), pp. 496–503. doi: 10.1161/01.res.87.6.496.

Köhler, R. et al. (2001) 'Impaired hyperpolarization in regenerated endothelium after balloon catheter injury.', Circulation research. United States, 89(2), pp. 174–179. doi: 10.1161/hh1401.093460.

Kong, B. W. C. et al. (2015) 'Reduced activity of SKC a and Na-K ATPase underlies the accelerated impairment of EDH-type relaxations in mesenteric arteries of aging spontaneously hypertensive rats.', Pharmacology research & perspectives, 3(3), p. e00150. doi: 10.1002/prp2.150.

Kornstein, S. G. and Parker, A. J. (1997) 'Menstrual migraines: etiology, treatment, and relationship to premenstrual syndrome.', Current opinion in obstetrics & gynecology. England, 9(3), pp. 154–159.

Kow, L.-M. and Pfaff, D. W. (2016) 'Rapid estrogen actions on ion channels: A survey in search for mechanisms.', Steroids, 111, pp. 46–53. doi: 10.1016/j.steroids.2016.02.018.

Kubisch, C. et al. (1999) 'KCNQ4, a novel potassium channel expressed in sensory outer hair cells, is mutated in dominant deafness', Cell. doi: 10.1016/S0092-8674(00)80556-5.

Kubo, M. et al. (1994) 'Atrial natriuretic factor and isosorbide dinitrate modulate the gating of ATP-sensitive K+ channels in cultured vascular smooth muscle cells.', Circulation research. United States, 74(3), pp. 471–476. doi: 10.1161/01.res.74.3.471.

Kubo, M., Quayle, J. M. and Standen, N. B. (1997) 'Angiotensin II inhibition of ATP-

sensitive K+ currents in rat arterial smooth muscle cells through protein kinase C', The Journal of physiology. Wiley Online Library, 503(3), pp. 489–496.

Kubo, Y. et al. (1993) 'Primary structure and functional expression of a mouse inward rectifier potassium channel.', Nature. England, 362(6416), pp. 127–133. doi: 10.1038/362127a0.

Kubo, Y. et al. (2005) 'International Union of Pharmacology. LIV. Nomenclature and molecular relationships of inwardly rectifying potassium channels.', Pharmacological reviews. United States, 57(4), pp. 509–526. doi: 10.1124/pr.57.4.11.

Kunichika, N. et al. (2004) 'Overexpression of TRPC1 enhances pulmonary vasoconstriction induced by capacitative Ca2+ entry.', American journal of physiology. Lung cellular and molecular physiology. United States, 287(5), pp. L962-9. doi: 10.1152/ajplung.00452.2003.

Kurata, H. T. and Fedida, D. (2006) 'A structural interpretation of voltage-gated potassium channel inactivation', Progress in Biophysics and Molecular Biology. doi: 10.1016/j.pbiomolbio.2005.10.001.

Kurt, A. H. and Buyukafsar, K. (2013) 'Vasoconstriction induced by G1, a G-protein-coupled oestrogen receptor1 (GPER-1) agonist, in the isolated perfused rat kidney.', European journal of pharmacology. Netherlands, 702(1–3), pp. 71–78. doi: 10.1016/j.ejphar.2013.01.020.

Kwak, Y. G. et al. (1999) 'Protein kinase A phosphorylation alters Kvbeta1.3 subunit-mediated inactivation of the Kv1.5 potassium channel.', The Journal of biological chemistry. United States, 274(20), pp. 13928–13932. doi: 10.1074/jbc.274.20.13928.

Kwan, C. Y. et al. (1994) 'Effects of sarcoplasmic reticulum calcium pump inhibitors on vascular smooth muscle.', Hypertension (Dallas, Tex. : 1979). United States, 23(1 Suppl), pp. I156-60. doi: 10.1161/01.hyp.23.1_suppl.i156.

LANDAU, R. L. and LUGIBIHL, K. (1958) 'Inhibition of the sodium-retaining influence of aldosterone by progesterone', The Journal of clinical endocrinology and metabolism. doi: 10.1210/jcem-18-11-1237.

Lange, W. et al. (2009) 'Refinement of the binding site and mode of action of the anticonvulsant Retigabine on KCNQ K+ channels.', Molecular pharmacology. United States, 75(2), pp. 272–280. doi: 10.1124/mol.108.052282.

Langer, P., Gründer, S. and Rüsch, A. (2003) 'Expression of Ca2+-activated BK channel mRNA and its splice variants in the rat cochlea.', The Journal of comparative neurology. United States, 455(2), pp. 198–209. doi: 10.1002/cne.10471.

Larsen, A. P. et al. (2008) 'Characterization of hERG1a and hERG1b potassium channels-a possible role for hERG1b in the I (Kr) current.', Pflugers Archiv :

European journal of physiology. Germany, 456(6), pp. 1137–1148. doi: 10.1007/s00424-008-0476-7.

Larsson, H. P. et al. (1996) 'Transmembrane movement of the shaker K+ channel S4.', Neuron. United States, 16(2), pp. 387–397. doi: 10.1016/s0896-6273(00)80056-2.

Laughlin, G. A., Barrett-Connor, E. and Bergstrom, J. (2008) 'Low serum testosterone and mortality in older men.', The Journal of clinical endocrinology and metabolism, 93(1), pp. 68–75. doi: 10.1210/jc.2007-1792.

Lee, S. et al. (2015) 'Heterogeneity in Kv7 channel function in the cerebral and coronary circulation', Microcirculation. doi: 10.1111/micc.12183.

Lees-Miller, J. P. et al. (1997) 'Electrophysiological characterization of an alternatively processed ERG K+ channel in mouse and human hearts.', Circulation research. United States, 81(5), pp. 719–726. doi: 10.1161/01.res.81.5.719.

Leo, M. D. et al. (2014) 'Dynamic regulation of β1 subunit trafficking controls vascular contractility.', Proceedings of the National Academy of Sciences of the United States of America, 111(6), pp. 2361–2366. doi: 10.1073/pnas.1317527111.

Leo, M. D. et al. (2015) 'Angiotensin II stimulates internalization and degradation of arterial myocyte plasma membrane BK channels to induce vasoconstriction.', American journal of physiology. Cell physiology, 309(6), pp. C392-402. doi: 10.1152/ajpcell.00127.2015.

Leonhardt, S. A., Boonyaratanakornkit, V. and Edwards, D. P. (2003) 'Progesterone receptor transcription and non-transcription signaling mechanisms.', Steroids. United States, 68(10–13), pp. 761–770. doi: 10.1016/s0039-128x(03)00129-6.

Lerche, C. et al. (2000) 'Molecular cloning and functional expression of KCNQ5, a potassium channel subunit that may contribute to neuronal M-current diversity.', The Journal of biological chemistry. United States, 275(29), pp. 22395–22400. doi: 10.1074/jbc.M002378200.

Lerche, C. et al. (2007) 'Chromanol 293B binding in KCNQ1 (Kv7.1) channels involves electrostatic interactions with a potassium ion in the selectivity filter.', Molecular pharmacology. United States, 71(6), pp. 1503–1511. doi: 10.1124/mol.106.031682.

Lesage, F. et al. (1996) 'TWIK-1, a ubiquitous human weakly inward rectifying K+ channel with a novel structure.', The EMBO journal, 15(5), pp. 1004–1011.

Lesage, F. et al. (1997) 'The structure, function and distribution of the mouse TWIK-1 K+ channel.', FEBS letters. England, 402(1), pp. 28–32. doi: 10.1016/s0014-5793(96)01491-3.

Leung, F. P. et al. (2008) 'Store-operated calcium entry in vascular smooth muscle.', British journal of pharmacology, 153(5), pp. 846–857. doi: 10.1038/sj.bjp.0707455.

Li, J. et al. (2008) 'Interactions, functions, and independence of plasma membrane STIM1 and TRPC1 in vascular smooth muscle cells.', Circulation research, 103(8),

pp. e97-104. doi: 10.1161/CIRCRESAHA.108.182931.

Li, R.-S. et al. (2016) 'TMEM16A contributes to angiotensin II-induced cerebral vasoconstriction via the RhoA/ROCK signaling pathway.', Molecular medicine reports. Greece, 13(4), pp. 3691–3699. doi: 10.3892/mmr.2016.4979.

Li, R. et al. (2013) 'Reduced anti-contractile effect of perivascular adipose tissue on mesenteric small arteries from spontaneously hypertensive rats: role of Kv7 channels.', European journal of pharmacology. Netherlands, 698(1–3), pp. 310–315. doi: 10.1016/j.ejphar.2012.09.026.

Li, T. et al. (2021) 'Structural Basis for the Modulation of Human KCNQ4 by Small-Molecule Drugs', Molecular Cell. Elsevier Inc., 81(1), pp. 25-37.e4. doi: 10.1016/j.molcel.2020.10.037.

Li, Y. et al. (2005) 'Regulation of Kv7 (KCNQ) K+ channel open probability by phosphatidylinositol 4,5-bisphosphate.', The Journal of neuroscience : the official journal of the Society for Neuroscience, 25(43), pp. 9825–9835. doi: 10.1523/JNEUROSCI.2597-05.2005.

Lin, Y. and Smrcka, A. V (2011) 'Understanding molecular recognition by G protein βγ subunits on the path to pharmacological targeting', Molecular pharmacology. ASPET, 80(4), pp. 551–557.

Lindman, J. et al. (2018) 'Microtubule Regulation of Kv7 Channels Orchestrates cAMP-Mediated Vasorelaxations in Rat Arterial Smooth Muscle.', Hypertension (Dallas, Tex. : 1979). United States, 71(2), pp. 336–345. doi: 10.1161/HYPERTENSIONAHA.117.10152.

Lindsey, S. H. et al. (2009) 'Chronic treatment with the G protein-coupled receptor 30 agonist G-1 decreases blood pressure in ovariectomized mRen2.Lewis rats.', Endocrinology, 150(8), pp. 3753–3758. doi: 10.1210/en.2008-1664.

Lindsey, S. H., Liu, L. and Chappell, M. C. (2014) 'Vasodilation by GPER in mesenteric arteries involves both endothelial nitric oxide and smooth muscle cAMP signaling', Steroids. Elsevier, 81, pp. 99–102.

Lipton, R. B. and Bigal, M. E. (2005) 'Migraine: epidemiology, impact, and risk factors for progression.', Headache. United States, 45 Suppl 1, pp. S3–S13. doi: 10.1111/j.1526-4610.2005.4501001.x.

Di Lisa, F. and Bernardi, P. (2006) 'Mitochondria and ischemia-reperfusion injury of the heart: Fixing a hole', Cardiovascular Research. doi: 10.1016/j.cardiores.2006.01.016.

Liu, B. et al. (2012) 'Concomitant activation of functionally opposing prostacyclin and thromboxane prostanoid receptors by cyclo-oxygenase-1-mediated prostacyclin synthesis in mouse arteries', Experimental Physiology, 97(7), pp. 895–904. doi: 10.1113/expphysiol.2011.063784.

Liu, B. et al. (2017) ‘Increased role of e prostanoid receptor-3 in prostacyclin-evoked contractile activity of spontaneously hypertensive rat mesenteric resistance arteries’, Scientific Reports. doi: 10.1038/s41598-017-09288-w.

Liu, D. et al. (2009) ‘Increased transient receptor potential canonical type 3 channels in vasculature from hypertensive rats.’, Hypertension (Dallas, Tex. : 1979). United States, 53(1), pp. 70–76. doi: 10.1161/HYPERTENSIONAHA.108.116947.

Liu, D. et al. (2015) ‘A vasoconstrictor response to COX-1-mediated prostacyclin synthesis in young rat renal arteries that increases in prehypertensive conditions’, American Journal of Physiology - Heart and Circulatory Physiology. doi: 10.1152/ajpheart.00150.2015.

Liu, W., Lou, X. and Ma, L. (2016) ‘Use of 3D pseudo-continuous arterial spin labeling to characterize sex and age differences in cerebral blood flow.’, Neuroradiology. Germany, 58(9), pp. 943–948. doi: 10.1007/s00234-016-1713-y.

Livak, K. J. and Schmittgen, T. D. (2001) ‘Analysis of relative gene expression data using real-time quantitative PCR and the 2(-Delta Delta C(T)) Method.’, Methods (San Diego, Calif.). United States, 25(4), pp. 402–408. doi: 10.1006/meth.2001.1262.

Logsdon, N. J. et al. (1997) ‘A Novel Gene, hKCa4, Encodes the Calcium-activated Potassium Channel in Human T Lymphocytes*’, Journal of Biological Chemistry, 272(52), pp. 32723–32726. doi: https://doi.org/10.1074/jbc.272.52.32723.

Lombard, J. H. et al. (1999) ‘Electrical and mechanical responses of rat middle cerebral arteries to reduced PO2 and prostacyclin’, American Journal of Physiology - Heart and Circulatory Physiology. doi: 10.1152/ajpheart.1999.276.2.h509.

Longden, T. A. and Nelson, M. T. (2015) ‘Vascular inward rectifier K+ channels as external K+ sensors in the control of cerebral blood flow’, Microcirculation. doi: 10.1111/micc.12190.

Lopatin, A. N., Makhina, E. N. and Nichols, C. G. (1994) ‘Potassium channel block by cytoplasmic polyamines as the mechanism of intrinsic rectification.’, Nature. England, 372(6504), pp. 366–369. doi: 10.1038/372366a0.

Lopatin, A. N. and Nichols, C. G. (1996) ‘[K+] dependence of open-channel conductance in cloned inward rectifier potassium channels (IRK1, Kir2.1).’, Biophysical journal, 71(2), pp. 682–694. doi: 10.1016/S0006-3495(96)79268-8.

Lopes, C. M. B. et al. (2007) ‘Protein kinase A modulates PLC-dependent regulation and PIP2-sensitivity of K+ channels.’, Channels (Austin, Tex.). United States, 1(2), pp. 124–134. doi: 10.4161/chan.4322.

Lorigo, M. et al. (2020) ‘Vascular mechanisms of testosterone: The non-genomic point of view’, The Journal of Steroid Biochemistry and Molecular Biology, 196, p. 105496. doi: https://doi.org/10.1016/j.jsbmb.2019.105496.

Loukotová, J., Kunes, J. and Zicha, J. (2002) ‘Gender-dependent difference in cell

calcium handling in VSMC isolated from SHR: the effect of angiotensin II.', Journal of hypertension. England, 20(11), pp. 2213–2219. doi: 10.1097/00004872-200211000-00021.

Lu, Y. et al. (2002) 'Contributions of Kv1.2, Kv1.5 and Kv2.1 subunits to the native delayed rectifier K(+) current in rat mesenteric artery smooth muscle cells.', Life sciences. Netherlands, 71(12), pp. 1465–1473. doi: 10.1016/s0024-3205(02)01922-7.

Lu, Z., Klem, A. M. and Ramu, Y. (2001) 'Ion conduction pore is conserved among potassium channels.', Nature. England, 413(6858), pp. 809–813. doi: 10.1038/35101535.

Lu, Z. and MacKinnon, R. (1994) 'Electrostatic tuning of Mg2+ affinity in an inward-rectifier K+ channel.', Nature. England, 371(6494), pp. 243–246. doi: 10.1038/371243a0.

Luksha, L. et al. (2006) 'The oestrogen receptor beta contributes to sex related differences in endothelial function of murine small arteries via EDHF.', The Journal of physiology, 577(Pt 3), pp. 945–955. doi: 10.1113/jphysiol.2006.121939.

Lund-Johansen, P. (1980) 'Haemodynamics in essential hypertension.', Clinical science (London, England : 1979). England, 59 Suppl 6, pp. 343s-354s. doi: 10.1042/cs059343s.

Lundby, A. et al. (2008) 'KCNE3 mutation V17M identified in a patient with lone atrial fibrillation.', Cellular physiology and biochemistry : international journal of experimental cellular physiology, biochemistry, and pharmacology. Germany, 21(1–3), pp. 47–54. doi: 10.1159/000113746.

Luo, Y. et al. (2008) 'Blood Pressure Characterization of Hypertensive and Control Rats for Cardiovascular Studies', AHA Atlanta. Available at: http://www.criver.com/files/pdfs/rms/shr/rm_rm_r_08_bp_characterization_of_hypertensive_and.aspx.

Lutz, S. et al. (2005) 'The guanine nucleotide exchange factor p63RhoGEF, a specific link between Gq/11-coupled receptor signaling and RhoA', Journal of Biological Chemistry. doi: 10.1074/jbc.M411322200.

Ma, D. et al. (2020) 'The Functional Availability of Arterial Kv7 Channels Is Suppressed Considerably by Large-Conductance Calcium-Activated Potassium Channels in 2- to 3-Month Old but Not in 10- to 15-Day Old Rats.', Frontiers in physiology, 11, p. 597395. doi: 10.3389/fphys.2020.597395.

Ma, M. M. et al. (2017) 'TMEM16A Contributes to Endothelial Dysfunction by Facilitating Nox2 NADPH Oxidase-Derived Reactive Oxygen Species Generation in Hypertension', Hypertension, 69(5), pp. 892–901. doi: 10.1161/HYPERTENSIONAHA.116.08874.

MacGregor, E. A. and Hackshaw, A. (2004) 'Prevalence of migraine on each day of the natural menstrual cycle.', Neurology. United States, 63(2), pp. 351–353. doi: 10.1212/01.wnl.0000133134.68143.2e.

Mackie, A. R. et al. (2008) 'Vascular KCNQ potassium channels as novel targets for the control of mesenteric artery constriction by vasopressin, based on studies in single cells, pressurized arteries, and in vivo measurements of mesenteric vascular resistance', Journal of Pharmacology and Experimental Therapeutics. doi: 10.1124/jpet.107.135764.

Main, M. J. et al. (2000) 'Modulation of KCNQ2/3 potassium channels by the novel anticonvulsant retigabine', Molecular Pharmacology. doi: 10.1124/mol.58.2.253.

Maingret, F. et al. (2002) 'Molecular basis of the voltage-dependent gating of TREK-1, a mechano-sensitive K(+) channel.', Biochemical and biophysical research communications. United States, 292(2), pp. 339–346. doi: 10.1006/bbrc.2002.6674.

Maiti, K. et al. (2011) 'G-1-activated membrane estrogen receptors mediate increased contractility of the human myometrium.', Endocrinology. United States, 152(6), pp. 2448–2455. doi: 10.1210/en.2010-0979.

Mall, M. et al. (2000) 'Role of KVLQT1 in Cyclic Adenosine Monophosphate–Mediated Cl− Secretion in Human Airway Epithelia', American Journal of Respiratory Cell and Molecular Biology. American Thoracic Society New York, NY, 23(3), pp. 283–289.

Mani, B. K. et al. (2011) 'Activation of vascular KCNQ (Kv7) potassium channels reverses spasmogen-induced constrictor responses in rat basilar artery.', British journal of pharmacology, 164(2), pp. 237–249. doi: 10.1111/j.1476-5381.2011.01273.x.

Mani, B. K. et al. (2013) 'Vascular KCNQ (Kv7) potassium channels as common signaling intermediates and therapeutic targets in cerebral vasospasm', Journal of Cardiovascular Pharmacology. doi: 10.1097/FJC.0b013e3182771708.

Mani, B. K. et al. (2016) 'Kv7.5 Potassium Channel Subunits Are the Primary Targets for PKA-Dependent Enhancement of Vascular Smooth Muscle Kv7 Currents', Molecular Pharmacology, 89(3), pp. 323–334. doi: 10.1124/mol.115.101758.

Mannuzzu, L. M., Moronne, M. M. and Isacoff, E. Y. (1996) 'Direct physical measure of conformational rearrangement underlying potassium channel gating.', Science (New York, N.Y.). United States, 271(5246), pp. 213–216. doi: 10.1126/science.271.5246.213.

Manoury, B., Tamuleviciute, A. and Tammaro, P. (2010) 'TMEM16A/anoctamin 1 protein mediates calcium-activated chloride currents in pulmonary arterial smooth muscle cells.', The Journal of physiology, 588(Pt 13), pp. 2305–14. doi: 10.1113/jphysiol.2010.189506.

Manville, R. W., Neverisky, D. L. and Abbott, G. W. (2017) 'SMIT1 Modifies KCNQ Channel Function and Pharmacology by Physical Interaction with the Pore.',

Biophysical journal, 113(3), pp. 613–626. doi: 10.1016/j.bpj.2017.06.055.

Maris, M. E. et al. (2005) 'Gender differences in blood pressure and heart rate in spontaneously hypertensive and Wistar-Kyoto rats', Clinical and Experimental Pharmacology and Physiology. doi: 10.1111/j.1440-1681.2005.04156.x.

Martens, J. R. and Gelband, C. H. (1996) 'Alterations in rat interlobar artery membrane potential and K+ channels in genetic and nongenetic hypertension.', Circulation research. United States, 79(2), pp. 295–301. doi: 10.1161/01.res.79.2.295.

Martín-Aragón Baudel, M. A. S. et al. (2020) 'Obligatory role for PKCδ in PIP(2) - mediated activation of store-operated TRPC1 channels in vascular smooth muscle cells.', The Journal of physiology, 598(18), pp. 3911–3925. doi: 10.1113/JP279947.

Martire, M. et al. (2004) 'M channels containing KCNQ2 subunits modulate norepinephrine, aspartate, and GABA release from hippocampal nerve terminals.', The Journal of neuroscience : the official journal of the Society for Neuroscience, 24(3), pp. 592–597. doi: 10.1523/JNEUROSCI.3143-03.2004.

Marty, A. (1981) 'Ca-dependent K channels with large unitary conductance in chromaffin cell membranes', Nature, 291(5815), pp. 497–500. doi: 10.1038/291497a0.

Marx, S. O. et al. (2002) 'Requirement of a macromolecular signaling complex for β adrenergic receptor modulation of the KCNQ1-KCNE1 potassium channel', Science. American Association for the Advancement of Science, 295(5554), pp. 496–499.

Masuda, K. et al. (2018) 'Testosterone-mediated upregulation of delayed rectifier potassium channel in cardiomyocytes causes abbreviation of QT intervals in rats', Journal of Physiological Sciences. doi: 10.1007/s12576-017-0590-4.

Mathiisen, T. M. et al. (2010) 'The perivascular astroglial sheath provides a complete covering of the brain microvessels: an electron microscopic 3D reconstruction.', Glia. United States, 58(9), pp. 1094–1103. doi: 10.1002/glia.20990.

Matsuda, K. et al. (2002) 'Colocalization and ligand-dependent discrete distribution of the estrogen receptor (ER) α and ERβ', Molecular Endocrinology. Oxford University Press, 16(10), pp. 2215–2230.

Mazzuca, M. Q. et al. (2015) 'Estrogen receptor subtypes mediate distinct microvascular dilation and reduction in [Ca2+]I in mesenteric microvessels of female rat.', The Journal of pharmacology and experimental therapeutics, 352(2), pp. 291–304. doi: 10.1124/jpet.114.219865.

McCallum, L. A. et al. (2011) 'The contribution of Kv7 channels to pregnant mouse and human myometrial contractility.', Journal of cellular and molecular medicine, 15(3), pp. 577–586. doi: 10.1111/j.1582-4934.2010.01021.x.

McCallum, L. A., Greenwood, I. A. and Tribe, R. M. (2008) 'Expression and function of Kv7 channels in murine myometrium throughout oestrous cycle', Pflügers Archiv -

European Journal of Physiology, 457(5), p. 1111. doi: 10.1007/s00424-008-0567-5.

McCallum, L. A., Greenwood, I. A. and Tribe, R. M. (2009) 'Expression and function of Kv7 channels in murine myometrium throughout oestrous cycle', Pflugers Archiv European Journal of Physiology. doi: 10.1007/s00424-008-0567-5.

McCobb, D. P. et al. (1995) 'A human calcium-activated potassium channel gene expressed in vascular smooth muscle.', The American journal of physiology. United States, 269(3 Pt 2), pp. H767-77. doi: 10.1152/ajpheart.1995.269.3.H767.

McCrohon, J. A. et al. (1997) 'Arterial reactivity is enhanced in genetic males taking high dose estrogens.', Journal of the American College of Cardiology. United States, 29(7), pp. 1432–1436. doi: 10.1016/s0735-1097(97)00063-6.

McCrossan, Z. A. and Abbott, G. W. (2004) 'The MinK-related peptides', Neuropharmacology. doi: 10.1016/j.neuropharm.2004.06.018.

McGahon, M. K. et al. (2007) 'Kv1.5 is a major component underlying the A-type potassium current in retinal arteriolar smooth muscle.', American journal of physiology. Heart and circulatory physiology, 292(2), pp. H1001-8. doi: 10.1152/ajpheart.01003.2006.

McGuire, J. J., Ding, H. and Triggle, C. R. (2001) 'Endothelium-derived relaxing factors: A focus on endothelium-derived hyperpolarizing factor(s)', Canadian Journal of Physiology and Pharmacology. doi: 10.1139/y01-025.

McManus, O. B. et al. (1995) 'Functional role of the beta subunit of high conductance calcium-activated potassium channels.', Neuron. United States, 14(3), pp. 645–650. doi: 10.1016/0896-6273(95)90321-6.

Meech, R. W. and STRUMWAS., F. (1970) 'Intracellular calcium injection activates potassium conductance in Aplysia nerve cells', in Federation Proceedings. FEDERATION AMER SOC EXP BIOL 9650 ROCKVILLE PIKE, BETHESDA, MD 20814-3998 USA, pp. A834-+.

Meera, P. et al. (1996) 'A calcium switch for the functional coupling between alpha (hslo) and beta subunits (KV,Ca beta) of maxi K channels.', FEBS letters. England, 382(1–2), pp. 84–88. doi: 10.1016/0014-5793(96)00151-2.

Messerli, F. H., Williams, B. and Ritz, E. (2007) 'Essential hypertension.', Lancet (London, England). England, 370(9587), pp. 591–603. doi: 10.1016/S0140-6736(07)61299-9.

Meyer, M. R. et al. (2009) 'Non-genomic regulation of vascular cell function and growth by estrogen.', Molecular and cellular endocrinology, 308(1–2), pp. 9–16. doi: 10.1016/j.mce.2009.03.009.

Meyer, M. R. et al. (2010) 'Dilation of epicardial coronary arteries by the G protein-coupled estrogen receptor agonists G-1 and ICI 182,780.', Pharmacology, 86(1),

pp. 58–64. doi: 10.1159/000315497.

Meyer, M. R. et al. (2012) ‘GPER regulates endothelin-dependent vascular tone and intracellular calcium.’, Life sciences, 91(13–14), pp. 623–627. doi: 10.1016/j.lfs.2012.01.007.

Miceli, F. et al. (1993) ‘KCNQ2-Related Disorders.’, in Adam, M. P. et al. (eds). Seattle (WA).

Michel, F. S., Man, R. Y. K. and Vanhoutte, P. M. (2007) ‘Increased spontaneous tone in renal arteries of spontaneously hypertensive rats.’, American journal of physiology. Heart and circulatory physiology. United States, 293(3), pp. H1673-81. doi: 10.1152/ajpheart.00289.2007.

Miki, T. et al. (2002) ‘Mouse model of Prinzmetal angina by disruption of the inward rectifier Kir6. 1’, Nature medicine. Nature Publishing Group, 8(5), pp. 466–472.

Mills, T. A. et al. (2015) ‘Activation of K<inf>V</inf>7 channels stimulates vasodilatation of human placental chorionic plate arteries’, Placenta, 36(6), pp. 638–644. doi: 10.1016/j.placenta.2015.03.007.

Mimuro, T. et al. (1998) ‘The attenuated effect of ATP-sensitive K+ channel opener pinacidil on renal haemodynamics in spontaneously hypertensive rats.’, European journal of pharmacology. Netherlands, 358(2), pp. 153–160. doi: 10.1016/s0014-2999(98)00573-1.

Ming, Z., Parent, R. and Lavallée, M. (1997) ‘Beta 2-adrenergic dilation of resistance coronary vessels involves KATP channels and nitric oxide in conscious dogs.’, Circulation. United States, 95(6), pp. 1568–1576. doi: 10.1161/01.cir.95.6.1568.

Mishra, J. S. et al. (2019) ‘Testosterone plays a permissive role in angiotensin II-induced hypertension and cardiac hypertrophy in male rats’, Biology of reproduction. Oxford University Press, 100(1), pp. 139–148.

Miyazaki, S. I. et al. (1974) ‘Analysis of non-linearity observed in the current-voltage relation of the tunicate embryo.’, The Journal of physiology, 238(1), pp. 55–77. doi: 10.1113/jphysiol.1974.sp010510.

Möller, C. and Netzer, R. (2006) ‘Effects of estradiol on cardiac ion channel currents.’, European journal of pharmacology. Netherlands, 532(1–2), pp. 44–49. doi: 10.1016/j.ejphar.2006.01.006.

Moncada, S. et al. (1976) ‘An enzyme isolated from arteries transforms prostaglandin endoperoxides to an unstable substance that inhibits platelet aggregation’, Nature. doi: 10.1038/263663a0.

Mondéjar-Parreño, G. et al. (2019) ‘Activation of Kv7 channels as a novel mechanism for NO/cGMP-induced pulmonary vasodilation’, British Journal of Pharmacology. doi: 10.1111/bph.14662.

Mondéjar-Parreño, G. et al. (2020) ‘Uncovered Contribution of Kv7 Channels to

Pulmonary Vascular Tone in Pulmonary Arterial Hypertension.', Hypertension (Dallas, Tex.: 1979). United States, 76(4), pp. 1134–1146. doi: 10.1161/HYPERTENSIONAHA.120.15221.

Morales-Cano, D. et al. (2015) 'Kv7 channels critically determine coronary artery reactivity: Left-right differences and down-regulation by hyperglycaemia', Cardiovascular Research, 106(1), pp. 98–108. doi: 10.1093/cvr/cvv020.

MOREY, K. A. et al. (1998) 'Oestrogen and progesterone inhibit the stimulated production of endothelin-1', Biochemical Journal. doi: 10.1042/bj3301097.

Mosca, L., Barrett-Connor, E. and Wenger, N. K. (2011) 'Sex/gender differences in cardiovascular disease prevention: what a difference a decade makes.', Circulation, 124(19), pp. 2145–2154. doi: 10.1161/CIRCULATIONAHA.110.968792.

Mulvany, M. (1977) 'Contractile properties of small arterial resistance vessels in spontaneously hypertensive and normotensive rats', Circulation Research, 41, pp. 19–26. doi: 10.1161/01.

Murphy, M. E. and Brayden, J. E. (1995) 'Nitric oxide hyperpolarizes rabbit mesenteric arteries via ATP-sensitive potassium channels.', The Journal of physiology, 486 (Pt 1(Pt 1), pp. 47–58. doi: 10.1113/jphysiol.1995.sp020789.

Nakamura, T. et al. (1988) 'Effects of pregnancy and hormone treatments on pressor response to angiotensin II in conscious rats', American Journal of Obstetrics and Gynecology. doi: 10.1016/S0002-9378(88)80186-8.

Namkoong, S. et al. (2005) 'Prostaglandin E2 stimulates angiogenesis by activating the nitric oxide/cGMP pathway in human umbilical vein endothelial cells', Experimental and Molecular Medicine. doi: 10.1038/emm.2005.72.

Nara, M. et al. (1998) 'Reconstitution of beta-adrenergic modulation of large conductance, calcium-activated potassium (maxi-K) channels in Xenopus oocytes. Identification of the camp-dependent protein kinase phosphorylation site.', The Journal of biological chemistry. United States, 273(24), pp. 14920–14924. doi: 10.1074/jbc.273.24.14920.

Nelson, M. T. (1993) 'Ca(2+)-activated potassium channels and ATP-sensitive potassium channels as modulators of vascular tone.', Trends in cardiovascular medicine. United States, 3(2), pp. 54–60. doi: 10.1016/1050-1738(93)90037-7.

Nelson, M. T. et al. (1997) 'Chloride channel blockers inhibit myogenic tone in rat cerebral arteries.', The Journal of physiology, 502 (Pt 2, pp. 259–64.

New, G. et al. (2000) 'Long-term oestrogen therapy is associated with improved endothelium-dependent vasodilation in the forearm resistance circulation of biological males.', Clinical and experimental pharmacology & physiology. Australia, 27(1–2), pp. 25–33. doi: 10.1046/j.1440-1681.2000.03195.x.

Neylon, C. B. et al. (1999) 'Molecular cloning and characterization of the intermediate-conductance Ca(2+)-activated K(+) channel in vascular smooth muscle: relationship between K(Ca) channel diversity and smooth muscle cell function.', Circulation research. United States, 85(9), pp. e33-43. doi: 10.1161/01.res.85.9.e33.

Neyroud, N. et al. (1997) 'A novel mutation in the potassium channel gene KVLQT1 causes the Jervell and Lange-Nielsen cardioauditory syndrome', Nature Genetics. doi: 10.1038/ng0297-186.

Ng, F. L. et al. (2011) 'Expression and function of the K + channel KCNQ genes in human arteries', British Journal of Pharmacology, 162(1), pp. 42–53. doi: 10.1111/j.1476-5381.2010.01027.x.

Nichols, C. G., Ho, K. and Hebert, S. (1994) 'Mg(2+)-dependent inward rectification of ROMK1 potassium channels expressed in Xenopus oocytes.', The Journal of physiology, 476(3), pp. 399–409. doi: 10.1113/jphysiol.1994.sp020141.

Nickenig, G. et al. (2000) 'Differential effects of estrogen and progesterone on AT(1) receptor gene expression in vascular smooth muscle cells.', Circulation. United States, 102(15), pp. 1828–1833. doi: 10.1161/01.cir.102.15.1828.

Nilius, B., Schwarz, G. and Droogmans, G. (1993) 'Modulation by histamine of an inwardly rectifying potassium channel in human endothelial cells.', The Journal of physiology, 472, pp. 359–371. doi: 10.1113/jphysiol.1993.sp019951.

Nilsson, M. E. et al. (2015) 'Measurement of a Comprehensive Sex Steroid Profile in Rodent Serum by High-Sensitive Gas Chromatography-Tandem Mass Spectrometry.', Endocrinology. United States, 156(7), pp. 2492–2502. doi: 10.1210/en.2014-1890.

Noma, A. (1983) 'ATP-regulated K+ channels in cardiac muscle', Nature. Nature Publishing Group, 305(5930), pp. 147–148.

Norel, X. (2007) 'Prostanoid receptors in the human vascular wall.', TheScientificWorldJournal, 7, pp. 1359–1374. doi: 10.1100/tsw.2007.184.

Novak, K. and Kaufman, S. (2017) 'Effects of pregnancy, estradiol, and progesterone on pressor responsiveness to angiotensin II', American Journal of Physiology-Regulatory, Integrative and Comparative Physiology. doi: 10.1152/ajpregu.1991.261.5.r1164.

Novella, S. et al. (2019) 'Mechanisms underlying the influence of oestrogen on cardiovascular physiology in women', Journal of Physiology, 597(19), pp. 4873–4886. doi: 10.1113/JP278063.

Nystoriak, M. A. et al. (2017) 'Heteromeric complexes of aldo-keto reductase auxiliary K(V)β subunits (AKR6A) regulate sarcolemmal localization of K(V)1.5 in coronary arterial myocytes.', Chemico-biological interactions, 276, pp. 210–217. doi:

10.1016/j.cbi.2017.03.011.

O'Mahony, F. et al. (2007) 'Female gender-specific inhibition of KCNQ1 channels and chloride secretion by 17β-estradiol in rat distal colonic crypts', Journal of Biological Chemistry. doi: 10.1074/jbc.M611682200.

O'Mahony, F. et al. (2009) 'Genomic priming of the antisecretory response to estrogen in rat distal colon throughout the estrous cycle.', Molecular endocrinology (Baltimore, Md.), 23(11), pp. 1885–1899. doi: 10.1210/me.2008-0248.

Obenauer, J. C., Cantley, L. C. and Yaffe, M. B. (2003) 'Scansite 2.0: Proteome-wide prediction of cell signaling interactions using short sequence motifs.', Nucleic acids research, 31(13), pp. 3635–3641. doi: 10.1093/nar/gkg584.

Ohanian, V., Gatfield, K. and Ohanian, J. (2005) 'Role of the actin cytoskeleton in G-protein-coupled receptor activation of PYK2 and paxillin in vascular smooth muscle', Hypertension. doi: 10.1161/01.HYP.0000167990.82235.3c.

Ohya, S. et al. (2003) 'Molecular variants of KCNQ channels expressed in murine portal vein myocytes: A role in delayed rectifier current', Circulation Research. doi: 10.1161/01.RES.0000070880.20955.F4.

Oliveras, A. et al. (2014) 'Functional assembly of Kv7.1/Kv7.5 channels with emerging properties on vascular muscle physiology', Arteriosclerosis, Thrombosis, and Vascular Biology. doi: 10.1161/ATVBAHA.114.303801.

Orie, N. N. and Clapp, L. H. (2011) 'Role of prostanoid IP and EP receptors in mediating vasorelaxant responses to PGI2 analogues in rat tail artery: Evidence for Gi/o modulation via EP3 receptors', European Journal of Pharmacology. doi: 10.1016/j.ejphar.2010.12.005.

Orie, N. N., Fry, C. H. and Clapp, L. H. (2006) 'Evidence that inward rectifier K+ channels mediate relaxation by the PGI2 receptor agonist cicaprost via a cyclic AMP-independent mechanism', Cardiovascular Research. doi: 10.1016/j.cardiores.2005.08.004.

Osol, G. et al. (2002) 'Myogenic tone, reactivity, and forced dilatation : a three- phase model of in vitro arterial myogenic behavior', American journal of physiology. Heart and circulatory physiology. doi: 10.1152/ajpheart.00634.2002.

Otsuka, K. et al. (2002) 'Functional contribution of voltage-dependent and Ca2+ activated K+ (BK(Ca)) channels to the relaxation of guinea-pig aorta in response to natriuretic peptides.', Journal of smooth muscle research = Nihon Heikatsukin Gakkai kikanshi. Japan, 38(4–5), pp. 117–129. doi: 10.1540/jsmr.38.117.

Owen, N. E. (1984) 'Regulation of Na/K/Cl cotransport in vascular smooth muscle cells.', Biochemical and biophysical research communications. United States, 125(2), pp. 500–508. doi: 10.1016/0006-291x(84)90568-0.

Pabbidi, M. R. et al. (2018) 'Sex differences in the vascular function and related

mechanisms: role of 17β-estradiol', American Journal of Physiology-Heart and Circulatory Physiology. American Physiological Society, 315(6), pp. H1499–H1518. doi: 10.1152/ajpheart.00194.2018.

Padilla, K. et al. (2009) 'The KCNQ2/3 selective channel opener ICA-27243 binds to a novel voltage-sensor domain site.', Neuroscience letters. Ireland, 465(2), pp. 138–142. doi: 10.1016/j.neulet.2009.08.071.

Pang, Y., Dong, J. and Thomas, P. (2015) 'Progesterone increases nitric oxide synthesis in human vascular endothelial cells through activation of membrane progesterone receptor-α.', American journal of physiology. Endocrinology and metabolism. United States, 308(10), pp. E899-911. doi: 10.1152/ajpendo.00527.2014.

Pant, S. et al. (2021) 'PIP(2)-dependent coupling of voltage sensor and pore domains in K(v)7.2 channel.', Communications biology, 4(1), p. 1189. doi: 10.1038/s42003-021-02729-3.

Panten, U. et al. (1989) 'Control of insulin secretion by sulfonylureas, meglitinide and diazoxide in relation to their binding to the sulfonylurea receptor in pancreatic islets.', Biochemical pharmacology. England, 38(8), pp. 1217–1229. doi: 10.1016/0006-2952(89)90327-4.

Park, K.-H. et al. (2005) 'Impaired KCNQ1-KCNE1 and phosphatidylinositol-4,5-bisphosphate interaction underlies the long QT syndrome.', Circulation research. United States, 96(7), pp. 730–739. doi: 10.1161/01.RES.0000161451.04649.a8.

Park, W. S. et al. (2005) 'Endothelin-1 acts via protein kinase C to block KATP channels in rabbit coronary and pulmonary arterial smooth muscle cells.', Journal of cardiovascular pharmacology. United States, 45(2), pp. 99–108. doi: 10.1097/01.fjc.0000150442.49051.f7.

Parsons, S. J. W. et al. (1994) 'The relative importance of nitric oxide and nitric oxide-independent mechanisms in acetylcholine-evoked dilatation of the rat mesenteric bed', British Journal of Pharmacology. doi: 10.1111/j.1476-5381.1994.tb17136.x.

Partiseti, M. et al. (1992) 'Differential regulation of voltage- and calcium-activated potassium channels in human B lymphocytes.', Journal of immunology (Baltimore, Md. : 1950). United States, 148(11), pp. 3361–3368.

Patel, A. J. et al. (1998) 'A mammalian two pore domain mechano-gated S-like K+ channel.', The EMBO journal, 17(15), pp. 4283–4290. doi: 10.1093/emboj/17.15.4283.

Patel, M. B. et al. (2016) 'Imaging Microvascular Dysfunction and Mechanisms for Female-Male Differences in CAD.', JACC. Cardiovascular imaging. United States, 9(4), pp. 465–482. doi: 10.1016/j.jcmg.2016.02.003.

Peppiatt-Wildman, C. M. et al. (2007) 'Endothelin-1 activates a Ca2+-permeable cation channel with TRPC3 and TRPC7 properties in rabbit coronary artery myocytes.',

The Journal of physiology, 580(Pt.3), pp. 755–764. doi: 10.1113/jphysiol.2006.126656.

Peredo, H. A., Feleder, E. C. and Adler-Graschinsky, E. (1997) 'Differential effects of acetylcholine and bradykinin on prostanoid release from the rat mesenteric bed: Role of endothelium and of nitric oxide', Prostaglandins Leukotrienes and Essential Fatty Acids. doi: 10.1016/S0952-3278(97)90567-6.

Peretz, A. et al. (2005) 'Meclofenamic acid and diclofenac, novel templates of KCNQ2/Q3 potassium channel openers, depress cortical neuron activity and exhibit anticonvulsant properties.', Molecular pharmacology. United States, 67(4), pp. 1053–1066. doi: 10.1124/mol.104.007112.

Peretz, A. et al. (2010) 'Targeting the voltage sensor of Kv7.2 voltage-gated K+ channels with a new gating-modifier.', Proceedings of the National Academy of Sciences of the United States of America, 107(35), pp. 15637–15642. doi: 10.1073/pnas.0911294107.

Peroz, D. et al. (2008) 'Kv7.1 (KCNQ1) properties and channelopathies.', The Journal of physiology, 586(7), pp. 1785–1789. doi: 10.1113/jphysiol.2007.148254.

Plane, F. et al. (2005) 'Heteromultimeric Kv1 channels contribute to myogenic control of arterial diameter.', Circulation research. United States, 96(2), pp. 216–224. doi: 10.1161/01.RES.0000154070.06421.25.

Plüger, S. et al. (2000) 'Mice with disrupted BK channel beta1 subunit gene feature abnormal Ca(2+) spark/STOC coupling and elevated blood pressure.', Circulation research. United States, 87(11), pp. E53-60. doi: 10.1161/01.res.87.11.e53.

Povstyan, O. V. et al. (2017) 'Synergistic interplay of Gβγ and phosphatidylinositol 4,5-bisphosphate dictates Kv7.4 channel activity', Pflugers Archiv European Journal of Physiology. doi: 10.1007/s00424-016-1916-4.

Prossnitz, E. R. and Barton, M. (2011) 'The G-protein-coupled estrogen receptor GPER in health and disease.', Nature reviews. Endocrinology, 7(12), pp. 715–726. doi: 10.1038/nrendo.2011.122.

Purtell, K. et al. (2012) 'The KCNQ1-KCNE2 K+ channel is required for adequate thyroid I− uptake.', FASEB journal : official publication of the Federation of American Societies for Experimental Biology, 26(8), pp. 3252–3259. doi: 10.1096/fj.12-206110.

Qin, J. et al. (2015) 'Sexually dimorphic phenotype of arteriolar responsiveness to shear stress in soluble epoxide hydrolase-knockout mice.', American journal of physiology. Heart and circulatory physiology, 309(11), pp. H1860-6. doi: 10.1152/ajpheart.00568.2015.

Quayle, J. M. et al. (1994) 'Calcitonin gene-related peptide activated ATP-sensitive K+ currents in rabbit arterial smooth muscle via protein kinase A.', The Journal of

physiology, 475(1), pp. 9–13. doi: 10.1113/jphysiol.1994.sp020045.

Quinn, K. V, Giblin, J. P. and Tinker, A. (2004) 'Multisite phosphorylation mechanism for protein kinase A activation of the smooth muscle ATP-sensitive K+ channel.', Circulation research. United States, 94(10), pp. 1359–1366. doi: 10.1161/01.RES.0000128513.34817.c4.

Qureshi, S. F. et al. (2013) 'Novel mutations of KCNQ1 in Long QT syndrome', Indian Heart Journal. doi: 10.1109/SAMPTA.2017.8024464.

Raab-Graham, K. F. and Vandenberg, C. A. (1998) 'Tetrameric subunit structure of the native brain inwardly rectifying potassium channel Kir 2.2.', The Journal of biological chemistry. United States, 273(31), pp. 19699–19707. doi: 10.1074/jbc.273.31.19699.

Randak, C. O. and Welsh, M. J. (2005) 'ADP inhibits function of the ABC transporter cystic fibrosis transmembrane conductance regulator via its adenylate kinase activity.', Proceedings of the National Academy of Sciences of the United States of America, 102(6), pp. 2216–2220. doi: 10.1073/pnas.0409787102.

Rapetti-Mauss, R. et al. (2013) 'Oestrogen promotes KCNQ1 potassium channel endocytosis and postendocytic trafficking in colonic epithelium', Journal of Physiology. doi: 10.1113/jphysiol.2013.251678.

Rapoport, R. M. and Williams, S. P. (1996) 'Role of prostaglandins in acetylcholine-induced contraction of aorta from spontaneously hypertensive and Wistar-Kyoto rats', Hypertension. doi: 10.1161/01.HYP.28.1.64.

Rathod, K. S. et al. (2017) 'Accelerated resolution of inflammation underlies sex differences in inflammatory responses in humans.', The Journal of clinical investigation, 127(1), pp. 169–182. doi: 10.1172/JCI89429.

Razandi, M. et al. (1999) 'Cell membrane and nuclear estrogen receptors (ERs) originate from a single transcript: studies of ERα and ERβ expressed in Chinese hamster ovary cells', Molecular endocrinology. Oxford University Press, 13(2), pp. 307–319.

Reading, S. A. et al. (2005) 'TRPC3 mediates pyrimidine receptor-induced depolarization of cerebral arteries', American Journal of Physiology-Heart and Circulatory Physiology. American Physiological Society, 288(5), pp. H2055–H2061.

Reckelhoff, J. F., Zhang, H. and Granger, J. P. (1998) 'Testosterone Exacerbates Hypertension and Reduces Pressure-Natriuresis in Male Spontaneously Hypertensive Rats', Hypertension. doi: 10.1161/01.HYP.31.1.435.

Reed, J. T. et al. (2020) 'Aging influences cerebrovascular myogenic reactivity and BK channel function in a sex-specific manner.', Cardiovascular research. England, 116(7), pp. 1372–1385. doi: 10.1093/cvr/cvz314.

Reinhart, P. H. et al. (1991) 'Modulation of calcium-activated potassium channels from rat brain by protein kinase A and phosphatase 2A.', The Journal of neuroscience :

the official journal of the Society for Neuroscience, 11(6), pp. 1627–1635. doi: 10.1523/JNEUROSCI.11-06-01627.1991.

Ren, J. et al. (2016) 'Role of BK(Ca) in Stretch-Induced Relaxation of Colonic Smooth Muscle.', BioMed research international, 2016, p. 9497041. doi: 10.1155/2016/9497041.

Restier, L., Cheng, L. and Sanguinetti, M. C. (2008) 'Mechanisms by which atrial fibrillation-associated mutations in the S1 domain of KCNQ1 slow deactivation of IKs channels.', The Journal of physiology, 586(17), pp. 4179–4191. doi: 10.1113/jphysiol.2008.157511.

Revankar, C. M. et al. (2005) 'A transmembrane intracellular estrogen receptor mediates rapid cell signaling', Science. American Association for the Advancement of Science, 307(5715), pp. 1625–1630.

Te Riet, L. et al. (2015) 'Hypertension: renin–angiotensin–aldosterone system alterations', Circulation research. Am Heart Assoc, 116(6), pp. 960–975.

Roberts, O. L. et al. (2013) 'Exchange protein activated by cAMP (Epac) induces vascular relaxation by activating Ca2+-sensitive K+ channels in rat mesenteric artery', Journal of Physiology, 591(20), pp. 5107–5123. doi: 10.1113/jphysiol.2013.262006.

Robertson, B. E. et al. (1993) 'cGMP-dependent protein kinase activates Ca-activated K channels in cerebral artery smooth muscle cells.', The American journal of physiology. United States, 265(1 Pt 1), pp. C299-303. doi: 10.1152/ajpcell.1993.265.1.C299.

Robinson, R. and Gardiner, M. (2000) 'Genetics of childhood epilepsy', Archives of Disease in Childhood. doi: 10.1136/adc.82.2.121.

Rodríguez-Moyano, M. et al. (2013) 'Urotensin-II promotes vascular smooth muscle cell proliferation through store-operated calcium entry and EGFR transactivation.', Cardiovascular research, 100(2), pp. 297–306. doi: 10.1093/cvr/cvt196.

Roepke, T. A. et al. (2011) 'Fasting and 17β-estradiol differentially modulate the M-current in neuropeptide Y neurons', Journal of Neuroscience, 31(33), pp. 11825–11835. doi: 10.1523/JNEUROSCI.1395-11.2011.

Romano, S. N. and Gorelick, D. A. (2018) 'Crosstalk between nuclear and G protein-coupled estrogen receptors.', General and comparative endocrinology, 261, pp. 190–197. doi: 10.1016/j.ygcen.2017.04.013.

Ronda, A. C., Buitrago, C. and Boland, R. (2010) 'Role of estrogen receptors, PKC and Src in ERK2 and p38 MAPK signaling triggered by 17β-estradiol in skeletal muscle cells.', The Journal of steroid biochemistry and molecular biology. England, 122(4), pp. 287–294. doi: 10.1016/j.jsbmb.2010.05.002.

de Rooij, J. et al. (1998) 'Epac is a Rap1 guanine-nucleotide-exchange factor directly

activated by cyclic AMP.', Nature. England, 396(6710), pp. 474–477. doi: 10.1038/24884.

Rostock, A. et al. (1996) 'D-23129: a new anticonvulsant with a broad spectrum activity in animal models of epileptic seizures.', Epilepsy research. Netherlands, 23(3), pp. 211–223. doi: 10.1016/0920-1211(95)00101-8.

Rubio-Gayosso, I. et al. (2000) '17Beta-estradiol increases intracellular calcium concentration through a short-term and nongenomic mechanism in rat vascular endothelium in culture.', Journal of cardiovascular pharmacology. United States, 36(2), pp. 196–202. doi: 10.1097/00005344-200008000-00009.

Sachyani, D. et al. (2014) 'Structural Basis of a Kv7.1 Potassium Channel Gating Module: Studies of the Intracellular C-Terminal Domain in Complex with Calmodulin', Structure. doi: 10.1016/j.str.2014.07.016.

Sadoshima, J. et al. (1988) 'Cyclic AMP modulates Ca-activated K channel in cultured smooth muscle cells of rat aortas.', The American journal of physiology. United States, 255(4 Pt 2), pp. H754-9. doi: 10.1152/ajpheart.1988.255.4.H754.

Sagara, Y. et al. (2007) 'Pressor response induced by central angiotensin II is mediated by activation of Rho/Rho-kinase pathway via AT1 receptors', Journal of Hypertension. doi: 10.1097/HJH.0b013e328010b87f.

Sakmann, B. and Trube, G. (1984) 'Conductance properties of single inwardly rectifying potassium channels in ventricular cells from guinea-pig heart.', The Journal of physiology, 347, pp. 641–657. doi: 10.1113/jphysiol.1984.sp015088.

Salata, J. J. et al. (1998) 'A novel benzodiazepine that activates cardiac slow delayed rectifier K+ currents.', Molecular pharmacology. United States, 54(1), pp. 220–230. doi: 10.1124/mol.54.1.220.

Salzer, I. et al. (2017) 'Phosphorylation regulates the sensitivity of voltage-gated Kv7.2 channels towards phosphatidylinositol-4,5-bisphosphate.', The Journal of physiology, 595(3), pp. 759–776. doi: 10.1113/JP273274.

Sandow, S. L. et al. (2002) 'Involvement of myoendothelial gap junctions in the actions of endothelium-derived hyperpolarizing factor', Circulation Research. doi: 10.1161/01.RES.0000019756.88731.83.

Sandow, S. L. et al. (2004) 'Developmental changes in myoendothelial gap junction mediated vasodilator activity in the rat saphenous artery', Journal of Physiology. doi: 10.1113/jphysiol.2003.058669.

Sandow, S. L. et al. (2006) 'Spatial separation of endothelial small- and intermediate-conductance calcium-activated potassium channels (KCa) and connexins: Possible relationship to vasodilator function?', Journal of Anatomy, 209(5), pp. 689–698. doi: 10.1111/j.1469-7580.2006.00647.x.

Sandow, S. L. et al. (2009) 'What's where and why at a vascular myoendothelial

microdomain signalling complex', Clinical and Experimental Pharmacology and Physiology. doi: 10.1111/j.1440-1681.2008.05076.x.

Sandow, S. L. et al. (2012) 'Myoendothelial Contacts, Gap Junctions, and Microdomains: Anatomical Links to Function?', Microcirculation, pp. 403–415. doi: 10.1111/j.1549-8719.2011.00146.x.

Sandow, S. L. and Grayson, T. H. (2009) 'Limits of isolation and culture: intact vascular endothelium and BKCa.', American journal of physiology. Heart and circulatory physiology. United States, 297(1), pp. H1-7. doi: 10.1152/ajpheart.00042.2009.

Sanguinetti, M. C. et al. (1996) 'Coassembly of K(V)LQT1 and minK (IsK) proteins to form cardiac I(Ks) potassium channel', Nature. doi: 10.1038/384080a0.

dos Santos, R. L. et al. (2014) 'Sex hormones in the cardiovascular system.', Hormone molecular biology and clinical investigation. Germany, 18(2), pp. 89–103. doi: 10.1515/hmbci-2013-0048.

Sausbier, M. et al. (2000) 'Mechanisms of NO/cGMP-dependent vasorelaxation.', Circulation research. United States, 87(9), pp. 825–830. doi: 10.1161/01.res.87.9.825.

Schenzer, A. et al. (2005) 'Molecular determinants of KCNQ (KV7) K+ channel sensitivity to the anticonvulsant retigabine', Journal of Neuroscience. doi: 10.1523/JNEUROSCI.0128-05.2005.

Schenzer, A. (2005) 'Molecular Determinants of KCNQ (Kv7) K+ Channel Sensitivity to the Anticonvulsant Retigabine', Journal of Neuroscience, 25(20), pp. 5051–5060. doi: 10.1523/JNEUROSCI.0128-05.2005.

Schmalz, F. et al. (1998) 'Molecular identification of a component of delayed rectifier current in gastrointestinal smooth muscles', American Journal of Physiology-Gastrointestinal and Liver Physiology. American Physiological Society Bethesda, MD, 274(5), pp. G901–G911.

Schmitt, N. et al. (2000) 'A recessive C-terminal Jervell and Lange-Nielsen mutation of the KCNQ1 channel impairs subunit assembly.', The EMBO journal, 19(3), pp. 332–340. doi: 10.1093/emboj/19.3.332.

Schnee, M. E. and Brown, B. S. (1998) 'Selectivity of linopirdine (DuP 996), a neurotransmitter release enhancer, in blocking voltage-dependent and calcium-activated potassium currents in hippocampal neurons', Journal of Pharmacology and Experimental Therapeutics.

Scholz, A., Gruss, M. and Vogel, W. (1998) 'Properties and functions of calcium-activated K+ channels in small neurones of rat dorsal root ganglion studied in a thin slice preparation.', The Journal of physiology, 513 (Pt 1(Pt 1), pp. 55–69. doi: 10.1111/j.1469-7793.1998.055by.x.

Schroeder, B. C., Waldegger, S., et al. (2000) 'A constitutively open potassium channel

formed by KCNQ1 and KCNE3.', Nature. England, 403(6766), pp. 196–199. doi: 10.1038/35003200.

Schroeder, B. C., Hechenberger, M., et al. (2000) 'KCNQ5, a novel potassium channel broadly expressed in brain, mediates M-type currents.', The Journal of biological chemistry. United States, 275(31), pp. 24089–24095. doi: 10.1074/jbc.M003245200.

Schroeder, B. C. et al. (2008) 'Expression cloning of TMEM16A as a calcium-activated chloride channel subunit.', Cell, 134(6), pp. 1019–29. doi: 10.1016/j.cell.2008.09.003.

Schubert, R. et al. (1996) 'Iloprost activates K(Ca) channels of vascular smooth muscle cells: Role of cAMP-dependent protein kinase', American Journal of Physiology - Cell Physiology. doi: 10.1152/ajpcell.1996.271.4.c1203.

Schubert, R. et al. (1997) 'Iloprost dilates rat small arteries: Role of K(ATP)- and K(Ca)-channel activation by cAMP-dependent protein kinase', American Journal of Physiology - Heart and Circulatory Physiology. doi: 10.1152/ajpheart.1997.272.3.h1147.

Schubert, R., Noack, T. and Serebryakov, V. N. (1999) 'Protein kinase C reduces the KCa current of rat tail artery smooth muscle cells.', The American journal of physiology. United States, 276(3), pp. C648-58. doi: 10.1152/ajpcell.1999.276.3.C648.

Schumacher, M. A. et al. (2001) 'Structure of the gating domain of a Ca2+-activated K+ channel complexed with Ca2+/calmodulin.', Nature. England, 410(6832), pp. 1120–1124. doi: 10.1038/35074145.

Schwake, M., Jentsch, T. J. and Friedrich, T. (2003) 'A carboxy-terminal domain determines the subunit specificity of KCNQ K+ channel assembly', EMBO Reports. doi: 10.1038/sj.embor.embor715.

Schwartz, P. J., Crotti, L. and Insolia, R. (2012) 'Long-QT syndrome: from genetics to management.', Circulation. Arrhythmia and electrophysiology, 5(4), pp. 868–877. doi: 10.1161/CIRCEP.111.962019.

Scotland, R. S. et al. (2005) 'Investigation of vascular responses in endothelial nitric oxide synthase/cyclooxygenase-1 double-knockout mice: key role for endothelium-derived hyperpolarizing factor in the regulation of blood pressure in vivo.', Circulation. United States, 111(6), pp. 796–803. doi: 10.1161/01.CIR.0000155238.70797.4E.

Seebohm, G. et al. (2007) 'Regulation of endocytic recycling of KCNQ1/KCNE1 potassium channels.', Circulation research. United States, 100(5), pp. 686–692. doi: 10.1161/01.RES.0000260250.83824.8f.

Seki, T. et al. (2017) 'Downregulation of Endothelial Transient Receptor Potential

Vanilloid Type 4 Channel and Small-Conductance of Ca2+-Activated K+ Channels Underpins Impaired Endothelium-Dependent Hyperpolarization in Hypertension.', Hypertension (Dallas, Tex. : 1979). United States, 69(1), pp. 143–153. doi: 10.1161/HYPERTENSIONAHA.116.07110.

Selles, J. et al. (2001) 'Progesterone and 17 β-estradiol acutely stimulate nitric oxide synthase activity in rat aorta and inhibit platelet aggregation', Life Sciences, 69(7), pp. 815–827. doi: https://doi.org/10.1016/S0024-3205(01)01174-2.

Senadheera, S. et al. (2012) 'Transient receptor potential canonical type 3 channels facilitate endothelium-derived hyperpolarization-mediated resistance artery vasodilator activity', Cardiovascular Research. doi: 10.1093/cvr/cvs208.

Shamgar, L. et al. (2006) 'Calmodulin is essential for cardiac IKS channel gating and assembly: impaired function in long-QT mutations.', Circulation research. United States, 98(8), pp. 1055–1063. doi: 10.1161/01.RES.0000218979.40770.69.

Shi, J. et al. (2017) 'Store-operated interactions between plasmalemmal STIM1 and TRPC1 proteins stimulate PLCβ1 to induce TRPC1 channel activation in vascular smooth muscle cells.', The Journal of physiology, 595(4), pp. 1039–1058. doi: 10.1113/JP273302.

Shi, W.-W. et al. (2012) 'K(ATP) channel action in vascular tone regulation: from genetics to diseases.', Sheng li xue bao : [Acta physiologica Sinica], 64(1), pp. 1–13.

Shi, W. et al. (2007) 'Arginine vasopressin inhibits Kir6.1/SUR2B channel and constricts the mesenteric artery via V1a receptor and protein kinase C.', American journal of physiology. Regulatory, integrative and comparative physiology. United States, 293(1), pp. R191-9. doi: 10.1152/ajpregu.00047.2007.

Shi, Y., Cui, N., et al. (2008) 'A short motif in Kir6.1 consisting of four phosphorylation repeats underlies the vascular KATP channel inhibition by protein kinase C.', The Journal of biological chemistry, 283(5), pp. 2488–2494. doi: 10.1074/jbc.M708769200.

Shi, Y., Chen, X., et al. (2008) 'cAMP-dependent protein kinase phosphorylation produces interdomain movement in SUR2B leading to activation of the vascular KATP channel.', The Journal of biological chemistry, 283(12), pp. 7523–7530. doi: 10.1074/jbc.M709941200.

Shihan, M., Bulldan, A. and Scheiner-Bobis, G. (2014) 'Non-classical testosterone signaling is mediated by a G-protein-coupled receptor interacting with Gnα11.', Biochimica et biophysica acta. Netherlands, 1843(6), pp. 1172–1181. doi: 10.1016/j.bbamcr.2014.03.002.

Shimizu, W. and Horie, M. (2011) 'Phenotypic manifestations of mutations in genes encoding subunits of cardiac potassium channels.', Circulation research. United States, 109(1), pp. 97–109. doi: 10.1161/CIRCRESAHA.110.224600.

Shimokawa, H. et al. (1996) 'The importance of the hyperpolarizing mechanism increases as the vessel size decreases in endothelium-dependent relaxations in rat mesenteric circulation', Journal of Cardiovascular Pharmacology. doi: 10.1097/00005344-199611000-00014.

Shvetsova, A. A. et al. (2019) 'Negative feedback regulation of vasocontraction by potassium channels in 10- to 15-day-old rats: Dominating role of K(v) 7 channels.', Acta physiologica (Oxford, England). England, 225(2), p. e13176. doi: 10.1111/apha.13176.

Sihn, C. R. et al. (2016) 'Mechanisms of calmodulin regulation of different isoforms of Kv7.4 K+channels', Journal of Biological Chemistry. doi: 10.1074/jbc.M115.668236.

De Silva, T. M. et al. (2009) 'Gender influences cerebral vascular responses to angiotensin II through Nox2-derived reactive oxygen species.', Stroke. United States, 40(4), pp. 1091–1097. doi: 10.1161/STROKEAHA.108.531707.

Silvestro, M. et al. (2021) 'Effectiveness and Safety of CGRP-mAbs in Menstrual-Related Migraine: A Real-World Experience.', Pain and therapy, 10(2), pp. 1203–1214. doi: 10.1007/s40122-021-00273-w.

Simoncini, T. et al. (2000) 'Interaction of oestrogen receptor with the regulatory subunit of phosphatidylinositol-3-OH kinase.', Nature, 407(6803), pp. 538–541. doi: 10.1038/35035131.

Simoncini, T. et al. (2004) 'Differential Signal Transduction of Progesterone and Medroxyprogesterone Acetate in Human Endothelial Cells', Endocrinology, 145(12), pp. 5745–5756. doi: 10.1210/en.2004-0510.

Sims, S. M. and Dixon, S. J. (1989) 'Inwardly rectifying K+ current in osteoclasts', American Journal of Physiology-Cell Physiology. American Physiological Society Bethesda, MD, 256(6), pp. C1277–C1282.

Sims, S. M., Singer, J. J. and Walsh, J. V. J. (1988) 'Antagonistic adrenergic-muscarinic regulation of M current in smooth muscle cells.', Science (New York, N.Y.). United States, 239(4836), pp. 190–193. doi: 10.1126/science.2827305.

Skaug, E.-A. et al. (2013) 'Age and gender differences of endothelial function in 4739 healthy adults: the HUNT3 Fitness Study.', European journal of preventive cardiology. England, 20(4), pp. 531–540. doi: 10.1177/2047487312444234.

Smirnov, S. V et al. (2002) 'Electrophysiologically distinct smooth muscle cell subtypes in rat conduit and resistance pulmonary arteries.', The Journal of physiology, 538(Pt 3), pp. 867–878. doi: 10.1113/jphysiol.2001.013003.

Smith, P. D. et al. (2008) 'KIR channels function as electrical amplifiers in rat vascular smooth muscle', Journal of Physiology. doi: 10.1113/jphysiol.2007.145474.

Soder, R. P. and Petkov, G. V (2011) 'Large conductance Ca2+-activated K+ channel activation with NS1619 decreases myogenic and neurogenic contractions of rat

detrusor smooth muscle', European Journal of Pharmacology, 670(1), pp. 252–259. doi: https://doi.org/10.1016/j.ejphar.2011.08.013.

Sonkusare, S. K. et al. (2016) 'Inward rectifier potassium (Kir2.1) channels as end-stage boosters of endothelium-dependent vasodilators', Journal of Physiology. doi: 10.1113/JP271652.

Splawski, I. et al. (2000) 'Spectrum of mutations in long-QT syndrome genes. KVLQT1, HERG, SCN5A, KCNE1, and KCNE2.', Circulation. United States, 102(10), pp. 1178–1185. doi: 10.1161/01.cir.102.10.1178.

Spoerri, E., Jentsch, J. and Glees, P. (1975) 'Apamin from bee venom. Effects of the neurotoxin on subcellular particles of neural cultures', FEBS Letters. doi: 10.1016/0014-5793(75)80006-8.

Stanfield, P. R., Nakajima, S. and Nakajima, Y. (2002) 'Constitutively active and G-protein coupled inward rectifier K+ channels: Kir2.0 and Kir3.0.', Reviews of physiology, biochemistry and pharmacology. Germany, 145, pp. 47–179. doi: 10.1007/BFb0116431.

Stanke-Labesque, F. et al. (2000) 'Furosemide inhibits thromboxane A2-induced contraction in isolated human internal mammary artery and saphenous vein.', Journal of cardiovascular pharmacology. United States, 35(4), pp. 531–537. doi: 10.1097/00005344-200004000-00003.

Stanke, F. et al. (1998) 'Frusemide inhibits angiotensin II-induced contraction on human vascular smooth muscle.', British journal of clinical pharmacology, 46(6), pp. 571–575. doi: 10.1046/j.1365-2125.1998.00820.x.

Stott, J. B., Barrese, V., et al. (2015) 'Contribution of Kv7 channels to natriuretic peptide mediated vasodilation in normal and hypertensive rats', Hypertension, 65(3), pp. 676–682. doi: 10.1161/HYPERTENSIONAHA.114.04373.

Stott, J. B., Povstyan, O. V., et al. (2015) 'G-protein βγ subunits are positive regulators of Kv7.4 and native vascular Kv7 channel activity', Proceedings of the National Academy of Sciences, 112(20), pp. 6497–6502. doi: 10.1073/pnas.1418605112.

Stott, J. B. et al. (2018) 'Investigating the Role of G Protein βγ in Kv7-Dependent Relaxations of the Rat Vasculature', Arteriosclerosis, thrombosis, and vascular biology. doi: 10.1161/ATVBAHA.118.311360.

Stott, J. B., Barrese, V. and Greenwood, I. A. (2016) 'Kv7 Channel Activation Underpins EPAC-Dependent Relaxations of Rat Arteries', Arteriosclerosis, Thrombosis, and Vascular Biology, 36(12), pp. 2404–2411. doi: 10.1161/ATVBAHA.116.308517.

Stott, J. B., Jepps, T. A. and Greenwood, I. A. (2014) 'KV7 potassium channels: A new therapeutic target in smooth muscle disorders', Drug Discovery Today, pp. 413–424. doi: 10.1016/j.drudis.2013.12.003.

Straub, S. V et al. (2006) 'Dynamic inositol trisphosphate-mediated calcium signals

within astrocytic endfeet underlie vasodilation of cerebral arterioles.', The Journal of general physiology, 128(6), pp. 659–669. doi: 10.1085/jgp.200609650.

Suessbrich, H. et al. (1996) 'Specific blockade of slowly activating I(sK) channels by chromanols -- impact on the role of I(sK) channels in epithelia.', FEBS letters. England, 396(2–3), pp. 271–275. doi: 10.1016/0014-5793(96)01113-1.

Suh, B.-C. and Hille, B. (2002) 'Recovery from muscarinic modulation of M current channels requires phosphatidylinositol 4,5-bisphosphate synthesis.', Neuron. United States, 35(3), pp. 507–520. doi: 10.1016/s0896-6273(02)00790-0.

Sun, X. et al. (2017) 'Calcium-activated BK(Ca) channels govern dynamic membrane depolarizations of horizontal cells in rodent retina.', The Journal of physiology, 595(13), pp. 4449–4465. doi: 10.1113/JP274132.

Sun, Y. et al. (2021) 'Sex Differences, Estrogen Metabolism and Signaling in the Development of Pulmonary Arterial Hypertension ', Frontiers in Cardiovascular Medicine , p. 1052. Available at: https://www.frontiersin.org/article/10.3389/fcvm.2021.719058.

Svalø, J. et al. (2012) 'K v7 positive modulators reduce detrusor overactivity and increase bladder capacity in rats', Basic and Clinical Pharmacology and Toxicology. doi: 10.1111/j.1742-7843.2011.00765.x.

Svalø, J. et al. (2015) 'Functional and molecular evidence for K<inf>v</inf>7 channel subtypes in human detrusor from patients with and without bladder outflow obstruction', PLoS ONE. doi: 10.1371/journal.pone.0117350.

Swica, Y. et al. (2018) 'Effects of oral conjugated equine estrogens with or without medroxyprogesterone acetate on incident hypertension in the Women's Health Initiative hormone therapy trials.', Menopause (New York, N.Y.), 25(7), pp. 753–761. doi: 10.1097/GME.0000000000001067.

Taglialatela, M. et al. (1994) 'Specification of pore properties by the carboxyl terminus of inwardly rectifying K+ channels.', Science (New York, N.Y.). United States, 264(5160), pp. 844–847. doi: 10.1126/science.8171340.

Taglialatela, M. et al. (1995) 'C-terminus determinants for Mg2+ and polyamine block of the inward rectifier K+ channel IRK1.', The EMBO journal, 14(22), pp. 5532–5541.

Taguchi, K., Kaneko, K. and Kubo, T. (2000) 'Protein kinase C modulates Ca2+-activated K+ channels in cultured rat mesenteric artery smooth muscle cells.', Biological & pharmaceutical bulletin. Japan, 23(12), pp. 1450–1454. doi: 10.1248/bpb.23.1450.

Takano, M. et al. (1998) 'Cytoplasmic terminus domains of Kir6.x confer different nucleotide-dependent gating on the ATP-sensitive K+ channel.', The Journal of physiology, 512 (Pt 2(Pt 2), pp. 395–406. doi: 10.1111/j.1469-7793.1998.395be.x.

Takeda, S. et al. (2006) 'Beating myocardium counteracts myogenic tone of coronary microvessels: involvement of ATP-sensitive potassium channels.', American

journal of physiology. Heart and circulatory physiology. United States, 291(6), pp. H3050-7. doi: 10.1152/ajpheart.00039.2006.

Takezawa, H. et al. (1994) 'Circadian and estrous cycle-dependent variations in blood pressure and heart rate in female rats.', The American journal of physiology. United States, 267(5 Pt 2), pp. R1250-6. doi: 10.1152/ajpregu.1994.267.5.R1250.

Tammaro, P. et al. (2004) 'Pharmacological evidence for a key role of voltage-gated K+ channels in the function of rat aortic smooth muscle cells.', British journal of pharmacology, 143(2), pp. 303–317. doi: 10.1038/sj.bjp.0705957.

Tan, C. O., Hamner, J. W. and Taylor, J. A. (2013) 'The role of myogenic mechanisms in human cerebrovascular regulation', Journal of Physiology. doi: 10.1113/jphysiol.2013.259747.

Tan, J. H., Al Abed, A. and Brock, J. A. (2007) 'Inhibition of KATP channels in the rat tail artery by neurally released noradrenaline acting on postjunctional alpha2-adrenoceptors.', The Journal of physiology, 581(Pt 2), pp. 757–765. doi: 10.1113/jphysiol.2007.129536.

Tanaka, Y. et al. (2006) 'Kv channels contribute to nitric oxide- and atrial natriuretic peptide-induced relaxation of a rat conduit artery.', The Journal of pharmacology and experimental therapeutics. United States, 317(1), pp. 341–354. doi: 10.1124/jpet.105.096115.

Tanaka, Y., Koike, K. and Toro, L. (2004) 'MaxiK channel roles in blood vessel relaxations induced by endothelium-derived relaxing factors and their molecular mechanisms', Journal of Smooth Muscle Research. doi: 10.1540/jsmr.40.125.

Tang, E. H. C. et al. (2008) 'The role of prostaglandin E and thromboxane-prostanoid receptors in the response to prostaglandin E2 in the aorta of Wistar Kyoto rats and spontaneously hypertensive rats', Cardiovascular Research. doi: 10.1093/cvr/cvm112.

Tatulian, L. et al. (2001) 'Activation of expressed KCNQ potassium currents and native neuronal M-type potassium currents by the anti-convulsant drug retigabine.', The Journal of neuroscience : the official journal of the Society for Neuroscience, 21(15), pp. 5535–5545. doi: 10.1523/JNEUROSCI.21-15-05535.2001.

Taylor, M. S. et al. (2003) 'Altered expression of small-conductance Ca2+-activated K+ (SK3) channels modulates arterial tone and blood pressure.', Circulation research. United States, 93(2), pp. 124–131. doi: 10.1161/01.RES.0000081980.63146.69.

Telezhkin, V. et al. (2013) 'A basic residue in the proximal C-terminus is necessary for efficient activation of the M-channel subunit Kv7.2 by $PI(4,5)P_2$.', Pflugers Archiv : European journal of physiology, 465(7), pp. 945–953. doi: 10.1007/s00424-012-1199-3.

Teng, B.-C. et al. (2016) 'Activation of neuronal Kv7/KCNQ/M-channels by the opener

QO58-lysine and its anti-nociceptive effects on inflammatory pain in rodents.', Acta pharmacologica Sinica, 37(8), pp. 1054–1062. doi: 10.1038/aps.2016.33.

Tep-areenan, P., Kendall, D. A. and Randall, M. D. (2002) 'Testosterone-induced vasorelaxation in the rat mesenteric arterial bed is mediated predominantly via potassium channels', British journal of pharmacology. Wiley Online Library, 135(3), pp. 735–740.

Testai, L. et al. (2016) 'Expression and function of Kv7.4 channels in rat cardiac mitochondria: possible targets for cardioprotection.', Cardiovascular research. England, 110(1), pp. 40–50. doi: 10.1093/cvr/cvv281.

Tharp, D. L. et al. (2014) 'Ovariectomy increases L-type Ca(2+) channel activity in porcine coronary smooth muscle.', Menopause (New York, N.Y.). United States, 21(6), pp. 661–668. doi: 10.1097/GME.0000000000000087.

Thomas-Gatewood, C. et al. (2011) 'TMEM16A channels generate Ca2+-activated Cl− currents in cerebral artery smooth muscle cells.', American journal of physiology. Heart and circulatory physiology, 301(5), pp. H1819-27. doi: 10.1152/ajpheart.00404.2011.

Thomas, G. P., Gerlach, U. and Antzelevitch, C. (2003) 'HMR 1556, a potent and selective blocker of slowly activating delayed rectifier potassium current', Journal of Cardiovascular Pharmacology. doi: 10.1097/00005344-200301000-00018.

Thomas, P. et al. (2005) 'Identity of an estrogen membrane receptor coupled to a G protein in human breast cancer cells.', Endocrinology. United States, 146(2), pp. 624–632. doi: 10.1210/en.2004-1064.

Thorneloe, K. S. et al. (2001) 'Molecular composition of 4-aminopyridine-sensitive voltage-gated K+ channels of vascular smooth muscle', Circulation research. Am Heart Assoc, 89(11), pp. 1030–1037.

Tiwari, S. et al. (2010) 'Sex differences in adaptive downregulation of pre-macula densa sodium transporters with ANG II infusion in mice', American Journal of Physiology-Renal Physiology. doi: 10.1152/ajprenal.00088.2009.

Traupe, T. et al. (2007) 'Distinct roles of estrogen receptors α and β mediating acute vasodilation of epicardial coronary arteries', Hypertension. Am Heart Assoc, 49(6), pp. 1364–1370.

Trinh, N. T. N. et al. (2007) 'Involvement of KATP and KvLQT1 K+ channels in EGF-stimulated alveolar epithelial cell repair processes.', American journal of physiology. Lung cellular and molecular physiology. United States, 293(4), pp. L870-82. doi: 10.1152/ajplung.00362.2006.

Trube, G. and Hescheler, J. (1984) 'Inward-rectifying channels in isolated patches of the heart cell membrane: ATP-dependence and comparison with cell-attached patches', Pflügers Archiv. Springer, 401(2), pp. 178–184.

Tsai, T.-C. et al. (2014) 'Urinary Bladder Relaxation through Activation of Imidazoline Receptors Induced by Agmatine is Increased in Diabetic Rats.', Lower urinary tract symptoms. Australia, 6(2), pp. 117–123. doi: 10.1111/luts.12031.

Tseng-Crank, J. et al. (1994) 'Cloning, expression, and distribution of functionally distinct Ca(2+)-activated K+ channel isoforms from human brain.', Neuron. United States, 13(6), pp. 1315–1330. doi: 10.1016/0896-6273(94)90418-9.

Tseng, S. et al. (1997) 'F-actin disruption attenuates agonist-induced [Ca2+], myosin phosphorylation, and force in smooth muscle', American Journal of Physiology - Cell Physiology. doi: 10.1152/ajpcell.1997.272.6.c1960.

Tsvetkov, D. et al. (2017) 'Do KV7.1 channels contribute to control of arterial vascular tone?', British Journal of Pharmacology. doi: 10.1111/bph.13665.

Tucker, S. J. et al. (1997) 'Truncation of Kir6.2 produces ATP-sensitive K+ channels in the absence of the sulphonylurea receptor.', Nature. England, 387(6629), pp. 179–183. doi: 10.1038/387179a0.

Tucker, S. J. et al. (1998) 'Molecular determinants of KATP channel inhibition by ATP.', The EMBO journal, 17(12), pp. 3290–3296. doi: 10.1093/emboj/17.12.3290.

Tunstall-Pedoe, H. et al. (1994) 'Myocardial infarction and coronary deaths in the World Health Organization MONICA Project. Registration procedures, event rates, and case-fatality rates in 38 populations from 21 countries in four continents', Circulation. doi: 10.1161/01.CIR.90.1.583.

Tuteja, D. et al. (2005) 'Differential expression of small-conductance Ca2+-activated K+ channels SK1, SK2, and SK3 in mouse atrial and ventricular myocytes.', American journal of physiology. Heart and circulatory physiology. United States, 289(6), pp. H2714-23. doi: 10.1152/ajpheart.00534.2005.

Tykocki, N. R., Boerman, E. M. and Jackson, W. F. (2017) 'Smooth muscle ion channels and regulation of vascular tone in resistance arteries and arterioles', Comprehensive Physiology. doi: 10.1002/cphy.c160011.

Unoki, H. et al. (2008) 'SNPs in KCNQ1 are associated with susceptibility to type 2 diabetes in East Asian and European populations.', Nature genetics. United States, 40(9), pp. 1098–1102. doi: 10.1038/ng.208.

Usselman, C. W., Stachenfeld, N. S. and Bender, J. R. (2016) 'The molecular actions of oestrogen in the regulation of vascular health', Experimental Physiology. doi: 10.1113/EP085148.

Vallon, V. et al. (2001) 'Role of KCNE1-dependent K+ fluxes in mouse proximal tubule.', Journal of the American Society of Nephrology : JASN. United States, 12(10), pp. 2003–2011. doi: 10.1681/ASN.V12102003.

Vallon, V. et al. (2005) 'KCNQ1-dependent transport in renal and gastrointestinal epithelia.', Proceedings of the National Academy of Sciences of the United States

of America, 102(49), pp. 17864–17869. doi: 10.1073/pnas.0505860102.

Vandenberg, C. A. (1987) 'Inward rectification of a potassium channel in cardiac ventricular cells depends on internal magnesium ions.', Proceedings of the National Academy of Sciences of the United States of America, 84(8), pp. 2560–2564. doi: 10.1073/pnas.84.8.2560.

Vandorpe, D. H. et al. (1998) 'cDNA cloning and functional characterization of the mouse Ca2+-gated K+ channel, mIK1. Roles in regulatory volume decrease and erythroid differentiation.', The Journal of biological chemistry. United States, 273(34), pp. 21542–21553. doi: 10.1074/jbc.273.34.21542.

Vetri, F. et al. (2012) 'Impairment of neurovascular coupling in type 1 diabetes mellitus in rats is linked to PKC modulation of BK(Ca) and Kir channels.', American journal of physiology. Heart and circulatory physiology, 302(6), pp. H1274-84. doi: 10.1152/ajpheart.01067.2011.

Villalobos, C. et al. (2004) 'SKCa channels mediate the medium but not the slow calcium-activated afterhyperpolarization in cortical neurons.', The Journal of neuroscience : the official journal of the Society for Neuroscience, 24(14), pp. 3537–3542. doi: 10.1523/JNEUROSCI.0380-04.2004.

Víteček, J. et al. (2012) 'Arginine-Based Inhibitors of Nitric Oxide Synthase: Therapeutic Potential and Challenges', Mediators of Inflammation. Edited by H. Bult. Hindawi Publishing Corporation, 2012, p. 318087. doi: 10.1155/2012/318087.

Wakatsuki, T. et al. (1992) 'Effects of vasopressin on ATP-sensitive and Ca(2+)-activated K+ channels of coronary arterial smooth muscle cells.', Japanese journal of pharmacology. Japan, 58 Suppl 2, p. 339P.

Wald, C. and Wu, C. (2010) 'Biomedical research. Of mice and women: the bias in animal models.', Science (New York, N.Y.). United States, pp. 1571–1572. doi: 10.1126/science.327.5973.1571.

Waldegger, S. et al. (1996) 'Inhibition of minK protein induced K+ channels in Xenopus oocytes by estrogens.', Pflugers Archiv European Journal of Physiology. Germany, 354(6), pp. 698–702. doi: 10.1007/s00424-008-0567-5.

Wallner, M., Meera, P. and Toro, L. (1999) 'Molecular basis of fast inactivation in voltage and Ca2+-activated K+ channels: a transmembrane beta-subunit homolog.', Proceedings of the National Academy of Sciences of the United States of America, 96(7), pp. 4137–4142. doi: 10.1073/pnas.96.7.4137.

Walsh, K. B. and Kass, R. S. (1988) 'Regulation of a heart potassium channel by protein kinase A and C', Science. American Association for the Advancement of Science, 242(4875), pp. 67–69.

Walsh, K. B. and Kass, R. S. (1991) 'Distinct voltage-dependent regulation of a heart-delayed IK by protein kinases A and C', American Journal of Physiology-Cell

Physiology, 261(6), pp. C1081–C1090.

Walsh, M. P. et al. (1982) 'Phosphorylation-dependent activated tension in skinned gizzard muscle fibers in the absence of Ca2+.', Journal of Biological Chemistry.

Walsh, M. P. (2011) 'Vascular Smooth muscle myosin light chain diphosphorylation: Mechanism, function, and pathological implications', IUBMB Life. doi: 10.1002/iub.527.

Walsh, M. P. and Cole, W. C. (2013) 'The role of actin filament dynamics in the myogenic response of cerebral resistance arteries', Journal of Cerebral Blood Flow and Metabolism. doi: 10.1038/jcbfm.2012.144.

Wang, A. W., Yang, R. and Kurata, H. T. (2017) 'Sequence determinants of subtype-specific actions of KCNQ channel openers.', The Journal of physiology, 595(3), pp. 663–676. doi: 10.1113/JP272762.

Wang, H. R. et al. (2011) 'Selective inhibition of the K ir2 family of inward rectifier potassium channels by a small molecule probe: The discovery, SAR, and pharmacological characterization of ML133', ACS Chemical Biology. doi: 10.1021/cb200146a.

Wang, H. S. et al. (1998) 'KCNQ2 and KCNQ3 potassium channel subunits: Molecular correlates of the M-channel', Science. doi: 10.1126/science.282.5395.1890.

Wang, Y. et al. (2006) 'Class II phosphoinositide 3-kinase α-isoform regulates Rho, myosin phosphatase and contraction in vascular smooth muscle', Biochemical Journal. doi: 10.1042/BJ20051471.

Wang, Y., Eldstrom, J. and Fedida, D. (2020) 'The I (Ks) Ion Channel Activator Mefenamic Acid Requires KCNE1 and Modulates Channel Gating in a Subunit-Dependent Manner.', Molecular pharmacology. United States, 97(2), pp. 132–144. doi: 10.1124/mol.119.117952.

Wassmann, K., Wassmann, S. and Nickenig, G. (2005) 'Progesterone antagonizes the vasoprotective effect of estrogen on antioxidant enzyme expression and function.', Circulation research. United States, 97(10), pp. 1046–1054. doi: 10.1161/01.RES.0000188212.57180.55.

Wei, A. D. et al. (2005) 'International Union of Pharmacology. LII. Nomenclature and molecular relationships of calcium-activated potassium channels.', Pharmacological reviews. United States, 57(4), pp. 463–472. doi: 10.1124/pr.57.4.9.

Wei, X. et al. (2018) 'The expression and function of KCNQ potassium channels in human chorionic plate arteries from women with normal pregnancies and pre-eclampsia', PLoS ONE. doi: 10.1371/journal.pone.0192122.

Wellman, G. C. et al. (1996) 'Gender differences in coronary artery diameter involve estrogen, nitric oxide, and Ca(2+)-dependent K+ channels.', Circulation research.

United States, 79(5), pp. 1024–1030. doi: 10.1161/01.res.79.5.1024.

Wellman, G. C. et al. (2001) 'Membrane depolarization, elevated Ca2+ entry, and gene expression in cerebral arteries of hypertensive rats', American Journal of Physiology - Heart and Circulatory Physiology, 281(6 50-6), pp. 2559–2567. doi: 10.1152/ajpheart.2001.281.6.h2559.

Wellman, G. C. and Bevan, J. A. (1995) 'Barium inhibits the endothelium-dependent component of flow but not acetylcholine-induced relaxation in isolated rabbit cerebral arteries.', The Journal of pharmacology and experimental therapeutics. United States, 274(1), pp. 47–53.

Werner, M. E. et al. (2005) 'Erectile dysfunction in mice lacking the large-conductance calcium-activated potassium (BK) channel.', The Journal of physiology, 567(Pt 2), pp. 545–556. doi: 10.1113/jphysiol.2005.093823.

Wersinger, E. et al. (2010) 'BK channels mediate cholinergic inhibition of high frequency cochlear hair cells.', PloS one, 5(11), p. e13836. doi: 10.1371/journal.pone.0013836.

Wesselman, J. P. et al. (1997) 'KCa-channel blockade prevents sustained pressure-induced depolarization in rat mesenteric small arteries.', The American journal of physiology. United States, 272(5 Pt 2), pp. H2241-9. doi: 10.1152/ajpheart.1997.272.5.H2241.

Weston, A. H. et al. (2010) 'Impairment of endothelial SK(Ca) channels and of downstream hyperpolarizing pathways in mesenteric arteries from spontaneously hypertensive rats.', British journal of pharmacology, 160(4), pp. 836–843. doi: 10.1111/j.1476-5381.2010.00657.x.

Westwood, F. R. (2008) 'The female rat reproductive cycle: a practical histological guide to staging.', Toxicologic pathology. United States, 36(3), pp. 375–384. doi: 10.1177/0192623308315665.

White, R. et al. (2001) 'Protein kinase A-dependent and -independent effects of isoproterenol in rat isolated mesenteric artery: interactions with levcromakalim.', The Journal of pharmacology and experimental therapeutics. United States, 298(3), pp. 917–924.

Whittle, B. J. et al. (2012) 'Binding and activity of the prostacyclin receptor (IP) agonists, treprostinil and iloprost, at human prostanoid receptors: Treprostinil is a potent DP 1 and EP 2 agonist', Biochemical Pharmacology. doi: 10.1016/j.bcp.2012.03.012.

Wickenden, A. D. et al. (2008) 'N-(6-chloro-pyridin-3-yl)-3,4-difluoro-benzamide (ICA-27243): a novel, selective KCNQ2/Q3 potassium channel activator.', Molecular pharmacology. United States, 73(3), pp. 977–986. doi: 10.1124/mol.107.043216.

Wilkins E. et al. (2017) European Cardiovascular Disease Statistics 2017 edition, European Heart Network, Brussels. doi: 978-2-9537898-1-2.

Wong, P. S., Roberts, R. E. and Randall, M. D. (2014) 'Sex differences in endothelial function in porcine coronary arteries: a role for H2O2 and gap junctions?', British journal of pharmacology, 171(11), pp. 2751–2766. doi: 10.1111/bph.12595.

Worley, P. F. et al. (2007) 'TRPC channels as STIM1-regulated store-operated channels.', Cell calcium, 42(2), pp. 205–211. doi: 10.1016/j.ceca.2007.03.004.

Wright, G. and Hurn, E. (1994) 'Cytochalasin inhibition of slow tension increase in rat aortic rings', American Journal of Physiology - Heart and Circulatory Physiology. doi: 10.1152/ajpheart.1994.267.4.h1437.

Wu, B.-N. et al. (2007) 'Hyposmotic challenge inhibits inward rectifying K+ channels in cerebral arterial smooth muscle cells.', American journal of physiology. Heart and circulatory physiology. United States, 292(2), pp. H1085-94. doi: 10.1152/ajpheart.00926.2006.

Wu, M. et al. (2010) A potent and selective small molecule Kir2.1 inhibitor, Probe Reports from the NIH Molecular Libraries Program.

Wu, X. and Davis, M. J. (2001) 'Characterization of stretch-activated cation current in coronary smooth muscle cells.', American journal of physiology. Heart and circulatory physiology. United States, 280(4), pp. H1751-61. doi: 10.1152/ajpheart.2001.280.4.H1751.

Wu, Y. et al. (2010) 'Structure of the gating ring from the human large-conductance Ca(2+)-gated K(+) channel.', Nature, 466(7304), pp. 393–397. doi: 10.1038/nature09252.

Wulff, H. et al. (2000) 'Design of a potent and selective inhibitor of the intermediate-conductance Ca2+-activated K+ channel, IKCa1: A potential immunosuppressant', Proceedings of the National Academy of Sciences of the United States of America. doi: 10.1073/pnas.97.14.8151.

Wuttke, T. V et al. (2005) 'The new anticonvulsant retigabine favors voltage-dependent opening of the Kv7.2 (KCNQ2) channel by binding to its activation gate.', Molecular pharmacology. United States, 67(4), pp. 1009–1017. doi: 10.1124/mol.104.010793.

Xi, Q. et al. (2008) 'IP3 constricts cerebral arteries via IP3 receptor–mediated TRPC3 channel activation and independently of sarcoplasmic reticulum Ca2+ release', Circulation research. Am Heart Assoc, 102(9), pp. 1118–1126.

Xia, X. M. et al. (1998) 'Mechanism of calcium gating in small-conductance calcium-activated potassium channels.', Nature. England, 395(6701), pp. 503–507. doi: 10.1038/26758.

Xiong, Q., Sun, H. and Li, M. (2007) 'Zinc pyrithione-mediated activation of voltage-gated KCNQ potassium channels rescues epileptogenic mutants.', Nature chemical biology. United States, 3(5), pp. 287–296. doi: 10.1038/nchembio874.

Xu, C. et al. (1999) 'Expression of voltage-dependent K(+) channel genes in mesenteric

artery smooth muscle cells.', The American journal of physiology. United States, 277(5), pp. G1055-63. doi: 10.1152/ajpgi.1999.277.5.G1055.

Xu, Q. et al. (2013) 'Structure of a Ca(2+)/CaM:Kv7.4 (KCNQ4) B-helix complex provides insight into M current modulation.', Journal of molecular biology, 425(2), pp. 378–394. doi: 10.1016/j.jmb.2012.11.023.

Xu, Y. et al. (2003) 'Molecular identification and functional roles of a Ca(2+)-activated K+ channel in human and mouse hearts.', The Journal of biological chemistry. United States, 278(49), pp. 49085–49094. doi: 10.1074/jbc.M307508200.

Y Schnitzler, M. M. et al. (2008) 'Gq-coupled receptors as mechanosensors mediating myogenic vasoconstriction', EMBO Journal. doi: 10.1038/emboj.2008.233.

Yamada, M. et al. (1997) 'Sulphonylurea receptor 2B and Kir6.1 form a sulphonylurea-sensitive but ATP-insensitive K+ channel.', The Journal of physiology, 499 (Pt 3(Pt 3), pp. 715–720. doi: 10.1113/jphysiol.1997.sp021963.

Yan, F.-F. et al. (2010) 'Role of Hsp90 in biogenesis of the beta-cell ATP-sensitive potassium channel complex.', Molecular biology of the cell, 21(12), pp. 1945–1954. doi: 10.1091/mbc.e10-02-0116.

Yan, J. et al. (2008) 'Profiling the phospho-status of the BKCa channel alpha subunit in rat brain reveals unexpected patterns and complexity.', Molecular & cellular proteomics : MCP, 7(11), pp. 2188–2198. doi: 10.1074/mcp.M800063-MCP200.

Yang, J., Jan, Y. N. and Jan, L. Y. (1995) 'Control of rectification and permeation by residues in two distinct domains in an inward rectifier K+ channel.', Neuron. United States, 14(5), pp. 1047–1054. doi: 10.1016/0896-6273(95)90343-7.

Yang, X.-P. and Reckelhoff, J. F. (2011) 'Estrogen, hormonal replacement therapy and cardiovascular disease.', Current opinion in nephrology and hypertension, 20(2), pp. 133–138. doi: 10.1097/MNH.0b013e3283431921.

Yang, Y. et al. (2007) 'Influence of sex, high-fat diet, and exercise training on potassium currents of swine coronary smooth muscle.', American journal of physiology. Heart and circulatory physiology. United States, 293(3), pp. H1553-63. doi: 10.1152/ajpheart.00151.2007.

Yang, Y. et al. (2013) 'IP3 decreases coronary artery tone via activating the BKCa channel of coronary artery smooth muscle cells in pigs.', Biochemical and biophysical research communications. United States, 439(3), pp. 363–368. doi: 10.1016/j.bbrc.2013.08.079.

Yasuda, K. et al. (2008) 'Variants in KCNQ1 are associated with susceptibility to type 2 diabetes mellitus.', Nature genetics. United States, 40(9), pp. 1092–1097. doi: 10.1038/ng.207.

Yau, M. C. et al. (2018) 'One drug-sensitive subunit is sufficient for a near-maximal retigabine effect in KCNQ channels.', The Journal of general physiology, 150(10),

pp. 1421–1431. doi: 10.1085/jgp.201812013.

Yeung, S. Y. M. et al. (2007) 'Molecular expression and pharmacological identification of a role for Kv7 channels in murine vascular reactivity', British Journal of Pharmacology, 151(6), pp. 758–770. doi: 10.1038/sj.bjp.0707284.

Yeung, S. Y. M. and Greenwood, I. A. (2005) 'Electrophysiological and functional effects of the KCNQ channel blocker XE991 on murine portal vein smooth muscle cells', British Journal of Pharmacology, 146(4), pp. 585–595. doi: 10.1038/sj.bjp.0706342.

Yip, K.-P. et al. (2018) 'Intraluminal pressure triggers myogenic response via activation of calcium spark and calcium-activated chloride channel in rat renal afferent arteriole.', American journal of physiology. Renal physiology, 315(6), pp. F1592–F1600. doi: 10.1152/ajprenal.00239.2018.

Yu (2013) 'Identification of a novel, small molecule activator of KCNQ1 channels.', in Probe Reports from the NIH Molecular Libraries Program [Internet].

Yu, H. et al. (2011) 'Discovery, Synthesis, and Structure Activity Relationship of a Series of N-Aryl- bicyclo[2.2.1]heptane-2-carboxamides: Characterization of ML213 as a Novel KCNQ2 and KCNQ4 Potassium Channel Opener.', ACS chemical neuroscience, 2(10), pp. 572–577. doi: 10.1021/cn200065b.

Yu, J. et al. (2012) 'Src kinase-mediates androgen receptor-dependent non-genomic activation of signaling cascade leading to endothelial nitric oxide synthase.', Biochemical and biophysical research communications. United States, 424(3), pp. 538–543. doi: 10.1016/j.bbrc.2012.06.151.

Yu, X. et al. (2011) 'Activation of G protein-coupled estrogen receptor induces endothelium-independent relaxation of coronary artery smooth muscle.', American journal of physiology. Endocrinology and metabolism, 301(5), pp. E882-8. doi: 10.1152/ajpendo.00037.2011.

Yu, X. et al. (2014) 'G protein-coupled estrogen receptor 1 mediates relaxation of coronary arteries via cAMP/PKA-dependent activation of MLCP', American Journal of Physiology-Endocrinology and Metabolism. American Physiological Society Bethesda, MD, 307(4), pp. E398–E407.

Yuan, P. et al. (2011) 'Open structure of the Ca2+ gating ring in the high-conductance Ca2+-activated K+ channel.', Nature, 481(7379), pp. 94–97. doi: 10.1038/nature10670.

Yuan, X. J. (1997) 'Role of calcium-activated chloride current in regulating pulmonary vasomotor tone', Am. J. Physiol., 16(5), pp. L959–L968.

Yue, P. et al. (1995) 'Testosterone relaxes rabbit coronary arteries and aorta', Circulation. doi: 10.1161/01.CIR.91.4.1154.

Yus-Najera, E., Santana-Castro, I. and Villarroel, A. (2002) 'The identification and characterization of a noncontinuous calmodulin-binding site in noninactivating

voltage-dependent KCNQ potassium channels.', The Journal of biological chemistry. United States, 277(32), pp. 28545–28553. doi: 10.1074/jbc.M204130200.

Zaika, O. et al. (2006) 'Angiotensin II regulates neuronal excitability via phosphatidylinositol 4,5-bisphosphate-dependent modulation of Kv7 (M-type) K+ channels.', The Journal of physiology, 575(Pt 1), pp. 49–67. doi: 10.1113/jphysiol.2006.114074.

Zaritsky, J. J. et al. (2000) 'Targeted disruption of Kir2.1 and Kir2.2 genes reveals the essential role of the inwardly rectifying K(+) current in K(+)-mediated vasodilation.', Circulation research. United States, 87(2), pp. 160–166. doi: 10.1161/01.res.87.2.160.

Zavaritskaya, O. et al. (2020) 'Vasodilation of rat skeletal muscle arteries by the novel BK channel opener GoSlo is mediated by the simultaneous activation of BK and K(v) 7 channels.', British journal of pharmacology, 177(5), pp. 1164–1186. doi: 10.1111/bph.14910.

Zaydman, M. A. et al. (2013) 'Kv7.1 ion channels require a lipid to couple voltage sensing to pore opening.', Proceedings of the National Academy of Sciences of the United States of America, 110(32), pp. 13180–13185. doi: 10.1073/pnas.1305167110.

Zhang, D. et al. (2021) 'ET-CORM Mediated Vasorelaxation of Small Mesenteric Arteries: Involvement of Kv7 Potassium Channels.', Frontiers in pharmacology, 12, p. 702392. doi: 10.3389/fphar.2021.702392.

Zhang, F. et al. (2013) 'Modulation of K(v)7 potassium channels by a novel opener pyrazolo[1,5-a]pyrimidin-7(4H)-one compound QO-58.', British journal of pharmacology, 168(4), pp. 1030–1042. doi: 10.1111/j.1476-5381.2012.02232.x.

Zhang, H. et al. (2003) 'PIP(2) activates KCNQ channels, and its hydrolysis underlies receptor-mediated inhibition of M currents.', Neuron. United States, 37(6), pp. 963–975. doi: 10.1016/s0896-6273(03)00125-9.

Zhang, J. and Shapiro, M. S. (2012) 'Activity-dependent transcriptional regulation of M-Type (Kv7) K(+) channels by AKAP79/150-mediated NFAT actions.', Neuron, 76(6), pp. 1133–1146. doi: 10.1016/j.neuron.2012.10.019.

Zhang, J. and Yan, J. (2014) 'Regulation of BK channels by auxiliary γ subunits.', Frontiers in physiology, 5, p. 401. doi: 10.3389/fphys.2014.00401.

Zhang, R. et al. (2012) 'Sex differences in mesenteric endothelial function of streptozotocin-induced diabetic rats: a shift in the relative importance of EDRFs.', American journal of physiology. Heart and circulatory physiology, 303(10), pp. H1183-98. doi: 10.1152/ajpheart.00327.2012.

Zhang, W., Du, L. and Gunst, S. J. (2010) 'The effects of the small GTPase RhoA on the muscarinic contraction of airway smooth muscle result from its role in regulating

actin polymerization', American Journal of Physiology - Cell Physiology. doi: 10.1152/ajpcell.00118.2010.

Zhang, X.-F., Gopalakrishnan, M. and Shieh, C.-C. (2003) 'Modulation of action potential firing by iberiotoxin and NS1619 in rat dorsal root ganglion neurons.', Neuroscience. United States, 122(4), pp. 1003–1011. doi: 10.1016/j.neuroscience.2003.08.035.

Zhang, Y. et al. (2021) 'Larger endothelium-dependent contractions in iliac arteries of adult SHRs are attributed to differential downregulation of TP and EP3 receptors in the vessels of WKYs and SHRs during the transition from adolescence to adulthood', European Journal of Pharmacology. doi: 10.1016/j.ejphar.2020.173828.

Zhao, H. et al. (2019) 'Overexpression of the medium-conductance calcium-activated potassium channel (SK4) and the HCN2 channel to generate a biological pacemaker.', Molecular medicine reports. Greece, 20(4), pp. 3406–3414. doi: 10.3892/mmr.2019.10591.

Zhao, L.-M. et al. (2014) 'Advanced glycation end products impair K(Ca)3.1- and K(Ca)2.3-mediated vasodilatation via oxidative stress in rat mesenteric arteries.', Pflugers Archiv : European journal of physiology. Germany, 466(2), pp. 307–317. doi: 10.1007/s00424-013-1324-y.

Zhong, X. Z., Harhun, M. I., et al. (2010) 'Participation of KCNQ (Kv7) potassium channels in myogenic control of cerebral arterial diameter', Journal of Physiology. doi: 10.1113/jphysiol.2010.192823.

Zhong, X. Z., Abd-Elrahman, K. S., et al. (2010) 'Stromatoxin-sensitive, heteromultimeric Kv2.1/Kv9.3 channels contribute to myogenic control of cerebral arterial diameter.', The Journal of physiology, 588(Pt 22), pp. 4519–4537. doi: 10.1113/jphysiol.2010.196618.

Zhu, Y., Bond, J. and Thomas, P. (2003) 'Identification, classification, and partial characterization of genes in humans and other vertebrates homologous to a fish membrane progestin receptor', Proceedings of the National Academy of Sciences. National Acad Sciences, 100(5), pp. 2237–2242.

Zhuang, W. and Yan, Z. (2020) 'The S2-S3 Loop of Kv7.4 Channels Is Essential for Calmodulin Regulation of Channel Activation.', Frontiers in physiology, 11, p. 604134. doi: 10.3389/fphys.2020.604134.

Zieba, B. J. et al. (2011) 'The cAMP-responsive Rap1 guanine nucleotide exchange factor, Epac, induces smooth muscle relaxation by down-regulation of RhoA activity', Journal of Biological Chemistry, 286(19), pp. 16681–16692. doi: 10.1074/jbc.M110.205062.

Zopf, Y. et al. (2008) 'Women encounter ADRs more often than do men.', European journal of clinical pharmacology. Germany, 64(10), pp. 999–1004. doi:

Chapter 10: Appendices

Received: 11 September 2018 | Revised: 19 December 2018 | Accepted: 5 January 2019

DOI: 10.1111/bph.14598

RESEARCH PAPER

TMEM16A is implicated in the regulation of coronary flow and is altered in hypertension

Henry R. Askew Page[1,2] | Thomas Dalsgaard[2] | Samuel N. Baldwin[1] | Thomas A. Jepps[2] | Oleksandr Povstyan[1] | Søren P. Olesen[2] | Iain A. Greenwood[1,2]

[1] Vascular Biology Research Centre, Institute of Molecular and Clinical Sciences, St George's University of London, London, UK

[2] Department of Biomedical Sciences, Faculty of Health Sciences, University of Copenhagen, Copenhagen, Denmark

Correspondence
Iain Greenwood, Vascular Biology Research Centre, Institute of Molecular and Clinical Sciences, St George's University of London, London SW17 0RE, UK.
Email: grenwood@sgul.ac.uk

Funding information
British Heart Foundation, Grant/Award Numbers: PG/14/57/30992 and FS/18/41/33762; Novo Nordisk, Grant/Award Number: 6553

Background and Purpose: Coronary artery disease leads to ischaemic heart disease and ultimately myocardial infarction. Thus, it is important to determine the factors that regulate coronary blood flow. Ca^{2+}-activated chloride channels contribute to the regulation of arterial tone; however, their role in coronary arteries is unknown. The aim of this study was to investigate the expression and function of the main molecular correlate of Ca^{2+}-activated chloride channels, TMEM16A, in rat coronary arteries.

Experimental Approach: We performed mRNA and protein analysis, electrophysiological studies of coronary artery myocytes, and functional studies of coronary artery contractility and coronary perfusion, using novel inhibitors of TMEM16A. Furthermore, we assessed whether any changes in expression and function occurred in coronary arteries from spontaneously hypertensive rats (SHRs).

Key Results: TMEM16A was expressed in rat coronary arteries. The TMEM16A-specific inhibitor, MONNA, hyperpolarised the membrane potential in U46619. MONNA, $T16A_{inh}$-A01, and Ani9 attenuated 5-HT/U46619-induced contractions. MONNA and $T16A_{inh}$-A01 also increased coronary flow in Langendorff perfused rat heart preparations. TMEM16A mRNA was increased in coronary artery smooth muscle cells from SHRs, and U46619 and 5-HT were more potent in arteries from SHRs than in those from normal Wistar rats. MONNA diminished this increased sensitivity to U46619 and 5-HT.

Conclusions and Implications: In conclusion, TMEM16A is a key regulator of coronary blood flow and is implicated in the altered contractility of coronary arteries from SHRs.

1 | INTRODUCTION

Coronary artery disease occurs when the narrowing of coronary arteries prevents sufficient cardiac perfusion. If left untreated, it can cause fatal myocardial infarctions. High BP is a major risk factor for coronary artery disease, and reducing BP is one of the best treatments to reduce or prevent coronary events. Cardiac perfusion is dictated by flow through the coronary arteries, which is determined by the contractile state of the vascular smooth muscle cells (VSMCs) as well as the presence of pathological impediments like atheroma or thrombi. Understanding what controls coronary artery smooth muscle contraction is necessary to comprehend what limits cardiac perfusion and to develop novel therapies.

TMEM16A (also known as ANO1) proteins contribute to the formation of chloride permeable channels that are activated by submicromolar concentrations of intracellular calcium (calcium-activated

Abbreviations: ACTA2, α2 smooth muscle actin; CaCC, calcium-activated chloride channel; CADD, combined annotation-dependent depletion; $I_{Cl(Ca)}$, calcium-activated chloride current; LAD, left anterior descending (coronary artery); PSS, physiological saline solution; SHR, spontaneously hypertensive rat; SNP, single nucleotide polymorphism; VGCC, voltage-gated calcium channel; VSMC, vascular smooth muscle cell

 © 2019 The British Pharmacological Society

chloride channels [CaCCs]). As VSMCs actively accumulate chloride ions (Cl^-), activating CaCCs leads to Cl^- efflux and membrane depolarisation sufficient to activate (VGCCs), and evoke contraction. Consequently, TMEM16A represents a possible factor in the development of vascular disease including hypertension, and targeting these channels may be a viable new therapy. While TMEM16A expression has been identified in several arteries (Dam, Boedtkjer, Aalkjaer, & Matchkov, 2014; Dam, Boedtkjer, Nyvad, Aalkjaer, & Matchkov, 2014; Davis et al., 2010; Manoury, Tamuleviciute, & Tammaro, 2010; Thomas-Gatewood et al., 2011), there are no data on TMEM16A in coronary arteries and whether it is altered in hypertension. Moreover, there is no information on the effect of recently developed TMEM16A-specific blockers in coronary arteries. The present study sought to address these points.

What is already known

- TMEM16A proteins contribute to calcium-activated chloride channels.
- Reducing TMEM16A activity reduces vasoconstriction in pulmonary and mesenteric arteries.

What this study adds

- TMEM16A blockers impaired vasoconstrictor responses in coronary artery and improved coronary blood flow.
- Coronary arteries from hypertensive rats exhibited raised TMEM16A and augmented vasoconstrictor sensitivity.

What is the clinical significance

- Targeting TMEM16A represents a new therapeutic target for ischaemic heart disease.

2 | METHODS

2.1 | Animals

All experiments were performed on the first- and second-order branches of the left anterior descending (LAD) coronary artery and first-order septal coronary arteries or third-order mesenteric arteries from male Wistar rats (aged 12–13 weeks, weighing 250–350 g; Charles River, Margate, UK; RRID:RGD_737929), killed by cervical dislocation in accordance with Schedule 1 of the UK Animal (Scientific Procedures) Act 1986. Spontaneously hypertensive rats (SHRs; Envigo, UK; RRID: RGD_724574) aged 12–13 weeks (weighing 250–300 g) were used as an acknowledged model of essential hypertension. Rats were housed according to ASPA 1986 regulations with 12:12-hr light : dark cycle; 19–22°C room temperature; room relative humidity within a range of 50 ± 10%; and received ad libidum water (changed at least twice weekly) and laboratory rodent diet. Bedding was LBS Aspen Classic woodchip. Coronary arteries were identified and dissected free of the heart. The pericardium was peeled away from the surface of the heart, and the right and left main coronary arteries were traced from the aortic root. Arteries were dissected free from myocardial tissue before they were used in any experiment. The LAD was identified as the main artery distal to the bifurcation at the left circumflex artery. The septal artery was identified by cutting away the right ventricular wall; whence, it could be seen running along the interventricular septum. The septal artery varied in its anatomical origin, sometimes arising from the right coronary artery and sometimes from the left. Animal studies are reported in compliance with the ARRIVE guidelines (Kilkenny, Browne, Cuthill, Emerson, & Altman, 2010) and with the recommendations made by the *British Journal of Pharmacology*.

2.2 | Expression studies

The expression of TMEM16A, as well as the reference genes ATP synthase B subunit (ATP5B), cytochrome C1, 14-3-3 protein ζ/δ, and GAPDH (predetermined by GeNorm [Biogazelle, Belgium] analysis), was measured by quantitative PCR (qPCR). The coronary artery smooth muscle cell (SMC) samples were obtained by cutting longitudinally along the dissected vessel and rubbing the lumen with a human hair. The vessel was then placed in 0.1% Triton X PBS for 1 min followed by three 1-min washes in fresh PBS to ensure removal of endothelium. The treated arteries were subsequently dispersed to a cell suspension as outline below before being spun down into a pellet and used for RNA extraction. Cardiac and endothelial cell-specific primers were designed to check for contamination of the SMC sample. For a full list of primers used in this study, see Table 1. The primer sequences for housekeeping genes used for the GeNorm were unavailable due to proprietary reasons. qPCR samples were run in duplicate to strengthen the reliability of the single value. Antibody AB53212 (AbCam, Cambridge, UK), used in previous studies (Pritchard, Leblanc, Albert, & Greenwood, 2014), was used for immunochemical and Western blot studies (Abcam Cat# ab53212, RRID:AB_883075).

2.3 | Functional studies

Wire myography was used to assess TMEM16A function in LAD coronary artery segments. Once the LAD coronary artery had been dissected free from surrounding cardiac tissue, segments were mounted onto the myograph (Danish MyoTech, Aarhus, Denmark) in physiological saline solution (PSS). The force elicited by the tension of the vessel wall on the wires was recorded using LabChart software (ADInstruments, UK). For simultaneous membrane potential recordings, coronary artery segments were impaled with sharp glass microelectrodes with resistances of 60–130 MΩ, pulled on a horizontal puller (P-97 Sutter Instrument Co., USA), that were filled with 3 mol·L^{-1} KCl. The reference electrode (flat-tip Ag/AgCl probe; Warner Instrument, USA) was submerged in the myograph chamber, and the amplifier was zeroed with the recording electrode lowered into the bath solution. Voltage was recorded at 1 kHz through an amplifier (Intra 767, WPI Ltd.) and A-D converter (PowerLab 4SP,

TABLE 1 Primer sequences used in qPCR experiments

Gene	Forward primers (+) (5′-3′) Reverse primers (−) (5′-3′)	Gene ID	Amplicon size (base pairs)
Tmem16a	CCCTGTTCGTTGCGTCCTT GCTCTGATGGCTACTGGTCTC	NM_001107564	121
Tmem16b	GGACGATGAGGATGATGAAGATAA GATAGACAATGACCCCAAAGACA	XM_017602863.1	128
Myh11	CAGTTGGACACTATGTCAGGGAAA ATGGAGACAAATGCTAATCAGCC	XM_017596998.1	78
Acta2	ATCCGATAGAACACGGCATC AGGCATAGAGGGACAGCACA	NM_031004.2	228
Tnni3	TGACCTGCGTGGCAAGTT TCCTTCTCAATGTCCTCCTTCT	NM_017144.2	153
Tnnt2	AGGAGGAAGGCTGAAGATGA CTCTCGCTCTGTCTGTCTCT	XM_006249842.3	126
Pecam1	CTCCTAAGAGCAAAGAGCAACTTC TACACTGGTATTCCATGTCTCTGG	NM_031591.1	100
Vwf	GTCGGAAGAGGAAGTGGACATT GGGCACACGCATGCGCTCTGTA	NM_053889.1	136

ADInstruments, New Zealand). Impalements were deemed suitable when there was an abrupt, negative deflection in potential, which rapidly returned to the pre-impalement level upon withdrawal from the cell. In both settings, the vessel segments were bathed in PSS (in mmol·L^{-1}: NaCl 119, KCl 4.5, $MgSO_4{\cdot}7H_2O$ 1.17, $NaH_2PO_4{\cdot}2H_2O$ 1.18, $NaHCO_3$ 25, glucose 5, and $CaCl_2$ 1.25), heated to 37°C, and aerated with 95% O_2 and 5% CO_2.

For Langendorff studies, the hearts were swiftly dissected, and the ascending aorta was tied onto a perfusion cannula attached to a vertical perfusion rig (Hugo Sachs Elektronik-Harvard Apparatus GmbH, Germany). This allowed retrograde perfusion of the heart. The heart was perfused at 80 mmHg with Krebs–Henseleit solution (in mmol·L^{-1}: 118 NaCl, 4.7 KCl, 2 $CaCl_2$, 1.2 KH_2PO_4, 1.2 Mg_2SO_4, 2 sodium pyruvate, 24.9 $NaHCO_3$, and 10 glucose, pH 7.45, aerated with 95% O_2 and 5% CO_2), heated to 37°C, and filtered through an in-line 0.45-μm Sterivex HV filter (Millipore A/S, Hellerup, Denmark). Coronary flow was measured using an ultrasonic flow meter probe (Transonic Systems Inc., Ithaca, USA) situated above the aortic cannula. Aortic pressure, coronary flow, ECG, and perfusate temperature were continuously monitored. Coronary flow was measured using a 16-channel PowerLab system (ADInstruments, Oxford, UK) and recorded by LabChart 7 software. The heart was left until the basal coronary flow had stabilised before any drugs were added to the perfusate.

2.4 | Single cell electrophysiology

Single smooth muscle cells (SMCs) were isolated from LAD coronary arteries by enzymatic treatment. The dissected vessel was placed into ice cold, Ca^{2+}-free dispersal PSS (in mmol·L^{-1}: NaCl 120, KCl 6, glucose 12, HEPES 10, and $MgCl_2$ 1.2, pH adjusted to 7.4 with NaOH). The solution was then supplemented with 1.75 mg·ml^{-1} collagenase IA, 0.9 mg·ml^{-1} protease X, 1 mg·ml^{-1} BSA, and 1 mg·ml^{-1} trypsin inhibitor and incubated at 37°C for 9 min. Following this, the vessels were washed with ice cold dispersal PSS 3 times. After the last wash, the tube was filled with 1 ml of dispersal PSS, and the vessel was triturated with a fire-polished, wide-bore Pasteur pipette to liberate the VSMCs mechanically. The resultant cell suspension was then supplemented with $CaCl_2$ to 0.75 mM and plated onto coverslips before being left to settle at 4°C before use.

Whole cell currents were recorded following amphotericin B permeabilisation (300 μg·ml^{-1}) in the absence and presence of 10 mmol·L^{-1} **caffeine**. Amphotericin was added to the pipette solution (in mmol·L^{-1}: CsCl 106, TEA-Cl 20, HEPES 10, and EGTA 10, pH adjusted to 7.2 with CsOH), which was refreshed every 2 hr for consistent amphotericin activity. The cells were superfused with bathing solution (in mmol·L^{-1}: NaCl 120, TEA-Cl 5, KCl 6, glucose 12, HEPES 10, $MgCl_2$ 1.2, and $CaCl_2$ 1.5, pH adjusted to 7.4 with NaOH). Currents evoked by caffeine application were recorded during a ramp protocol which stepped to −100 mV from a −50-mV holding potential and steadily increased to +100 mV over 2 s. MONNA was applied in the caffeine-free bathing solution before the protocol was repeated in the presence of both drugs. Where possible, drugs were applied while recording from the same cell as the initial caffeine application. Cells were always compared to same day controls. Similar experiments were performed on pulmonary artery cells where the calcium-activated chloride current ($I_{Cl(Ca)}$) has been characterised extensively (Manoury et al., 2010; Pritchard et al., 2014).

2.5 | Statistical analysis and blinding

For all graphs, the error bars represent SEM of no less than 5 independent data points. Each data point represents data collected from one animal. Data from myography experiments are expressed as a

percentage of the peak contraction in response to a maximal concentration of U46619 or 5-HT, or the peak of the first high K^+-induced contraction/EC_{80}-induced contraction. This is to control for variation in the overall contractility of the vessel segment. Similarly, in the Langendorff experiments, data are expressed as percentage change in flow to control for varying heart sizes and therefore innate differences in coronary flow. Randomisation of samples was undertaken in the functional experiments by scrambling the vessel segments before mounting them into the myograph chambers. In this way, vessel segments from higher or lower down the coronary artery branch were randomised to whether they were subjected to treatment or control conditions. Blinding of the experiments was impractical due to the experimenter adding differing concentrations of drugs to the set-ups. Concentration-effect curves were log transformed to reduce the skew, and curves were fitted to the data using four-parameter, non-linear regression curve fitting in GraphPad Prism (version 7.0b; GraphPad Prism, RRID:SCR_002798) with the following formula: Y = Bottom + (Top − Bottom)/(1 + 10 ^ ((LogEC50 − X)*HillSlope)) where x is [agonist] (in log M), Y is the percentage of the peak contraction mentioned above, Top refers to F_{max} (maximal percentage), Bottom refers to F_{min} (average percentage contraction at lowest concentration of agonist), and the Hill Slope is variable. Comparisons of responses ± blocker versus same day/animal controls were compared by two-way ANOVA, followed by a post hoc test (Bonferroni) for multiple comparisons. Peak contraction studies ± inhibitor and ±Cl^- were compared to same day/animal controls using Student's paired or unpaired two-tailed *t* test where appropriate. Comparisons between Wistars and SHRs were made using data from earlier experiments in order to reduce animal numbers. Therefore, data were not paired for analysis, and the *n* numbers are not equal. Statistical significance is defined as $P < 0.05$ (*).The data and statistical analysis comply with the recommendations of the *British Journal of Pharmacology* on experimental design and analysis in pharmacology.

2.6 | Reagents

All drugs and reagents were purchased from Sigma-Aldrich (Dorset, UK) unless otherwise stated. MONNA, T16Ainh-A01, and Ani9 (Tocris, UK) block Cl^- currents that were generated by the overexpression of TMEM16A or endogenous TMEM16A currents with IC_{50}s of about 0.1, 1, and 0.1 μM, respectively (Namkung, Phuan, & Verkman, 2011; Oh et al., 2013; Seo et al., 2016).

2.7 | Nomenclature of targets and ligands

Key protein targets and ligands in this article are hyperlinked to corresponding entries in http://www.guidetopharmacology.org, the common portal for data from the IUPHAR/BPS Guide to PHARMACOLOGY (Harding et al., 2018), and are permanently archived in the Concise Guide to PHARMACOLOGY 2017/18 (Alexander et al., 2017a,b).

3 | RESULTS

3.1 | TMEM16A is expressed in rat coronary arteries

qPCR revealed expression of Tmem16a and extremely low expression of the close orthologue Tmem16b in LAD and septal coronary arteries (Figure 1a). The relative level of Tmem16a expression was higher than mesenteric arteries but lower than pulmonary arteries (Figure 1b) where CaCCs have been well characterised (Angermann, Forrest, Greenwood, & Leblanc, 2012; Davis et al., 2013; Greenwood, Ledoux, & Leblanc, 2001; Greenwood, Ledoux, Sanguinetti, Perrino, & Leblanc, 2004; Manoury et al., 2010; Piper & Greenwood, 2003; Pritchard et al., 2014; Q. Wang, Hogg, & Large, 1992; Wiwchar, Ayon, Greenwood, & Leblanc, 2009; Yuan, 1997). In Western blot studies (Figure 1c), untransfected and GFP-tagged TMEM16A transfected HEK293 cells were used to further validate anti-TMEM16A antibody AB53212 for use in immunocytochemical/histochemical experiment. Rat pulmonary artery lysates were also used as the expression of TMEM16A has previously been characterised here (Pritchard et al., 2014; Sun, Xia, Paudel, Yang, & Sham, 2012). Antibody AB53212 produced a band close to the theoretical MW for TMEM16A protein (~120 kDa) in lysates from rat pulmonary artery and the two HEK cell samples. A band was also detected around 145 kDa in lysates of HEK cells transfected with GFP-tagged TMEM16A. No band was detected at these MWs from rat coronary artery ($n = 3$ complete isolations, where each isolation consisted of three rats worth of arteries). The distribution of TMEM16A encoded protein was investigated in isolated coronary artery SMCs. Figure 1d shows representative images of TMEM16A staining. Imaging of cells incubated with the TMEM16A antibody AB53212 (Figure 1d, i–iv) showed disperse TMEM16A staining throughout the cytoplasm with more intense punctate regions both centrally and around the extremities of the cell (examples indicated by Arrows 1 and 2). Expression of TMEM16A protein was also observed in transverse sections of coronary arteries in situ (Figure 1e) delineated by α-smooth muscle actin staining (indicated by Arrows 1 and 3). TMEM16A was also detected in the surrounding, troponin-positive myocardium.

These data show that TMEM16A is expressed in coronary artery SMCs.

3.2 | TMEM16A activation is integral to agonist-induced contraction of rat coronary arteries

When LAD coronary artery segments were incubated in a low chloride PSS, contractions to both U46619 and 5-HT were reduced considerably (Figure 2a,b, respectively). Bathing LAD coronary artery segments in high K^+-PSS produced robust and reproducible contractions that were not affected by incubation with 10-μmol·L^{-1} MONNA (Figure 2c) suggesting that the agent did not directly inhibit VGCCs. Application of U46619 and 5-HT produced concentration-dependent contractions with approximate EC_{50} values of 37 ± 7 nmol·L^{-1} ($n = 27$) and 207 ± 56 nmol·L^{-1} ($n = 12$),

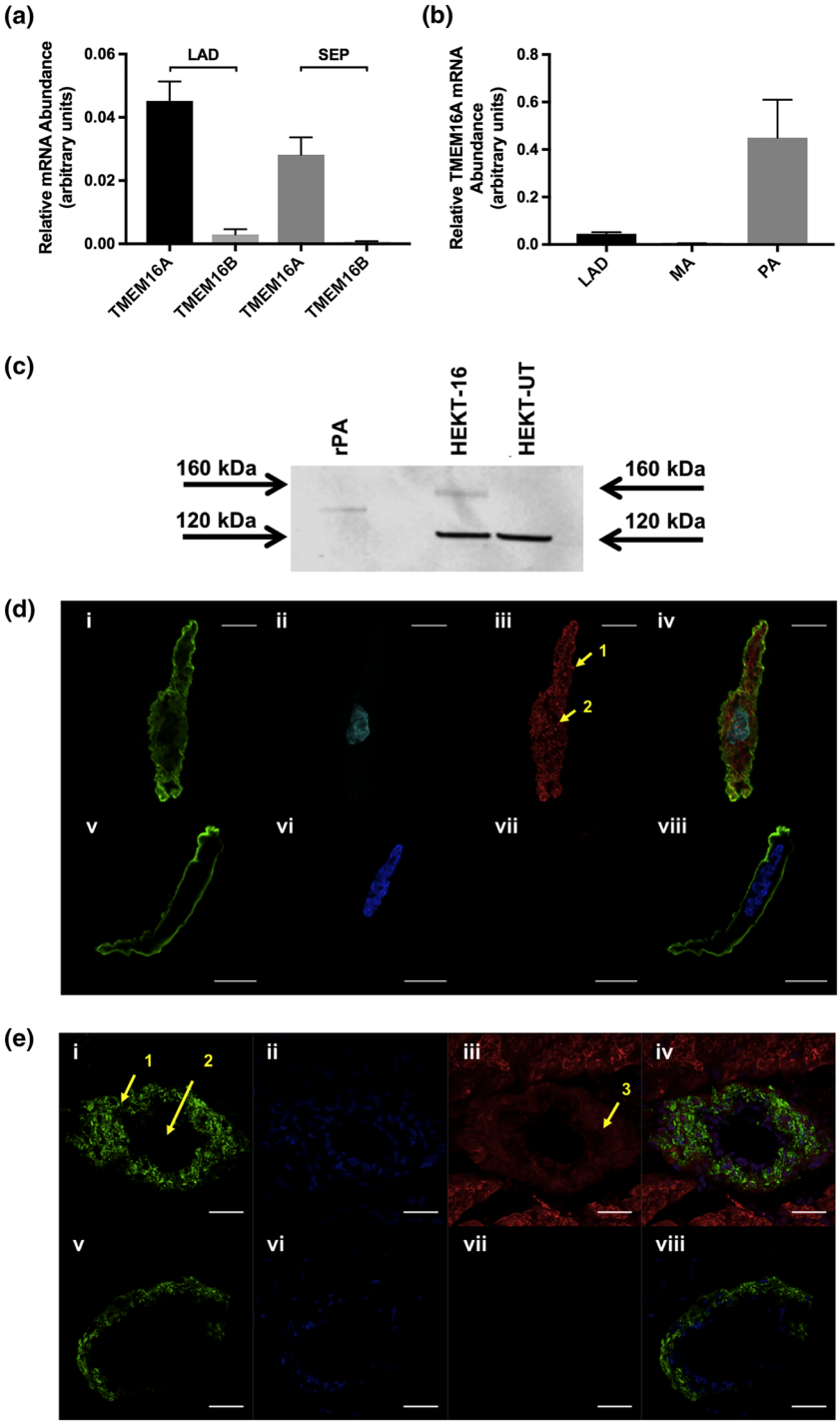

FIGURE 1 Tmem16a is expressed in rat coronary arteries. (a) Abundance of Tmem16a and Tmem16b mRNA relative to predetermined house-keeping genes in left anterior descending (LAD) and septal coronary arteries. *n* = 3 where *n* is a pooled sample of arteries from at least three rats. (b) Abundance of Tmem16a mRNA relative to predetermined house-keeping genes in LAD coronary arteries, mesenteric arteries, and pulmonary arteries. *n* = 3 where *n* is a pooled sample of arteries from at least three rats. (c) Western blot with anti-TMEM16A antibody AB53212 on lysates from rat pulmonary artery, TMEM16A-GFP-transfected HEK293 cells, and untransfected HEK293 cells. Each rat sample constitutes three rats worth of tissue. (d) Single isolated vascular smooth muscle cells (VSMCs) from LAD coronary arteries with anti-TMEM16A antibody AB53212 (i–iv). Cells are co-stained with anti-α-smooth muscle actin (i and v), DAPI (ii and vi), anti-TMEM16A (iii), and a composite image (iv and viii). Arrows highlight small hotspots of intense staining. Images v–viii show a single VSMC isolated from a LAD coronary artery that was not incubated with an anti-TMEM16A primary antibody. Images are representative of at least three cells from arteries of three rats. Scale bar is 10 μm. (e) Images of a 16-μm-thick slice of a rat heart where a coronary artery can be seen in situ, stained with anti-α-smooth muscle actin (i and v), DAPI (ii and vi), +anti-TMEM16A (iii), −anti-TMEM16A (vii), and a composite image (iv and viii). Arrows 1 and 3 indicate the arterial wall within the myocardial tissue, and Arrow 2 highlights the lumen of the vessel. Images are representative of slices from two rats and two to three arteries per rat. Scale bar is 30 μm

respectively. These contractions were abolished by prior incubation with 10-nmol·L^{-1} **nicardipine** (Figure S1) indicating that activation of **VGCCs** was crucial for contractions brought about by both U46619 and 5-HT. Application of MONNA inhibited the contractile response to U46619 and 5-HT in a concentration-dependent manner (Figure 2d–g). The inhibitory effect of MONNA was not reliant upon a functional endothelium (Figure 2i,j) and was not altered by incubation with a cocktail of K^+ channel blockers (Figure 2H).

3.3 | Effect of T16A$_{inh}$-A01 and Ani9 on contraction of LAD coronary arteries

High K^+-induced contractions of LAD coronary artery segments were significantly inhibited by pre-incubation with 10-μmol·L^{-1} T16A$_{inh}$-A01 (Figure 3b). While 3-μmol·L^{-1} T16A$_{inh}$-A01 and Ani9 did not cause statistically significant attenuations in the high K^+-induced contractions, there was a trend for them to be reduced (Figure 3b,a, respectively). In further experiments, Ani9 caused a small but significant attenuation

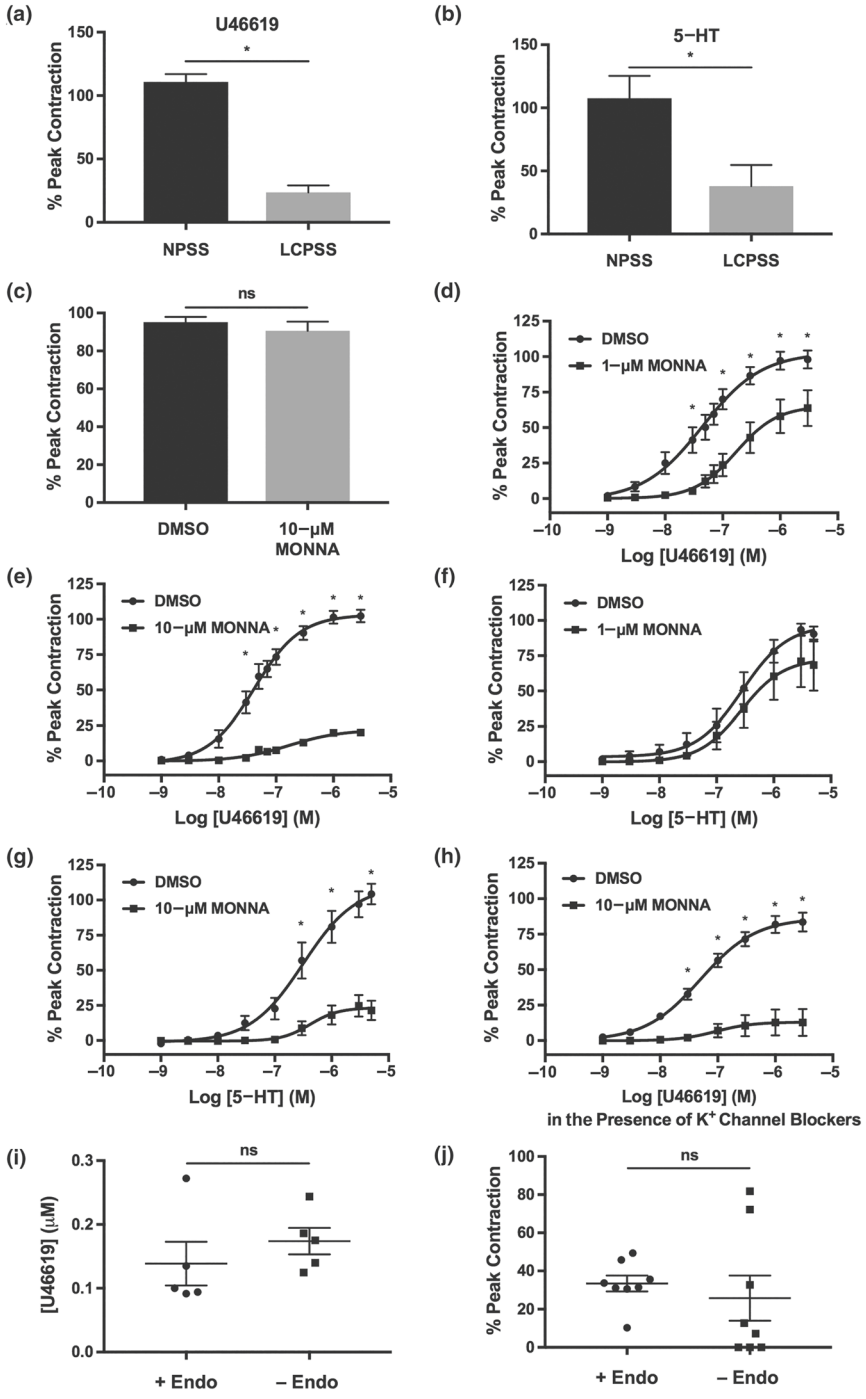

FIGURE 2 Inhibition of TMEM16A significantly attenuates coronary artery function. Bar charts showing that contractions of coronary arteries to (a) U46619 and (b) 5-HT were significantly smaller when the segments were bathed in low chloride physiological saline solution (LCPSS); n = 7 for U46619 and n = 6 for 5-HT. (c) Pre-incubation of 10 μmol·L^{-1} MONNA had no effect on the KPSS-induced contraction in LADCA segments; n = 6 for both DMSO and MONNA. (d) Pre-incubation with 1 μmol·L^{-1} MONNA caused a significant attenuation of the U46619-induced response in left anterior descending (LAD) coronary arterials segments (n = 8 for both DMSO and 1 μmol·L^{-1} MONNA), while pre-incubation with 10 μmol·L^{-1} MONNA significantly reduced the ability of the vessel to contract to (e) U46619 (n = 8 for both DMSO and 10 μmol·L^{-1} MONNA). (f) Pre-incubation with 1 μmol·L^{-1} MONNA did not cause a significant attenuation of the 5-HT-induced response in LAD coronary arterial segments (n = 6 for both DMSO and 1 μmol·L^{-1} MONNA), while pre-incubation of 10 μmol·L^{-1} MONNA significantly reduced the ability of the vessel to contract to (g) 5-HT (n = 8 for both DMSO and 10 μmol·L^{-1} MONNA). (h) Concentration effect curves of U46619 in LADCA segments in the presence of K^+ channel blockers were significantly attenuated after incubation with 10 μmol·L^{-1} MONNA; n = 8 for both. (i) Scatter graph indicating that the EC_{50} of U46619 in LAD coronary artery segments in the presence of 10 μmol·L^{-1} MONNA were similar in both endothelium intact and denuded segments. Data are expressed as mean EC_{50} of U46619 ± SEM (in 10 μmol·L^{-1} MONNA), n = 5 for both. (j) The maximal contraction evoked by U46619 in LADCA segments incubated with 10 μmol·L^{-1} MONNA was not different between endothelium intact and endothelium denuded segments; n = 5 for both. All data are expressed as mean ± SEM. Statistical significance is defined as $^*P < 0.05$

in the U46619-induced contraction although, given the data in Figure 3 a, it is difficult to say whether this was due solely to TMEM16A inhibition (Figure 3c). $T16A_{inh}$-A01 caused leftward shifts in the U46619 concentration effect curves in LAD coronary artery segments at both 3 and 10 μmol·L^{-1} (Figure 3d,e). Interestingly, the effect of pre-incubation with 3-μmol·L^{-1} $T16A_{inh}$-A01 was more marked than that with 10-μmol·L^{-1} $T16A_{inh}$-A01 and 3-μmol·L^{-1} Ani9. 10-μmol·L^{-1} $T16A_{inh}$-A01 also caused an inhibition of 5-HT-induced contractions in LAD coronary arteries (Figure 3f). This inhibition of U46619- and 5-HT-induced contractions with 10-μmol·L^{-1} $T16A_{inh}$-A01 was also seen in septal coronary arteries (Figure S2). Given the data in Figure 2 c–j where MONNA did not cause an effect on the high K^+-induced contractions, and its effect on agonist-induced contractions was independent of endothelium and was unchanged in the present of a cocktail of potassium channel blockers, we decided to focus on MONNA for further studies.

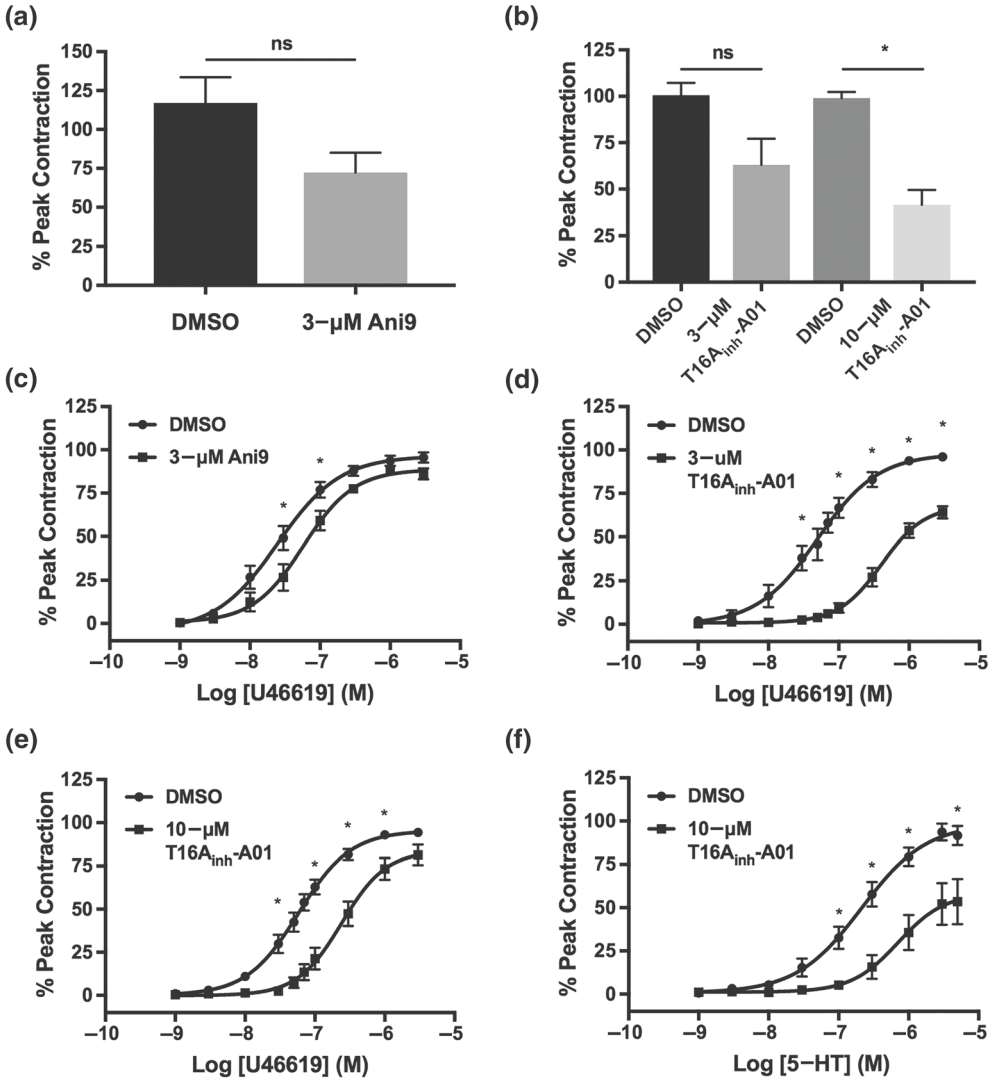

FIGURE 3 Effect of other TMEM16A inhibitors on coronary artery contractility. (a) Pre-incubation with 3 μmol·L^{-1} Ani9 did not cause a significant attenuation of the high K^+-induced contraction of coronary arteries (n = 5 for both DMSO and 3 μmol·L^{-1} Ani9). (b) While pre-incubation with 3 μmol·L^{-1} T16A$_{inh}$-A01 did not cause a significant attenuation of high K^+-induced contraction of coronary arteries (n = 5 for both DMSO and 3 μmol·L^{-1} T16A$_{inh}$-A01), pre-incubation with 10 μmol·L^{-1} T16A$_{inh}$-A01 reduced the contractility considerably (n = 12 for both DMSO and 10 μmol·L^{-1} T16A$_{inh}$-A01). (c) U46619 concentration effect curves were significantly attenuated in the presence of 3 μmol·L^{-1} Ani9 (n = 6 for both DMSO and 3 μmol·L^{-1} Ani9), (d) 3 μmol·L^{-1} T16A$_{inh}$-A01 (n = 9 for both DMSO and 3 μmol·L^{-1} T16A$_{inh}$-A01), and (e) 10 μmol·L^{-1} T16A$_{inh}$-A01 (n = 10 for both DMSO and 10 μmol·L^{-1} T16A$_{inh}$-A01). (f) 5-HT concentration effect curves were also significantly impaired in the presence of 10 μmol·L^{-1} T16A$_{inh}$-A01 (n = 7 for both DMSO and 10-μmol·L^{-1} T16A$_{inh}$-A01). All data are expressed as mean ± SEM. Statistical significance is defined as *P < 0.05

3.4 | Involvement of TMEM16A in coronary perfusion

The influence of TMEM16A channels on coronary blood flow in whole hearts was investigated using a Langendorff preparation. Application of either MONNA or T16A$_{inh}$-A01 (10 nmol·L^{-1}–1 μmol·L^{-1}) enhanced coronary flow (Figure 4a) without any effect on cardiac parameters. The QT and RR intervals recorded during these experiments can be seen in Tables 2 and 3. MONNA (1 μmol·L^{-1}) also prevented the decreased coronary flow produced by infusion of U46619 (10 nmol·L^{-1}, Figure 4b,c). These data show that pharmacologically disabling TMEM16A improves coronary blood flow.

3.5 | MONNA attenuates caffeine-evoked chloride currents in coronary artery VSMCs and decreases membrane potential of U46619-constricted coronary arteries

In line with previous studies investigating CaCCs (Greenwood et al., 2001), **caffeine** was used to mobilise Ca^{2+} from the sarcoplasmic reticulum and evoke $I_{Cl(Ca)}$. Reproducible caffeine-evoked chloride currents were recorded in LAD coronary artery VSMCs in the absence, but not in the presence, of 10-μmol·L^{-1} MONNA (Figure 5a). Caffeine evoked considerably larger currents in similar experiments on pulmonary artery SMCs (Figure S3). In sharp microelectrode recordings on whole

TABLE 2 Cardiac parameters from Langendorff experiments

Treatment	QT (ms)	RR interval (ms)	Coronary flow ($ml \cdot min^{-1}$)
Vehicle	69 ± 6	182 ± 18	11.9 ± 0.1
MONNA (μM)			
0.01	66 ± 7	166 ± 15	12.1 ± 0.2
0.03	72 ± 8	182 ± 15	12.2 ± 0.2
0.1	63 ± 5	173 ± 17	12.8 ± 0.4
0.3	64 ± 6	176 ± 20	14.3 ± 0.4*
1	74 ± 8	191 ± 20	20.7 ± 1.0*
Vehicle	72 ± 7	173 ± 14	12.4 ± 0.6
U46619 (μM)			
0.01	62 ± 5	167 ± 17	8.8 ± 0.2*
MONNA + U46619 (μM)			
1.0 + 0.1	66 ± 8	177 ± 19	11.6 ± 0.2#

Note: QT and RR intervals were extrapolated from ECG recorded by LabChart. Coronary flow was measured directly with ultrasonic flow meter probe. Data are expressed as mean ± SEM, n = 5–6. Paired t test.

*P < 0.05 from vehicle.

#P < 0.05 from U46619.

TABLE 3 Cardiac parameters from Langendorff experiments

Treatment	QT (ms)	RR interval (ms)	Coronary flow ($ml \cdot min^{-1}$)
Vehicle	64 ± 9	174 ± 20	9.9 ± 0.1
$T16A_{inh}$-A01 (μM)			
0.01	62 ± 7	168 ± 19	9.9 ± 0.1
0.03	65 ± 9	179 ± 21	10.2 ± 0.1
0.1	73 ± 8	174 ± 21	10.2 ± 0.2
0.3	72 ± 8	166 ± 22	11.1 ± 0.3*
1	64 ± 8	151 ± 28	12.9 ± 0.3*

Note: QT and RR intervals were extrapolated from ECG recorded by LabChart. Coronary flow was measured directly with ultrasonic flow meter probe. Data are expressed as mean ± SEM, n = 5. Paired t test.

*P < 0.05 from vehicle.

LAD coronary arteries, application of an EC_{50} concentration of U46619 contracted arteries with an associated depolarisation of the membrane potential (Figure 5b). Application of 10-$\mu mol \cdot L^{-1}$ MONNA caused membrane potential repolarisation (Figure 5b). This change in membrane potential was accompanied by a simultaneous decrease in wall tension.

3.6 | Altered expression of TMEM16A in SHR coronary artery SMCs

SMCs were isolated from coronary arteries as described above. The cleanliness of the SMC preparation was confirmed by qPCR analysis of cardiac and endothelial cell-specific markers (troponin T2, troponin I3, Von Willebrand factor, and platelet and endothelial cell adhesion marker). Tmem16a expression was greatest in the SMC sample and at low levels in ventricular tissue and endothelial cells. The SMC samples were highly positive for the smooth muscle markers α2 smooth muscle actin (Acta2), and myosin heavy chain 11, while comparatively negligible levels of expression of the cardiac and endothelial cell-specific markers were found in the SMC sample. All data for these experiments can be found in Figure S4. This established that the SMC sample was free from cardiac and endothelial contamination. qPCR analysis showed a ~fourfold increase in expression of Tmem16a in the coronary artery SMCs of SHRs when compared to Wistar controls (Figure 6a). Importantly, Tmem16a expression in ventricular tissue, where protein staining can be seen (Figure 1e, iii), was not increased in the hearts from SHRs (Figure 6b). This finding adds further credence to the fact that the results seen in Figure 6a are not due to any contribution from cardiac myocytes.

3.7 | Altered function of TMEM16A in SHR LAD coronary arteries

Functional experiments revealed that LAD segments had a greater sensitivity to U46619 and 5-HT compared to segments from normotensive rats contracting more in response to lower concentrations without a change in the maximal contractile response (Figure 7c,d, respectively); 30-$nmol \cdot L^{-1}$ 5-HT caused a contraction of 0.12 ± 0.05 mN in LAD coronary artery segments of Wistars, while it caused a much bigger contraction of 1.23 ± 0.32 mN in those of SHRs (P = 0.0018), equivalent to a ~10-fold increase in contraction. This increased sensitivity was abolished by application of 10-$\mu mol \cdot L^{-1}$ MONNA (Figure 7b). Similar effects were seen in the U46619 contraction study (Figure 7a). In addition, LAD segments from SHRs exhibited a higher level of spontaneously developed basal tone, which was abrogated by 10-$\mu mol \cdot L^{-1}$ MONNA (Figure 7i). In contrast, the overall contractility of LAD coronary artery segments from SHRs in response to U46619 and 5-HT was less sensitive to inhibition by MONNA than in LAD coronary arteries from normotensive rats (Figure 7e–h). This is reflected in the mean EC_{50} values highlighted in Table 4. In summary, expression of Tmem16a mRNA is higher in coronary arteries from SHRs that was associated with a MONNA-sensitive increase in basal tone and responsiveness to low concentrations of U46619 and 5-HT.

4 | DISCUSSION

This study is the first to identify expression of TMEM16A in coronary arteries and implicate it in determination of coronary perfusion. In addition, we report changes in TMEM16A expression and function in coronary arteries from hypertensive rats.

We show that MONNA, at concentrations that inhibit TMEM16A mediated Cl^- currents in overexpression systems, inhibited $I_{Cl(Ca)}$ in coronary artery myocytes, attenuated contractions produced by

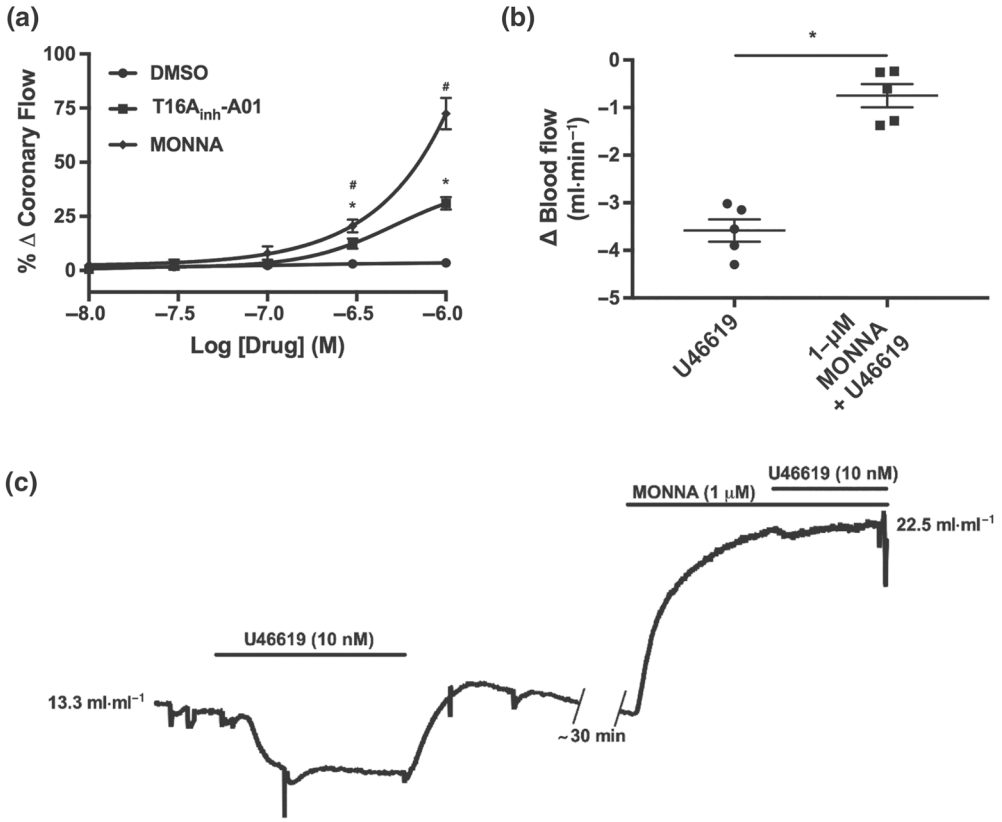

FIGURE 4 Inhibition of TMEM16A significantly increases coronary flow. (a) Application of MONNA and T16A$_{inh}$-A01 caused a concentration-dependent increase in coronary flow (n = 6 for MONNA, n = 5 for T16A$_{inh}$-A01, and n = 5 for DMSO). Pre-incubation with 1 μmol·L^{-1} MONNA prevented U46619-induced reductions in coronary flow (b) (n = 5 for both conditions). (c) Shows a representative trace from the experiment described in (b). All data are expressed as mean ± SEM. Statistical significance is defined as $^*P < 0.05$

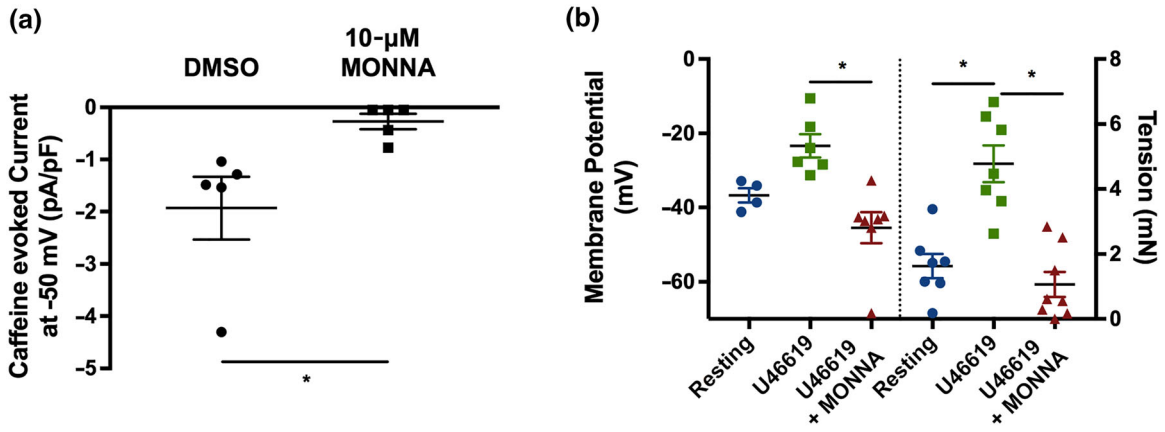

FIGURE 5 The scatter plot shows the increase in current evoked from left anterior descending coronary artery vascular smooth muscle cells, at a holding potential of −50 mV, upon application of 10 mmol·L^{-1} caffeine in the absence and presence of 10 μmol·L^{-1} MONNA; n = 5. Scatter graph showing the membrane potential (left, mV), and evoked contraction (right, mN) in resting, +U46619, and +U46619 + 10 μmol·L^{-1} MONNA; n = 4 for resting E_M, n = 6 for E_M in U46619, and n = 7 for E_M in U46619 + 10 μmol·L^{-1} MONNA, and n = 7 for tension recordings in resting and U46619, and n = 8 in U46619 + 10 μmol·L^{-1} MONNA. All data are expressed as mean ± SEM. Statistical significance is defined as $^*P < 0.05$

U46619 and 5-HT, reversed membrane depolarisation produced by U46619, inhibited spontaneously induced basal tone, and improved coronary blood flow. These anti-contractile effects were not dependent upon a functional endothelium, nor were they affected by incubation of the coronary artery with several K^+-channel blockers. Moreover, they did not reflect a direct block of calcium channels as contractions produced by high K^+ solutions were not affected by MONNA, although two other TMEM16A blockers, T16A$_{inh}$-A01 and Ani9, did affect high K^+ spasms moderately. Incubation of the coronary arteries in low Cl^- bathing solution also attenuated 5-HT-

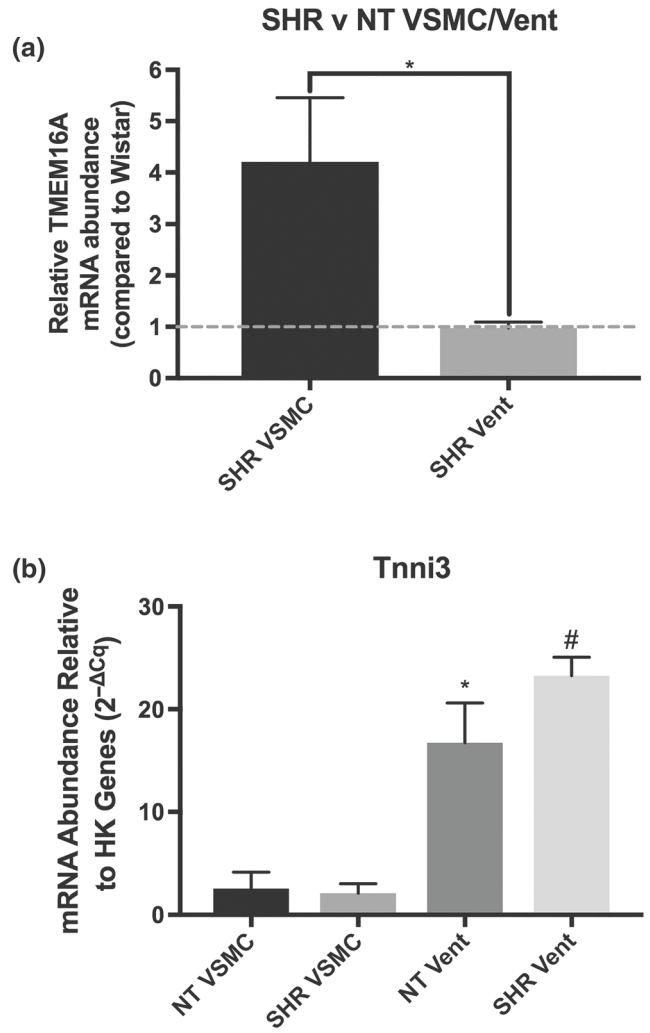

FIGURE 6 Increased expression of Tmem16a in coronary arteries from spontaneously hypertensive rats (SHRs). (a) Tmem16a mRNA is expressed at levels approximately fourfold greater in coronary arteries smooth muscle cells from SHRs when compared to Wistar rats. There was no increase in Tmem16a expression in the ventricular tissue from SHRs. (b) The expression of the cardiac-specific marker troponin I3 (Tnni3) was expressed at negligible levels in the coronary artery vascular smooth muscle cell (VSMC) samples of both Wistar rats and SHRs, and expression was significantly greater in the ventricular tissue of the same rats (*for Wistar tissues, # for SHR tissues). All data are expressed as mean ± SEM of at least five separate rat samples. Statistical significance is defined as $P < 0.05$

and U46619-induced contractions considerably. These consolidated data provide evidence that activation of TMEM16A-comprising Cl^- channels produces sufficient depolarisation to increase calcium channel opening and produce vasoconstriction in response to two different receptor agonists as well as at rest in certain conditions. By inference, these data implicate TMEM16A channels as key determinants of coronary perfusion. However, Boedtkjer, Kim, Jensen, Matchkov, and Andersson (2015) have challenged the specificity of $T16A_{inh}$-A01 and, to a lesser extent, that of MONNA. They reported no difference in contractions of rat mesenteric arteries to noradrenaline in the absence or presence of Cl^- in the PSS. Moreover, 10 $\mu mol \cdot L^{-1}$ of both $T16A_{inh}$-A01 and MONNA inhibited the Cl^--independent contraction seen in the mesenteric arteries, indicating that these two inhibitors abrogate contractility of these vessels in the absence of a functional chloride gradient. Our data in coronary arteries concur with their finding that $T16A_{inh}$-A01 relaxed rat mesenteric arteries contracted with a high extracellular K^+-containing (60 $mmol \cdot L^{-1}$) saline solution. This supports the Boedtkjer et al. (2015) proposal that this agent inhibited vasospasm by means other than inhibiting $I_{Cl(Ca)}$, with direct blockade of calcium channels most likely. However, our data did not emulate the low Cl^- experiment findings of Boedtkjer et al. (2015), and we have no explanation for these differences. Our extensive characterisation of MONNA gave us no reason to doubt its specificity for TMEM16A. Nonetheless, it is curious that so many purportedly TMEM16A-specific inhibitors also cause a decrease in the high K^+-induced contraction. Interestingly, a reduction in high K^+-induced contraction and expression of VGCCs has been reported upon TMEM16A knockdown in rat mesenteric arteries (Dam, Boedtkjer, Aalkjaer, et al., 2014; Dam, Boedtkjer, Nyvad, et al., 2014), and more recently, constitutive TMEM16A-targetted siRNA down-regulation was associated with a concurrent decrease in L-type voltage-gated Ca^{2+} channel protein expression (Jensen et al., 2018). This questions whether $T16A_{inh}$-A01 and Ani9 are indeed blocking TMEM16A and causing a similar effect to that of TMEM16A knockdown. It could be possible that TMEM16A has a regulatory function that modulates other ion channels, as suggested in Jensen et al. (2018). CFTR, another Cl^- channel, negatively regulates CaCCs in bovine pulmonary arteries (Wei et al., 1999). Furthermore, it indicates that TMEM16A could be coupled to VSMC contraction in ways other than the direct depolarising effect of $I_{Cl(Ca)}$. Indeed, a recent paper has implicated TMEM16A in the RhoA/Rho-associated protein kinase (ROCK) signalling pathway (Li et al., 2016). This could possibly account for the results seen in the Cl^--free experiments in Boedtkjer et al. (2015) where noradrenaline-induced contractions of mesenteric artery were still sensitive to TMEM16A inhibitors.

We observed an increase of TMEM16A transcript in coronary and arteries from SHRs, which exhibited a greater level of spontaneous basal tone development. Furthermore, we show that U46619 and 5-HT were more effective at eliciting contraction at lower concentrations (10 and 30 $nmol \cdot L^{-1}$, respectively) in arteries from SHRs and these responses along with the heightened basal tone were abrogated by MONNA. Interestingly, our study shows that inhibition of TMEM16A was less effective against maximal contractions in arteries from SHRs compared to Wistar controls, similar to a previous report by B. Wang, Li, Huai, and Qu (2015). These results suggest that the increase in contractility of coronary arteries from SHRs could be due to the increased expression of TMEM16A causing greater depolarisation and therefore Ca^{2+} influx. In support of this hypothesis, VSMC-specific knockout of TMEM16A reduced systemic BP and attenuated the development of hypertension in mice (Heinze et al., 2014), and knockdown of TMEM16A with siRNA prevented the increase in systolic BP in SHRs (B. Wang et al., 2015). Furthermore,

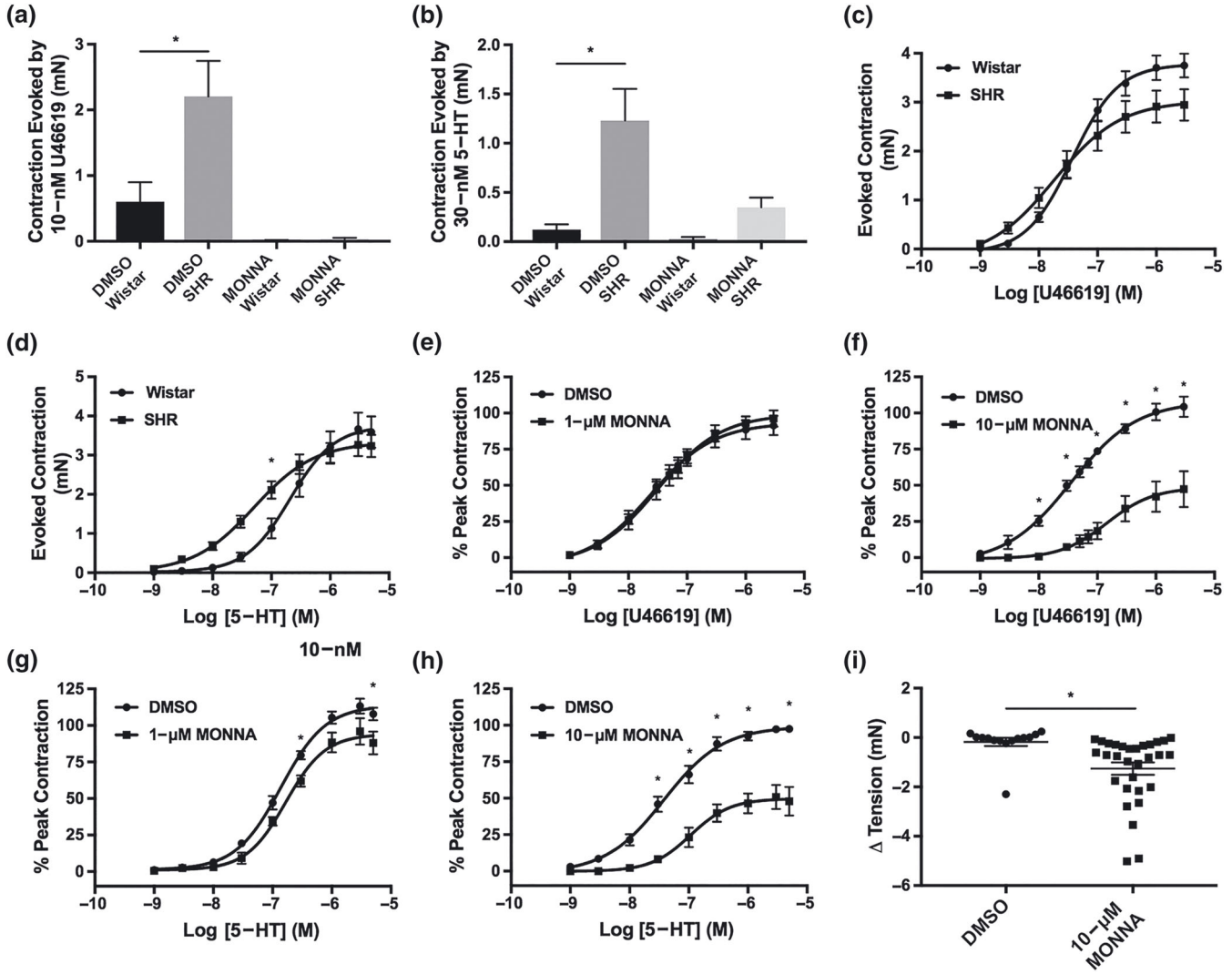

FIGURE 7 Altered function of TMEM16A in left anterior descending (LAD) coronary arteries from spontaneously hypertensive rats (SHRs). (a) Increases in contractility of LAD coronary arteries from SHRs in response to lower concentrations of U46619 (n = 8 for Wistar and n = 6 for SHRs) and 5-HT (b) (n = 9 for Wistars and n = 7 for SHRs) were abolished by pre-incubation with 10 μmol·L^{-1} MONNA. LAD coronary arteries from SHRs were more sensitive to constriction with U46619 (n = 27 for Wistar and n = 16 for SHR) and 5-HT (n = 12 for Wistar and n = 13 in SHRs) (c and d). (e) Pre-incubation with 1 μmol·L^{-1} MONNA has no effect on the U46619 concentration effect curve in LAD coronary artery segments of SHRs. (f) Pre-incubation with 10 μmol·L^{-1} MONNA significantly attenuates the ability of the vessel to constrict to U46619. (g) Pre-incubation with 1 μmol·L^{-1} MONNA has a small but significant effect on the 5-HT concentration-effect curve in LAD coronary artery segments of SHRs. (h) Pre-incubation with 10 μmol·L^{-1} MONNA significantly attenuates the ability of the vessel to constrict to 5-HT. (i) Basal tone developed in LAD coronary artery segments of SHRs was significantly suppressed by application of 10 μmol·L^{-1} MONNA. All data are expressed as mean ± SEM. Statistical significance is defined as $^*P < 0.05$

pulmonary arteries from animals with monocrotaline- or chronic hypoxia-induced hypertension have increased TMEM16A protein and $I_{Cl(Ca)}$ density (Forrest et al., 2012; Sun et al., 2012). Ideally, we would like to show increased protein expression by Western blot in the coronary arteries of SHRs, similar to studies in other arteries of SHRs (B. Wang et al., 2015). However, we were not able to detect a band at ~120 kDa in lysates from coronary artery or mesenteric artery even though robust staining was detected in immunocytochemical studies with the validated anti-TMEM16A antibody, AB53212. These findings suggest that the molecular isoforms of TMEM16A may differ in different arteries with the pulmonary artery exhibiting the conventional full-length form. A truncated isoform of TMEM16A has been identified in the interstitial cells of Cajal of patients with diabetic gastroparesis (Mazzone et al., 2011), and future studies will focus on the relative abundance of these truncated variants over the full-length form in arterial regulation.

Since inhibiting TMEM16A improved coronary perfusion any up-regulation in expression or activation efficiency would narrow coronary arteries, contributing to the development of coronary artery disease. Given the strong association between hypertension

TABLE 4 Mean EC_{50}s of U46619 and 5-HT in coronary arteries from Wistar and spontaneously hypertensive rats in the presence and absence of different concentrations of the TMEM16A-specific inhibitor MONNA

	DMSO	1 μM MONNA	10 μM MONNA
U46619 EC_{50} ± SEM (nM)			
NT	50.1 ± 8	172.7 ± 32	167.1 ± 234
SHR	30.0 ± 5	31.2 ± 86	145.5 ± 73
5-HT (nM; ±SEM)			
NT	258.2 ± 82	254.9 ± 67	415.1 ± 213
SHR	73.3 ± 10	167.0 ± 28	107.7 ± 37

Note: SHR, spontaneously hypertensive rat.

and coronary artery disease, we suggest that these findings have important implications in the pathogenesis of coronary artery disease and that targeting TMEM16A may not only prove an effective mechanism to reduce BP but also increase coronary artery blood flow and cardiac perfusion. Interrogation of a UK Biobank database containing >400,000 individuals identified a novel single nucleotide polymorphism (SNP) in the coding region of the TMEM16A gene that is strongly associated with the pathogenesis of essential hypertension. We performed combined annotation-dependent depletion (CADD) analysis of all 51 loci identified to be associated with essential hypertension in the UK Biobank and found that the SNP associated with TMEM16A (rs2186797) was the most deleterious of all SNPs associated with hypertension (see Table **S1**). CADD prioritises functional, deleterious, and pathogenic variants across many categories, and CADD scores of ≥20 are predictive of the 1% most deleterious substitutions to the human genome. This analysis of the large data set provided by the UK Biobank provides powerful support for TMEM16A in the pathogenesis of hypertension that consolidates animal studies with TMEM16A-deficient mice (Heinze et al., 2014) and the pharmacological or molecular disabling of TMEM16A. Importantly, the caveat must be made that the functional impact of the SNP in question on TMEM16A is not currently known. Future studies will investigate how this variant may change the structure and function of the TMEM16A protein, so it is possible to hone in on what it is that leads to pathology. The future impact of this could be dramatic if the defect in TMEM16A can be rectified pharmacologically. Interestingly, it is not the first time that this gene variant of TMEM16A has been reported in relation to a cardiovascular pathology. Shiffman et al. (2006) found that the allele frequency of the rs2186797 TMEM16A gene variant was significantly increased in patients with early-onset myocardial infarction (Shiffman et al., 2006)—an observation made pertinent by the findings of the present study. More recently, a different variant of TMEM16A, rs7127129, was identified as being associated with changes in the aortic root diameter of patients with heart failure (Wild et al., 2017). Recent investigations have resolved the atomic structure of murine TMEM16A transmembrane domains which could facilitate identifying how these SNPs cause functional variation. Given the noteworthy CADD score of the rs2186797 variant (>21), the expressional and functional changes of TMEM16A in coronary arteries from SHRs outlined above, and the other reports of TMEM16A SNPs in cardiovascular disease, as well as previous reports of TMEM16A's role in animal models of hypertension, there is a plethora of evidence to suggest that irregularities in expression and function of TMEM16A contribute to cardiovascular pathology.

In conclusion, this study provides evidence for an important role of TMEM16A in rat coronary arteries under normal physiological circumstances but also in the pathophysiology of hypertension. Future studies will help clarify the role of TMEM16A in the vasculature and in cardiovascular diseases, not only as an ion channel regulating $I_{Cl(Ca)}$ but also as a multifunctional protein, which may modulate the function of other ion channels. Furthermore, investigations of the functional impact of the SNP in the TMEM16A coding region could help to elucidate how this SNP contributes to the pathology of hypertension in humans.

ACKNOWLEDGEMENTS

The authors would like to thank Professor Christian Aalkjær, University of Aarhus, for the use of the membrane potential recording equipment, and Dr Vincenzo Barrese, St. George's University of London, for his expert advice on the qPCR experiments.

T.D. was funded by Novo Nordsk Foundation (Grant 6553). awarded to I.A.G. O.P and N.S were funded by British Heart Foundation awards to I. A. G.

AUTHOR CONTRIBUTIONS

H.R.A.P. designed and implemented all experiments, analysed data, and drafted the manuscript. T.D., S.N.B., T.A.J., and O.P. undertook experiments and generated data. S. P.O. was involved with funding provision. I.A.G. oversaw project, provided funding, and constructed the manuscript.

CONFLICT OF INTEREST

The authors declare no conflicts of interest.

DECLARATION OF TRANSPARENCY AND SCIENTIFIC RIGOUR

This Declaration acknowledges that this paper adheres to the principles for transparent reporting and scientific rigour of preclinical research as stated in the *BJP* guidelines for Design & Analysis, Immunoblotting and Immunochemistry, and Animal Experimentation, and as recommended by funding agencies, publishers, and other organisations engaged with supporting research.

ORCID

Henry R. Askew Page https://orcid.org/0000-0001-8521-6828
Thomas Dalsgaard https://orcid.org/0000-0002-3712-1741
Samuel N. Baldwin https://orcid.org/0000-0002-3796-6090

Thomas A. Jepps https://orcid.org/0000-0002-9903-714X
Iain A. Greenwood https://orcid.org/0000-0002-0603-0492

REFERENCES

Alexander, S. P. H., Kelly, E., Marrion, N. V., Peters, J. A., Faccenda, E., Harding, S. D., … Collaborators, C. G. T. P. (2017a). The Concise Guide to PHARMACOLOGY 2017/18: Other ion channels. *British Journal of Pharmacology*, *174*(S1), S195–S207. https://doi.org/10.1111/bph.13881

Alexander, S. P. H., Kelly, E., Marrion, N. V., Peters, J. A., Faccenda, E., Harding, S. D., … Collaborators, C. G. T. P. (2017b). The Concise Guide to PHARMACOLOGY 2017/18: Transporters. *British Journal of Pharmacology*, *174*(S1), S360–S446. https://doi.org/10.1111/bph.13883

Angermann, J. E., Forrest, A. S., Greenwood, I. A., & Leblanc, N. (2012). Activation of Ca^{2+}-activated Cl^- channels by store-operated Ca^{2+} entry in arterial smooth muscle cells does not require reverse-mode Na^+/Ca^{2+} exchange. *Canadian Journal of Physiology and Pharmacology*, *90*(7), 903–921. http://doi.org/10.1139/y2012-081

Boedtkjer, D. M. B., Kim, S., Jensen, A. B., Matchkov, V. M., & Andersson, K. E. (2015). New selective inhibitors of calcium-activated chloride channels—T16Ainh-A01, CaCCinh-A01, and MONNA—What do they inhibit? *British Journal of Pharmacology*. http://doi.org/10.1111/bph.13201, *172*, 4158–4172.

Dam, V. S., Boedtkjer, D. M., Aalkjaer, C., & Matchkov, V. (2014). The bestrophin- and TMEM16A-associated Ca^{2+}-activated Cl^- channels in vascular smooth muscles. *Channels*, *8*(4), 361–369. http://doi.org/10.4161/chan.29531

Dam, V. S., Boedtkjer, D. M. B., Nyvad, J., Aalkjaer, C., & Matchkov, V. (2014). TMEM16A knockdown abrogates two different Ca^{2+}-activated Cl^- currents and contractility of smooth muscle in rat mesenteric small arteries. *Pflügers Archiv: European Journal of Physiology*, *466*(7), 1391–1409. http://doi.org/10.1007/s00424-013-1382-1

Davis, A. J., Forrest, A. S., Jepps, T. A., Valencik, M. L., Wiwchar, M., Singer, C. A., … Leblanc, N. (2010). Expression profile and protein translation of TMEM16A in murine smooth muscle. *American Journal of Physiology. Cell Physiology*, *299*(5), C948–C959. http://doi.org/10.1152/ajpcell.00018.2010

Davis, A. J., Shi, J., Pritchard, H. A. T., Chadha, P. S., Leblanc, N., Vasilikostas, G., … Greenwood, I. A. (2013). Potent vasorelaxant activity of the TMEM16A inhibitor $T16A_{inh}$-A01. *British Journal of Pharmacology*, *168*(3), 773–784. http://doi.org/10.1111/j.1476-5381.2012.02199.x

Forrest, A. S., Joyce, T. C., Huebner, M. L., Ayon, R. J., Wiwchar, M., Joyce, J., … Leblanc, N. (2012). Increased TMEM16A-encoded calcium-activated chloride channel activity is associated with pulmonary hypertension. *American Journal of Physiology. Cell Physiology*, *303*(12), C1229–C1243. http://doi.org/10.1152/ajpcell.00044.2012

Greenwood, I. A., Ledoux, J., & Leblanc, N. (2001). Differential regulation of Ca^{2+}-activated Cl^- currents in rabbit arterial and portal vein smooth muscle cells by Ca^{2+}-calmodulin-dependent kinase. *The Journal of Physiology*, *534*(Pt. 2), 395–408. https://doi.org/10.1111/j.1469-7793.2001.00395.x

Greenwood, I. A., Ledoux, J., Sanguinetti, A., Perrino, B. A., & Leblanc, N. (2004). Calcineurin Aα, but not Aβ, augments $I_{Cl(Ca)}$ in rabbit pulmonary artery smooth muscle cells. *The Journal of Biological Chemistry*, *279*(37), 38830–38837. https://doi.org/10.1074/jbc.M406234200

Harding, S. D., Sharman, J. L., Faccenda, E., Southan, C., Pawson, A. J., Ireland, S., … NC-IUPHAR (2018). The IUPHAR/BPS Guide to PHARMACOLOGY in 2018: Updates and expansion to encompass the new guide to IMMUNOPHARMACOLOGY. *Nucleic Acids Research*, *46*(D1), D1091–D1106. http://doi.org/10.1093/nar/gkx1121

Heinze, C., Seniuk, A., Sokolov, M. V., Huebner, A. K., Klementowicz, A. E., Szijártó, I. A., … Hübner, C. A. (2014). Disruption of vascular Ca^{2+}-activated chloride currents lowers blood pressure. *The Journal of Clinical Investigation*, *124*(2), 675–686. http://doi.org/10.1172/JCI70025

Jensen, A. B., Joergensen, H. B., Dam, V. S., Kamaev, D., Boedtkjer, D., Füchtbauer, E.-M., … Matchkov, V. V. (2018). Variable contribution of TMEM16A to tone in murine arterial vasculature. *Basic & Clinical Pharmacology & Toxicology*, *123*(1), 30–41. http://doi.org/10.1111/bcpt.12984

Kilkenny, C., Browne, W., Cuthill, I. C., Emerson, M., & Altman, D. G. (2010). Animal research: Reporting *in vivo* experiments: The ARRIVE guidelines. *British Journal of Pharmacology*, *160*, 1577–1579.

Li, R.-S., Wang, Y., Chen, H.-S., Jiang, F.-Y., Tu, Q., Li, W.-J., & Yin, R.-X. (2016). TMEM16A contributes to angiotensin II-induced cerebral vasoconstriction via the RhoA/ROCK signaling pathway. *Molecular Medicine Reports*, *13*(4), 3691–3699. http://doi.org/10.3892/mmr.2016.4979

Manoury, B., Tamuleviciute, A., & Tammaro, P. (2010). TMEM16A/anoctamin 1 protein mediates calcium-activated chloride currents in pulmonary arterial smooth muscle cells. *The Journal of Physiology*, *588*(Pt 13), 2305–2314. http://doi.org/10.1113/jphysiol.2010.189506

Mazzone, A., Bernard, C. E., Strege, P. R., Beyder, A., Galietta, L. J. V., Pasricha, P. J., … Farrugia, G. (2011). Altered expression of Ano1 variants in human diabetic gastroparesis. *The Journal of Biological Chemistry*, *286*(15), 13393–13403. https://doi.org/10.1074/jbc.M110.196089

Namkung, W., Phuan, P.-W., & Verkman, A. S. (2011). TMEM16A inhibitors reveal TMEM16A as a minor component of calcium-activated chloride channel conductance in airway and intestinal epithelial cells. *The Journal of Biological Chemistry*, *286*(3), 2365–2374. https://doi.org/10.1074/jbc.M110.175109

Oh, S.-J., Hwang, S. J., Jung, J., Yu, K., Kim, J., Choi, J. Y., … Lee, C. J. (2013). MONNA, a potent and selective blocker for transmembrane protein with unknown function 16/anoctamin-1. *Molecular Pharmacology*, *84*(5), 726–735. https://doi.org/10.1124/mol.113.087502

Piper, A. S., & Greenwood, I. A. (2003). Anomalous effect of anthracene-9-carboxylic acid on calcium-activated chloride currents in rabbit pulmonary artery smooth muscle cells. *British Journal of Pharmacology*, *138*(1), 31–38. http://doi.org/10.1038/sj.bjp.0705000

Piper, A. S., & Large, W. A. (2003). Multiple conductance states of single Ca^{2+}-activated Cl^- channels in rabbit pulmonary artery smooth muscle cells. *The Journal of Physiology*, *547*(Pt 1), 181–196. http://doi.org/10.1113/jphysiol.2002.033688

Pritchard, H. A. T., Leblanc, N., Albert, A. P., & Greenwood, I. A. (2014). Inhibitory role of phosphatidylinositol 4,5-bisphosphate on TMEM16A-encoded calcium-activated chloride channels in rat pulmonary artery. *British Journal of Pharmacology*, *171*(18), 4311–4321. http://doi.org/10.1111/bph.12778

Seo, Y., Lee, H. K., Park, J., Jeon, D.-K., Jo, S., Jo, M., & Namkung, W. (2016). Ani9, a novel potent small-molecule ANO1 inhibitor with negligible effect on ANO2. *PLoS ONE*, *11*(5), e0155771. http://doi.org/10.1371/journal.pone.0155771

Shiffman, D., Rowland, C. M., Louie, J. Z., Luke, M. M., Bare, L. A., Bolonick, J. I., … Devlin, J. J. (2006). Gene variants of VAMP8 and HNRPUL1 are associated with early-onset myocardial infarction. *Arteriosclerosis, Thrombosis, and Vascular Biology*, *26*(7), 1613–1618. http://doi.org/10.1161/01.ATV.0000226543.77214.e4

Sun, H., Xia, Y., Paudel, O., Yang, X.-R., & Sham, J. S. K. (2012). Chronic hypoxia-induced upregulation of Ca^{2+}-activated Cl^- channel in pulmonary arterial myocytes: A mechanism contributing to enhanced vasoreactivity. *The Journal of Physiology*, *590*(Pt 15), 3507–3521. http://doi.org/10.1113/jphysiol.2012.232520

Thomas-Gatewood, C., Neeb, Z. P., Bulley, S., Adebiyi, A., Bannister, J. P., Leo, M. D., & Jaggar, J. H. (2011). TMEM16A channels generate Ca^{2+}-activated Cl^- currents in cerebral artery smooth muscle cells. *American Journal of Physiology. Heart and Circulatory Physiology*, *301*(5), H1819–H1827. http://doi.org/10.1152/ajpheart.00404.2011

Wang, B., Li, C., Huai, R., & Qu, Z. (2015). Overexpression of ANO1/TMEM16A, an arterial Ca^{2+}-activated Cl^- channel, contributes to spontaneous hypertension. *Journal of Molecular and Cellular Cardiology*, *82*, 22–32. http://doi.org/10.1016/j.yjmcc.2015.02.020

Wang, Q., Hogg, R. C., & Large, W. A. (1992). Properties of spontaneous inward currents recorded in smooth muscle cells isolated from the rabbit portal vein. *The Journal of Physiology*, *451*, 525–537. https://doi.org/10.1113/jphysiol.1992.sp019177

Wei, L., Vankeerberghen, A., Cuppens, H., Eggermont, J., Cassiman, J. J., Droogmans, G., & Nilius, B. (1999). Interaction between calcium-activated chloride channels and the cystic fibrosis transmembrane conductance regulator. *Pflügers Archiv: European Journal of Physiology*, *438*(5), 635–641. https://doi.org/10.1007/s004249900108

Wild, P. S., Felix, J. F., Schillert, A., Teumer, A., Chen, M.-H., Leening, M. J. G., … Dörr, M. (2017). Large-scale genome-wide analysis identifies genetic variants associated with cardiac structure and function. *Journal of Clinical Investigation*, *127*(5), 1798–1812. http://doi.org/10.1172/JCI84840

Wiwchar, M., Ayon, R., Greenwood, I., & Leblanc, N. (2009). Phosphorylation alters the pharmacology of Ca^{2+}-activated Cl^- channels in rabbit pulmonary arterial smooth muscle cells. *British Journal of Pharmacology*, *158*(5), 1356–1365. http://doi.org/10.1111/j.1476-5381.2009.00405.x

Yuan, X. J. (1997). Role of calcium-activated chloride current in regulating pulmonary vasomotor tone. *The American Journal of Physiology*, *272*(5 Pt 1), L959–L968. https://doi.org/10.1152/ajplung.1997.272.5.L959

SUPPORTING INFORMATION

Additional supporting information may be found online in the Supporting Information section at the end of the article.

How to cite this article: Askew Page HR, Dalsgaard T, Baldwin SN, et al. TMEM16A is implicated in the regulation of coronary flow and is altered in hypertension. *Br J Pharmacol*. 2019;176:1635–1648. https://doi.org/10.1111/bph.14598

Arteriosclerosis, Thrombosis, and Vascular Biology

BASIC SCIENCES

SMIT (Sodium-Myo-Inositol Transporter) 1 Regulates Arterial Contractility Through the Modulation of Vascular Kv7 Channels

Vincenzo Barrese, Jennifer B. Stott, Samuel N. Baldwin, Gema Mondejar-Parreño, Iain A. Greenwood

OBJECTIVE: The SMIT1 (sodium:myo-inositol transporter 1) regulates myo-inositol movement into cells and responses to hypertonic stimuli. Alteration of myo-inositol levels has been associated with several diseases, including hypertension, but there is no evidence of a functional role of SMIT1 in the vasculature. Recent evidence showed that in the nervous system SMIT1 interacted and modulated the function of members of the Kv7 family of voltage-gated potassium channels, which are also expressed in the vasculature where they regulate arterial contractility. Therefore, in this study, we evaluated whether SMIT1 was functionally relevant in arterial smooth muscle.

APPROACH AND RESULTS: Immunofluorescence and polymerase chain reaction experiments revealed that SMIT1 was expressed in rat renal and mesenteric vascular smooth muscle cells. Isometric tension recordings showed that incubation of renal arteries with raffinose and myo-inositol (which increases SMIT1 expression) reduced the contractile responses to methoxamine, an effect that was abolished by preincubation with the pan-Kv7 blocker linopirdine and by molecular knockdown of Kv7.4 and Kv7.5. Knockdown of SMIT1 increased the contraction of renal arteries induced by methoxamine, impaired the response to the Kv7.2–Kv7.5 activator ML213 but did not interfere with the relaxant responses induced by openers of other potassium channels. Proximity ligation assay showed that SMIT1 interacted with heteromeric channels formed by Kv7.4 and Kv7.5 proteins in both renal and mesenteric vascular smooth muscle cells. Patch-clamp experiments showed that incubation with raffinose plus myo-inositol increased Kv7 currents in vascular smooth muscle cells.

CONCLUSIONS: SMIT1 protein is expressed in vascular smooth muscle cells where it modulates arterial contractility through an association with Kv7.4/Kv7.5 heteromers.

GRAPHIC ABSTRACT: A graphic abstract is available for this article.

Key Words: KCNQ ■ Kv7 ■ myo-inositol ■ SLC5A3 ■ SMIT1

Downloaded from http://ahajournals.org by on January 22, 2022

The cyclic polyol myo-inositol is an organic osmolyte that plays a pivotal role in many cell types, regulating their response to hypertonic environments. Intracellular levels of myo-inositol are tightly controlled by the activity of membrane transporters belonging to the SLC5A (solute carrier family 5A) that mediate the influx of substrates along with sodium. Two SMIT (sodium:myo-inositol transporter) have been cloned and named SMIT1 (SLC5A3)[1] and SMIT2 (SLC5A11).[2] Since their first identification in the kidney, myo-inositol transporters have been found in several other tissues including the brain, liver, pancreas, placenta, heart and skeletal muscle.[3,4] Expression of SMIT1 is upregulated by extracellular hypertonicity via transcriptional mechanisms, resulting in enhanced uptake of myo-inositol by cells. This prevents an increase in the concentration of inorganic ions without perturbing the activity of macromolecules.[5] Alterations of SMIT1 function have been associated with

Correspondence to: Vincenzo Barrese, MD, PhD, Department of Neuroscience, Reproductive Science and Dentistry, University of Naples Federico II, Bldg 19, 9th floor, Via Pansini, 5, 80131 Naples, Italy. Email vincenzo.barrese@unina.it

The Data Supplement is available with this article at https://www.ahajournals.org/doi/suppl/10.1161/ATVBAHA.120.315096.

For Sources of Funding and Disclosures, see page 2479.

© 2020 The Authors. *Arteriosclerosis, Thrombosis, and Vascular Biology* is published on behalf of the American Heart Association, Inc., by Wolters Kluwer Health, Inc. This is an open access article under the terms of the Creative Commons Attribution License, which permits use, distribution, and reproduction in any medium, provided that the original work is properly cited.

Arterioscler Thromb Vasc Biol is available at www.ahajournals.org/journal/atvb

Nonstandard Abbreviations and Acronyms

CHO	Chinese hamster ovary
PIP_2	phosphatidylinositol-4,5-bisphosphate
SLC5A	solute carrier family 5A
SMIT1	sodium:myo-inositol transporter 1
TonEBP	tonicity responsive enhancers binding protein
TRPC1	transient receptor potential C1 channel
VSMC	vascular smooth muscle cells

several diseases, including Down syndrome, Alzheimer disease, and mood disorders.[6] Moreover, alterations of myo-inositol metabolism have been observed in other diseases, such as epilepsy,[7,8] stroke,[9] and diabetes mellitus.[10] Administration of myo-inositol has been proposed as a potential therapeutic strategy in these conditions.

In addition to its osmotic role, myo-inositol is a substrate for the biosynthesis of phosphatidylinositol, a membrane molecule that is the precursor of phosphatidylinositol-4,5-bisphosphate (PIP_2), a key modulator of many ion channels.[6,11] Consequently, myo-inositol transporters may have a profound effect on ion channel activity. Regulation of ion channels function in the vasculature, in particular K^+ channels, is a key mechanism modulating arterial contractility.

KCNQ-encoded potassium channels (Kv7.1–7.5) are important regulators of cellular activity in neurons, cardiac myocytes, epithelia, and smooth muscle cells, which have an exquisite reliance upon local PIP_2 levels.[12] Within the vasculature, Kv7.1, Kv7.4, and Kv7.5 are the main subunit expressed, have been shown to regulate arterial contractility at rest, and contribute to receptor-mediated vasorelaxation.[12,13] Recently, SMIT1 has been shown to interact with Kv7.1, Kv7.2, and Kv7.3 resulting in increased activity of the channels.[8,14] These so-called chansporter complexes[15] have been implicated as key determinants of neuronal activity,[8,16,17] suggesting a tight link between regulation of osmolarity and cell excitability. Acute exposure to hypertonic solution causes vasodilation in several arterial beds including skeletal muscle arterioles, mesenteric and coronary arteries, through poorly defined mechanisms.[18–20] Moreover, increased urinary depletion of myo-inositol has been observed in diabetic patients and in animal models of metabolic diseases including hypertension.[21,22] However, there is little data about the expression of myo-inositol transporters in the arteries,[23] and there is no evidence about their functional role in vascular smooth muscle cells (VSMCs). We, therefore, set out to establish expression of SMIT1 in VSMCs and ascertaining if modifying SMIT1 levels altered arterial contractility potentially through an interaction with Kv7 channels.

Highlights

- The myo-inositol transporter SMIT1 (sodium:myo-inositol transporter 1) modulates arterial contractility.
- SMIT1 interacts with Kv7.4/Kv7.5 heteromeric channels in the vasculature and affect their function.
- This is the first evidence of the interaction of a transporter with a K^+ channel in the vasculature.

MATERIALS AND METHODS

Please see the Major Resources Table in the Data Supplement. Detailed methods are available in the Data Supplement. The authors declare that all supporting data are available within the article (and its Data Supplement files).

Arteries

Main conduit renal and third-order mesenteric arteries were microdissected and cleaned of adherent fat in ice-cold Krebs solution, as previously described.[24] Arteries were incubated in DMEM/F-12 culture medium (Sigma Aldrich, Dorset, United Kingdom) supplemented with 1% penicillin-streptomycin (Sigma Aldrich, Dorset, United Kingdom) in a 37°C incubator with 5% CO_2 for 16 hours (for myo-inositol/raffinose treatments) or 48 hours (for gene-silencing experiments). In double knockdown experiments, arteries were incubated in the morpholinos transfection mix for 32 hours and then incubated in medium containing either vehicle or raffinose plus myo-inositol for 16 hours.

Cell Culture

Chinese Hamster Ovary (CHO) cells were maintained in DMEM supplemented with 10% (v/v) FBS, 2 mmol/L L-glutamine, and 1% (v/v) penicillin/streptomycin (Sigma Aldrich, Dorset, United Kingdom) in a 37°C incubator with 5% CO_2. CHO cells were plated in 6-well dish and transfected with pcDNA3.1-KCNQ4, pcDNA3.1-KCNQ5, pcDNA3.1-SMIT1, and pGFP (green fluorescent protein; pMaxCloningTM Vector, Lonza, Basel, Switzerland) plasmids using Lipofectamine 2000 (Thermo Fisher, Paisley, United Kingdom), according to the manufacturer's instructions. CHO cells were used 24 hours after transfection.

Isolation of Vascular Smooth Muscle Cells

VSMCs were isolated as previously described.[24] Arteries were digested with collagenase type IA (2 mg/mL) and protease type X (1 mg/mL). For quantitative polymerase chain reaction (PCR) experiments, VSMCs were prepared to ensure removal of endothelium as previously described.[25]

Gene Knockdown

Knockdown of Kv7.4, Kv7.5, and SMIT1 in renal and mesenteric arteries was performed by transfection with morpholino oligonucleotides as described in vessels previously.[26] Targeting and scrambled (control) morpholino oligonucleotides (5 μmol/L; Genetools, Oregon) were mixed in Opti-MEM and transfected using Lipofectamine 2000 (Thermo Fisher, Paisley, United Kingdom).

Downloaded from http://ahajournals.org by on January 22, 2022

RNA Extraction, Reverse Transcription and Quantitative PCR

Total RNA was extracted from arteries using Monarch Total RNA Miniprep Kit (New England Biolabs, Hitchin, United Kingdom), according to the manufacturer's instruction, and reverse transcribed to cDNA using Luna Script RT Super Mix (New England Biolabs, Hitchin, United Kingdom). Quantitative PCR experiments were run in CFX96 Real-Time PCR Detection System (Bio-Rad, Hertfordshire, United Kingdom) using the SYBR-Green detection technique and specific primers (Table I in the Data Supplement), as previously described.[24]

Immunofluorescence

VSMCs were fixed with 3% paraformaldehyde, treated with 0.1 mol/L glycine, and incubated with primary antibodies overnight at 4°C, as previously described.[16] Coverslips were then washed with PBS and incubated for 1 hour with secondary antibodies conjugated to Alexa Fluor 488 or Alexa Fluor 567. Coverslips were analyzed with a Nikon A1R confocal microscope (Nikon Instruments Europe BV, Amsterdam, Netherlands). Corrected total cell fluorescence was calculated using ImageJ software as elsewhere described.[27] The number of cells analyzed is indicated by n, whereas N represents the number of animals used.

Patch-Clamp Recordings

All current recordings were made with an Axopatch 200B and a Digidata 1322A (Axon Instruments, Burlingame, CA). For renal VSMCs, membrane Kv currents were measured using perforated whole-cell voltage-clamp by including amphotericin B in the pipette solution (final concentration of 200 µg/mL) at room temperature (21°C–23°C).

Wire Myography

Segments of renal arteries (≈2 mm) were mounted in a wire myograph (Danish Myo Technology, Aarhus, Denmark) for isometric tension recording.[28] Concentration-effect curves for methoxamine (30 nmol/L–30 µmol/L) or KCl (10–120 mmol/L) were constructed to evaluate arterial contractility after the experimental treatments. Data were recorded and analyzed using LabChart 7 (ADInstruments, Dunedin, New Zealand).

Proximity Ligation Assay

Proximity ligation assay (PLA) was used to assess protein-protein interactions as previously described using validated antibodies.[24,26] Analysis of midcell xy sections was performed using ImageJ software. For PLA in CHO cells, the number of puncta per cell was calculated by dividing the total number of dots by the number of nuclei in the microscopic field.

Drugs

Specific activators of different potassium channels were used at submaximal concentrations derived from previous work. These were the Kv7.2–7.5 activators ML213 and retigabine[29] (Tocris Bioscience, Bristol, United Kingdom), the Kv7.1 activator RL-3[30] (Sigma Aldrich, Dorset, United Kingdom), the K_{ATP} activator levcromakalim[31] (Tocris Bioscience, Bristol, United Kingdom), and the BK_{Ca} activator NS11021[32] (Tocris Bioscience, Bristol, United Kingdom). Specific blockers of Kv7 channels (XE991,[24] linopirdine and HMR1556[33]), SMIT1 (phlorizin[8]), and the G-protein-gated inwardly rectifying K^+ channels (Tertiapin Q[34]) were purchased from Tocris Bioscience, Bristol, United Kingdom.

Statistical Analysis

All data are expressed as mean±SEM. One- or 2-way ANOVA test followed by a Bonferroni, Dunnett, or Tukey multiple comparisons test, and Student *t* test (paired or unpaired) were used to determine statistical significance between groups, according to the different experiments. The significance level for statistic tests was 0.05 (differences were considered statistically significant when $P<0.05$).

RESULTS

SMIT1 Is Expressed in Rat VSMCs

Immunofluorescence experiments on freshly dispersed arterial VSMCs isolated from rat renal and mesenteric arteries were performed to determine whether SMIT1 was present in vascular smooth muscle cells. Images in Figure 1A show that SMIT1 was expressed in renal and mesenteric VSMCs, with a predominantly peripheral, membrane-like distribution. Quantitative PCR in purified renal VSMCs showed an abundant expression of SMIT1 (slc5a3), whereas levels of SMIT2 (slc5a11) were negligible (Figure 1B).

Modulation of SMIT1 Levels Regulates Arterial Contractility

Renal arteries were incubated overnight with different treatments known to potentiate or reduce SMIT1 function and expression,[17] and vascular reactivity was evaluated by measuring contractions to increasing concentration of the α1-adrenergic receptors agonist methoxamine (30 nmol/L–30 µmol/L). Incubation of renal arteries with a SMIT1-specific morpholino oligonucleotide reduced SMIT1 expression by ≈40% (Figure 2A, left) and produced a left-shift in the concentration-response curve for methoxamine with respect to control (at 1 µmol/L methoxamine: 40±8% of maximal contraction with SMIT1-morpholino; 14±5% for scrambled control; Figure 2A, right). Neither 3-hour nor 16-hour (overnight) incubation with the SMIT1 transport inhibitor phlorizin (500 µmol/L) modified methoxamine-induced contraction of renal artery (Figure I in the Data Supplement).

Previous studies showed that SMIT1 abundance in neuronal cell membranes is increased by bathing solutions made hypertonic by addition of raffinose.[17,23] Overnight incubation of renal arteries with 150 mmol/L raffinose plus the transporter substrate myo-inositol (1 mmol/L) increased SMIT1 fluorescence intensity in VSMCs by ≈140% with respect to controls (Figure 2B, left) and reduced concentration-dependent contractions to methoxamine (at

Downloaded from http://ahajournals.org by on January 22, 2022

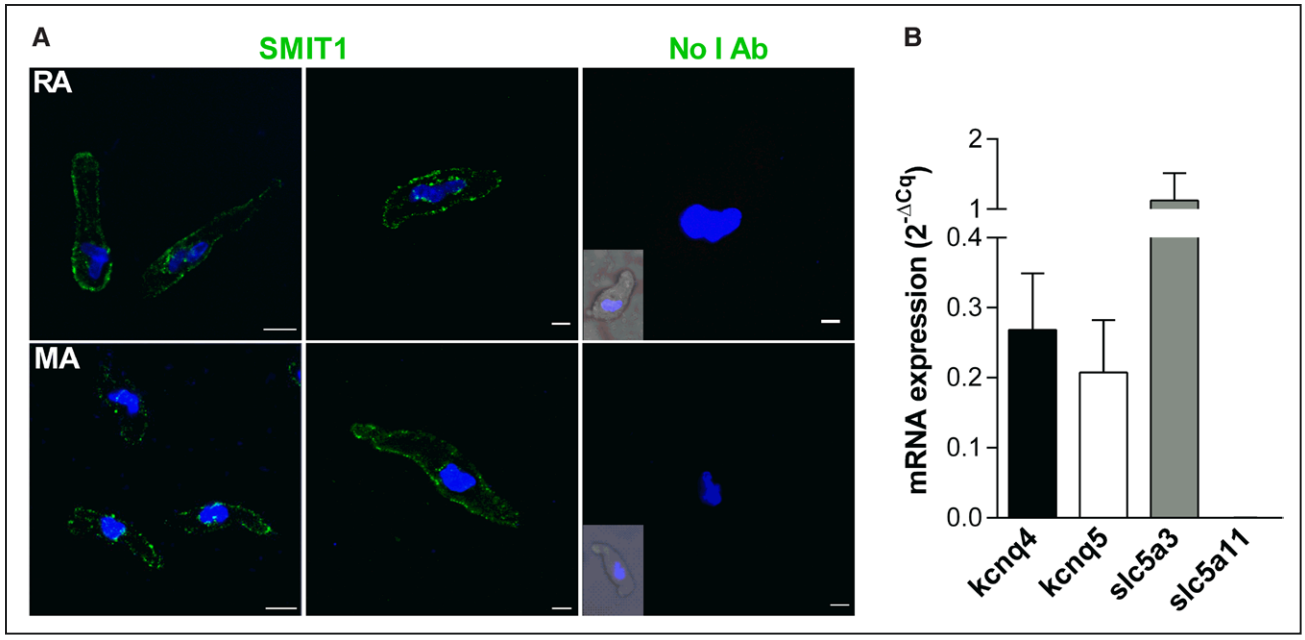

Figure 1. Expression of SMIT1 (sodium:myo-inositol transporter 1) in vascular smooth muscle cells (VSMCs). **A**, Representative immunofluorescence showing the expression of SMIT1 protein in VSMCs isolated from renal arteries (RA, **top**) and mesenteric arteries (MA, **bottom**). The **right**-most parts show the staining in absence of the SMIT1 antibody (No I Ab). The insets show a brightfield image of the cell. Nuclei (DAPI [4',6-diamidino-2-phenylindole, dihydrochloride] staining, blue) are also shown. Scale bar=10 µm (**left**-most parts) and 5 µm (other parts). **B**, Quantitative polymerase chain reaction showing the expression of the transcripts encoding for Kv7.4 (kcnq4), Kv7.5 (kcnq5), SMIT1 (slc5a [solute carrier family 5A] 3) and SMIT2 (slc5a11) in VSMCs isolated from renal arteries. Data are expressed using the $2^{-\Delta Cq}$ formula (N=5).

1 µmol/L methoxamine: 10±3% of maximal contraction with raffinose plus myo-inositol; 39±10% for control; Figure 2B). Incubation with raffinose alone also inhibited contractions to methoxamine, although to a lesser extent as raffinose plus myo-inositol (at 1 µmol/L methoxamine: 20±7% of maximal contraction; Figure 2B). In contrast, overnight incubation with myo-inositol alone did not affect renal artery contractility. Addition of the SMIT1 transport inhibitor phlorizin (500 µmol/L) had a small effect on the anticontractile action of raffinose plus inositol (Figure IIA in the Data Supplement). Moreover, wortmannin (10 nmol/L), that depletes PIP_2 levels, partially prevented the right-shift of the concentration-response curve to methoxamine induced by raffinose plus myo-inositol, being effective only at 3 µmol/L methoxamine (82±4% of maximal contraction in wortmannin and raffinose plus myo-inositol; 54±12% in raffinose+myo-inositol; Figure IIB in the Data Supplement).

Incubation or renal arteries with raffinose plus myo-inositol did not modify the contractile response induced by 60 mmol/L KCl (Figure 2C, left). When exposed to increasing concentration of KCl (10–120 mmol/L), incubation of renal arteries with raffinose plus myo-inositol caused a reduction of the contraction only at lower KCl concentration with respect to controls (at 40 mmol/L KCl: 46±7 of maximal contraction with raffinose plus myo-inositol; 80±11% in control), a result consistent with the involvement of K^+ channels in mediating the effects on arterial contractility induced by raffinose plus myo-inositol (Figure 2C, right).

Overall, these results show that augmenting membrane expression of SMIT1 attenuated vasoconstrictor responses with a mechanism that was partly dependent on increased intracellular availability of myo-inositol.

SMIT1 Selectively Modulates the Functional Impact of Specific Kv7 Subunits

Having established that SMIT1 modulates arterial function, we investigated whether these effects occurred through the regulation of the activity of K^+ channels, which are key regulators of arterial contractility. To this aim, we evaluated whether modulating SMIT1 levels interfered with the ability of several activators of different K^+ channel classes found in the vasculature to counteract the vasoconstriction of renal artery segments induced by 10 µmol/L methoxamine (Figure 3A). Under control conditions methoxamine-induced contractions were reduced by preincubation with the Kv7.2–Kv7.5 activator ML213 (3 µmol/L; 24±3% of first contraction to methoxamine), the Kv7.1-specific activator RL-3 (3 µmol/L; 65±13%), the K_{ATP}- opener levcromakalim (3 µmol/L; 57±18%), and the BK_{Ca} activator NS11021 (3 µmol/L; 84±2%; Figure 3B through 3E, black bars). Knockdown of SMIT1 caused a significant impairment of the ML213 effect on methoxamine-induced contraction (49±7% of first contraction to methoxamine, Figure 3B, white bars), whereas no changes were observed in the responses to the other K^+ channels activators (RL-3: 75±10%; LEV: 67±12%; NS11021: 83±11%; Figure 3C through 3E, white bars). In contrast to the knockdown studies,

Downloaded from http://ahajournals.org by on January 22, 2022

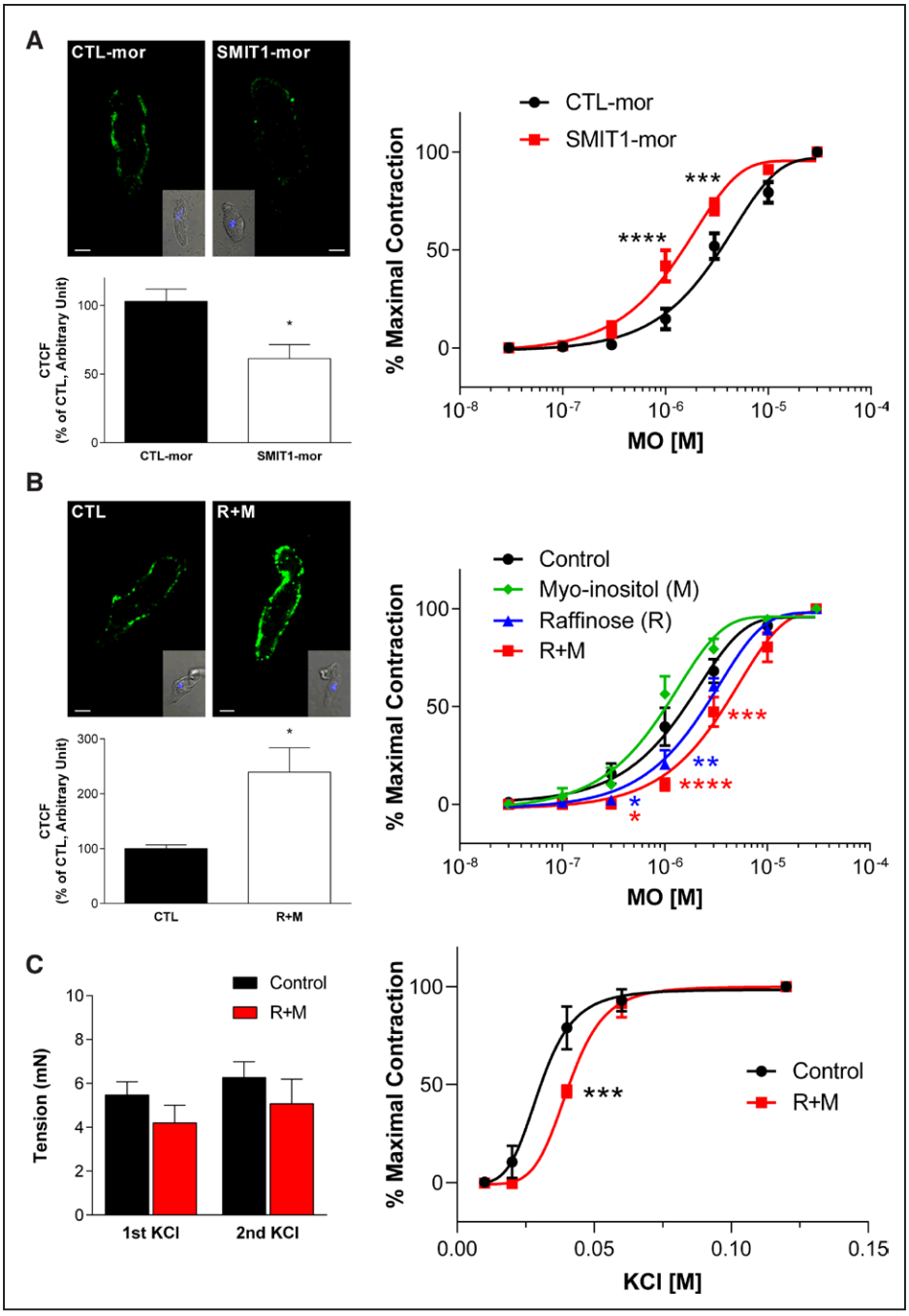

Figure 2. Effects of the modulation of SMIT1 (sodium:myo-inositol transporter 1) levels on arterial contractility.
A, **left**, representative images showing the immunostaining of SMIT1 in renal vascular smooth muscle cells (VSMCs) incubated with a scrambled (CTL-mor) or an anti-SMIT1 morpholino oligonucleotide (SMIT1-mor). The insets show brightfield images of the cells. Scale bar=5 µm. The graph shows the quantification of SMIT1 fluorescence intensities measured as corrected total cell fluorescence (CTCF) and expressed as percentage of control (CTL-mor). Data are expressed as mean±SEM. *P<0.05 vs respective controls; n=28 cells for CTL-mor and 30 cells for SMIT1-mor obtained from 3 different preparations (N=3). **Right**, isometric tension recordings showing the effects of increasing concentration of methoxamine (MO) in segments of renal arteries after 48 h incubation with CTL-mor (black line) or SMIT1-mor (red line). Data are shown as percentage of the contraction obtained with 30 µmol/L MO. Data are expressed as mean±SEM. ***P<0.001; ****P<0.0001 vs controls; N=13 for CTL-mor and 16 for SMIT1-mor. **B**, **left**, representative images showing the immunostaining of SMIT1 in renal VSMCs incubated with vehicle (CTL) or raffinose plus myo-inositol (R+M). The insets show brightfield images of the cells. Scale bar=5 µm. The graph shows the quantification of SMIT1 fluorescence intensities measured as CTCF and expressed as percentage of control. Data are expressed as mean±SEM. *P<0.05 vs respective controls; n=28 cells for CTL and 30 cells for R+M from 3 different preparations (N=3) per experimental group. **Right**, isometric tension recordings showing the effects of increasing concentration of MO in segments of renal arteries after 16 h incubation with vehicle (control, black line, N=10), 1 mmol/L myo-inositol (M, green line, N=6), 150 mmol/L raffinose (R, blue line; N=8), or 150 mmol/L raffinose plus 1 mmol/L myo-inositol (R+M, red line, N=10). Data are shown as percentage of the contraction obtained with 30 µmol/L MO. Data are expressed as mean±SEM. *P<0.05; **P<0.01; ***P<0.001; ****P<0.0001 vs controls. (*Continued*)

Downloaded from http://ahajournals.org by on January 22, 2022

increasing SMIT1 levels by incubation with raffinose and myo-inositol did not alter the vasorelaxant properties of any of the selected K^+ channels openers when compared with their respective controls (Figure III in the Data Supplement). To further investigate the possible involvement of Kv7 channels in the anticontractile effect of SMIT1, we performed myography experiments with the pan-Kv7 blocker linopirdine. Application of linopirdine (1–3 μmol/L) contracted renal arteries considerably less in segments incubated with raffinose and myo-inositol (Figure 4A) and abrogated the reduced contraction to methoxamine produced by treatment with raffinose and myo-inositol (Figure 4B). Similar effects were not seen with the selective Kv7.1 blocker HMR1556 (1 μmol/L; Figure 4B) nor tertiapin Q (1 μmol/L), a blocker of the inward-rectifier K^+ channel GIRK (Figure IV in the Data Supplement).

To further investigate the involvement of Kv7.4 and Kv7.5 channels in mediating the effects of SMIT1 on arterial contractility, we reduced Kv7.4 and Kv7.5 channels levels with morpholino oligonucleotides (Q4/Q5-mor). Knockdown of Kv7.4 and Kv7.5 prevented the rightward-shift of the concentration-response curves for methoxamine and KCl (Figure 5A and 5B) induced by incubation with raffinose plus myo-inositol. The effective knockdown of Kv7.4 and Kv7.5 channels was confirmed by the lack of vasorelaxant effects of the Kv7 activator retigabine (10 μmol/L) in arteries transfected with morpholinos targeting Kv7.4 and Kv7.5 (Figure 5C). Overall, these data show that SMIT1 influences vascular contractility via a mechanism dependent, in part, on Kv7.4/Kv7.5.

SMIT1 Interacts With Heteromeric Kv7.4–Kv7.5 Channels

Our myography data suggests that SMIT1 modulates vascular reactivity through altering Kv7 channel activity. The impairment of the ML213-dependent relaxation in SMIT1-silenced arteries and the lack of effect of the Kv7.1-selective drugs (RL-3, HMR1556), along with the impairment of raffinose plus myo-inositol effects in Kv7.4/Kv7.5–silenced arteries suggest the involvement of Kv7.4 and Kv7.5 subunits. Therefore, we performed PLA to investigate whether SMIT1 interacted with Kv7 channel subunits. PLA puncta were detected in VSMCs from renal and mesenteric arteries for both Kv7.4-SMIT1 and Kv7.5-SMIT1 couples (Figure 6A). Interestingly, SMIT1 also interacted with the ancillary KCNE4 subunit that is abundant in VSMCs and colocalizes with Kv7.4/Kv7.5 channels[35] (Figure VA in the Data Supplement). To get insight into the dynamic changes of these interactions when SMIT1 expression was upregulated, we evaluated the PLA puncta for Kv7.4-SMIT1 and Kv7.5-SMIT1 in renal arteries incubated with raffinose plus myo-inositol. Enhancing SMIT1 expression increased the number of PLA puncta for Kv7.4-SMIT1 and Kv7.5-SMIT1 by ≈60 and ≈85%, respectively. Treatment with raffinose plus myo-inositol did not modify the interaction of SMIT1 with the voltage-gated K^+ channel Kv2.1 or the interaction of Kv7.4 or Kv7.5 with the TRPC1 (transient receptor potential C1 channel; Figure 6B), suggesting a preferential interaction between SMIT1 and Kv7.4/Kv7.5 channels in these experimental settings.

We then performed further experiments to evaluate the molecular determinant of the interaction between SMIT1 and Kv7 channels by analyzing the PLA puncta for Kv7.4-SMIT1 and Kv7.5-SMIT1 when Kv7 subunits were knocked down with morpholino oligonucleotides. As shown in Figure 6C, morpholino targeting Kv7.4 (Q4-mor) reduced the number of interactions of SMIT1 with Kv7.4 (≈60%) and Kv7.5 (≈50%) in renal arteries. Similarly, a morpholino targeted to Kv7.5 (Q5-mor) reduced SMIT1-Kv7.4 and SMIT1-Kv7.5 interactions by ≈50%. Both morpholinos reduced the number of PLA punctae observed when antibodies for Kv7.4 and Kv7.5 were used with respect to control condition (Figure 6C). Similar results were observed in VSMCs isolated from mesenteric arteries (Figure VB in the Data Supplement). To get further insight into the stoichiometry of these interactions, we performed PLAs on CHO cells overexpressing homomeric Kv7.4 or Kv7.5 channels and heteromeric channels formed by Kv7.4 and Kv7.5. Although PLA signals were detected for Kv7.5-SMIT1 in CHO cells transfected with Kv7.5 only, the number of Kv7.4-SMIT1 interactions in CHO transfected with Kv7.4 was not significantly different from background signals. Interestingly, a significant increase in PLA puncta for Kv7.4 and SMIT1 was detected when Kv7.4 and Kv7.5 were coexpressed in CHO cells (Figure VC in the Data Supplement). These results suggest that SMIT1 interacts with heteromeric channels formed by Kv7.4 and Kv7.5.

SMIT1 Effects on Kv7-Mediated Currents

In studies on CHO cells, the amplitude of currents produced by the overexpression of Kv7.4 and Kv7.5 was not altered by coexpression with SMIT1 (Figure 7A), but there was a small but nonsignificant effect on the voltage-dependence of activation ($V_{1/2}$=−10.6±4.0 mV for Kv7.4/7.5; $V_{1/2}$=−16.1±3.4 for Kv7.4/7.5 plus SMIT1; n=8 per group; P=0.32). In studies on native K^+ currents in isolated renal artery smooth muscle cells, increasing SMIT1 expression by overnight incubation of the artery in

Figure 2 Continued. C, **left**, isometric tension recordings showing the effects of 60 mmol/L KCl in renal arteries after 16 h incubation with vehicle (control, black bars, N=20), or 150 mmol/L raffinose plus 1 mmol/L myo-inositol (R+M, red bars, N=22). Arteries were challenged with 2 independent KCl stimuli. **Right**, Isometric tension recordings showing the effects of increasing concentration of KCl in segments of renal arteries after 16 h incubation with vehicle (control, black line) or 150 mmol/L raffinose plus 1 mmol/L myo-inositol (R+M, red line). Data are shown as percentage of the contraction obtained with 120 mmol/L KCl. Data are expressed as mean±SEM. ***P<0.001; ****P<0.0001 vs controls; N=6 per experimental group.

Downloaded from http://ahajournals.org by on January 22, 2022

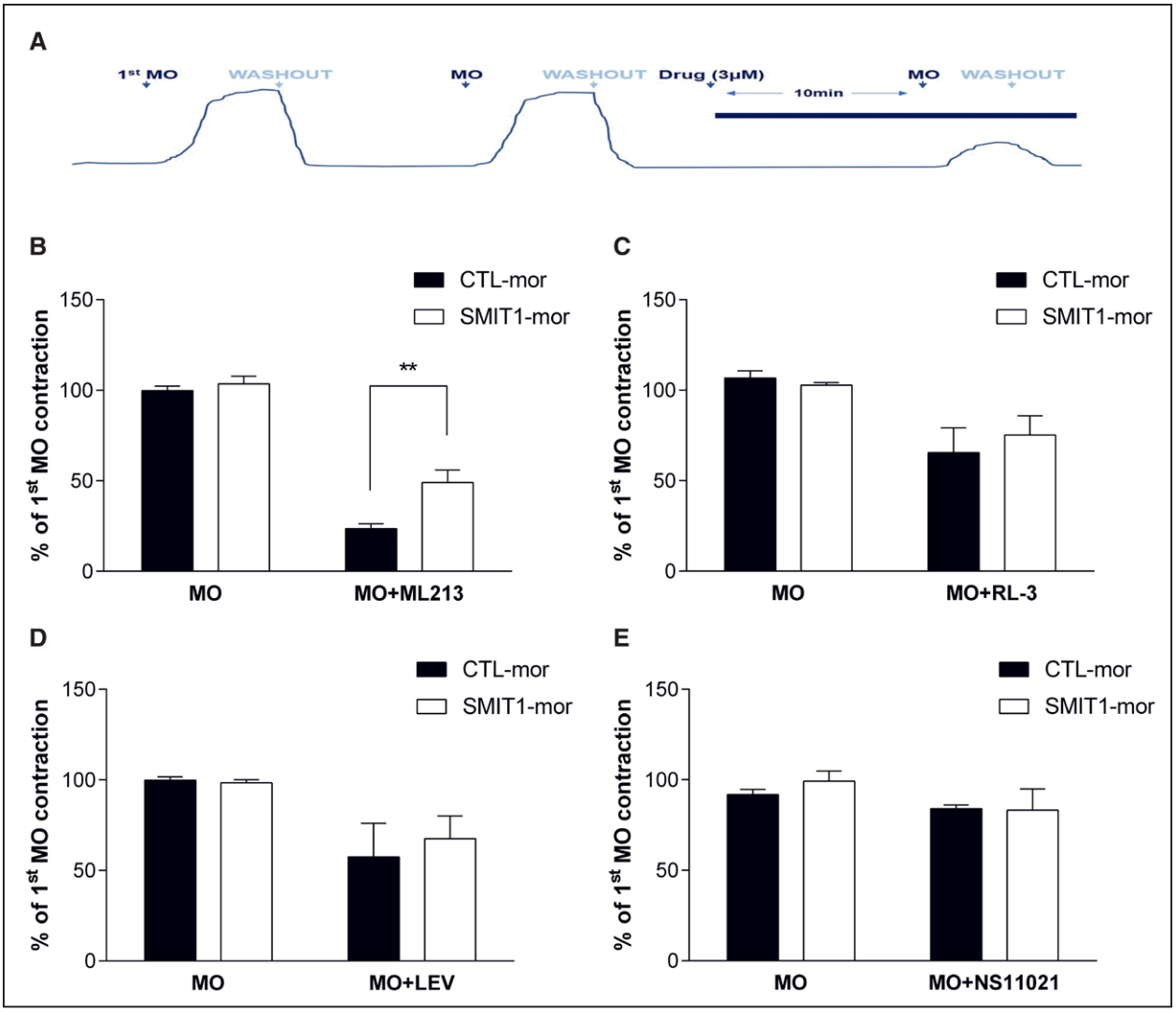

Figure 3. Effects of SMIT1 (sodium:myo-inositol transporter 1)-silencing on K+ channels activators.
A, Representative image showing the protocol used for isometric tension recordings. After 2 stimulations with 10 µmol/L methoxamine (MO), segments of renal arteries were incubated for 10 min with K^+ channels activators (all used at a concentration of 3 µmol/L) and then stimulated again with MO. **B**–**E**, Quantification of the responses to MO in the presence of ML213 (**B**, N=9), RL-3 (**C**, N=6), levcromakalim (**D**, N=5), or NS11021 (**E**, N=4) in renal arteries incubated with a scrambled (CTL-mor) or an anti-SMIT1 morpholino oligonucleotide (SMIT1-mor). Data are expressed as mean±SEM. and shown as percentage of the contraction to the first stimulation with MO (see **A**). The responses to the second incubation of MO before the incubation with the activators (MO) are also shown. $^{**}P<0.01$.

raffinose plus inositol increased XE991-sensitive currents compared with control (Figure 7B and 7C). Raffinose plus inositol had no effect on the membrane capacitance (raffinose plus myo-inositol: 33±1.4 pF; control: 36.0±2.8 pF).

These results show that in identical recording conditions augmenting SMIT1 increased Kv7 currents in VSMCs.

DISCUSSION

SMIT1 Regulates Arterial Contractility

In this study, we identified that SMIT1 mRNA and protein are expressed in VSMCs, and altering SMIT1 levels regulated arterial contractility mainly through the modulation of Kv7 channels. Introduction of a morpholino targeting SMIT1 reduced SMIT1 abundance and enhanced vasoconstrictor responses, whereas exposure to hypertonic medium that increased SMIT1 expression reduced arterial contractility. These data provide the first evidence that SMIT1 protein is expressed in the vasculature and has a functional role in the regulation of arterial contractility.

Our results show that methoxamine in raffinose-incubated arteries was less effective compared to arteries incubated in isotonic conditions. These effects were not due to a direct effect of the hypertonicity produced by raffinose because acute application had no relaxant effect and the inhibitory effect was maintained after bathing in isotonic medium for over an hour. We speculated this

Downloaded from http://ahajournals.org by on January 22, 2022

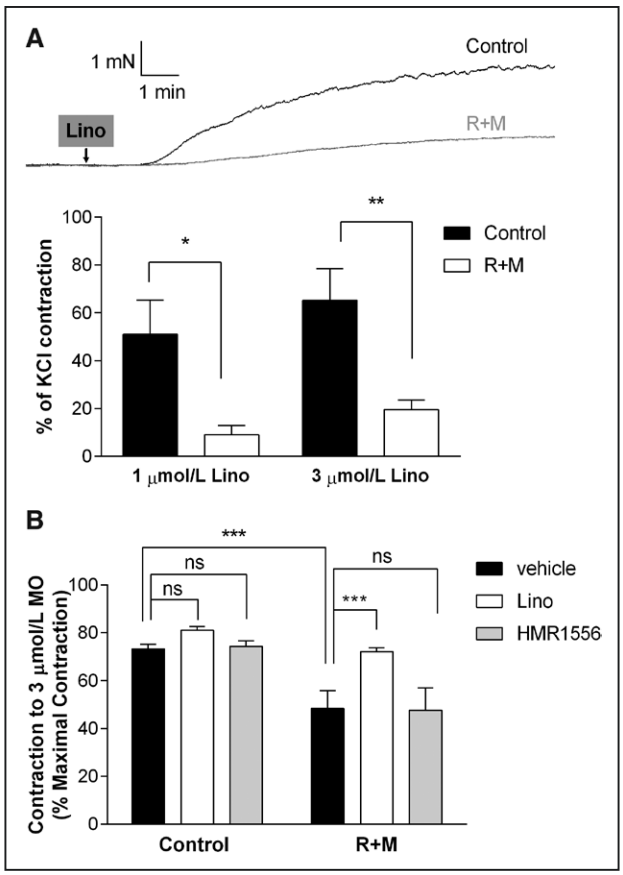

Figure 4. Effects of enhanced SMIT1 (sodium:myo-inositol transporter 1) expression on Kv7 channels blockers.
A, **top**, representative traces showing the effects on isometric tension recordings of the pan-Kv7 blocker linopirdine (3 µmol/L) in renal arteries after 16 h incubation with vehicle (black line) or raffinose plus myo-inositol (R+M; gray line). **Bottom**, bar graphs showing the contraction to linopirdine (1 and 3 µmol/L) of renal arteries incubated for 16 h with vehicle (control, black bars) or R+M (white bars) in wire-myography experiments. Data are expressed as mean±SEM and shown as percentage of the initial contraction to 60 mmol/L KCl. **P*<0.05, ***P*<0.01; N=10 per experimental group. **B**, bar graphs showing the effects of methoxamine (3 µmol/L) in the presence of dimethyl sulfoxide (DMSO; vehicle, black bars), 3 µmol/L linopirdine (Lino, white bars) or 1 µmol/L HMR1556 (gray bars) on isometric tension recordings of renal arteries incubated for 16 h with vehicle (control) or R+M. Data are expressed as mean±SEM and shown as percentage of the contraction to 30 µmol/L methoxamine. ****P*<0.001; ns=not significant; N=10 per experimental group.

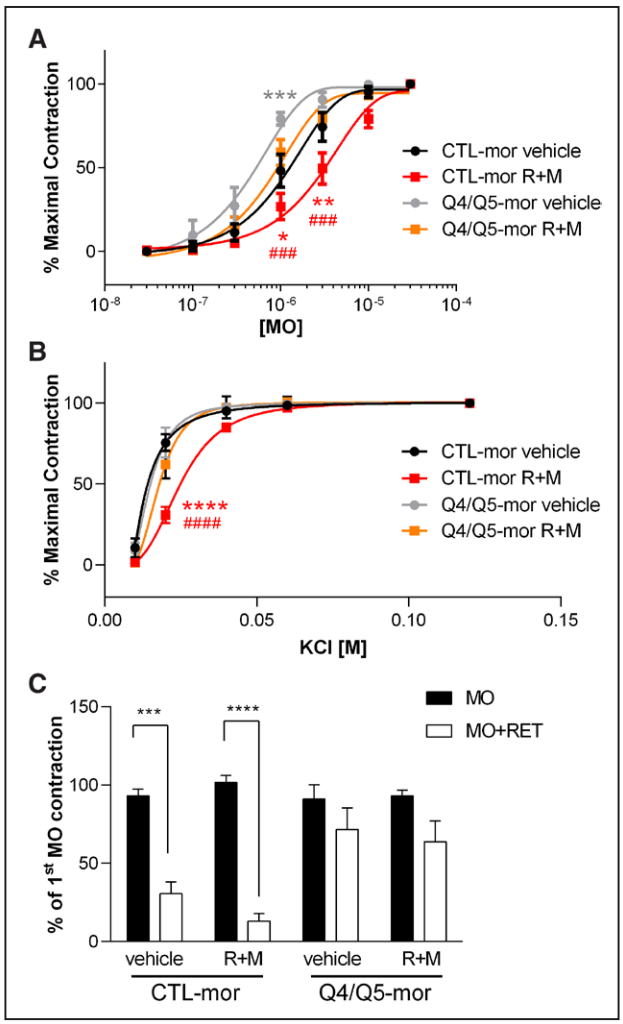

Figure 5. Effects of enhanced SMIT1 (sodium:myo-inositol transporter 1) expression and silencing of Kv7.4 and Kv7.5 in renal arteries.
Isometric tension recordings showing the effects of increasing concentration of methoxamine (MO, **A**) or KCl (**B**) in segments of renal arteries transfected with a scrambled morpholino (CTL-mor) or 2 morpholinos targeting Kv7.4 and Kv7.5 (Q4/Q5-mor). 32 h after the transfection, arteries were incubated for 16 h with either vehicle (black and gray lines) or 150 mmol/L raffinose plus 1 mmol/L myo-inositol (raffinose plus myo-inositol [R+M]; red and orange lines). Data are shown as percentage of the contraction obtained with 30 µmol/L MO (**A**) or 120 mmol/L KCl (**B**). Data are expressed as mean±SEM. **P*<0.05; ***P*<0.01: *****P*<0.0001 vs CTL-mor vehicle; ###*P*<0.001; ####*P*<0.0001 vs Q4/Q5-mor R+M; N=6 for vehicle incubated arteries and 8 for Q4/Q5-mor arteries. **C**, Bar graph showing the effects of the Kv7 activator retigabine (RET) in Kv7.4 and Kv7.5-silenced arteries. At the end of the experiments shown in **A** and **B**, arteries were challenged twice with 10 µmol/L MO alone (second MO contraction is shown with black bars) and then with MO in the presence of 10 µmol/L RET (white bars). Data are expressed as mean±SEM and shown as percentage of the contraction to the first stimulation with MO. *****P*<0.0001; N=6 for vehicle incubated arteries and 8 for Q4/Q5-mor arteries.

might be due to increased SMIT1 activity as raffinose (and hyperosmolarity in general) induces the activity of the transcription factor TonEBP (tonicity responsive enhancers binding protein) that increases the expression of SMIT1.[5] Consistent with this hypothesis, we observed greater membrane abundance of SMIT1 in renal artery smooth muscle cells following incubation with raffinose plus myo-inositol similar to previous reports in neurons.[17] Further support for a direct role of SMIT1 in the regulation of vascular contractility was provided by the observation that SMIT1-silenced arteries were significantly more contractile than control arteries. Consequently, there is a correlation between changes in SMIT1 abundance and contractile responses to methoxamine concurrent with

Downloaded from http://ahajournals.org by on January 22, 2022

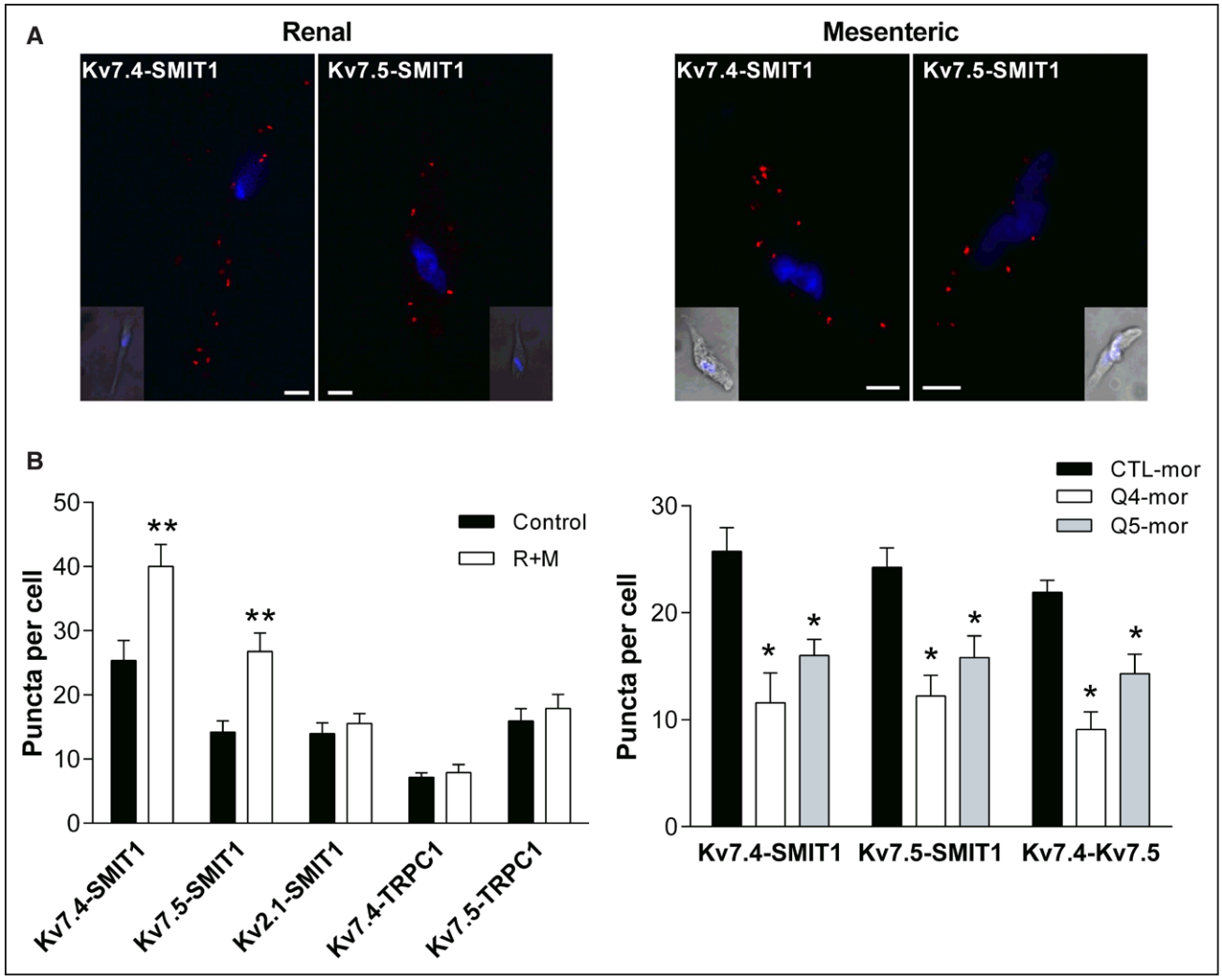

Figure 6. Interaction of SMIT1 (sodium:myo-inositol transporter 1) with vascular Kv7 channels.
A, Proximity Ligation Assays (PLAs) showing the interaction of SMIT1 with Kv7.4 and Kv7.5 in vascular smooth muscle cells (VSMCs) isolated from renal and mesenteric arteries. The insets show a brightfield image of the cell. Nuclei (DAPI [4',6-diamidino-2-phenylindole, dihydrochloride] staining, blue) are also shown. Scale bar=5 µm. **B**, Bar graphs showing the interactions of Kv7.4, Kv7.5, and SMIT1 with Kv2.1 and TRPC1 (transient receptor potential C1 channel) in VSMCs isolated from renal arteries incubated for 16 h with vehicle (control, black bars) or 150 mmol/L raffinose plus 1 mmol/L myo-inositol (raffinose plus myo-inositol [R+M], white bars). Data represent the mean number of PLA signals per midcell xy section, expressed as mean±SEM. n=26–36 cells from 3 to 4 rats (N=3–4) per experimental point in 3–4 sessions. **P*<0.05 vs respective controls. **C**, Bar graphs showing the interaction between Kv7.4-SMIT1, Kv7.5-SMIT1, and Kv7.4–Kv7.5 in renal VSMCs. Arteries were incubated with a scrambled morpholino (CTL-mor, black bars), a morpholino targeting Kv7.4 (Q4-mor, white bars), or a morpholino against Kv7.5 (Q5-mor, gray bars). Data represent the mean number of PLA signals per midcell xy section, expressed as mean±SEM. n=26–36 cells from 3 to 4 rats (N=3–4) per experimental point in 3 to 4 sessions. **P*<0.05 vs respective controls (CTL-mor).

SMIT1 regulating arterial contractility. These effects do not appear to be mediated primarily by increased availability of intracellular myo-inositol as administration of myo-inositol alone did not mimic the effect of raffinose, and blockade of SMIT1 transport with phlorizin did not prevent the effects on arterial contractility.

SMIT1 Induces Vasorelaxation Through the Activation of Heteromeric Kv7.4–Kv7.5 Channels

Raffinose plus inositol inhibited contractions produced by lower concentration of K^+ (≤40 mmol/L) but not higher concentrations consistent with an effect involving K^+ channels. Opening of K^+ channels hyperpolarizes the cell membrane potential thus reducing the activation of voltage-gated calcium channels and the consequent influx of calcium ions that is necessary for VSMCs contraction. VSMCs express a wide range of K^+ channels that regulate arterial contractility,[36,37] but considerable evidence have been accumulated for a key role of Kv7.4/7.5 channels in the regulation of basal arterial diameter and also the active response to receptor agonists.[38] Thus, the pan-Kv7 blockers linopirdine and XE991 contract most arteries, whereas Kv7.1-specific blockers like HMR1556 do not show a clear effect on vascular tone.[12] Impairment of Kv7.4 function and expression have been observed in

Downloaded from http://ahajournals.org by on January 22, 2022

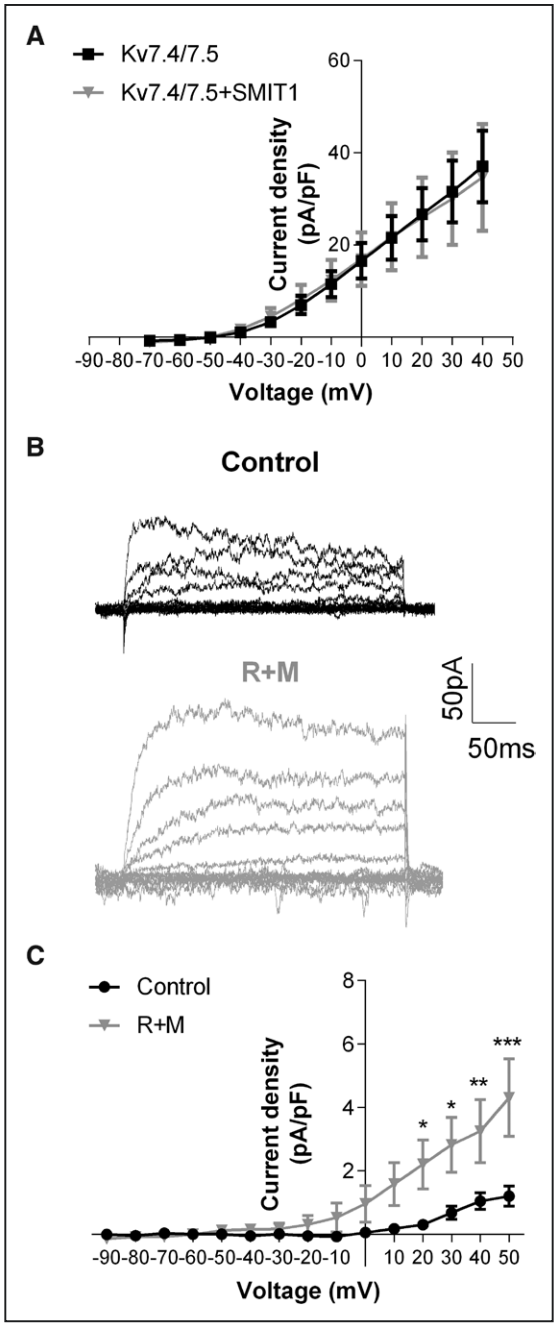

Figure 7. Effects of SMIT1 (sodium:myo-inositol transporter 1) on Kv7.4/Kv7.5-mediated currents.
A, Mean current-voltage relationship in Chinese Hamster Ovary cells transfected with plasmids encoding for Kv7.4 and Kv7.5 plus a GFP (green fluorescent protein)-encoding plasmid (black line) or a plasmid encoding for SMIT1 (gray line). Data are expressed as mean±SEM. n=8 per experimental group. **B**, representative traces showing XE-991 sensitive currents in vascular smooth muscle cells (VSMCs) isolated from renal arteries incubated for 16 h with vehicle (control, black traces) or 150 mmol/L raffinose plus 1 mmol/L myo-inositol (raffinose plus myo-inositol [R+M], gray traces). **C**, Mean current-voltage relationship of the XE991-sensitive current in VSMCs isolated from renal arteries incubated for 16 h with vehicle (control, black line) or 150 mmol/L raffinose plus 1 mmol/L myo-inositol (R+M, gray line). Data are expressed as mean±SEM. n=7 cells for control and 8 cells for R+M, obtained from 8 animals in 8 experimental sessions. **P*<0.05; ***P*<0.01; ****P*<0.001 vs control.

2 animal models of hypertension such as spontaneously hypertensive rats and angiotensin II–infused mice,[33,39,40] and trafficking of Kv7.4 subunits to the plasma membrane is altered upon stimulation with angiotensin II.[24] Reduction of Kv7 function has also been observed in coronary arteries exposed to high glucose.[41] Evidence from functional and molecular studies have highlighted that Kv7.4 and Kv7.5 form a heteromeric channel that is the main Kv7 species in VSMCs,[42,43] with the participation of the accessory subunit KCNE4.[35]In the present study, knockdown of SMIT1 attenuated the anticontractile effect of the Kv7.2–Kv7.5 specific activator ML213 but did not alter the effectiveness of activators of Kv7.1 (RL-3), BK_{Ca} (NS11021) or K_{ATP} (levcromakalim). The anticontractile effect of increasing SMIT1 levels was prevented by linopirdine but not the Kv7.1 specific blocker HMR1556 nor tertiapin Q, a blocker of PIP_2-sensitive GIRK channels. A role for Kv7.4 and 7.5 was consolidated by the use of morpholinos targeting Kv7.4 and Kv7.5 that abrogated the inhibitory effect of raising raffinose plus myo-inositol. Interestingly, the effects of ML213 were not potentiated after raffinose and myo-inositol incubation. A possible explanation is that overexpression of SMIT1 heightened the activity of Kv7.4/Kv7.5 sufficiently to negate the stimulatory effect of Kv7 activators. The fact that linopirdine was less able to contract resting arteries incubated with raffinose and myo-inositol supports this hypothesis, although it is possible that other mechanisms involved in arterial contraction might be affected by the increased expression of SMIT1.

A crucial role for Kv7 channels was corroborated by patch-clamp experiments showing that incubation with raffinose and myo-inositol increased the amplitude of Kv7 currents (XE991-sensitive component) in renal VSMCs. Interestingly, when we recorded the effects of SMIT1 on Kv7.4/Kv7.5 currents in heterologous systems, we observed only a trend to increase voltage-sensitivity of the Kv7.4/Kv7.5 channels that was quantitatively similar to that induced by SMIT1 on Kv7.2/Kv7.3 heteromeric channels (≈7 mV),[14] but we were not able to show that overexpression of SMIT1 alone directly affected the current amplitude of heteromeric Kv7.4/Kv7.5 channels. The discrepancy between patch-clamp data from VSMCs and CHO cells may reflect a different molecular architecture of the Kv7.4/Kv7.5 channels in the CHO cells compared with arterial smooth muscle cells. In particular, the ancillary subunit KCNE4, which our PLA experiments show interacts with SMIT1 in VSMCs, coassembles with Kv7 channels and alters their function.[35] Because KCNE subunits modulate the binding of SMIT1 to Kv7.2,[14] the possibility exists that the lack of effect of SMIT1 overexpression in CHO cells was due to the absence of KCNE4 subunits that could modify SMIT1 interaction with the Kv7.4/Kv7.5 channels. Alternatively, the relative increase in SMIT1 with respect to Kv7 channels in CHO cells is likely to be very different than the situation in

Downloaded from http://ahajournals.org by on January 22, 2022

smooth muscle cells following raffinose-induced SMIT1 increase. Moreover, we cannot rule out the possibility that additional proteins known to interact with Kv7 channels[12] might mediate the functional consequences exerted by SMIT1 on Kv7 channels in arteries. Regardless, modulation of SMIT1 protein levels has a marked impact on renal artery reactivity mediated through an increase in Kv7.4/7.5 activity.

Overexpression of SMIT1 potentiates Kv7.1, Kv7.2, and Kv7.3 channels activity by a physical interaction with the channel pore that induces a conformational change affecting the gating and pharmacological properties of Kv7 subunits in the absence of myo-inositol[14] and via a PIP_2-dependent mechanism that requires extracellular inositol.[16,17] Our data suggest that both the physical interaction of SMIT1 and Kv7 channels and localized increase in PIP_2 via enhanced myo-inositol transport play a role in the regulation of Kv7.4/Kv7.5 channels by SMIT1 in the vasculature. Thus, phlorizin, which prevents SMIT1 transport function and wortmannin, that depletes PIP_2, only partially prevented the effects on contractility exerted by the incubation with raffinose plus myo-inositol. Furthermore, raffinose alone altered arterial contractility. Synergistic interplay of PIP_2 with other regulators of Kv7 channels, such as G-protein βγ subunits, have been previously shown to potentiate Kv7.4 currents[44]; therefore, the possibility exists that the interaction of SMIT1 with Kv7.4/Kv7.5 induces a conformational change of the channel that facilitates the binding of PIP_2.

SMIT1 Resides in Close Proximity to Kv7.4 and Kv7.5

Physical interaction of SMIT1 with Kv7.1, Kv7.2, and Kv7.3 have been shown in overexpression systems, neurons, and choroid plexus epithelium, where they reciprocally regulate their function.[8,16,17] Our data showed that in VSMCs SMIT1 resided in close proximity (<40 nm) with both Kv7.4 and Kv7.5 subunits, as well as the accessory subunit KCNE4. Interestingly, PLA also showed that SMIT1 overexpression selectively increased the interaction between SMIT1 and Kv7.4/Kv7.5, without affecting the interaction of these proteins with other molecular partners, such as Kv2.1 or TRPC1. In particular, our PLA data show a preferential interaction of SMIT1 with heteromeric Kv7.4/Kv7.5 channels because knockdown of either Kv7.4 or Kv7.5 reduced the interaction of SMIT1 with both Kv7 subunits, consistent with the reduction of Kv7.4–Kv7.5 heteromers induced by Kv7 subunits silencing. The preferential interaction of SMIT1 with the heteromeric channels is also suggested by PLA data from overexpression system showing that SMIT1-Kv7.4 interaction occurred only when both Kv7 subunits were expressed in CHO cells. These data are consistent with previous evidence showing that SMIT1 neither coimmunoprecipitated with Kv7.4 nor affected the currents mediated by Kv7.4 homomeric channels.[8] Assembly of heteromeric Kv7 channels occurs very early during protein trafficking to the plasma membrane and is responsible for increased channel insertion and enhanced Kv7-mediated currents.[45,46] PLA data in overexpression system also suggest that the molecular determinants responsible for this interaction are localized within Kv7.5 because only the Kv7.5 subunit was able to interact with SMIT1 in homomeric conformation, although the possibility exists that SMIT1 binds a complex region resulting from the heteromeric assembly of Kv7.4 and Kv7.5 subunits. Interestingly, interaction of Kv7.5 with SMIT1 seemed to be reduced when Kv7.4 and Kv7.5 were coexpressed in CHO cells. A recent study identified the pore region of Kv7.2 as necessary and sufficient for SMIT1 binding to this subunit. However, the authors suggested that the docking site for SMIT1 on Kv7.2 was large enough to allow further binding of the ancillary KCNE subunits which could, in turn, modulate SMIT1 interaction.[14] Therefore, the possibility exists that a complex interaction between Kv7.4, Kv7.5, and KCNE4 might occur in VSMCs, possibly increasing the interaction of SMIT1 with Kv7.4/Kv7.5 in native cells. Further studies are needed to identify the molecular determinants of SMIT1 binding on vascular Kv7 channels and clarify the stoichiometry of this interaction. Irrespective of these issues, these data are, to our knowledge, the first evidence of the interaction of an organic osmolyte transporter and a potassium channel in the vasculature.

Conclusions

Crosstalk between members of the transporters- and ion channels families has been unveiled recently, highlighting a high degree of functional and physical interaction that has led to the creation of the term chansporter.[15] Here, we describe for the first time a functional and molecular interaction between a myo-inositol transporter and a potassium channels in the vasculature that affects arterial contractility. Such interaction might provide an explanation for the changes in vascular reactivity observed in hyperosmolarity, a condition occurring in pathologies, such as diabetes mellitus.

In conclusion, our data unveil a novel mechanism regulating arterial reactivity and highlight a new potential strategy in the treatment of vascular disease.

ARTICLE INFORMATION

Received December 17, 2019; accepted August 3, 2020.

Affiliations

Vascular Research Centre, Institute of Molecular & Clinical Sciences, St George's, University of London, United Kingdom (V.B., J.B.S., S.N.B., I.A.G.). Department of Neuroscience, Reproductive Science and Dentistry, University of Naples Federico II, Italy (V.B.). Department of Pharmacology and Toxicology. School of Medicine, Universidad Complutense de Madrid, Spain (G.M.-P.).

Downloaded from http://ahajournals.org by on January 22, 2022

Acknowledgments

We acknowledge the Biological Research Facility for animal services, and the Image Resource Facility for assistance with confocal imaging, both at St George's University of London. We thank Professor Geoffrey W. Abbott (University of California, Irvine, United States) for the SMIT1 (sodium:myo-inositol transporter 1) plasmid and scientific discussions.

Sources of Funding

J.B. Stott was funded by a British Heart Foundation grant (PG/15/97/31862) awarded to I.A. Greenwood. S.N. Baldwin was funded by a British Heart Foundation grant (FS/18/41/33762) awarded to I.A. Greenwood. G. Mondejar-Parreño was funded by Ciber Enfermedades Respiratorias, CIBERES, grant (New markets and Therapeutic Targets for the Diagnosis and Treatment of Pulmonary Hypertension, EMPATHY project).

Disclosures

None.

REFERENCES

1. Kwon HM, Yamauchi A, Uchida S, Preston AS, Garcia-Perez A, Burg MB, Handler JS. Cloning of the cDNa for a Na+/myo-inositol cotransporter, a hypertonicity stress protein. *J Biol Chem*. 1992;267:6297–6301.
2. Hitomi K, Tsukagoshi N. cDNA sequence for rkST1, a novel member of the sodium ion-dependent glucose cotransporter family. *Biochim Biophys Acta*. 1994;1190:469–472. doi: 10.1016/0005-2736(94)90110-4
3. Berry GT, Mallee JJ, Kwon HM, Rim JS, Mulla WR, Muenke M, Spinner NB. The human osmoregulatory Na+/myo-inositol cotransporter gene (SLC5A3): molecular cloning and localization to chromosome 21. *Genomics*. 1995;25:507–513. doi: 10.1016/0888-7543(95)80052-n
4. Roll P, Massacrier A, Pereira S, Robaglia-Schlupp A, Cau P, Szepetowski P. New human sodium/glucose cotransporter gene (KST1): identification, characterization, and mutation analysis in ICCA (infantile convulsions and choreoathetosis) and BFIC (benign familial infantile convulsions) families. *Gene*. 2002;285:141–148. doi: 10.1016/s0378-1119(02)00416-x
5. Miyakawa H, Woo SK, Dahl SC, Handler JS, Kwon HM. Tonicity-responsive enhancer binding protein, a rel-like protein that stimulates transcription in response to hypertonicity. *Proc Natl Acad Sci USA*. 1999;96:2538–2542. doi: 10.1073/pnas.96.5.2538
6. Schneider S. Inositol transport proteins. *FEBS Lett*. 2015;589:1049–1058. doi: 10.1016/j.febslet.2015.03.012
7. Kotaria N, Kiladze M, Zhvania MG, Japaridze NJ, Bikashvili T, Solomonia RO, Bolkvadze T. The protective effect of myo-inositol on hippocamal cell loss and structural alterations in neurons and synapses triggered by kainic acid-induced status epilepticus. *Cell Mol Neurobiol*. 2013;33:659–671. doi: 10.1007/s10571-013-9930-y
8. Abbott GW, Tai KK, Neverisky DL, Hansler A, Hu Z, Roepke TK, Lerner DJ, Chen Q, Liu L, Zupan B, et al. KCNQ1, KCNE2, and Na+-coupled solute transporters form reciprocally regulating complexes that affect neuronal excitability. *Sci Signal*. 2014;7:ra22. doi: 10.1126/scisignal.2005025
9. Villalba H, Shah K, Albekairi TH, Sifat AE, Vaidya B, Abbruscato TJ. Potential role of myo-inositol to improve ischemic stroke outcome in diabetic mouse. *Brain Res*. 2018;1699:166–176. doi: 10.1016/j.brainres.2018.08.028
10. Li SYT, Cheng STW, Zhang D, Leung PS. Identification and functional implications of sodium/myo-inositol cotransporter 1 in pancreatic β-cells and type 2 diabetes. *Diabetes*. 2017;66:1258–1271. doi: 10.2337/db16-0880
11. Hille B, Dickson EJ, Kruse M, Vivas O, Suh BC. Phosphoinositides regulate ion channels. *Biochim Biophys Acta*. 2015;1851:844–856. doi: 10.1016/j.bbalip.2014.09.010
12. Barrese V, Stott JB, Greenwood IA. KCNQ-encoded potassium channels as therapeutic targets. *Annu Rev Pharmacol Toxicol*. 2018;58:625–648. doi: 10.1146/annurev-pharmtox-010617-052912
13. Haick JM, Byron KL. Novel treatment strategies for smooth muscle disorders: Targeting Kv7 potassium channels. *Pharmacol Ther*. 2016;165:14–25. doi: 10.1016/j.pharmthera.2016.05.002
14. Manville RW, Neverisky DL, Abbott GW. SMIT1 modifies KCNQ channel function and pharmacology by physical interaction with the pore. *Biophys J*. 2017;113:613–626. doi: 10.1016/j.bpj.2017.06.055
15. Neverisky DL, Abbott GW. Ion channel-transporter interactions. *Crit Rev Biochem Mol Biol*. 2015;51:257–267. doi: 10.3109/10409238.2016.1172553
16. Neverisky DL, Abbott GW. KCNQ-SMIT complex formation facilitates ion channel-solute transporter cross talk. *FASEB J*. 2017;31:2828–2838. doi: 10.1096/fj.201601334R
17. Dai G, Yu H, Kruse M, Traynor-Kaplan A, Hille B. Osmoregulatory inositol transporter SMIT1 modulates electrical activity by adjusting PI(4,5)P 2 levels. *Proc Natl Acad Sci*. 2016;113:E3290–E3299.
18. Massett MP, Koller A, Kaley G. Hyperosmolality dilates rat skeletal muscle arterioles: role of endothelial K(ATP) channels and daily exercise. *J Appl Physiol (1985)*. 2000;89:2227–2234. doi: 10.1152/jappl.2000.89.6.2227
19. Ishizaka H, Kuo L. Endothelial ATP-sensitive potassium channels mediate coronary microvascular dilation to hyperosmolarity. *Am J Physiol*. 1997;273(1 Pt 2):H104–H112. doi: 10.1152/ajpheart.1997.273.1.H104
20. Aalkjaer C, Mortensen FV, Jensen PE, Nielsen H. The role of [Ca2+] i, membrane potential and pHi in the relaxation of rat mesenteric arteries to hyperosmolar acetate. *Pflugers Arch*. 1998;436:705–711. doi: 10.1007/s004240050692
21. Hong JH, Jang HW, Kang YE, Lee JH, Kim KS, Kim HJ, Park KR, Ku BJ. Urinary chiro- and myo-inositol levels as a biological marker for type 2 diabetes mellitus. *Dis Markers*. 2012;33:193–199. doi: 10.3233/DMA-2012-0925
22. Chang H-H, Chao H-N, Walker CS, Choong S-Y, Phillips A, Loomes KM. Renal depletion of myo -inositol is associated with its increased degradation in animal models of metabolic disease. *Am J Physiol-Ren Physiol*. 2015;309:F755–F763.
23. Sotoda Y, Negoro M, Wakabayashi I. Involvement of decreased myo-inositol transport in lipopolysaccharide-induced depression of phosphoinositide hydrolysis in vascular smooth muscle. *FEBS Lett*. 2002;519:227–230. doi: 10.1016/s0014-5793(02)02747-3
24. Barrese V, Stott JB, Figueiredo HB, Aubdool AA, Hobbs AJ, Jepps TA, McNeish AJ, Greenwood IA. Angiotensin II promotes KV7.4 channels degradation through reduced interaction with HSP90 (Heat Shock Protein 90). *Hypertension*. 2018;71:1091–1100. doi: 10.1161/HYPERTENSIONAHA.118.11116
25. Askew Page HR, Dalsgaard T, Baldwin SN, Jepps TA, Povstyan O, Olesen SP, Greenwood IA. TMEM16A is implicated in the regulation of coronary flow and is altered in hypertension. *Br J Pharmacol*. 2019;176:1635–1648. doi: 10.1111/bph.14598
26. Stott JB, Barrese V, Suresh M, Masoodi S, Greenwood IA. Investigating the role of G protein βγ in Kv7-dependent relaxations of the rat vasculature. *Arterioscler Thromb Vasc Biol*. 2018;38:2091–2102. doi: 10.1161/ATVBAHA.118.311360
27. Burgess A, Vigneron S, Brioudes E, Labbé JC, Lorca T, Castro A. Loss of human Greatwall results in G2 arrest and multiple mitotic defects due to deregulation of the cyclin B-Cdc2/PP2A balance. *Proc Natl Acad Sci USA*. 2010;107:12564–12569. doi: 10.1073/pnas.0914191107
28. Chadha PS, Zunke F, Zhu H-L, Davis AJ, Jepps TA, Olesen SP, Cole WC, Moffatt JD, Greenwood IA. Reduced KCNQ4-encoded voltage-dependent potassium channel activity underlies impaired β-adrenoceptor–mediated relaxation of renal arteries in hypertension. *Hypertension*. 2012;59:877–884.
29. Jepps TA, Bentzen BH, Stott JB, Povstyan OV, Sivaloganathan K, Dalby-Brown W, Greenwood IA. Vasorelaxant effects of novel Kv 7.4 channel enhancers ML213 and NS15370. *Br J Pharmacol*. 2014;171:4413–4424. doi: 10.1111/bph.12805
30. Chadha PS, Zunke F, Davis AJ, Jepps TA, Linders JT, Schwake M, Towart R, Greenwood IA. Pharmacological dissection of K(v)7.1 channels in systemic and pulmonary arteries. *Br J Pharmacol*. 2012;166:1377–1387. doi: 10.1111/j.1476-5381.2012.01863.x
31. Haba M, Hatakeyama N, Kinoshita H, Teramae H, Azma T, Hatano Y, Matsuda N. The modulation of vascular ATP-sensitive K+ channel function via the phosphatidylinositol 3-kinase-Akt pathway activated by phenylephrine. *J Pharmacol Exp Ther*. 2010;334:673–678. doi: 10.1124/jpet.110.167775
32. Shi L, Zhang H, Chen Y, Liu Y, Lu N, Zhao T, Zhang L. Chronic exercise normalizes changes in Cav 1.2 and KCa 1.1 channels in mesenteric arteries from spontaneously hypertensive rats. *Br J Pharmacol*. 2015;172:1846–1858. doi: 10.1111/bph.13035
33. Stott JB, Barrese V, Jepps TA, Leighton EV, Greenwood IA. Contribution of Kv7 channels to natriuretic peptide mediated vasodilation in normal and hypertensive rats. *Hypertension*. 2015;65:676–682. doi: 10.1161/HYPERTENSIONAHA.114.04373
34. Li Q, Pang M, Zhu M, Chen L. G-protein-gated inwardly-rectifying K+ channels and large-conductance calcium-activated K+ channels are involved in C-type natriuretic peptide-mediated vasodilation in human arteries. *Int Heart J*. 2019;60:168–174. doi: 10.1536/ihj.18-004
35. Jepps TA, Carr G, Lundegaard PR, Olesen SP, Greenwood IA. Fundamental role for the KCNE4 ancillary subunit in Kv7.4 regulation of arterial tone. *J Physiol*. 2015;593:5325–5340. doi: 10.1113/JP271286

Downloaded from http://ahajournals.org by on January 22, 2022

36. Tykocki NR, Boerman EM, Jackson WF. Smooth muscle ion channels and regulation of vascular tone in resistance arteries and arterioles. *Compr Physiol*. 2017;7:485–581. doi: 10.1002/cphy.c160011
37. Byron KL, Brueggemann LI. Kv7 potassium channels as signal transduction intermediates in the control of microvascular tone. *Microcirculation*. 2018;25:e12419.
38. Stott JB, Jepps TA, Greenwood IA. K(V)7 potassium channels: a new therapeutic target in smooth muscle disorders. *Drug Discov Today*. 2014;19:413–424. doi: 10.1016/j.drudis.2013.12.003
39. Jepps TA, Chadha PS, Davis AJ, Harhun MI, Cockerill GW, Olesen SP, Hansen RS, Greenwood IA. Downregulation of Kv7.4 channel activity in primary and secondary hypertension. *Circulation*. 2011;124:602–611. doi: 10.1161/CIRCULATIONAHA.111.032136
40. Carr G, Barrese V, Stott JB, Povstyan OV, Jepps TA, Figueiredo HB, Zheng D, Jamshidi Y, Greenwood IA. MicroRNA-153 targeting of KCNQ4 contributes to vascular dysfunction in hypertension. *Cardiovasc Res*. 2016;112:581–589. doi: 10.1093/cvr/cvw177
41. Morales-Cano D, Moreno L, Barreira B, Pandolfi R, Chamorro V, Jimenez R, Villamor E, Duarte J, Perez-Vizcaino F, Cogolludo A. Kv7 channels critically determine coronary artery reactivity: left-right differences and downregulation by hyperglycaemia. *Cardiovasc Res*. 2015;106:98–108. doi: 10.1093/cvr/cvv020
42. Brueggemann LI, Mackie AR, Cribbs LL, Freda J, Tripathi A, Majetschak M, Byron KL. Differential protein kinase C-dependent modulation of Kv7.4 and Kv7.5 subunits of vascular Kv7 channels. *J Biol Chem*. 2014;289:2099–2111. doi: 10.1074/jbc.M113.527820
43. Chadha PS, Jepps TA, Carr G, Stott JB, Zhu HL, Cole WC, Greenwood IA. Contribution of kv7.4/kv7.5 heteromers to intrinsic and calcitonin gene-related peptide-induced cerebral reactivity. *Arterioscler Thromb Vasc Biol*. 2014;34:887–893. doi: 10.1161/ATVBAHA.114.303405
44. Povstyan OV, Barrese V, Stott JB, Greenwood IA. Synergistic interplay of Gβγ and phosphatidylinositol 4,5-bisphosphate dictates Kv7.4 channel activity. *Pflugers Arch*. 2017;469:213–223. doi: 10.1007/s00424-016-1916-4
45. Etxeberria A, Santana-Castro I, Regalado MP, Aivar P, Villarroel A. Three mechanisms underlie KCNQ2/3 heteromeric potassium M-channel potentiation. *J Neurosci*. 2004;24:9146–9152. doi: 10.1523/JNEUROSCI.3194-04.2004
46. Soldovieri MV, Castaldo P, Iodice L, Miceli F, Barrese V, Bellini G, Miraglia del Giudice E, Pascotto A, Bonatti S, Annunziato L, et al. Decreased subunit stability as a novel mechanism for potassium current impairment by a KCNQ2 C terminus mutation causing benign familial neonatal convulsions. *J Biol Chem*. 2006;281:418–428. doi: 10.1074/jbc.M510980200

Downloaded from http://ahajournals.org by on January 22, 2022

frontiers in Physiology

ORIGINAL RESEARCH
published: 07 December 2020
doi: 10.3389/fphys.2020.598779

K_V7 Channel Expression and Function Within Rat Mesenteric Endothelial Cells

Samuel N. Baldwin[1], Shaun L. Sandow[2], Gema Mondéjar-Parreño[3], Jennifer B. Stott[1] and Iain A. Greenwood[1]**

[1] *Vascular Biology Research Centre, Institute of Molecular and Clinical Sciences, St George's University of London, London, United Kingdom,* [2] *Biomedical Science, School of Health and Sports Science, University of the Sunshine Coast, Maroochydore, QLD, Australia,* [3] *Department of Pharmacology and Toxicology, School of Medicine, Complutense University of Madrid, Madrid, Spain*

OPEN ACCESS

Edited by:
Francesco Miceli, University of Naples Federico II, Italy

Reviewed by:
Vincenzo Calderone, University of Pisa, Italy
Nikita Gamper, University of Leeds, United Kingdom

***Correspondence:**
Iain A. Greenwood
grenwood@sgul.ac.uk
Samuel N. Baldwin
m1405629@sgul.ac.uk

Specialty section:
This article was submitted to Membrane Physiology and Membrane Biophysics, a section of the journal Frontiers in Physiology

Received: *25 August 2020*
Accepted: *13 November 2020*
Published: *07 December 2020*

Citation:
Baldwin SN, Sandow SL, Mondéjar-Parreño G, Stott JB and Greenwood IA (2020) K_V7 Channel Expression and Function Within Rat Mesenteric Endothelial Cells. Front. Physiol. 11:598779. doi: 10.3389/fphys.2020.598779

Background and Purpose: Arterial diameter is dictated by the contractile state of the vascular smooth muscle cells (VSMCs), which is modulated by direct and indirect inputs from endothelial cells (ECs). Modulators of KCNQ-encoded k_V7 channels have considerable impact on arterial diameter and these channels are known to be expressed in VSMCs but not yet defined in ECs. However, expression of k_V7 channels in ECs would add an extra level of vascular control. This study aims to characterize the expression and function of K_V7 channels within rat mesenteric artery ECs.

Experimental Approach: In rat mesenteric artery, KCNQ transcript and K_V7 channel protein expression were determined via RT-qPCR, immunocytochemistry, immunohistochemistry and immunoelectron microscopy. Wire myography was used to determine vascular reactivity.

Key Results: KCNQ transcript was identified in isolated ECs and VSMCs. $K_V7.1$, $K_V7.4$ and $K_V7.5$ protein expression was determined in both isolated EC and VSMC and in whole vessels. Removal of ECs attenuated vasorelaxation to two structurally different $K_V7.2$-5 activators S-1 and ML213. $K_{IR}2$ blockers ML133, and $BaCl_2$ also attenuated S-1 or ML213-mediated vasorelaxation in an endothelium-dependent process. K_V7 inhibition attenuated receptor-dependent nitric oxide (NO)-mediated vasorelaxation to carbachol, but had no impact on relaxation to the NO donor, SNP.

Conclusion and Implications: In rat mesenteric artery ECs, $K_V7.4$ and $K_V7.5$ channels are expressed, functionally interact with endothelial $K_{IR}2.x$ channels and contribute to endogenous eNOS-mediated relaxation. This study identifies K_V7 channels as novel functional channels within rat mesenteric ECs and suggests that these channels are involved in NO release from the endothelium of these vessels.

Keywords: pharmacology, vascular biology, endothelial cell, K_V7 channel, K_{IR} channel, carbachol

INTRODUCTION

KCNQ-encoded K_V7 channels are key regulators of arterial reactivity. Within the vasculature, of the five KCNQ subtypes, KCNQ4 is predominantly expressed, followed by KCNQ5 > KCNQ1; with little to no contribution from KCNQ2/3 (Ohya et al., 2003; Yeung et al., 2007; Ng et al., 2011). In human and rodent blood vessels K_V7 channels contribute to resting tone (Ohya et al., 2003; Yeung et al., 2007; Mackie et al., 2008; Ng et al., 2011), whereby their blockers such as linopirdine or XE991 produce contractions or enhance vasoconstrictor responses. In addition, a range of K_V7 channel activators including retigabine, S-1 and ML213 are effective relaxants of pre-contracted arterial tone. Furthermore, K_V7 channels also represent functional end targets for a myriad of endogenous vasoactive responses, wherein channel activity is impaired during PKC-mediated vasoconstriction (Brueggemann et al., 2006) and enhanced as a result of cGMP and cAMP dependent receptor-mediated vasodilation (e.g., Chadha et al., 2012; Khanamiri et al., 2013; Stott et al., 2014, 2015; Mani et al., 2016; Brueggemann et al., 2018; Mondéjar-Parreño et al., 2019). To date, vascular K_V7 channel studies have focused predominantly on vascular smooth muscle cells (VSMCs) or whole arteries, and as a result it is currently unclear whether endothelial cells (ECs) express K_V7 channels and if so, what their functional role may be.

Endothelial cells form the inner layer of blood vessels and constitute a paracrine signaling platform which regulates VSMC contractility, vascular resistance and ultimately blood flow through the release of nitric oxide (NO), prostacyclin, epoxyeicosatrienoic acid and others; including the generation and spread of endothelium-derived hyperpolarization (EDH) (McGuire et al., 2001). Myoendothelial (ME) projections within fenestrations (holes) of the internal elastic lamina (IEL) facilitate the presence gap junctions (MEGJs) at a proportion of such sites (∼50% in adult rat 1st–3rd order 'large' mesenteric arteries; MA; Sandow et al., 2009) which permits heterocellular electrochemical coupling via connexin proteins (Sandow et al., 2012). These sites enable the transfer of EC-derived signals via the flow of both small molecules < ∼1 kDa and current between the cells. In endothelium-dependent relaxation of rat MA, a fundamental role for small/intermediate conductance calcium-activated potassium (SK_{Ca} and IK_{Ca}, respectively; Sandow et al., 2006; Dora et al., 2008), transient receptor potential canonical type 3 (Senadheera et al., 2012), inwardly rectifying potassium channels ($K_{IR}2$) (Goto et al., 2004), as well as inositol-1,3,4 trisphosphate receptor/s (Fukao et al., 1997) has been demonstrated.

Identification of K_V7 expression in ECs would open up a new layer of vascular control by these channels and is a necessary requisite for understanding the role of these channels in vascular health and disease. This study aims to ascertain whether rat mesenteric ECs express K_V7 channels, and if so, what their functional implications may be. This study shows that K_V7 channels are expressed in rat mesenteric artery ECs and contribute to both K_V7 activator-mediated relaxation via a potential functional interaction with $K_{IR}2$ channels and endothelial NO synthase (eNOS)-dependent axis of carbachol (CCh)-mediated vasorelaxation.

Abbreviations: 4-AP, 4-aminopyridine; Acta2, α-smooth muscle actin-2; CCh, carbachol; cGMP, cyclic guanosine monophosphate; Cq, quantification cycle; CYC1, cytochrome C1; EC, endothelial cell; EDH, endothelium derived hyperpolarization; GAPD, glyceraldehyde-3-phosphate dehydrogenase; eNOS, endothelial nitric oxide synthase; IK_{Ca}, intermediate conductance calcium-activated potassium channel; IEL, internal elastic lamina; K_{IR}, inwardly rectifying potassium channel; K_V, voltage-gated potassium channel; L-NAME, L-nitroarginine methyl ester; MA, mesenteric artery; MO, methoxamine; Myh11, myosin heavy chain 11; NO, nitric oxide; PECAM-1, platelet endothelial cell adhesion molecule-1; RT-qPCR, reverse-transcription quantitative polymerase chain reaction; SEM, standard error of the mean; SK_{Ca}, small conductance calcium-activated potassium channel; SNP, *S*-nitroprusside; TEA, tetraethylammonium; VSMC, vascular smooth muscle cell; vWBF, von-Willebrand factor.

MATERIALS AND METHODS

Animal Models

Experiments were performed on MA from Male Wistar rats (Charles River, Margate, United Kingdom) ages 11–14 weeks (200–350 g) from the Biological Research Facility, St George's, London, United Kingdom; and from the Animal Resources Center, Perth, Australia. Animals were housed in cages with free access to water and food (RM1; Dietex Inter-national, United Kingdom) *ad libitum*, with a 12-h light/dark cycle and constant temperature and humidity (21 ± 1°C; 50% ± 10% humidity) in accordance with the Animal (Scientific Procedures) Act 1986, the guidelines of the National Health and Medical Research Council of Australia and the UNSW Animal Ethics and Experimentation Committee (AEEC #18/86B). Animals were kept in LSB Aspen woodchip bedding. Animals were culled by either cervical dislocation with secondary confirmation via cessation of the circulation by femoral artery severance or were anesthetized with sodium pentathol (intraperitoneal, 100 mg/kg) in accordance with Schedule 1 of the ASPA 1986.

Either whole mesenteric plexus or 2nd/3rd/4th order MA were used with vessel order identified from the second bifurcation of the superior MA. Arteries were dissected, cleaned of fat and adherent tissue and stored on ice within physiological salt solution (PSS) of the following composition (mmol-L^{-1}); 119 NaCl, 4.5 KCl, 1.17 $MgSO_4.7H_20$, 1.18 NaH_2PO_4, 25 $NaHCO_3$, 5 glucose, 1.25 $CaCl_2$.

Reverse Transcription Quantitative Polymerase Chain Reaction

Second and third order MA segments were enzymatically digested to obtain either freshly isolated ECs (as previous, Greenberg et al., 2016) or VSMCs. Briefly, vessels were washed in Hanks' Balanced Salt Solution (HBSS; ThermoFisher Scientific, GIBCO, 14170-088) containing 50 μmol-L^{-1} $CaCl_2$ for 5 min at 37°C, the media was then replaced in HBSS containing 50 μmol-L^{-1} $CaCl_2$ with 1 mg/mL collagenase IA (Sigma Aldrich, C9891, United Kingdom) for 15 min at 37°C. Vessels were washed

in HBSS containing 50 μmol-L^{-1} $CaCl_2$ for 10 min at 37°C. The supernatant was removed and the vessels suspended in fresh HBSS containing 75 μmol-L^{-1} $CaCl_2$. For RT-qPCR, ECs were dissociated using a wide-bore smooth-tipped pipette and identified under the microscope (x10) as sheets of cells independent from the vessel which were harvested and stored separately from the residual VSMCs.

mRNA from both isolated ECs and VSMCs was extracted using Monarch Total RNA Miniprep Kit (New England BioLabs, Ipswich, MA, United States) and reverse transcribed via LunaScript RT SuperMix Kit (New England BioLabs, Ipswich, MA, United States). Quantitative analysis of relative gene expression was assessed via CFX-96 Real-Time PCR Detection System (BioRad, Hertfordshire, United Kingdom). Samples were run in duplicate to account for variation. Samples were run in BrightWhite qPCR plate (Primer Design, Camberley, United Kingdom), with each well containing 20 μL of reaction solution containing: 10 μL of PrecisionPLUS qPCR Master Mix (Primer Design, Camberley, United Kingdom), 300 nmol-L^{-1} of gene specific target primer (Thermofisher scientific, Waltham, MA, United States) and 10 ng of cDNA sample made up to 20 μL total volume with nuclease free water. Run protocol: (1) activation step (15 min:95°C), (2) denaturation step (15 s: 94°C), (3) annealing step (30 s: 55°C), and (4) extension step (30 s: 70°C). Steps 2- 4 were repeated x 40. Quantification cycle (Cq) was determined via Bio-Rad CFX96 Manager 3.0. Cq values were normalised to housekeeper genes expressed as a $2^{-\Delta Cq}$ when compared to appropriate reference genes including 14-3-3 Zeta (YWHAZ) and glyceraldehyde-3-phosphate dehydrogenase (GAPD). Cell isolation for VSMCs and ECs was validated by either positive expression of VSMC specific marker α-actin 2 (*Acta2)* or EC specific marker-platelet endothelial cell adhesion molecule-1 *(Pecam-1)* respectively. See **Table 1** for a list of the primers used in the following (Jepps et al., 2011; Askew Page et al., 2019; ThermoFisher Scientific).

TABLE 1 | RT-qPCR primer sequences.

Gene	(+) Forward primer sequence (–) Reverse primer sequence	Gene accession number	Amplicon (bp)
Acta2	ATCCGATAGAACACGGCATC AGGCATAGAGGGACAGCACA	NM_031004.2	228
Pecam1	CTCCTAAGAGCAAAGAGCAACTTC TACACTGGTATTCCATGTCTCTGG	NM_031591.1	100
Kcnq1	TGGGTCTCATCTTCTCCTCC GTAGCCAATGGTGGTGACTG	NM_032073	124
Kcnq2	AAGAGCAGCATCGGCAAAAA GGTGCGTGAGAGGTTAGTAGCA-	NM_133322	101
Kcnq3	CAGCAAAGAACTCATCACCG ATGGTGGCCAGTGTGATCAG	AF091247	161
Kcnq4	GAATGAGCAGCTCCCAGAAG AAGCTCCAGCTTTTCTGCAC	XM_233477.8	133
Kcnq5	AACTGATGAGGAGGTCGGTG GATGACCGTGACCTTCCAGT	XM_001071249.3	120

Immunocytochemistry

Freshly dispersed ECs (as above), together with residual VSMCs were left for 1hr before use. Cells were then fixed in 4% paraformaldehyde (Sigma-Aldrich, United Kingdom) in PBS for 20 min at RT as previously described (Barrese et al., 2018a). Cells were treated with 0.1 mol-L^{-1} glycine for 5 min and incubated for 1 h with blocking solution (PBS-0.1% Triton X-100-10% bovine serum albumin) at RT. Following incubation overnight at 4°C with primary antibodies (**Table 2**) diluted in blocking solution (anti-PECAM-1 for ECs, anti-α-actin for VSMCs and anti-$K_V7.1$, $K_V7.4$, and $K_V7.5$ channel for ECs/VSMCs), cells were then washed for 20 min with PBS, incubated for 1 h at RT with the secondary conjugated antibodies diluted in blocking solution. Excess secondary antibody was removed by washing with PBS and cells mounted using media containing 4′,6-diamidino-2-phenylindole (DAPI) for nuclear counterstaining. Using triple staining, ECs and VSMC were differentiated via the following: ECs were positive for anti PECAM-1 and negative for anti-α-actin; while VSMC was positive for anti-α-actin and negative for anti-PECAM-1 (data not shown). Cells were analyzed using a Zeiss LSM 510 Meta argon/krypton laser scanning confocal microscope (Image Resource Facility, St George's University, London).

Cell Culture

Chinese Hamster Ovary (CHO) cells were maintained in DMEM supplemented with 10% fetal bovine serum, 2 mmol-L^{-1} L-glutamine, and 1% penicillin/streptomycin (Sigma Aldrich, Dorset, United Kingdom) and maintained at 37°C with 5% CO_2 in an incubator. Cells were plated in a 24-well plate, incubated for 24hr then transfected with either $K_V7.1$, $K_V7.4$ or $K_V7.5$ plasmids using Lipofecamine 2000 (Thermofisher, Paisley, United Kingdom) as described previously (Barrese et al., 2018a). After 24 h, cells were fixed and stained as described above.

Immunohistochemistry

Animals were anesthetized with sodium pentathol (intraperitoneal, 100 mg/kg) and perfusion fixed (Sandow et al., 2004) in 2% paraformaldehyde in 0.1 mol-L^{-1} PBS. Third to 4th order MA segments were dissected, opened laterally and pinned as a sheet to a Sylgard dish. Segments were washed in PBS (3 × 5 min), incubated in blocking buffer (PBS with 1% BSA and 0.2% Triton) at room temperature (RT) for 2 h and then overnight with primary antibody (**Table 2**) in blocking buffer at 4°C, washed again (3 × 5 min with gentle agitation), and incubated in secondary antibody (**Table 2**; matched to the respective primary) in PBS with 0.1% Triton in PBS for 2 h at RT. Tissue was mounted on slides in anti-fade media containing propidium iodide (PI) or DAPI (**Table 2**) and imaged with uniform confocal settings. Incubation of tissue with secondary only was used as a 'zero' setting for confocal imaging. Controls involved substitution of primary with isotype control, with concentration (where provided by manufacturer) matched, or 10-fold higher than the respective antibody of interest (**Table 2**). Working Ab dilutions were prepared in accordance with previous work (Jepps et al., 2009; Chadha et al., 2012). Confocal image

TABLE 2 | Immunocyto/histochemistry reagents and use (Jepps et al., 2009; Chadha et al., 2012).

Reagent purpose	Detail	Source	Predicted MW, kDa	Epitope	[used]	Peptide availability	Raised in
Primary antibodies	Kv7.1/KCNQ1	Pineda Antikörper-Service, Germany	75	N-terminus	1:100	No	Rabbit
	Kv7.4/KCNQ4	NeuroMab, cat no 75-082, 1 mg/ml	77	Hu aa 2-77, clone N4/36 IgG	1:200 (5 μg/ml)	No	Mouse
	Kv7.4/KCNQ4*	Abcam, ab65797, lot GR94754, whole serum	77	N' domain	1:100 not available	No	Rabbit
	Kv7.5/KCNQ5*	Millipore ABN1372-q2476155; 1 ml/ml	∼103	Human IgG	1:100 (10 μg/ml)	No	Rabbit
	PECAM-1/CD31	Santa Cruz Biotechnology, Sc-1506, 200 μg/ml	130	699–727 aa at the C-terminus	1:100 (2 μg/ml)	–	Goat
	SM-α-actin	Sigma Aldrich A2547	∼42	N-terminal	(1:100) not available	–	Mouse
Nuclear labels/cell patency markers	DAPI, Vectasheild	Vectorlabs	–	Nucleic acid		–	–
	propidium iodide (PI)	Sigma, P4170	–	Nucleic acid	10 nM	–	–
Immuno-histochemistry secondary antibodies	Mouse 568	Abcam, ab175700, lot GR320062-4, 2 mg/ml	–	IgG	1:100 (20 μg/ml)	–	Donkey
	Rabbit 546	Thermofisher, A-11035	–	IgG	1:100 (20 μg/ml)	–	Goat
	Rabbit 633	Merck, SAB4600132, lot 15C0423, 2 mg/ml	–	IgG	1:100 (20 μg/ml)	–	Donkey
Immuno-cytochemistry secondary antibodies	Mouse 488	Thermofisher, A21202, 2 mg/mL	–	IgG	1:100 (0.02 mg/ml)	–	Donkey
	Rabbit 568	Thermofisher, A10042, 2 mg/mL	–	IgG	1:100 (0.02 mg/ml)	–	Donkey
	Goat 633	Thermofisher, A21082, 2 mg/mL	–	IgG	1:100 (0.02 mg/ml)	–	Donkey
Isotype controls	Mouse IgG	ThermoFisher, 10400C	–	IgG	5 mg/ml	–	Mouse
	Rabbit IgG	ThermoFisher, S31235	–	IgG	10 mg/ml	–	Rabbit
Immunoelectron microscopy secondary antibodies	5 nm Au anti- rabbit	Merck, G7277, lot SLB3882V	–	IgG	1:100	–	Goat
	10 nm Au anti- rabbit	Merck, G7402	–	IgG	1:100	–	Goat

CD31, cluster of differentiation 31; DAPI, 4',6-diamidino-2-phenylindole; PECAM, platelet endothelial cell adhesion molecule.

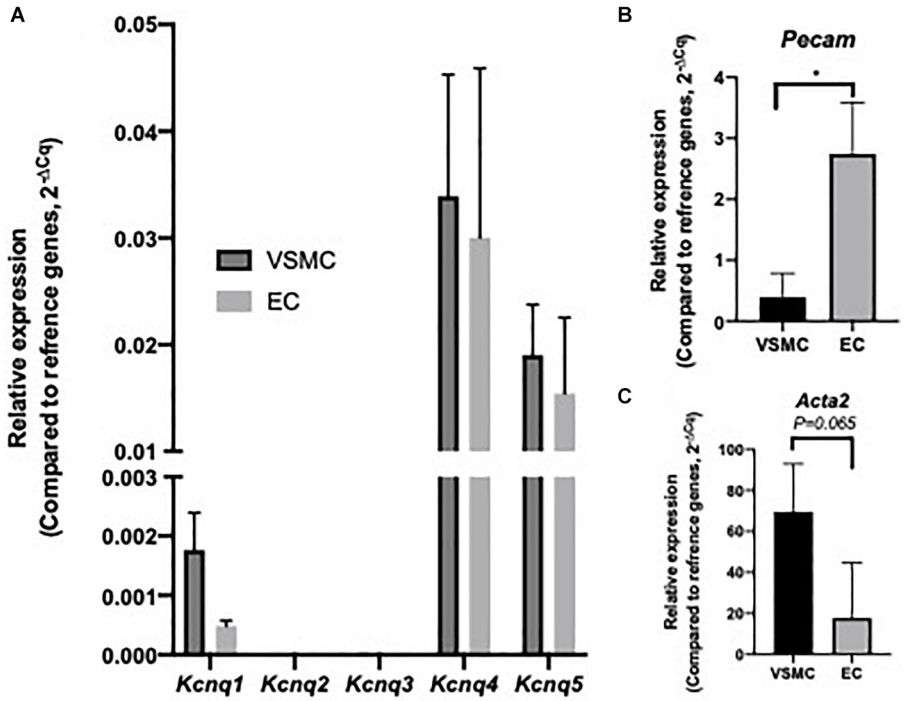

FIGURE 1 | Expression profile of *Kcnq* genes within isolated rat mesenteric vascular smooth muscle cells (VSMCs) and endothelial cells (ECs). RT-qPCR analysis of relative expression of *Kcnq1-5* in isolated VSMCs and ECs **(A)**. Cell specific markers *Acta2* and *Pecam,* for VSMCs and ECs respectively, were measured to determine sample purity **(B,C)**. Values expressed as mean ± SEM of ($2^{-\Delta Cq}$) of ΔCq values generated from appropriate housekeeper genes ($n = 3$). Statistical significance is defined as $^*P < 0.05$ **(B,C)**.

stacks were collected at 0.2 μm intervals. The optimal rinsing protocol was determined by incubating in secondary only; and rinsing after successive 5 min incubations until fluorescence was reduced to background. Note that if this was not done secondary alone was specifically and highly localized to IEL hole sites; as potential false positives at such sites; suggesting that such sites have an affinity for IgG-secondary label alone.

Electron Microscopy

Animals were anesthetized as above and perfusion fixed in 0.2% glutaraldehyde and 2% paraformaldehyde in 0.1 mol-L^{-1} PBS (pH 7.4). MA segments (∼2 mm in length) were washed (3 × 5 min) and processed in a Leica EMPACT 2 high-pressure freezer using 0.7% low melting agarose as a cryoprotectant. Samples were then freeze-substituted in a Leica AFS2 into 0.2% uranyl acetate in 95% acetone (from −85 to −50°C) and infiltrated with Lowicryl (at −50°C), before UV polymerization (2 days each at −50 and 20°C; Zechariah et al., 2020). Conventional transmission electron microscopy (TEM) was conducted using standard procedures (Sandow et al., 2002, 2004).

Individual serial transverse sections (∼100 nm) were mounted on Formvar-coated slot grids and processed for antigen localization as for confocal immunohistochemistry (per above and **Table 2**). The secondary used was 5 or 10 nmol-L^{-1} colloidal gold-conjugated antibody (1:40; 2 h) in 0.01% Tween-20. Sections were imaged at x10-40,000 on a JEOL transmission electron microscope at 16 MP (Emsis, Morada G3). Background gold label density was determined from randomly selected (4x) 1 × 1 μm regions per sample of lumen and IEL, compared to the same sized regions of interest in EC profiles.

Wire Myography

Second order MA segments (∼2 mm in length) were mounted on 40 μm diameter tungsten wire in a tension myograph chamber (Danish Myo Technology, Arhus, Denmark) containing 5 mL of PSS (composition, as above) oxygenated with 95% O_2 and 5% CO_2 at 37°C. Vessels then underwent a passive force normalization process to achieve an internal luminal circumference at a transmural pressure of 100 mmHg (13.3 kPa) to standardize pre-experimental conditions (Mulvany and Halpern, 1976). Force generated was first amplified by a PowerLab (ADInstruments, Oxford, United Kingdom), and recorded by LabChart software (ADInstruments, Oxford, United Kingdom). Vessels were then challenged with 60 mmol-L^{-1} [K^+] to determine viability, and then constricted with 10 μmol-L^{-1} methoxamine (MO), an α-1 adrenoreceptor agonist, EC integrity was then determined via addition of 10 μmol-L^{-1} carbachol (CCh), a synthetic acetylcholine analog. Vessels displaying ≥ 90% vasorelaxation in response to CCh were considered EC positive (EC+). Vessels were denuded of ECs by gently passing a human hair through the lumen. Vessels expressing ≤ 10% vasorelaxation in response to CCh were considered EC negative (EC−). During functional investigations,

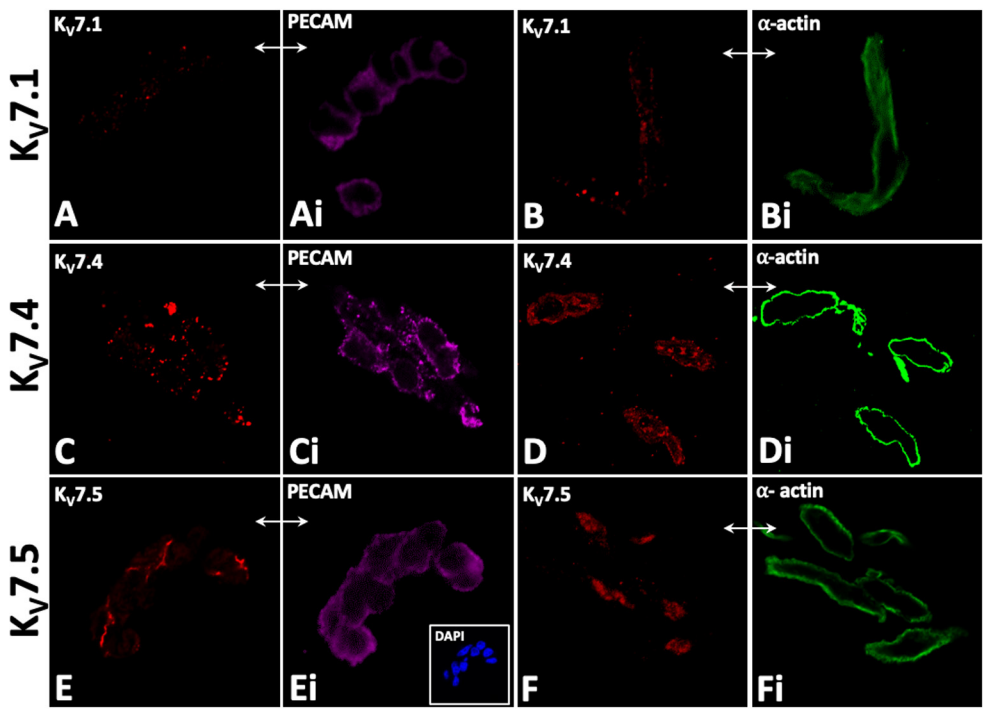

FIGURE 2 | Immunocytochemistry demonstrates K_V7.1, K_V7.4, and 7_V.5 localization in rat mesenteric artery isolated endothelial (EC; **A,C,E**) and smooth muscle cells (SMC; **B,D,F**). Punctate labelling for Kv7.1, Kv7.4, and 7.5 was present in isolated EC and SMCs (**A,C,E** and **B,D,F**). PECAM and smooth muscle a-actin were used as markers for isolated endothelial and smooth muscle cells, respectively (**Ai,Ci,Ei** and **Bi,Di,Fi** respectively); e.g. comparative-same cells, double arrows, **A–Fi**). 4′,6-diamidino-2-phenylindole (DAPI; e.g. inset, **C**) were used as nuclear markers to verify cell patency. *n* = 4–6, representative of different source tissue **(A–Fi)**. Double arrows from insets indicate same panel as main, but to different marker.

all vessels were pre-constricted with the thromboxane A2 receptor agonist U46619 (300 nmol-L^{-1}) to elicit an EC_{80} contraction. Concentration-dependent relaxant responses to S-1 (0.1–10 μmol-L^{-1}), ML213 (0.1–10 μmol-L^{-1}), ML277 (0.03–10 μmol-L^{-1}), CCh (0.3–10 μmol-L^{-1}) and *S*-nitroprusside (SNP; 0.01–3 μmol-L^{-1}) were determined in the presence and absence of ECs, linopirdine (10 μmol-L^{-1}), HMR-1556 (10 μmol-L^{-1}), carbenoxolone (100 μmol-L^{-1}), ML133 (20 μmol-L^{-1}), barium chloride ($BaCl_2$; 100 μmol-L^{-1}), L-nitroarginine methyl ester (L-NAME; 100 μmol-L^{-1}), TRAM34 (1 μmol-L^{-1}), Apamin (10 nmol-L^{-1}), 4-aminopyridine (4-AP; 1 mmol-L^{-1}), and tetraethylamonium (TEA; 1 mmol-L^{-1}).

Data and Statistical Analysis

All functional figures express mean data from at least 5 animals ± standard error of the mean (SEM). Experiments comparing groups of unequal numbers are present due to technical failure or expiry of tissue during isometric tension recording. For functional experiments involving cumulative concentrations, a transformed data set was generated using; X = Log(X), to reduce representative skew. A four parametric linear regression analysis was then performed using the following equation; [Log(Agonist) vs. response – variable slope (four parameters bottom/hillslope/top/EC_{50})] using GraphPad Prism (Version 8.2.0) to fit a concentration effect curve (CEC) to the figure. For data comparing multiple groups, a two way-ANOVA followed by a *post hoc* Bonferonni test in order to account for type 1 errors in multiple comparisons was performed for comparison of mean values. For data comparing two groups, an unpaired parametric T-test was was performed. Significance values are represented as follows; $P < 0.05$ (*). *n* = (x), number of animals used. *N* = (x), number of segments used. The data and statistical analysis comply with the recommendations on experimental design and analysis in pharmacology (Curtis et al., 2018).

RESULTS

Identification of K_V7 Channels Within MA ECs

Initial investigation sought to identify *Kcnq*/K_V7 transcript and protein within MA ECs. Transcript levels for *Kcnq1-5* and EC and VSMC markers were determined in cell lysates from isolated MA VSMC and EC (per Methods). Both ECs and VSMCs expressed *Kcnq4* > *Kcnq5* > *Kcnq1* with no expression of *Kcnq2/3* (**Figure 1A**) similar to previous studies (Ohya et al., 2003; Yeung et al., 2007; Ng et al., 2011). However, a comparative reduction in the relative abundance of *Kcnq1* was observed in MA ECs when compared to VSMCs (**Figure 1A**). Cell isolation efficiency is demonstrated by a reduction in EC marker *Pecam*

within VSMCs cell lysates when compared to ECs ($P \leq 0.05$) and a reduction in VSMCs marker *Acta2* in EC cell lysates when compared to VSMCs ($P = 0.065$, **Figures 1B,C**).

K_V7.1, K_V7.4, and K_V7.5 were detected in isolated ECs by immunodetection (**Figures 2A,C,E**). K_V7.4 had a punctate distribution in isolated ECs (**Figure 2C**) whereas K_V7.5 label appeared to be predominantly cytoplasmic with some diffuse label around the nucleus (**Figure 2E**). Similar to previous reports (Zhong et al., 2010; Oliveras et al., 2014; Mills et al., 2015; Morales-Cano et al., 2015; Barrese et al., 2018a). K_V7.1, K_V7.4, and 7.5 were also identified in isolated MA VSMCs (**Figures 2B,D,F**). K_V7.1 staining in ECs was negligible compared to VMSCs (**Figures 2A,B**). ECs and VSMCs were identified by positive expression of either PECAM (**Figures 2Ai,Ci,Ei**) or α-actin (**Figures 2Bi,Di,Fi**) respectively. Antibody specificity was determined via positive staining in CHO cells transfected with purported target and negative staining in non-transfected control cells (**Supplementary Figure 1**). Importantly, as ion channel expression can alter in isolated cells K_V7.4 and K_V7.5 were also detected in both ECs and VSMCs in *en face* whole-mount arteries (**Figures 3A,B,E,F**). Notably, both K_V7.4 and 7.5 were expressed at a proportion of IEL hole sites at an apparently higher level than the associated EC membrane label (**Figures 3C,D,G,H**). We also detected K_V7.4 and K_V7.5 in EC by immuno-gold electron microscopy (**Supplementary Figure 2**). These studies identify K_V7.4 and K_V7.5 in ECs as well as smooth muscle cells.

Removal of ECs Modulates K_V7.2-5 Activator Efficacy

A comprehensive pharmacological analysis was undertaken to determine if K_V7 channels have a functional role in MA ECs via a reductive approach. Initially, the effects of K_V7 channel modulators were examined in endothelium intact or denuded MAs. The structurally dissimilar K_V7.2–7.5 activators S-1 and ML213 interact with the same pharmacophore centered around a tryptophan in the S5 domain (Schenzer, 2005; Bentzen et al., 2006; Brueggemann et al., 2014; Jepps et al., 2014). ML277 is a potent activator of K_V7.1 (Yu et al., 2013) with a 100-fold increase in selectivity for K_V7.1 compared to K_V7.2-5 (Yu et al., 2013). Consistent with previous findings (Chadha et al., 2012; Jepps et al., 2014), S-1- and ML213-mediated vasorelaxation was ablated by pre-incubation with 10 μmol-L^{-1} of the pan-K_V7 channel inhibitor linopirdine (Schnee and Brown, 1998; **Figures 4A,B,D**). Relaxation produced by 10–300 nmol-L^{-1} ML277 were also prevented by pre-incubation with linopirdine (**Figure 4C**). However, relaxation produced by concentrations > 1 μmol-L^{-1} ML277 was not attenuated by linopirdine and are therefore not mediated by K_V7.1 activation.

Endothelial removal for the following experiments was confirmed by ablation of vasorelaxation in response to 10 μmol-L^{-1} CCh (**Figure 5A**). Endothelium denudation by mechanical abrasion has no impact on the peak contraction produced by 300 nmol-L^{-1} U46619 (**Figure 5B**), but significantly attenuated the potency of S-1 mediated vasorelaxation increasing EC_{50} from

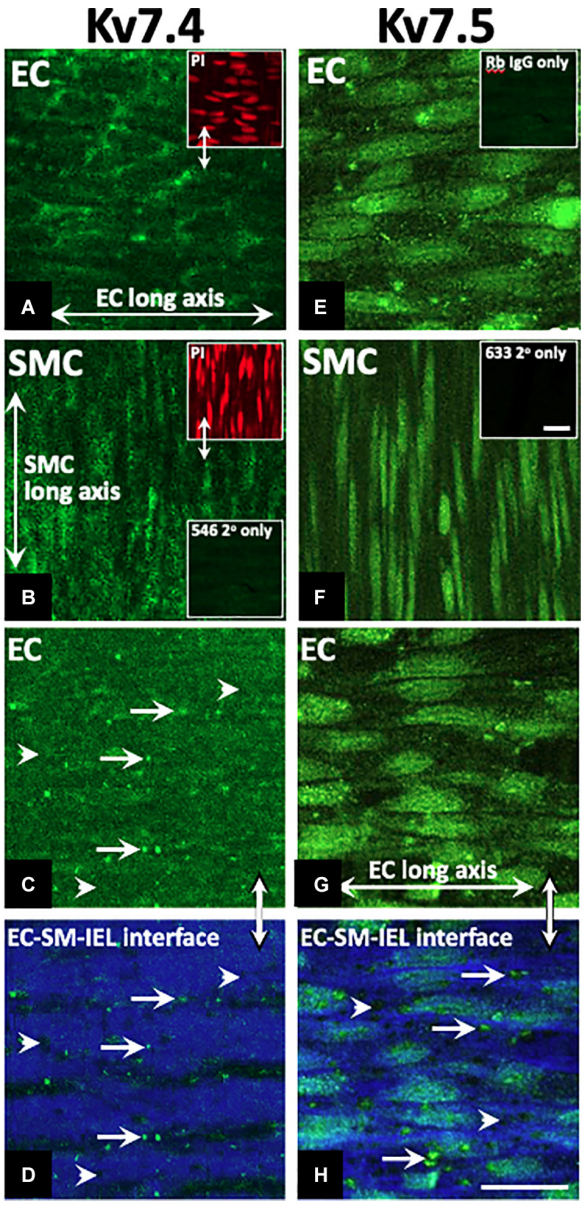

FIGURE 3 | Immunohistochemistry demonstrates Kv7.4 and 7.5 localization in rat mesenteric artery endothelium (EC) and smooth muscle cells (SMCs) with a focus on internal elastic lamina (IEL) hole sites in whole mount tissue. Whole mounts of confocal stacks through the EC and SMC of K_V7.4 (**A,B**, respectively) and Kv7.5 (**E,F**, respectively). Confocal image stacks through the luminal EC to SM border **(C,G)** show diffuse/punctate K_V7.4/K_V7.5 across the cell membrane with some punctate higher-level fluorescence at localized sites (e.g. full arrows; **C**). When single images were taken at the EC-IEL-SM interface **(D,H)**, punctate higher-level fluorescence densities were present (e.g. **D,H** arrows; **H**, higher magnification inset) at *a proportion* of IEL hole sites (e.g., **D,H** arrowheads). Propidium iodide (PI; e.g., upper left inset, **A,B**) were used as nuclear markers to verify cell and layer patency. Incubation in secondary only separately for each of the 3 fluorophores (**Table 2**; e.g. lower left inset, **B**; inset, **F**) were used to set 'zero' confocal settings. Incubation in isotype IgG control only (e.g., **E**, inset) showed fluorescence equivalent to secondary alone (e.g., **B**, lower inset; **F**, inset). $n = 4$, representative of different source. Longitudinal vessel axis, left to right. Double arrows indicate same site, but at different focal planes **(C,D,G,H)**, and location of inset **(D)**. Bar, 25 μm.

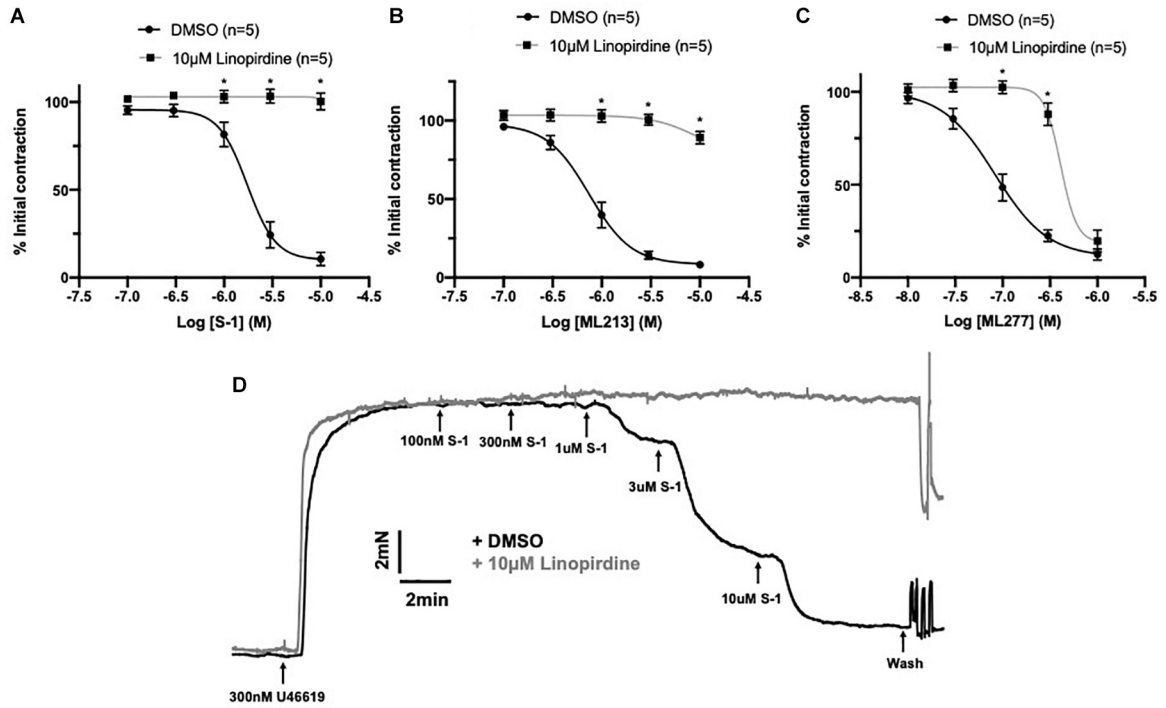

FIGURE 4 | Sensitivity of Kv7 activator relaxations to 10 μmol-L^{-1} linopirdine. In vessels pre-incubated in DMSO solvent control, K_V7.2-5 channel activators S-1 and ML213 relax pre-constricted arterial tone (300 nmol-L^{-1} U46619; black) and are ablated by pre-incubation with pan K_V7 channel inhibitor linopirdine (10 μmol-L^{-1}; gray; n = 5; **A,B**). In vessels pre-incubated in DMSO solvent control, K_V7.1 channel activator ML277 relaxes pre-constricted arterial tone (300 mol-L^{-1} U46619; black) and is ablated by linopirdine (10 μmol-L^{-1}; gray) to a threshold of 300 nmol-L^{-1} ML277 (n = 5; **C**). A representative trace of S-1-mediated vasorelaxation ± 10 μmol-L^{-1} linopirdine **(D)**. All values are expressed as mean + SEM. A two-way statistical ANOVA with a *post hoc* Bonferroni test was used to generate significance values. Statistical significance is defined as $^*P < 0.05$ **(A–C)**.

2 ± 0.2 μmol-L^{-1} to 3 ± 0.7 μmol-L^{-1} (**Figures 5C,D**). S-1 mediated relaxation was also impaired via the non-selective gap junction inhibitor carbenoxolone (Tare et al., 2002) (water E_{max} = 6.11 ± 1.82% vs. carbenoxolone E_{max} = 18.7 ± 3.25%; **Figure 5E**). In addition, the potency of ML213 was also impaired by endothelial removal (EC(+) EC_{50} = 1 ± 0.2 μmol-L^{-1} vs. EC(−) EC_{50} = 3 ± 0.2 μmol-L^{-1}; **Figure 5F**) in a fashion analogous to S-1. However, the linopirdine-sensitive relaxation produced by ML277 was not affected by endothelial removal (**Figure 5G**).

EC K_{IR} Channels Modulate K_V7.2-5 Activator Sensitivity

Having identified that the presence of the endothelium modulates responses to K_V7 activators, experiments were performed to identify the underlying mechanism/s involved. *Murine* endothelial KCNJ2-encoded K_{IR}2.1 channels have been identified as 'signal boosters' that enhance EC-derived relaxation (Sonkusare et al., 2016). Comparatively, the current literature regarding *rat* mesenteric K_{IR}2 channels is limited. In brief, rat MA endothelium expresses K_{IR}2.1 (Dora et al., 2008), inwardly rectifying Ba^{2+} sensitive channels are restricted to the endothelial layer (Crane et al., 2003a) and K_{IR} channels contribute to acetylcholine-mediated responses (Goto et al., 2004). We propose that like mice, rat mesenteric ECs express functional K_{IR}2 channels that propagate EC signals in a similar process. Therefore, we performed a series of studies investigating the effect of two characterized K_{IR}2 blockers, $BaCl_2$ (Hagiwara et al., 1978) and ML133 (Wang et al., 2011) on K_V7 activator-mediated vasorelaxation.

In arteries with a functional endothelium, K_{IR}2 blockers, $BaCl_2$ (100 μmol-L^{-1}) and ML133 (20 μmol-L^{-1}), significantly impaired relaxations produced by S-1 (**Figure 6A**, EC_{50} = DMSO, 1.89 ± 0.2 μmol-L^{-1}/$BaCl_2$, 2.3 ± 0.31 μmol-L^{-1}; **Figure 6B**, EC_{50} = DMSO, 0.52 ± 0.12 μmol-L^{-1}/ML133, 3.1 ± 1.5 μmol-L^{-1}) and ML213 (**Figures 6C,D**, EC_{50} = DMSO, 0.9 ± 0.3 μmol/L^{-1}/$BaCl_2$, 2.2 ± 0.5 μmol/L^{-1}/ML133, 2.5 ± 0.25 μmol-L^{-1}) when compared to DMSO solvent control (**Figures 6A–D**). No attenuation of the response to ML277 was observed when pre-incubated with either blocker (**Figures 6E,F**), consistent with EC removal. Furthermore, in arteries where the endothelium had been removed neither ML133 nor $BaCl_2$ had any effect on ML213 mediated relaxations (**Figures 6G,H**).

IK_{Ca}/SK_{Ca} Inhibitors Had No Impact on K_V7 Activator Mediated Relaxation

Endothelial IK_{Ca} and SK_{Ca} channels contribute to relaxation responses in rat MA (Crane et al., 2003b). Thus, it is feasible that K_V7 channels interact with other key endothelial

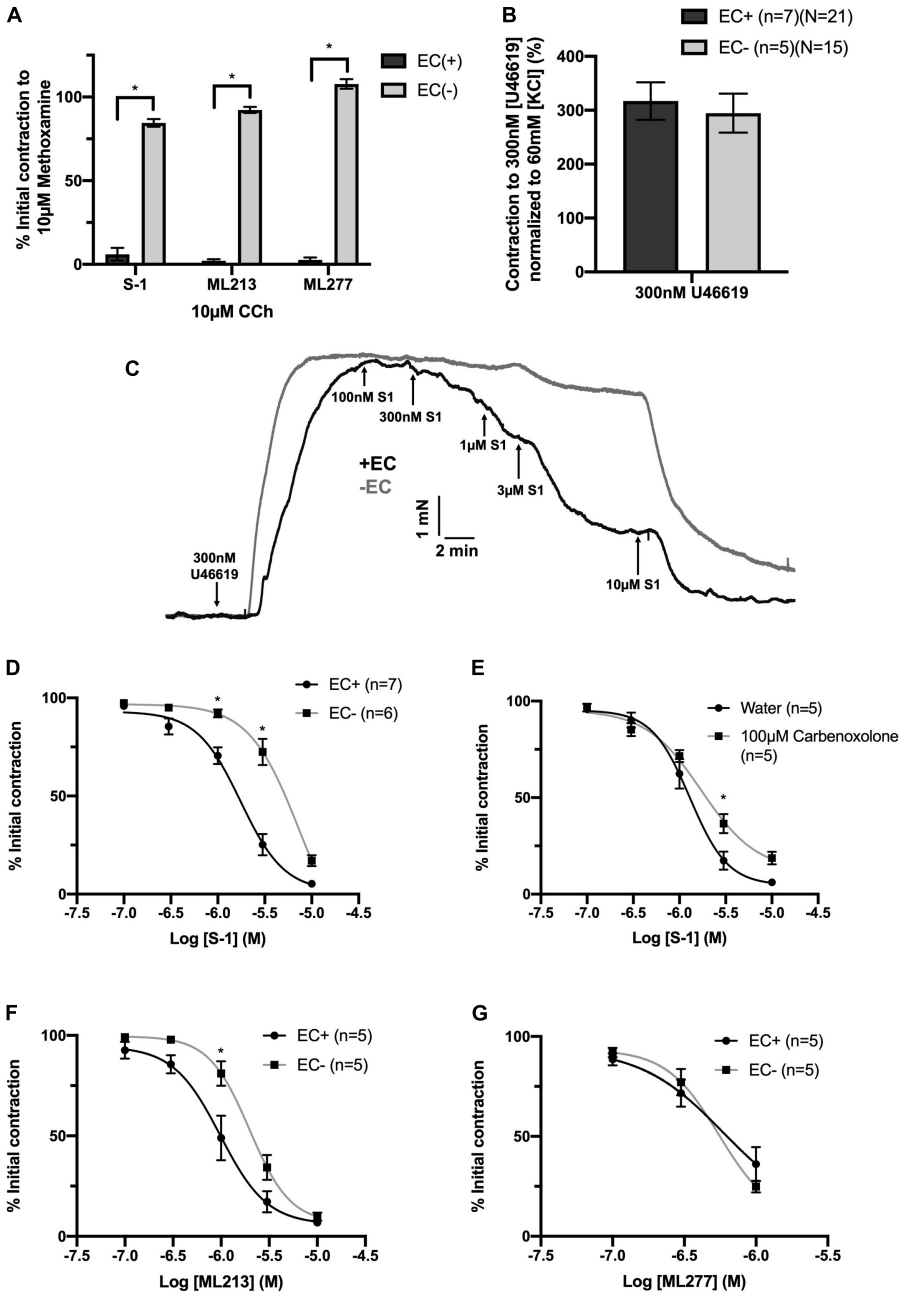

FIGURE 5 | $K_V7.2$-5 channel activator mediated vasorelaxation was significantly attenuated by EC removal. Removal of ECs ablated vasorelaxation in response to 10 μmol-L^{-1} CCh following pre-constriction with 10 μmol-L^{-1} MO **(A)**. Removal of ECs (gray) has no effect on vasoconstriction to U46619 (300 nmol-L^{-1}) when normalized to vasoconstriction to KCl (60 mmol-L^{-1}; n = 5–7; n = 15-21; **B**). Representative trace of EC S-1-mediated vasorelaxation in EC(–) denuded vessels (gray) vs. EC(+) vessels (black; **C**). S-1-mediated vasorelaxation was significantly attenuated by EC removal and 100 μmolL^{-1} carbenoxolone (gray; n = 5–7; **D,E**). ML213 but not ML277-mediated vasorelaxation was significantly attenuated by EC removal (gray; n = 5–7; **D,E**). Removal of ECs (gray) has no effect on ML277 within its range of linopirdine sensitivity (n = 5; **F**). All values are expressed as mean + SEM **(A–G)**. A two-way statistical ANOVA with a *post hoc* Bonferroni test was used to generate significance values. Statistical significance is defined as $^*P < 0.05$ **(A–G)**.

potassium channels; particularly those expressed within microdomains (Sandow et al., 2009). However, consistent with previous reports (Jepps et al., 2016), pre-incubation with a combination of IK_{Ca} inhibitor TRAM-34 (1 μmol-L^{-1}; Wulff et al., 2000) and SK_{Ca} inhibitor apamin (100 nmol-L^{-1}; Spoerri et al., 1975) had no effect on K_V7 activator mediated vasorelaxation (**Figures 7A–C**). These data suggest that the endothelium-dependent increase in potency to the K_V7 activators involves endothelial K_{IR}, but not IK_{Ca} or SK_{Ca} channels.

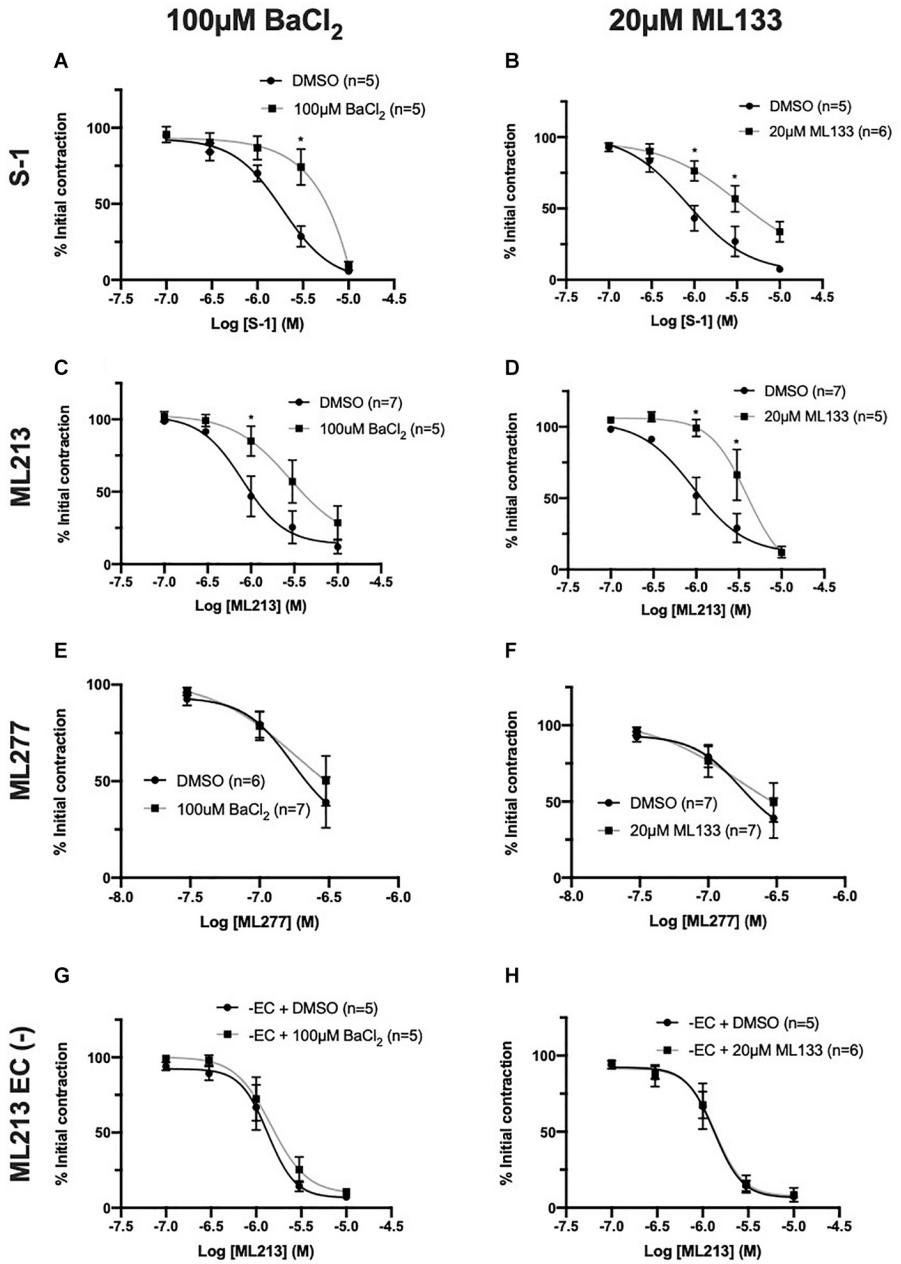

FIGURE 6 | $K_V7.2$-5 channel activator-mediated vasorelaxation was attenuated by two structurally different K_{IR} channel blockers, $BaCl_2$ and ML133, but not In EC denuded vessels. $K_V7.2$-5 channel activator S-1 and ML213 effects were significantly attenuated by pre-incubation with the $K_{IR}2$ channel inhibitor $BaCl_2$ (100 μmol-L^{-1}; black; n = 5–7; **A,C**). $K_V7.2$-5 channel activator S-1 and ML213 effects were significantly attenuated by pre-incubation with a selective K_{Ir} 2.1 channel inhibitor, ML133 (20 μmol-L^{-1}; gray; n = 5–7; **B,D**). $K_V7.1$ channel activator ML277-mediated vasorelaxation was not affected by pre-incubation with either $BaCl_2$ (100 μmol-L^{-1}) or ML133 (20 μmol-L^{-1}; gray; n = 6–7; **E,F**). In EC denuded vessels, $K_V7.2$-5 channel activator ML213 responses were not affected by pre-incubation with either $K_{IR}2$ channel inhibitor $BaCl_2$ (100 μmol-L^{-1}; gray; n = 5; **G**) or ML133 (20 μmol-L^{-1}; gray; n = 5–6; **H**). All values are expressed as mean + SEM **(A–H)**. A two-way statistical ANOVA with a *post hoc* Bonferroni test was used to generate significance values. Statistical significance is defined as $^*P < 0.05$ **(A–H)**.

K_V7 Channels Contribute to CCh Evoked Vasorelaxation

The expression of functional K_V7 channels within ECs begs the question - do they contribute to EC-derived responses? Acetylcholine produces endothelium-dependent relaxation through NO-, EDH- and prostanoid-dependent mechanisms in rat MA (Parsons et al., 1994; Shimokawa et al., 1996; Peredo et al., 1997).

A distinct rightward shift in the sensitivity to vasorelaxation in response to CCh, a synthetic acetylcholine analog, was

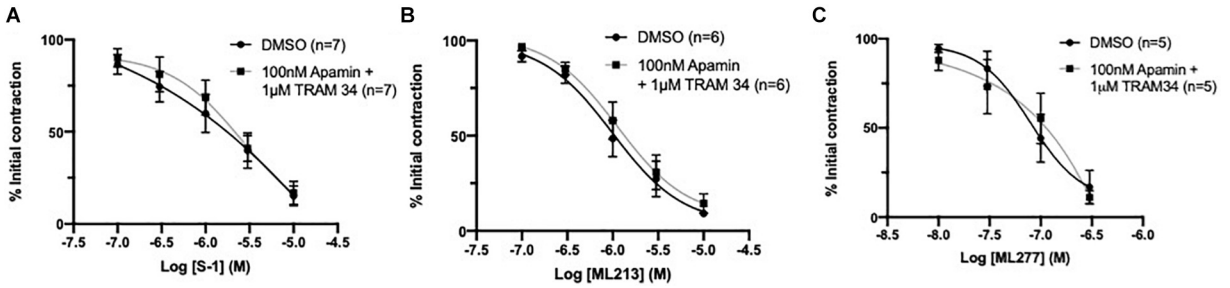

FIGURE 7 | K_V7 channel activator mediated vasorelaxation was not affected by preincubation with IK_{Ca}/SK_{Ca} channel antagonists. Pre-incubation with both IK_{Ca} channel inhibitor TRAM34 (1 μmol-L^{-1}) and SK_{Ca} channel inhibitor Apamin (100 nmol-L^{-1}) had no effect on S-1, ML213 nor ML277 mediated vasorelaxation (n = 5–7; gray, **A–C**). All values are expressed are expressed as mean values ± SEM. A two-way statistical ANOVA with a *post hoc* Bonferroni test was used to generate significance values; no significant values were observed **(A–C)**.

produced by the eNOS inhibitor L-NAME (100 μmol-L^{-1}) when compared to DMSO control (EC_{50} DMSO = 0.59 ± 0.1 μmol-L^{-1}; L-NAME = 0.94 ± 0.1 μmol-L^{-1}; **Figure 8A**). A combination IK_{Ca} and SK_{Ca} inhibitors, TRAM-34 (1 μmol-L^{-1}) and apamin (100 nmol-L^{-1}) respectively, suppress EDH in rat MA, and produced greater attenuation (EC_{50} TRAM34/apamin = 1.5 ± 0.7 μmol-L^{-1}; **Figure 8A**) when compared to L-NAME. Pre-incubating vessels with the pan K_V7 channel inhibitor linopirdine (10 μmol-L^{-1}) significantly attenuated CCh-mediated relaxation when compared to DMSO control (EC_{50} DMSO = 0.2 ± 0.08 μmol-L^{-1}; linopirdine = 0.7 ± 0.3 μmol-L^{-1}; **Figure 8B**). In contrast, pre-incubating vessels with either the $K_V7.1$ specific inhibitor HMR-1556 (10 μmol-L^{-1}) or a combination of non-specific K_V channel inhibitors TEA (1 mmol-L^{-1}; Choi et al., 1991) and 4-AP (1 mmol-L^{-1}; Kurata and Fedida, 2006) had no significant effect on CCh-evoked vasorelaxation (**Figures 8C,D**).

Additionally, CCh-evoked relaxations were significantly attenuated in vessels pre-incubated in TRAM34/apamin (1 μmol-L^{-1}/100 nmol-L^{-1}) and linopirdine (10 μmol-L^{-1}) compared to vessels only pre-incubated in TRAM34/apamin alone (EC_{50} DMSO = 0.24 ± 0.05 μmol-L^{-1}; TRAM34/Apamin = 0.27 ± 0.03 μmol-L^{-1}; TRAM34/Apamin + linopirdine = 0.61 ± 0.2 μmol-L^{-1}; **Figure 8E**). In contrast, linopirdine failed to attenuate CCh relaxation in arteries pre-incubated with L-NAME (100 μmol-L^{-1}; **Figure 8F**), thus suggesting K_V7 contribution to eNOS sensitive proportion of CCh-mediated relaxation.

Furthermore, the present data demonstrates that pre-incubation with linopirdine (10 μmol-L^{-1}) has no effect on vasorelaxation produced by the NO-donor SNP (**Figure 8G**). However, in contrast with previous reports (Jepps et al., 2016), pre-incubation with L-NAME (100 μmol-L^{-1}) significantly attenuated $K_V7.2$-5 activator mediated vasorelaxation (**Figure 8H**).

DISCUSSION

The present study identified *Kcnq1, Kcnq4,* and *Kcnq5* transcripts in EC marker expressing cells and the consequent $K_V7.1$, $K_V7.4$, and $K_V7.5$ protein in isolated and whole mount rat MA ECs/VSMCs. Functionally, the present study demonstrates that the relaxation produced by two structurally different $K_V7.2$-5 activators, but not a $K_V7.1$ activator, were modulated by the presence of the endothelium and gap junction inhibition. Said relaxation was also sensitive to $K_{IR}2$ inhibition, which was dependent on the presence of ECs, suggestive of a novel functional interaction between K_V7 and endothelial $K_{IR}2.x$ channels. Furthermore, the present data suggest that $K_V7.4/K_V7.5$ channels contribute to the NO-mediated axis of CCh-evoked endothelium-dependent relaxation downstream of eNOS. Thus, K_V7 channels are expressed in ECs, when pharmacologically upregulated, are functionally coupled to other EC potassium channels in rat MA and contribute to endothelium-derived responses.

K_V7 Channel Expression and Function Within ECs

Kv7 channel modulators have considerable impact on arterial tone. In VSMCs, active K_V7 channels hyperpolarize the membrane potential, decreasing voltage-dependent calcium channel (VDCC) open probability and extracellular calcium influx resulting in relaxation. Within rodent models, the pharmacopeia of K_V7 channel modulators has revealed $K_V7.4$ and 7.5 channels are; (1) key determinants of resting vascular tone via regulation of resting membrane potential; (2) upregulated during cGMP and cAMP/EPAC/PKA-mediated vasodilation; (3) suppressed via PKC-mediated vasoconstriction. Comparatively, no functional role for $K_V7.1$ has been identified in arteries (see Barrese et al., 2018b; Byron and Brueggemann, 2018 for review). A caveat of these observations is a lack of differentiation between VSMCs and ECs. However, recently K_V7 channels were identified in pig coronary artery ECs (Chen et al., 2016), the novel findings presented here expand on these findings and demonstrate K_V7 transcript and channel expression, functional activity and contribution to EC-derived vasodilatory signaling cascades in rat MA endothelium.

In most arteries, the endothelium and smooth muscle are electrochemically linked via MEGJs formed from connexin proteins within heterocellular communicating microdomains

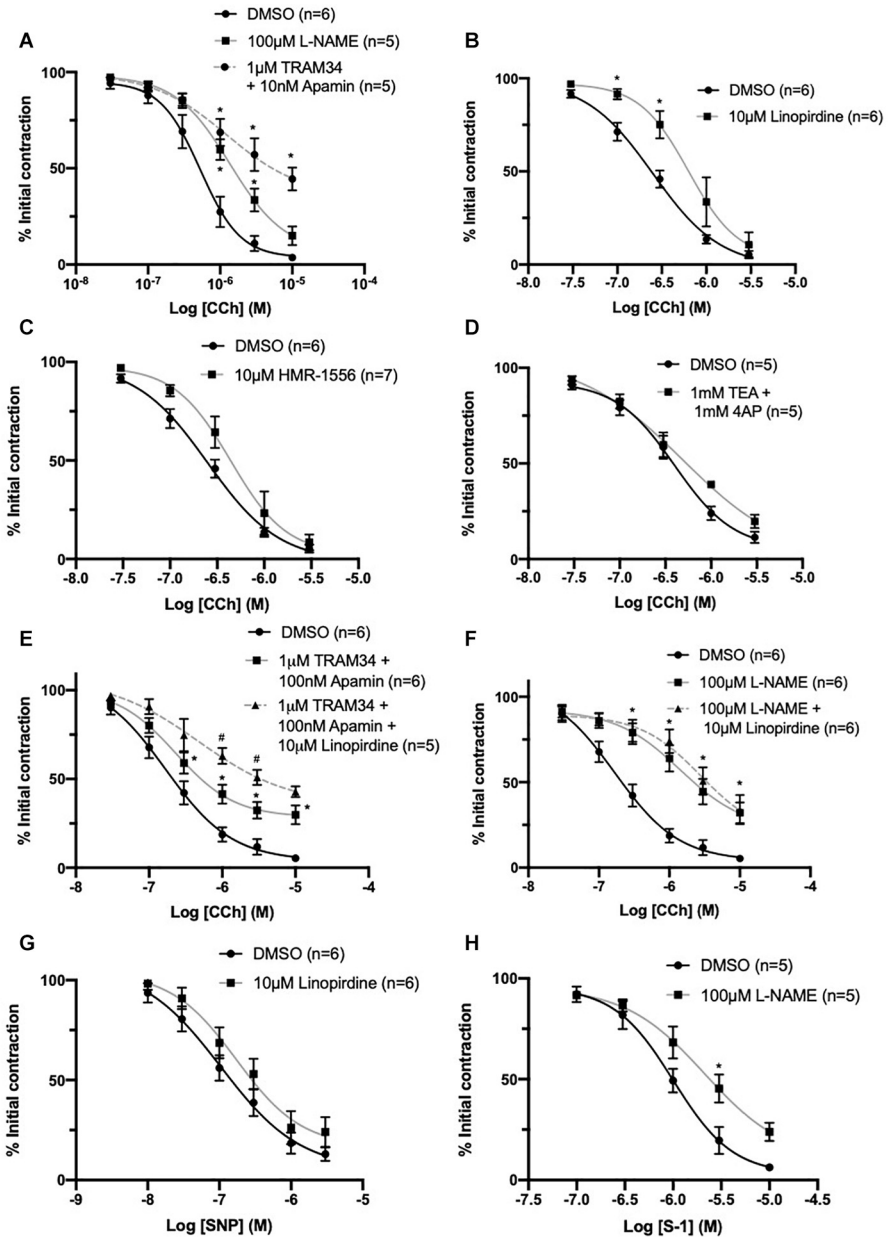

FIGURE 8 | CCh evoked vasorelaxation is mediated through both eNOS and IK_{Ca}/SK_{Ca} channels and is partially attenuated by inhibition of K_V7 channels upstream of NO. Both eNOS inhibitor L-nitroarginine methyl ester (L-NAME; 100 μmol-L^{-1}; gray) and IK_{Ca}/SK_{Ca} channel inhibitors TRAM-34 (1 μmol-L^{-1})/apamin (100 nmol-L^{-1}; red, dashed line) significantly attenuated CCh mediated vasorelaxation (n = 5–6; **A**). The pan K_V7 channel inhibitor linopirdine (10 μmol-L^{-1}; gray) significantly attenuated CCh mediated vasorelaxation (n = 6; **B**). The $K_V7.1$ channel inhibitor HMR-1556 (10 μmol-L^{-1}; gray) did not modulate CCh-mediated vasorelaxation (n = 6; **C**). A combination of non-specific K^+ channel inhibitors 4-aminopyridine (4-AP; 1 mmol-L^{-1}) and tetraethylammonium (TEA; 1 mmol-L^{-1}; gray) did not modulate CCh-mediated vasorelaxation (n = 5; **D**). Additive attenuation to CCh-evoked relaxation in the presence of TRAM-34 (1 μmol-L^{-1})/apamin (100 nmol-L^{-1}) + linopirdine (10 μmol-L^{-1}; gray, dashed line) was observed when compared to vessels pre-incubated in only TRAM34/apamin (gray; n = 5–6; **E**). No additive attenuation to CCh evoked vasorelaxation was observed between vessels pre-incubated in L-NAME (100 μmol-L^{-1}) + linopirdine (10 μmol-L^{-1}; gray, dashed line) when compared with L-NAME (100 μmol-L^{-1}; gray; n = 5; **F**). SNP-mediated vasorelaxation was no effected by the pan-K_V7 channel inhibitor linopirdine (10 μmol-L^{-1}; gray) when compared to DMSO solvent control (black; **G**). $K_V7.2$-5 channel activator S-1 was significantly attenuated by pre-incubation with eNOS inhibitor L-NAME (100 μmol-L^{-1}; gray; n = 5; **H**). All values are expressed as mean + SEM. A two-way statistical ANOVA with a *post hoc* Bonferroni test was used to generate significance values (*, drug v DMSO solvent control; #=Group B vs. Group C) Statistical significance is defined as $^{\#/*}P < 0.05$ **(A–H)**.

present within holes in the IEL (see Sandow et al., 2012 for review). Via these connections, current injection in to ECs passes into VSMCs (Sandow et al., 2002) supporting the presence of such coupling. The present data suggests a potential role for electrochemical heterocellular communication during $K_V7.2$-5 activator-mediated vasorelaxation (**Figure 9**). This conjecture is

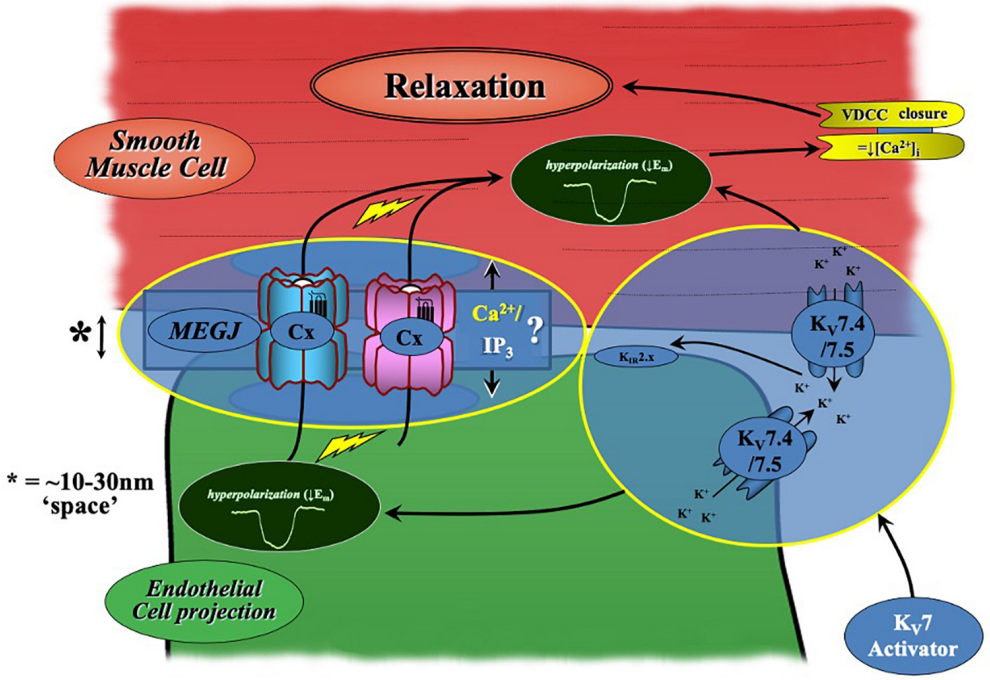

FIGURE 9 | Schematic of K_V7.2-5 activator-mediated vasorelaxation. K_V7.2-5 activator-mediated vasorelaxation occurs predominantly via K_V7.4/7.5 activation within VSMCs. However, our findings suggest a novel contribution of endothelial-K_V7.4/7.5 channels to K_V7.2-5 activator mediated responses which augments relaxation. A process which is sensitive to both gap-junction and endothelial-K_{IR}2.x inhibition (modified from Senadheera et al., 2012).

supported by apparently higher level expression of K_V7.4/K_V7.5 in a proportion of IEL holes than that at the EC membrane as well as a significant attenuation of relaxation of pre-constricted arterial tone by two structurally different K_V7.2-5 activators in the absence of ECs and presence of a (putative) gap junction inhibitor. In contrast, EC removal had no impact on K_V7.1 activator-mediated vasorelaxation, which was observed in conjunction with reduced expression of *Kcnq1* transcript and K_V7.1 labeling within ECs compared to VSMCs. Collectively suggesting that only K_V7.4/K_V7.5 channels of the K_V7 sub-family are functionally expressed within MA ECs. An extrapolation of these results indicates a novel role for K_V7.4/K_V7.5 channels in the regulation of EC membrane potential within myoendothelial projections. It is plausible, that localized EC K_V7 channels negate the influx of depolarization from VSMCs into the endothelium, providing tight regulation of EC V_m during VSMC contraction. However, further studies would be required to validate this hypothesis.

A Novel Functional Interaction With Endothelial K_{IR} Channels

K_{IR}2.x channels have been characterized in a variety of rat vascular beds including cerebral and coronary arteries (Smith et al., 2008), where their selective inhibition by Ba^{2+} revealed K_{IR} channel amplification of a K^+ channel activator conductance (Smith et al., 2008). However, there is a degree of conflict regarding the role of K_{IR}2.x channels within rat MAs. As above, Ba^{2+} sensitive currents and K_{IR}2.x expression has been demonstrated in rat MA ECs (Crane et al., 2003a) which are purported to contribute to K_{Ca} mediated-hyperpolarization during ACh-derived EC-dependent responses (Goto et al., 2004). In contrast, Smith et al. (2008) demonstrated that within 3rd order MAs, ACh-mediated K^+ conductance-dependent relaxation was insensitive to Ba^{2+}, indicating that K_{IR}2.x channels do not augment K^+ conductance in these vessels during receptor-mediated vasodilation.

In the present study, significant attenuation of both S-1 and ML213 K_V7.2-5 activator-mediated vasorelaxation was found following pre-incubation with two structurally different K_{IR}2.x blockers ML133 (Wu et al., 2010) and Ba^{2+} (Hagiwara et al., 1978) when compared to a solvent control. ML133 has been identified via high-throughput and mutagenesis investigation as a novel inhibitor of K_{IR}2.1 channels via D172 and I176 residues within the M2 region of K_{IR}2.1 (Wang et al., 2011) with an IC_{50} of 1.8 μmol-L^{-1} at pH 7.4, with little to no effect against other K_{IR}2.x family members (Wu et al., 2010; Wang et al., 2011). Presently, ML133 is the most selective inhibitor of the K_{IR}2 family. In analogous fashion to our endothelium denudation experiments, no effect was seen on the K_V7.1 activator ML277-mediated vasorelaxation; implying a specific interplay with K_V7.4 and 7.5 channels. Furthermore, K_{IR}2 blockers had no effect on K_V7.2–7.5 activator-mediated relaxation in EC-denuded arteries, supporting the notion that functional K_{IR}2 channels (in the rat MA bed) are restricted to the endothelium (Crane et al., 2003b). The present study suggests that pharmacological activation of

endothelial $K_V7.4/7.5$ channels also activates an endothelial $K_{IR}2$ channels, increasing K^+ conductance, which in turn accounts for a proportion of EC augmentation of $K_V7.2$-5 activator-mediated vasorelaxation (**Figure 9**). This may be due to a localized increase in potassium ion concentration in the proximity of the $K_{IR}2$ channels or an alternative modulation. However, based on the findings described by Goto et al. (2004) and Smith et al. (2008), the collective data suggest that this phenomenon is dependent on the branch order of MA. Furthermore, it remains unclear if this occurs during receptor mediated signaling, or if it is only present during pharmacological activation of endothelial K_V7 channels.

A primary concern for identification of novel functional interactions between ion channels using pharmacological tools is potential off-target effects. However, K_V7 activator-mediated relaxation in vessels pre-incubated in 10 μmol-L^{-1} linopirdine was abolished. If S-1 or ML213 were activating non-K_V channels such as K_{IR}, a degree of relaxation would still be observed in the presence of linopirdine. The present findings therefore suggest that both S-1 and ML213 work exclusively via K_V7 channels and that attenuation of their response within rat MA occurs via a novel functional coupling of $K_V7.4/7.5$ and $K_{IR}2$ within ECs.

The Contribution of K_V7 Channels to CCh Evoked Relaxations Within Rat MA

Our findings demonstrate that both NO- and EDH-dependent signaling contributes to CCh-mediated vasodilation, though the main contributor to endothelial-dependent vasodilation in 2nd order MA appears to be EDH, consistent with previous studies (Shimokawa et al., 1996). In light of the significant impact of K_V7 inhibition on CCh-mediated vasorelaxation during the suppression of EDH, the present study suggests that K_V7 channels contribute to the eNOS sensitive axis of CCh-evoked relaxation within rat MA.

However, in a similar manner to rat renal artery (Stott et al., 2015), rat MA K_V7 channels do not represent downstream targets of NO signaling as K_V7 inhibition does not impair NO-donor SNP-mediated relaxation. However, eNOS inhibition does impair relaxation to a K_V7 activator, potentially implying K_V7 channel involvement in the production or release of NO in response to CCh. Interestingly, this appears to be a vascular bed specific phenomenon, as L-NAME has no effect on K_V7 activator-mediated relaxation within rat penile artery (Jepps et al., 2016).

Limitations

Ideally, direct functional evidence for a functional role of K_v7 channels in ECs would be provided by either single cell electrophysiology of sharp microelectrode impalement in whole arteries. However, this was not possible within the constraints of this study. Instead, we inferred a functional role for EC K_v7 channels using a reductive approach, i.e., comparison of functional responses without or with EC ablation. These studies implicate K_v7 channels as functional component of the EC physiology that merit consideration in future studies.

CONCLUSION

In conclusion, the present data reveal that mesenteric ECs express $K_V7.4/K_V7.5$ channels and their presence boosts K_V7 activator-mediated relaxation. Furthermore, the data indicated a novel functional interaction with endothelial $K_{IR}2$ channels and support the proposition that endothelial K_V7 channels contribute to endogenous endothelium-derived responses. These findings highlight the complex nature of the vascular response to K_V7 channel upregulation and emphasize the importance of these channels to vascular signaling. The present data are consistent with K_V7 channels representing a novel therapeutic target in endothelial dysfunction.

DATA AVAILABILITY STATEMENT

The original contributions presented in the study are included in the article/**Supplementary Material**, further inquiries can be directed to the corresponding author/s.

ETHICS STATEMENT

The animal study was reviewed and approved by UNSW Animal Ethics and Experimentation Committee (AEEC #18/86B). For investigations performed at St George's University, London, investigators strictly adhered to the Animal (Scientific Procedures) Act 1986.

AUTHOR CONTRIBUTIONS

SB, SS, GM-P, and JS performed the research. IG and JS designed the research study. SS contributed essential reagents or tools. SB, SS, and GM-P analyzed the data. SB and IG wrote the manuscript. All the authors contributed to the article and approved the submitted version.

FUNDING

SB was funded by the British Heart Foundation (Grant #FS/18/41/33762) awarded to IG.

ACKNOWLEDGMENTS

The authors would like to thank Miss Aditi Gunjal for her excellent assistance in wire myography.

SUPPLEMENTARY MATERIAL

The Supplementary Material for this article can be found online at: https://www.frontiersin.org/articles/10.3389/fphys.2020.598779/full#supplementary-material

REFERENCES

Askew Page, H. R., Dalsgaard, T., Baldwin, S. N., Jepps, T. A., Povstyan, O., Olesen, S. P., et al. (2019). TMEM16A is implicated in the regulation of coronary flow and is altered in hypertension. *Br. J. Pharmacol.* 176, 1635–1648. doi: 10.1111/bph.14598

Barrese, V., Stott, J. B., Figueiredo, H. B., Aubdool, A. A., Hobbs, A. J., Jepps, T. A., et al. (2018b). Angiotensin II Promotes $K_V7.4$ channels degradation through reduced interaction with HSP90. *Hypertension* 71, 1091–1100. doi: 10.1161/HYPERTENSIONAHA.118.11116

Barrese, V., Stott, J. B., and Greenwood, I. A. (2018a). KCNQ-encoded potassium channels as therapeutic targets. *Ann. Rev. Pharmacol. Toxicol.* 58, 625–648. doi: 10.1146/annurev-pharmtox-010617-052912

Bentzen, B. H., Schmitt, N., Calloe, K., Dalby Brown, W., Grunnet, M., and Olesen, S. P. (2006). The acrylamide (S)-1 differentially affects Kv7 (KCNQ) potassium channels. *Neuropharmacology* 51, 1068–1077. doi: 10.1016/j.neuropharm.2006.07.001

Brueggemann, L. I., Cribbs, L. L., Schwartz, J., Wang, M., Kouta, A., and Byron, K. L. (2018). Mechanisms of PKA-dependent potentiation of Kv7.5 channel activity in human airway smooth muscle cells. *Int. J. Mol. Sci.* 12:2223. doi: 10.3390/ijms19082223

Brueggemann, L. I., Haick, J. M., Cribbs, L. L., and Byron, K. L. (2014). Differential activation of vascular smooth muscle Kv7.4, Kv7.5, and Kv7.4/7.5 channels by ML213 and ICA-069673. *Mol. Pharmacol.* 86, 330–341. doi: 10.1124/mol.114.093799

Brueggemann, L. I., Moran, C. J., Barakat, J. A., Yeh, J. Z., Cribbs, L. L., and Byron, K. L. (2006). Vasopressin stimulates action potential firing by protein kinase C-dependent inhibition of KCNQ5 in A7r5 rat aortic smooth muscle cells. *AJP Heart Circ. Physiol.* 292, H1352–H1363. doi: 10.1152/ajpheart.00065.2006

Byron, K. L., and Brueggemann, L. I. (2018). Kv7 potassium channels as signal transduction intermediates in the control of microvascular tone. *Microcirculation* 25:e12419. doi: 10.1111/micc.12419

Chadha, P. S., Zunke, F., Zhu, H. L., Davis, A. J., Jepps, T. A., Olesen, S. P., et al. (2012). Reduced KCNQ4-encoded voltage-dependent potassium channel activity underlies impaired β-adrenoceptor-mediated relaxation of renal arteries in hypertension. *Hypertension* 59, 877–884. doi: 10.1161/HYPERTENSIONAHA.111.187427

Chen, X., Li, W., Hiett, S. C., and Obukhov, A. G. (2016). Novel Roles for Kv7 channels in shaping histamine-induced contractions and bradykinin-dependent relaxations in Pig Coronary Arteries. *PLoS One* 11:e1048569. doi: 10.1371/journal.pone.0148569

Choi, K. L., Aldricht, R. W., Yellen, G., and Hughes, H. (1991). Tetraethylammonium blockade distinguishes two inactivation mechanisms in voltage-activated Ki channels. *Proc. Natl. Acad. Sci. U. S. A.* 88, 5092–5095. doi: 10.1073/pnas.88.12.5092

Crane, G. J., Gallagher, N., Dora, K. A., and Garland, C. J. (2003a). Small- and intermediate-conductance calcium-activated K+ channels provide different facets of endothelium-dependent hyperpolarization in rat mesenteric artery. *J. Physiol.* 553(Pt 1), 183–189. doi: 10.1113/jphysiol.2003.051896

Crane, G. J., Walker, S. D., Dora, K. A., and Garland, C. J. (2003b). Evidence for a differential cellular distribution of inward rectifier K channels in the rat isolated mesenteric artery. *J. Vasc. Res.* 40, 159–168. doi: 10.1159/000070713

Curtis, M. J., Alexander, S., Cirino, G., Docherty, J. R., George, C. H., Giembycz, M. A., et al. (2018). Experimental design and analysis and their reporting II: updated and simplified guidance for authors and peer reviewers. *Br. J. Pharmacol.* 175, 987–993. doi: 10.1111/bph.14153

Dora, K. A., Gallagher, N. T., McNeish, A., and Garland, C. J. (2008). Modulation of endothelial cell KCa3.1 channels during endothelium-derived hyperpolarizing factor signaling in mesenteric resistance arteries. *Circ. Res.* 102, 1247–1255. doi: 10.1161/CIRCRESAHA.108.172379

Fukao, M., Hattori, Y., Kanno, M., Sakuma, I., and Kitabatake, A. (1997). Sources of Ca2+ in relation to generation of acetylcholine-induced endothelium-dependent hyperpolarization in rat mesenteric artery. *Br. J. Pharmacol.* 120, 1328–1334. doi: 10.1038/sj.bjp.0701027

Goto, K., Rummery, N. M., Grayson, T. H., and Hill, C. E. (2004). Attenuation of conducted vasodilatation in rat mesenteric arteries during hypertension: role of inwardly rectifying potassium channels. *J. Physiol.* 561(Pt 1), 215–231. doi: 10.1113/jphysiol.2004.070458

Grayson, T. H., Chadha, P. S., Bertrand, P. P., Chen, H., Morris, M. J., Senadheera, S., et al. (2013). Increased caveolae density and caveolin-1 expression accompany impaired NO-mediated vasorelaxation in diet-induced obesity. *Histochem. Cell Biol.* 139, 309–321. doi: 10.1007/s00418-012-1032-2

Greenberg, H. Z. E., Shi, J., Jahan, K. S., Martinucci, M. C., Gilbert, S. J., Ho, W. S., et al. (2016). Stimulation of calcium-sensing receptors induces endothelium-dependent vasorelaxations via nitric oxide production and activation of IKCa channels. *Vasc. Pharmacol.* 80, 75–84. doi: 10.1016/j.vph.2016.01.001

Hagiwara, S., Miyazaki, S., Moody, W., and Patlak, J. (1978). Blocking effects of barium and hydrogen ions on the potassium current during anomalous rectification in the starfish egg. *J. Physiol.* 279, 167–185. doi: 10.1113/jphysiol.1978.sp012338

Howitt, L., Hilton Grayson, T., Morris, M. J., Sandow, S. L., and Murphy, T. V. (2012). Dietary obesity increases NO and inhibits BKCa-mediated, endothelium-dependent dilation in rat cremaster muscle artery: association with caveolins and caveolae. *Am. J. Physiol. Heart Circ. Physiol.* 302, H2464–H2476. doi: 10.1152/ajpheart.00965.2011

Jepps, T. A., Bentzen, B. H., Stott, J. B., Povstyan, O. V., Sivaloganathan, K., Dalby-Brown, W., et al. (2014). Vasorelaxant effects of novel Kv7.4 channel enhancers ML213 and NS15370. *Br. J. Pharmacol.* 171, 4413–4424. doi: 10.1111/bph.12805

Jepps, T. A., Chadha, P. S., Davis, A. J., Harhun, M. I., Cockerill, G. W., Olesen, S. P., et al. (2011). Downregulation of Kv7.4 channel activity in primary and secondary hypertension. *Circulation* 124, 602–611. doi: 10.1161/CIRCULATIONAHA.111.032136

Jepps, T. A., Greenwood, I. A., Moffatt, J. D., Sanders, K. M., and Ohya, S. (2009). Molecular and functional characterization of K_v7 K^+ channel in murine gastrointestinal smooth muscles. *Am. J. Physiol. Gastrointest. Liver Physiol.* 297, G107–G115. doi: 10.1152/ajpgi.00057.2009

Jepps, T. A., Olesen, S. P., Greenwood, I. A., and Dalsgaard, T. (2016). Molecular and functional characterization of Kv7 channels in penile arteries and corpus cavernosum of healthy and metabolic syndrome rats. *Br. J. Pharmacol.* 173, 1478–1490. doi: 10.1111/bph.13444

Khanamiri, S., Soltysinska, E., Jepps, T. A., Bentzen, B. H., Chadha, P. S., Schmitt, N., et al. (2013). Contribution of K_v7 channels to basal coronary flow and active response to ischemia. *Hypertension* 62, 1090–1097. doi: 10.1161/HYPERTENSIONAHA.113.01244

Kurata, H. T., and Fedida, D. (2006). A structural interpretation of voltage-gated potassium channel inactivation. *Prog. Biophys. Mol. Biol.* 92, 185–208. doi: 10.1016/j.pbiomolbio.2005.10.001

Mackie, A. R., Brueggemann, L. I., Henderson, K. K., Shiels, A. J., Cribbs, L. L., Scrogin, K. E., et al. (2008). Vascular KCNQ potassium channels as novel targets for the control of mesenteric artery constriction by vasopressin, based on studies in single cells, pressurized arteries, and in vivo measurements of mesenteric vascular resistance. *J. Pharmacol. Exp. Ther.* 325, 475–483. doi: 10.1124/jpet.107.135764

Mani, B. K., Robakowski, C., Brueggemann, L. I., Cribbs, L. L., Tripathi, A., Majetschak, M., et al. (2016). Kv7.5 potassium channel subunits are the primary targets for PKA-dependent enhancement of vascular smooth muscle Kv7 Currents. *Mol. Pharmacol.* 89, 323–334. doi: 10.1124/mol.115.101758

McGuire, J. J., Ding, H., and Triggle, C. R. (2001). Endothelium-derived relaxing factors: a focus on endothelium-derived hyperpolarizing factor(s). *Can. J. Physiol. Pharmacol.* 79, 443–470. doi: 10.1139/y01-025

Mills, T. A., Greenwood, S. L., Devlin, G., Shweikh, Y., Robinson, M., Cowley, E., et al. (2015). Activation of K_V7 channels stimulates vasodilatation of human placental chorionic plate arteries. *Placenta* 36, 638–644. doi: 10.1016/j.placenta.2015.03.007

Mondéjar-Parreño, G., Moral-Sanz, J., Barreira, B., De la Cruz, A., Gonzalez, T., Callejo, M., et al. (2019). Activation of Kv7 channels as a novel mechanism for NO/cGMP-induced pulmonary vasodilation. *Br. J. Pharmacol.* 176, 2131–2145. doi: 10.1111/bph.14662

Morales-Cano, D., Moreno, L., Barreira, B., Pandolfi, R., Chamorro, V., Jimenez, R., et al. (2015). Kv7 channels critically determine coronary artery reactivity: left-right differences and down-regulation by hyperglycaemia. *Cardiovasc. Res.* 106, 98–108. doi: 10.1093/cvr/cvv020

Mulvany, M. J., and Halpern, W. (1976). Mechanical properties of vascular smooth muscle cells *in situ*. *Nature* 260, 617–619. doi: 10.1038/260617a0

Ng, F. L., Davis, A. J., Jepps, T. A., Harhun, M. I., Yeung, S. Y., Wan, A., et al. (2011). Expression and function of the K + channel KCNQ genes in human arteries. *Br. J. Pharmacol.* 162, 42–53. doi: 10.1111/j.1476-5381.2010.01027.x

Ohya, S., Sergeant, G. P., Greenwood, I. A., and Horowitz, B. (2003). Molecular variants of KCNQ channels expressed in murine portal vein myocytes: a role in delayed rectifier current. *Circ. Res.* 92, 1016–1023. doi: 10.1161/01.RES.0000070880.20955.F4

Oliveras, A., Roura-Ferrer, M., Solé, L., De La Cruz, A., Prieto, A., Etxebarria, A., et al. (2014). Functional assembly of Kv7.1/Kv7.5 channels with emerging properties on vascular muscle physiology. *Arterioscler. Thromb. Vasc. Biol.* 23, 1522–1530. doi: 10.1161/ATVBAHA.114.303801

Parsons, S. J. W., Hill, A., Waldron, G. J., Plane, T., and Garland, C. J. (1994). The relative importance of nitric oxide and nitric oxide—independent mechanisms in acetylcholine—evoked dilatation of the rat mesenteric bed. *Br. J. Pharmacol.* 113, 1275–1280. doi: 10.1111/j.1476-5381.1994.tb17136.x

Peredo, H. A., Feleder, E. C., and Adler-Graschinsky, E. (1997). Differential effects of acetylcholine and bradykinin on prostanoid release from the rat mesenteric bed: role of endothelium and of nitric oxide. *Prostaglandins Leukot. Essent. Fatty Acids* 56, 253–258. doi: 10.1016/S0952-3278(97)90567-6

Sandow, S. L., Goto, K., Rummery, N. M., and Hill, C. E. (2004). Developmental changes in myoendothelial gap junction mediated vasodilator activity in the rat saphenous artery. *J. Physiol.* 556(Pt 3), 875–886. doi: 10.1113/jphysiol.2003.058669

Sandow, S. L., Haddock, R. E., Hill, C. E., Chadha, P. S., Kerr, P. M., Welsh, D. G., et al. (2009). What's where and why at a vascular myoendothelial microdomain signalling complex. *Clin. Exp. Pharmacol. Physiol.* 36, 67–76. doi: 10.1111/j.1440-1681.2008.05076.x

Sandow, S. L., Neylon, C. B., Chen, M. X., and Garland, C. J. (2006). Spatial separation of endothelial small- and intermediate-conductance calcium-activated potassium channels (KCa) and connexins: possible relationship to vasodilator function? *J. Anat.* 209, 689–698. doi: 10.1111/j.1469-7580.2006.00647.x

Sandow, S. L., Senadheera, S., Bertrand, P. P., Murphy, T. V., and Tare, M. (2012). Myoendothelial contacts, gap junctions, and microdomains: anatomical links to function? *Microcirculation* 19, 403–415. doi: 10.1111/j.1549-8719.2011.00146.x

Sandow, S. L., Tare, M., Coleman, H. A., Hill, C. E., and Parkington, H. C. (2002). Involvement of myoendothelial gap junctions in the actions of endothelium-derived hyperpolarizing factor. *Circ. Res.* 90, 1108–1113. doi: 10.1161/01.RES.0000019756.88731.83

Schenzer, A. (2005). Molecular Determinants of KCNQ (Kv7) K+ channel sensitivity to the anticonvulsant retigabine. *J. Neurosci.* 25, 5051–5060. doi: 10.1523/JNEUROSCI.0128-05.2005

Schnee, M. E., and Brown, B. S. (1998). Selectivity of linopirdine (DuP 996), a neurotransmitter release enhancer, in blocking voltage-dependent and calcium-activated potassium currents in hippocampal neurons. *J. Pharmacol. Exp. Ther.* 286, 709–717.

Senadheera, S., Kim, Y., Grayson, T. H., Toemoe, S., Kochukov, M. Y., Abramowitz, J., et al. (2012). Transient receptor potential canonical type 3 channels facilitate endothelium-derived hyperpolarization-mediated resistance artery vasodilator activity. *Cardiovasc. Res.* 95, 439–447. doi: 10.1093/cvr/cvs208

Shimokawa, H., Yasutake, H., Fujii, K., Owada, M. K., Nakaike, R., Fukumoto, Y., et al. (1996). The importance of the hyperpolarizing mechanism increases as the vessel size decreases in endothelium-dependent relaxations in rat mesenteric circulation. *J. Cardiovasc. Pharmacol.* 28, 703–711. doi: 10.1097/00005344-199611000-00014

Smith, P. D., Brett, S. E., Luykenaar, K. D., Sandow, S. L., Marrelli, S. P., Vigmond, E. J., et al. (2008). KIR channels function as electrical amplifiers in rat vascular smooth muscle. *J. Physiol.* 586, 1147–1160. doi: 10.1113/jphysiol.2007.145474

Sonkusare, S. K., Dalsgaard, T., Bonev, A. D., and Nelson, M. T. (2016). Inward rectifier potassium (Kir2.1) channels as end-stage boosters of endothelium-dependent vasodilators. *J. Physiol.* 594, 3271–3285. doi: 10.1113/JP271652

Spoerri, E., Jentsch, J., and Glees, P. (1975). Apamin from bee venom. Effects of the neurotoxin on subcellular particles of neural cultures. *FEBS Lett.* 52, 143–147. doi: 10.1016/0014-5793(75)80006-8

Stott, J. B., Barrese, V., Jepps, T. A., Leighton, E. V., and Greenwood, I. A. (2015). Contribution of Kv7 channels to natriuretic peptide mediated vasodilation in normal and hypertensive rats. *Hypertension* 65, 676–682. doi: 10.1161/HYPERTENSIONAHA.114.04373

Stott, J. B., Jepps, T. A., and Greenwood, I. A. (2014). K_V7 potassium channels: a new therapeutic target in smooth muscle disorders. *Drug Discov. Today* 19, 413–424. doi: 10.1016/j.drudis.2013.12.003

Tare, M., Coleman, H. A., and Parkington, H. C. (2002). Glycyrrhetinic derivatives inhibit hyperpolarization in endothelial cells of guinea pig and rat arteries. *Am. J. Physiol. Heart Circ. Physiol.* 282, H335–H341. doi: 10.1152/ajpheart.2002.282.1.H335

Wang, H. R., Wu, M., Yu, H., Long, S., Stevens, A., Engers, D. W., et al. (2011). Selective inhibition of the Kir2 family of inward rectifier potassium channels by a small molecule probe: The discovery, SAR, and pharmacological characterization of ML133. *ACS Chem. Biol.* 6, 845–856. doi: 10.1021/cb200146a

Wu, M., Wang, H., Yu, H., Makhina, E., Xu, J., Dawson, E. S., et al. (2010). "A potent and selective small molecule Kir2.1 inhibitor," in *Probe Reports from the NIH Molecular Libraries Program*, (Bethesda, MD: National Center for Biotechnology Information).

Wulff, H., Miller, M. J., Hänsel, W., Grissmer, S., Cahalan, M. D., and Chandy, K. G. (2000). Design of a potent and selective inhibitor of the intermediate- conductance Ca2+-activated K+ channel, IKCa1: a potential immunosuppressant. *Proc. Natl. Acad. Sci. U. S. A.* 97, 8151–8156. doi: 10.1073/pnas.97.14.8151

Yeung, S. Y. M., Pucovský, V., Moffatt, J. D., Saldanha, L., Schwake, M., Ohya, S., et al. (2007). Molecular expression and pharmacological identification of a role for Kv7 channels in murine vascular reactivity. *Br. J. Pharmacol.* 151, 758–770. doi: 10.1038/sj.bjp.0707284

Yu, H., Lin, Z., Xu, K., Huang, X., Long, S., Wu, M., et al. (2013). "Identification of a novel, small molecule activator of KCNQ1 channels," in *Probe Reports from the NIH Molecular Libraries Program*, (Bethesda, MD: National Center for Biotechnology Information).

Zechariah, A., Tran, C. H. T., Hald, B. O., Sandow, S. L., Sancho, M., Kim, M. S. M., et al. (2020). Intercellular conduction optimizes arterial network function and conserves blood flow homeostasis during cerebrovascular challenges. *Arterioscler. Thromb. Vasc. Biol.* 40, 733–750. doi: 10.1161/ATVBAHA.119.313391

Zhong, X. Z., Harhun, M. I., Olesen, S. P., Ohya, S., Moffatt, J. D., Cole, W. C., et al. (2010). Participation of KCNQ (Kv7) potassium channels in myogenic control of cerebral arterial diameter. *J. Physiol.* 588(Pt 17), 3277–3293. doi: 10.1113/jphysiol.2010.192823

Conflict of Interest: The authors declare that the research was conducted in the absence of any commercial or financial relationships that could be construed as a potential conflict of interest.

Copyright © 2020 Baldwin, Sandow, Mondéjar-Parreño, Stott and Greenwood. This is an open-access article distributed under the terms of the Creative Commons Attribution License (CC BY). The use, distribution or reproduction in other forums is permitted, provided the original author(s) and the copyright owner(s) are credited and that the original publication in this journal is cited, in accordance with accepted academic practice. No use, distribution or reproduction is permitted which does not comply with these terms.

A small molecule inhibitor of the chloride channel TMEM16A blocks vascular smooth muscle contraction and lowers blood pressure in spontaneously hypertensive rats

see commentary on page 269

Onur Cil[1], Xiaolan Chen[2,3], Henry R. Askew Page[4], Samuel N. Baldwin[4], Maria C. Jordan[5], Pyone Myat Thwe[6], Marc O. Anderson[6], Peter M. Haggie[2,3], Iain A. Greenwood[4], Kenneth P. Roos[5] and Alan S. Verkman[2,3]

[1]Department of Pediatrics, University of California, San Francisco, San Francisco, California, USA; [2]Department of Medicine, University of California, San Francisco, San Francisco, California, USA; [3]Department of Physiology, University of California, San Francisco, San Francisco, California, USA; [4]Vascular Biology Research Centre, Institute of Molecular and Clinical Sciences, St. George's University of London, London, UK; [5]Department of Physiology, University of California, Los Angeles, Los Angeles, California, USA; and [6]Department of Chemistry and Biochemistry, San Francisco State University, San Francisco, California, USA

Hypertension is a major cause of cardiovascular morbidity and mortality, despite the availability of antihypertensive drugs with different targets and mechanisms of action. Here, we provide evidence that pharmacological inhibition of TMEM16A (ANO1), a calcium-activated chloride channel expressed in vascular smooth muscle cells, blocks calcium-activated chloride currents and contraction in vascular smooth muscle *in vitro* and decreases blood pressure in spontaneously hypertensive rats. The acylaminocycloalkylthiophene TMinh-23 fully inhibited calcium-activated TMEM16A chloride current with nanomolar potency in Fischer rat thyroid cells expressing TMEM16A, and in primary cultures of rat vascular smooth muscle cells. TMinh-23 reduced vasoconstriction caused by the thromboxane mimetic U46619 in mesenteric resistance arteries of wild-type and spontaneously hypertensive rats, with a greater inhibition in spontaneously hypertensive rats. Blood pressure measurements by tail-cuff and telemetry showed up to a 45-mmHg reduction in systolic blood pressure lasting for four-six hours in spontaneously hypertensive rats after a single dose of TMinh-23. A minimal effect on blood pressure was seen in wild-type rats or mice treated with TMinh-23. Five-day twice daily treatment of spontaneously hypertensive rats with TMinh-23 produced sustained reductions of 20-25 mmHg in daily mean systolic and diastolic blood pressure. TMinh-23 action was reversible, with blood pressure returning to baseline in spontaneously hypertensive rats by three days after treatment discontinuation. Thus, our studies provide validation for TMEM16A as a target for antihypertensive therapy and demonstrate the efficacy of TMinh-23 as an antihypertensive with a novel mechanism of action.

Correspondence: *Onur Cil, Department of Pediatrics, University of California, San Francisco, 513 Parnassus Avenue, HSE 1244, San Francisco, California 94143, USA. E-mail: onur.cil@ucsf.edu*

Received 16 July 2020; revised 3 February 2021; accepted 5 March 2021; published online 6 April 2021

Kidney International (2021) **100,** 311–320; https://doi.org/10.1016/j.kint.2021.03.025

KEYWORDS: antihypertensives; hypertension; vasodilators

Copyright © 2021, International Society of Nephrology. Published by Elsevier Inc. All rights reserved.

Translational Statement

Hypertension is a major risk factor for cardiovascular diseases and renal failure. Despite the availability of antihypertensive drugs with different mechanisms of action, hypertension remains a significant clinical problem. There is an unmet need for novel antihypertensives to control blood pressure, particularly for patients with resistant hypertension. Herein, we characterize and show proof-of-concept efficacy of a small-molecule inhibitor of vascular smooth muscle calcium-activated chloride channel TMEM16A (transmembrane member 16A or anoctamin-1). TMEM16A inhibitor prevented vasoconstriction in isolated arteries, reduced blood pressure in spontaneously hypertensive rats, and had a sustained antihypertensive effect with long-term administration. TMEM16A inhibition is a novel approach for the treatment of hypertension.

Hypertension, affecting >25% of the global adult population and 1 in 3 US adults, is a major risk factor for coronary artery disease, stroke, heart failure, and renal failure.[1,2] Drug treatment of hypertension reduces the probability of cardiovascular events, with more intensive blood pressure (BP) control correlating with reduced cardiovascular morbidity and mortality.[1,3] Hypertension remains a major problem despite the availability of antihypertensive drugs with different targets and mechanisms of action. Of patients receiving antihypertensive medications, 12% to 15% have resistant disease and 8% have uncontrolled hypertension despite being treated with ≥3 different classes of

antihypertensives.[4,5] There is an unmet need for antihypertensive drugs with novel mechanisms of action to better control hypertension and reduce cardiovascular morbidity and mortality.

TMEM16A (transmembrane member 16A or anoctamin-1) is a Ca^{2+}-activated Cl^- channel expressed in vascular smooth muscle cells,[6–9] as well as in airway smooth muscle, gastrointestinal pacemaker cells, and various epithelial cell types.[10] Because vascular smooth muscle cells actively accumulate Cl^-,[11] TMEM16A activation leads to Cl^- efflux and membrane depolarization that results in secondary activation of ion channels that modulate vasoconstriction, including voltage-dependent Ca^{2+} channels (VDCCs).[12] TMEM16A knockout in mice decreases *in vitro* contractile responses to angiotensin II in aortic strips, reduces BP, and attenuates the hypertensive response to angiotensin II.[13] *In vitro* studies using a low-potency TMEM16A inhibitor[14] showed relaxation in mouse arteries in response to methoxamine.[7] Whether pharmacologic TMEM16A inhibition may be efficacious for treatment of hypertension *in vivo* has not been investigated.

Our group recently identified, and optimized by medicinal chemistry, TMEM16A inhibitor TM_{inh}-23 (Figure 1a), which showed nanomolar potency and good selectivity and pharmacologic properties.[15,16] Herein, we investigated its efficacy in blocking vascular smooth muscle contraction *in vitro* and reducing BP in a rat model of hypertension.

METHODS

Chemicals

TM_{inh}-23 (2-bromodifluoroacetylamino-5,6,7,8-tetrahydro-4H-cyclohepta[b]thiophene-3-carboxylic acid o-tolylamide) (Figure 1a, originally named 10bm in a previous study[15]) was synthesized in 3 steps, as described,[15] and had >95% purity determined by high-performance liquid chromatography analysis at 254 nm. Other chemicals were purchased from Sigma-Aldrich, unless indicated otherwise.

Short-circuit current measurements

Short-circuit current measurements were done on Fischer rat thyroid cells stably expressing human TMEM16A. Cells were cultured, as described,[15] and grown as tight monolayers on inserts (12-mm diameter, 0.4-μm polyester membrane; Corning Life Sciences). For measurement of short-circuit current, cells were mounted in Ussing chambers and a basolateral-to-apical Cl^- gradient was applied, as described.[15] Basolateral chambers were filled with bicarbonate-buffered Ringer solution (pH 7.4, in mM: 120 NaCl, 5 KCl, 1 $MgCl_2$, 1 $CaCl_2$, 10 D-glucose, 5 HEPES, and 25 $NaHCO_3$). For the apical chamber solution, 120 mM NaCl was replaced by 60 mM NaCl and 60 mM Na-gluconate. The solutions were aerated with 95% O_2/5% CO_2 and maintained at 37°C. Short-circuit current was measured using an EVC4000 multi-channel voltage clamp (World Precision Instruments) via Ag/AgCl electrodes and 3 M KCl agar bridges. Cells were preincubated with TM_{inh}-23 for 10 minutes before addition of 1 μM ionomycin (Alfa Aesar) to increase cytoplasmic Ca^{2+} concentration. All compounds were added to both apical and basolateral bathing solutions.

TMEM16A function in rat pulmonary artery smooth muscle cells

Primary cultures of rat pulmonary artery smooth muscle cells (RPASMCs) were purchased from Sigma-Aldrich and cultured according to the manufacturer's protocols. For experiments, RPASMCs were grown for 48 to 96 hours in a SensoPlate 96 well glass-bottom, black-walled microplate (Greiner Bio-One) and transduced with EYFP-H148Q/I152L/F46L using lentivirus. One day after transduction, RPASMCs were washed twice with phosphate-buffered saline, incubated in 100 μl phosphate-buffered saline, and transferred to Nikon TE2000 microscope (Nikon Inc.). To measure TMEM16A function, cells were imaged for 5 seconds before the addition of 100 μl of phosphate-buffered saline, in which NaCl was replaced by NaI with 100 mM adenosine triphosphate (ATP) to stimulate TMEM16A activity. TM_{inh}-23 inhibition was studied by preincubation with different concentrations of TM_{inh}-23 for 10 minutes before addition of iodide and ATP.

Cellular toxicity

RPASMCs were plated in black-walled, clear-bottom tissue culture plates at a density of 20,000 cells/well. After 48 hours in culture, cells were incubated with 3 μM TM_{inh}-23, 0.1% dimethylsulfoxide (vehicle control), or 20% dimethylsulfoxide (positive control) for 24 hours for assay of cell viability using Alamar blue (ThermoFischer Scientific), according to the manufacturer's instructions.

Animals

Spontaneously hypertensive rats (SHRs; male and female; aged 16–20 weeks) and wild-type Wistar rats (male and female; aged 16–20 weeks) were purchased from Charles River Laboratories. Wild-type CD1 mice (male and female; aged 10–14 weeks) were bred in house. All animal experiments were approved by the respective Institutional Animal Care and Use Committees at each institution. Rats and mice were housed in communal cages with 12-hour light-dark cycle (light period: 7 AM–7 PM). During recording days for telemetry experiments, rats were housed individually with free access to food and water.

Tail-cuff BP measurements

BP was measured by tail cuff in SHRs, wild-type Wistar rats, and wild-type CD1 mice using a Visitech BP-2000 instrument (Visitech Systems Inc.). Animals were acclimatized to tail-cuff measurements by performing daily BP measurements for 5 to 7 days until BP stabilized. After acclimatization, each animal underwent a baseline BP measurement and then was treated with 10 mg/kg TM_{inh}-23 (i.p.; in saline containing 5% dimethylsulfoxide and 10% Kolliphor HS) or vehicle under light isoflurane anesthesia, from which animals recovered quickly (<2 minutes). BP was measured at 15 minutes and 1, 2, and 4 hours after treatments. In SHRs, BP was also measured at 6 and 24 hours after treatment. BP measurements were made in awake animals placed in a restrainer on a heated platform in a quiet room. For each measurement, after 3 initial test measurements (not used for analysis), 20 serial measurements were done and averaged to determine BP. Baseline BP measurements were done at approximately 10:00 AM everyday, followed by i.p. injections and subsequent BP measurements.

Telemetry studies

BP and electrocardiogram (ECG) recordings were made in awake, freely moving SHRs and wild-type rats using an implanted radio telemetry device (HD-S11; Data Sciences Intl). The devices were

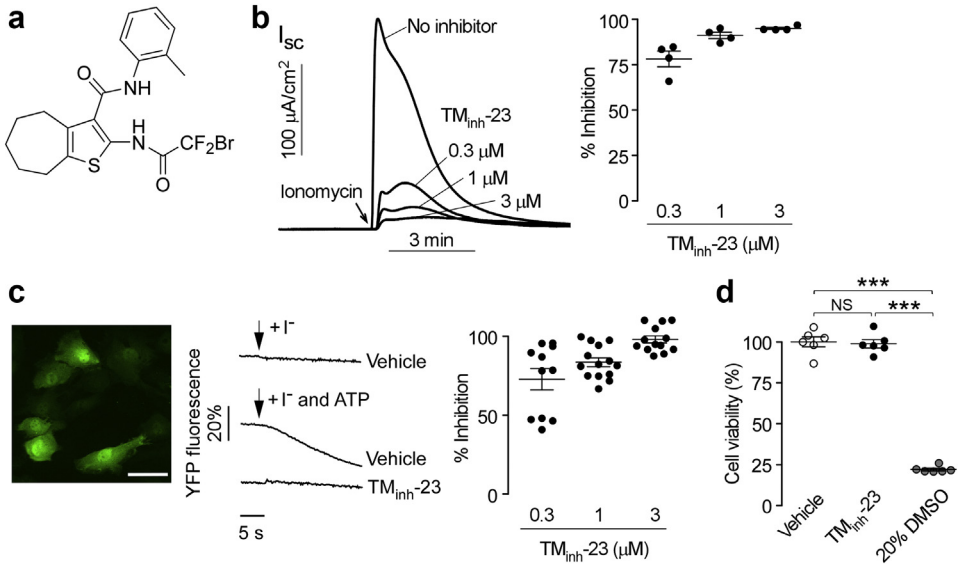

Figure 1 | 2-Bromodifluoroacetylamino-5,6,7,8-tetrahydro-4H-cyclohepta[b]thiophene-3-carboxylic acid o-tolylamide (TM_{inh}-23) pretreatment blocks Ca^{+2}-activated Cl^- secretion in Fischer rat thyroid (FRT) cells and rat primary vascular smooth muscle cells. (**a**) Chemical structure of TM_{inh}-23. (**b**) FRT cells expressing transmembrane member 16A or anoctamin-1 (TMEM16A) were pretreated with indicated concentrations of TM_{inh}-23 for 10 minutes before the addition of ionomycin (1 μM). Original data are shown on the left, and averaged data (mean ± SEM; n = 4) are shown on the right. (**c**) (Left) Rat pulmonary artery smooth muscle cells (RPASMCs) transduced with lentivirus to express halide-sensing yellow fluorescent protein (YFP; bar = 50 μm). (Middle) YFP fluorescence quenching in response to the extracellular addition of iodide, with or without adenosine triphosphate (ATP) and 3 μM TM_{inh}-23. (Right) Summary of the percentage inhibition of I- influx by TM_{inh}-23 in RPASMCs (mean ± SEM; n = 11–14). (**d**) Cell viability assayed by Alamar blue in RPASMCs incubated for 24 hours with vehicle control (0.1% dimethylsulfoxide [DMSO]) or 3 μM TM_{inh}-23. The 20% DMSO was used as positive control. Data are given as mean ± SEM, n = 6 wells per group, 1-way analysis of variance and *post hoc* Newman-Keuls multiple comparisons test. ***$P < 0.001$, NS, not significant. To optimize viewing of this image, please see the online version of this article at www.kidney-international.org.

surgically implanted in the abdomen, and the biopotential leads were placed adjacent to the heart in a lead II arrangement, as described.[17] The BP catheter was inserted in the abdominal aorta. Data recording began after full recovery via an antenna receiver under the cage interfaced to a computer system. ECG and pressure waveforms were acquired once every minute with the DSI Ponemah V6.2 software (Data Sciences Intl) before, during, and after TM_{inh}-23 or vehicle treatments. Data were subsequently analyzed for arterial BP (systolic, diastolic, and mean), heart rate, and ECG.

After animal recovery and acclimatization for 2 weeks, baseline telemetry recording was done for 1 to 2 days before each experiment. To assess short-term effect of TM_{inh}-23 on BP, SHRs and wild-type rats were treated with a single dose of TM_{inh}-23 (10 mg/kg; i.p.) or vehicle around noon under light isoflurane anesthesia and recordings were made for the next 24 hours. In long-term studies, SHRs were administered 10 mg/kg TM_{inh}-23 twice daily (i.p.; daily injections done approximately at 10 AM and 4 PM under light isoflurane anesthesia) for 5 days.

In vitro vascular smooth muscle contraction

Experiments were done on third-order mesenteric arteries from SHRs and wild-type rats or segments of thoracic aorta from wild-type rats (all of Wistar background). Wire or pin myography was used to assess function of mesenteric artery and aorta segments, respectively. After dissection, arterial segments were mounted on tungsten wires in a myograph (Danish MyoTech) in physiological salt solution (pH 7.4), which contained (in mM): 119 NaCl, 4.5 KCl, 1.17 $MgSO_4$, 1.18 NaH_2PO_4, 25 $NaHCO_3$, 5 glucose, and 1.25 $CaCl_2$. The force elicited by tension of the vessel wall on the wires/pins was recorded using LabChart software (ADInstruments). All vessels were subjected to normalization, where they were incrementally stretched to determine the resting diameter of the vessel lumen under a transmural pressure of 100 mm Hg. The vessels were then set to 90% of this diameter as this was considered the ideal passive stretch for active tension development. Following a 30-minute postnormalization equilibration period, the segments were challenged with physiological salt solution containing 60 mM K^+ (replacing Na^+) to determine maximum contractility. After washout and restabilization of tension, the concentration-response for U46619 induced contractions was measured. All contraction responses were normalized and reported as percentage contraction induced by physiological salt solution containing 60 mM K^+.

Statistical analysis

Experiments with 2 groups were analyzed using Student's *t* test; for ≥3 groups, analysis was done with 1-way analysis of variance and *post hoc* Newman-Keuls multiple comparisons test. $P < 0.05$ was considered statistically significant.

RESULTS

TM_{inh}-23 inhibition of Ca^{2+}-activated TMEM16A Cl^- conductance

As reported previously, the small-molecule inhibitor TM_{inh}-23 (Figure 1a) is a chemically stable compound with drug-like physicochemical properties, which inhibited ATP-activated TMEM16A Cl^- conductance with nanomolar potency.[15] To confirm that TMEM16A inhibition by TM_{inh}-23 is

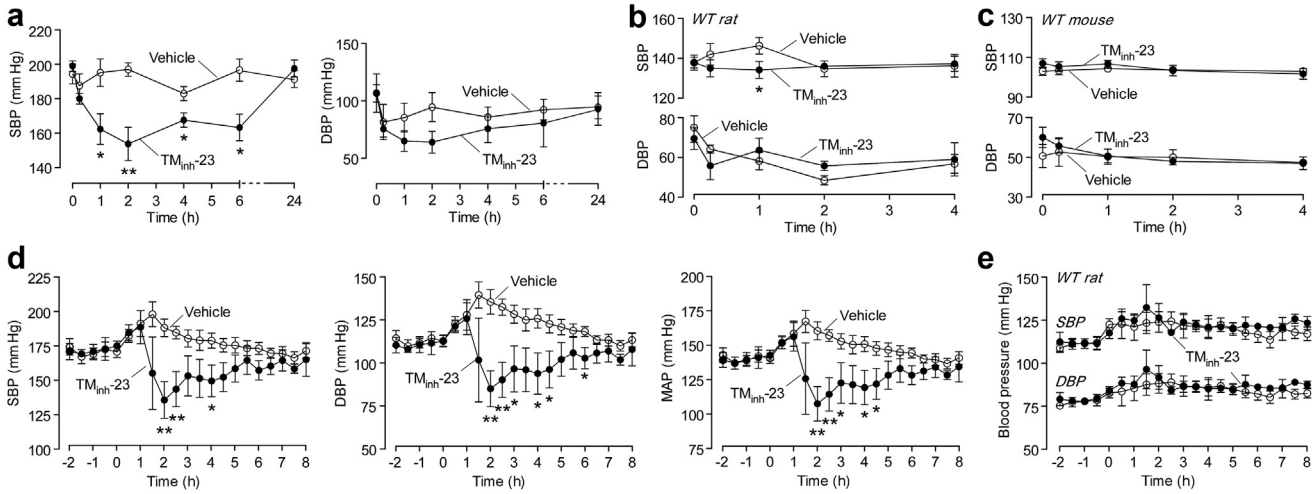

Figure 2 | Single-dose 2-bromodifluoroacetylamino-5,6,7,8-tetrahydro-4H-cyclohepta[b]thiophene-3-carboxylic acid o-tolylamide (TM_{inh}-23) lowers blood pressure (BP) in spontaneously hypertensive rats (SHRs), but not in wild-type (WT) rats or mice. (**a**) Tail-cuff systolic blood pressure (SBP; left) and diastolic blood pressure (DBP; right) in SHRs administered TM_{inh}-23 or vehicle at time 0 (mean ± SEM; n = 5 rats per group). (**b**) Tail-cuff BP in WT Wistar rats administered TM_{inh}-23 (10 mg/kg; i.p.) or vehicle at time 0 (mean ± SEM; n = 6 rats per group). (**c**) Tail-cuff BP in WT CD1 mice administered TM_{inh}-23 (10 mg/kg; i.p.) or vehicle at time 0 (mean ± SEM; n = 3 mice per group). (**d**) Telemetry BP in SHRs administered TM_{inh}-23 or vehicle at time 0 (mean ± SEM; n = 3–6 rats per group). (**e**) Telemetry BP in WT Wistar rats administered TM_{inh}-23 or vehicle at time 0 (mean ± SEM; n = 3 rats per group). The Student's *t* test was used. $^*P < 0.05$, $^{**}P < 0.01$ compared with the vehicle group; all other comparisons between groups are not significant. Each data point represents the average of all measurements in the preceding 30-minute period in panels (**d**) and (**e**). MAP, mean arterial pressure.

independent of purinergic signaling, short-circuit current measurements of TMEM16A Cl^- conductance were done in Fischer rat thyroid cells expressing TMEM16A in response to elevation of intracellular Ca^{2+} concentration by the calcium ionophore ionomycin. TM_{inh}-23 pretreatment largely blocked Cl^- secretion at 300 nM with near complete inhibition at 1 and 3 μM (Figure 1b). The effects of TM_{inh}-23 were also investigated in primary cultures of rat vascular smooth muscle cells that were transduced with a halide-sensing yellow fluorescent protein using lentivirus. Yellow fluorescent protein fluorescence decreased in response to an I^- gradient when in the presence of the Ca^{2+} agonist ATP (Figure 1c). TM_{inh}-23 pretreatment inhibited the ATP-stimulated I^- entry, with complete inhibition at 3 μM. To rule out TM_{inh}-23 toxicity in these experiments, Alamar blue assay showed no effect of 24-hour incubation with 3 μM TM_{inh}-23 on the viability of primary rat vascular smooth muscle cells (Figure 1d). Prior pharmacokinetics measurements in mice showed sustained therapeutic TM_{inh}-23 serum concentrations for at least 4 hours following a single i.p. dose at 10 mg/kg.[16] Preliminary studies in rats showed a similar TM_{inh}-23 pharmacokinetic profile following a single i.p. dose at 10 mg/kg (data not shown). These studies provided a rational basis for compound dosing in the animal experiments below.

TM_{inh}-23 efficacy in reducing BP, as measured by tail cuff

To investigate TM_{inh}-23 action on BP, initial measurements were made by tail cuff in SHRs and wild-type rats, as well as in wild-type mice. In SHRs, TM_{inh}-23 at 10 mg/kg administered i.p. produced up to an ~45–mm Hg decrease in systolic BP (SBP) compared with vehicle control, with peak response at 120 minutes after injection (Figure 2a, left). SBP was significantly reduced in SHRs for at least 6 hours after treatment and returned to baseline by 24 hours, indicating reversibility of the TM_{inh}-23 effect. There was also a trend in reduction of diastolic BP (DBP) with TM_{inh}-23 treatment (Figure 2a, right), although the differences were not statistically significant, in part because of large variability in DBP, as the tail-cuff method can have limited accuracy in measuring DBP.[18,19]

In vehicle-treated wild-type rats, there was a small increase in SBP of ~9 mm Hg at 60 minutes after injection (Figure 2b), which may be due to distress and/or pain related to anesthesia, i.p. injections, and restraining. TM_{inh}-23 slightly lowered SBP at 60 minutes compared with vehicle treatment ($P = 0.04$), with no effect on DBP. In wild-type mice, TM_{inh}-23 did not significantly affect SBP or DBP (Figure 2c).

Pharmacodynamics of single-dose TM_{inh}-23 in reducing BP, as measured by telemetry

As the tail-cuff method has recognized limitations, it is generally considered as a screening method suitable for detection of relatively large BP changes. Telemetry is the gold standard method for continuous measurement of BP in freely moving rodents, providing unambiguous data without significant confounding variables, such as restraining.[20]

Telemetric monitoring was done in freely moving SHRs and wild-type rats to assess TM_{inh}-23 pharmacodynamics. After acclimatization and baseline BP measurement, rats were administered a single dose of TM_{inh}-23 (10 mg/kg; i.p.) or vehicle. In SHRs, TM_{inh}-23 produced substantial drops in

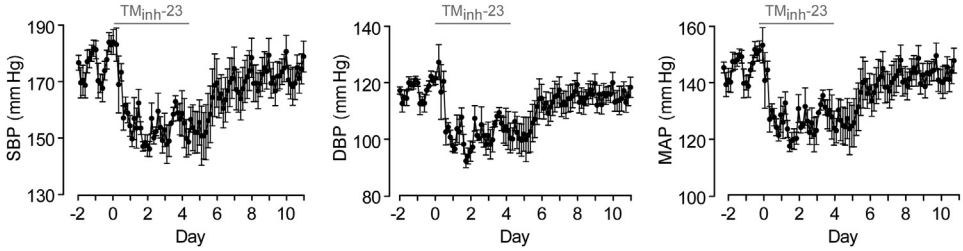

Figure 3 | Long-term 2-bromodifluoroacetylamino-5,6,7,8-tetrahydro-4H-cyclohepta[b]thiophene-3-carboxylic acid o-tolylamide (TM_{inh}-23) treatment causes sustained decreases in blood pressure (BP) in spontaneously hypertensive rats (SHRs). Telemetry BP in SHRs with twice daily TM_{inh}-23 (10 mg/kg; i.p.) treatment for 5 days, starting on day 0. The TM_{inh}-23 treatment period is shown as a horizontal gray bar above each graph. Each data point is the average of all measurements in the preceding 3-hour period (mean ± SEM; n = 4 rats). DBP, diastolic blood pressure; MAP, mean arterial pressure; SBP, systolic blood pressure.

SBP, DBP, and mean arterial pressure (MAP) compared with vehicle treatment, with peak effect at 120 minutes (Figure 2d), in general agreement with the tail-cuff studies. BP values returned to baseline levels within 6 to 8 hours after treatment. In agreement with results using the tail-cuff method, TM_{inh}-23 had little or no effect on BP in wild-type rats (Figure 2e).

Long-term TM_{inh}-23 treatment in SHRs causes sustained reduction in BP

In long-term studies, SHRs treated with 10 mg/kg TM_{inh}-23 (i.p.) twice daily had sustained reductions in BP that returned to baseline levels at 3 to 4 days after discontinuation of treatment (raw data presented in Figure 3). As can be seen in the raw data, there was significant physiological diurnal variation in BP, which was analyzed by calculating average daily BP (Figure 4a). Further analysis also calculated daily daytime (7 AM–7 PM) and nighttime (7 PM–7 AM) average BP (Figure 4b). TM_{inh}-23 decreased daily mean SBP, DBP, and MAP by 20 to 25 mm Hg during the 5-day treatment period, with gradual return to baseline values over 3 to 4 days after treatment cessation (Figure 4a). TM_{inh}-23 reduced both average daytime and nighttime BP (Figure 4b), indicating sustained antihypertensive efficacy.

The effect of TM_{inh}-23 treatment on heart rate and ECG was also studied. Long-term TM_{inh}-23 treatment resulted in increased heart rate during the first 2 to 3 days of the 5-day treatment period, which then returned to near baseline values (Figure 5a, left). The daily average heart rate after treatment cessation was slightly lower than baseline values (Figure 5a, middle), which was primarily due to slight reduction in nocturnal heart rate (Figure 5a, right). ECG analysis showed slightly reduced PR interval, QRS duration, and QT interval at day 2 of TM_{inh}-23 treatment, as expected from the increased heart rate. Each ECG parameter returned to baseline after treatment cessation (Figure 5b).

TM_{inh}-23 inhibits vascular smooth muscle contraction in *ex vivo* rat resistance arteries

To investigate the antihypertensive mechanism of TM_{inh}-23, isometric vascular smooth muscle contractions in response to a vasoconstrictor (thromboxane mimetic U46619) were studied in mesenteric resistance arteries, which are critical for BP regulation. TM_{inh}-23 largely, but incompletely, inhibited the U46619-induced vasoconstriction in mesenteric resistance arteries, even at 3 μM (Figure 6a and b). TM_{inh}-23 effect was also investigated on contractions induced by high K^+, which is thought to depolarize vascular smooth muscle cells independent of calcium-activated chloride channels (CaCCs) and cause vasoconstriction by activating VDCCs. The high K^+ response in mesenteric arteries was biphasic, with an initial peak followed by a smaller plateau (Figure 6a). Interestingly, the high K^+ response was also inhibited by TM_{inh}-23 (Figure 6a and c). The TM_{inh}-23 effect was reversible, as seen from the return of high K^+ response to pretreatment values after washout (Figure 6a, bottom trace).

Contractions were also measured in mesenteric resistance arteries from SHRs. TM_{inh}-23 completely inhibited maximum U46619-induced vasoconstriction in SHR mesenteric arteries at 3 μM (Figure 7a and b). Consistent with the greater BP-lowering effect *in vivo* in SHRs, TM_{inh}-23 inhibited maximum U46619-induced contractions significantly more in mesenteric arteries from SHRs than wild-type rats (Figure 7c, left). Contractions induced by lower U46619 concentrations (100 nM) in SHR arteries were even more sensitive to TM_{inh}-23, compared with wild-type rats (Figure 7c, right). As seen in wild-type rats, TM_{inh}-23 also inhibited high K^+-induced vasoconstriction in SHR mesenteric arteries (Figure 7d).

TM_{inh}-23 has minimal effect on *ex vivo* rat aorta smooth muscle contraction

In contrast to the results in rat resistance arteries, in aorta, TM_{inh}-23 pretreatment slightly reduced U46619-induced contractions (by ~20%) even at a high concentration of 3 μM (Figure 8a and b; $P = 0.14$). TM_{inh}-23 pretreatment had no effect on high K^+-induced vasoconstriction in aorta (Figure 8a and c). These findings suggest that TMEM16A inhibition preferentially prevents vasoconstriction in rat resistance arteries but not in aorta, noting that the latter have minimal contribution to BP.

DISCUSSION

TMEM16A inhibition by a small-molecule drug candidate markedly reduced BP in a rat model of hypertension, offering

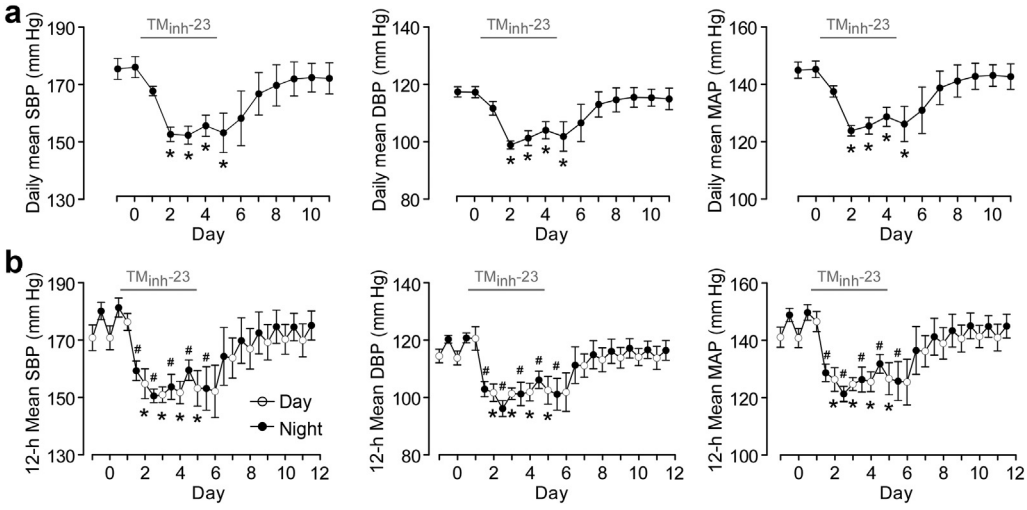

Figure 4 | Long-term 2-bromodifluoroacetylamino-5,6,7,8-tetrahydro-4H-cyclohepta[b]thiophene-3-carboxylic acid o-tolylamide (TM_{inh}-23) treatment causes sustained decreases in 24-hour average, daytime, and nighttime blood pressure (BP) in spontaneously hypertensive rats (SHRs). (**a**) Daily mean BP (measured by telemetry) in SHRs with twice daily TM_{inh}-23 (10 mg/kg; i.p.) treatment for 5 days, starting on day 0 (mean ± SEM; n = 4 rats), Student's *t* test, **P* < 0.05 compared with day 0. (**b**) Diurnal variation in blood pressure in SHRs. Open circles show average daytime BP (7 AM–7 PM), and closed circles represent average nighttime BP (7 PM–7 AM). The TM_{inh}-23 treatment period is shown as a horizontal gray bar above each graph (mean ± SEM; n = 4 rats). Student's *t* test was used. **P* < 0.05 compared with daytime BP on day 0; #*P* < 0.05 compared with nighttime BP on day 0. DBP, diastolic blood pressure; MAP, mean arterial pressure; SBP, systolic blood pressure.

proof of concept for pharmacologic inhibition of TMEM16A by a small molecule for antihypertensive therapy with a novel mechanism of action. An interesting observation was the large reductions in BP of SHRs with TMEM16A inhibition, although there was minimal effect in wild-type rats and mice. This differential effect may in part be a consequence of differences in TMEM16A expression and/or activity between SHRs and wild-type rodents. A recent study showed 4-fold increased TMEM16A expression in smooth muscle cells of coronary arteries in SHRs compared with wild-type rats.[21] Herein, we found that mesenteric arteries from SHRs were considerably more sensitive to TMEM16A inhibition than

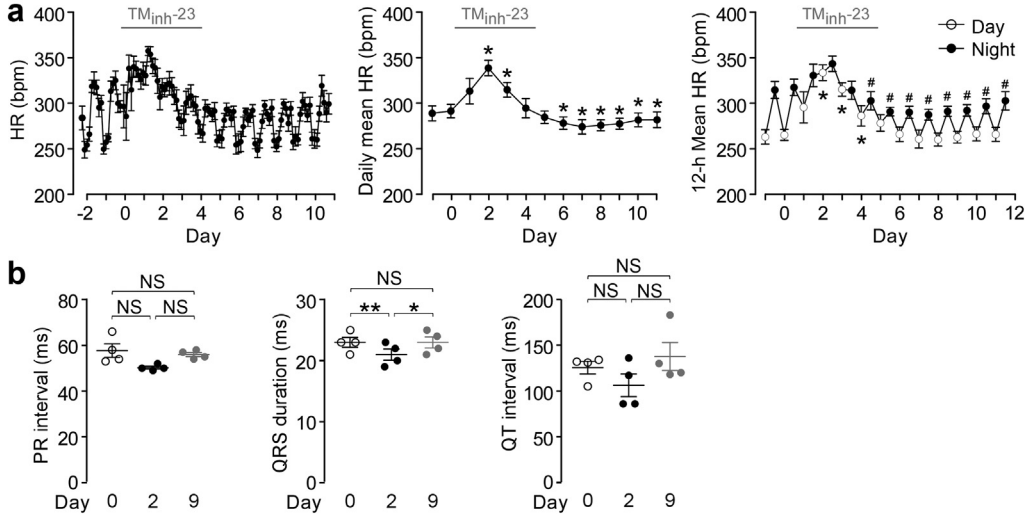

Figure 5 | Heart rate (HR) and electrocardiogram (ECG) with long-term 2-bromodifluoroacetylamino-5,6,7,8-tetrahydro-4H-cyclohepta[b]thiophene-3-carboxylic acid o-tolylamide (TM_{inh}-23) treatment in spontaneously hypertensive rats (SHRs). (**a**) (Left) HR in SHRs with twice daily TM_{inh}-23 (10 mg/kg; i.p.) treatment for 5 days, starting on day 0. Each data point is the average of all measurements in the preceding 3-hour period. (Middle) Daily mean HR in SHRs. **P* < 0.05 compared with day 0. (Right) Diurnal variation in HR in SHRs. Open circles show average daytime (7 AM–7 PM) HR, and closed circles represent average nighttime (7 PM–7 am) HR (mean ± SEM; n = 4 rats). Student's *t* test was used. **P* < 0.05 compared with average daytime HR on day 0; #*P* < 0.05 compared with average nighttime HR on day 0. The TM_{inh}-23 treatment period is shown as a horizontal gray bar above each graph. (**b**) ECG parameters in SHRs with twice daily TM_{inh}-23 (10 mg/kg; i.p.) treatment for 5 days, starting on day 0 (mean ± SEM; n = 4 rats). One-way analysis of variance with *post hoc* Newman-Keuls multiple comparison test was used. **P* < 0.05, ***P* < 0.01. Bpm, beats per minute; NS, not significant.

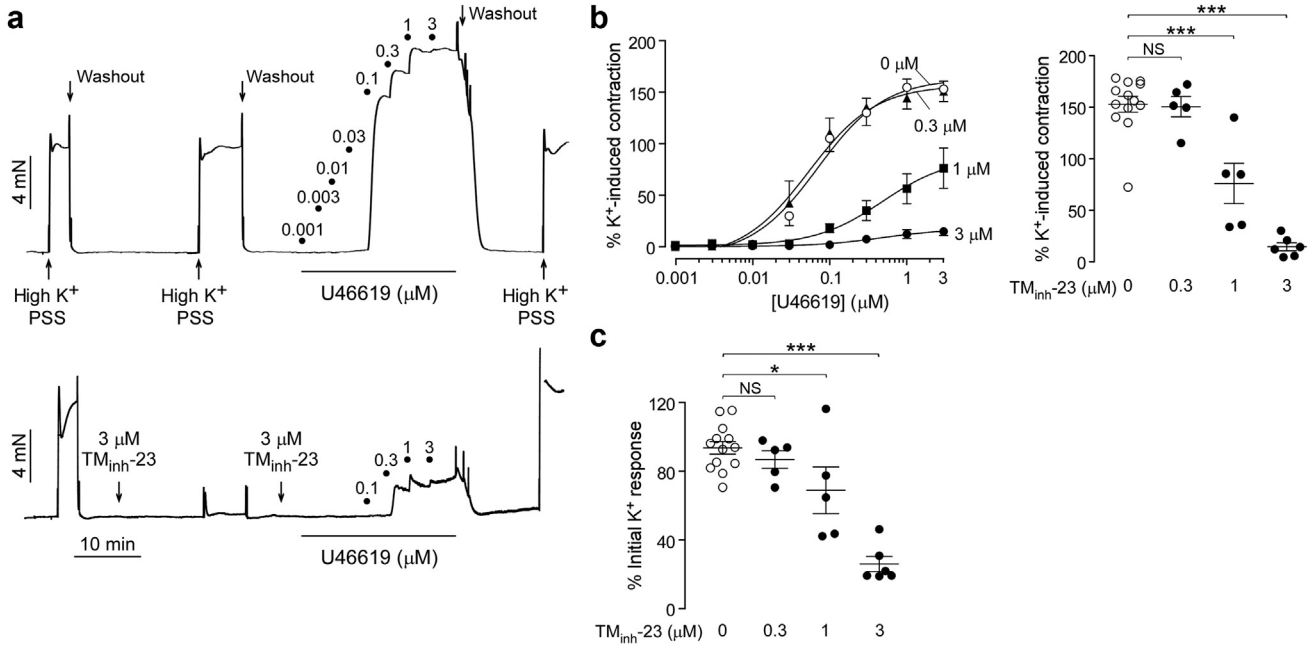

Figure 6 | 2-Bromodifluoroacetylamino-5,6,7,8-tetrahydro-4H-cyclohepta[b]thiophene-3-carboxylic acid o-tolylamide (TM_{inh}-23) blocks vascular smooth muscle contractions in mesenteric resistance arteries of wild-type rats. (**a**) Representative traces showing isometric contractions in response to high K^+ (60 mM) and increasing concentrations of U46619 in rat mesenteric arteries treated with vehicle (0.1% dimethylsulfoxide; top) or 3 μM TM_{inh}-23 (bottom). (**b**) (Left) U46619 concentration-response curves at indicated concentrations of TM_{inh}-23. (Right) Maximum U46619 response in the presence of different concentrations of TM_{inh}-23. (**c**) High K^+-induced peak contraction responses as a function of TM_{inh}-23 concentration. N = 5 to 13 experiments per group; 1-way analysis of variance with *post hoc* Newman-Keuls multiple comparison test was used. $^*P < 0.05$, $^{***}P < 0.001$. NS, not significant; PSS, physiological salt solution.

arteries from wild-type rats, which may explain the greater *in vivo* BP-lowering efficacy of TM_{inh}-23 in SHRs versus wild-type rats. Another explanation for the greater BP-lowering effect of TM_{inh}-23 in SHRs may be the markedly increased peripheral vascular resistance in SHRs compared with wild-type rats.[22]

TMEM16A expression in vascular smooth muscle is species and artery dependent. In mice, TMEM16A is strongly expressed in aorta, with some studies reporting relatively little expression in small resistance arteries,[6,13,23] whereas others reported comparable TMEM16A expression in aorta and small mesenteric resistance arteries.[7] In rats, TMEM16A is expressed throughout the arterial system, including small resistance arteries.[21,24] We found herein that TMEM16A inhibition by a selective small-molecule inhibitor largely blocked vascular smooth muscle contraction in rat mesenteric resistance arteries, suggesting TMEM16A as the major CaCC in these vessels. Interestingly, TMEM16A inhibition had limited effect on vasoconstriction in rat aorta, which might be due to the presence of alternative, non-TMEM16A CaCC(s) in this segment. This idea is supported by an earlier study showing 50% reduction in norepinephrine-induced vasoconstriction in rat aortic strips using the nonselective CaCC inhibitor niflumic acid.[25] Because resistance arteries are key regulators of vascular tone and peripheral arterial resistance,[26] our findings suggest that the mechanism of antihypertensive action by TM_{inh}-23 is likely vasodilatation in resistance arteries. Similar to rats, TMEM16A is expressed in small resistance arteries of humans,[7] supporting the potential antihypertensive efficacy of TMEM16A inhibition in humans.

Elevation in extracellular K^+ results in vascular smooth muscle cell depolarization, which opens VDCCs and causes vasoconstriction. This action has been presumed to be independent of CaCCs. We found that TM_{inh}-23 inhibited high K^+-induced vasoconstriction responses in rat mesenteric resistance arteries, but not aorta. Similarly, earlier studies reported 40% to 60% lower high K^+-induced contraction responses in rat coronary arteries in the presence of other small-molecule TMEM16A inhibitors[21] or in rat mesenteric arteries with TMEM16A knockdown.[27] Consistent with lack of TM_{inh}-23 effect in rat aorta herein, previous studies showed no effect of the nonselective CaCC inhibitor niflumic acid on high K^+-induced vasoconstriction in rat aortic strips.[25] Our findings, together with these earlier studies, suggest a potential functional interplay between TMEM16A and VDCCs in rat resistance arteries but not aorta. There is now evidence that the TMEM16A protein may directly alter VDCC activity, as vascular L-type Ca^{+2} channels were downregulated by TMEM16A small interfering RNA knockdown or in a constitutive mouse model.[23,27] TMEM16A has also been implicated in angiotensin II–mediated vascular effects through increased Rho kinase activity in cerebral arteries.[28] TMEM16A inhibition might therefore exert its antihypertensive effects by several different mechanisms in addition to inhibition of Cl^- conductance.

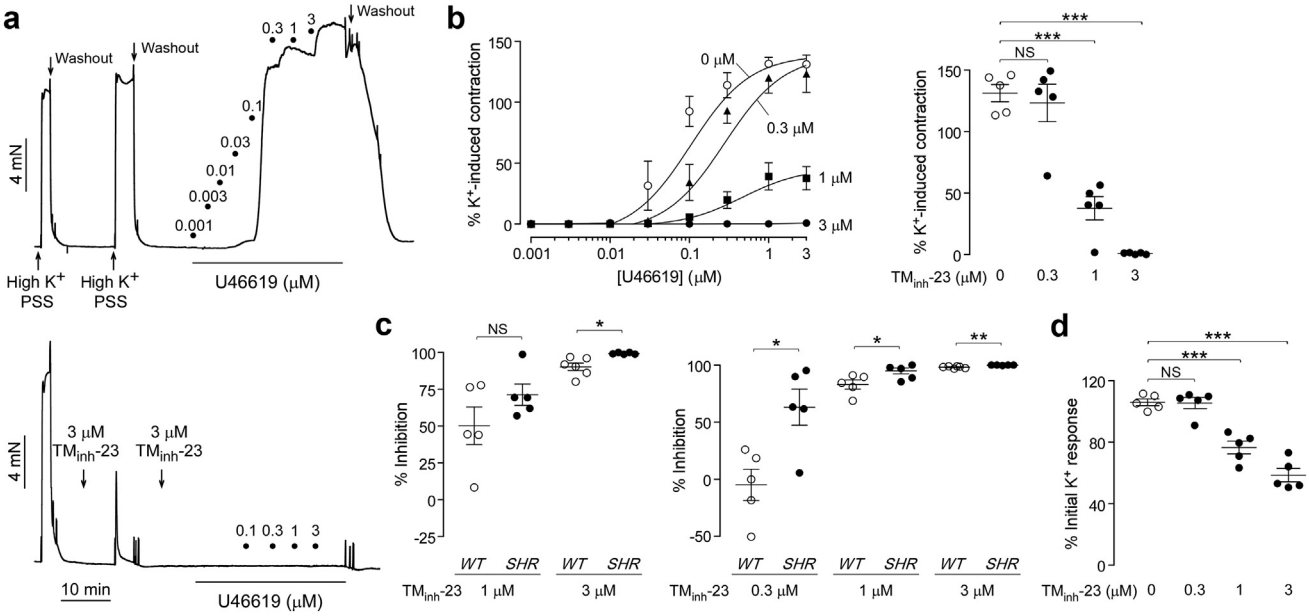

Figure 7 | 2-Bromodifluoroacetylamino-5,6,7,8-tetrahydro-4H-cyclohepta[b]thiophene-3-carboxylic acid o-tolylamide (TM_{inh}-23) blocks vascular smooth muscle contractions in mesenteric resistance arteries of spontaneously hypertensive rats (SHRs). (**a**) Representative traces showing isometric contractions in response to high K^+ (60 mM) and increasing concentrations of U46619 in mesenteric arteries from SHRs treated with vehicle (0.1% dimethylsulfoxide; top) or 3 μM TM_{inh}-23 (bottom). (**b**) (Left) U46619 concentration-response curves at indicated concentrations of TM_{inh}-23. (Right) Maximum U46619 response in the presence of indicated concentrations of TM_{inh}-23. (**c**) (Left) Percentage inhibition of maximal U46619 response in the presence of 1 or 3 μM TM_{inh}-23 in wild-type (WT) and SHR mesenteric arteries. (Right) Percentage inhibition of the 100 nM U46619 response in the presence of TM_{inh}-23 in WT and SHR mesenteric arteries. (**d**) High K^+-induced peak contraction responses as a function of TM_{inh}-23 concentration. N = 5 to 6 experiments per group; Student's *t* test was used for (**c**), and 1-way analysis of variance with *post hoc* Newman-Keuls multiple comparison test was used for (**b**) and (**d**). $^*P < 0.05$, $^{**}P < 0.01$, and $^{***}P < 0.001$. NS, not significant; PSS, physiological salt solution.

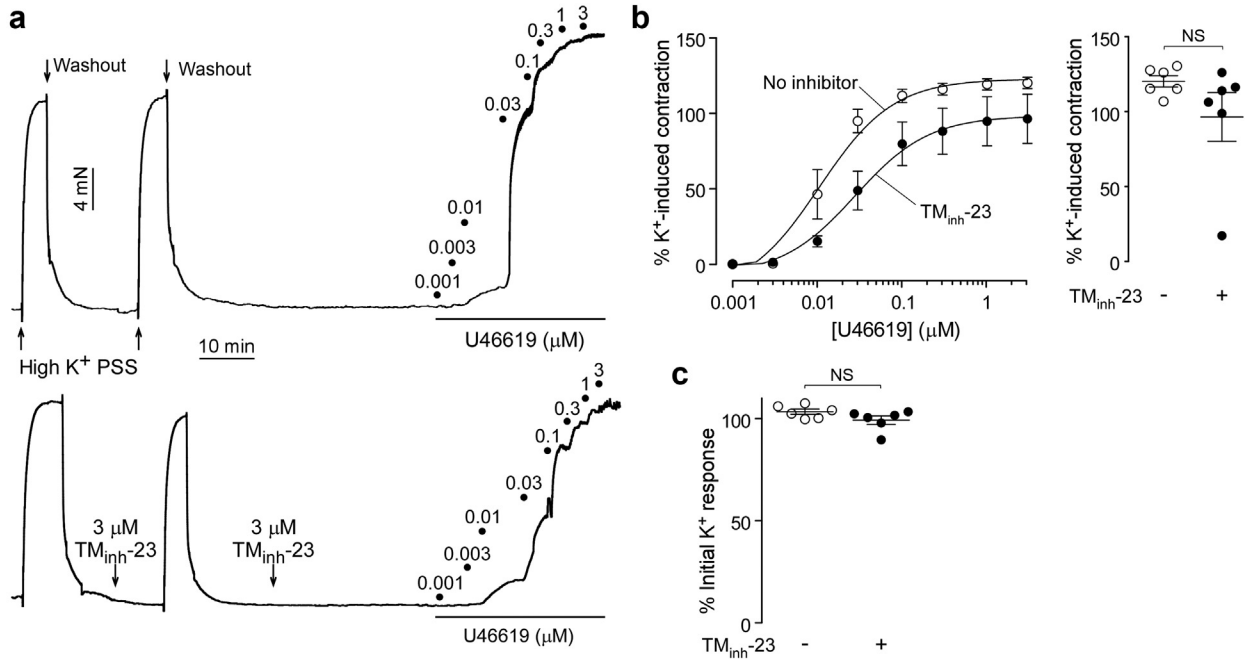

Figure 8 | 2-Bromodifluoroacetylamino-5,6,7,8-tetrahydro-4H-cyclohepta[b]thiophene-3-carboxylic acid o-tolylamide (TM_{inh}-23) effect on vascular smooth muscle contractions in wild-type rat aorta. (**a**) Representative traces showing isometric contractions in response to high K^+ (60 mM) and U46619 in rat aorta treated with vehicle (top) or 3 μM TM_{inh}-23 (bottom). (**b**) (Left) U46619 concentration-response curves in the absence or presence of 3 μM TM_{inh}-23. (Right) Maximum U46619 response in the absence or presence of 3 μM TM_{inh}-23. (**c**) High K^+-induced peak contraction in the absence or presence of 3 μM TM_{inh}-23. N = 6 experiments per group; Student's *t* test was used. NS, not significant; PSS, physiological salt solution.

TM_{inh}-23 treatment in SHRs produced a transient increase in heart rate, which is likely due to the baroreceptor reflex in response to BP reduction, as reported for other vasodilators, such as calcium channel blockers.[29] Earlier studies reported expression of TMEM16A and other putative CaCCs in mouse ventricle[30] and human left ventricular cardiomyocytes.[31] CaCC inhibition by the nonselective compound 9-anthracene carboxylic acid reduced phase 1 repolarization of the action potential in isolated canine cardiomyocytes, with increased incidence of early after-depolarizations,[32] suggesting that CaCC currents might have antiarrhythmic effects. In contrast, earlier TMEM16A inhibitors had no effect on cardiac parameters whilst they increased coronary blood flow in isolated Langendorff experiments.[21] Herein, we found that 5-day TM_{inh}-23 treatment did not produce ECG changes other than the expected shortened intervals associated with increased heart rate. Future studies investigating the potential cardiac effects of TMEM16A inhibitors might be informative.

TMEM16A inhibition is a unique antihypertensive mechanism that targets the initial depolarization of vascular smooth muscle cells in response to intracellular Ca^{+2} elevation. TMEM16A inhibitors can thus potentially have additive effect with other vasodilatory antihypertensives, such as Ca^{+2} channel blockers, which target downstream mechanisms. In addition, the rapid onset of TM_{inh}-23 action makes TMEM16A inhibitors potentially suitable for treatment of hypertensive emergencies in the hospital setting.

Several limitations of the study herein are noted. Although the data support TMEM16A inhibition to relax mesenteric resistance arteries, possible regional differences in the vasorelaxant response in the systemic circulation remain unknown. Of note, we found vasorelaxant effects of TM_{inh}-23 in rat pulmonary arteries as well, which suggests the potential utility of TMEM16A inhibitors in pulmonary hypertension, because increased TMEM16A expression and activity appear to be an important pathologic mechanism in this condition.[33] As TMEM16A is expressed in various tissues in addition vascular smooth muscle, off-target effects of TMEM16A inhibition are possible, depending on inhibitor tissue distribution. Data in knockout or inhibitor-treated mice suggest possible actions of TMEM16A inhibition on airway smooth muscle to cause bronchodilation,[34] on gastrointestinal pacemaker cells to inhibit gastric motility,[16] and on secretory epithelia to reduce saliva[35] and tear fluid secretion.[36] Although these off-target actions may be of lesser concern for short-term TMEM16A inhibition therapy of hypertensive emergencies, they warrant careful evaluation for long-term therapy. Further medicinal chemistry (e.g., prodrug strategies) may promote preferential inhibitor targeting to vascular smooth muscle.

In conclusion, the TMEM16A inhibitor TM_{inh}-23 was efficacious in reducing BP in a rat model of hypertension. This compound, or alternative TMEM16A inhibitors, may be useful for treatment of hypertension as first-in-class antihypertensives with a novel mechanism of action.

DISCLOSURE

All the authors declared no competing interests.

ACKNOWLEDGEMENTS

This work was supported by grants from the American Heart Association (18POST33990365 and Stephanie Watts Career Development Award) and the National Institutes of Health (DK126070 and DK072517).

AUTHOR CONTRIBUTIONS

OC and ASV conceived the study; OC performed the short-circuit current experiments; OC, XC, MCJ, and KPR performed the blood pressure measurements in animals; OC and KPR analyzed the blood pressure data; HRAP, SNB, and IAG performed the *in vitro* vascular smooth muscle experiments and analyzed the data; MOA and PMT synthesized and purified the TMEM16A inhibitor; PMH performed the human vascular smooth muscle cell experiments and analyzed the data; OC wrote the article; HRAP, IAG, KPR, and ASV revised the article; all authors reviewed the article.

REFERENCES

1. James PA, Oparil S, Carter BL, et al. 2014 Evidence-based guideline for the management of high blood pressure in adults: report from the panel members appointed to the Eighth Joint National Committee (JNC 8). *JAMA*. 2014;311:507–520.
2. Vital signs: awareness and treatment of uncontrolled hypertension among adults - United States, 2003–2010. *MMWR Morb Mortal Wkly Rep*. 2012;61:703–709.
3. The SPRINT Research Group. A randomized trial of intensive versus standard blood-pressure control. *N Engl J Med*. 2015;373:2103–2116.
4. Persell SD. Prevalence of resistant hypertension in the United States, 2003-2008. *Hypertension*. 2011;57:1076–1080.
5. Sim JJ, Bhandari SK, Shi J, et al. Characteristics of resistant hypertension in a large, ethnically diverse hypertension population of an integrated health system. *Mayo Clin Proc*. 2013;88:1099–1107.
6. Davis AJ, Forrest AS, Jepps TA, et al. Expression profile and protein translation of TMEM16A in murine smooth muscle. *Am J Physiol Cell Physiol*. 2010;299:C948–C959.
7. Davis AJ, Shi J, Pritchard HAT, et al. Potent vasorelaxant activity of the TMEM16A inhibitor T16A(inh) -A01. *Br J Pharmacol*. 2013;168:773–784.
8. Manoury B, Tamuleviciute A, Tammaro P. TMEM16A/anoctamin 1 protein mediates calcium-activated chloride currents in pulmonary arterial smooth muscle cells. *J Physiol*. 2010;588:2305–2314.
9. Thomas-Gatewood C, Neeb ZP, Bulley S, et al. TMEM16A channels generate Ca^{2+}-activated Cl^- currents in cerebral artery smooth muscle cells. *Am J Physiol Heart Circ Physiol*. 2011;301:H1819–H1827.
10. Kamaleddin MA. Molecular, biophysical, and pharmacological properties of calcium-activated chloride channels. *J Cell Physiol*. 2018;233:787–798.
11. Chipperfield AR, Harper AA. Chloride in smooth muscle. *Prog Biophys Mol Biol*. 2000;74:175–221.
12. Leblanc N, Ledoux J, Saleh S, et al. Regulation of calcium-activated chloride channels in smooth muscle cells: a complex picture is emerging. *Can J Physiol Pharmacol*. 2005;83:541–556.
13. Heinze C, Seniuk A, Sokolov MV, et al. Disruption of vascular Ca2+-activated chloride currents lowers blood pressure. *J Clin Invest*. 2014;124:675–686.
14. Namkung W, Phuan PW, Verkman AS. TMEM16A inhibitors reveal TMEM16A as a minor component of calcium-activated chloride channel conductance in airway and intestinal epithelial cells. *J Biol Chem*. 2011;286:2365–2374.
15. Truong EC, Phuan PW, Reggi AL, et al. Substituted 2-acylaminocycloalkylthiophene-3-carboxylic acid arylamides as inhibitors of the calcium-activated chloride channel transmembrane protein 16A (TMEM16A). *J Med Chem*. 2017;60:4626–4635.
16. Cil O, Anderson MO, Yen R, et al. Slowed gastric emptying and improved oral glucose tolerance produced by a nanomolar-potency inhibitor of calcium-activated chloride channel TMEM16A. *FASEB J*. 2019;33:11247–11257.

17. Jordan MC, Zheng Y, Ryazantsev S, et al. Cardiac manifestations in the mouse model of mucopolysaccharidosis I. *Mol Genet Metab*. 2005;86:233–243.
18. Feng M, Whitesall S, Zhang Y, et al. Validation of volume–pressure recording tail-cuff blood pressure measurements. *Am J Hypertens*. 2008;21:1288–1291.
19. Zhao X, Ho D, Gao S, et al. Arterial pressure monitoring in mice. *Curr Protoc Mouse Biol*. 2011;1:105–122.
20. Luft FC. Men, mice, and blood pressure: telemetry? *Kidney Int*. 2019;96:31–33.
21. Askew Page HR, Dalsgaard T, Baldwin SN, et al. TMEM16A is implicated in the regulation of coronary flow and is altered in hypertension. *Br J Pharmacol*. 2019;176:1635–1648.
22. Mulvany MJ. Do resistance vessel abnormalities contribute to the elevated blood pressure of spontaneously-hypertensive rats? a review of some of the evidence. *Blood Vessels*. 1983;20:1–22.
23. Jensen AB, Joergensen HB, Dam VS, et al. Variable contribution of TMEM16A to tone in murine arterial vasculature. *Basic Clin Pharmacol Toxicol*. 2018;123:30–41.
24. Wang B, Li C, Huai R, et al. Overexpression of ANO1/TMEM16A, an arterial Ca+2-activated Cl- channel, contributes to spontaneous hypertension. *J Mol Cell Cardiol*. 2015;82:22–32.
25. Criddle DN, de Moura RS, Greenwood IA, et al. Effect of niflumic acid on noradrenaline-induced contractions of the rat aorta. *Br J Pharmacol*. 1996;118:1065–1071.
26. Tykocki NR, Boerman EM, Jackson WF. Smooth muscle ion channels and regulation of vascular tone in resistance arteries and arterioles. *Compr Physiol*. 2017;7:485–581.
27. Dam VS, Boedtkjer DMB, Nyvad J, et al. TMEM16A knockdown abrogates two different Ca(2+)-activated Cl (-) currents and contractility of smooth muscle in rat mesenteric small arteries. *Pflugers Arch*. 2014;466:1391–1409.
28. Li RS, Wang Y, Chen HS, et al. TMEM16A contributes to angiotensin II-induced cerebral vasoconstriction via the RhoA/ROCK signaling pathway. *Mol Med Rep*. 2016;13:3691–3699.
29. Behuliak M, Bencze M, Polgárová K, et al. Hemodynamic response to gabapentin in conscious spontaneously hypertensive rats. *Hypertension*. 2018;72:676–685.
30. Ye Z, Wu MM, Wang CY, et al. Characterization of cardiac anoctamin1 Ca^{2+}-activated chloride channels and functional role in ischemia-induced arrhythmias. *J Cell Physiol*. 2015;230:337–346.
31. Horváth B, Váczi K, Hegyi B, et al. Sarcolemmal Ca(2+)-entry through L-type Ca(2+) channels controls the profile of Ca(2+)-activated Cl(-) current in canine ventricular myocytes. *J Mol Cell Cardiol*. 2016;97:125–139.
32. Hegyi B, Horváth B, Váczi K, et al. Ca(2+)-activated Cl(-) current is antiarrhythmic by reducing both spatial and temporal heterogeneity of cardiac repolarization. *J Mol Cell Cardiol*. 2017;109:27–37.
33. Papp R, Nagaraj C, Zabini D, et al. Targeting TMEM16A to reverse vasoconstriction and remodelling in idiopathic pulmonary arterial hypertension. *Eur Respir J*. 2019;53:1800965.
34. Huang F, Zhang H, Wu M, et al. Calcium-activated chloride channel TMEM16A modulates mucin secretion and airway smooth muscle contraction. *Proc Natl Acad Sci U S A*. 2012;109:16354–16359.
35. Catalán MA, Kondo Y, Peña-Munzenmayer G, et al. A fluid secretion pathway unmasked by acinar-specific Tmem16A gene ablation in the adult mouse salivary gland. *Proc Natl Acad Sci U S A*. 2015;112:2263–2268.
36. Yu D, Thelin WR, Rogers TD, et al. Regional differences in rat conjunctival ion transport activities. *Am J Physiol Cell Physiol*. 2012;303:C767–C780.

Received: 28 June 2021 | Revised: 21 September 2021 | Accepted: 19 October 2021

DOI: 10.1111/bph.15722

RESEARCH ARTICLE

Sexual dimorphism in prostacyclin-mimetic responses within rat mesenteric arteries: A novel role for $K_V7.1$ in shaping IP receptor-mediated relaxation

Samuel N. Baldwin | **Elizabeth A. Forrester** | **Lauren McEwan** | **Iain A. Greenwood**

Molecular and Clinical Sciences Research Institute, St. George's University, London, UK

Correspondence
Samuel N. Baldwin, Molecular and Clinical Sciences Research Institute, St. George's University, Cranmer Terrace, London SW17 0RE, UK.
Email: m1405629@sgul.ac.uk

Funding information
British Heart Foundation, Grant/Award Numbers: #FS/18/41/33762, FS/18/41/33762

Background and Purpose: Prostacyclin mimetics express potent vasoactive effects via prostanoid receptors that are not unequivocally defined, as to date no study has considered sex as a factor. The aim of this study was to determine the contribution of IP and EP_3 prostanoid receptors to prostacyclin mimetic iloprost-mediated responses, whether $K_V7.1$–5 channels represent downstream targets of selective prostacyclin-IP-receptor agonist MRE-269 and the impact of the oestrus cycle on vascular reactivity.

Experimental Approach: Within second-order mesenteric arteries from male and female Wistar rats, we determined (1) relative mRNA transcripts for EP_{1-4} (*Ptger*$_{1-4}$), IP (*Ptgi*) and TXA_2 (*Tbxa*) prostanoid receptors via RT-qPCR; (2) the effect of iloprost, MRE-269, isoprenaline and ML277 on precontracted arterial tone in the presence of inhibitors of prostanoid receptors, potassium channels and the molecular interference of $K_V7.1$ via wire-myograph; (3) oestrus cycle stage via histological changes in cervical cell preparations.

Key Results: Iloprost evoked a biphasic response in male mesenteric arteries, at concentrations ≤100 nmol·L^{-1} relaxing, then contracting the vessel at concentration ≥300 nmol·L^{-1}, a process attributed to IP and EP_3 receptors respectively. Secondary contraction was absent in the females, which was associated with a reduction in *Ptger3*. Pharmacological inhibition and molecular interference of $K_V7.1$ significantly attenuated relaxations produced by the selective IP receptor agonist MRE-269 in male and female Wistar in dioestrus/metoestrus, but not pro-oestrus/oestrus.

Conclusions and Implications: Stark sexual dimorphisms in iloprost-mediated vasoactive responses are present within mesenteric arteries. $K_V7.1$ is implicated in IP receptor-mediated vasorelaxation and is impaired by the oestrus cycle.

KEYWORDS
GPCR, Iloprost, Kv7, MRE-269, Prostacyclin, Sex, Vascular

This is an open access article under the terms of the Creative Commons Attribution License, which permits use, distribution and reproduction in any medium, provided the original work is properly cited.
© 2021 The Authors. *British Journal of Pharmacology* published by John Wiley & Sons Ltd on behalf of British Pharmacological Society.

1 | INTRODUCTION

Prostacyclin (PGI_2), a product **cyclooxygenase-1 (COX-1)** and **cyclooxygenase-2 (COX-2)** metabolism of **arachidonic acid**, has anti-thrombotic, anti-inflammatory and potent vasodilatory properties attributed to the activation of G_s-coupled **prostanoid (IP) receptor** signalling. PGI_2 and stable analogues, including **iloprost**, however bind to a plethora of G-protein coupled receptors (GPCR) including $EP_{1,2,3,4}$, IP, **TP**, **FP** and **DP_1** (Katusic et al., 2012), though with different affinities. For instance, in human and rat pulmonary arteries, iloprost binds to IP/EP_1 with high affinity, FP > $EP_{3/4}$ with moderate affinity and DP_1 > EP_2 > TP with low affinity (Whittle et al., 2012). As such, the potential effect of PGI_2/iloprost within the vasculature includes both $EP_{1/3}$/FP prostanoid receptor-evoked contraction (Kobayashi et al., 2011; Orie & Clapp, 2011; Tang et al., 2008) and EP_4/IP prostanoid receptor-mediated relaxation (e.g. Dumas et al., 1997; Lombard et al., 1999; Schubert et al., 1996, 1997). These diverse responses to prostacyclin mimetics remain largely uncharacterized and, moreover, few studies have considered sex as a factor when characterizing prostacyclin-memetic mediated vascular responses.

Previously, large conductance **calcium activated potassium channels ($K_{Ca}1.1$/BK_{Ca}**; Schubert et al., 1997), **ATP-sensitive potassium channels (K_{ATP}**; Lombard et al., 1999; Schubert et al., 1997) and **inwardly rectifying potassium channels (K_{IR}**; Orie et al., 2006) have been identified as the downstream targets of IP receptor-mediated vasorelaxation. Voltage-gated potassium channels encoded by *KCNQ1-5* genes (termed **$K_V7.1$-5** channels) are voltage-gated potassium channels with a negative threshold for activation that have well-identified roles in maintaining resting excitability in neurones, cardiac myocytes, epithelia and smooth muscle cells (Barrese et al., 2018). Of the five subtypes genes, ***Kcnq1***, ***4*** and ***5*** are robustly expressed in arterial smooth muscle (Barrese et al., 2020; Mackie et al., 2008; Yeung et al., 2007) and blockers of the expressed channels elicit contraction or enhanced vasoconstrictor response (e.g. Mackie et al., 2008; Yeung et al., 2007). K_V7 channels are also key functional components of vasorelaxations generated by several agonists of G_s-linked receptors including β-**adrenoceptor**s (Chadha, Zunke, Zhu, et al., 2012; Stott et al., 2016), **calcitonin gene-related peptide receptors** (Chadha et al., 2014; Stott et al., 2018) and **adenosine receptors** (Khanamiri et al., 2013). Additionally, novel findings implicate sexual dimorphisms in channel physiology (Abbott & Jepps, 2016; Alzamora et al., 2011) and pathophysiology (Berg, 2018).

As the contribution of K_V7 channels to prostanoid receptor-mediated relaxations is unknown, we sought to determine whether K_V7 channels were involved with prostacyclin mimetic-mediated responses in rat mesenteric arteries from aged-matched male and female rats. This artery was chosen because (1), K_V7 expression has been established (Jepps et al., 2011, 2015; Mackie et al., 2008), (2) K_V7 activators are effective relaxants (Jepps et al., 2014), (3) a role for K_V7 channels in $G_{\alpha s}$-linked responses has been identified (e.g. Lindman et al., 2018; Stott et al., 2016, 2018) and (4), endothelium dependent production of PGI_2 mediates concomitant IP receptor-mediated relaxation (Liu et al., 2012) and TP/EP_3-mediated contraction (Liu et al., 2012, 2017). Moreover, in line with Docherty et al. (2019), we investigated possible sex difference as nothing is known about the impact of sex on prostanoid-mediated vascular responses. To circumvent the short half-life of prostacyclin, we characterized the contribution of EP_3 and IP receptors to responses mediated by its stable analogue iloprost and defined the contribution of K_V7 channels to IP receptor-mediated vasorelaxation using a selective IP receptor agonist, **MRE-269**. Our data demonstrate a striking sex-dependent difference in response to iloprost and a role for $K_V7.1$ channels in shaping IP receptor-evoked vasorelaxation within rat mesenteric arteries, which is oestrus cycle sensitive.

What is already known

- The prostacyclin analogue iloprost evokes vasoactive responses through a myriad of receptors.
- K_V7 channels are targets of endogenous vasoactive signalling cascades.

What does this study add

- Iloprost evoked biphasic relaxant-contrail responses in males, which is absent in females.
- $K_V7.1$ inhibition impairs MRE-269 mesenteric arteries relaxation which is affected by the oestrus cycle.

What is the clinical significance

- Sex must be considered as a factor when considering prostacyclin mimetics as a therapeutic tool.

2 | METHODS

2.1 | Animal models

Animal studies are reported in compliance with the ARRIVE guidelines (Percie du Sert et al., 2020) and with the recommendations made by the *British Journal of Pharmacology* (Lilley et al., 2020). Experiments were performed on arteries from male and female Wistar rats (RRID: RGD_734476, Charles River, Margate, UK) ages 11–14 weeks (200–350 g) housed at the Biological Research Facility, St George's, London, UK. A maximum of 5 rats were housed in NKP cages with free access to water and food (RM1; Dietex Inter-national, UK) with a 12-h light/dark cycle and constant temperature and humidity (21 ± 1°C; 50% ± 10% humidity) in accordance with the Animal (Scientific Procedures)

Act 1986. Animals were kept in LSB Aspen woodchip bedding. Animals were killed by cervical dislocation with secondary confirmation via cessation of the circulation by femoral artery severance in accordance with Schedule 1 of the ASPA 1986.

For the following investigations, second-order mesenteric arteries were used, identified as the second bifurcation of the superior mesenteric artery. Arteries were dissected, cleaned of fat and adherent tissue and stored on ice in physiological salt solution (PSS) of the following composition (mmol·L^{-1}): 119 NaCl, 4.5 KCl, 1.17 $MgSO_4{\cdot}7H_20$, 1.18 NaH_2PO_4, 25 $NaHCO_3$, 5 glucose, 1.25 $CaCl_2$.

2.2 | Oestrus cycle stage determination

After killing, 50 µl of PSS was inserted into the vaginal canal via a 2- to 200-µl pipette tip and flushed four to six times to liberate cells from the surface of the cervix and then stored on ice; 25 µl of the subsequent cell suspension was mounted on a glass slide and examined under light microscopy (×10 to ×20 magnification). Previously described changes in cervical cell histology allowed for the determination of oestrus cycle stage (Cora et al., 2015) as either (in order of the 4–5 day cycle) pro-oestrus, oestrus, metoestrous or dioestrus. Cycle stage determination was performed post-experiment during functional investigation as a means of blinding; this was not possible during molecular techniques.

2.3 | Wire myography

For functional investigations, ~2-mm arterial segments were mounted on a 40-µm tungsten steel wire within a myograph chamber (Danish Myo Technology, Arhus, Denmark) containing 5 ml of PSS (composition described above) oxygenated with 95% O_2 and 5% CO_2 at 37°C. Vessels then underwent a passive force normalization process to achieve an internal luminal circumference at a transmural pressure of 100 mmHg (13.3 kPa) to standardize pre-experimental conditions (Mulvany, 1977). Force generated was first amplified by a PowerLab (ADInstruments, Oxford, UK) and then recorded via LabChart software (RRID:SCR_017551; ADInstruments, Oxford, UK). Vessels were then challenged with isotonic high K^+ physiological salt solution (K^+PSS) of the following composition (mmol·L^{-1}): 63.5 NaCl, 60 KCl, 1.17 $MgSO_4{\cdot}7H_20$, 1.18 NaH_2PO_4, 25 $NaHCO_3$, 5 glucose, 1.25 $CaCl_2$, to determine viability. Vessels were then constricted with 10 µmol·L^{-1} **methoxamine**, an **α_1-adrenoreceptor** agonist, and endothelial cell integrity was determined via vasorelaxation in response to 10 µmol·L^{-1} of the synthetic acetylcholine analogue, **carbachol**, prior to investigation. Subsequently, vessels were preconstricted with 300 nmol·L^{-1} thromboxane A_2 mimetic **U46619**. Following which single dose responses or cumulative concentration effect curve were generated in response to either prostacyclin mimetic iloprost (0.001–3 µmol·L^{-1}), IP receptor agonists **selexipag** (0.03–3 µmol·L^{-1})/MRE-269 (0.01–1/0.01–3 µmol·L^{-1}), β-adrenoreceptor agonist **isoprenaline** (0.03–3 µmol·L^{-1}) or K_V7.1 activator **ML277**. Vessels were pre-incubated in the presence or absence of a combination of solvent control dimethyl sulphoxide (DMSO) or antagonists of the following: - IP prostanoid receptor-**CAY10441 (RO1138452**; 100 nmol·L^{-1}); EP_3 prostanoid receptor-**L-798,106** (300 nmol·L^{-1}); pan-K_V7 channel, **linopirdine** (10 µmol·L^{-1}); K_V7.1, **HMR-1556** (10 µmol·L^{-1}); **adenylate cyclase** ,SQ22,562 (10 µmol·L^{-1}); **PKA**, Rp-8-Br-cAMP/KT5720 (1 µmol·L^{-1}); **EPAC** (100 nmol·L^{-1}); $G_{\beta\gamma}$, M119K (10 µmol·L^{-1}); BK_{Ca}/K_{Ca}1.1, **iberiotoxin** (100 nmol·L^{-1}); K_{ATP}, **glibenclamide** (1 µmol·L^{-1}) for a period of 10 min.

2.4 | Reverse transcription quantitative polymerase chain reaction

mRNA from whole mesenteric arteries was extracted using Monarch Total RNA Miniprep Kit (New England BioLabs, Ipswich, Massachusetts, USA) and reverse transcribed via LunaScript RT SuperMix Kit (New England BioLabs, Ipswich, Massachusetts, USA). Quantitative analysis of relative gene expression was determined via CFX-96 Real-Time PCR Detection System (RRID:SCR_018064, BioRad, Hertfordshire, UK). Samples were run in BrightWhite qPCR plate (Primer Design, Camberley, UK) in combination with PrecisionPLUS qPCR Master Mix (Primer Design, Camberley, UK), 300 nmol·L^{-1} of gene specific target primer (Thermofisher scientific, Waltham, Massachusetts, USA) and 10-ng cDNA as per manufacturers instruction. Quantification cycle (Cq) was determined via Bio-Rad CFX96 Manager 3.0. Cq values are expressed as normalized values to appropriate, stable, housekeeper genes ($2^{-\Delta Cq}$) calnexin (*Canx*) and cytochrome C1 (*Cyc1*) chosen for their stable, and similar Cq values. Housekeeper genes were acquired from Primer Design (Camberley, UK); as such, for proprietary reasons, the sequences are not disclosed. See Table 1 for a list of primers used in the following investigation.

2.5 | Morpholino transfection

Knockdown of K_V7.1 in whole mesenteric arteries was performed by transfection with morpholinos that prohibit protein translation but do not affect transcript levels (see Barrese et al., 2020; Jepps et al., 2015). Either K_V7.1 morpholino nucleotides or mismatch controls (5 µmol·L^{-1}, RRID:SCR_005663, Genetools, USA) were mixed with Lipofectamine 2000 (ThermoFisher, Paisley, UK) and Opti-MEM (Sigma, UK) and left at room temperature for 2 h. Morpholino/Lipofectamine/Opti-MEM mixture was added to Dulbecco's modified Eagle medium (DMEM) F-12 (Sigma, UK) containing 1% penicillin/streptomycin. Arteries were added and left for 48 h at 37°C with 5% CO_2.

2.6 | Immunocytochemistry

The Immuno-related procedures used comply with the recommendations made by the *British Journal of Pharmacology* (Alexander et al., 2018). Vascular smooth muscle cells were isolated from morpholino-transfected mesenteric arteries via incubation in isolation PSS of the following composition (mmol·L^{-1}): 120 NaCl, 6 KCl,

TABLE 1 RT-qPCR primer sequences

Gene name	(+) Forward primer sequence 3′-5′ (−) Reverse primer sequence 5′-3′	Gene accession number	Amplicon	Concentration
EP_1 (*Ptger1*)	(+) AGTTCGAACGTTGGTCACGA (−) TAAGGTTGCAGCATTGTGCG	NM_001278475.1	112	300 nmol·L^{-1}
EP_2 (*Ptger2*)	(+) TATGCTCCCTGCCTTTCACAA (−) GGAGGTCCCACTTTTCCTTT	NM_031088.2	72	300 nmol·L^{-1}
EP_3 (*Ptger3*)	(+) GTGCAATTCCTTCCTAATCGCC (−) TCAGGTTGTTCATCATCTGGCA	NM_012704.1	122	300 nmol·L^{-1}
EP_4 (*Ptger4*)	(+) ATGAGCATTGAGCGCTACCT (−) AGATGCATAGACGGCGAAGA	NM_032076.3	102	300 nmol·L^{-1}
IP (*Ptgir*)	(+) TGACACTTTCGCCTTCGCTA (−) TAGATGGCAGGCAAAGCCAA	NP_001071112.1	156	300 nmol·L^{-1}
TXA2 (*Tbxa2r*)	(+) TTGACATTCCCAGGCCCAAA (−) ACGTGATAAGGGGGTCAACA	NM_017054.2	141	300 nmol·L^{-1}
Clnexin (*Canx*)	N/A (Primer design, Camberley, UK)			300 nmol·L^{-1}
Cytochrome C1 (*Cyc1*)	N/A (Primer design, Camberley, UK)			300 nmol·L^{-1}

12 glucose, 10 HEPEs and 1.2 $MgCl_2$ supplemented with 1.75 mg·ml^{-1} Collagenase Type IA, 0.9 mg·ml^{-1} protease, 1 mg·ml^{-1} trypsin inhibitor and 1 mg·ml^{-1} bovine serum albumin (Sigma, UK) at 37°C for 17 min. Vessels then underwent mechanical trituration by wide bore glass pipette to liberate vascular smooth muscle cells. The subsequent cell suspension was plated onto 13-mm coverslips in a 24-well plate, supplemented with an equal volume of Ca^{2+} (2.5 mmol·L^{-1}) containing PSS and left to attach for 1 h.

Vascular smooth muscle cells were fixed in 3% paraformaldehyde for 15 min and then stored at 4°C in PBS prior to staining. Cells were then incubated in the following: 100 mmol·L^{-1} glycine in PBS, 5 min; blocking solution (PBS containing 0.1% Triton X-100 and 10% FBS in PBS), 45 min; primary antibody (K_V7.1, 1:100, Rabbit, Pineda Antikörper-Service, Germany), overnight at 4°C. The following day, cells were incubated in secondary antibody (Goat anti-rabbit IgG [H + L] cross-absorbed secondary antibody, Alexa Fluro™ 568, 1:100, Goat, RRID:AB_143157, ThermoFisher, UK), then mounted in Vectasheild (Sigma, P4170). Cells were imaged via Nikon A1R confocal microscope (inverted) on Ti2 chassis (Image Resource Facility, St George's University, London), and total cell fluorescence was analysed using ImageJ (RRID:SCR_003070) software.

2.7 | Cell culture

The K_V7.1 antibody was validated using Chinese Hamster Ovarian (CHO) cells (RRID:CVCL_0213) overexpressing KCNQ1. CHO cells were grown in DMEM/F-12 (Sigma, UK) supplemented in 1% penicillin/streptomycin in an incubator with 5% CO_2 at 37°C. CHO cells were incubated with either a total of 3 μg of plasmid containing *Kcnq1* (University of Copenhagen, Denmark) in a Lipofectamine 2000/Opti-MEM mixture (*Kcnq1*-transfected CHO), or lipofectamine/Opti-MEM only for 24 h (nontransfected CHO). Cells were mounted onto glass coverslips, fixed and stained for K_V7.1 as above. Antibody specificity demonstrated by positive staining for K_V7.1 (Pineda Antikörper-Service, Germany) in *Kcnq1*-transfected CHO cells (Figure S1A), but not non-transfected CHO cells (Figure S1B).

2.8 | Materials

All drugs for the following investigation were procured from Tocris Bioscience (Oxford, UK). Excluding CAY-10441 and MRE-269, which were acquired from Cayman chemical (Michigan, USA), Rp-8-Br-cAMP which was aquired from Sigma-Aldrich (UK) and M119K which was provided by the National Cancer Institute Drug Development Programme. All drugs were dissolved in DMSO and final vehicle concentrations were always ≤0.01. For materials regarding morpholino transfection, immunodetection or RT-qPCR, see relevant sections above.

2.9 | Data and statistical analysis

All values are expressed as mean ± standard error of the mean (SEM) for no less than five independent data points, excluding measurement of total cell fluorescence during immunocytochemistry, in which 10 cells were measured per cell. For isometric tension recordings, single dose responses to iloprost are expressed as (%) change from stable tone in response to 300 nmol·L^{-1} U46619, contractions from basal tone are expressed as (%) contraction when normalized to vasoconstriction to 10 μmol·L^{-1} methoxamine and all cumulative concentration effect curves are expressed as (%) stable contraction in response to 300 nmol·L^{-1} U46619. This is to account for changes in vessel contractility. For functional experiments involving cumulative concentration effect curves, a transformed data set was generated using; X = Log(X), to reduce representative skew. Following which, either a four parametric linear regression analysis was performed using either (Log(Agonist) vs. response variable slope [four parameters Bottom/Hillslope/top/EC_{50}]) using GraphPad Prism (RRID:SCR_002798, Version 9.0.0) to fit a cumulative concentration effect curve to the figure.

When generating data with morpholino-transfected arteries, the investigator was blinded, whereby a second researcher would mount the vessels and then post-investigation reveals which arteries had been transfected with scrambled control or *Kcnq1* targeted morpholino. Blinding for the remaining investigations was impractical because researchers were working in isolation during the COVID-19 pandemic. However, vessel segments were cut prior to mounting during isometric tension recording and invert in an Eppendorf suspended in PSS. In doing so, vessel segments either proximal or distal to the bifurcation from first-order mesenteric arteries were randomly selected for drug treatments. For data comparing multiple groups, a paired Student's t-test or a two-way ANOVA was performed for comparison of mean values. If statistical significance was achieved up two-way ANOVA ($P < 0.5$), a post hoc Bonferonni (for comparing one condition against control) test or Dunnett's (for comparing multiple conditions against control) test was also performed to generate corrected significance values. Significant values are represented as $P < 0.05$ (*/#). Sample sizes subject to statistical analysis contain at least 5 animals per group, where n= number of independent values. Investigations expressing groups. Investigations expressing groups of unequal numbers were gathered due to technical failure or an artefact of cycle stage determination post-experiment during functional investigations. The data and statistical analysis comply with the recommendations of the *British Journal of Pharmacology* on experimental design and analysis in pharmacology in accordance with Curtis et al. (2018).

2.10 | Nomenclature of targets and ligands

Key protein targets and ligands in this article are hyperlinked to corresponding entries in the IUPHAR/BPS Guide to PHARMACOLOGY http://www.guidetopharmacology.org and are permanently archived in the Concise Guide to PHARMACOLOGY 2021/22 (Alexander, Christopoulos, et al., 2021; Alexander, Mathie, et al., 2021).

3 | RESULTS

3.1 | Iloprost-mediated vasoactive responses

In mesenteric arteries from male rats stably contracted by U46619 (300 nmol·L^{-1}), iloprost (0.1–3 μmol·L^{-1}) evoked a biphasic response, producing relaxation at lower concentrations followed by contraction at concentrations >300 nmol·L^{-1} (Figure 1a,b, black). This phenomenon was notably absent in mesenteric arteries from female rats, wherein iloprost only evoked concentration-dependent vasorelaxation (Figure 1a,b, red). See representative traces in Figure 1a. Application of solvent control had negligible effect on established tone in mesenteric arteries from either male or female rats (Figure 1b). For concentration effect curves generated in response to iloprost on precontracted tone, see Figure S2. Prostacyclin-mediated relaxations are conventionally mediated via activation of IP receptors, while EP_3 receptors have been implicated in contractile responses to iloprost in mesenteric arteries from hypertensive rats (Liu et al., 2017). To establish the role of these receptors in the biphasic or monophasic response observed in male and female rats, respectively, vessels were preincubated in either EP_3 receptor antagonist L-798,106 (300 nmol·L^{-1}) or IP receptor antagonist CAY-10441 (100 nmol·L^{-1}).

In the presence of the EP_3 receptor antagonist L-798,106, 1 μmol·L^{-1} iloprost-mediated contraction was converted to a relaxation (Figure 2a). In mesenteric arteries from females, EP_3 receptor blockade had no effect (Figure 2a). In the presence of IP receptor antagonist CAY-10441, 0.3 μmol·L^{-1} iloprost-mediated relaxation was abolished in both groups (Figure 3a,b; $P \geq 0.05$). Similarly, 3 μmol·L^{-1} iloprost evoked significantly greater contraction from

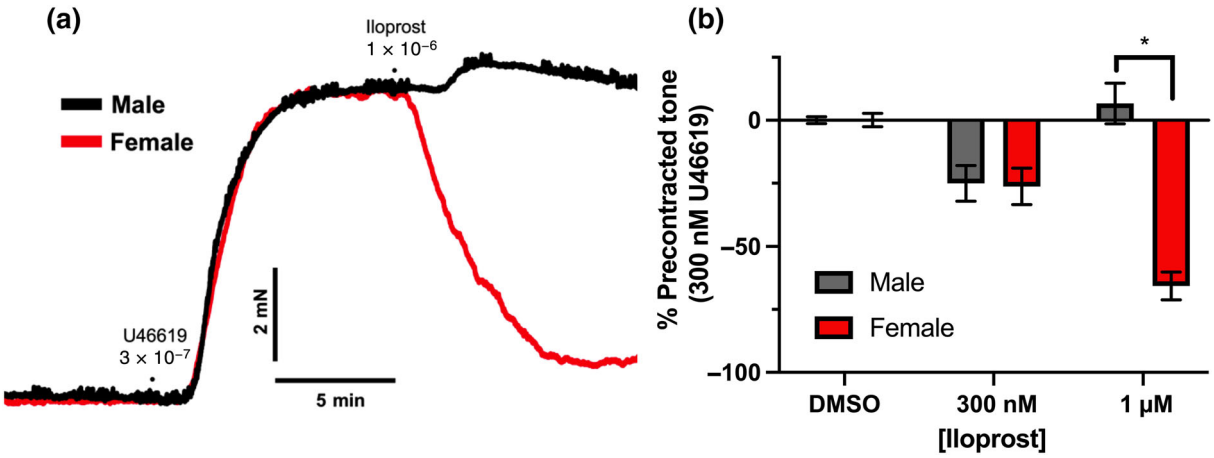

FIGURE 1 Iloprost evokes biphasic vasoactive responses within male, but not female mesenteric arteries. Representative traces of iloprost (0.3–1 μmol·L^{-1}) mediated vasoactive responses on precontracted tone (300 nmol·L^{-1} U46619) within mesenteric arteries from male (a; black) or female (a; red) Wistar rats. Mean data for DMSO solvent control and iloprost-mediated vasoactive responses on precontracted (300 nmol·L^{-1} U46619) mesenteric arteries (a; 0.3–1 μmol·L^{-1}; $n = 6–8$). All values are expressed as mean ± SEM. A two-way statistical ANOVA with a post-hoc Bonferroni test was used to generate significance values ($^*P < 0.05$). n = number of animals used

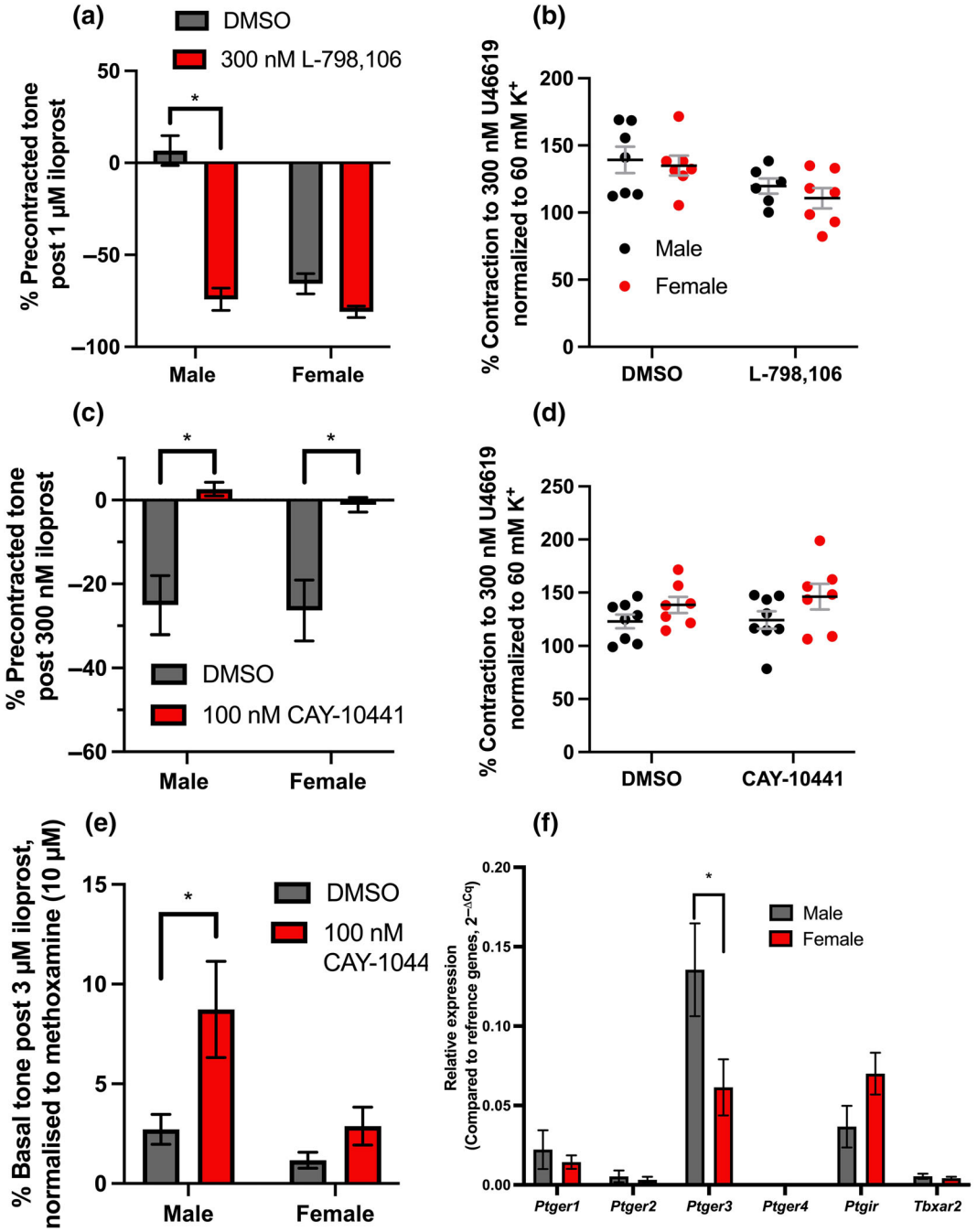

FIGURE 2 Iloprost-mediated contraction and relaxation is blocked by EP_3 and IP receptor-mediated inhibition, respectively. Mean data for iloprost-mediated vasoactive responses (a, 1 µmol·L^{-1}; c, 300 nmol·L^{-1}) within precontracted (300 nmol·L^{-1} U46619) mesenteric arteries from male and female rats preincubated in either solvent control (DMSO; a,c; $n = 6–8$), 300 nmol·L^{-1} L-798,106 (a; $n = 6–8$) or 100 nmol·L^{-1} CAY-10441 (c; $n = 6–8$). Scatter graph showing individual and mean values of stable precontracted tone from male and female arteries prior to adding iloprost to the chamber (b,d). Mean data for vasoconstriction from base line tension in response to 3 µmol·L^{-1} iloprost in male (black; $n = 7$) and female (red; $n = 10$) mesenteric arteries in the presence of DMSO or 100 nmol·L^{-1} CAY-10441 normalized to peak contraction in response to 10 µmol·L^{-1} methoxamine (e). Relative gene expression of prostanoid receptors (*Ptger1–4* = $EP_{1–4}$, *Ptgi* = IP, *Tbxar2* = TXA_2) normalized to stable housekeeper genes (*Canx*, *Cyc1*) expressed as $2^{-\Delta Cq}$ from male (black; $n = 5$) and female (red; $n = 5–10$) whole mesenteric artery lysates (f). A two-way statistical ANOVA with a post-hoc Bonferroni test was used to generate significant values ($^*P < 0.05$). n = number of animals used

base-line tone in mesenteric arteries from male rats preincubated in CAY-10441 when compared to mesenteric arteries from female rats (Figure 3e). No differences were observed in precontracted tone in vessels preincubated in either L-798,106 or CAY-10441 when compared to DMSO solvent control or between the sexes (Figure 2b/d). Subsequently, we performed quantitative PCR to determine the relative expression of prostanoid receptors (Table 1) in the mesenteric arteries from both sexes. Figure 2.F shows that expression of *Ptger2/4*

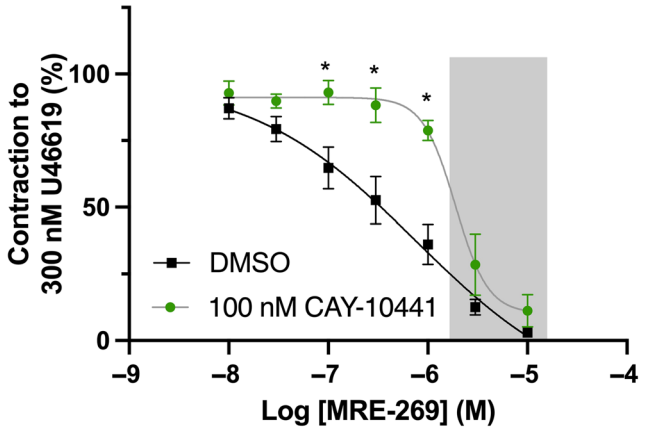

FIGURE 3 MRE-269 relaxation is inhibited by CAY-10441 to a threshold of 1 μmol·L^{-1} in male mesenteric arteries. Mean data of MRE-269 (0.01–10 μmol·L^{-1}) mediated relaxation of precontracted arterial tone (300 nmol·L^{-1}) in vessels preincubated in DMSO solvent control (black; $n = 7$) or 100 nmol·L^{-1} CAY-10441 ($n = 5$) in male mesenteric arteries. Grey box demonstrates non-CAY-10441 sensitive MRE-269-mediated relaxation. All values are expressed as mean ± SEM. A two-way statistical ANOVA with a post-hoc Bonferroni test was used to generate significant values ($^*P < 0.05$). n = number of animals used

($EP_{2/4}$) was negligible in mesenteric arteries from both sexes compared to *Ptger3* > *Ptgir* > *Ptger1* (EP_3; IP; EP_1), which were well expressed (Figure 2f). However, *Ptger3* was expressed at significantly lower level in mesenteric arteries from female rats compared to mesenteric arteries from males (Figure 2f). Thus, our data demonstrate that iloprost-mediated relaxation in rat mesenteric arteries occurs predominantly via IP receptors, while contraction was caused by activation of EP_3 receptors. Additionally, the absence of a biphasic response to iloprost in female mesenteric arteries was associated with a comparably smaller effect of EP_3 receptor inhibition on iloprost-mediated relaxation and a reduction in *Ptger3* expression.

3.2 | Characterizing MRE-269-mediated relaxation

As iloprost has a plethora of potential targets, we used the clinically available IP receptor agonist, selexipag (NS-304), to delineate the mechanisms underlying IP-mediated relaxation. Application of selexipag produced concentration-dependent relaxations of precontracted mesenteric arteries from male rats (Figure S3). However, this effect was insensitive to preincubation with IP receptor antagonist CAY-10441 (Figure S3) thus, selexipag effects are non-IP

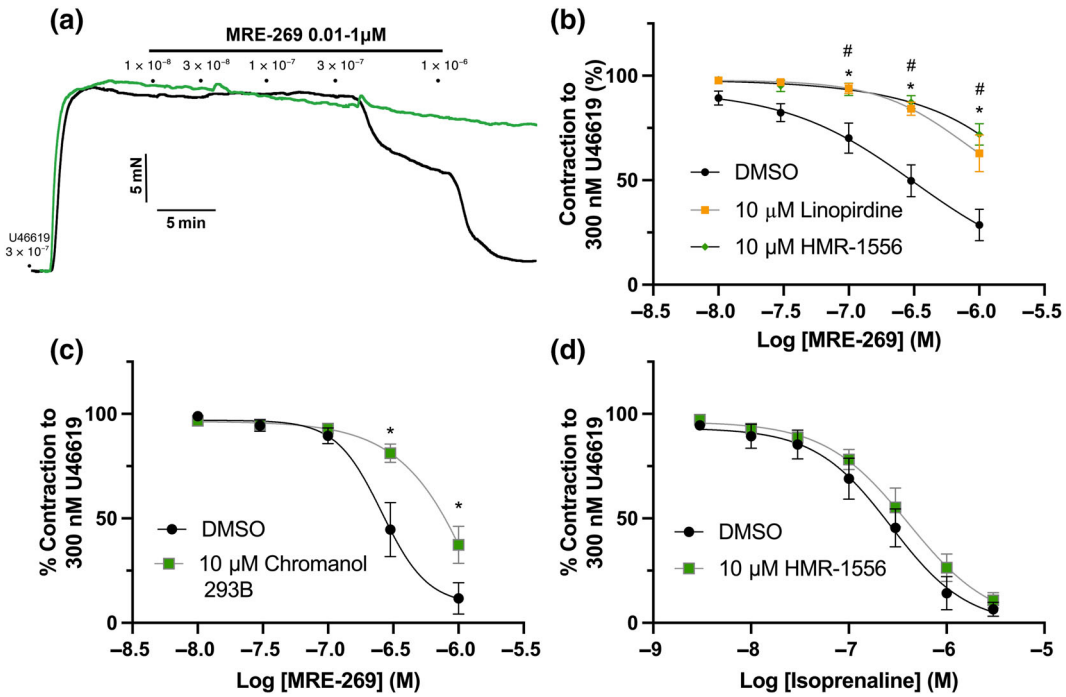

FIGURE 4 Linopirdine and HMR-1556 attenuate MRE-269-mediated vasorelaxation in mesenteric arteries from male and female rats. Representative traces of MRE-269-mediated (0.01–1 μmol·L^{-1}) relaxation of precontracted tone (300 nmol·L^{-1} U46619) within mesenteric arteries preincubated in either DMSO solvent control (a; black) or 10 μmol·L^{-1} $K_V7.1$ specific blocker HMR-1556 (a; green) from male Wistar rats. Mean data for MRE-269-mediated vasorelaxation (0.01–1 μmol·L^{-1}) of precontracted tone (300 nmol·L^{-1} U46619) within mesenteric arteries preincubated in either DMSO (b; black) solvent control, 10 μmol·L^{-1} pan-K_V7 channel blocker linopirdine (b; yellow) or HMR-1556 (b; green) or 10 μmol·L^{-1} $K_V7.1$ seelective blocker Chromanol 293B (c; green; $n = 7$–10). Mean data for isoprenaline-mediated relaxation in vessels preincubated in DMSO (black) or 10 μmol·L^{-1} HMR-1556 (green) in male mesenteric arteries (d; $n = 9$). All values are expressed as mean ± SEM (a–f). A two-way statistical ANOVA with a post-hoc Dunnet (b) or Bonferroni (c,d) test was used to generate significant values ($^*P < 0.05$). n = number of animals used

receptor dependent. It is now known that in the body, selexipag is metabolized into the active compound, inhibited by CAY-10441 pre-incubation up to threshold of 1 μmol·L^{-1}. At higher concentrations, the MRE-269-mediated relaxation was not sensitive to CAY-10441 and therefore does not involve IP receptor activation. This non-IP receptor-mediated relaxation is highlighted by the grey box in Figure 3 and in the following investigations, MRE-269 was used at concentrations ≤1 μmol·L^{-1} to ensure only IP receptor-mediated effects were investigated.

3.3 | A novel role for K_V7.1 in shaping IP receptor-selective agonists in mesenteric arteries

Kv7 channels, especially Kv7.4 and Kv7.5, are functional endpoints for several G_s-linked receptors (see Barrese et al., 2020; Byron & Brueggemann, 2018). As such, we characterized the potential contribution of K_V7 channels to IP-receptor selective MRE-269-mediated relaxation. In mesenteric arteries from male rats, MRE-269-mediated relaxation was significantly attenuated by preincubation with the pan-K_V7 channel inhibitor linopirdine (10 μmol·L^{-1}; yellow) when compared to DMSO (Figure 4, black). Strikingly, preincubation with the K_V7.1 selective inhibitor HMR-1556 (10 μmol·L^{-1}) also inhibited MRE-269-induced relaxations to the same extent as linopirdine (Figure 4a,b, green;). The structurally dissimilar K_V7.1 inhibitor chromanol 293B (3S,4R-293B) also significantly attenuated MRE-269-mediated relaxation of male mesenteric arteries (Figure 4c). In contrast and consistent with previous reports (Stott et al., 2016), relaxations of mesenteric arteries induced by the mixed β-adrenoceptor agonist isoprenaline were not affected by pre-incubation with 10 μmol·L^{-1} HMR-1556 (Figure 4d).

To corroborate the contribution of K_V7.1 to IP receptor-mediated vasorelaxation, we transfected mesenteric arteries with morpholinos that prevent translation of Kv7.1 or a scrambled control. Immunocytochemistry with an antibody for K_V7.1 validated by overexpression studies (Figure S1) showed a significant reduction in total cell fluorescence (A.U) in *Kcnq1* morpholino-transfected arteries when compared to mismatch control (Figure 5a–c). Functionally, arteries incubated

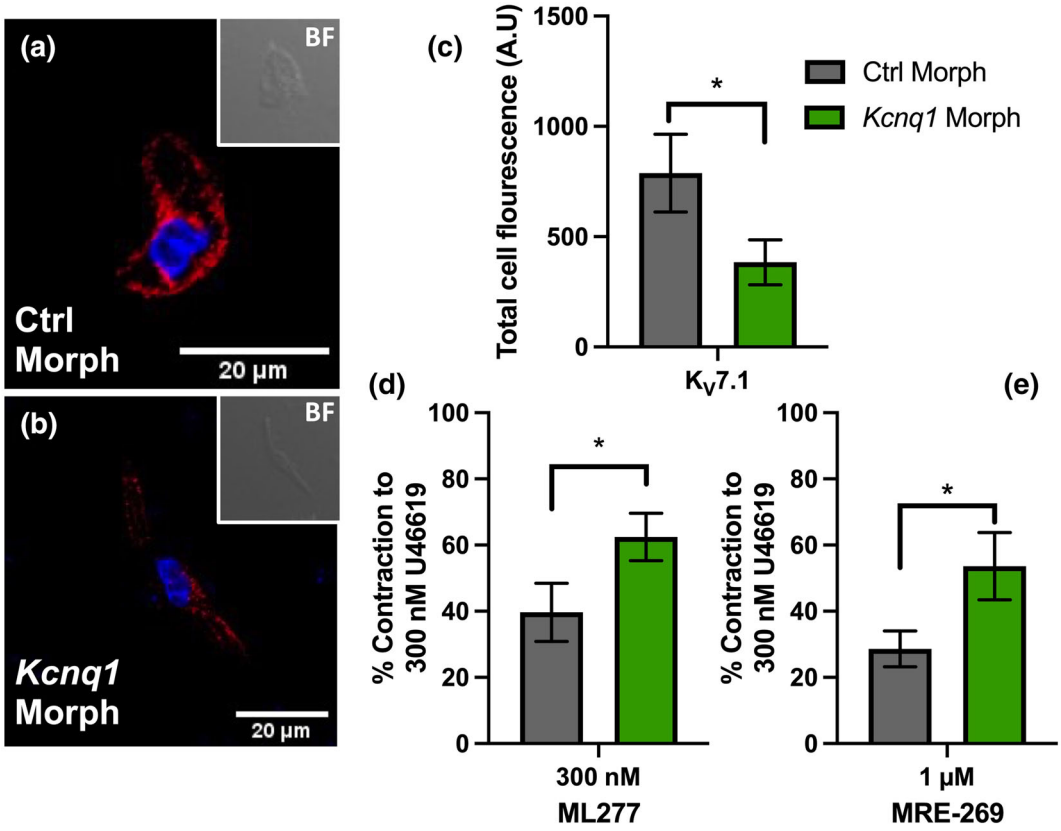

FIGURE 5 Molecular interference of *Kcnq1* via targeted morpholino knockdown impairs MRE-269-mediated relaxation. Representative immunofluorescence showing K_V7.1 in isolated vascular smooth muscle cells from either scrambled control (Ctrl morph; a) or *Kcnq1* (*Kcnq1* morph; b) morpholino-transfected mesenteric arteries. K_V7.1 shown in red, nuclear staining in blue (DAPI [4′,6-diamidino-2-phenylindole, dihydrochloride]). Insets show brightfield (BF) images of the cell. Mean data for total cell fluorescence measured in arbitrary units (A.U) for Ctrl morph (grey; $n = 3$; $N = 10$) and *Kcnq1* morph (green; $n = 3$; $N = 10$; d) transfected cells. Mean data for 300 nmol·L^{-1} ML277-mediated relaxation ($n = 7$; e). Mean data for 1 μmol·L^{-1} MRE-269-mediated relaxation ($n = 7$; f). All values are expressed as mean ± SEM (a–f). A paired Student's *t*-test was used to generate significant values (*$P < 0.05$). n = number of animals used, N = number of cells per biological repeat

with mismatch control produced a significantly greater relaxant response to 300 nmol·L^{-1} K_V7.1 activator ML277 (Baldwin et al., 2020; Yu et al., 2013) compared to *Kcnq1* morpholino-transfected arteries (Figure 5d). Similarly, relaxation produced by 1 μmol·L^{-1} MRE-269 was greater in arteries transfected with mismatch control morpholino when compared *Kcnq1* morpholino-transfected arteries (Figure 5e). Thus, a reduction in K_V7.1 protein was observed in conjunction with an attenuated relaxation by MRE-269.

Subsequently, we aimed to determine the signalling cascade activated in response to IP receptor stimulation. Previously, Schubert et al. (1996) demonstrated that iloprost-evoked hyperpolarization of rat tail artery vascular smooth muscle cells is mediated via G_s–cyclic adenosine 3′-5′-monophosphate (cAMP)–protein kinase A (PKA) stimulation of potassium currents (Schubert et al., 1996) in a process attributed to IP receptors, although not fully defined. Here, we similarly demonstrate that adenylate cyclase inhibitor SQ22,562 (10 μmol·L^{-1}) and PKA inhibitors Rp8 (1 μmol·L^{-1}) and KT5720 (1 μmol·L^{-1}) significantly attenuated MRE-269-mediated relaxation (1 μmol·L^{-1}; $P \geq 0.05$; Figure 6a–c). In addition, inhibition of an alternative secondary signalling molecule activated by G_s–cAMP, exchange protein directly activated by cAMP (EPAC), via **ESI-09** had no effect

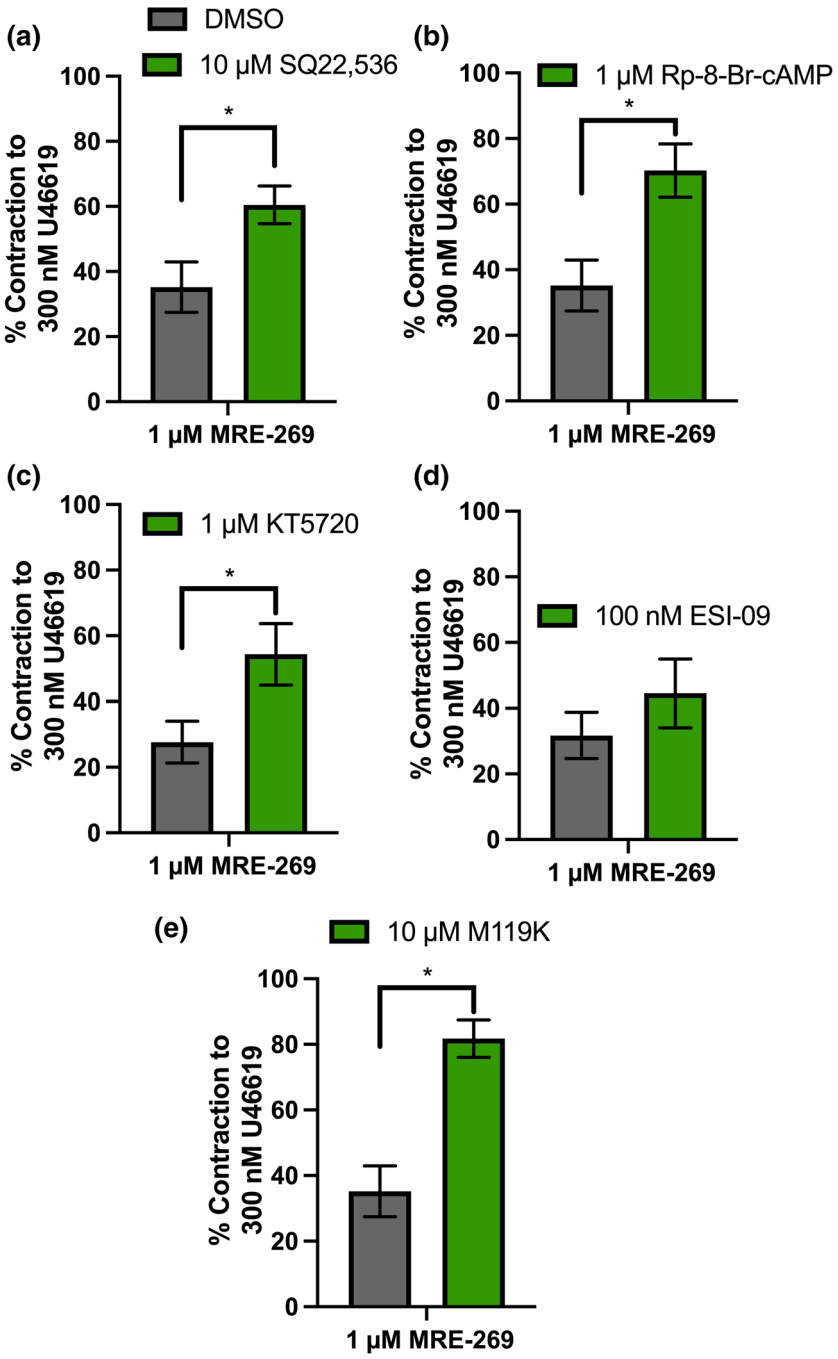

FIGURE 6 MRE-268-mediated relaxation is sensitive to adenylate cyclase, Gβγ and protein kinase A inhibition, but not effector protein activated by cAMP in male rat mesenteric arteries. Mean data for MRE-269-mediated vasorelaxation (1 μmol·L^{-1}) of precontracted tone (300 nmol·L^{-1} U46619) within mesenteric arteries preincubated in either DMSO (a–e; $n = 9$; grey) solvent control or inhibitors of the following (green); adenylate cyclase–SQ22,562 (10 μmol·L^{-1}; $n = 7$; a), protein kinase A–Rp-8-Br-cAMP (1 μmol·L^{-1}; $n = 5$; b)/KT5720 (1 μmol·L^{-1}; $n = 8$; c), effector protein inhibited by cAMP–ES09 (100 nmol·L^{-1}; $n = 8$; d) and Gβγ–ML119K (1 μmol·L^{-1}; $n = 7$; e). All values are expressed as mean ± SEM (a–e). An unpaired Students *t*-test was used to generate significant values ($^*P < 0.05$). n = number of animals used

(100 nmol·L^{-1}; Figure 6d). Finally, $G_{\beta\gamma}$ inhibition by M119K (1 μmol·L^{-1}) also significantly attenuated MRE-269-mediated relaxation (Figure 6e).

BK_{Ca} and K_{ATP} channels have also been identified as downstream targets of cAMP-PKA-dependent relaxations evoked by iloprost (Schubert et al., 1997). Here, we demonstrate that BK_{Ca} inhibitor iberiotoxin (100 nmol·L^{-1}) but not K_{ATP} inhibitor glibenclamide (1 μmol·L^{-1}) partially inhibited MRE-269-mediated relaxation in male mesenteric arteries (Figure S4A,B), though this failed to reach statistical significance.

3.4 | Oestrus cycle-dependent shifts in the sensitivity of MRE-269-mediated vasorelaxation to K_V7 channel modulators

The pan K_V7 channel inhibitor linopirdine and $K_V7.1$ channel inhibitor HMR-1556 also significantly attenuated MRE-269-mediated relaxation in mesenteric arteries from female rats when compared to DMSO solvent control (Figure 7a;), though the latter to a smaller degree when compared to linopirdine. However, we observed two-distinct populations of possible responses to MRE-269-mediated relaxation and its subsequent sensitivity to K_V7 channel modulators, categorized into rats in dioestrus/metestrus or proestrus/oestrus (Pro/Est). Oestrus cycle stage was identified by defined histological changes in cells lifted from the cervix after killing (as per methods; Cora et al., 2015). Both the pan-K_V7 channel inhibitor linopirdine and $K_V7.1$ selective inhibitor HMR-1556 impaired MRE-269-mediated relaxation to the same degree in arteries from female in dioestrus/metestrus (Figure 7b) but had no effect in arteries from rats in proestrus/oestrus (Figure 7c). Moreover, MRE-269-mediated relaxation in arteries from female proestrus/oestrus rats was significantly less sensitive to the IP-selective agonist than arteries from rats in dioestrus/metestrus (Figure 7d;). However, we observed no differences in $K_V7.1$ activator ML277 (0.1–0.3 μmol·L^{-1}) mediated relaxation on precontracted tone between the separated groups (Figure 7e). These data reveal an oestrus cycle stage-dependent regulation of the contribution of $K_V7.1$ to IP receptor-mediated relaxation, which underpins diminished sensitivity to MRE-269-mediated relaxation during proestrus/oestrus.

4 | DISCUSSION

To our knowledge, the present study is the first to highlight sex as a factor in the arterial response to prostacyclin mimetics. The study shows that application of iloprost to pre-contacted mesenteric arteries from male rats produced bimodal responses, relaxation at low concentrations, followed by contraction at higher concentrations, whereas mesenteric arteries from female arteries presented with monophasic relaxation only. In arteries from both sexes the relaxant effect of iloprost was enhanced by EP_3 receptor antagonist L-798106 and was blocked by IP receptor antagonist CAY-10441. Our data demonstrated iloprost-mediated contractions in mesenteric arteries from male rats were more efficacious when compared to vessels from females, correlating with a higher level of *Ptger*$_3$ expression. Finally, our data show that the selective IP receptor agonist MRE-269 was a potent relaxant of precontracted mesenteric arteries from both sexes. This relaxation was inhibited by both the pan-K_V7 blocker linopirdine and $K_V7.1$ selective blocker HMR-1556 in arteries from males and dioestrus/metestrus females but strikingly not proestrus/oestrus rats. These findings are the first observation of $K_V7.1$ as a downstream target of an endogenous vasoactive signalling cascade and reveal oestrus cycle-dependent regulation of K_V7 channels within the vasculature.

4.1 | Iloprost-evoked vasoconstriction

While principally regarded as a vasodilator, PGI_2 mediates both relaxation and contraction of smooth muscle (Dusting et al., 1977; Liu et al., 2017; Moncada et al., 1976). PGI_2 has subsequently been identified as an endothelial-derived contracting factor produced in response to acetylcholine within rat aorta (Gluais et al., 2005), mesenteric (Liu et al., 2017), iliac (Zhang et al., 2021) and renal arteries (Zhang et al., 2021) in a process attributed to the activation of both EP and TP prostanoid receptors. Consistent with Liu et al. (2017), we show that high concentrations of iloprost-evoked contractions were blocked by the EP_3 receptor antagonist L-798,106. As iloprost has a low affinity for TP receptors (Whittle et al., 2012), TP receptor knockout has no effect on PGI_2-mediated contraction in mesenteric arteries (Liu et al., 2017) and all vessels in this study were precontracted with U46619, a TP receptor agonist. TP receptors were not considered for the scope of this investigation. Additionally, EP_1 receptor agonists do not elicit contractions in male mesenteric arteries (Kobayashi et al., 2011), and in agreement with previous findings (Kobayashi et al., 2011), a reduced expression of *Ptger1* was observed when compared to *Ptger3*. Furthermore, iloprost had negligible contractile effect in mesenteric arteries from female rats, which was associated with a lower expression level of *Ptger3* in these arteries.

4.2 | $K_V7.1$ underpins IP receptor-mediated relaxation

Our data show that relaxations of mesenteric arteries mediated by low concentrations of iloprost were driven primarily through CAY-10441-sensitive IP receptor activation. We subsequently showed that CAY-10441-sensititve relaxations produced by the selective IP receptor agonist MRE-269 were impaired by the selective K_V7 channel blocker, linopirdine. Within the vasculature, of the five subtypes, *Kcnq4* > *Kcqn5* > *Kcnq1* are the principally expressed transcripts with little to no expression of *Kcnq2/3* (Chadha, Zunke, Zhu, et al., 2012; Jepps et al., 2011; Yeung et al., 2007). $K_V7.4$/$K_V7.5$ alone however are implicated in the regulation of the resting

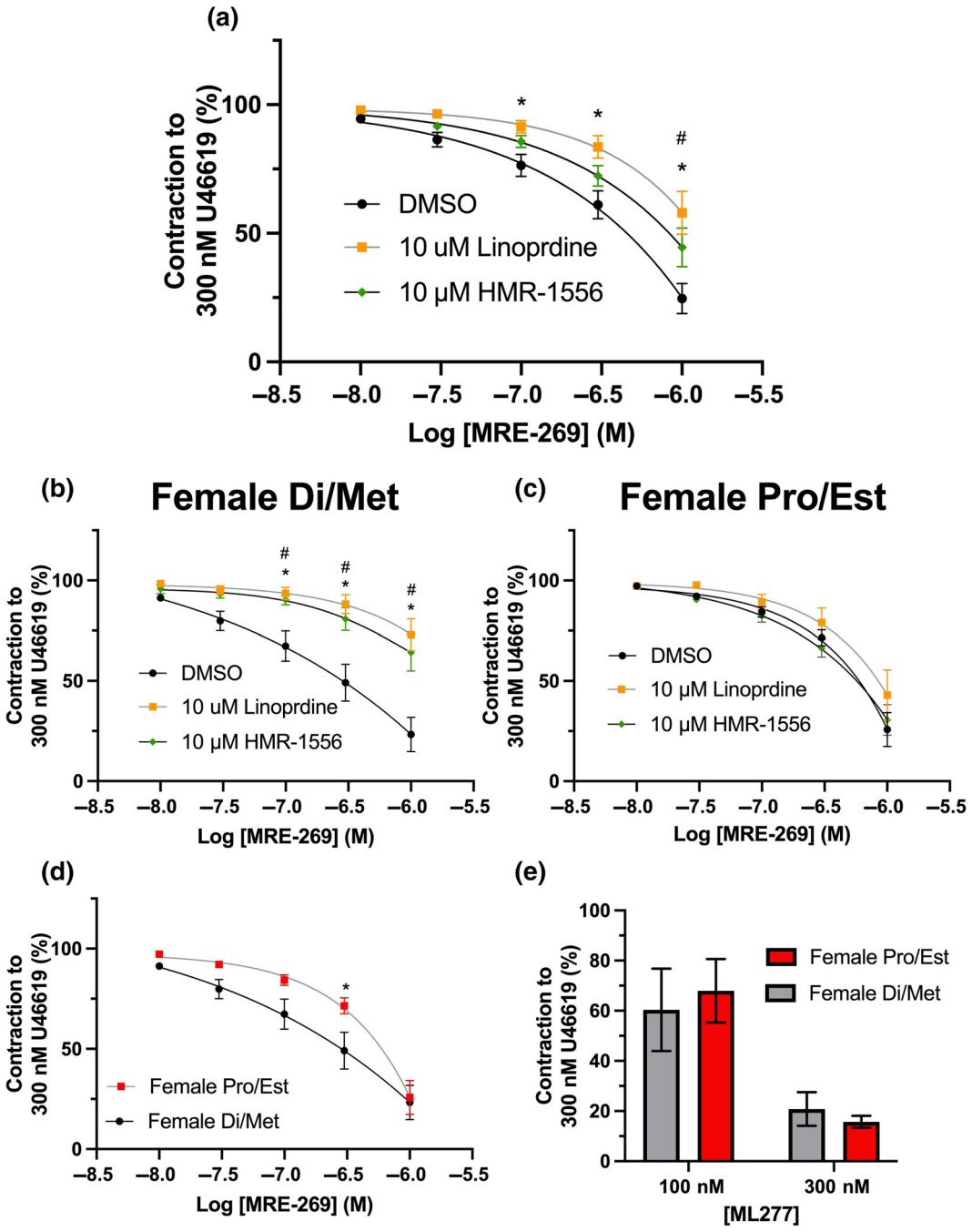

FIGURE 7 K_V7 channel inhibition attenuates MRE-269-mediated vasorelaxation in mesenteric arteries from dioestrus/metestrus (Di/Met), but not proestrus/oestrus (Pro/Est) female rats. Mean data for MRE-269-mediated vasorelaxation (0.01–1 µmol·L^{-1}) within mesenteric arteries preincubated in DMSO solvent control (a–c; black), 10 µmol·L^{-1} pan K_V7 channel inhibitor linopirdine (a–c; yellow) or 10 µmol·L^{-1} $K_V7.1$ specific inhibitor HMR-1556 (a–c; green) from female Wistar rats. Data are expressed as either all female (a), female Di/Met (n = 5–7; b) and female Pro/Est (n = 6–8; c). MRE-269 (0.01–1 µmol·L^{-1}; d) and ML277 (0.01–0.03 µmol·L^{-1}) mediated relaxation in vessels from either female Pro/Est (red; n = 6–8) or female Di/Met (black; n = 5–6). All values are expressed as mean ± SEM (a–e). A two-way statistical ANOVA with a post-hoc Dunnett's test (a–c) or Bonferroni test (d,e) was used to generate significant values ($^*P < 0.05$). n = number of animals used

membrane potential (Mackie et al., 2008) and basal tone (Mackie et al., 2008; Ng et al., 2011). In addition, pharmacological inhibition or molecular knockdown of $K_V7.4/7.5$ impairs relaxations to many different relaxants including isoprenaline, calcitonin gene-related peptide (CGRP), adenosine (G_s linked), atrial natriuretic peptide (ANP; cGMP linked) and adipose derived relaxant factors in several arteries (Byron & Brueggemann, 2018; Chadha et al., 2014; Gollasch, 2017; Khanamiri et al., 2013; Morales-Cano et al., 2015; Stott et al., 2016; Stott, Barrese, et al., 2015). Our data suggest that IP receptor activation in male mesenteric arteries involves another GPCR that also

relies on K_V7 channels for functional responses. In contrast to previous reports (Lombard et al., 1999; Schubert et al., 1997) IP receptor-mediated relaxation was not affected by K_{ATP} nor BK_{Ca} blockade. However, this discrepancy is potentially accounted for by a difference in vascular model used, as Lombard et al. (1999) investigated the rat middle cerebral artery and Schubert et al. (1997) used the rat tail artery.

Surprisingly, MRE-269-evoked CAY-10441-sensitive relaxations in mesenteric arteries from male rats were also potently inhibited by two structurally dissimilar $K_V7.1$ selective inhibitors (HMR-1556, chromanol 293B) and molecular knockdown of the channel. In contrast to $K_V7.4/K_V7.5$, the role of $K_V7.1$ within the vasculature remains enigmatic. Though $K_V7.1$ is expressed within vascular smooth muscle cells (Baldwin et al., 2020; Chadha, Zunke, Zhu, et al., 2012; Tsvetkov et al., 2017) and $K_V7.1$ selective activators RL-1 and ML277 are effective relaxants of precontracted arterial tone (Baldwin et al., 2020; Chadha, Zunke, Davis, et al., 2012), $K_V7.1$ has not been identified as the downstream target of any endogenous vasoactive signalling cascades (Chadha et al., 2014; Stott et al., 2016; Stott, Barrese, et al., 2015). Yet in the present study, HMR-1556 produced as full an inhibition as linopirdine, which suggests $K_V7.1$, and not $K_V7.4/7.5$, contributes to MRE-269-mediated relaxations. Under the same conditions, the mixed β-adrenoceptor agonist isoprenaline produced relaxations that were not HMR1556 sensitive. Thus, our findings appear not to be an off-target effect of HMR-1556. Moreover, a role for $K_V7.1$ in MRE-269-mediated relaxation was substantiated by morpholino-induced reduction in $K_V7.1$ protein levels. While further work is required to validate these findings, to our knowledge, the first to describe an effect on vascular reactivity by $K_V7.1$ inhibition is our data. Additionally, our data support the notion that IP receptor-mediated responses are cAMP-PKA mediated. In agreement with previous work done by our lab (Stott et al., 2016, 2018; Stott, Povstyan, et al., 2015), we demonstrate that relaxations that are mediated PKA, but not EPAC, are also sensitive to $G_{\beta\gamma}$ inhibition. The identification of $G_{\beta\gamma}$ contribution to IP receptor-mediated relaxation adds new complexity to the vascular response and gives credence to the novel role of $G_{\beta\gamma}$ in the functional relationship between GPCRs and K_V7s.

To date, comparably little is known as to how K_V7 channels operate within the female. However, K_V7 has been shown to regulate both human and murine myometrium (McCallum et al., 2009) and human chorionic plate artery (Mills et al., 2015) contractility. Intriguingly, while MRE-269-mediated relaxation was attenuated by linopirdine and HMR-1556 in arteries from female rats, the effect of the latter was far smaller than in the male. When separated into oestrus cycle stages, arteries from females in dioestrus/metestrus expressed sensitivities to HMR-1556 and linopirdine equivalent to the male, whereas arteries from females in proestrus/oestrus were entirely insensitive to either. However, $K_V7.1$ activator-ML277-mediated relaxation was insensitive to changes in the oestrus cycle. As the functional output of pharmacological activation of the channel remains the same, the data indicate an oestrus cycle-dependent impairment of $K_V7.1$ channel coupling to IP receptor-mediated relaxation. Oestrus cycle-dependent regulation of vascular reactivity is a known but incompletely understood phenomenon (Jaimes et al., 2019) largely attributed to endogenous sex-hormones, primarily, **17-β oestradiol.** 17-β oestradiol negatively regulates $K_V7.1$ in distal colic crypt cells and cardiac myocytes (Alzamora et al., 2011; O'Mahony et al., 2007; Rapetti-Mauss et al., 2013; Waldegger et al., 1996). As previous work demonstrates that within the Wistar rat, oestradiol peaks within pro-oestrus rats followed by comparably little to none in oestrus, metestrus and dioestrus (Nilsson et al., 2015), we propose that during pro-oestrus, oestradiol levels rise, impairing $K_V7.1$ coupling to IP receptor during proestrus/oestrus phase, thus reducing the potency of MRE-269-mediated relaxation and its HMR-1556/linopirdine sensitivity, which does not recover until dioestrus/metestrus. Our data imply an oestrus cycle.

4.3 | Perspectives

Sexual dimorphisms in cardiovascular physiology and pathophysiology are known (Pabbidi et al., 2018), whereby women express a cardioprotective factor or factors that differentiates the aetiology of vascular disease between age-matched men and women. Chronic **aldosterone** treatment in male Wistar–Kyoto rats induces hypertension through endothelial dysfunction attributed to upregulated COX-2 production of PGI_2 (Blanco-Rivero et al., 2005). Diminished EP_3-mediated contraction/expression in female rats may potentially negate the pathophysiological levels of PGI_2 production observed by Blanco-Rivero et al. (2005), contributing to the known cardioprotective phenotype expressed by females, though further work is required to validate this hypothesis.

5 | CONCLUSION

The data of the present study demonstrate a remarkable sexual dimorphism in the vascular response to synthetic prostacyclin analogues and highlight the importance of considering sex as a determinant in vascular physiology. Strikingly, the potent relaxations to the selective IP receptor agonist MRE-269 were sensitive to the Kv7.1-selective blocker HMR1556 in mesenteric arteries from males and females in dioestrus/metestrus but not at all in proestrus/oestrus. These novel findings demonstrate both a functional role for $K_V7.1$ in receptor mediated vascular reponses and cyclical changes in K_V7 channel activity across the oestrus cycle, and form the basis of future investigations.

ACKNOWLEDGEMENT

S.N.B was funded by the British Heart Foundation (Grant #FS/18/41/33762) awarded to I.A.G.

AUTHOR CONTRIBUTIONS

S.N.B designed and implemented all experiments. S.N.B, E.A.F and L. M performed experiments, generated and analysed data. S.N.B and I.A.G drafted the manuscript. I.A.G oversaw the project and prepared the submission of the paper. I.A.G provided funding.

CONFLICT OF INTEREST

The authors declare no conflict of interest.

DECLARATION OF TRANSPARENCY AND SCIENTIFIC RIGOUR

This Declaration acknowledges that this paper adheres to the principles for transparent reporting and scientific rigour of preclinical research as stated in the *BJP* guidelines for Design & Analysis, Immunoblotting and Immunochemistry and Animal Experimentation, and as recommended by funding agencies, publishers and other organizations engaged with supporting research.

DATA AVAILABILITY STATEMENT

The data generated herein are available upon reasonable request to the corresponding author.

ORCID

Samuel N. Baldwin https://orcid.org/0000-0002-3796-6090
Elizabeth A. Forrester https://orcid.org/0000-0002-2164-103X
Lauren McEwan https://orcid.org/0000-0002-1983-2574
Iain A. Greenwood https://orcid.org/0000-0002-0603-0492

REFERENCES

Abbott, G. W., & Jepps, T. A. (2016). Kcne4 deletion sex-dependently alters vascular reactivity. *Journal of Vascular Research*, *53*, 138–148. https://doi.org/10.1159/000449060

Alexander, S. P., Christopoulos, A., Davenport, A. P., Kelly, E., Mathie, A., Peters, J. A., Veale, E. L., Armstrong, J. F., Faccenda, E., Harding, S. D., Pawson, A. J., Southan, C., Davies, J. A., Abbracchio, M. P., Alexander, W., Al-hosaini, K., Bäck, M., Barnes, N. M., Bathgate, R., … Ye, R. D. (2021). THE CONCISE GUIDE TO PHARMACOLOGY 2021/22: G protein-coupled receptors. *British Journal of Pharmacology*, *178*(S1), S27–S156. https://doi.org/10.1111/bph.15538

Alexander, S. P., Mathie, A., Peters, J. A., Veale, E. L., Striessnig, J., Kelly, E., Armstrong, J. F., Faccenda, E., Harding, S. D., Pawson, A. J., Southan, C., Davies, J. A., Aldrich, R. W., Attali, B., Baggetta, A. M., Becirovic, E., Biel, M., Bill, R. M., Catterall, W. A., … Zhu, M. (2021). THE CONCISE GUIDE TO PHARMACOLOGY 2021/22: Ion channels. *British Journal of Pharmacology*, *178*(S1), S157–S245. https://doi.org/10.1111/bph.15539

Alexander, S. P. H., Roberts, R. E., Broughton, B. R. S., Sobey, C. G., George, C. H., Stanford, S. C., … Ahluwalia, A. (2018). Goals and practicalities of immunoblotting and immunohistochemistry: A guide for submission to the *British Journal of Pharmacology*. *British Journal of Pharmacology*, *175*, 407–411. https://doi.org/10.1111/bph.14112

Alzamora, R., O'Mahony, F., Bustos, V., Rapetti-Mauss, R., Urbach, V., Cid, L. P., Sepúlveda, F. V., & Harvey, B. J. (2011). Sexual dimorphism and oestrogen regulation of KCNE3 expression modulates the functional properties of KCNQ1 K^+ channels. *Journal of Physiology*, *589*, 5091–5107. https://doi.org/10.1113/jphysiol.2011.215772

Baldwin, S. N., Sandow, S. L., Mondéjar-Parreño, G., Stott, J. B., & Greenwood, I. A. (2020). KV7 channel expression and function within rat mesenteric endothelial cells. *Frontiers in Physiology*, *11*(December), 1–16. https://doi.org/10.3389/fphys.2020.598779

Barrese, V., Stott, J. B., Baldwin, S. N., Mondejar-Parreño, G., & Greenwood, I. A. (2020). SMIT (sodium-myo-inositol transporter) 1 regulates arterial contractility through the modulation of vascular Kv7 channels. *Arteriosclerosis, Thrombosis, and Vascular Biology*, *40*(10), 2468–2480. https://doi.org/10.1161/ATVBAHA.120.315096

Barrese, V., Stott, J. B., & Greenwood, I. A. (2018). KCNQ-Encoded Potassium Channels as Therapeutic Targets. *Annual review of pharmacology and toxicology*, *58*, 625–648. https://doi.org/10.1146/annurev-pharmtox-010617-052912

Berg, T. (2018). Kv7(KCNQ)-K^+-channels influence total peripheral resistance in female but not male rats, and hamper catecholamine release in hypertensive rats of both sexes. *Frontiers in Physiology*, *9*, 117. https://doi.org/10.3389/fphys.2018.00117

Blanco-Rivero, J., Cachofeiro, V., Lahera, V., Aras-Lopez, R., Márquez-Rodas, I.´., Salaices, M., Xavier, F. E., Ferrer, M., & Balfagón, G. (2005). Participation of prostacyclin in endothelial dysfunction induced by aldosterone in normotensive and hypertensive rats. *Hypertension*, *46*(1), 107–112. https://doi.org/10.1161/01.HYP.0000171479.36880.17

Byron, K. L., & Brueggemann, L. I. (2018). Kv7 potassium channels as signal transduction intermediates in the control of microvascular tone. *Microcirculation*, *25*, e12419. https://doi.org/10.1111/micc.12419

Chadha, P. S., Jepps, T. A., Carr, G., Stott, J. B., Zhu, H. L., Cole, W. C., & Greenwood, I. A. (2014). Contribution of Kv7.4/Kv7.5 heteromers to intrinsic and calcitonin gene-related peptide-induced cerebral reactivity. *Arteriosclerosis, Thrombosis, and Vascular Biology*, *34*(4), 887–893. https://doi.org/10.1161/ATVBAHA.114.303405

Chadha, P. S., Zunke, F., Davis, A. J., Jepps, T. A., Linders, J. T. M., Schwake, M., Towart, R., & Greenwood, I. A. (2012). Pharmacological dissection of Kv7.1 channels in systemic and pulmonary arteries. *British Journal of Pharmacology*, *166*, 1377–1387. https://doi.org/10.1111/j.1476-5381.2012.01863.x

Chadha, P. S., Zunke, F., Zhu, H. L., Davis, A. J., Jepps, T. A., Olesen, S. P., Cole, W. C., Moffatt, J. D., & Greenwood, I. A. (2012). Reduced KCNQ4-encoded voltage-dependent potassium channel activity underlies impaired β-adrenoceptor-mediated relaxation of renal arteries in hypertension. *Hypertension*, *59*, 877–884. https://doi.org/10.1161/HYPERTENSIONAHA.111.187427

Cora, M. C., Kooistra, L., & Travlos, G. (2015). Vaginal cytology of the laboratory rat and mouse: Review and criteria for the staging of the estrous cycle using stained vaginal smears. *Toxicologic Pathology*, *43*, 776–793. https://doi.org/10.1177/0192623315570339

Curtis, M. J., Alexander, S., Cirino, G., Docherty, J. R., George, C. H., Giembycz, M. A., Hoyer, D., Insel, P. A., Izzo, A. A., Ji, Y., MacEwan, D. J., Sobey, C. G., Stanford, S. C., Teixeira, M. M., Wonnacott, S., & Ahluwalia, A. (2018). Experimental design and analysis and their reporting II: Updated and simplified guidance for authors and peer reviewers. *British Journal of Pharmacology*, *175*, 987–993. https://doi.org/10.1111/bph.14153

Docherty, J. R., Stanford, S. C., Panattieri, R. A., Alexander, S. P. H., Cirino, G., George, C. H., Hoyer, D., Izzo, A. A., Ji, Y., Lilley, E., & Sobey, C. G. (2019). Sex: A change in our guidelines to authors to ensure that this is no longer an ignored experimental variable. *British Journal of Pharmacology*, *176*(21), 4081–4086. https://doi.org/10.1111/bph.14761

Dumas, M., Dumas, J. P., Rochette, L., Advenier, C., & Giudicelli, J. F. (1997). Role of potassium channels and nitric oxide in the effects of iloprost and prostaglandin E1 on hypoxic vasoconstriction in the isolated perfused lung of the rat. *British Journal of Pharmacology*, *120*, 405–410. https://doi.org/10.1038/sj.bjp.0700912

Dusting, G. J., Moncada, S., & Vane, J. R. (1977). Prostacyclin (PGI2) is a weak contractor of coronary arteries of the pig. *European Journal of Pharmacology*, *45*, 301–304. https://doi.org/10.1016/0014-2999(77)90014-0

Gluais, P., Lonchampt, M., Morrow, J. D., Vanhoutte, P. M., & Feletou, M. (2005). Acetylcholine-induced endothelium-dependent contractions in the SHR aorta: The Janus face of prostacyclin. *British Journal of Pharmacology*, *146*, 834–845. https://doi.org/10.1038/sj.bjp.0706390

Gollasch, M. (2017). Adipose-vascular coupling and potential therapeutics. *Annual Review of Pharmacology and Toxicology*, *57*, 417–436. https://doi.org/10.1146/annurev-pharmtox-010716-104542

Jaimes, L., Vinet, R., Knox, M., Morales, B., Benites, J., Laurido, C., & Martínez, J. (2019). A review of the actions of endogenous and exogenous vasoactive substances during the estrous cycle and pregnancy in rats. *Animals : An Open Access Journal from MDPI*, *9*(6), 288. https://doi.org/10.3390/ani9060288

Jepps, T. A., Bentzen, B. H., Stott, J. B., Povstyan, O. V., Sivaloganathan, K., Dalby-Brown, W., & Greenwood, I. A. (2014). Vasorelaxant effects of novel Kv7.4 channel enhancers ML213 and NS15370. *British Journal of Pharmacology*, *171*(19), 4413–4424. https://doi.org/10.1111/bph.12805

Jepps, T. A., Carr, G., Lundegaard, P. R., Olesen, S. P., & Greenwood, I. A. (2015). Fundamental role for the KCNE4 ancillary subunit in Kv7.4 regulation of arterial tone. *Journal of Physiology*, *593*, 5325–5340. https://doi.org/10.1113/JP271286

Jepps, T. A., Chadha, P. S., Davis, A. J., Harhun, M. I., Cockerill, G. W., Olesen, S. P., Hansen, R. S., & Greenwood, I. A. (2011). Downregulation of Kv7.4 channel activity in primary and secondary hypertension. *Circulation*, *124*, 602–611. https://doi.org/10.1161/CIRCULATIONAHA.111.032136

Katusic, Z. S., Santhanam, A. V., & He, T. (2012). Vascular effects of prostacyclin: Does activation of PPARδ play a role? *Trends in Pharmacological Sciences*, *33*, 559–564. https://doi.org/10.1016/j.tips.2012.05.005

Khanamiri, S., Soltysinska, E., Jepps, T. A., Bentzen, B. H., Chadha, P. S., Schmitt, N., Greenwood, I. A., & Olesen, S. P. (2013). Contribution of KV7 channels to basal coronary flow and active response to ischemia. *Hypertension*, *62*(6), 1090–1097. https://doi.org/10.1161/HYPERTENSIONAHA.113.01244

Kobayashi, K., Murata, T., Hori, M., & Ozaki, H. (2011). Prostaglandin E2-prostanoid EP3 signal induces vascular contraction via nPKC and ROCK activation in rat mesenteric artery. *European Journal of Pharmacology*, *660*, 375–380. https://doi.org/10.1016/j.ejphar.2011.03.032

Lilley, E., Stanford, S. C., Kendall, D. E., Alexander, S. P. H., Cirino, G., Docherty, J. R., George, C. H., Insel, P. A., Izzo, A. A., Ji, Y., Panettieri, R. A., Sobey, C. G., Stefanska, B., Stephens, G., Teixeira, M., & Ahluwalia, A. (2020). ARRIVE 2.0 and the British Journal of Pharmacology: Updated guidance for 2020.

Lindman, J., Khammy, M. M., Lundegaard, P. R., Aalkjær, C., & Jepps, T. A. (2018). Microtubule regulation of Kv7 channels orchestrates cAMP-mediated vasorelaxations in rat arterial smooth muscle. *Hypertension (Dallas, Tex.: 1979)*, *71*, 336–345. https://doi.org/10.1161/HYPERTENSIONAHA.117.10152

Liu, B., Luo, W., Zhang, Y., Li, H., Zhang, J., Tan, X. R., & Zhou, Y. (2012). Concomitant activation of functionally opposing prostacyclin and thromboxane prostanoid receptors by cyclo-oxygenase-1-mediated prostacyclin synthesis in mouse arteries. *Experimental Physiology*, *97*(7), 895–904. https://doi.org/10.1113/expphysiol.2011.063784

Liu, B., Zhan, M., Zhang, Y., Li, H., Wu, X., Zhuang, F., Luo, W., & Zhou, Y. (2017). Increased role of e prostanoid receptor-3 in prostacyclin-evoked contractile activity of spontaneously hypertensive rat mesenteric resistance arteries. *Scientific Reports*, *7*(1), 8927. https://doi.org/10.1038/s41598-017-09288-w

Lombard, J. H., Liu, Y., Fredricks, K. T., Bizub, D. M., Roman, R. J., & Rusch, N. J. (1999). Electrical and mechanical responses of rat middle cerebral arteries to reduced PO2 and prostacyclin. *American Journal of Physiology - Heart and Circulatory Physiology*, *276*, H509–H516. https://doi.org/10.1152/ajpheart.1999.276.2.h509

Mackie, A. R., Brueggemann, L. I., Henderson, K. K., Shiels, A. J., Cribbs, L. L., Scrogin, K. E., & Byron, K. L. (2008). Vascular KCNQ potassium channels as novel targets for the control of mesenteric artery constriction by vasopressin, based on studies in single cells, pressurized arteries, and in vivo measurements of mesenteric vascular resistance. *Journal of Pharmacology and Experimental Therapeutics*, *325*, 475–483. https://doi.org/10.1124/jpet.107.135764

McCallum, L. A., Greenwood, I. A., & Tribe, R. M. (2009). Expression and function of Kv7 channels in murine myometrium throughout oestrous cycle. *Pflügers Archiv / European Journal of Physiology*, *457*, 1111–1120. https://doi.org/10.1007/s00424-008-0567-5

Mills, T. A., Greenwood, S. L., Devlin, G., Shweikh, Y., Robinson, M., Cowley, E., Hayward, C. E., Cottrell, E. C., Tropea, T., Brereton, M. F., Dalby-Brown, W., & Wareing, M. (2015). Activation of K_V7 channels stimulates vasodilatation of human placental chorionic plate arteries. *Placenta*, *36*(6), 638–644. https://doi.org/10.1016/j.placenta.2015.03.007

Moncada, S., Gryglewski, R., Bunting, S., & Vane, J. R. (1976). An enzyme isolated from arteries transforms prostaglandin endoperoxides to an unstable substance that inhibits platelet aggregation. *Nature*, *263*, 663–665. https://doi.org/10.1038/263663a0

Morales-Cano, D., Moreno, L., Barreira, B., Pandolfi, R., Chamorro, V., Jimenez, R., Villamor, E., Duarte, J., Perez-Vizcaino, F., & Cogolludo, A. (2015). Kv7 channels critically determine coronary artery reactivity: Left-right differences and down-regulation by hyperglycaemia. *Cardiovascular Research*, *106*(1), 98–108. https://doi.org/10.1093/cvr/cvv020

Mulvany, M. (1977). Contractile properties of small arterial resistance vessels in spontaneously hypertensive and normotensive rats. *Circulation Research*, *41*, 19–26. https://doi.org/10.1161/01

Ng, F. L., Davis, A. J., Jepps, T. A., Harhun, M. I., Yeung, S. Y., Wan, A., Reddy, M., Melville, D., Nardi, A., Khong, T. K., & Greenwood, I. A. (2011). Expression and function of the K^+ channel KCNQ genes in human arteries. *British Journal of Pharmacology*, *162*(1), 42–53. https://doi.org/10.1111/j.1476-5381.2010.01027.x

Nilsson, M. E., Vandenput, L., Tivesten, Å., Norlén, A.-K., Lagerquist, M. K., Windahl, S. H., Börjesson, A. E., Farman, H. H., Poutanen, M., Benrick, A., Maliqueo, M., Stener-Victorin, E., Ryberg, H., & Ohlsson, C. (2015). Measurement of a comprehensive sex steroid profile in rodent serum by high-sensitive gas chromatography-tandem mass spectrometry. *Endocrinology*, *156*, 2492–2502. https://doi.org/10.1210/en.2014-1890

O'Mahony, F., Alzamora, R., Betts, V., LaPaix, F., Carter, D., Irnaten, M., & Harvey, B. J. (2007). Female gender-specific inhibition of KCNQ1 channels and chloride secretion by 17β-estradiol in rat distal colonic crypts. *Journal of Biological Chemistry*, *282*, 24563–24573. https://doi.org/10.1074/jbc.M611682200

Orie, N. N., & Clapp, L. H. (2011). Role of prostanoid IP and EP receptors in mediating vasorelaxant responses to PGI2 analogues in rat tail artery: Evidence for Gi/o modulation via EP3 receptors. *European Journal of Pharmacology*, *654*, 258–265. https://doi.org/10.1016/j.ejphar.2010.12.005

Orie, N. N., Fry, C. H., & Clapp, L. H. (2006). Evidence that inward rectifier K^+ channels mediate relaxation by the PGI2 receptor agonist cicaprost via a cyclic AMP-independent mechanism. *Cardiovascular Research*, *69*, 107–115. https://doi.org/10.1016/j.cardiores.2005.08.004

Pabbidi, M. R., Kuppusamy, M., Didion, S. P., Sanapureddy, P., Reed, J. T., & Sontakke, S. P. (2018). Sex differences in the vascular function and related mechanisms: Role of 17β-estradiol. *American Journal of Physiology. Heart and Circulatory Physiology*, *315*(6), H1499–H1518. https://doi.org/10.1152/ajpheart.00194.2018

Percie du Sert, N., Hurst, V., Ahluwalia, A., Alam, S., Avey, M. T., Baker, M., Browne, W. J., Clark, A., Cuthill, I. C., Dirnagl, U., Emerson, M., Garner, P., Holgate, S. T., Howells, D. W., Karp, N. A., Lazic, S. E., Lidster, K., MacCallum, C. J., Macleod, M., … Würbel, H. (2020). The ARRIVE guidelines 2.0: Updated guidelines for reporting animal research. *Experimental Physiology*, *105*(9), 1459–1466. https://doi.org/10.1113/EP088870

Rapetti-Mauss, R., O'Mahony, F., Sepulveda, F. V., Urbach, V., & Harvey, B. J. (2013). Oestrogen promotes KCNQ1 potassium channel

endocytosis and postendocytic trafficking in colonic epithelium. *Journal of Physiology*, *591*, 2813–2831. https://doi.org/10.1113/jphysiol.2013.251678

Schubert, R., Serebryakov, V. N., Engel, H., & Hopp, H. H. (1996). Iloprost activates K (Ca) channels of vascular smooth muscle cells: Role of cAMP-dependent protein kinase. *American Journal of Physiology - Cell Physiology*, *271*, C1203–C1211. https://doi.org/10.1152/ajpcell.1996.271.4.c1203

Schubert, R., Serebryakov, V. N., Mewes, H., & Hopp, H. H. (1997). Iloprost dilates rat small arteries: Role of K (ATP)- and K (Ca)-channel activation by cAMP-dependent protein kinase. *American Journal of Physiology - Heart and Circulatory Physiology*, *272*, H1147–H1156. https://doi.org/10.1152/ajpheart.1997.272.3.h1147

Stott, J. B., Barrese, V., & Greenwood, I. A. (2016). Kv7 channel activation underpins EPAC-dependent relaxations of rat arteries. *Arteriosclerosis, Thrombosis, and Vascular Biology*, *36*(12), 2404–2411. https://doi.org/10.1161/ATVBAHA.116.308517

Stott, J. B., Barrese, V., Jepps, T. A., Leighton, E. V., & Greenwood, I. A. (2015). Contribution of Kv7 channels to natriuretic peptide mediated vasodilation in normal and hypertensive rats. *Hypertension*, *65*, 676–682. https://doi.org/10.1161/HYPERTENSIONAHA.114.04373

Stott, J. B., Barrese, V., Suresh, M., Masoodi, S., & Greenwood, I. A. (2018). Investigating the role of G protein βγ in Kv7-dependent relaxations of the rat vasculature. *Arteriosclerosis, Thrombosis, and Vascular Biology*, *38*, 2091–2102. https://doi.org/10.1161/ATVBAHA.118.311360

Stott, J. B., Povstyan, O. V., Carr, G., Barrese, V., & Greenwood, I. A. (2015). G-protein βγ subunits are positive regulators of Kv7.4 and native vascular Kv7 channel activity. *Proceedings of the National Academy of Sciences*, *112*, 6497–6502. https://doi.org/10.1073/pnas.1418605112

Tang, E. H. C., Jensen, B. L., Skott, O., Leung, G. P. H., Feletou, M., Man, R. Y. K., & Vanhoutte, P. M. (2008). The role of prostaglandin E and thromboxane-prostanoid receptors in the response to prostaglandin E2 in the aorta of Wistar Kyoto rats and spontaneously hypertensive rats. *Cardiovascular Research*, *78*, 130–138. https://doi.org/10.1093/cvr/cvm112

Tsvetkov, D., Kaßmann, M., Tano, J. Y., Chen, L., Schleifenbaum, J., Voelkl, J., Lang, F., Huang, Y., & Gollasch, M. (2017). Do KV7.1 channels contribute to control of arterial vascular tone? *British Journal of Pharmacology*, *174*, 150–162. https://doi.org/10.1111/bph.13665

Waldegger, S., Lang, U., Herzer, T., Suessbrich, H., et al. (1996). Inhibition of minK protein induced K^+ channels in Xenopus oocytes by estrogens. *Pflügers Archiv / European Journal of Physiology*, *457*, 1111–1120. https://doi.org/10.1007/s00424-008-0567-5

Whittle, B. J., Silverstein, A. M., Mottola, D. M., & Clapp, L. H. (2012). Binding and activity of the prostacyclin receptor (IP) agonists, treprostinil and iloprost, at human prostanoid receptors: Treprostinil is a potent DP 1 and EP 2 agonist. *Biochemical Pharmacology*, *84*, 68–75. https://doi.org/10.1016/j.bcp.2012.03.012

Yeung, S. Y. M., Pucovský, V., Moffatt, J. D., Saldanha, L., Schwake, M., Ohya, S., & Greenwood, I. A. (2007). Molecular expression and pharmacological identification of a role for Kv7 channels in murine vascular reactivity. *British Journal of Pharmacology*, *151*(6), 758–770. https://doi.org/10.1038/sj.bjp.0707284

Yu, H., Lin, Z., Xu, K., Huang, X., Long, S., Wu, M., McManus, O. B., & Le Engers, J, Mattmann, M.E., Engers, D.W., Le, U.M., Lindsley, C. W., Hopkins, C. R., & Li, M. (2013). Identification of a novel, small molecule activator of KCNQ1 channels. In: Probe Reports from the NIH Molecular Libraries Program [Internet].

Zhang, Y., Luo, W., Li, H., Yu, G., Luo, H., Leng, J., Ge, J., Zeng, R., Guo, T., Yin, Y., Zhou, Y., & Liu, B. (2021). Larger endothelium-dependent contractions in iliac arteries of adult SHRs are attributed to differential downregulation of TP and EP3 receptors in the vessels of WKYs and SHRs during the transition from adolescence to adulthood. *European Journal of Pharmacology*, *893*, 173828. https://doi.org/10.1016/j.ejphar.2020.173828

SUPPORTING INFORMATION

Additional supporting information may be found in the online version of the article at the publisher's website.

How to cite this article: Baldwin, S. N., Forrester, E. A., McEwan, L., & Greenwood, I. A. (2022). Sexual dimorphism in prostacyclin-mimetic responses within rat mesenteric arteries: A novel role for $K_V7.1$ in shaping IP receptor-mediated relaxation. *British Journal of Pharmacology*, 1–15. https://doi.org/10.1111/bph.15722